Final Report

GULF OF MEXICO COMPREHENSIVE SYNTHETIC BASED MUDS MONITORING PROGRAM VOLUME II: TECHNICAL

October 2004

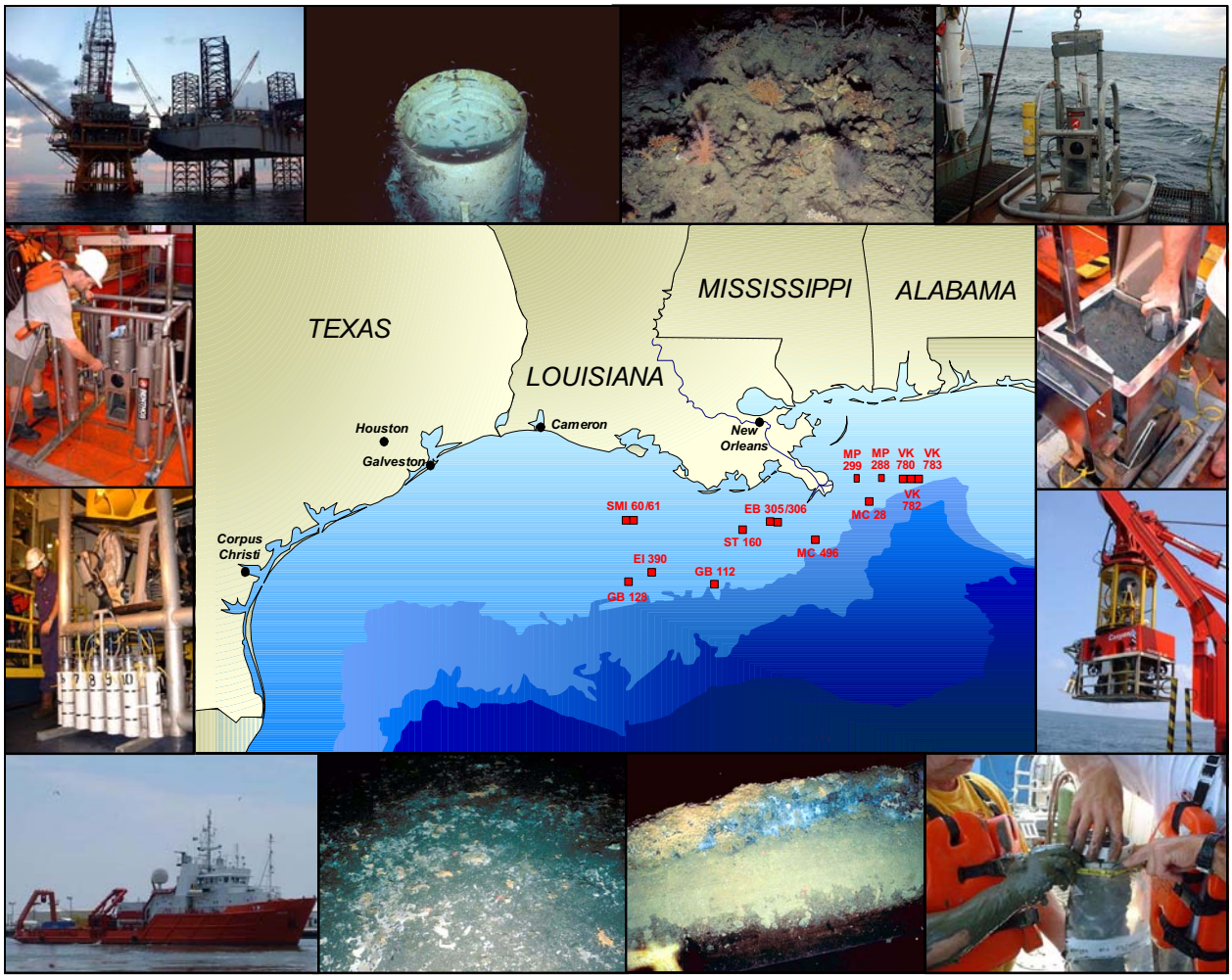

Prepared for

SBM Research Group

Submitted to

James P. Ray
Shell Global Solutions U.S.
Westhollow Technology Center
3333 Highway 6 South
Houston, Texas 77082
Telephone: (281) 544-6165

Prepared by

Continental Shelf Associates, Inc.
759 Parkway Street
Jupiter, Florida 33477
Telephone: (561) 746-7946

Final Report

GULF OF MEXICO COMPREHENSIVE SYNTHETIC BASED MUDS MONITORING PROGRAM VOLUME II: TECHNICAL

October 2004

Prepared for

SBM Research Group

Submitted to

James P. Ray
Shell Global Solutions U.S.
Westhollow Technology Center
3333 Highway 6 South
Houston, Texas 77082
Telephone: (281) 544-6165

Prepared by

Continental Shelf Associates, Inc.
759 Parkway Street
Jupiter, Florida 33477
Telephone: (561) 746-7946

TABLE OF CONTENTS

TABLE OF CONTENTS
(Continued)

Page

TABLE OF CONTENTS
(Continued)

Page

TABLE OF CONTENTS
(Continued)

Page

TABLE OF CONTENTS
(Continued)

Page

TABLE OF CONTENTS
(Continued)

Page

TABLE OF CONTENTS
(Continued)

Page

VOLUME III: APPENDICES

TABLE OF CONTENTS
(Continued)

Page

LIST OF TABLES

LIST OF TABLES
(Continued)

LIST OF TABLES
(Continued)

LIST OF TABLES
(Continued)

LIST OF TABLES
(Continued)

LIST OF TABLES
(Continued)

LIST OF TABLES
(Continued)

LIST OF TABLES
(Continued)

LIST OF TABLES
(Continued)

LIST OF FIGURES

LIST OF FIGURES
(Continued)

LIST OF FIGURES
(Continued)

LIST OF FIGURES
(Continued)

LIST OF FIGURES
(Continued)

LIST OF FIGURES
(Continued)

LIST OF FIGURES
(Continued)

LIST OF FIGURES
(Continued)

LIST OF FIGURES
(Continued)

LIST OF FIGURES
(Continued)

LIST OF FIGURES
(Continued)

LIST OF FIGURES
(Continued)

LIST OF FIGURES
(Continued)

LIST OF FIGURES
(Continued)

LIST OF PHOTOS

LIST OF PHOTOS
(Continued)

LIST OF PHOTOS
(Continued)

LIST OF ACRONYMS

AAS	atomic absorption spectrometry
ANOVA	analysis of variance
API	American Petroleum Institute
ASTM	American Society for Testing and Materials
BI	biotic index
BVA	Barry A. Vittor & Associates, Inc.
CAS	Columbia Analytical Services, Inc.
CC	Chesapeake Cultures
CL	clay
CNESS	chord-normalized expected species shared
CRM	certified reference material
CSA	Continental Shelf Associates, Inc.
CTD	conductivity/temperature/depth
CV	coefficient of variation
CVAAS	cold vapor atomic absorption spectrometry
DGPS	differential global positioning system
DISC	discretionary
DIW	deionized water
DO	dissolved oxygen
DP	dynamic positioning
DQO	data quality objective
EI	Eugene Island
ELG	Effluent Limitation Guideline
EW	Ewing Bank
FAAS	flame atomic absorption spectrometry
FF	far-field
FIT	Florida Institute of Technology
GB	Garden Banks
GC/MS	gas chromatography/mass spectrometry
GFAAS	graphite furnace atomic absorption spectrometry
GIS	geographic information system
HSD	Honest Significant Difference
IASPSO	International Association for the Physical Sciences of the Ocean
ICP-MS	inductively-coupled plasma-mass spectrometry
ID	internal diameter
IO	internal olefin
JCPDS	Joint Committee on Powder Diffraction Studies
KD	Kuderna-Danish
LAO	linear alpha olefin
LARS	launch and recovery system
LGL	LGL Ecological Research Associates, Inc.
LPIL	lowest practical identification level
LSA	logarithmic series alpha
MC	Mississippi Canyon
MDL	method detection limit
MDS	multidimensional scaling
MF	mid-field
MMS	Minerals Management Service

LIST OF ACRONYMS
(Continued)

MP	Main Pass
MS/MSD	matrix spike/matrix spike duplicate
MSL	Battelle Marine Sciences Laboratory
NAD	North American Datum
NADAS	navigation and data acquisition system
NESS	normalized expected species shared
NF	near-field
NIST	National Institute of Standards and Technology
NIVA	Norwegian Institute of Water Research
NOAA	National Oceanic and Atmospheric Administration
NPDES	National Pollutant Discharge Elimination System
NRC	National Research Council
OBM	oil based mud
OMZ	oxygen minimum zones
PAO	poly alpha olefin
PFTBA	perfluorotributylamine
QA/QC	quality assurance/quality control
RF	response factor
RIS	recovery internal standards
ROV	remotely operated vehicle
RPD	redox potential discontinuity
RSD	relative standard deviation
RTR	ratio-to-reference
SBF	synthetic based fluid
SBM	synthetic based mud
SD	standard deviation
SE	standard error
SICL	sitly clay
SIS	surrogate internal standards
SMI	South Marsh Island
SOP	standard operating procedure
SPI	sediment profile imaging
SRM	standard reference material
ST	South Timbalier
TMS	tether management system
TOC	total organic carbon
TPH	total petroleum hydrocarbons
USBL	ultra short base line
USDOI	U.S. Department of the Interior
USEPA	U.S. Environmental Protection Agency
UTM	Universal Transverse Mercator
UV	ultraviolet
VK	Viosca Knoll
WBM	water based mud

ACKNOWLEDGMENTS

The Gulf of Mexico Comprehensive Synthetic Based Muds (SBM) Monitoring Program was sponsored by the SBM Research Group participants (listed below), the U.S. Department of Energy, and the Minerals Management Service. The members of this consortium are gratefully acknowledged for their respective support of this project.

- Agip Petroleum Co. Inc.
- Amerada Hess
- Anadarko Petroleum Corporation
- Apache Corporation
- ATP Oil & Gas Corporation
- Baker Hughes INTEQ
- Baroid Drilling Fluids
- BHP Billiton Petroleum (Americas) Inc.
- BP Exploration & Production, Inc (including Vastar Resources)
- BP Chemicals
- British-Borneo Exploration, Inc.
- Burlington Resources Offshore Inc.
- Callon Petroleum Operating Company
- Challenger Minerals, Inc.
- ChevronTexaco U.S.A. Inc.
- ConocoPhillips Petroleum
- Denbury Resources, Inc.
- Devon Energy (formerly Santa Fe Snyder Corporation)
- Dominion Exploration & Production (formerly CNG Producing Company)
- EEX Corporation
- Elf E&P USA Inc.
- El Paso Production (formerly Sonat Exploration GOM Inc.)
- Energy Partners Ltd/Hall Houston Oil Company
- EOG Resources
- ExxonMobil Corporation
- Forest Oil Corporation
- Hunt Oil Company
- IP Petroleum Company, Inc.
- Kerr-McGee Oil & Gas Corporation
- LLOG Exploration Company, L.L.C.
- Magnum Hunter Production, Inc.
- Marathon Oil Company
- Mariner Energy, Inc.
- Maxus (U.S.) Exploration Company
- McMoRan Exploration Co.
- M-I L.L.C.
- Mossgas (Pty) Limited c/o Alcochem, Inc.
- Murphy Exploration & Production Company
- Newfield Exploration Company
- Nexen Petroleum (formerly CXY Energy)

- Occidental Oil & Gas
- Ocean Energy, Inc.
- PetroBras America Inc.
- PetroCanada Corp.
- PetroQuest Energy, Inc.
- Pioneer Natural Resources USA, Inc.
- Samedan Oil Corporation
- SASOL Technology (Pty) Ltd
- Seneca Resources Corporation
- Shell Offshore Inc.
- Shrieve Chemical Products Co
- Spinnaker Exploration Company
- Statoil Exploration (US) Inc.
- Stone Energy Corporation
- Taylor Energy Company
- Union Oil Company of California
- Walter Oil & Gas Corporation.
- Westport Resources Corporation
- W&T Offshore, Inc.

The following individuals served as the technical working group to advise the project. They are gratefully acknowledged for their support and guidance during the project.

- Dr. James Ray (Chair)
- Dr. Joseph P. Smith (Co-Chair)
- Dr. Robert Ayers
- Dr. Kris Bansal
- Dr. Mary Boatman
- Ms. Nancy Comstock
- Dr. Andrew Glickman
- Dr. John Hall
- Ms. Cheryl Hood
- Dr. Bela James
- Ms. Gail Korenaga
- Dr. Jose Limia
- Mr. Ed Malachosky
- Dr. Robert McNeil
- Dr. Tim Nedwed
- Mr. Mike Parker
- Dr. Thomas Purcell
- Mr. Steven Rabke
- Dr. Larry Reitsema

REPORT ORGANIZATION

This report is organized into three volumes. The first volume consists of the Executive Summary, introductory chapters, and the synthesis of the project findings. Volume I is composed of the following:

	EXECUTIVE SUMMARY
Chapter 1	INTRODUCTION
Chapter 2	SITE SELECTION AND DESCRIPTION
Chapter 3	FIELD METHODOLOGY
Chapter 4	SYNTHESIS AND INTEGRATION
Chapter 5	REFERENCES*

The second volume consists of the technical support for the project findings. Volume II is composed of the following:

Chapter 6	GEOPHYSICAL DATA
Chapter 7	NANNOFOSSILS, SEDIMENTOLOGY, AND VISUAL CUTTINGS ANALYSIS
Chapter 8	THE ORGANIC CHEMISTRY OF SYNTHETIC BASED FLUID RESIDUES AND TOTAL PETROLEUM HYDROCARBONS IN SEDIMENTS
Chapter 9	METALS AND REDOX CHEMISTRY IN SEDIMENTS
Chapter 10	SEDIMENT TOXICITY
Chapter 11	SEDIMENT PROFILE IMAGING
Chapter 12	MACROINFAUNA
Chapter 13	REFERENCES*

Volume III contains the appendices. These are the following:

Appendix A	LOCATIONS OF SAMPLING SITES
Appendix B	HYDROGRAPHIC DATA FOR SAMPLING CRUISES 1 AND 2
Appendix C	ANALYTICAL RESULTS FOR NANNOFOSSIL ANALYSIS, GRAIN SIZE ANALYSIS, AND VISUAL CUTTINGS ANALYSIS FOR SAMPLING CRUISES 1 AND 2
Appendix D	TOTAL PETROLEUM HYDROCARBON AND SYNTHETIC BASED FLUID CONCENTRATIONS FOR SAMPLING CRUISES 1 AND 2
Appendix E	TRACE METAL, TOTAL ORGANIC CARBON, AND QUALITY ASSURANCE/QUALITY CONTROL DATA FOR THE SCREENING CRUISE AND SAMPLING CRUISES 1 AND 2; VERTICAL PROFILES FOR SEDIMENT CORES FOR CONCERNATIONS OF ALUMINUM, BARIUM, TOTAL ORGANIC CARBON, SYNTHETIC BASED FLUID, IRON, AND MANGANESE FOR SAMPLING CRUISES 1 AND 2; SEDIMENT PROFILE DATA (O_2, pH, and Eh) FOR SAMPLING CRUISES 1 AND 2; AND PORE WATER DATA FOR SAMPLING CRUISES 1 AND 2
Appendix F	SEDIMENT TOXICITY
Appendix G	SEDIMENT PROFILE IMAGE DATA
Appendix H	BENTHIC INFAUNAL DATA
Appendix I	PREVIOUS PROJECT REPORTS

* Chapters 5 and 13 contain all references cited in both Volumes I and II.

Chapter 6
GEOPHYSICAL DATA

Alan D. Hart
Continental Shelf Associates, Inc.

6.1 INTRODUCTION

This chapter describes the findings of swath bathymetry and side-scan sonar surveys that were conducted at four continental shelf and four continental slope study sites during the Screening Cruise (August 2000). This section of the report focuses on addressing the fate aspect of the overall objective of assessing the fate and effects of discharged SBM cuttings at continental shelf and continental slope sites in the Gulf of Mexico. Previous industry practices in the North Sea permitted discharges of cuttings from oil-based systems, and the characteristics of the discharges resulted in large cuttings piles accumulating at the discharge points. This raised an important question regarding the fate of Gulf of Mexico discharges—are large SBM cuttings piles accumulating underneath platforms in the Gulf of Mexico? To address this important issue, swath bathymetry data and side-scan sonar data were collected at each of eight study sites, and the results are presented in the following sections.

6.2 METHODOLOGY

Swath bathymetry data and side-scan sonar data were collected during the Screening Cruise with an ROV following the methods described in Chapter 3. As stated in Chapter 3, the resolutions of the swath bathymetry data and the side-scan sonar data were 1 and 2 m, respectively. Bathymetry data from each study site were contoured with Surfer Version 8.1 (Golden Software, Inc., Golden, CO). The resolution of the swath bathymetry data was 1 m. Mosaics of the side-scan data were prepared by David Evans and Associates, Inc. These mosaics were examined for differences in reflectivity, which could imply the presence of cuttings.

6.3 RESULTS AND DISCUSSION

6.3.1 Continental Shelf Sites

6.3.1.1 Garden Banks 128. Eight wells were drilled at this site prior to the Screening Cruise. An estimated volume of 4,697 bbl of SBM cuttings had been discharged, and the last well was drilled in April 1999. Results of the swath bathymetry collected at GB 128 are shown as a contour plot in Figure 6-1. The discharge site was located in an area that gradually sloped deeper toward the southeast. Water depths at this study site ranged from about 190 to 194 m. Examination of the side-scan sonar data collected around the GB 128 study site (Figure 6-2) revealed evidence of drilling activity. Scarring on the seafloor was noted, perhaps associated with anchors/cables. There was no evidence of cuttings piles in the vicinity of the discharge site based on the swath bathymetry or side-scan sonar data.

6.3.1.2 Main Pass 288. Three SBM wells had been drilled within 50 m of the MP 288 study site center prior to the Screening Cruise, and a total of 1,309 bbl of SBM cuttings had been discharged. The last of these SBM wells was drilled in March 1998. Twenty-three WBM wells were drilled within 50 m of the study site center between 1976 and 1987 at MP 288. Discharges from most of these wells were between 1,000 and 2,000 bbl of cuttings.

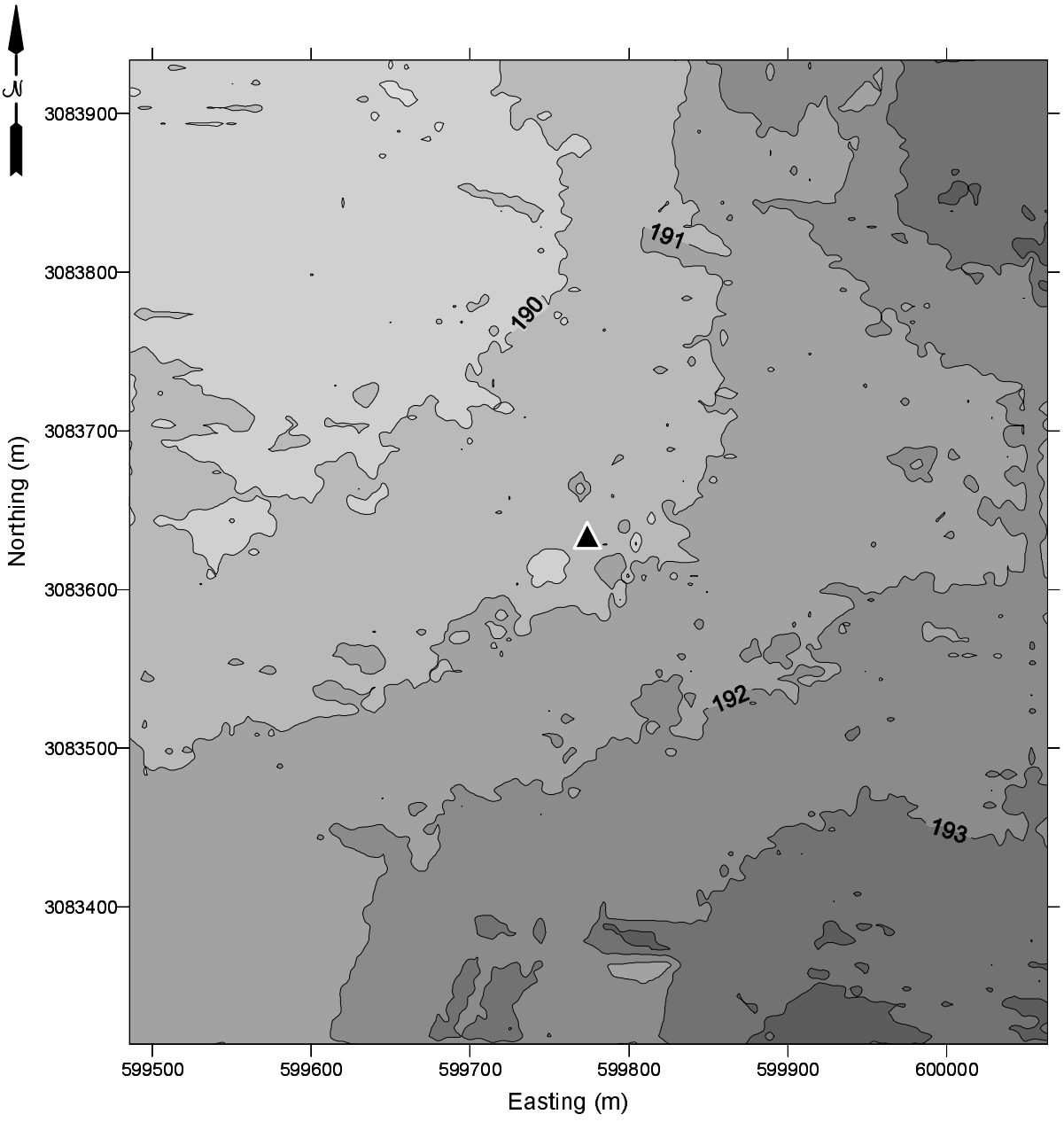

Figure 6-1. Bathymetry in the vicinity of the Garden Banks 128 study site. Geodesy is UTM, Zone 15N, NAD 27.

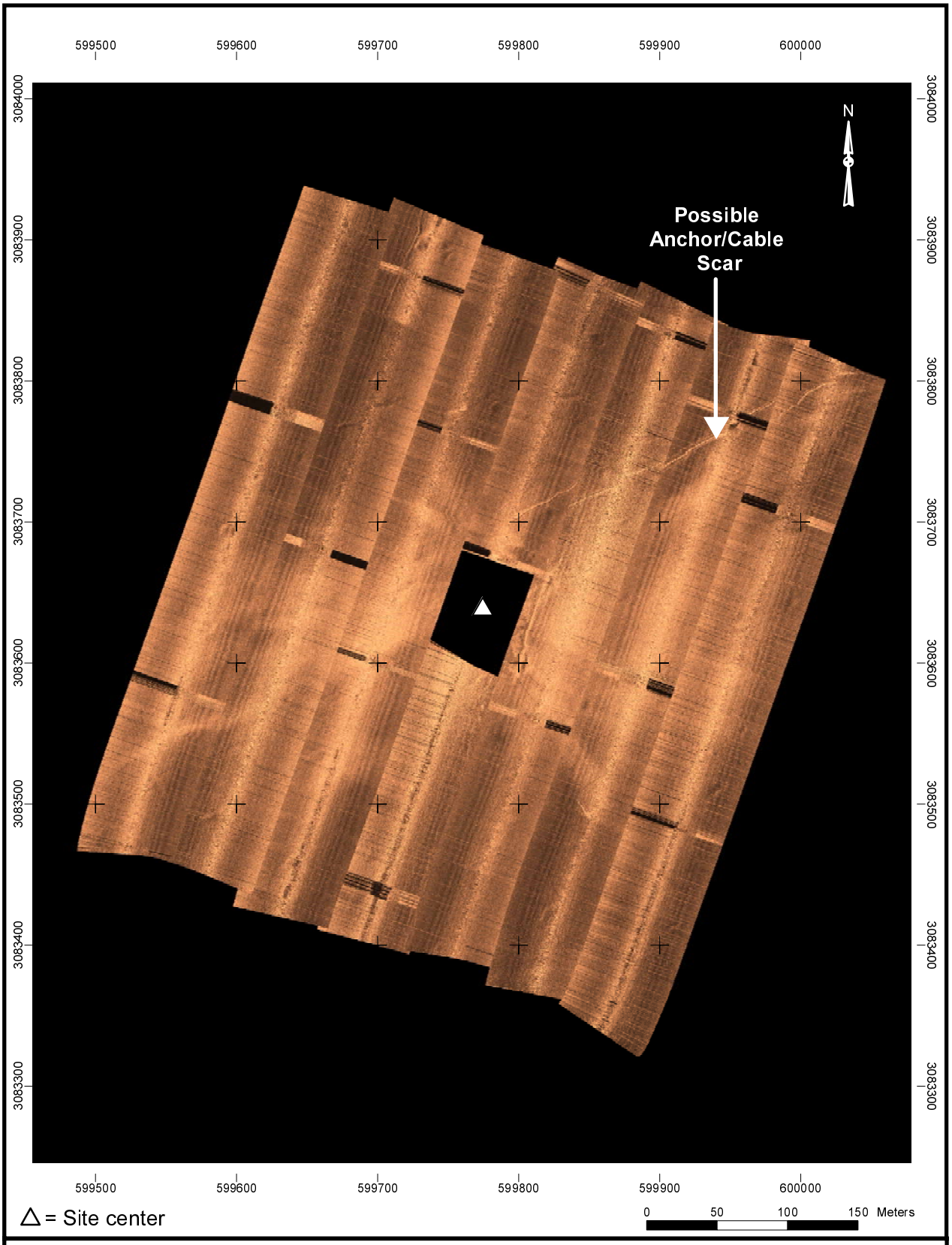

Figure 6-2. Mosaic of side-scan sonar imagery collected in the vicinity of the Garden Banks 128 study site.

The seafloor in the vicinity of MP 288 deepened from north to south (Figure 6-3). There was a difference in the reflectivity observed in the side-scan sonar data collected near the MP 288 discharge site compared to farther away from the discharge site (Figure 6-4). This may indicate the presence of coarse material such as drill cuttings near the discharge site. Neither the swath bathymetry nor the side-scan sonar, however, indicated that cuttings had accumulated to the point that they projected above the ambient sediments.

6.3.1.3 Main Pass 299. Three SBM wells had been drilled within 50 m of the center of the MP 299 study site. The total estimated quantity of discharged SBM cuttings was 966 bbl, and the last well was drilled in April 2000. An additional 14 WBM wells were drilled within 50 m of the site center between 1985 and 2000. Discharges from most of these wells were between 2,000 and 4,000 bbl of cuttings.

The MP 299 discharge site was located on relatively flat seafloor (Figure 6-5). Water depths in the very near vicinity of the discharge point were slightly greater than the surrounding seafloor, and there was evidence of some shallow holes near the discharge site. There was some shadowing northeast of the site center observed with the side-scan sonar, possibly indicating drilling-related activity (Figure 6-6). However, there was no evidence of cuttings piles in the swath bathymetry or the side-scan sonar data.

6.3.1.4 Viosca Knoll 780. Eight wells had been drilled at VK 780 prior to the Screening Cruise. The last of these was drilled in July 1999. There was a hole several meters deep observed in the near vicinity of the VK 780 discharge site (Figure 6-7). A small mound that was several meters higher than the surrounding seafloor was observed south-southeast of the discharge point. It is unlikely that this was a drill cuttings mound because there were a number of similar features observed farther from the discharge point. The side-scan sonar imagery indicated some shading on the seafloor around the discharge point, which may have been related to drilling activities (Figure 6-8). Neither the swath bathymetry nor the side-scan sonar indicated that cuttings piles occurred in the vicinity of the VK 780 discharge site.

6.3.2 Continental Slope Sites

6.3.2.1 Green Canyon 112. An estimated quantity of 3,570 bbl of SBM cuttings was discharged from a single SBM well that had been drilled at the center of the GC 112 site in December 1997. Another SBM well was drilled approximately 50 m south of the site center in March 1997. This well discharged 1,900 bbl of SBM cuttings. An additional 3,500 bbl of WBM cuttings were discharged from these wells.

Bathymetry at this study site was irregular, sloping distinctly deeper toward the southeast (Figure 6-9). Depths ranged from less than 525 m to greater than 545 m. Contours of the swath bathymetry data indicated a small mound was located west of the central coordinates of the study sites. Because there are similar features at other locations in the swath bathymetry record at this location, this feature cannot be definitively identified as a cuttings pile. Side-scan sonar showed a difference in reflectivity at and south of the discharge point compared to the surrounding areas, which may indicate the presence of coarse-grained material such as cuttings (Figure 6-10). Evidence of potential cuttings piles was limited to the small mound west of the site center. No large accumulations were identified.

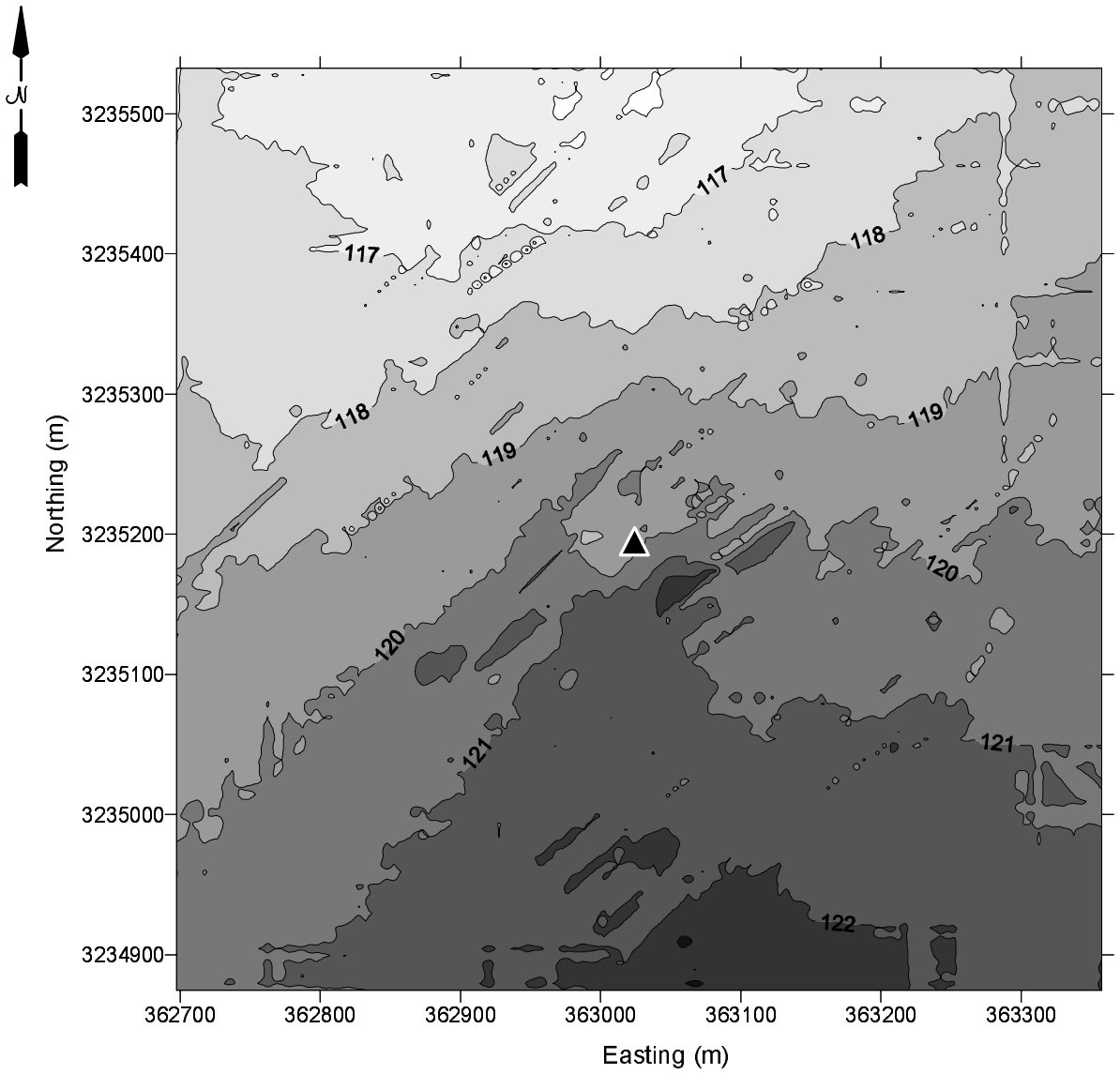

▲ = Site center

Figure 6-3. Bathymetry in the vicinity of the Main Pass 288 study site. Geodesy is UTM, Zone 16N, NAD 27.

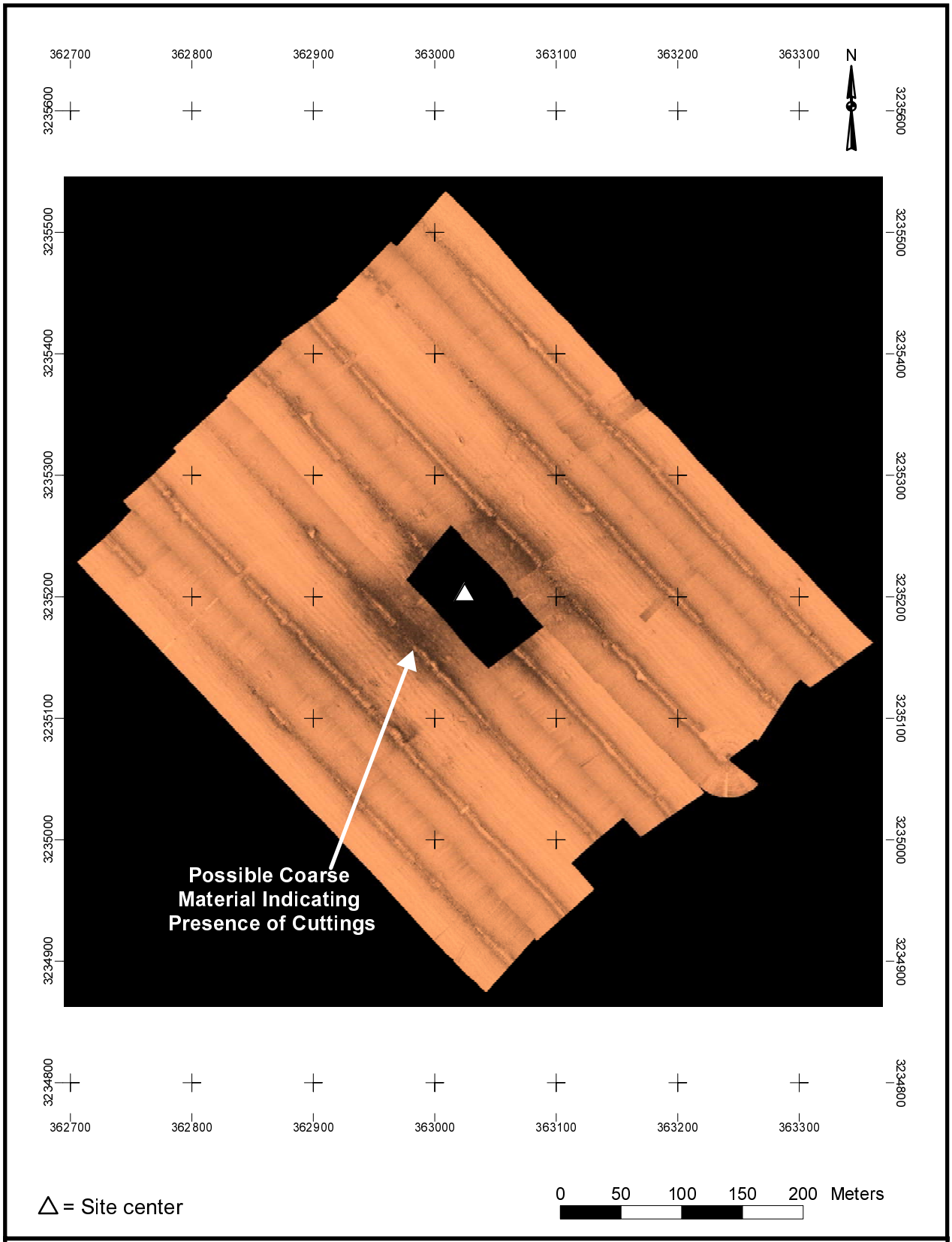

Figure 6-4. Mosaic of side-scan sonar imagery collected in the vicinity of the Main Pass 288 study site.

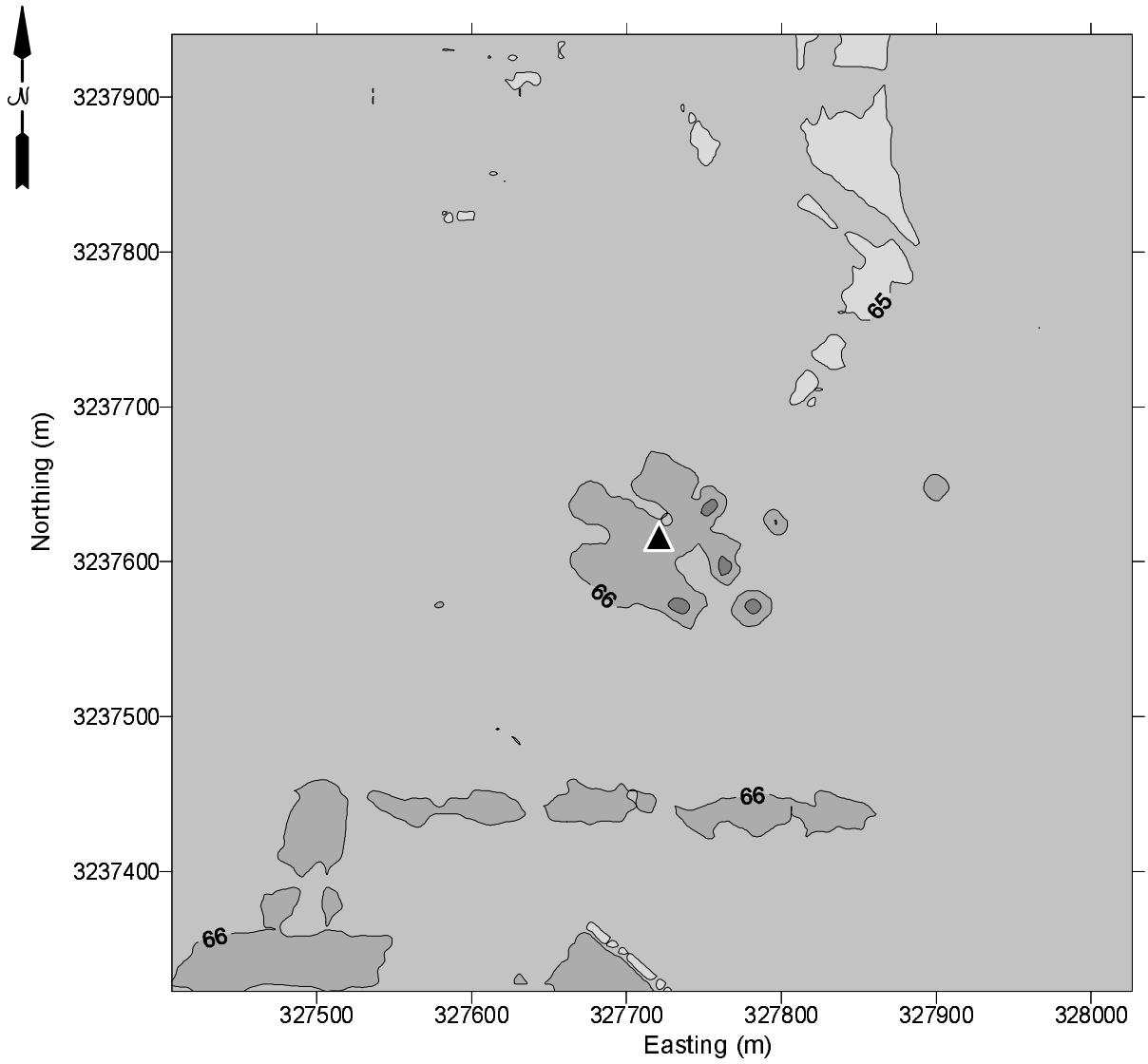

▲ = Site center

Figure 6-5. Bathymetry in the vicinity of the Main Pass 299 study site. Geodesy is UTM, Zone 16N, NAD 27.

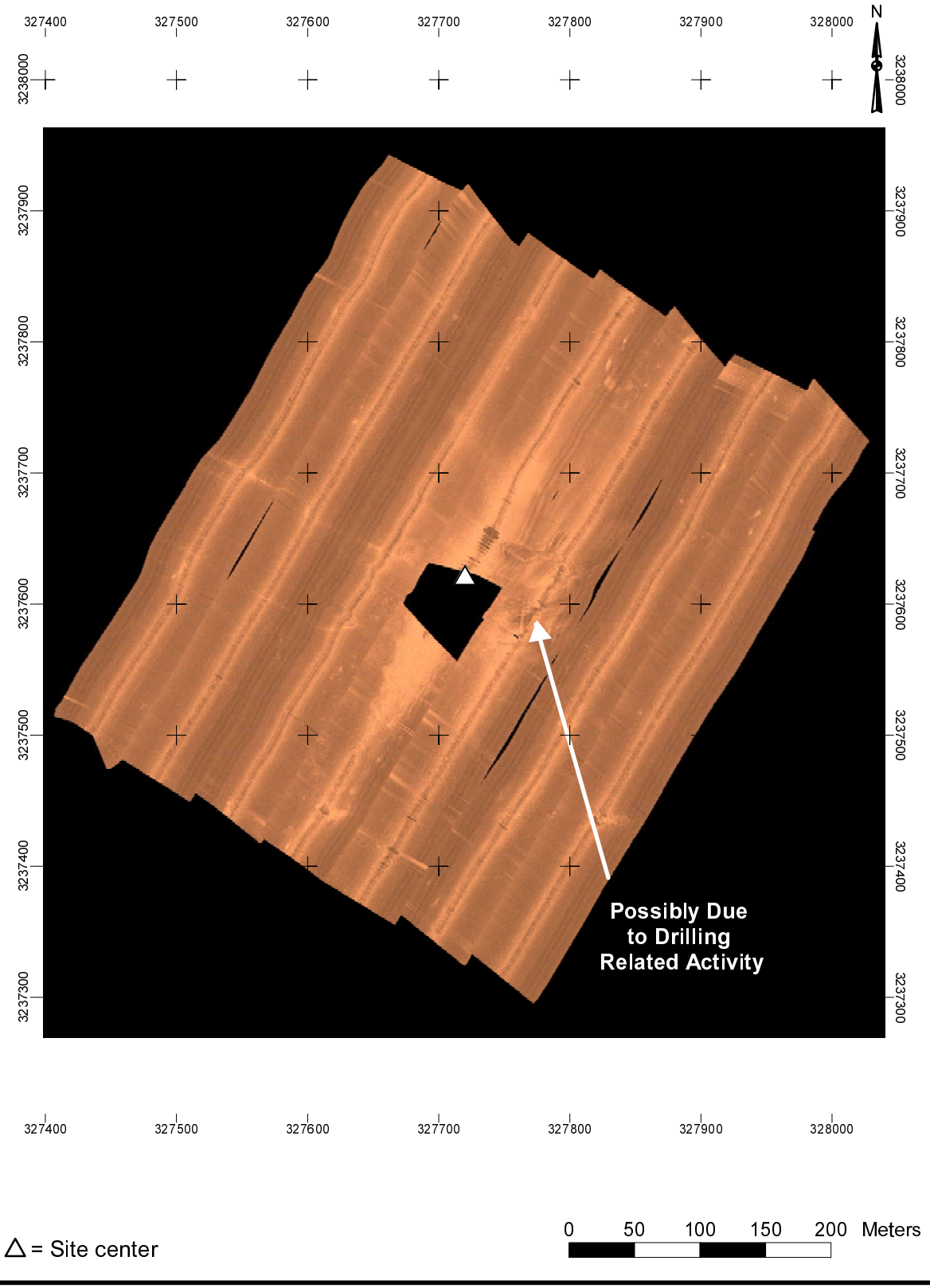

Figure 6-6. Mosaic of side-scan sonar imagery collected in the vicinity of the Main Pass 299 study site.

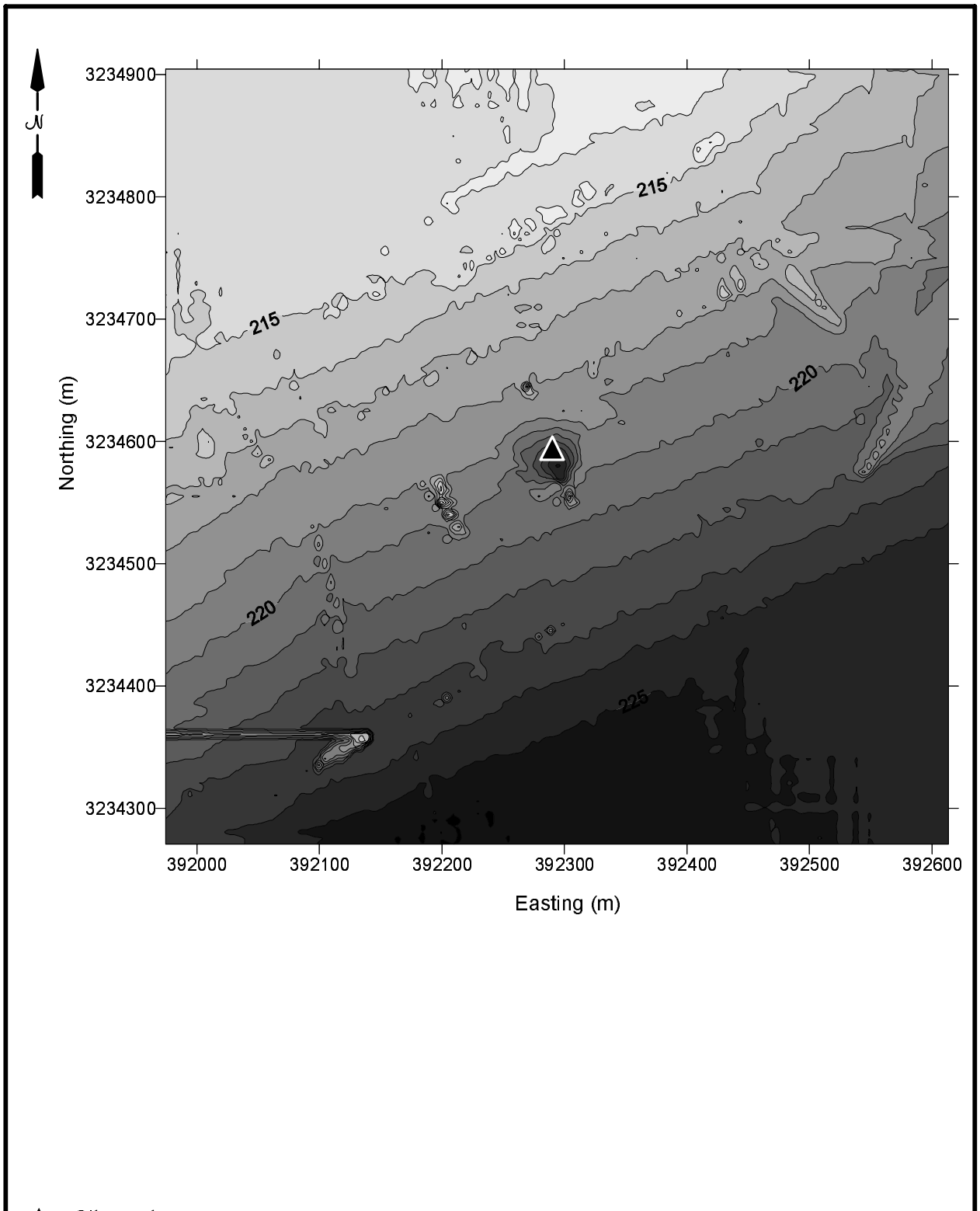

Figure 6-7. Bathymetry in the vicinity of the Viosca Knoll 780 study site. Geodesy is UTM, Zone 16N, NAD 27.

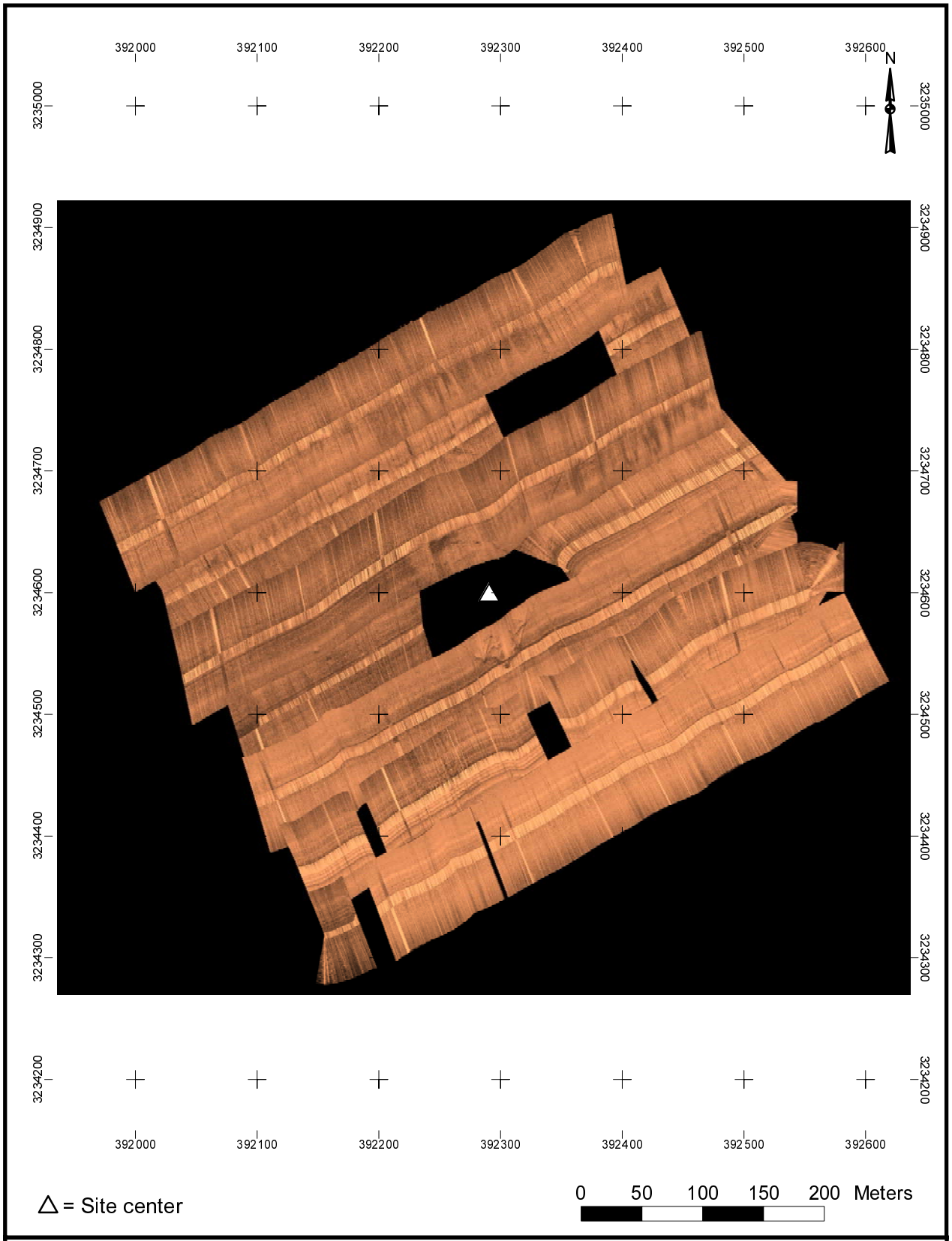

Figure 6-8. Mosaic of side-scan sonar imagery collected in the vicinity of the Viosca Knoll 780 study site.

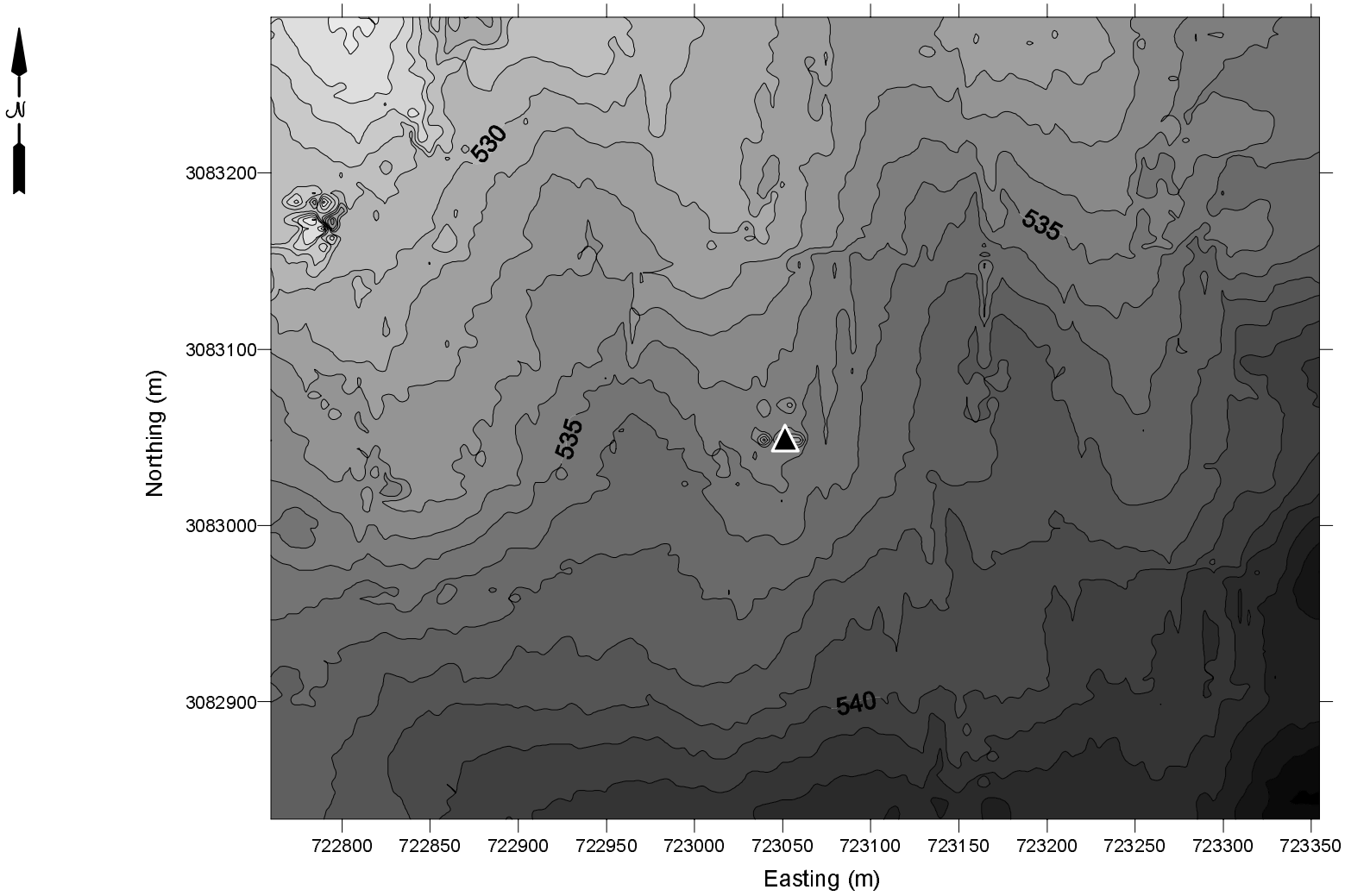

Figure 6-9. Bathymetry in the vicinity of the Green Canyon 112 study site. Geodesy is UTM, Zone 15N, NAD 27.

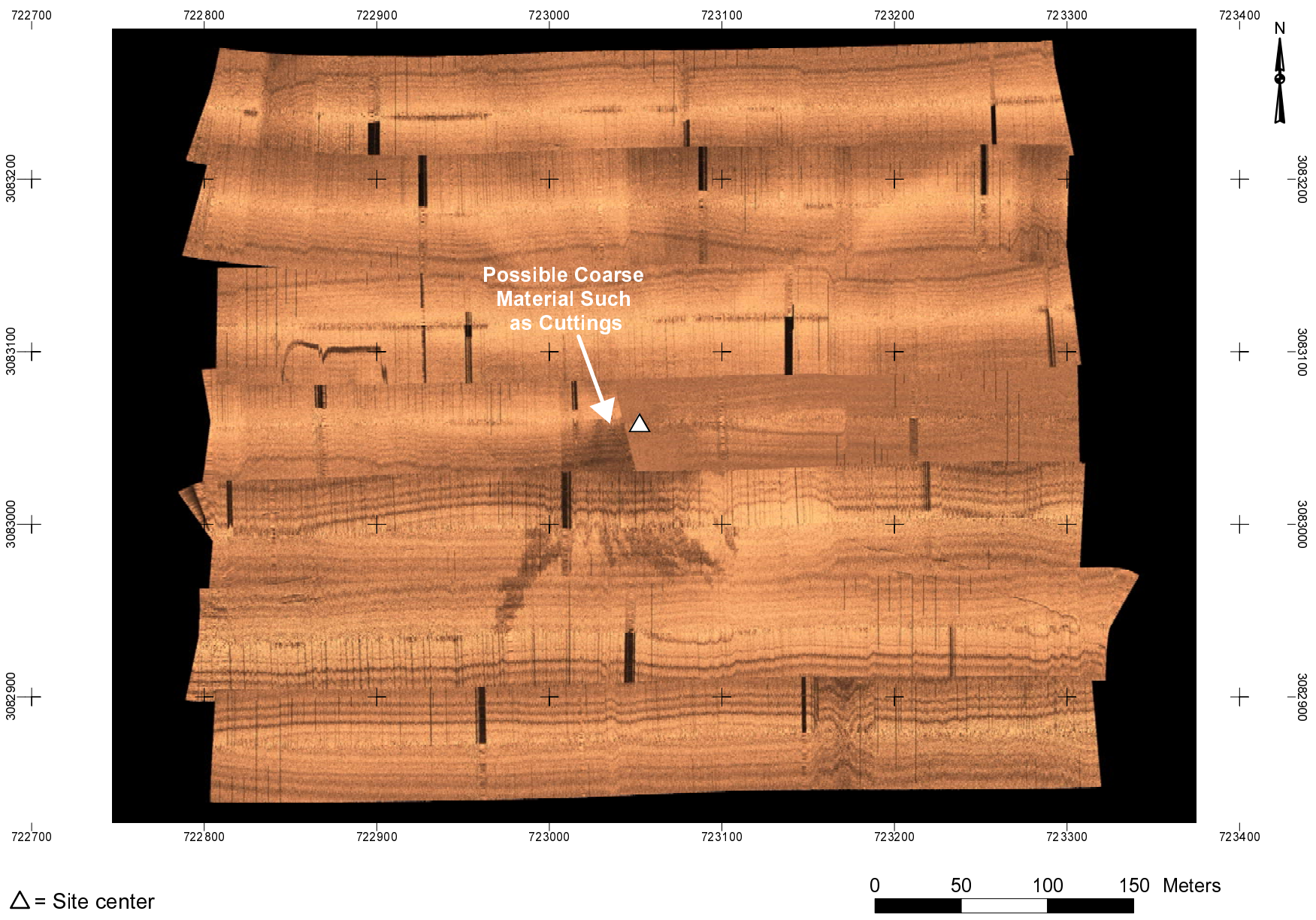

Figure 6-10. Mosaic of side-scan sonar imagery collected in the vicinity of the Green Canyon 112 study site.

6.3.2.2 Mississippi Canyon 28. Seven wells had been drilled at this site prior to the Screening Cruise. The last well was drilled in 1998. The estimated quantity of SBM cuttings discharged was 5,150 bbl. Bathymetry at the MC 28 study site sloped from about 554 m northwest of the discharge point to greater than 570 m southeast of the discharge point (Figure 6-11). There was a notable feature that rose distinctly above the seafloor east-southeast of the discharge point. Discussion with the operator revealed that this feature was the subsurface structure associated with this production site. Information from the operator revealed that the dimensions of the manifold/template are approximately 46.3 m x 24.4 m x 14.6 m (152 ft x 80 ft x 48 ft). The corners of the subsurface structure are shown on Figure 6-11. The presence of this structure also was evident in the side-scan sonar imagery (Figure 6-12). There was no evidence of mounds that could be interpreted as cuttings piles.

6.3.2.3 Mississippi Canyon 496. One well had been drilled at MC 496 in October 1998 prior to the Screening Cruise, and the quantity of discharged SBM cuttings was 1,674 bbl. An additional 5,045 bbl of WBM cuttings were discharged from this well.

Water depths at the MC 496 study site ranged from less than 540 m to greater than 554 m (Figure 6-13). There was no evidence of any mound in the vicinity of the discharge point at the study site. The results of the side-scan sonar survey at this site likewise did not clearly indicate the presence of cuttings (Figure 6-14).

6.3.2.4 Viosca Knoll 783. Prior to the Screening Cruise, one well had been drilled at this site in October 1995, and an estimated 436 bbl of SBM cuttings were discharged. The mound indicated by the swath bathymetry data at the discharge point in VK 783 (Figure 6-15) was not due to an accumulation of cuttings. A well head protruding approximately 2 m above the seafloor was acoustically detected and confirmed visually at this location. Its appearance in the bathymetry contour plot as a mound is an artifact of the contouring algorithm. The side-scan sonar data confirmed this feature at the location of the discharge point (Figure 6-16). There were differences in the reflectivity near the discharge point that may indicate the presence of some cuttings on the seafloor, but there was no evidence of a cuttings mound.

6.4 SUMMARY

Swath bathymetry and side-scan sonar data were collected at eight study sites during the Screening Cruise. Four study sites were located on the continental shelf, and four study sites were located in deeper water on the continental slope. There were indications at some locations of drilling-related discharges; however, there were no cuttings accumulations of significant relief detected. Based on the sensitivities of the instrumentation used to collect the swath bathymetry and side-scan sonar data, cuttings accumulations of 1 m or greater would have been detected. These observations are in contrast to those from the North Sea. In the central and northern parts of the United Kingdom Sector of the North Sea, cuttings piles have been documented around approximately 60 multiwell platforms. Most of these wells were drilled with oil based fluids. Piles up to 26 m high have been observed, but most were less than 10 m high (Cordah, 1998). The presence of cuttings piles in the North Sea may in part be due to shunting of discharges to near the seafloor, which decreases the area of the seafloor over which cuttings accumulate and increases the mass of cuttings deposited per unit area near the discharge point (Neff et al., 2000). Another factor contributing to the large cuttings piles in the North Sea is the size of the reservoirs. Typical North Sea oil fields are large compared to Gulf of Mexico oil fields. This results in many wells being drilled from a single location. In the Gulf of Mexico, typical reservoirs are smaller, so fewer wells are drilled at a single location.

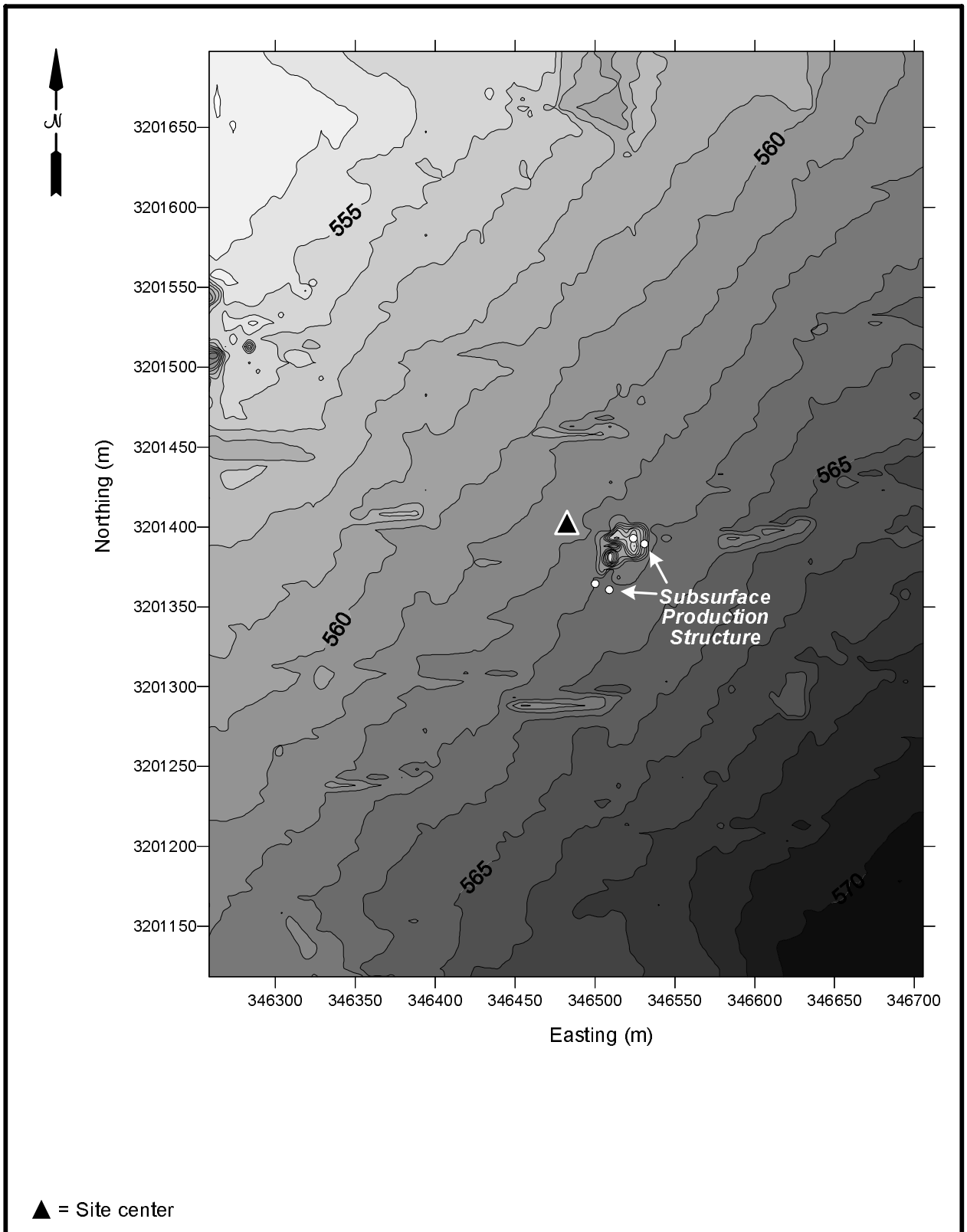

Figure 6-11. Bathymetry in the vicinity of the Mississippi Canyon 28 study site. Geodesy is UTM, Zone 16N, NAD 27.

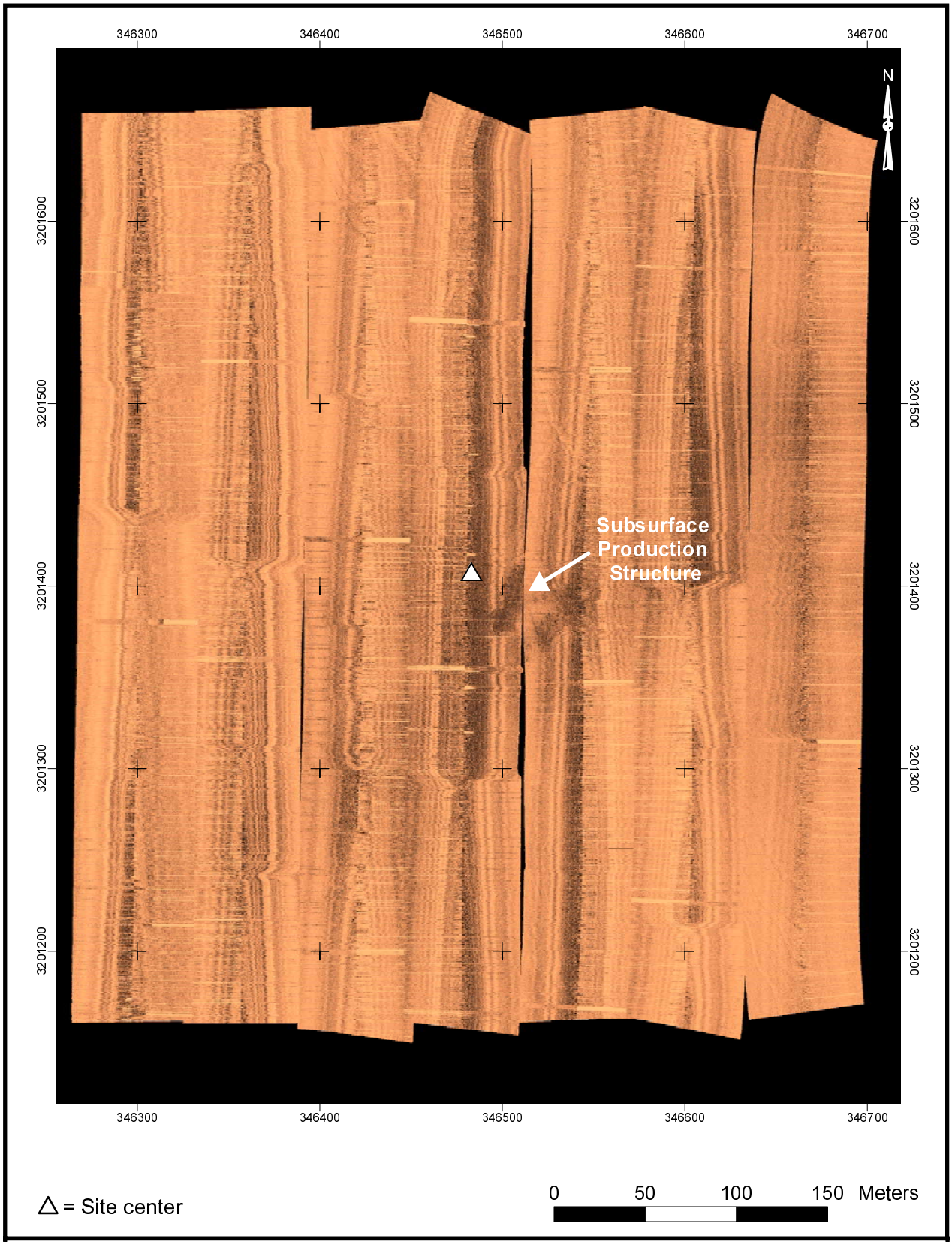

Figure 6-12. Mosaic of side-scan sonar imagery collected in the vicinity of the Mississippi Canyon 28 study site.

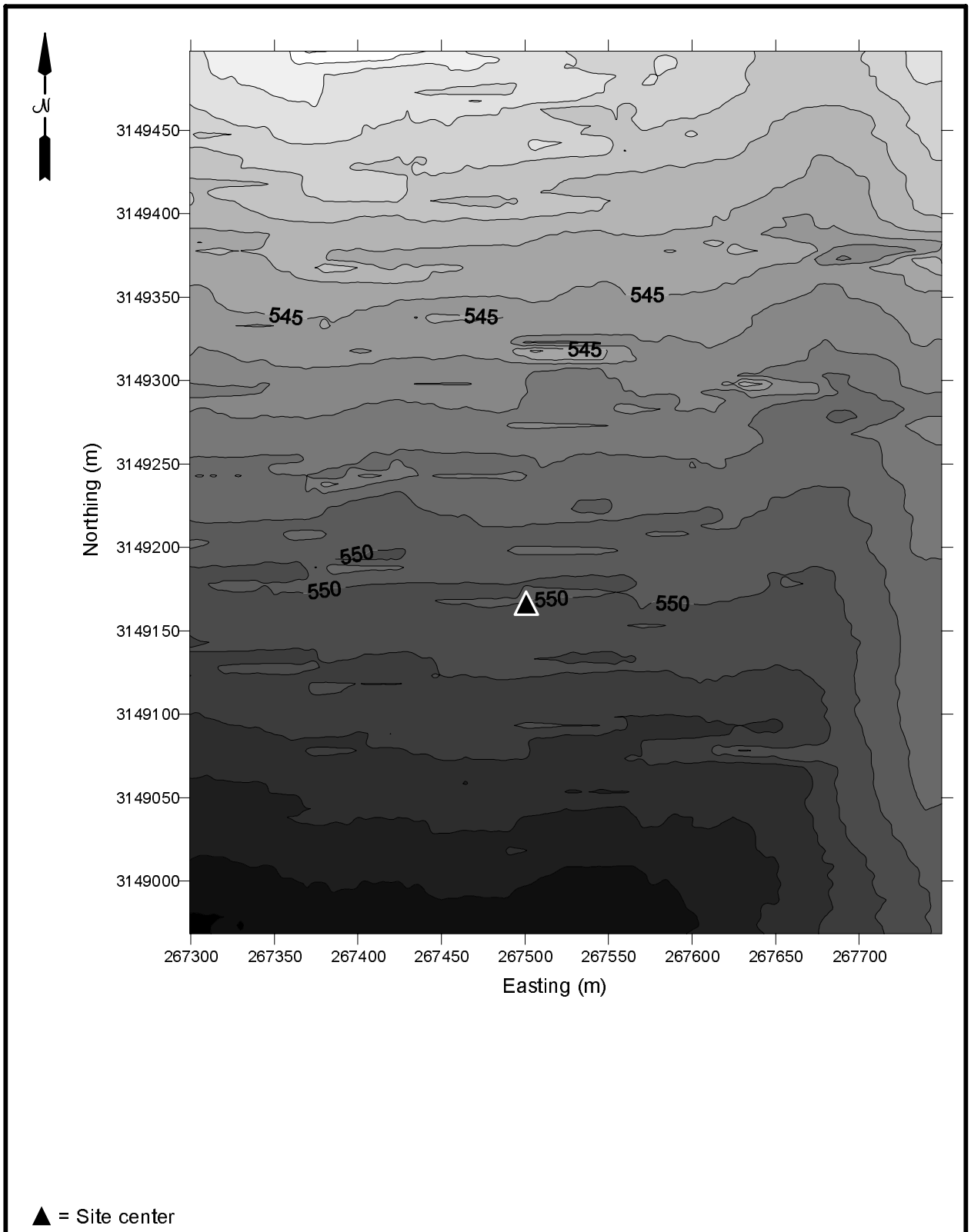

Figure 6-13. Bathymetry in the vicinity of the Mississippi Canyon 496 study site. Geodesy is UTM, Zone 16N, NAD 27.

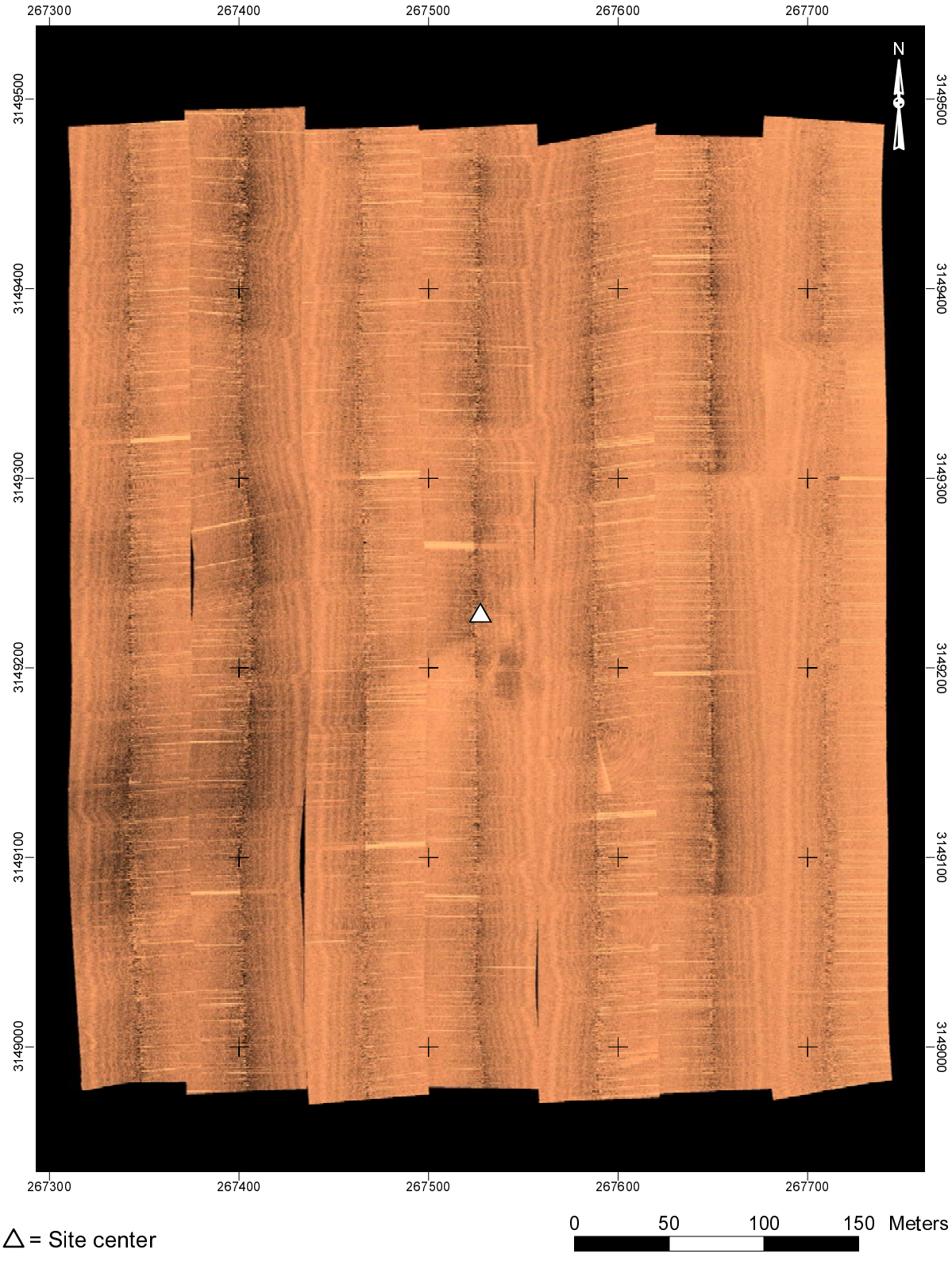

Figure 6-14. Mosaic of side-scan sonar imagery collected in the vicinity of the Mississippi Canyon 496 study site.

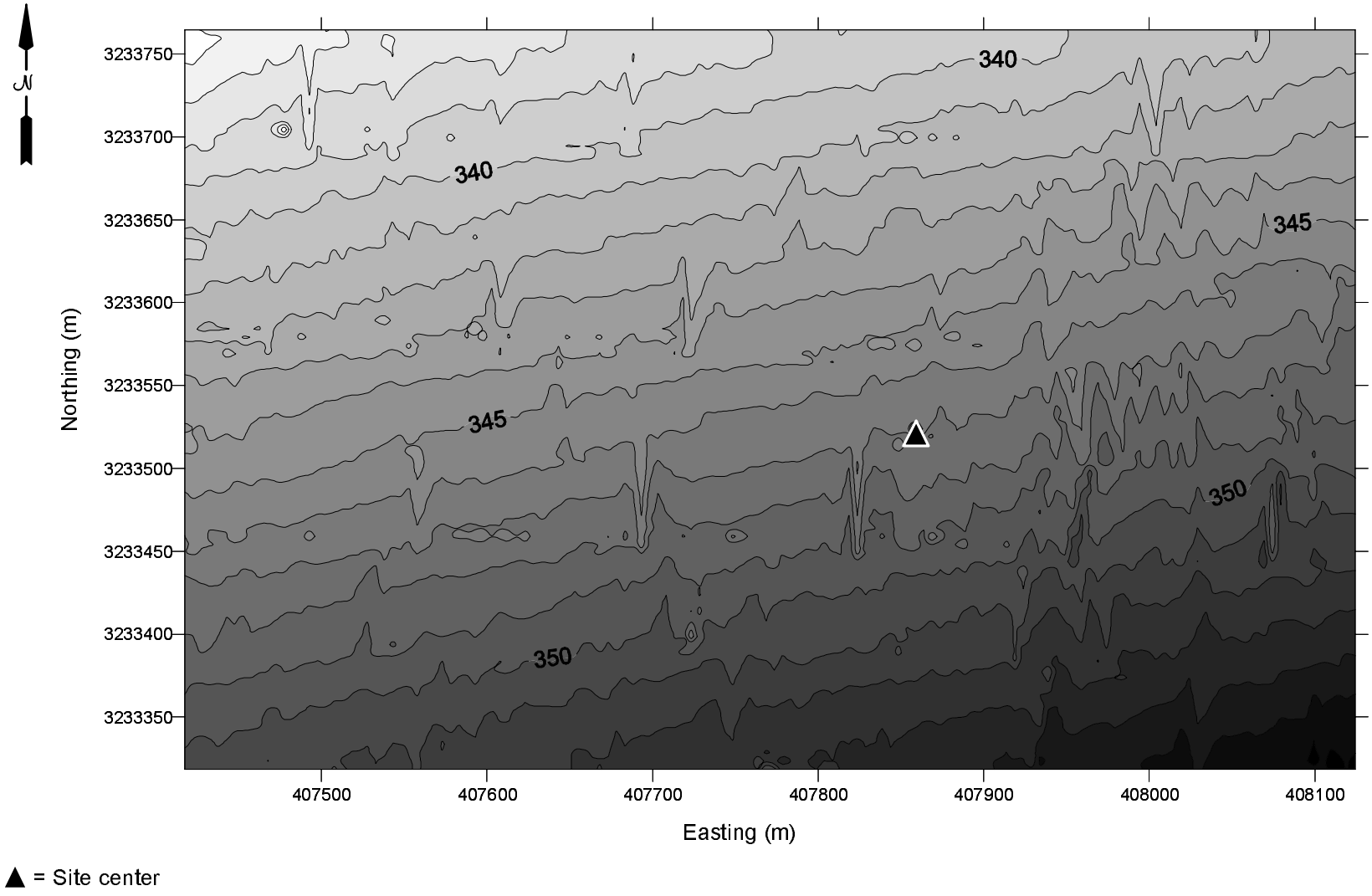

Figure 6-15. Bathymetry in the vicinity of the Viosca Knoll 783 study site. Geodesy is UTM, Zone 16N, NAD 27.

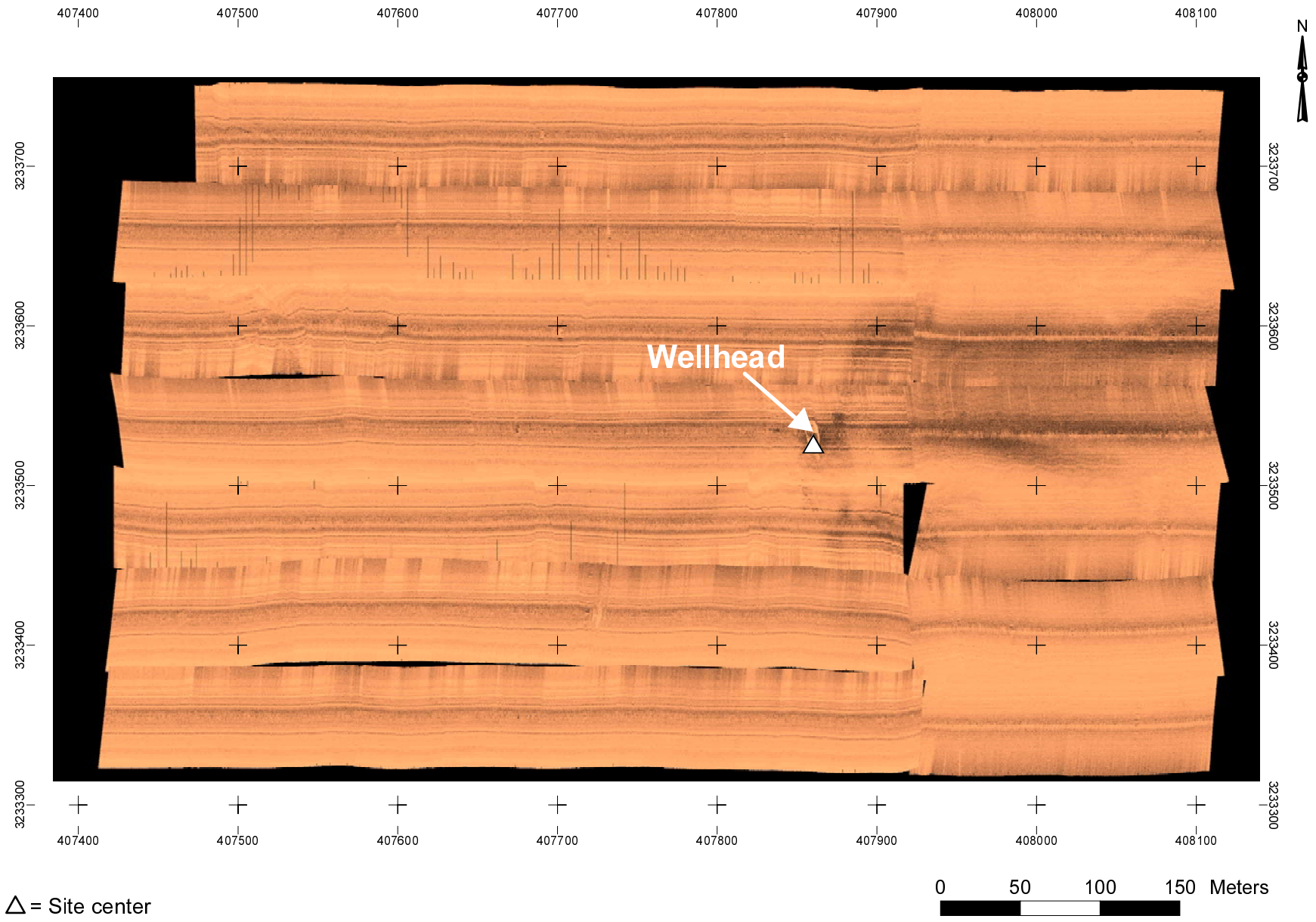

Figure 6-16. Mosaic of side-scan sonar imagery collected in the vicinity of the Viosca Knoll 783 study site.

Chapter 7
NANNOFOSSILS, SEDIMENTOLOGY, AND VISUAL CUTTINGS ANALYSIS

Wayne C. Isphording and Murlene W. Clark
University of South Alabama
and
Alan D. Hart
Continental Shelf Associates, Inc.

7.1 INTRODUCTION

One of the objectives of this study was to determine the thickness and areal extent of SBM cuttings accumulations on the seafloor near continental shelf and continental slope discharge sites in order to evaluate the fate and effects of discharged SBM cuttings. Therefore, it was important to determine the presence of cuttings. Wells often are initially drilled with WBM systems, and the muds and cuttings are generally discharged overboard. In contrast, only cuttings with a very small portion of adhering muds can be discharged overboard when an SBM system is in use. The SBF adhering to discharged cuttings potentially could become separated from discharged cuttings over time due to physical processes. It is therefore important to understand the distribution of cuttings on the seafloor as well as that of SBM to evaluate the effects of cuttings, the effects of SBM, and the effects of cuttings with adhering SBM.

To assist in the delineation of cuttings distributions on the seafloor around the study sites, sediment samples were collected for analysis of nannofossils, sediment grain size, clay mineralogy, and visual cuttings. As discussed in Chapter 1, sediment grain size samples were collected during the Screening Cruise and both Sampling Cruises. Clay mineralogy samples were collected only during the Screening Cruise because evaluation of the Screening Cruise data indicated that this methodology did not effectively identify cuttings, although it was successful in identifying the presence of barium sulfate, an important component of heavier drilling muds. Clay mineralogy analysis was subsequently replaced by nannofossils analysis for the two Sampling Cruises. Samples for visual cuttings analysis were collected during the two Sampling Cruises. In this chapter, the methodologies and results of these different approaches to evaluating the presence of cuttings on the seafloor are presented.

7.2 NANNOFOSSILS

Nannofossils are microscopic plates produced by certain species of yellow-brown algae (Chrysophyta). These plates are intricate in design and range in size from 1 to 50 μm. Each day, for unknown reasons, certain algal cells in this group produce a surface covering of individual plates made of calcium carbonate (Figure 7-1). At night, these plates (collectively called nannofossils) drop to the seafloor to become part of the geologic record. Nannofossils exhibit magnificent diversity and a capacity for rapid evolutionary change. These qualities allow nannofossils to be used as marker species in order to indicate the geologic age of sediments. Nannofossils originated in the Early Jurassic and have been a common sedimentary component in the Gulf of Mexico basin throughout the Cenozoic.

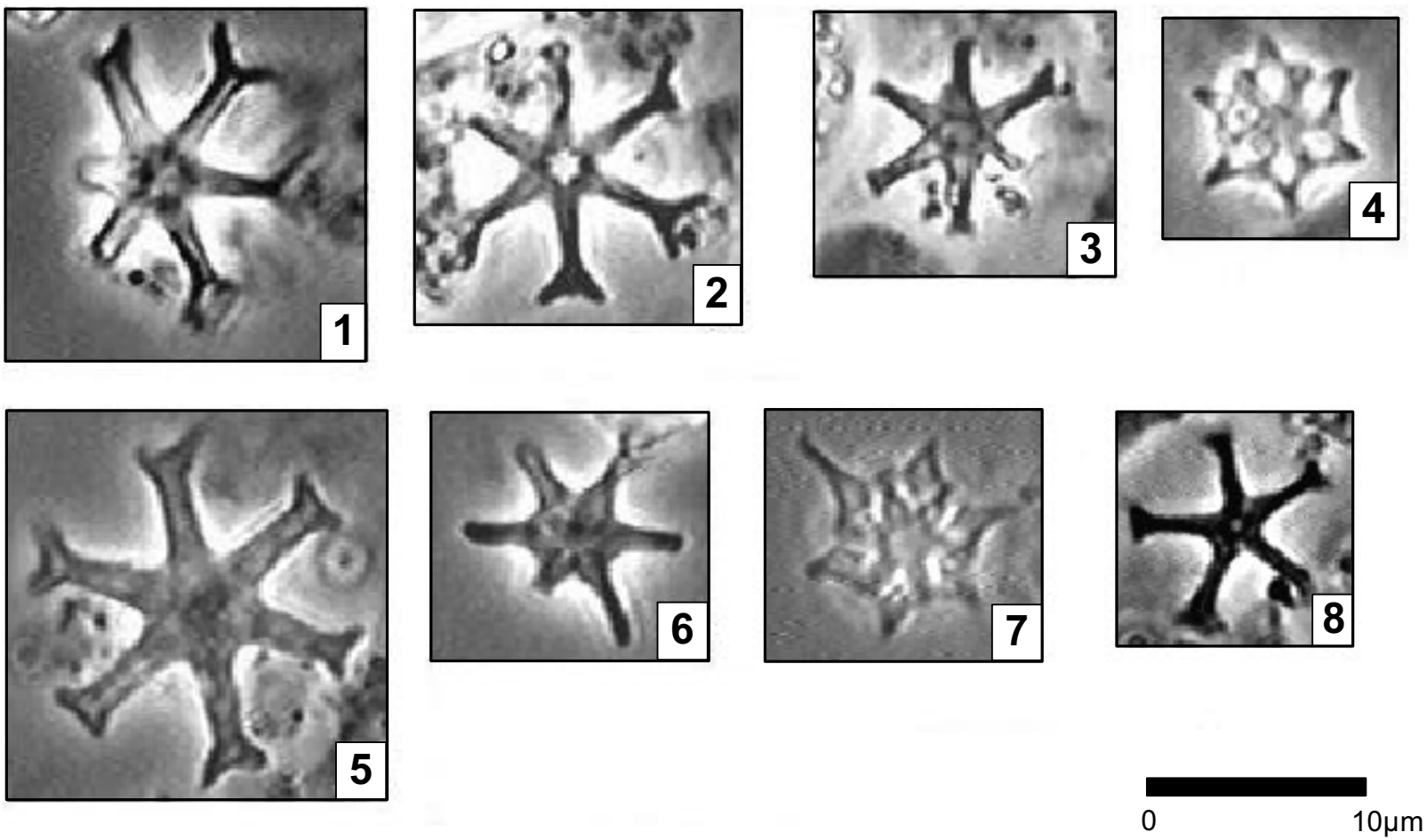

Figure 7-1. Nannofossils of the genus *Discoaster.*

The nannofossil assemblage present in the Gulf of Mexico today has evolved through time from older assemblages that are easily identifiable in well cuttings. Because progressively older sediments are encountered with depth, marker species are encountered from youngest to oldest as drilling proceeds. Should marker species older than the Recent or latest Pleistocene occur in surface box core samples, they are out of place stratigraphically and are designated in this report as anachronous.

The age of the fossils contained in this report is expressed in terms of the geologic time scale (Figure 7-2). The geologic time scale was developed in order to evaluate the age of sedimentary layers relative to other rocks on Earth. This scale simply tells the order in which the rock layers of the Earth were deposited. Because the geologic time scale is a relative tool, it was not related to the concept of absolute age before the advent of radiometric dating techniques. Radiometric dating subsequently has been applied to the boundaries recognized in the geologic time scale, and a correlation between the two time scales has been established, i.e., a sample designated as Miocene is considered to have an absolute age of between 5.2 and 23.3 million years.

Anachronous nannofossils can be introduced into surface sediments by drilling activity as well as by other methods that do not require human intervention. Because nannofossils are microscopic particles, they can be winnowed from the seafloor and transported in the water column by strong currents. Slumping and erosion of deep sea channels also may act to expose and facilitate the reworking of previously deposited nannofossils. The distribution pattern of anachronous nannofossils in the present study has revealed that anachronous forms are more abundant in near-field samples and occur only rarely in far-field samples. This pattern suggests that the anachronous forms in this study are less likely to have been introduced by global transport of resuspended material from slumped areas or eroded channels that have cut into older sediments. Sampling locations are probably far enough away from the shelf edge to avoid significant problems with natural reworking of this kind.

Eight sites associated with oil wells in the Gulf of Mexico were sampled in order to determine the nannofossil content of the surface sediments. Sampling was conducted at four continental shelf locations (MP 299, MP 288, EI 346, and ST 160) and four continental slope locations (MC 496, EW 963, GC 112, and VK 783). Box core samples were taken in near-field (0 to 100 m), mid-field (100 to 250 m), and far-field (3,000 to 6,000 m) proximity to the drilling site on which each sampling location was centered. In theory, anachronous nannofossils introduced through drilling activity would cluster in samples closest to the drilling source. This pattern was indeed observed at MC 496, VK 783, GC 112, and EI 346. The other locations contained only rare occurrences of anomalous forms, with the exception of MP 299, which contained none at all.

In order to determine whether anachronous forms were present in the area in the recent geologic past, the substrate was examined at four stations per site, to depths that ranged between 10 and 20 cm. Anachronous forms were rare below 6 to 8 cm subbottom, which suggests that these forms were more recently introduced into the area and have not been long-term components of natural sedimentation patterns.

Eon	Era	Period	Epoch	Age (Ma)*
Phanerozoic	Cenozoic	Quaternary	Holocene	0.01
			Pleistocene	1.64
		Neogene	Pliocene	5.2
			Miocene	23.3
		Palaeogene	Oligocene	35.4
			Eocene	56.5
			Palaeocene	65.0
	Mesozoic	Cretaceous		145.6
		Jurassic		208.0
		Triassic		245.0
	Palaeozoic	Permian		290.0
		Carboniferous		362.5
		Devonian		408.5
		Silurian		439.0
		Ordovician		510.0
		Cambrian		570.0
Proterozoic				2,500
Archean				4,000

*Millions of years.

Figure 7-2. Geologic time scale based on Harland et al. (1990).

Splits of all samples examined for nannofossil content were washed through a 63-µm sieve, dried, and examined through a binocular microscope for the presence of glass spheres. The glass spheres found in this study were contained in the 125- and 250-µm sieve fractions and appear to be transparent and perfectly spherical. Glass spheres of this type are used during normal drilling practices as a drilling mud additive. Glass spheres found in this study may be analogous to those described on the web site of a major supplier of drilling products as glass spheres that are designed for oil drilling mud applications to reduce friction and torque within deviated holes. Solid glass spheres act as tiny ball bearings to reduce friction and differential pressure. The glass beads are a transparent, solid soda lime glass, free of pits and air bubbles and have compressive strengths in excess of 10,000 psi. The glass spheres are chemically inert and do not affect the chemical characteristics of the mud system (www.pqcorp.com/applications/Drilling-application.asp).

The occurrence of glass spheres at each location is recorded on Tables 7-1, 7-2, and 7-3 by the use of the letter "S." Glass spheres proved to be a common sedimentary component in all areas, especially EI 346, MC 496, VK 783, and MP 299. The glass spheres did not show any marked distribution pattern among near-field, mid-field, and far-field stations.

7.2.1 Study Methods

In this study, a total of 288 surface box cores was examined for nannofossil content from Sampling Cruises 1 and 2, conducted a year apart. A combined total of 36 samples from each location was recovered. Samples from both cruises showed similar results with respect to the distribution of anachronous nannofossils. A total of 124 additional samples was retrieved during Sampling Cruise 2 from subsurface depths of up to 20 cm.

Sampling Cruise 1 samples were placed in individual plastic bags and kept refrigerated until opening. Samples from Sampling Cruise 2 also were refrigerated but were double-bagged as an added protection against contamination. Samples were opened in the laboratory after thoroughly washing the exterior of each plastic bag. A portion of each sample was transferred into a plastic cup to which distilled water was added. In order to isolate the correct size fraction for nannofossil study, the sample was stirred and allowed to settle for 10 seconds. The suspended portion was decanted into a second plastic cup and allowed to settle again for 30 seconds. A drop of liquid from the bottom of the cup was placed on a glass cover slip, which was allowed to dry on a hot plate. The cover slip was then affixed to a labeled glass slide using Loctite mounting medium.

Each slide was examined with an Olympus BHT microscope using a polarizing objective of 100 power. At least ten traverses were made per slide (more if nannofossil abundance was low). The presence of anomalous marker species in each sample is shown in Tables 7-1, 7-2, and 7-3, and the abundances of important species were catalogued in range charts located in Appendix C. Individual species abundances, recorded on the range charts, were estimated by the following designation: V-very rare, three or less per slide; R-rare, one per traverse; F-frequent, one every three fields of view; C-common, one per field of view; A-abundant, ten or more per field of view; and VA-very abundant, one hundred or more per field of view. Anachronous specimens never occurred in numbers greater than the very rare designation, except in one sample shown in Appendix C (MC 496, NF-3 – Sampling Cruise 2). The actual count of anachronous nannofossils from Sampling Cruise 2 samples, with the exception of MC 496 NF-3, is recorded in Appendix C.

Table 7-1. Occurrence of nannofossils and/or glass spheres at each site during Sampling Cruise 1.

Station	Eugene Island 346	Main Pass 288	Main Pass 299	South Timbalier 160	Ewing Bank 963	Green Canyon 112	Mississippi Canyon 496	Viosca Knoll 783
NF-1	N					N	N	N S
NF-2	N S		S			N	N S	
NF-3	N S		S			N	N	N
NF-4	N S					N	N S	N S
NF-5	N S			N			N S	N S
NF-6		N					N S	N
MF-1	S	S					N S	N S
MF-2	S					N	S	N
MF-3							S	N S
MF-4	S			S				N
MF-5	S			S		N	N	S
MF-6	N		S				N	S
FF-1								S
FF-2	S		S	N			S	
FF-3	N S		S					
FF-4	N					S		
FF-5								
FF-6			S				S	

N = Nannofossil marker/markers older than Holocene.
S = Glass sphere/spheres present, which are associated with drilling practices.
Blank spaces indicate samples were free of anachronous fossils or glass spheres.

Table 7-2. Occurrence of nannofossils and/or glass spheres at each site during Sampling Cruise 2.

Station	Eugene Island 346	Main Pass 288	Main Pass 299	South Timbalier 160	Ewing Bank 963	Green Canyon 112	Mississippi Canyon 496	Viosca Knoll 783
NF-1	S N	S	S			S N	N	
NF-2	S	S N	S			S N	N	N
NF-3	S N		S	S	N	N	N	
NF-4	S N		S		N	N	S N	S N
NF-5	S N	S	S				N	N
NF-6	S N				S		N	N
MF-1	S N							
MF-2		N					N	N
MF-3							S	
MF-4	S N	S	S	S		N		
MF-5	S N		S					S
MF-6	S		S				S	N
FF-1			S			N	S	
FF-2			S		S			S
FF-3	S		S		S N	N		S
FF-4	S					S	S	S
FF-5	S				S			
FF-6	S		S	S	S	N	S	

N = Nannofossil marker/markers older than Holocene.
S = Glass sphere/spheres present, which are associated with drilling practices.
Blank spaces indicate samples were free of anachronous fossils or glass spheres.

Table 7-3. Occurrence of nannofossils and/or glass spheres at sites from Sampling Cruise 2.

Eugene Island 346		Main Pass 288		Main Pass 299		South Timbalier 160		Ewing Bank 963		Green Canyon 112		Mississippi Canyon 496		Viosca Knoll 783	
NF-1		NF-1		NF-2		NF-6		NF-1		NF-1		NF-1		NF-1	
0-2 cm	S N	0-2 cm	S	0-2 cm	S	0-2 cm		0-2 cm		0-2 cm	S N	0-2 cm	N	0-2 cm	
2-4 cm	N	2-4 cm		2-4 cm		2-4 cm		2-4 cm		2-4 cm	S	2-4 cm	N	2-4 cm	
4-6 cm	N	4-6 cm		4-6 cm	S	4-6 cm		4-6 cm		4-6 cm		4-6 cm	N	4-6 cm	
6-8 cm		6-8 cm		6-8 cm		6-8 cm		6-8 cm		6-8 cm		6-8 cm		6-8 cm	
8-10 cm		8-10 cm		8-10 cm	S	8-10 cm		8-10 cm		8-10 cm		8-10 cm		8-10 cm	
FF-1		FF-1		FF-1		FF-6		FF-1		FF-1		FF-1		FF-1	
0-2 cm		0-2 cm		0-2 cm	S	0-2 cm		0-2 cm		0-2 cm	N	0-2 cm	S	0-2 cm	
2-4 cm		2-4 cm		2-4 cm		2-4 cm	S	2-4 cm		2-4 cm	N	2-4 cm		2-4 cm	
4-6 cm	S	4-6 cm		4-6 cm	S	4-6 cm		4-6 cm		4-6 cm	N	4-6 cm	S	4-6 cm	
6-8 cm		6-8 cm		6-8 cm		6-8 cm		6-8 cm		6-8 cm		6-8 cm		6-8 cm	
8-10 cm	S N	8-10 cm		8-10 cm	S	8-10 cm	S	8-10 cm		8-10 cm		8-10 cm		8-10 cm	
DISC-1		DISC-1		DISC-1				DISC-1		DISC-1		DISC-1			
0-2 cm	S N	0-2 cm		0-2 cm	S			0-2 cm		0-2 cm	N	0-2 cm	S		
2-4 cm		2-4 cm		2-4 cm	S			2-4 cm		2-4 cm	N	2-4 cm			
4-6 cm		4-6 cm		4-6 cm				4-6 cm		4-6 cm		4-6 cm			
6-8 cm	S	6-8 cm		6-8 cm				6-8 cm		6-8 cm		6-8 cm			
16-18 cm		8-10 cm		10-12 cm				18-20 cm		18-20 cm		8-10 cm			
DISC-2		DISC-2		DISC-2				DISC-2		DISC-2		DISC-2			
0-2 cm	S N	0-2 cm		0-2 cm	S			0-2 cm	N	0-2 cm		0-2 cm			
2-4 cm	S N	2-4 cm		2-4 cm	S			2-4 cm	N	2-4 cm		2-4 cm			
4-6 cm		4-6 cm		4-6 cm	S			4-6 cm	S N	4-6 cm		4-6 cm			
6-8 cm	N	6-8 cm		6-8 cm				6-8 cm	S N	6-8 cm		6-8 cm			
8-10 cm		12-14 cm		14-16 cm				16-18 cm	S	18-20 cm		8-10 cm			

N = Nannofossil marker/markers older than Holocene.
S = Glass sphere/spheres present, which are associated with drilling practices.
Blank spaces indicate samples were free of anachronous fossils or glass spheres.

7.2.2 Results and Discussion

7.2.2.1 Eugene Island 346. The EI 346 sampling area was is located in 92 m of water where anachronous nannofossils were present in significant numbers. The anachronous assemblage contained markers that ranged in age from Eocene through Early Pleistocene. Anachronous forms were most prevalent at near-field and mid-field stations (Appendix C, Figures C-1 and C-2) but occurred in some of the far-field stations as well (Appendix C, Figures C-3 and C-4). This pattern of anachronous nannofossil distribution may be linked to drilling activity.

Anachronous nannofossils were recognized in Sampling Cruise 1 near-field samples NF-1, NF-2, NF-3, NF-4, and NF-5 by the presence of a mix of Plio-Pleistocene markers, which included discoasters *Sphenolithus abies* and *Calcidiscus macintyrei* as well as rare Miocene forms such as *S. moriformis* and *Cyclicargolithus floridanus*. Rare anachronous fossils of Eocene to Miocene age occurred in samples FF-3 and MF-6 from Sampling Cruise 1. No more than one to two older specimens per slide were encountered.

Sampling Cruise 2 near-field samples contained anachronous markers at all stations except NF-2. The anachronous assemblage was similar to that encountered in Sampling Cruise 1 samples in that it also was defined by a mix of Plio-Pleistocene markers and older Miocene forms such as *S. moriformis*, *S. heteromorphus*, *Dictyococcites bisectus*, and *C. floridanus*. Sampling Cruise 2 mid-field samples MF-1, MF-4, and MF-5 contained a similar mixed assemblage. Samples examined at depth revealed multiple occurrences of anachronous forms, mainly in the top 1 to 6 cm at NF-1 and DISC-2. The suite of samples at DISC-1 contained only one anachronous form in the top 2 cm, and FF-1 samples contained only a single specimen at a depth of 10 cm.

7.2.2.2 Main Pass 288. The MP 288 sampling area occurred in a water depth of 119 m. The presence of anachronous nannofossils was noted at only three surface box core sampling locations (see Appendix C, Figures C-5 and C-6). Sampling Cruise 1 sample NF-6 contained one specimen of *S. abies*, Sampling Cruise 2 sample MF-2 contained a single specimen of *Discoaster variabilis*, and Sampling Cruise 2 sample NF-2 contained one discoaster fragment. The incidence of anachronous nannofossils at this location is considered minimal in spite of the high volume of cuttings discharged near the site center. Discharged cuttings may have been too young at this location to be differentiated from recent sediments.

7.2.2.3 Main Pass 299. The MP 299 sampling area occurred in close proximity to the Mississippi River Delta at a water depth of 60 m. The fact that no anachronous nannofossils were observed in MP 299 samples suggests that discharge from the Mississippi River (which theoretically could carry suspended fossils from older land sections) is not a likely source of the anachronous fossils observed in this study. The high volumes of discharged cuttings reported at this site seem inconsistent with the absence of anachronous nannofossils. Discharged sediments may have been too young to distinguish from recent sediments at this location.

7.2.2.4 South Timbalier 160. At a water depth of 37 m, ST 160 was the shallowest of all locations examined. Sampling Cruise 1 samples NF-5 and FF-2 each contained a single anachronous form of Paleogene age (Appendix C, Figures C-7 and C-8). No anachronous nannofossils were observed in Sampling Cruise 2 samples. Because nannofossils are better suited to the environmental conditions present in deep water, nannofossils in general were less abundant at this location than at any other in the study.

7.2.2.5 Ewing Bank 963. The EW 963 samples were retrieved from 540 m of water. No anachronous nannofossils were encountered at this location from Sampling Cruise 1. Sampling Cruise 2 samples contained only isolated occurrences of Plio-Pleistocene fossils at Stations NF-3, NF-4, and FF-3. Samples at DISC-2 contained multiple occurrences of anachronous forms to a depth of 6 to 8 cm. The distribution of Ewing Bank stations with anachronous forms is plotted in Appendix C, Figures C-14 and C-15.

7.2.2.6 Green Canyon 112. The GC 112 sampling area is located in a water depth of 534 m. Anachronous nannofossils were concentrated in the near-field samples of both cruises (Appendix C, Figures C-11 and C-12). Anachronous nannofossils also occurred sporadically in three mid-field stations (Appendix C, Figures C-11 and C-12) as well as in two far-field stations (Appendix C, Figure C-13). Anachronous nannofossils that ranged in age from Oligocene to Early Pliocene often occurred on the same slide. These mixed fossil assemblages were concentrated primarily in near-field samples, which suggests a relationship with nearby drilling activity. Sampling Cruise 1 samples yielded higher numbers of anachronous nannofossils than those retrieved on Sampling Cruise 2. Sampling locations examined at depth on Sampling Cruise 2 revealed the presence of anachronous Plio-Pleistocene forms to a depth of 6 cm at FF-1 and to a depth of 4 cm at DISC-1.

Sampling Cruise 1 samples from Stations NF-1, NF-2, NF-3, NF-4, MF-2, and MF-5 contained decidedly older nannofossils (Oligocene-Miocene) mixed with anachronous forms of Pliocene age. Several anachronous specimens usually were encountered per slide. Forms representative of this assemblage are *S. heteromorphus*, *S. belemnos*, *S. distentus*, *S. ciperoensis*, *C. floridanus*, *D. variabilis*, and *Reticulofenestra pseudoumbilica*.

Fewer anachronous forms were discovered at GC 112 on Sampling Cruise 2; however, such forms clearly were present at many of the Sampling Cruise 2 sampling locations. Samples from NF-1, NF-2, NF-3, and NF-4 contained low numbers of Plio-Pleistocene markers. Sample MF-4 contained a single specimen of *C. floridanus*, as did sample FF-3. A single discoaster fragment was recorded from sample FF-6.

7.2.2.7 Mississippi Canyon 496. Samples from MC 496 were taken from a water depth of approximately 556 m. Anachronous nannofossils were more abundant at this location than at any other in the study (Appendix C). A rich clustering of anachronous forms occurred primarily in near-field samples. Mid-field samples contained sporadic occurrences of anachronous fossils, and far-field samples contained no anachronous forms at all. This pattern, seen in Appendix C, Figures C-16 and C-17, strongly indicates that older sediments were introduced into the environment through drilling activity.

Samples from Stations NF-1, NF-2, NF-3, NF-4, NF-5, and NF-6 from both cruises contained anachronous nannofossil assemblages of Plio-Pleistocene age. Sample NF-3 from Sampling Cruise 2 was so rich in *Pseudoemiliania lacunosa* and *C. macintyrei* that it must be classified as Early Pleistocene in age. Sample MF-2 from Sampling Cruise 2 and samples MF-1, MF-5, and MF-6 from Sampling Cruise 1 also contained markers from the Pliocene and Early Pleistocene such as *C. macintyrei*, *S. abies*, and *Discoaster* spp. Far-field samples from both cruises contained a normal Holocene assemblage with no anachronous forms. Samples examined at depth contained anachronous forms only at NF-1 to a depth of 6 cm.

7.2.2.8 Viosca Knoll 783. The VK 783 was located at an intermediate water depth of 338 m. Samples collected from VK 783 contained consistent occurrences of anachronous nannofossils in near-field and mid-field samples from both cruises. No far-field anomalies were recognized.

The pattern of rich near-field and diminishing mid-field abundances of anachronous forms seen in Appendix C, Figures C-9 and C-10 suggests a link to drilling activity.

A mixture of Eocene through Miocene fossils was present at the rate of one or two specimens per slide in samples NF-3, NF-4, NF-5, NF-6, MF-1, MF-3, and MF-4 from Sampling Cruise 1. Pliocene to Early Pleistocene nannofossils were present in Sampling Cruise 1 samples NF-1, NF-3, NF-6, and MF-2. During Sampling Cruise 2, anachronous Plio-Pleistocene forms were recorded in near-field samples NF-2 through NF-6, with the exception of NF-3, where one broken specimen of Miocene age (*C. floridanus*) was encountered. Sample MF-2 contained a single specimen of *C. macintyrei*, and MF-6 contained a single specimen of *Discoaster quinqueramus*. Samples examined at depth on Sampling Cruise 2 revealed no suspect forms. The presence of fossils from multiple epochs in VK 783 samples further indicates drilling activity as the source.

7.3 SEDIMENTOLOGY

7.3.1 Laboratory Methodology

Samples for mineralogical and sedimentological analysis from the Screening Cruise were sent to the Sedimentology Laboratory, Department of Earth Sciences, University of South Alabama in the form of two 250-mL plastic jars (one each for mineralogy and sediment grain size) in freezer lockers containing “blue ice” to maintain a maximum temperature of 0°C. Subsequent samples from Sampling Cruises 1 and 2 were supplied in WHIRL-PAC® bags that were similarly sent and refrigerated. All samples, on receipt, were immediately transferred to a constant temperature (4°C) room where the samples remained until analyses were initiated. Sample analysis was carried out by first bringing the samples to room temperature and then allowing individual samples to air dry completely. Once dried, the samples were subjected to preliminary disaggregation by being gently broken into fragments of less than 5-mm size using a rubber-tipped policeman. Next, the sample was split to approximately 50 g using a standard riffle splitter. The split sample then was processed to obtain the particle size analysis.

7.3.1.1 Grain Size Analysis. Sediment grain size distributions were measured by the sieve and hydrometer method described in Table 7-4. The data quality objectives (DQOs) originally requested for this phase of the investigation were as follows:

- Measurement (Parameter): grain size
- Reporting Units: cumulative percent
- Method Detection Limit: 0.1 µm
- Precision (±%): 5
- Accuracy (±%): NA
- Quality Control Samples: random selection of 5% samples
- Acceptance Criteria: ±10% in each size fraction
- Corrective Action: sieve replacement

Table 7-4. Sieve and hydrometer analysis procedure (ASTM D 422-63, Modified).

1. Air dry sample if possible; otherwise dry in oven at 110°F (maximum).

2. If consolidated, disaggregate sample using a rubber policeman (do not use a mortar and pestle as this will cause breakage of grains and alter the natural size properties of the sample).

3. Split the sample into a representative portion using the laboratory riffle sample splitter. Weigh out approximately 40 g and record weight to nearest 0.01 g. Do not attempt to obtain a weight of *exactly* 40 g as this will bias the sample.

4. Place the sample in a Mason jar and add approximately 300 mL distilled (or deionized) water. Add 20 mL of a 10% sodium hexametaphosphate (by volume) solution. Stir and let stand for 6 hours (or overnight).

5. Transfer the sample to a soils stirrer and stir on *medium speed* for 5 minutes.

6. Pour the sample into a 1 L hydrometer cylinder. Use a wash bottle to ensure that all sample has been transferred into the hydrometer cylinder.

7. Bring the cylinder to a volume of approximately 800 to 900 mL with distilled (deionized) water. Let stand for 6 hours and check for flocculation. If flocculation is observed, add an additional 20 ml of the 10% sodium hexametaphosphate solution, stir, and let stand again for 6 hours.

8. If no flocculation is observed after 6 hours, the samples can be brought to a 1 L volume and a normal hydrometer analysis can be performed. Readings are taken using a 152H ASTM hydrometer (following initial vigorous stirring of the sample) at the following intervals: 2, 5, 15, 60, 240, 720, and 1,200 minutes. The temperature of the sample also must be recorded when each reading is taken to correct for the viscosity of water.

9. Following the 1,200 minute reading, the sample is then washed through a 230 mesh (62.5 μm) or 270 mesh (53 μm) sieve. That retained on the sieve is washed onto a drying pan and oven dried. The oven-dried material is then subjected to a standard sieve analysis (see ASTM Method D 422-63) using either a whole phi or half phi interval.

10. Standard practice is to then calculate the measures of central tendency (mean diameter and median diameter) and dispersion (coefficient of sorting, skewness, and kurtosis) using either the methods of Krumbein and Pettijohn (1938), Inman (1952), and Folk and Ward (1957).

11. Quality Assurance/Quality Control Procedure: Five percent of the total number of samples analyzed are selected randomly for duplicate analysis. Agreement of the duplicate analysis for *all* size fractions analyzed must be within ±10%.

- **NOTE**: If flocculation is still taking place, it has probably resulted from either (1) the sample contains dissolved salt adhering to the grains or (2) excessive organics are present. If (1), the sample will have to be treated by dialysis; if (2), the sample should be pre-treated with 30% hydrogen peroxide to remove the organic component.

Although the precision for the sieve-hydrometer method used here is ±5%, an accuracy figure cannot be cited because no method exists that truly defines the particle distribution in the colloidal range (i.e., sub -0.1 μm). To assure that maximum precision was being attained, a random selection of 5% of all samples supplied was re-run and compared with the original analyses. A difference in results of no more than 10% for any given size fraction was deemed acceptable.

7.3.1.2 Clay Mineral Analysis. Identification of mineral phases present in samples is based upon methodologies developed by the Joint Committee on Powder Diffraction Studies (JCPDS) and involves indexing the peak positions (i.e., determining the spacing of atomic planes) on diffractograms and then comparing these to standards either developed by the JCPDS or produced from known and optically verified samples in this laboratory. As such, they are not amenable to a definition of DQOs because the terms Precision, Accuracy, Quality Control, Acceptance Criteria, and Corrective Action are meaningless and non-definable for X-ray diffraction analyses. The only objective that can be truly addressed is "Method Detection Limit." Textbooks can be cited that note that individual mineral phases can be identified if the phase is present in an abundance of 5% or greater. Even this must be accompanied by caveats.

Depending on the matrix, it may be possible in some samples to detect specific mineral phases at the "sub-1% level." However, if the phase is poorly crystalline, a detection level in the range of 5% to 8% is more likely. Naturally, if the phase is non-crystalline, it cannot be detected by X-ray diffraction, even if it comprises 100% of the sample.

The DQOs for this phase of the investigation were as follows:

- Measurement (Parameter): Phase 0.1%
- Reporting Units: name of phase
- Method Detection Limit: variable
- Precision (±%): NA
- Accuracy (±%): dependent on degree of crystallinity
- Quality Control Samples: NA
- Acceptance Criteria: NA
- Corrective Action: compound identification

7.3.2 Results

7.3.2.1 Screening Cruise Analyses. A review of the size analyses carried out on near-field, mid-field, and far-field samples from this cruise indicated that the great bulk of all samples would be classified as “silty clays” according to Shepard’s (1954) classification. Shepard’s classification would be preferred for characterizing most of the sediments in the study areas because gravel-size particles are largely absent. Hence, this classification provides a better descriptor for each sample (Figure 7-3). Further, because of the limited number of samples obtained from near-field, mid-field, and far-field stations, the median diameter would be preferred over the mean diameter as a measure of the central tendency of the particle size distribution. The reason for this is that the mean diameter is affected to a much greater degree by aberrant extreme values, while the median is either unaffected or affected to a much lesser extent. X-ray diffraction analysis was employed to characterize the crystalline mineral phases that were present in the 95 samples supplied. While all of the samples consisted of mixtures of the clay minerals kaolinite, illite (clay mica), and the Smectite Group mineral montmorillonite, 12 of the samples also were observed to contain detectable barite. Numerous investigations

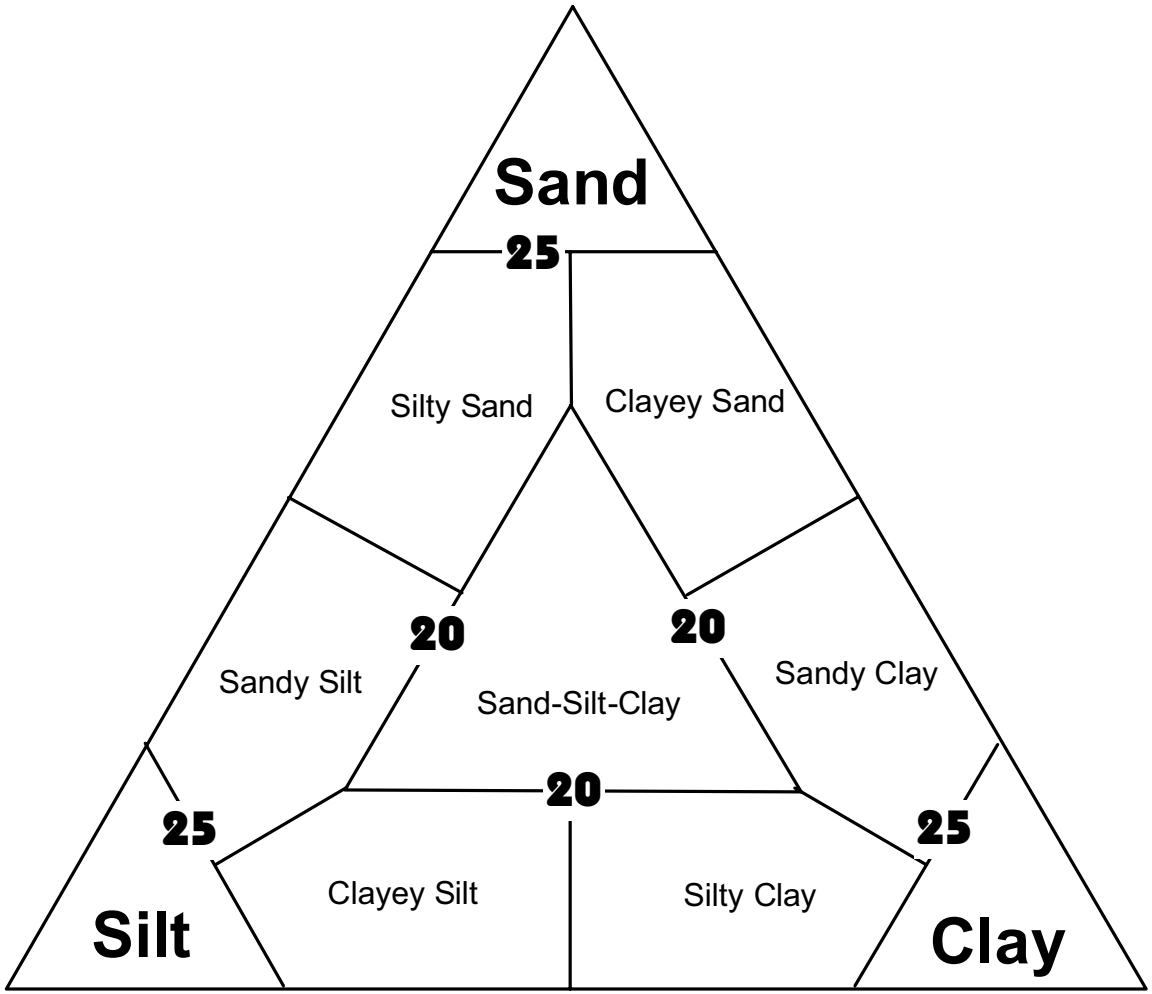

Figure 7-3. Sediment texture classification (Shepard, 1954). Numbers refer to percentages of different end member components.

have confirmed that barite is totally absent in the heavy minerals fraction of Recent (and older) northern Gulf of Mexico detrital sediments (see Russell, 1937; Cogen, 1940; Goldstein, 1942; Rosen, 1969; Isphording, 1983) Hence, where present, the mineral is tied to its use in drilling operations.

While barium can be detected easily by standard analytical procedures, care must be taken when interpreting chemical analyses of samples. Barium is the 14th most abundant element in the earth's crust and is a common, though minor, constituent of all marine sediments. Only its presence in the form of barite can be used to associate the sediment with drilling wastes. Though some tendency was observed for samples that contained detectable barite to be associated with coarse textured sediments (possible cuttings), there were exceptions observed that would prevent any categorical association of grain size and barite from being made. Also, the lack of barite on sample X-ray diffractograms cannot be used to exclude the possibility that some barite might be present. X-ray diffractogram manufacturers will generally cite a "sensitivity" for their instruments at detection levels for various minerals at about 5%. This is a conservative estimate, however, and it is usually possible to detect a mineral's presence at or below this level. Barite, for example, has been detected in Mobile Bay sediments in quantities of less than 1% (and often at 0.5%).

7.3.2.1.1 Garden Banks 128. This site is located at a depth of 192 m (630 ft) on the gently southeastward sloping continental shelf. Texturally, samples ranged from clay to sand-silt-clay mixtures. Coarsest sediments were associated with near-field samples. Median diameter ranged from 0.2 to 8.3 μm. Far-field samples were generally finer in texture (0.7 to 2.6 μm), but the differences were minor, at best. Barite was observed in diffractograms at two near-field stations (the Discretionary Site east of the wellhead and at NF-3 south of the wellhead). The mineral also was observed at FF-1, also located southwest of the wellhead.

7.3.2.1.2 Main Pass 288. This site, located at a water depth of 119 m (390 ft) and on a relatively flat plane, contained the coarsest-grained sediments of all samples analyzed. Half of the ten samples examined were classified as sand-silt-clay, reflecting the coarser detritus being supplied by the nearby Mississippi River source. Near-field (and mid-field) samples, however, were distinctly coarser in texture than were far-field samples, and the extremely coarse texture of NF-3 (39.8 μm median diameter, 24.5% sand) may, in part, reflect discharged cuttings. Similar coarse textured sediments also were observed at NF-1 and NF-2. Barite was observed in only one sample, which was collected from the Discretionary Site located immediately northeast of the drillsite.

7.3.2.1.3 Main Pass 299. This site is located less than 20 mi due east of the mouth of the Mississippi River at a depth of 60 m (197 ft) on a topographically near-horizontal surface. Sediment samples here were finer-grained than those from MP 288 but typically contained higher levels of sand than were found at most of the other sites (reflecting the proximity of this site to the mouth of the Mississippi River). Most of the samples were characterized as silty clay, except for MF-3, which was sand-silt-clay. The latter also contained the highest level of sand-size material (20.1%). Barite was observed in two samples: NF-3, collected immediately southwest of the wellhead, and FF-3, collected north-northwest of the site.

7.3.2.1.4 Viosca Knoll 780. This site is at a water depth of 210 m (689 ft) on a relatively smooth plain that slopes toward the south-southwest. Near-field samples ranged in median diameter from less than 1 μm (NF-2) to over 7 μm (Discretionary Site), and the

latter also was characterized by detectable barite. Far-field samples were all of considerably finer texture, with median diameters of less than 1 μm. FF-3 contained the highest percentage of clay-size (<4 μm) material of any of the 95 samples analyzed (83.4%).

7.3.2.1.5 Viosca Knoll 783. This site was located approximately 50 mi south of Mobile Bay, Alabama at a depth of 338 m (1,109 ft). As such, it was the most easterly of the sites being investigated. Far-field samples were typically coarser in texture than near-field samples (especially those to the north of the wellhead), and this likely reflects the influence of sediments derived from a Mobile River source rather than a Mississippi River source. No barite was observed in any of the samples.

7.3.2.1.6 Green Canyon 112. Water depth at this site was 534 m (1,752 ft). The topographical relief was more irregular than at other sites and sloped toward the south. Texturally, all samples would be classified as either silty clay or clayey silt. Only slight differences were noted between near-field and far-field samples, but again, the far-field samples were slightly finer in texture. Barite was observed on diffractograms from two near-field sites (the Discretionary Site and NF-1), both of which lay to the east of the wellhead.

7.3.2.1.7 Mississippi Canyon 28. This drillsite is located at a depth of 558 m (1,830 ft) on a distinctly southeast sloping, smooth topographical plain approximately 25 mi due east of the mouth of the Mississippi River. Sediments from samples from this location were finer in texture than all other sites analyzed and typically possessed median diameters of less than 1 μm. As such, all occurred in either the clay field of the Shepard triangle or in the silty clay field. Near-field samples were of slightly coarser texture, but differences were generally minor. No barite was detected in any of the diffractograms examined.

7.3.2.1.8 Mississippi Canyon 496. The water depth at this site was 556 m (1,824 ft) with a smooth topography that sloped toward the south. Samples were almost entirely silty clays, and median diameters were nearly identical. One near-field sample east of the wellhead (NF-2) was somewhat anomalous in possessing a median diameter approximately three times that of all other samples; this sample also was characterized by easily detectable barite on the X-ray diffractogram.

7.3.2.2 Sampling Cruises 1 and 2. X-ray diffraction analyses were not conducted on samples collected during Sampling Cruises 1 and 2. Hence, the following discussion will review only the particle size distribution analyses that were performed on the samples supplied. These results are presented in Appendix C. Because no strong correlation was observed between grain size and the presence of barite in the Screening Cruise samples, grain size alone cannot be used as an indicator of drilling-related materials unless 1) anomalous grain sizes also are accompanied by the presence of pre-Holocene nannofossils (or glass spheres that are a common additive to drilling muds) or 2) surrounding sediments (e.g., mid-field and/or far-field) are of a significantly different (i.e., finer) grain size. Under these circumstances, the sediments may well indicate presence of non-indigenous materials.

7.3.2.2.1 Sampling Cruise 1.

Eugene Island 346. Size analyses from this site generally were different for near-, mid-, and far-field samples. Near-field and mid-field samples possessed a distinctly higher

content of sand-size particles when compared with far-field samples. This also was reflected in significantly higher median diameters for the near- and mid-field samples. These observations, when combined with the observed presence of both nannofossils and/or glass spheres in most near-field and mid-field samples, provided strong evidence that materials associated with drilling operations are present at these sites. Non-indigenous materials (nannofossils/glass spheres) also were observed in three of the six far-field samples.

Main Pass 288. Presence of drilling-related material was indicated only in one near-field sample (NF-6) by fossil evidence. Particle size analyses, however, identified a major anomaly in a number of far-field samples. Samples FF-1 and FF-3 contained the highest level of sand-size material (>95%) and largest median diameters (>200 µm) observed at any of the drilling sites in this investigation. Whether this is a drilling-related phenomenon, however, is open to speculation. Examination of the size analyses of core samples taken at FF-3 shows that similar-grained sediment is present to a depth of at least 10 cm. It is unlikely that any such drilling discharges from this site could have been carried nearly 3,000 m from the drillsite and accumulated to this thickness.

Main Pass 299. No significant differences were observed in overall particle median diameters nor sand-silt-clay ratios when near-, mid-, and far-field samples were examined. Glass spheres were observed in samples collected from NF-2, NF-3, MF-6, FF-1, FF-2, and FF-6; however, these may well have been carried by the prevailing currents from other sites where drilling operations had been carried out.

South Timbalier 160. Sediment samples from Stations NF-1, NF-2, and NF-3 possessed somewhat larger median diameters than other near-field samples, and quantities of sand- and clay-size components in these samples were different from all other samples at this site. While only one sample (NF-5) showed the presence of pre-Holocene nannofossils (and two mid-field samples contained glass spheres), there is a strong likelihood that some drilling-related materials are present in the sediments (near-field and far-field) at this site. The quantity of drilling-related materials was significantly less than that observed at Viosca Knoll, Eugene Island, and Mississippi Canyon.

Ewing Bank 963. No sediment textural differences were observed for near-, mid-, and far-field samples from this site. Sample NF-5 did possess a larger median diameter than all other near- and mid-field samples, but the difference was not deemed truly anomalous. Supporting this was the fact that no samples were observed at either near-, mid-, or far-field stations that contained pre-Holocene nannofossils (or glass spheres).

Green Canyon 112. Two anomalous near-field samples (NF-1 and NF-4) were observed that possessed markedly higher median diameters and significantly higher sand percentages than all other samples from this site. Presence of drilling wastes is the likely cause, and this is supported by the presence of pre-Holocene nannofossils in these samples. While no textural anomalies were observed in other samples from this location, pre-Pleistocene fossils were observed in samples from NF-2, NF-3, MF-2, and MF-5.

Mississippi Canyon 496. Far-field samples from this site are, again, finer in texture than either near-field or mid-field samples. This is particularly apparent when sand-silt-clay ratios are examined. Far-field samples typically were higher in clay-size particles and lower in silt-size components. Although not conclusive in indicating drilling-related

materials in near-field and mid-field samples, when combined with the fact that all near-field and all but one (MF-4) mid-field sample were found to contain pre-Holocene nannofossils and/or glass spheres, the conclusion can be drawn that the identified samples also contain materials in part derived from drilling operations. As with the above described Eugene Island samples, far-field samples also had presence of drilling-related materials.

Viosca Knoll 783. Samples from the near-field, mid-field, and far-field zones could not be differentiated on the basis of grain size analyses. The accumulation of drilling-related materials was indicated by the presence of nannofossils and/or glass spheres in all but one of the near-field samples and in all mid-field samples.

7.3.2.2.2 Sampling Cruise 2.

As with Sampling Cruise 1, sedimentological evidence of drilling-related materials in bottom sediments was based upon the observation of samples having anomalous textural characteristics. No X-ray diffraction analyses were performed, but the data were compared with nannofossil information in order to maximize the likelihood that the possible presence of drilling discharges at the different sites could be identified.

Eugene Island 346. Coarse-grained sediments (median diameters >10 μm, sand percentages >20%) were associated with a number of near-field samples. Sediment textures became gradually finer away from the site center, and this, combined with extensive glass spheres (found in nearly all samples) and the presence of pre-Holocene nannofossils in numerous near-field samples and some mid-field samples, would strongly indicate that drilling materials were present at this site. A similar conclusion was reached for samples collected during the Sampling Cruise 1 operations.

Main Pass 288. As was observed for Sampling Cruise 1, definite anomalies were identified at this location; in fact, the coarsest textured samples found throughout the entire study area were observed here. Unlike MP 299, however, these extremely coarse-grained sediments (median diameters >200 μm, sand percentages >95%) were found in far-field samples and not in near-field or mid-field samples. Although glass spheres occurred in a few samples, the anomalies were largely an artifact of the vagaries of the depositional environment.

Main Pass 299. Possible presence of drilling-related material at this site was indicated by the fact that both median diameters and percentages of sand were higher at most near-field stations (and several of the mid-field stations) than they were farther from the site center at far-field stations. Though by no means conclusive, the fact that four near-field and three mid-field stations also were characterized by glass spheres would lend support to the conclusion that the site was disturbed by drilling activity. It should be noted here that the same thing was observed on Sampling Cruise 1.

South Timbalier 160. This site offered little evidence for the presence of drilling materials other than sparse occurrence of glass spheres. No pre-Holocene nannofossils were observed in samples, and sediment grain size distributions were similar for samples collected throughout the site. Essentially all of the samples were silty clay, and the only sediment trend observed was a slight coarsening of median diameters toward the northwest of the site center. It is likely that this was simply a reflection of the greater proximity of these stations (FF-1, FF-5, and FF-6) to a nearer shore environment, and as

was the case following examination of Sampling Cruise 1 samples, the site appears to be free of drilling-related materials.

Ewing Bank 963. Samples examined from this cruise were similar to those from Sampling Cruise 1 in that no major differences were observed when near-, mid-, and far-field samples were examined. While pre-Holocene nannofossils were observed in samples NF-3, NF-4, and FF-3 (and glass spheres were present in a few samples), conclusive evidence of presence of drilling materials in bottom sediment was largely lacking.

Green Canyon 112. Several near-field samples from this site possessed distinctly large median particle diameters (8 to 34 µm). Mid-field particle diameters were smaller (1.5 to 7 µm) and were similar to those of far-field samples. The presence of pre-Holocene nannofossils in samples NF-1, NF-2, NF-3, NF-4, MF-4, and FF-3 would support a conclusion that drilling discharges were present. A similar conclusion was reached following examination of Sampling Cruise 1 samples.

Mississippi Canyon 496. Samples from this site showed ample evidence of cuttings by the presence of nannofossils in near-field samples, although this was not strongly reflected in the particle size analyses. While there was some evidence that a gradation in grain size from coarse to fine was present in near-field, mid-field, and far-field samples, the trend was by no means strong. Nannofossil results here provided the strongest evidence for the presence of cuttings.

Viosca Knoll 783. As was the case with samples from MC 496, no distinct sediment trends were present that would support a belief that cuttings were present at this site. Nannofossil evidence, however, argues to the contrary. Analysis of the particle size distribution was inconclusive, largely because two significant sources of detrital sediment affect this area; both a Mississippi River source and a Mobile River source have imprinted a sediment signature here. Hence, any conclusions as to likelihood of occurrence of cuttings should be based on the presence of pre-Holocene nannofossils in the sediments or evidence from some other analytical method.

7.4 VISUAL CUTTINGS ANALYSIS

Visual cuttings analysis was used as another means to assess the fate of cuttings. The analysis consisted of a visual inspection of sediment samples under a microscope by a trained mud engineer to characterize its constituents and to determine whether or not cuttings were present in the sample.

7.4.1 Methodology

Analysis of visual cuttings was conducted by Sperry-Sun. Each sample initially was examined under plain light illumination using overhead fluorescent light as well as an incandescent lamp to determine sample color. Sample color was determined by comparison to the Geological Society of America's Rock Color Chart, equipped with Munsell standard color chips. While still in the original shipping container (WHIRL-PAC® bag), a sample was placed in a UV box to check for any fluorescence, which was noted in the work notes. Any samples in translucent or non-clear containers were transferred to a glass Pyrex dish for examination in the UV box. Any material exhibiting fluorescence was treated with 1,1,1,trichloroethane, which helps the observer to differentiate between the yellow-gold-blue/white fluorescence of petroleum based oils and the

dull olive fluorescence characteristic of the emulsifiers in SBMs. There were some samples that, although exhibiting no fluorescence attributable to either petroleum based oils or SBMs, had either an oily odor or a sheen. This was attributed to the presence of small amounts of partially degraded or weathered SBMs and noted as "slight trace synthetic based mud, no fluorescence despite presence." Samples were poured from the sample container into a Pyrex dish and examined with a binocular microscope under plain light. Any visible features were noted at this time. The entire sample was then gently washed through a 40-mesh and 200-mesh sieve system to separate silt-size or larger components from the mud fraction of the sample. These coarser and finer fractions then were removed from the sieves and viewed under the microscope to determine the nature of the particles, the relative percentages of each, and any other information that could be determined with the microscope. The presence of shale or sandstone particles or other materials not characteristic of normal marine sediments was recorded as an indication of the presence of cuttings in the sample. All sample handling equipment was cleaned before the next sample was analyzed. All data were recorded on the work notes, checked for accuracy, and entered on the spreadsheet as required.

7.4.2 Results

The results of the visual cuttings analysis at each of the study sites are summarized in the following discussion. Specific results for each analysis are presented in Appendix C.

7.4.2.1 Continental Shelf Study Sites.

7.4.2.1.1 Eugene Island 346.

For the samples collected at EI 346 during Sampling Cruise 1, fine-grained sediments dominated at the far-field stations and at most of the mid-field stations (Table 7-5). Considerable portions of silt/sand-sized particles were observed at three mid-field stations and all near-field stations. There was evidence of cuttings at all stations in the near-field zone and at some stations in the mid-field zone. None of the far-field stations had evidence of cuttings based on the visual cuttings analysis. Trace fluorescence at two near-field stations, one mid-field station, and a far-field station indicated that trace amounts of SBF may have been present.

For Sampling Cruise 2, fine-grained sediments dominated at all stations in the near-field and far-field and at all but one mid-field station. Cuttings were observed at four near-field stations and four mid-field stations. Cuttings were consistently absent from the far-field stations. Evidence of SBF was not observed at any of the stations during Sampling Cruise 2.

7.4.2.1.2 Main Pass 288.

Fine-grained sediment was the principal constituent of the near-field and mid-field sediment samples collected during Sampling Cruise 1 at MP 288 (Table 7-6). Three far-field stations were dominated by silt/sand-sized particles, and the remainder were principally fine-grained sediments. Cuttings were present at all near-field and mid-field stations, occurring commonly in most. Only one sample showed a corresponding indication of the presence of SBF. Cuttings were observed at one of the far-field stations, but there was no indication of SBF.

Fine-grained sediments dominated in all samples collected during Sampling Cruise 2. There were no indications of the presence of cuttings or SBF in these samples.

Table 7-5. Summary of the results from visual cuttings analysis of sediment samples collected at Eugene Island 346 during Sampling Cruises 1 and 2.

Sampling Cruise	Station	General Characteristics	Cuttings	Fluorescence Indicating Presence of Synthetic Based Muds
1	NF-1	60% moderate yellowish black mud with very abundant black sulfides; 40% silt/sand-size particles	Present (shale/sandstone/siltstone fragments)	Trace minor fluorescence
1	NF-2	60% moderate yellowish black mud with trace black sulfides; 40% silt/sand-size particles	Present (shale/siltstone fragments)	None
1	NF-3	50% moderate yellowish brown mud with abundant black sulfides; 50% silt/sand-size particles	Present (shale fragments)	None
1	NF-4	50% dark yellowish brown mud with moderate black sulfides; 50% silt/sand-size particles	Present (shale fragments)	None
1	NF-5	50% moderate yellowish black mud with very abundant black sulfides; 50% silt/sand-size particles	Present (shale fragments)	Trace minor fluorescence
1	NF-6	60% dark yellowish brown mud with trace black sulfides; 40% silt/sand-size particles	Present (shale/siltstone fragments)	None
1	MF-1	70% moderate yellowish brown mud with moderate black sulfides; 30% silt/sand-size particles	Present (shale fragments)	None
1	MF-2	80% dark yellowish brown mud with trace black sulfides	Present (shale fragments)	None
1	MF-3	80% dark yellowish brown mud	Present (shale fragments)	None
1	MF-4	85% dark yellowish brown mud	None	None
1	MF-5	60% dark yellowish brown mud; 40% silt/sand-size particles	Present (shale fragments)	None
1	MF-6	40% moderate yellowish brown mud with very abundant black sulfides; 60% silt/sand-size particles	Present (shale/siltstone fragments)	Trace fluorescence
1	FF-1	80% dark yellowish brown mud	None	None

Table 7-5. (Continued).

Sampling Cruise	Station	General Characteristics	Cuttings	Fluorescence Indicating Presence of Synthetic Based Muds
1	FF-2	90% moderate yellowish brown mud with trace black sulfides	None	Trace synthetic oil based mud; Trace fluorescence
1	FF-3	90% dark yellowish brown mud	None	None
1	FF-4	90% dark yellowish brown mud	None	None
1	FF-5	90% dark yellowish brown mud	None	None
1	FF-6	85% dark yellowish brown mud	None	None
2	NF-1	90% light olive gray mud	None	None
2	NF-2	90% light olive gray mud	Present (sandstone cuttings)	None
2	NF-3	90% light olive gray to dark gray mud	Present (sandstone cuttings)	None
2	NF-4	90% dark gray mud	Present (sandstone/siltstone cuttings)	None
2	NF-5	90% light olive gray to dark gray mud	Present (siltstone cuttings)	None
2	NF-6	85% olive black mud	None	None
2	MF-1	90% light olive gray mud	Trace	None
2	MF-2	95% light olive gray mud	Present (shale/sandstone cuttings)	None
2	MF-3	95% light olive gray mud	None	None
2	MF-4	50% olive gray to grayish olive mud; 50% silt/sand-size particles	None	None
2	MF-5	90% light olive gray mud	Present (sandstone cuttings)	None
2	MF-6	95% olive gray to grayish olive mud	Very slight trace	None
2	FF-1	95% light olive gray mud	None	None
2	FF-2	95% light olive gray mud	None	None
2	FF-3	95% light olive gray mud	None	None
2	FF-4	95% light olive gray mud	None	None
2	FF-5	95% light olive gray mud	None	None
2	FF-6	95% light olive gray mud	None	None

Table 7-6. Summary of the results from visual cuttings analysis of sediment samples collected at Main Pass 288 during Sampling Cruises 1 and 2.

Sampling Cruise	Station	General Characteristics	Cuttings	Fluorescence Indicating Presence of Synthetic Based Muds
1	NF-1	80% light to moderate olive brown mud	Present (shale/sandstone fragments)	None
1	NF-2	80% moderate olive brown mud with yellow/brown iron oxide streaks	Common	None
1	NF-3	75% light olive gray mud with yellow/brown iron oxide streaks	Common	None
1	NF-4	80% light olive gray mud with yellow/brown iron oxide streaks	Common	None
1	NF-5	60% light olive gray mud with brown/black streaks and iron oxide stain; 40% silt/sand-size particles	Common	None
1	NF6	50% light olive gray mud with brown/black streaks and iron oxide stain; 50% silt/sand-size particles	Common	None
1	MF-1	90% light olive brown mud with brown iron oxide streaks and trace black sulfide	Less common	Slight trace fluorescence
1	MF-2	90% light to moderate olive brown mud with brown streaks	Common	None
1	MF-3	85% light to moderate olive brown mud with brown streaks	Common	None
1	MF-4	85% light to moderate olive brown mud	Common	None
1	MF-5	80% light olive brown mud	Common	None
1	MF-6	85% light to moderate olive brown mud with brown streaks	Rare	None
1	FF-1	20% light olive gray mud; 80% silt/sand-size particles	Very common	None
1	FF-2	95% light olive gray mud with brown/black streaks	None	None

Table 7-6. (Continued).

Sampling Cruise	Station	General Characteristics	Cuttings	Fluorescence Indicating Presence of Synthetic Based Muds
1	FF-3	20% moderate yellowish brown mud with brown/black streaks; 80% silt/sand-size particles	None	None
1	FF-4	90% dark yellowish brown mud	None	None
1	FF-5	90% moderate to dark yellowish brown mud	None	None
1	FF-6	20% moderate to dark yellowish brown mud with black streaks; 80% silt/sand-size particles	None	None
2	NF-1	95% light olive gray mud	None	None
2	NF2	90% light olive gray mud	None	None
2	NF-3	95% light olive gray silt	None	None
2	NF-4	95% light olive gray silt	None	None
2	NF-5	95% dark olive gray silt	None	None
2	NF-6	95% light olive gray silt	None	None
2	MF-1	95% dark olive brown mud	None	None
2	MF-2	95% light olive gray mud	None	None
2	MF-3	95% dark olive gray mud	None	None
2	MF-4	95% light olive brown mud	None	None
2	MF-5	95% dark olive gray mud	None	None
2	MF-6	95% dark olive gray mud	None	None
2	FF-1	95% dark gray mud	None	None
2	FF-2	95% light olive green mud	None	None
2	FF-3	95% light olive gray mud	None	None
2	FF-4	95% olive gray mud	None	None
2	FF-5	90% olive gray mud	None	None
2	FF-6	95% light olive gray mud	None	None

7.4.2.1.3 Main Pass 299. Fine-grained sediments dominated all sediment samples collected during Sampling Cruise 1 at MP 299, and cuttings were detected in all samples, irrespective of zone (Table 7-7). This is not particularly unexpected as MP 299 is one of the most heavily drilled blocks in the Gulf of Mexico. However, indications of SBF were observed in only two near-field samples.

Fine-grained sediments also dominated all sediment samples collected during Sampling Cruise 2 at MP 299. Cuttings were observed in one near-field sample and two mid-field samples, in contrast to the ubiquitous presence observed during Sampling Cruise 1. There were no indications of SBF in any samples collected during Sampling Cruise 2.

7.4.2.1.4 South Timbalier 160. Although yellowish brown fine-grained sediments dominated the sediment samples collected at ST 160 during Sampling Cruise 1, the most notable general characteristic was the abundant presence of black sulfides in all near-field samples, which corresponded to the presence of trace residue of SBF in these near-field samples (Table 7-8). Cuttings were detected in all but one sample.

As was the case for Sampling Cruise 1, fine-grained sediments dominated all samples collected during Sampling Cruise 2. In contrast to Sampling Cruise 1, cuttings and SBF were not detected by visual cuttings analysis in sediment samples collected at ST 160 during Sampling Cruise 2.

7.4.2.2 Continental Slope Study Sites.

7.4.2.2.1 Green Canyon 112. During Sampling Cruise 1, fine-grained sediments dominated at most GC 112 stations, but various streaks were observed in the samples collected in the near-field and mid-field zones (Table 7-9). Cuttings were present at five of six near-field stations, occurring commonly at three. There were indications of the presence of SBF at four near-field stations. Cuttings also were common at three mid-field stations during Sampling Cruise 1, and SBF was detected at two stations in this zone. Although there were trace quantities of cuttings present at two far-field stations, no SBF was detected at the stations in this zone.

Fine-grained sediments dominated in all samples collected during Sampling Cruise 2. There were no indications of the presence of cuttings or SBF in these samples.

7.4.2.2.2 Mississippi Canyon 496. Samples collected in the near-field at MC 496 during Sampling Cruise 1 were predominantly fine-grained sediments with streaks of sulfide (Table 7-10). Cuttings were detected in all but one of the samples collected in this zone, but presence of SBF was not indicated in any of the near-field samples. Similar results were observed for the samples collected in the mid-field zone. Shale/siltstone fragments in four of the far-field samples may have indicated the presence of cuttings, but the presence of SBF was not indicated in any of these samples.

Fine-grained sediments dominated in all samples collected during Sampling Cruise 2. There were no indications of the presence of cuttings or SBF in these samples.

Table 7-7. Summary of the results from visual cuttings analysis of sediment samples collected at Main Pass 299 during Sampling Cruises 1 and 2.

Sampling Cruise	Station	General Characteristics	Cuttings	Fluorescence Indicating Presence of Synthetic Based Muds
1	NF-1	90% light olive brown to gray mud	Present (slight trace of shale/sandstone/siltstone fragments)	None
1	NF-2	90% moderate olive brown mud with brown iron oxide streaks	Some	None
1	NF-3	85% moderate olive brown mud with brown iron oxide streaks, trace black sulfides	Moderate	Mild fluorescence
1	NF-4	95% light olive gray mud	Some	None
1	NF-5	90% light olive gray mud	Moderate	None
1	NF-6	85% greenish black mud	Common	Minor fluorescence
1	MF-1	90% light olive gray mud	Trace	None
1	MF-2	90% grayish black mud with brown/orange iron oxide streaks	Trace	None
1	MF-3	90% light olive gray to moderate olive brown mud with brown and black streaks	Moderate	None
1	MF-4	90% light olive gray mud with brown and black streaks	Moderate	None
1	MF-5	90% light olive gray mud with brown streaks	Minor	None
1	MF-6	90% grayish black to light olive brown mud with iron oxide stain	Moderate	None
1	FF-1	95% light olive gray mud with dark brown streaks	Trace	None
1	FF-2	95% light olive gray mud with dark brown streaks	Trace	None
1	FF-3	90% light olive gray to dark gray mud with black streaks	Trace	None
1	FF-4	90% light olive gray mud with black spots and dark brown streaks	Trace	None
1	FF-5	90% light olive gray mud with brown streaks	Trace	None

Table 7-7. (Continued).

Sampling Cruise	Station	General Characteristics	Cuttings	Fluorescence Indicating Presence of Synthetic Based Muds
1	FF-6	90% light olive gray mud with dark brown streaks	Trace	None
2	NF-1	90% light olive gray silt/clay	None	None
2	NF-2	90% light olive gray silt/clay	Slight trace	None
2	NF-3	95% light olive gray silt	None	None
2	NF-4	95% light olive gray silt	None	None
2	NF-5	95% light olive gray silt	None	None
2	NF-6	95% light olive gray silt	None	None
2	MF-1	95% light olive gray mud	None	None
2	MF-2	95% light olive gray mud	Very slight trace	None
2	MF-3	95% light olive gray mud	Present (shale cuttings)	None
2	MF-4	95% light olive gray mud	None	None
2	MF-5	95% light olive gray mud	None	None
2	MF-6	95% light olive gray mud	None	None
2	FF-1	95% olive gray mud	None	None
2	FF-2	95% olive gray mud	None	None
2	FF-3	95% olive gray mud	None	None
2	FF-4	95% olive gray mud	None	None
2	FF-5	95% light olive gray mud	None	None
2	FF-6	95% light olive gray mud	None	None

Table 7-8. Summary of the results from visual cuttings analysis of sediment samples collected at South Timbalier 160 during Sampling Cruises 1 and 2.

Sampling Cruise	Station	General Characteristics	Cuttings	Fluorescence Indicating Presence of Synthetic Based Muds
1	NF-1	90% dark yellowish brown mud with abundant black sulfides	Present (shale/sandstone fragments)	Slight trace synthetic oil based mud; no fluorescence despite presence
1	NF-2	80% moderate yellowish brown mud with abundant black sulfides	Present (shale/sandstone/siltstone)	Slight trace synthetic oil based mud; no fluorescence despite presence
1	NF-3	80% moderate yellowish brown mud with abundant black sulfides	Present (shale/sandstone/siltstone)	Slight trace synthetic oil based mud; no fluorescence despite presence
1	NF-4	90% moderate yellowish brown mud with abundant black sulfides	Present (shale/siltstone/silt)	Slight trace residual synthetic oil based mud; no fluorescence despite presence
1	NF-5	80% dark yellowish brown mud with abundant black sulfides	Present (shale/sandstone/siltstone)	Slight trace residual synthetic oil based mud; no fluorescence despite presence
1	NF-6	85% moderate yellowish brown mud with abundant black sulfides	Present (shale fragments)	None
1	MF-1	95% moderate yellowish brown mud	Present (few ½-cm shale cuttings)	None
1	MF-2	90% moderate yellowish brown mud	Present (slight trace of shale)	None
1	MF-3	95% moderate yellowish brown mud	None	None
1	MF-4	90% moderate yellowish brown mud	Present (shale fragments)	None
1	MF-5	80% moderate yellowish brown mud	Present (gumbo shale lumps)	None
1	MF-6	90% moderate yellowish brown mud	Present (shale fragments)	None
1	FF-1	95% moderate yellowish brown mud	Present (shale fragments)	None
1	FF-2	90% moderate yellowish brown mud	Present (trace shale fragments)	None
1	FF-3	95% moderate yellowish brown mud	Present (trace shale fragments)	None
1	FF-4	95% moderate yellowish brown mud	Present (trace shale fragments)	None
1	FF-5	90% moderate yellowish brown mud	Present (gumbo shale lumps)	None
1	FF-6	95% moderate yellowish brown mud	Present (shale fragments)	None
2	NF-1	95% light olive gray and dark gray mud	None	None
2	NF-2	95% light olive gray mud	None	None
2	NF-3	95% pale brown mud	None	None
2	NF-4	95% dark gray mud	None	None
2	NF-5	95% olive gray mud	None	None

Table 7-8. (Continued).

Sampling Cruise	Station	General Characteristics	Cuttings	Fluorescence Indicating Presence of Synthetic Based Muds
2	NF-6	95% olive gray mud	None	None
2	MF-1	95% light olive gray mud	None	None
2	MF-2	95% light olive gray mud	None	None
2	MF-3	95% light olive gray mud	None	None
2	MF-4	95% light olive gray mud	None	None
2	MF-5	95% light olive gray mud	None	None
2	MF-6	95% light olive gray mud	None	None
2	FF-1	95% olive gray mud	None	None
2	FF-2	95% olive gray mud	None	None
2	FF-3	95% light olive gray mud	None	None
2	FF-4	95% light olive gray mud	None	None
2	FF-5	95% light olive gray mud	None	None
2	FF-6	95% light olive gray mud	None	None

Table 7-9. Summary of the results from visual cuttings analysis of sediment samples collected at Green Canyon 112 during Sampling Cruises 1 and 2.

Sampling Cruise	Station	General Characteristics	Cuttings	Fluorescence Indicating Presence of Synthetic Based Muds
1	NF-1	50% dark gray mud with moderate brown streaks; 50% silt/sand-size particles	None	Slight trace moderate fluorescence
1	NF-2	90% light olive gray mud with medium gray streaks	Common	None
1	NF-3	85% light olive gray mud with brown/orange streaks	Present	None
1	NF-4	80% gray to black mud with yellow/gray spots	Present	Trace moderate fluorescence
1	NF-5	80% light olive gray mud with brown/black streaks and iron oxide stain	Common	Slight trace mild fluorescence
1	NF-6	85% light olive gray mud with brown/black streaks and iron oxide stain	Common	Slight trace mild fluorescence
1	MF-1	90% light olive gray to grayish black mud with iron oxide streaks	Common	Trace mild fluorescence
1	MF-2	80% light olive gray mud with black streaks and iron oxide stain	Common	None
1	MF-3	90% moderate to dark yellowish brown mud	None	None
1	MF-4	85% moderate to dark yellowish brown mud	None	None
1	MF-5	85% light olive gray to dark gray with black streaks and iron oxide stain	Common	Slight trace mild fluorescence
1	MF-6	90% moderate to dark yellowish brown mud	None	None
1	FF-1	90% moderate brown mud	None	None
1	FF-2	90% moderate brown mud	Slight trace	None
1	FF-3	90% moderate brown mud	Trace	None
1	FF-4	90% moderate brown to moderate yellowish brown mud	Slight trace	None

Table 7-9. (Continued).

Sampling Cruise	Station	General Characteristics	Cuttings	Fluorescence Indicating Presence of Synthetic Based Muds
1	FF-5	85% moderate brown mud	None	None
1	FF-6	90% moderate brown mud	None	None
2	NF-1	90% olive gray mud	None	None
2	NF-2	95% dark olive gray	None	None
2	NF-3	95% dark gray mud	None	None
2	NF-4	95% dark gray mud	None	None
2	NF-5	95% dark gray mud	None	None
2	NF-6	90% dark gray mud	None	None
2	MF-1	95% light brown mud	None	None
2	MF-2	90% olive green mud	None	None
2	MF-3	95% olive green mud	None	None
2	MF-4	90% light olive gray mud	None	None
2	MF-5	90% dark brown to black mud	None	None
2	MF-6	90% light olive gray mud	None	None
2	FF-1	95% olive gray mud	None	None
2	FF-2	95% olive gray mud	None	None
2	FF-3	95% olive gray mud	None	None
2	FF-4	95% olive gray mud	None	None
2	FF-5	95% dark yellow brown mud	None	None
2	FF-6	95% dark yellow brown mud	None	None

Table 7-10. Summary of the results from visual cuttings analysis of sediment samples collected at Mississippi Canyon 496 during Sampling Cruises 1 and 2.

Sampling Cruise	Station	General Characteristics	Cuttings	Fluorescence Indicating Presence of Synthetic Based Muds
1	NF-1	75% dark yellowish brown mud with trace black sulfide streaks	Present (shale/siltstone cuttings)	None
1	NF-2	75% dark yellowish brown mud with abundant black sulfide streaks	Present (shale/siltstone cuttings)	None
1	NF-3	80% dark yellowish brown mud with abundant black sulfide streaks	None	None
1	NF-4	70% moderate yellowish brown mud with abundant black sulfides	Present (shale/siltstone cuttings)	None
1	NF-5	75% moderate yellowish brown mud with abundant (75%) black sulfides	Present (shale fragments)	None
1	NF-6	90% dark yellowish brown mud with trace black sulfides	Present (shale/siltstone cuttings)	None
1	MF-1	90% dark yellowish brown mud	Present (shale cuttings)	None
1	MF-2	90% dark yellowish brown mud	Present (shale/siltstone cuttings)	None
1	MF-3	90% dark yellowish brown mud with abundant black sulfides	Present (shale/siltstone fragments)	None
1	MF-4	90% dark yellowish brown mud with trace black sulfides	Present (shale/siltstone fragments)	None
1	MF-5	90% dark yellowish brown mud with trace black sulfides	Present (shale/siltstone fragments)	None
1	MF-6	90% dark yellowish brown mud	None	None
1	FF-1	90% dark yellowish brown mud	None	None
1	FF-2	95% dark yellowish brown mud	Present (shale/siltstone fragments)	None
1	FF-3	95% dark yellowish brown mud	Present (shale/siltstone fragments)	None
1	FF-4	95% dark yellowish brown mud	Present (shale/siltstone fragments)	None
1	FF-5	95% dark yellowish brown mud	Present (shale/siltstone fragments)	None
1	FF-6	90% dark yellowish brown mud	None	None
2	NF-1	95% dark yellowish brown mud	None	None
2	NF-2	95% dark yellowish brown mud	None	None

Table 7-10. (Continued).

Sampling Cruise	Station	General Characteristics	Cuttings	Fluorescence Indicating Presence of Synthetic Based Muds
2	NF-3	90% dark yellowish brown mud	None	None
2	NF-4	90% dark yellowish brown mud	None	None
2	NF-5	90% dark yellowish brown mud	None	None
2	NF-6	90% dark yellowish brown mud	None	None
2	MF-1	95% dark yellowish brown mud	None	None
2	MF-2	95% dark yellowish brown mud	None	None
2	MF-3	95% dark yellowish brown mud	None	None
2	MF-4	95% dark yellowish brown mud	None	None
2	MF-5	95% dark yellowish brown mud	None	None
2	MF-6	95% dark yellowish brown mud	None	None
2	FF-1	95% dark yellow brown mud	None	None
2	FF-2	95% dark yellow brown mud	None	None
2	FF-3	95% light olive gray mud	None	None
2	FF-4	95% dark yellow brown mud	None	None
2	FF-5	95% dark yellow brown mud	None	None
2	FF-6	95% dark yellowish brown mud	None	None

7.4.2.2.3 Ewing Bank 963. At EW 963, fine-grained sediments dominated at most stations, but various streaks were observed in the samples collected in the near-field and mid-field zones during Sampling Cruise 1 (Table 7-11). Cuttings were present at five of six near-field stations, but there were no indications of the presence of SBF in the near-field zone. Cuttings also were detected at five mid-field stations during Sampling Cruise 1. SBF was observed in this zone during Sampling Cruise 1. There were no indications of cuttings or SBF in the samples collected in the far-field zone.

Fine-grained sediments dominated in all samples collected during Sampling Cruise 2. There were no indications of the presence of cuttings or SBF in these samples.

7.4.2.2.4 Viosca Knoll 783. Fine-grained sediment was the dominant constituent of the samples collected at VK 783 during Sampling Cruise 1 (Table 7-12). Cuttings were detected in all samples, but there was no indication of the presence of SBF. Similarly, fine-grained sediments dominated in the samples collected during Sampling Cruise 2. Cuttings were detected in all of the samples collected in the near-field, at two stations in the mid-field, and at one station in the far-field.

7.5 SUMMARY

Sediment samples were collected in the vicinity of four continental shelf discharge sites and four continental slope discharge sites during the two Sampling Cruises for the detection of drill cuttings using three methods: nannofossils analysis, sediment grain size analysis, and visual cuttings analysis. A summary of the results from the visual cuttings analysis and the nannofossils analysis (including the presence of glass spheres) is presented in Table 7-13. There was evidence that cuttings occurred in the near-field and mid-field at MC 496, VK 783, GC 112, and EI 346 during Sampling Cruise 1. Cuttings were not frequently observed in the far-field at these sites. For Sampling Cruise 2, the occurrence of cuttings at these sites was less frequent compared to Sampling Cruise 1. Overall, these results indicated that cuttings occurred primarily in the near vicinity (<250 m) of the discharge sites.

The results of the sediment grain size analysis were of very limited use. Additional information from the nannofossils analysis was necessary to interpret the grain size results as it was related to the presence of cuttings. Because no strong correlation was observed between grain size and the presence of barite in the Screening Cruise samples, grain size alone cannot be used as an indicator of drilling-related materials unless 1) anomalous grain sizes also are accompanied by the presence of pre-Holocene nannofossils (or glass spheres that are a common additive to drilling muds) or 2) surrounding sediments (e.g., mid-field and/or far-field) are of a significantly different (i.e., finer) grain size. Under these circumstances, the sediments may indicate presence of non-indigenous materials.

Table 7-11. Summary of the results from visual cuttings analysis of sediment samples collected at Ewing Bank 963 during Sampling Cruises 1 and 2.

Sampling Cruise	Station	General Characteristics	Cuttings	Fluorescence Indicating Presence of Synthetic Based Muds
1	NF-1	80% moderate olive brown mud with gray/olive streaks and oxide stains	None	None
1	NF-2	80% moderate olive brown mud with black and moderate brown streaks	Present (shale fragments)	None
1	NF-3	90% light olive gray mud with gray/brown and oxide streaks	Present (minor shale fragments)	None
1	NF-4	80% dark gray mud with yellow/gray streaks	Present (shale/sandstone fragments)	None
1	NF-5	90% light olive gray mud with moderate olive brown and dark gray streaks	Present (minor shale fragments)	None
1	NF-6	95% light olive gray mud	Present (3 pieces shale cuttings)	None
1	MF-1	80% moderate olive brown mud with black sulfide and orange/yellow oxide streaks	Present (shale fragments)	None
1	MF-2	90% moderate olive brown mud with black sulfide and orange/yellow oxide streaks	Present (very small shale cuttings)	None
1	MF-3	85% olive gray to moderate olive brown mud	Present (minor shale/siltstone fragments)	None
1	MF-4	80% olive gray to moderate olive brown mud	None	None
1	MF-5	75% moderate olive brown mud with orange-yellow oxide and olive gray streaks	Present (shale fragments)	None
1	MF-6	90% moderate olive brown mud with olive-gray streaks	Present (trace shale fragments)	None
1	FF-1	95% dark yellowish brown mud	None	None
1	FF-2	85% dark yellowish brown mud	None	None
1	FF-3	90% dark yellowish brown mud	None	None
1	FF-4	85% dark yellowish brown mud	None	None
1	FF-5	90% moderate olive brown mud with black sulfide and orange/yellow oxide streaks	None	None
1	FF-6	90% moderate olive brown mud	None	None
2	NF-1	95% dark yellowish brown mud	None	None

Table 7-11. (Continued).

Sampling Cruise	Station	General Characteristics	Cuttings	Fluorescence Indicating Presence of Synthetic Based Muds
2	NF-2	95% dark yellowish brown mud	None	None
2	NF-3	95% dark yellowish brown mud	None	None
2	NF-4	95% light olive gray mud	None	None
2	NF-5	95% light olive gray mud	None	None
2	NF-6	95% dark yellowish brown mud	None	None
2	MF-1	95% dark yellowish brown mud	None	None
2	MF-2	95% dark yellowish brown mud	None	None
2	MF-3	95% dark yellowish brown mud	None	None
2	MF-4	95% dark yellowish brown mud	None	None
2	MF-5	95% dark yellowish brown mud	None	None
2	MF-6	95% dark yellowish brown mud	None	None
2	FF-1	95% dark yellowish brown mud	None	None
2	FF-2	95% dark yellowish brown mud	None	None
2	FF-3	95% dark yellowish brown mud	None	None
2	FF-4	95% dark yellowish brown mud	None	None
2	FF-5	95% dark yellowish brown mud	None	None
2	FF-6	95% light olive gray mud	None	None

Table 7-12. Summary of the results from visual cuttings analysis of sediment samples collected at Viosca Knoll 783 during Sampling Cruises 1 and 2.

Sampling Cruise	Station	General Characteristics	Cuttings	Fluorescence Indicating Presence of Synthetic Based Muds
1	NF-1	95% dark yellowish brown mud	Trace	None
1	NF-2	95% dark yellowish brown mud	Trace	None
1	NF-3	90% dark yellowish brown mud	Trace	None
1	NF-4	90% dark yellowish brown mud	Slight trace	None
1	NF-5	90% dark yellowish brown mud	Slight trace	None
1	NF-6	90% dark yellowish brown mud	Trace	None
1	MF-1	90% moderate olive brown mud	Very slight trace	None
1	MF-2	90% moderate olive brown mud	Present	None
1	MF-3	95% moderate olive brown mud	Present	None
1	MF-4	85% moderate olive brown mud	Trace	None
1	MF-5	90% moderate olive brown mud	Trace	None
1	MF-6	90% moderate olive brown mud	Trace	None
1	FF-1	95% moderate olive brown mud	Trace	None
1	FF-2	95% moderate olive brown mud	Trace	None
1	FF-3	90% moderate olive brown mud	Trace	None
1	FF-4	85% moderate olive brown mud	Trace	None
1	FF-5	85% moderate olive brown mud	Trace	None
1	FF-6	90% moderate olive brown mud	Trace	None
2	NF-1	95% olive gray mud	Present (shale cuttings)	None
2	NF-2	95% dark yellowish brown mud	Slight trace	None
2	NF-3	95% light olive gray mud	Slight trace	None
2	NF-4	95% dark yellowish brown mud	Trace	None
2	NF-5	95% dark yellowish brown mud	Trace	None
2	NF-6	95% dark yellowish brown mud	Trace	None
2	MF-1	95% dark yellowish brown mud	None	None
2	MF-2	95% dark yellowish brown mud	None	None
2	MF-3	95% dark yellowish brown mud	None	None
2	MF-4	95% dark yellowish brown mud	Present (shale cuttings)	None

Table 7-12. (Continued).

Sampling Cruise	Station	General Characteristics	Cuttings	Fluorescence Indicating Presence of Synthetic Based Muds
2	MF-5	95% moderate olive brown mud	None	None
2	MF-6	95% dark yellowish brown mud	Present (shale cuttings)	None
2	FF-1	95% dark yellowish brown mud	None	None
2	FF-2	95% dark yellowish brown mud	Present (slight trace shale cuttings)	None
2	FF-3	95% dark yellowish brown mud	None	None
2	FF-4	95% dark yellowish brown mud	None	None
2	FF-5	95% dark yellowish brown mud	None	None
2	FF-6	95% dark yellowish brown mud	None	None

Table 7-13. Summary of results of analysis of sediments for cuttings solids, anachronous nannofossils, and glass spheres.

Site	Indicator	Sampling Cruise 1			Sampling Cruise 2		
		NF	MF	FF	NF	MF	FF
Eugene Island 346	Cuttings	+	+	-	+	~	-
	Fossils	+	~	~	+	~	-
	Spheres	+	+	~	+	~	~
Main Pass 288	Cuttings	+	+	~	-	-	-
	Fossils	~	-	-	~	~	-
	Spheres	-	-	-	~	~	-
Main Pass 299	Cuttings	+	+	~	~	~	-
	Fossils	-	-	-	-	-	-
	Spheres	~	~	~	+	~	~
Ewing Bank 963	Cuttings	+	+	-	-	-	-
	Fossils	-	-	-	~	-	-
	Spheres	-	-	-	~	-	+
South Timbalier 160	Cuttings	+	+	+	-	-	-
	Fossils	~	-	~	-	-	-
	Spheres	-	~	-	~	~	~
Viosca Knoll 783	Cuttings	+	+	+	+	~	~
	Fossils	+	+	-	+	~	~
	Spheres	~	+	~	~	~	~
Green Canyon 112	Cuttings	+	~	~	-	-	-
	Fossils	+	~	-	~	~	~
	Spheres	-	-	~	~	-	~
Mississippi Canyon 496	Cuttings	+	+	+	-	-	-
	Fossils	+	~	-	+	~	-
	Spheres	+	~	~	~	~	~

- = Indications in no samples.
~ = Indications in half or less of samples.
+ = Indications in majority of samples.

FF = Far-field.
MF = Mid-field.
NF = Near-field.

Chapter 8
THE ORGANIC CHEMISTRY OF SYNTHETIC BASED FLUID RESIDUES AND TOTAL PETROLEUM HYDROCARBONS IN SEDIMENTS

Allen D. Uhler and Richard M. Uhler
Battelle Memorial Institute
and
Alan D. Hart
Continental Shelf Associates, Inc.

8.1 INTRODUCTION

This chapter describes the findings of SBF residues and TPH in sediments from the four continental shelf and four continental slope study sites collected during Sampling Cruises 1 and 2 (May 2001 and May 2002, respectively). Specifications for the study sites are presented in Table 8-1. Synthetic based fluids are composed of well characterized chemical compounds synthesized specifically to provide drilling muds with excellent wellbore lubricity and added temperature stability that, in conjunction with other mud additives, reduce potential for differential sticking and low formation damage in offshore drilling operations. The base fluids can include olefins, ethers, esters, and acetals (Uhler and Neff, 1998). When SBFs are mixed with specially formulated mixtures of water, natural clays and/or polymers, weighting agents, and other materials, the resulting product is referred to as an SBM. There are a number of SBM products currently in use or proposed for use by the oil and gas industry (Candler et al., 1993; Bloys et al., 1994; Veil et al., 1996). These muds are less toxic and more readily biodegraded than OBMs, while retaining many of the technical advantages of the OBMs (Park et al., 1993, Veil et al., 1996).

Table 8-1. Study site specifications.

Study Site	Acronym Used in Data Reporting	Drillsite Type	Nominal Water Depth (m)	Synthetic Based Fluid Used in Drilling
Main Pass 299	MP 299	Continental Shelf	60	LAO
Main Pass 288	MP 288	Continental Shelf	119	IO
Eugene Island 346	EI 346	Continental Shelf	92	IO
South Timbalier 160	ST 160	Continental Shelf	37	IO
Viosca Knoll 783	VK 783	Continental Slope	338	Ester
Mississippi Canyon 496	MC 496	Continental Slope	556	IO
Ewing Bank 963	EW 963	Continental Slope	540	IO
Green Canyon 112	GC 112	Continental Slope	534	IO

IO = Internal olefin.
LAO = Linear alpha olefin.

This section of the report focuses on addressing two principal goals of the Gulf of Mexico Comprehensive Synthetic Based Muds Monitoring Program, namely 1) to determine the spatial distribution of SBM cuttings residues in the vicinity of selected continental shelf and continental slope drillsites and 2) to assess any temporal changes in the distributions and concentrations of SBM cuttings residues in sediments proximal to drillsites.

In order to address two of the principal goals of the Gulf of Mexico Comprehensive Synthetic Based Muds Monitoring Program, sediment samples were collected at varying distances from the well points at each of the eight study sites at two different times after drilling. The rationale and details of this sampling design are described in Chapter 1. Briefly, sediment samples were collected proximal to the eight study sites at two points in time; one set was collected in May 2001 (Sampling Cruise 1), and another set a year later in May 2002 (Sampling Cruise 2). At each test site, sediments were collected in a stratified random method at distances ranging across the near-field (within a 100-m radius of the platform or drillsite), mid-field (100- to 250-m radius from the platform or drillsite), and far-field (3,000- to 6,000-m radius from the platform or drillsite). The sampling grids at each study area were re-randomized between Sampling Cruises 1 and 2. Surface sediment (0 to 2 cm) subsamples were collected at all sampling locations; residues of SBFs found in these samples can be used to describe the spatial extent of SBM cuttings around each study site. At certain study sites, a limited number of depth-discrete sediment samples (0 to 2 cm; 2 to 4 cm; 4 to 6 cm; 6 to 8 cm; 8 to 10 cm) were obtained; residues of SBFs in these samples can be used to judge depth profiles of SBM cuttings at locations proximal to the selected drillsites.

8.2 METHODS OF ANALYSIS FOR SYNTHETIC BASED FLUID RESIDUES AND TOTAL PETROLEUM HYDROCARBON RESIDUES IN SEDIMENT

Subsamples of sediment collected from the eight study sites were analyzed for TPH and SBF residues using high resolution GC/MS techniques. The principal advantage of using GC/MS as a determinative tool in this study is that the method allows 1) identification of the presence of SBF(s) in a sample, 2) identification of the type(s) of SBF residue (e.g., IO, LAO, ester) in a sample, and 3) discrimination between SBF components from other types of hydrocarbons (be they petroleum or naturally occurring) that may be present in the sediments.

In this study, TPH in sediment as measured by GC/MS is defined as those hydrocarbons between *n*-C_{10} and *n*-C_{36} that can be extracted and measured in the sediment samples. Practically, this measurement detects and quantifies petroleum (including crude and most refined products such as diesel, residual fuels, and lubricating-range materials), SBF hydrocarbons, and certain biogenic (naturally occurring) hydrocarbons, e.g., plant waxes. Sediments that contain residues of SBF will have a TPH value that reflects the SBF content (as described below, represented by a rather narrow hydrocarbon range) *plus* any other petroleum or natural hydrocarbons found in the sediment outside that SBF carbon-range window.

Synthetic based fluid residue in sediment as measured by GC/MS is defined as the concentration of hydrocarbons found in specific patterns that can be matched to an authentic SBF standard, after those hydrocarbons have been extracted from a sediment. In this investigation, three different SBFs were used to develop wells at the eight study sites: an LAO, an IO, and an ester formulation.

Each of these SBFs has distinct GC “patterns” of synthetic hydrocarbons that can be distinguished from non-SBF hydrocarbons (Figure 8-1). As described below, specific identification and quantitation criteria were used to measure SBF residues in sediment samples.

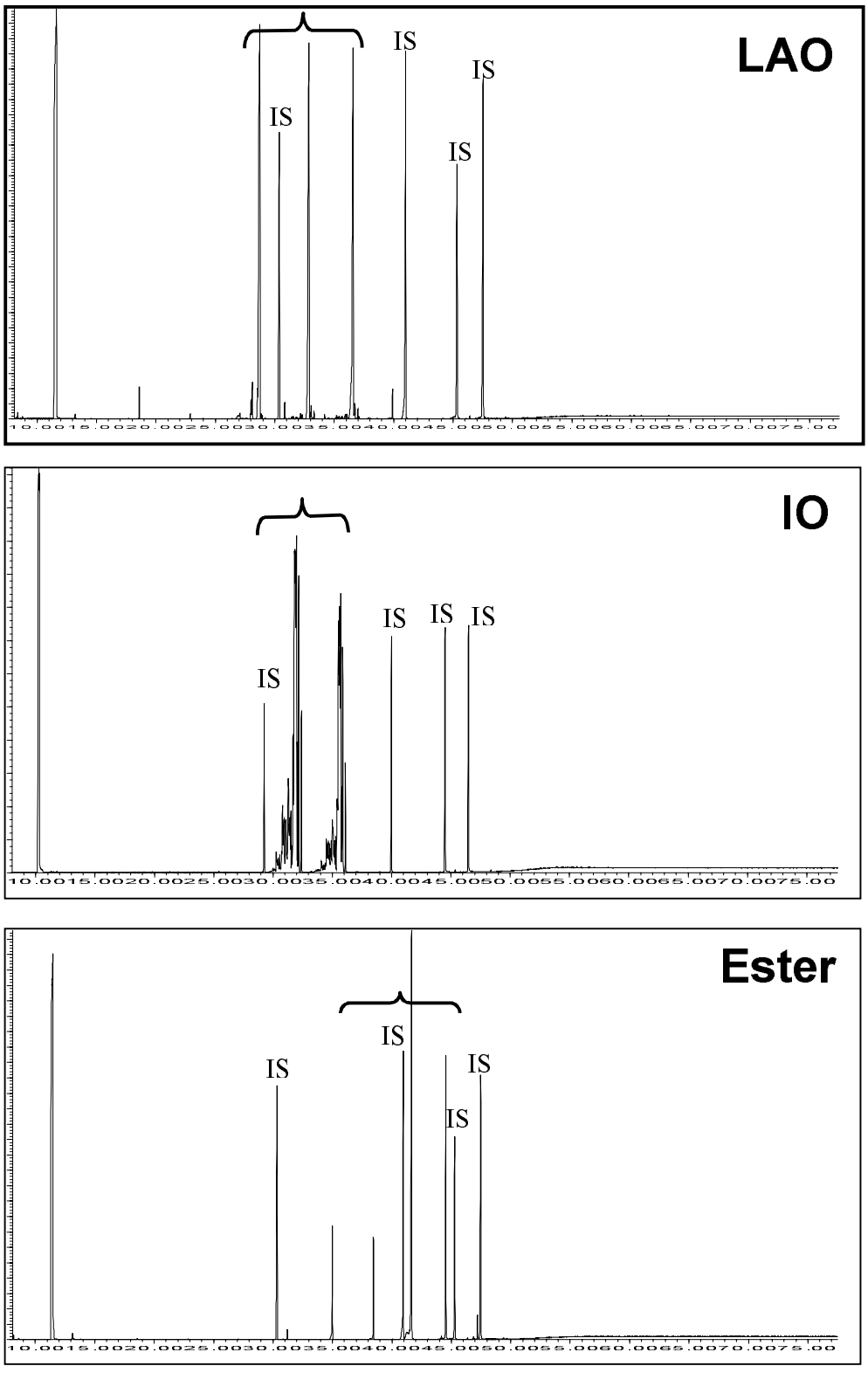

Figure 8-1. Gas chromatography/mass spectrometry chromatograms of synthetic based fluid (SBF) reference standards. Retention time windows for the SBF are marked with brackets. Analytical internal standard labeled as "IS."

8.2.1 Chemical Analysis of Sediments for TPH and SBF

Sediment samples were extracted following National Oceanic and Atmospheric Administration (NOAA) National Status and Trends analytical methods (NOAA, 1998), which are codified in Battelle Standard Operating Procedure (SOP) 5-203, *Extraction of Soil/Sediment Samples for Petroleum Analysis*. A 5-g aliquot of homogenized sediment was removed for percent moisture determination. Approximately 25 g of homogenized sediment were placed in a glass extraction jar, spiked with the appropriate surrogate internal standards (SIS), n-tetracosane-d50 and hexamethylbenzene, combined with solvent (methylene chloride) and sodium sulfate, shaken on a rotary action shaker table for 12 hours, centrifuged, and the solvent decanted into an Erlenmeyer flask. Two additional solvent addition/shake procedures were performed, one for 4 hours and the final for half an hour. The combined extracts were concentrated using Kuderna-Danish (KD) and nitrogen concentration techniques. The concentrated extract was treated with activated copper to remove elemental sulfur. Gravimetric analysis was performed on all near-field samples and any others that appeared contaminated so as to determine the potential total oil content and assist in the necessary dilution of samples. The final extract was spiked with the appropriate recovery internal standards (RIS), 5α-androstane and alternate RIS, chrysene-d_{12}, and analyzed by GC/MS for TPH and SBF.

Sample extracts were analyzed for TPH and SBF by GC/MS following Battelle SOP 5-157, *Identification and Quantification of Polynuclear Aromatic Hydrocarbons by Gas Chromatography/Mass Spectrometry*. The GC/MS was operated in the full scan mode. The system was tuned prior to use with perfluorotributylamine (PFTBA). The GC/MS was equipped with a 60-m DB-5 column (0.25-mm internal diameter [ID] and 0.25-µm film thickness), and a split/splitless inlet (with electronic pressure control) operated in the splitless mode. The GC/MS conditions for the analysis were 1) initial column temperature: 35°C; 2) initial hold time: 5 minutes; 3) program rate: 6°/minute; 4) final column temperature: 320°C; 5) final hold time: 25 minutes; 6) injector temperature: 300°C; 7) detector temperature: 280°C; and 8) mass range scanned: 50 to 550 m/z.

Separate multilevel calibrations (minimum of 5 points each) were prepared for TPH analysis and for analysis of each SBF (IO, LAO, ester). Specific SBF products were used as chromatographic reference and calibration standards for chemical analysis:

- LAO: Bio-Base 250, Shrieve Chemical Products;
- IO: C16/C18 Internal Olefin, Chevron Chemical Company; and
- Ester: Petrofree, Baroid Drilling Fluids, Inc.

For TPH analysis, the average response factor (RF) for individual *n*-alkanes between *n*-C_{10} and *n*-C_{36} was used to quantify the response of total hydrocarbons. For individual base fluids, a response factor was generated relative to the response of the major synthetic hydrocarbon compounds found in each SBF formulation. The alkane calibration solution was composed of selected *n*-alkanes between *n*-C_{10} and *n*-C_{36}, as well as pristane and phytane. Target alkane analyte concentrations in the calibration standard solutions ranged from 1 to 100 ng/µL. Base fluid calibrations ranged from approximately 10 to 1,800 ng/µL. A respective mid-level calibration check standard was analyzed at least every 10 samples to monitor instrument response relative to the initial calibration.

The SBF calibrations were based on manufacturer-specific reference formulations. Among different manufacturers, there are distinct differences in the relative distribution of the synthetic chemical isomers that comprise a particular SBF formulation. As such, there can be some small (but measurable) systematic differences between the SBF measured in a field sample residue when another manufacturer's fluid is used as the analytical reference. The comparison shown in Figure 8-2 of gas chromatograms of IO fluids for ChevronTexaco IO-1618, Amodrill 1000, and the Chevron Chemical Company fluid used as a calibration reference in this study shows that both the ChevronTexaco IO-1618 and Amodrill 1000 are very similar IO formulations dominated by C_{16} and C_{18} internal olefin isomers and the Amodrill 1000 contains a small but measurable amount of C_{20} IO isomers that do not appear in the ChevronTexaco IO-1618 (or the Chevron Chemical Company fluid formulation used as a calibration standard in this study). The important implication of this fact is that if Amodrill 1000 residues were present in sediments measured in this program, there would be an inherent bias in the difference between measured values of SBF and TPH, e.g., the measured TPH concentration would be higher than the measured SBF concentration (even though the SBF and TPH concentrations should in theory be equivalent in the absence of other hydrocarbons). The reason for this bias is that the portion of the SBF composed of the C_{20} IO isomers would be quantified as TPH instead of SBF, resulting in an apparently higher relative concentration of TPH than SBF. While this kind of analytical bias is unavoidable (it would be impractical to prepare SBF instrument calibrations for every possible SBF formulation potentially encountered in environmental samples), knowledge of this potential bias aids in the interpretation of observations made later in this chapter about the relative differences in measured SBF and TPH concentrations in sediments from this study.

There are significant differences in the GC/MS response factors for synthetic hydrocarbons containing olefins and esters as compared to that for the normal (saturated) hydrocarbons (i.e., synthetic hydrocarbons respond significantly differently than normal hydrocarbons in a GC/MS analysis). The consequence of this fact for this study is that there is an inherent systematic difference between TPH measurements (which are based on average response factors for normal alkanes, a reasonable proxy for naturally occurring hydrocarbons) and SBF measurements (which are based on average response factors for particular synthetic fluids). In certain sediments from this study where the proportion of total hydrocarbons in the sample is dominated by the synthetic fluid hydrocarbons, the SBF concentration can appear as a value larger than the corresponding TPH measurement. Nonetheless, the comparison between TPH and SBF results is extremely useful in understanding what hydrocarbon assemblages are driving the hydrocarbon burden in the sediments.

Quantification of TPH and SBF concentration in the samples was performed by the method of internal standards. The recovery internal standard, 5α-androstane, was used to quantify the TPH and the specific SBF (IO, LAO, or ester), as well as to quantify the surrogates, hexamethylbenzene and *n*-tetracosane-d_{50}. When the concentration of the analyte exceeded the calibration range of the system, the sample was diluted and reanalyzed. All data were reported in mg/kg on a dry weight basis.

A reporting limit of 1 mg/kg (dry weight basis) for TPH and SBF was used for this investigation. This reporting limit was chosen because it was 1) equivalent to the concentration of the lowest instrument calibration standard and 2) it represented a concentration at which the instrument analysts could confidently identify and measure the chromatographic patterns of the synthetic fluid in a sediment sample.

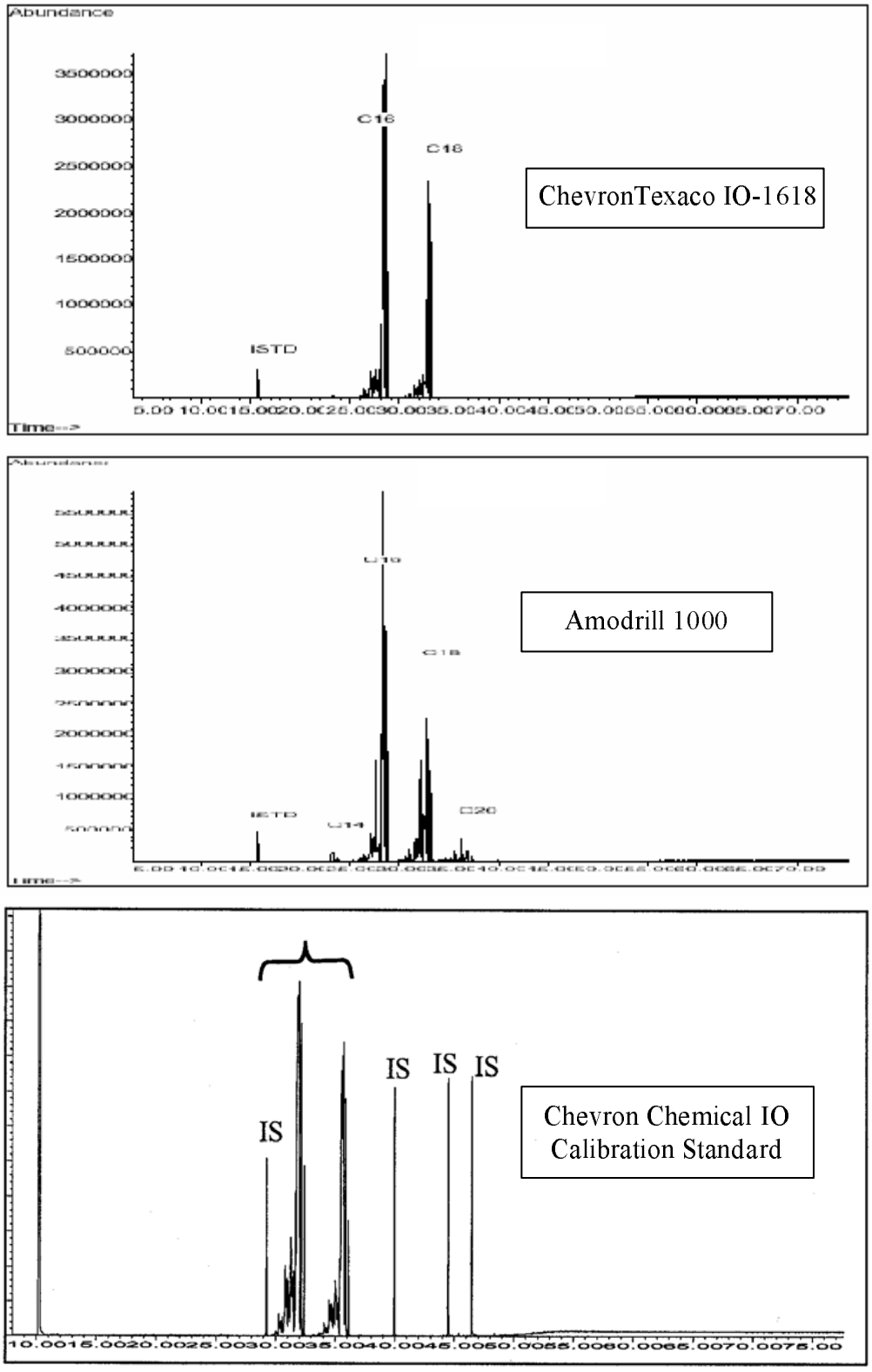

Note that the detectable amounts of C_{20} isomers in the Amodrill 1000 formulation are not present in the ChevronTexaco IO-1618 or the instrument calibration standard.

Figure 8-2. Comparative chromatograms of ChevronTexaco IO-1618, Amodrill 1000, and the Chevron Chemical Company IO fluid, which was used as a standard for synthetic based fluid analyses in this study.

Appropriate quality control (QC) samples and QC measures were followed in this analytical program. Quality control samples, analyzed with every batch of 20 or fewer field samples, included procedural blanks (to document lack of laboratory contamination during sample preparation), laboratory control samples (to document method accuracy and precision), and matrix spike/matrix spike duplicate (MS/MSD: representative field samples spiked with SBF and carried through the analytical procedure to document method accuracy with authentic field samples). Specific DQOs and corrective measures were established and adhered to during the course of the laboratory analyses (Table 8-2).

Table 8-2. Analytical data quality objectives (DQOs) and corrective actions.

Quality Control Type/Parameter	DQO Targets	Comment/Corrective Action
Procedural Blank	<5x RL, or associated samples must be >10x blank concentration.	Review with Project Manager; re-analyze or explain other corrective action in project records and qualify data appropriately.
Laboratory Control Sample or Blank Spike Recovery	40%-120% recovery	Review with Project Manager; re-analyze or explain other corrective action in project records and qualify data appropriately.
Matrix Spike (MS) Recovery	40%-120% recovery	Analyte concentration in MS must be >5x background concentration to be used for data quality assessment. Review with Project Manager; re-analyze or explain other corrective action in project records and qualify data appropriately.
Matrix Spike/Spike Duplicate Precision	<30% relative percent difference (RPD)	Analyte concentration in MS must be >5x background concentration to be used for data quality assessment. Review with Project Manager, re-analyze or explain other corrective action in project records and qualify data appropriately.
Sample Duplicates	<30% RPD	Analyte concentration in MS must be >10x MDL concentration to be used for data quality assessment. Review with Project Manager, re-analyze or explain other corrective action in project records and qualify data appropriately.
Laboratory Control Sample	40%-120% recovery	Review with Project Manager, re-analyze or explain other corrective action in project records and qualify data appropriately.
Surrogate Compound Recovery	40%-120% recovery	Review with Project Manager, re-analyze or justify in project records.
Independent Check Sample	±15%	Review with Project Manager, re-analyze or explain other corrective action in project records and qualify data appropriately.
Instrument Calibrations Initial (minimum of 5-point) Continuing Calibration Check	GC/FID: <25% RSD for response factors (RFs) (15% average) <25% difference vs. initial RF (15% on average)	Review with Project Manager, re-analyze/calibrate or explain other corrective action in project records and qualify data appropriately. At least every 10 samples. Minimally middle and end of each batch.

GC-FID = Gas chromatography-flame ionization detection.

8.3 RESULTS

The concentrations of TPH and SBF residues measured in sediments from the eight study sites, expressed in milligrams of hydrocarbons per kilogram of dry sediment (mg/kg; ppm), are tabulated in Appendix D. The results from both Sampling Cruise 1 (May 2001) and Sampling Cruise 2 (May 2002) are presented in Tables D-1 to D-8. A summary of TPH and SBF residues measured in the near-field, mid-field, and far-field zones of the continental shelf study sites is presented in Table 8-3. Similarly, a summary of TPH and SBF residues measured in the near-field, mid-field, and far-field zones of the continental slope study sites is listed in Table 8-4.

Table 8-3. Means, standard deviations, minimums, and maximums for total petroleum hydrocarbons (TPH) and synthetic based fluid (SBF) in the 0 to 2 cm sediment layer from samples collected at continental shelf sites for Sampling Cruises 1 and 2.*

	Sampling Cruise 1		Sampling Cruise 2	
	TPH (mg/kg)	SBF (mg/kg)	TPH (mg/kg)	SBF (mg/kg)
Main Pass 299				
Near-field				
Mean	619	322	44	4.5
Standard Deviation	1,000	762	14	7.6
Minimum	55	1.2	21	<1
Maximum	2,650	1,879	59	20
Mid-field				
Mean	122	3.1	64	2.0
Standard Deviation	47	2.5	23	2.4
Minimum	77	<1	40	<1
Maximum	201	6.8	109	6.8
Far-field				
Mean	11	NA	45	NA
Standard Deviation	13	NA	10	NA
Minimum	<1	<1	29	<1
Maximum	35	<1	58	<1
Main Pass 288				
Near-field				
Mean	551	196	38	2.0
Standard Deviation	379	172	9	1.0
Minimum	118	6.7	25	<1
Maximum	1,020	404	51	3.6
Mid-field				
Mean	85	4.6	78	18
Standard Deviation	49	6.0	115	37
Minimum	9	<1	22	1.3
Maximum	157	16	311	93
Far-field				
Mean	24	NA	10	NA
Standard Deviation	19	NA	7.5	NA
Minimum	7.9	<1	2.3	<1
Maximum	51	<1	21	<1

Table 8-3. (Continued).

	Sampling Cruise 1		Sampling Cruise 2	
	TPH (mg/kg)	SBF (mg/kg)	TPH (mg/kg)	SBF (mg/kg)
Eugene Island 346				
Near-field				
Mean	13,900	12,900	2,150	925
Standard Deviation	19,800	19,600	2,370	1,100
Minimum	280	178	71	22
Maximum	48,000	47,500	5,120	2,340
Mid-field				
Mean	1,460	1,000	122	40
Standard Deviation	2,240	1,730	83	34
Minimum	49	4.8	30	3.5
Maximum	5,520	4,290	250	95
Far-field				
Mean	17	NA	10	NA
Standard Deviation	3.3	NA	10	NA
Minimum	13	<1	3.2	<1
Maximum	21	<1	29	<1
South Timbalier 160				
Near-field				
Mean	5,460	4,790	254	236
Standard Deviation	5,100	5,010	385	442
Minimum	853	499	21	2.1
Maximum	14,600	14,200	972	1,110
Mid-field				
Mean	71	2.0	51	1.3
Standard Deviation	12	2.4	12	0.5
Minimum	61	<1	41	<1
Maximum	93	6.8	73	2.2
Far-field				
Mean	41	NA	35	1.3
Standard Deviation	11	NA	11	0.6
Minimum	29	<1	22	<1
Maximum	61	<1	51	2.5

NA = Not applicable.
*Mean and standard deviation were computed with concentrations below detection limits = 0 mg/kg.

Table 8-4. Means, standard deviations, minimums, and maximums for total petroleum hydrocarbons (TPH) and synthetic based fluid (SBF) in the 0 to 2 cm sediment layer from samples collected at continental slope sites for Sampling Cruises 1 and 2.*

	Sampling Cruise 1		Sampling Cruise 2	
	TPH (mg/kg)	SBF (mg/kg)	TPH (mg/kg)	SBF (mg/kg)
Mississippi Canyon 496				
Near-field				
Mean	5,520	4,060	159	65
Standard Deviation	7,910	5,390	209	89
Minimum	48	10	14	3.7
Maximum	20,500	11,200	541	213
Mid-field				
Mean	725	379	99	45
Standard Deviation	403	286	184	94
Minimum	228	79	1.2	<1
Maximum	1,090	817	471	236
Far-field				
Mean	22	NA	47	1.0
Standard Deviation	7	NA	9	0.04
Minimum	13	<1	34	<1
Maximum	32	<1	62	1.1
Ewing Bank 963				
Near-field				
Mean	2,670	1,750	365	172
Standard Deviation	3,550	2,340	377	124
Minimum	114	43	79	36
Maximum	9,770	6,410	1,060	371
Mid-field				
Mean	1,250	620	353	99
Standard Deviation	1,300	820	476	147
Minimum	77	11	41	<1
Maximum	3,390	2,120	1,210	371
Far-field				
Mean	3.6	NA	16	NA
Standard Deviation	4.8	NA	11	NA
Minimum	<1	<1	8	NA
Maximum	13	<1	36	<1

Table 8-4. (Continued).

	Sampling Cruise 1		Sampling Cruise 2	
	TPH (mg/kg)	SBF (mg/kg)	TPH (mg/kg)	SBF (mg/kg)
Green Canyon 112				
Near-field				
Mean	18,200	11,500	6,370	4,050
Standard Deviation	40,000	25,400	7,490	4,580
Minimum	324	37	563	284
Maximum	99,800	63,300	20,400	12,300
Mid-field				
Mean	867	519	3,220	1,750
Standard Deviation	885	558	6,010	3,570
Minimum	40	<1	22	1.2
Maximum	1,990	1,180	15,300	8,990
Far-field				
Mean	35	1.2	28	NA
Standard Deviation	6	0.5	14	NA
Minimum	29	<1	18	<1
Maximum	46	2.2	55	<1
Viosca Knoll 783				
Near-field				
Mean	55	4.4	53	5.9
Standard Deviation	22	4.6	15	5.3
Minimum	30	<1	35	<1
Maximum	93	13	80	14
Mid-field				
Mean	46	7.1	52	1.1
Standard Deviation	34	15	13	0.2
Minimum	26	<1	35	<1
Maximum	115	38	64	1.6
Far-field				
Mean	39	NA	30	NA
Standard Deviation	11	NA	13	NA
Minimum	26	<1	20	<1
Maximum	57	<1	55	<1

NA = Not applicable.
*Mean and standard deviation were computed with concentrations below detection limits = 0 mg/kg.

These data are displayed graphically in Figures 8-3 through 8-10 for the continental shelf and continental slope study site groups, respectively. In these figures, the data are arranged first by sampling zone (i.e., near-field, mid-field, far-field) and then, within each sampling zone, by decreasing TPH concentration. In this manner, it is possible to quickly identify the stations within a sampling zone that have the highest (or lowest) TPH and/or SBF concentrations. Refer to Chapter 3 for maps depicting the specific sediment sampling locations within each sampling zone during each cruise for each of the eight study areas.

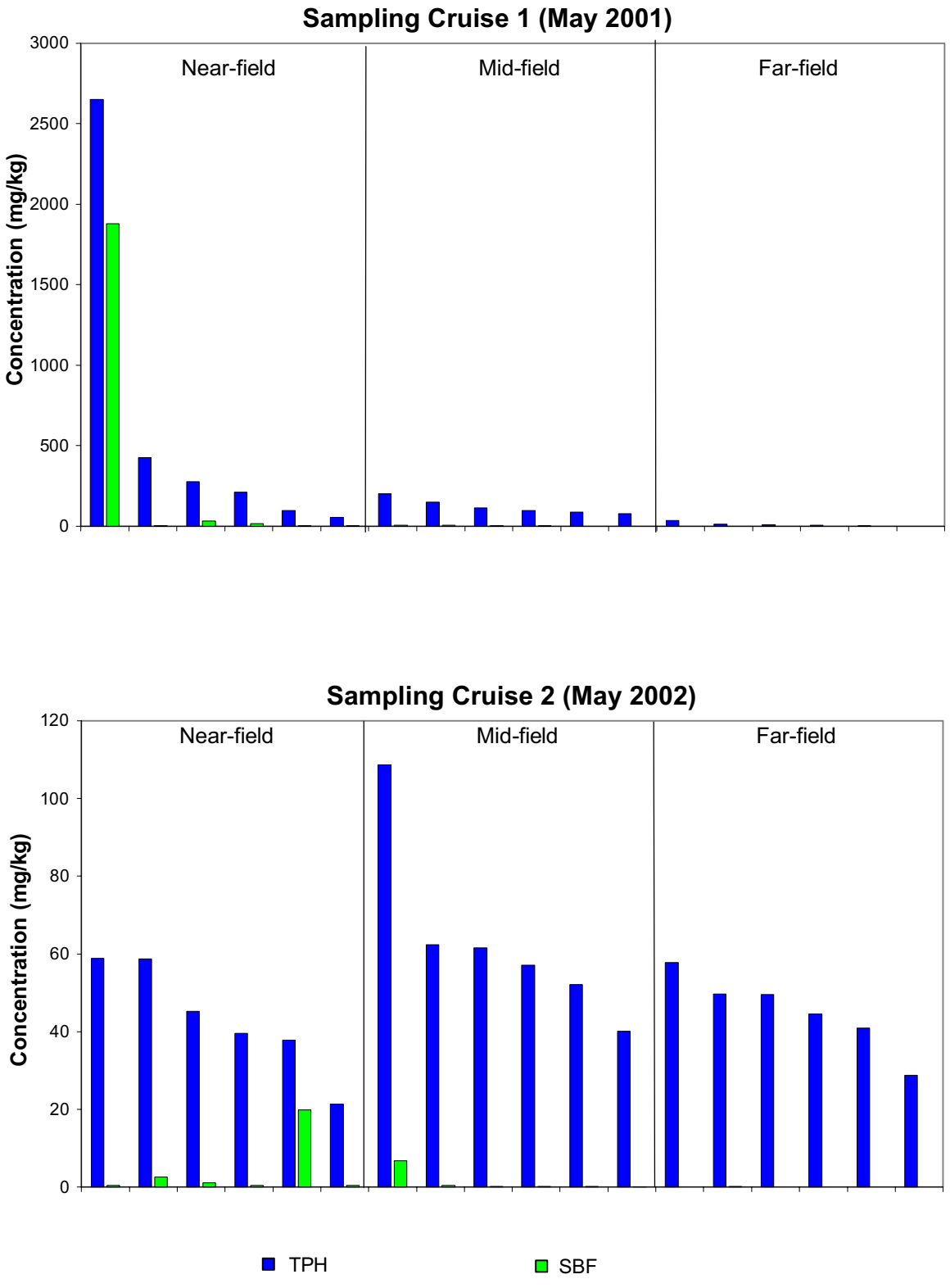

Figure 8-3. Distribution of total petroleum hydrocarbons (TPH) and synthetic based fluid (SBF) at Main Pass 299.

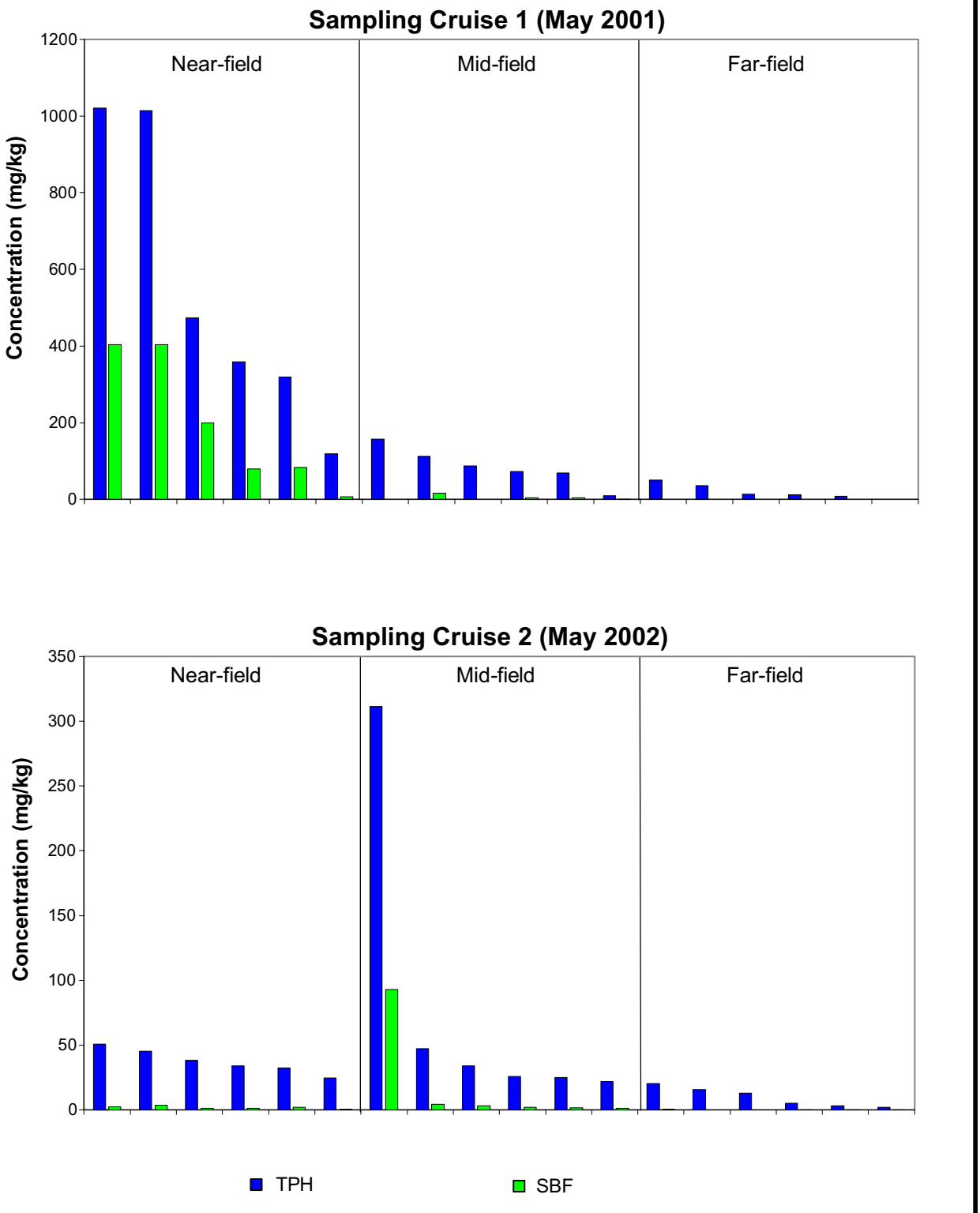

Figure 8-4. Distribution of total petroleum hydrocarbons (TPH) and synthetic based fluid (SBF) at Main Pass 288.

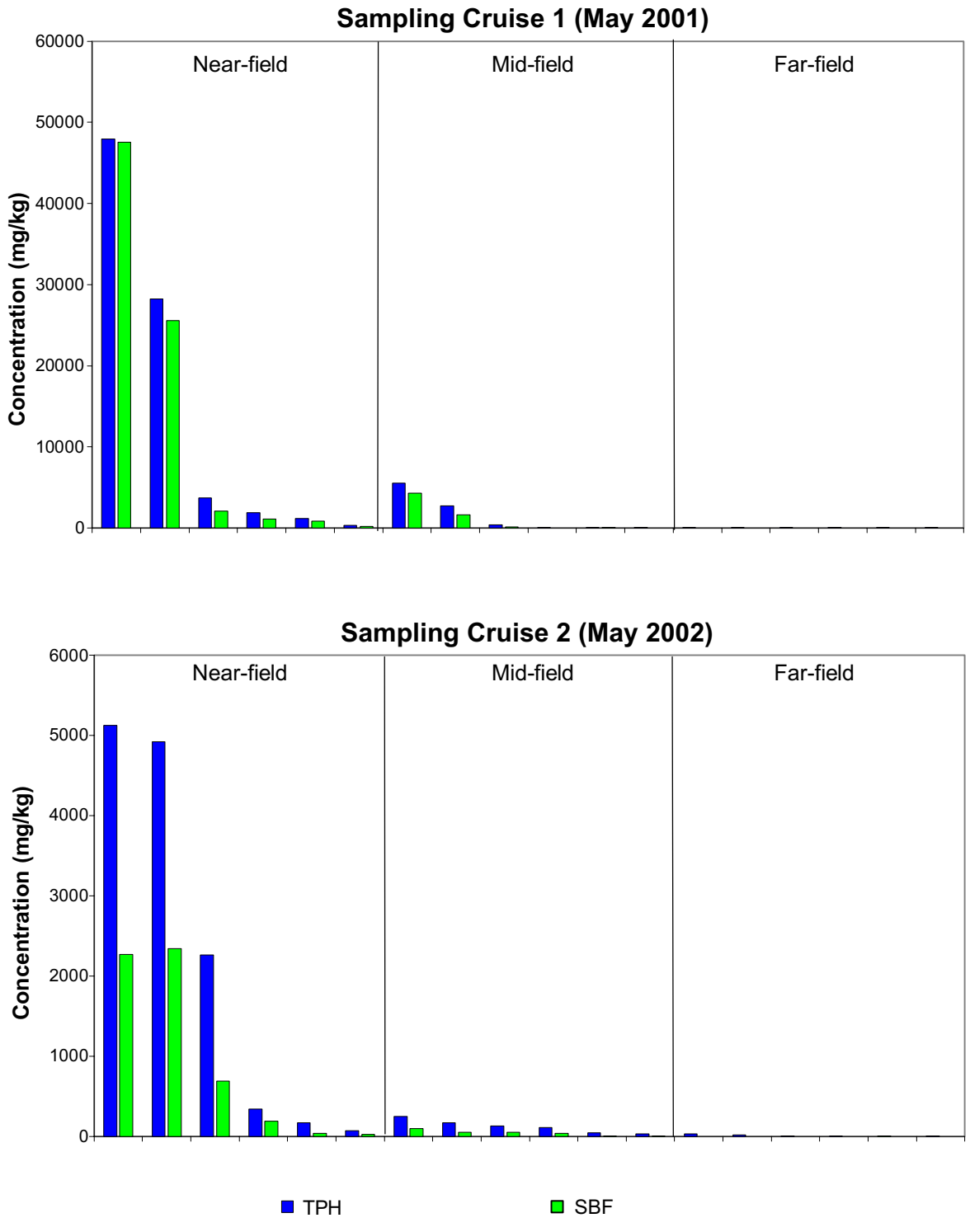

Figure 8-5. Distribution of total petroleum hydrocarbons (TPH) and synthetic based fluid (SBF) at Eugene Island 346.

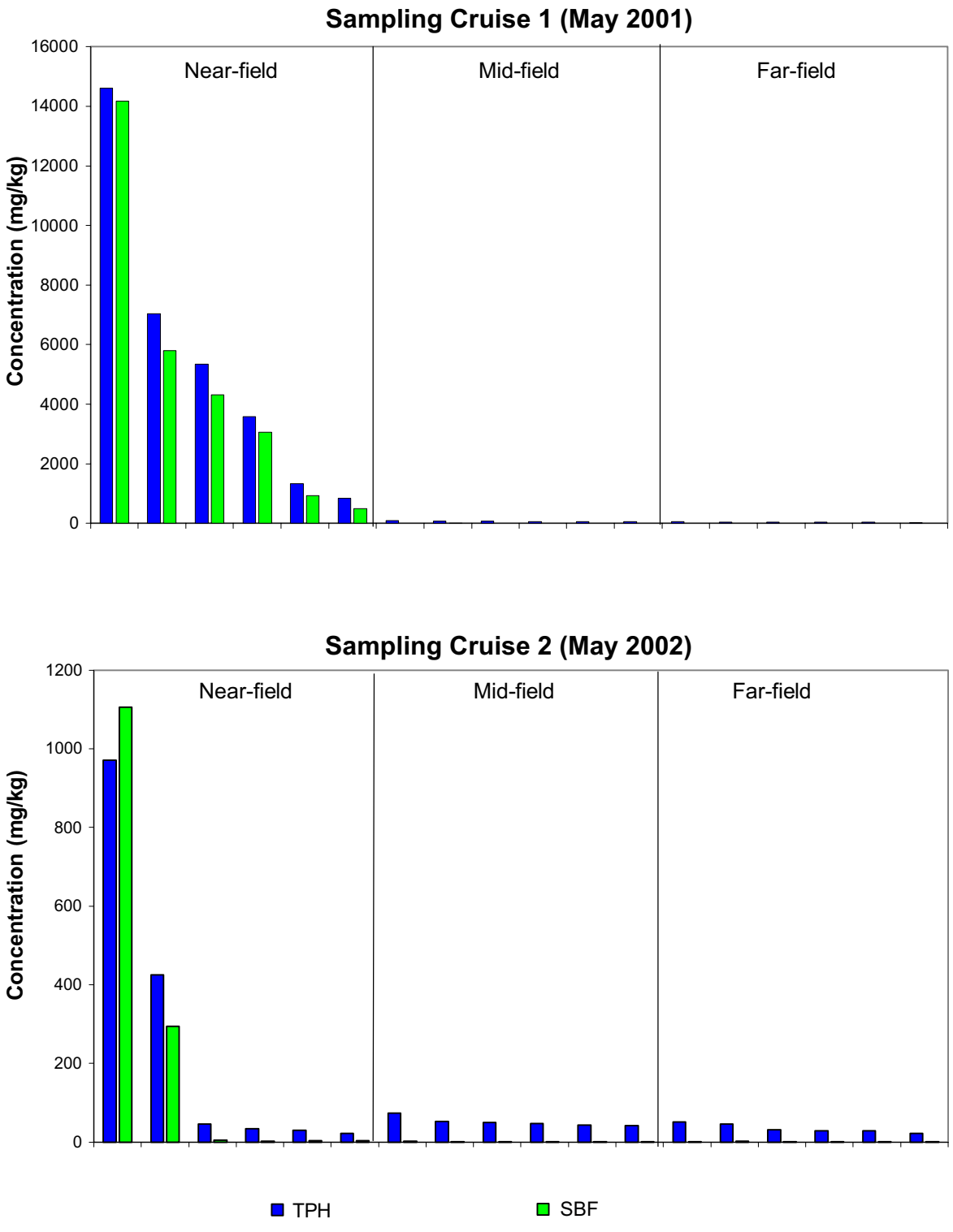

Figure 8-6. Distribution of total petroleum hydrocarbons (TPH) and synthetic based fluid (SBF) at South Timbalier 160.

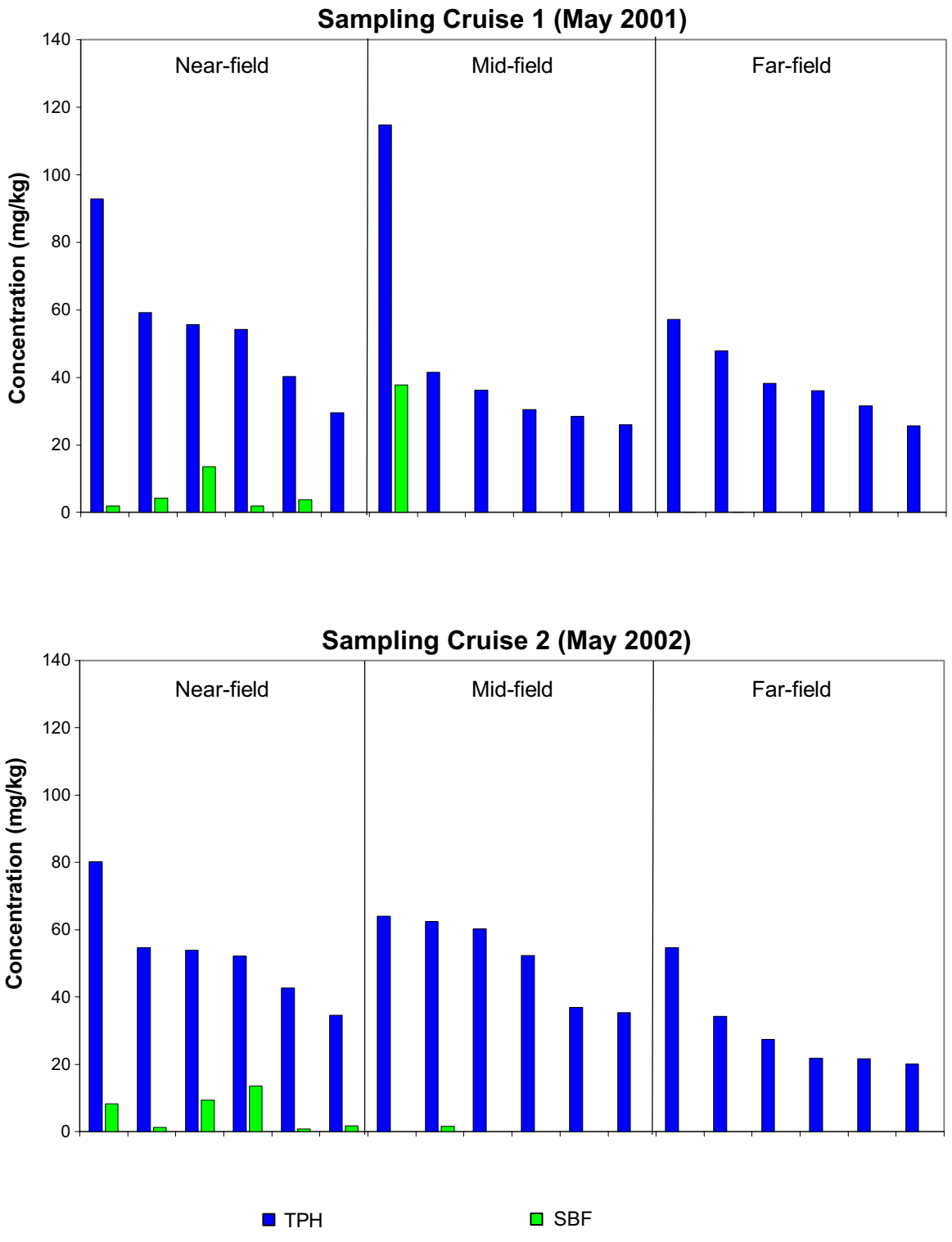

Figure 8-7. Distribution of total petroleum hydrocarbons (TPH) and synthetic based fluid (SBF) at Viosca Knoll 783.

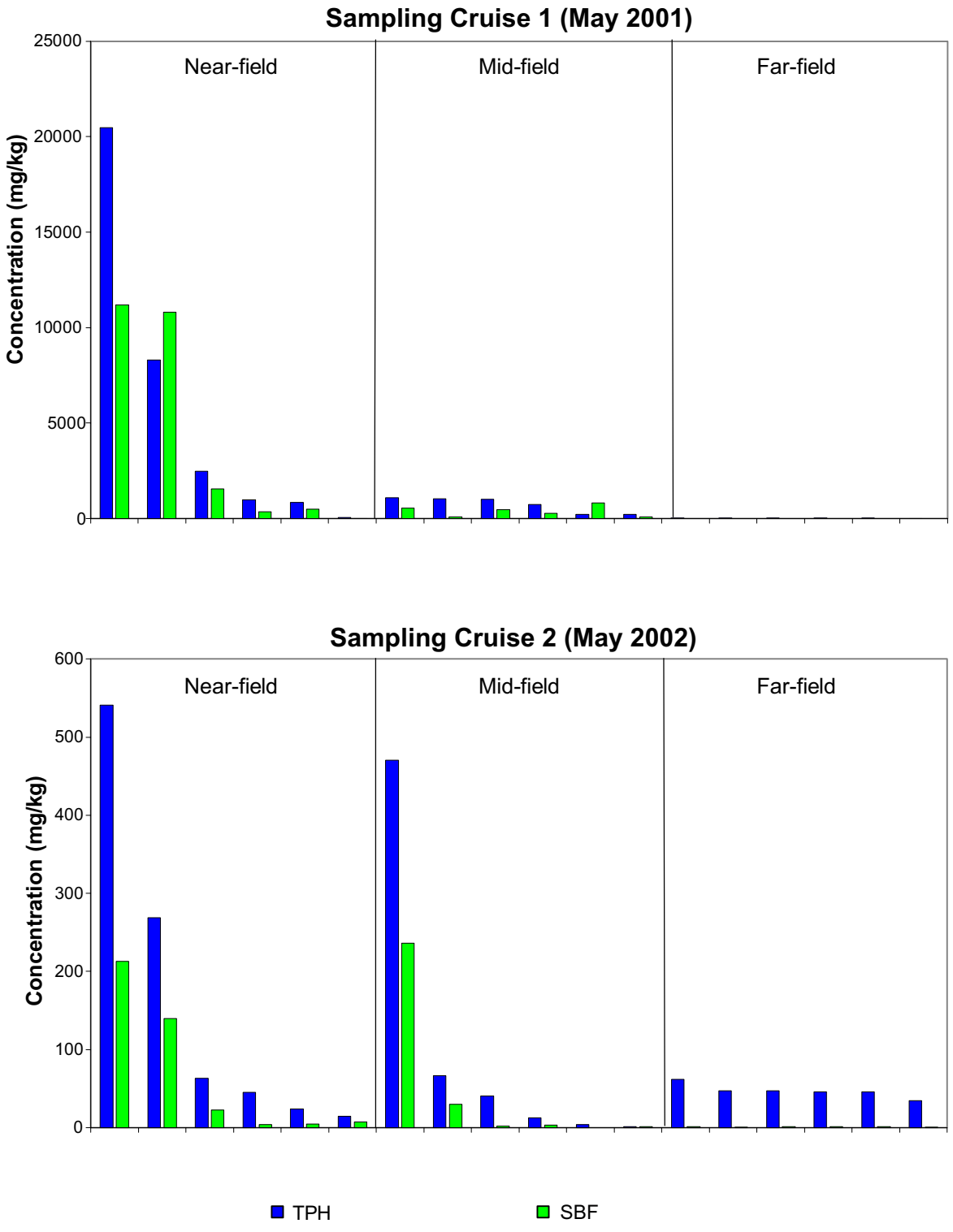

Figure 8-8. Distribution of total petroleum hydrocarbons (TPH) and synthetic based fluid (SBF) at Mississippi Canyon 496.

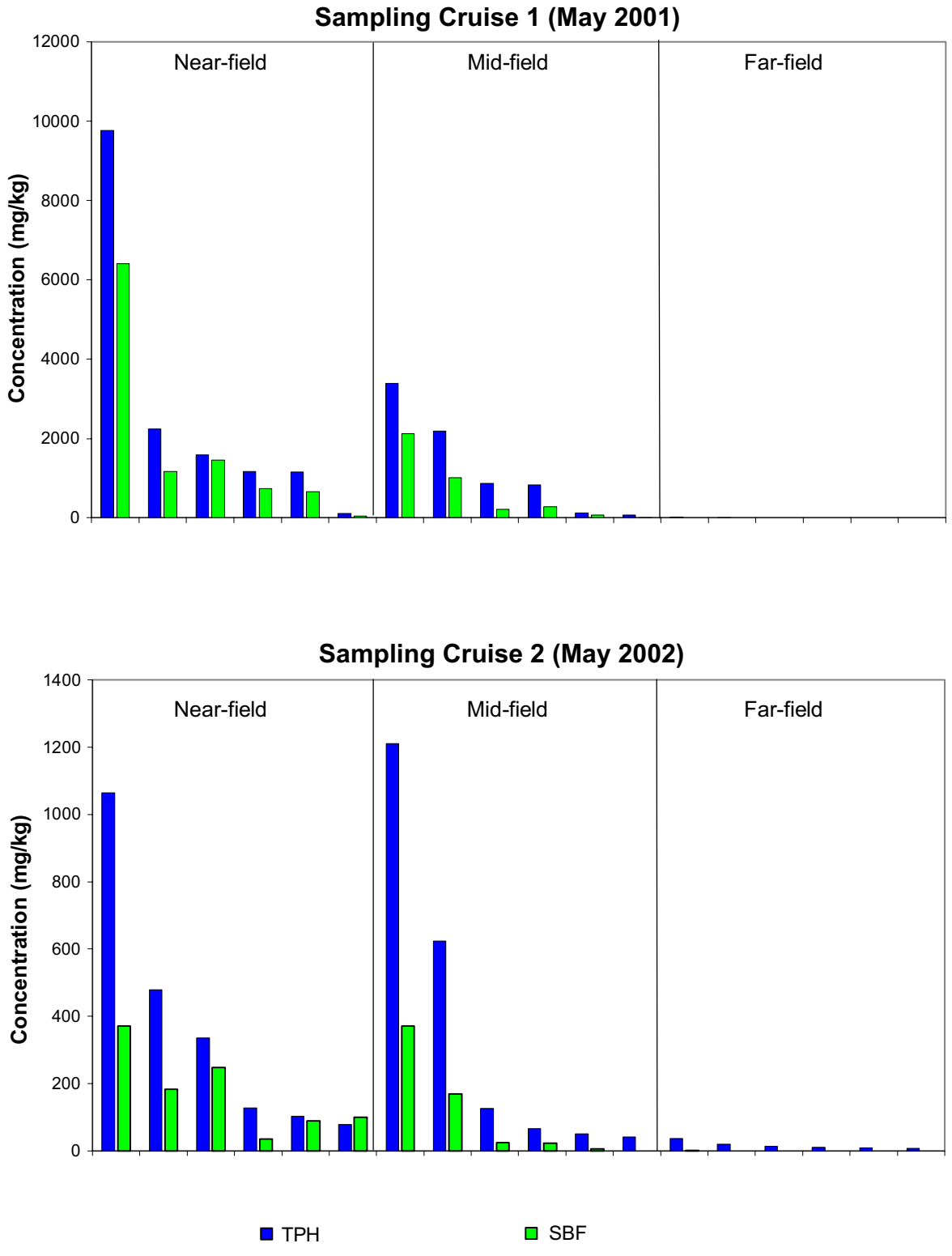

Figure 8-9. Distribution of total petroleum hydrocarbons (TPH) and synthetic based fluid (SBF) at Ewing Bank 963.

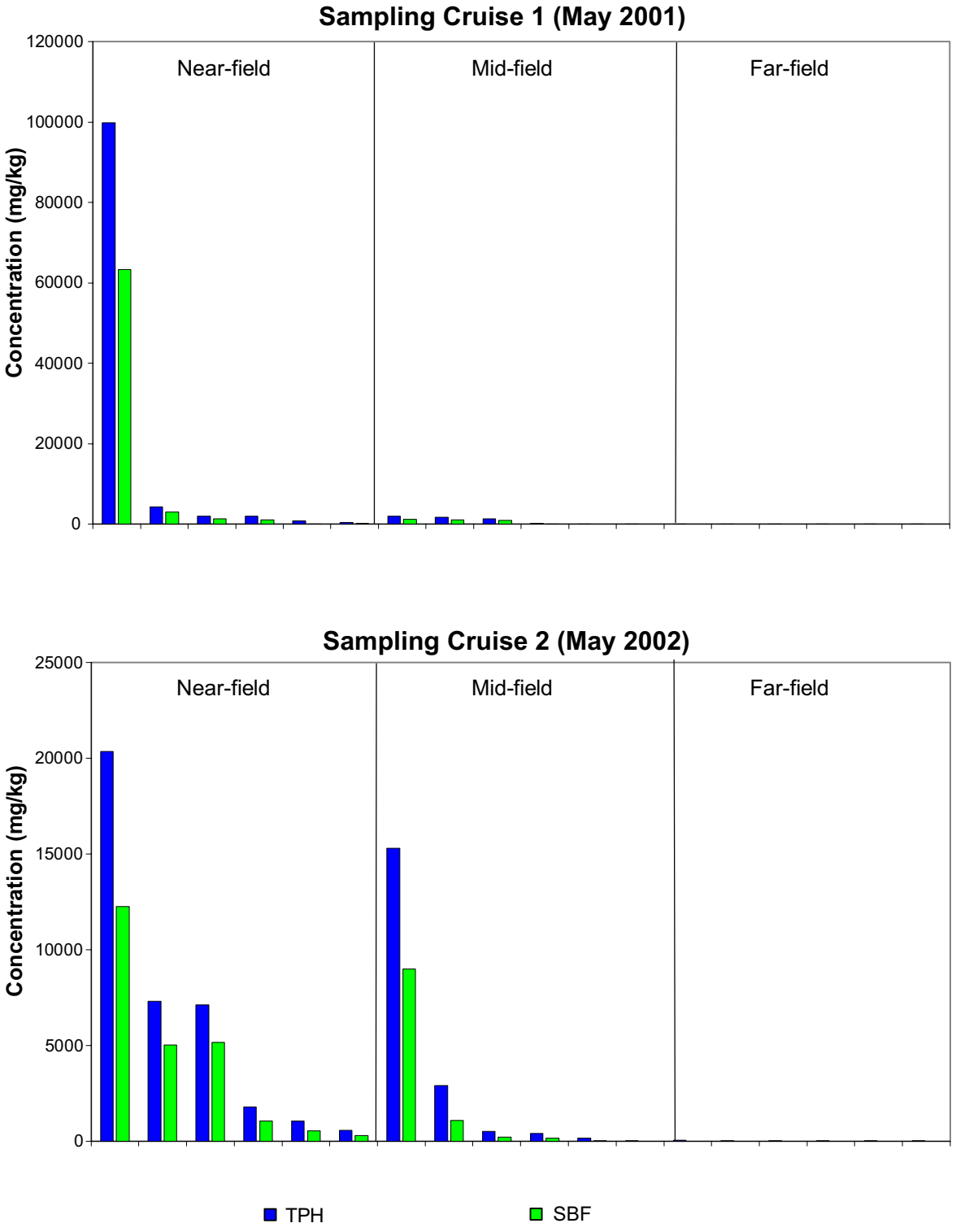

Figure 8-10. Distribution of total petroleum hydrocarbons (TPH) and synthetic based fluid (SBF) at Green Canyon 112.

8.3.1 Background Conditions at Far-field Sampling Areas

The data presented in Appendix D indicate that there is no evidence for systematic occurrence of SBF residues in the far-field surface sediments of the study sites. Between the two cruises, a total of 96 far-field samples was analyzed, yet only 5 far-field surficial sediment samples were found to contain measurable amounts of SBF residues. These five findings are all low level residues between 1 and 2.5 mg/kg SBF. The findings of low levels of SBF in far-field stations included one at the GC 112 study site (2 mg/kg at FF-5 during Sampling Cruise 1), two at MC 496 (1.1 mg/kg at both FF-1 and FF-2 during Sampling Cruise 2), and two at ST 160 (1.0 and 2.5 mg/kg at FF-2 and FF-1, respectively, during Sampling Cruise 2).

During Sampling Cruise 1, SBF residues were detected at GC 112 Station FF-5, which was selected for depth-discrete sampling. No SBF residues were detected in the first three sections of this core (surface, 0 to 2 cm, 4 to 6 cm); approximately 15 mg/kg of SBF were found in the 6 to 8 cm section and 4 mg/kg of SBF were found in the 8 to 10 cm section. The SBF concentration profile in this core is difficult to rationalize. This observation raises the possibility that these subcore sections might have been contaminated with low-level residues of SBF during sample handling and likely did not represent actual field conditions. Even in the face of this curious anomaly, the overall far-field data set from Sampling Cruises 1 and 2 indicate that these surficial sediments are excellent surrogates of background conditions in the study areas.

The “background” or ambient concentrations of TPH in surficial sediments of the far-field environs of both the continental shelf and continental slope study sites are low—less than 50 mg/kg (Table 8-5). In the absence of anthropogenic hydrocarbon inputs (for example, oil and gas operations), marine sediments in the Gulf of Mexico contain TOC at concentrations that span approximately 0.1% to 1% (Brownlow, 1979). Typically, only a portion of the total organic matter is extractable and measurable as TPH by GC. The 50 mg/kg of TPH measured in the “background” sediments is consistent with low TOC-burdened sediments. The background concentrations of TPH are generally consistent across the continental shelf and continental slope study sites.

Table 8-5. Total petroleum hydrocarbon (TPH) concentrations at far-field background stations.

Drillsite	Drillsite Type	Sampling Cruise 1 TPH (mg/kg)	Sampling Cruise 2 TPH (mg/kg)
Eugene Island 346	Continental Shelf	17	10
Main Pass 299	Continental Shelf	41	45
Main Pass 288	Continental Shelf	16	10
South Timbalier 160	Continental Shelf	41	35
Green Canyon 112	Continental Slope	33	28
Mississippi Canyon 496	Continental Slope	20	47
Ewing Bank 963	Continental Slope	5	16
Viosca Knoll 783	Continental Slope	39	30

8.3.2 Continental Shelf Study Sites

Wells at three of the four continental shelf study sites—MP 288, EI 346, and ST 160—were completed with IO SBMs. This trio of drillsites generally exhibits similar spatial patterns of TPH and SBF in sediment, particularly for Sampling Cruise 1 (Figures 8-4 through 8-6). For Sampling Cruise 1, SBF residues were found in all of the near-field surface sediments. Concentrations of SBF were below detection limits in 8 of 18 mid-field samples. The highest SBF concentrations were found in the near-field at all three of these sites. At these three study sites, TPH concentrations tracked with SBF concentrations but were generally higher than the corresponding SBF concentrations. The differences between measured SBF and TPH concentrations are discussed below. By Sampling Cruise 2, a similar pattern for SBF and TPH residues was evident, but the concentrations of both these analytes had diminished substantially. For example, TPH and SBF concentrations for near-field sediments at EI 346 dropped from about 48,000 mg/kg to about 2,000 to 5,000 mg/kg. A similar diminution in SBF and TPH concentrations between the two cruises was seen for MP 288 and ST 160.

The most likely reason that TPH concentrations were greater than corresponding SBF concentrations in these samples is the fact that there are subtle but noticeable differences in the makeup of the SBF residues found in the sediments versus those used for the analytical instrument calibration standard (see Section 8.2.1). C_{20} isomers arising from certain formulations of IO drilling fluid (but not present in the instrument calibration standards used in this study) are clearly visible in the majority of field sediments taken from platforms drilled with IO fluid. These synthetic C_{20} isomers contributed to the measured TPH (even though they actually are SBF components). Figure 8-11 shows a representative example of a gas chromatogram of a field sample that exhibits these features—in this case, a sediment from the near-field of EI 346. Here, the C_{20} synthetic isomers are clearly evident in the gas chromatogram.

Another likely contributor to excess TPH versus SBF is the presence of naturally occurring hydrocarbons that are present outside the chromatographic window of the SBF, such as those found in the background (reference) sediment samples. In fact, naturally occurring hydrocarbons consistent with background can be seen in the gas chromatogram shown in Figure 8-11. In this example, the presence of both the C_{20} synthetic isomers and the naturally occurring hydrocarbons result in a TPH concentration measurably higher than the corresponding SBF concentration.

Another possible reason why TPH concentrations could have been higher than SBF in field sediments—the presence of crude or refined petroleum residues—was discounted because there was no chromatographic evidence for crude or refined petroleum in any of the sediments collected in this study.

Main Pass 299 was drilled with an LAO mud. During Sampling Cruise 1, elevated TPH and LAO was detected in near-field and mid-field stations; by Sampling Cruise 2, TPH concentrations in the near-field and mid-field essentially reached background concentrations. During Sampling Cruise 2, SBF concentrations were much lower than measured in Sampling Cruise 1. For example, the highest concentration of SBF during Sampling Cruise 1 was 1,879 mg/kg (Station NF-6); during Sampling Cruise 2, the highest SBF concentration was about 20 mg/kg (Station NF-3).

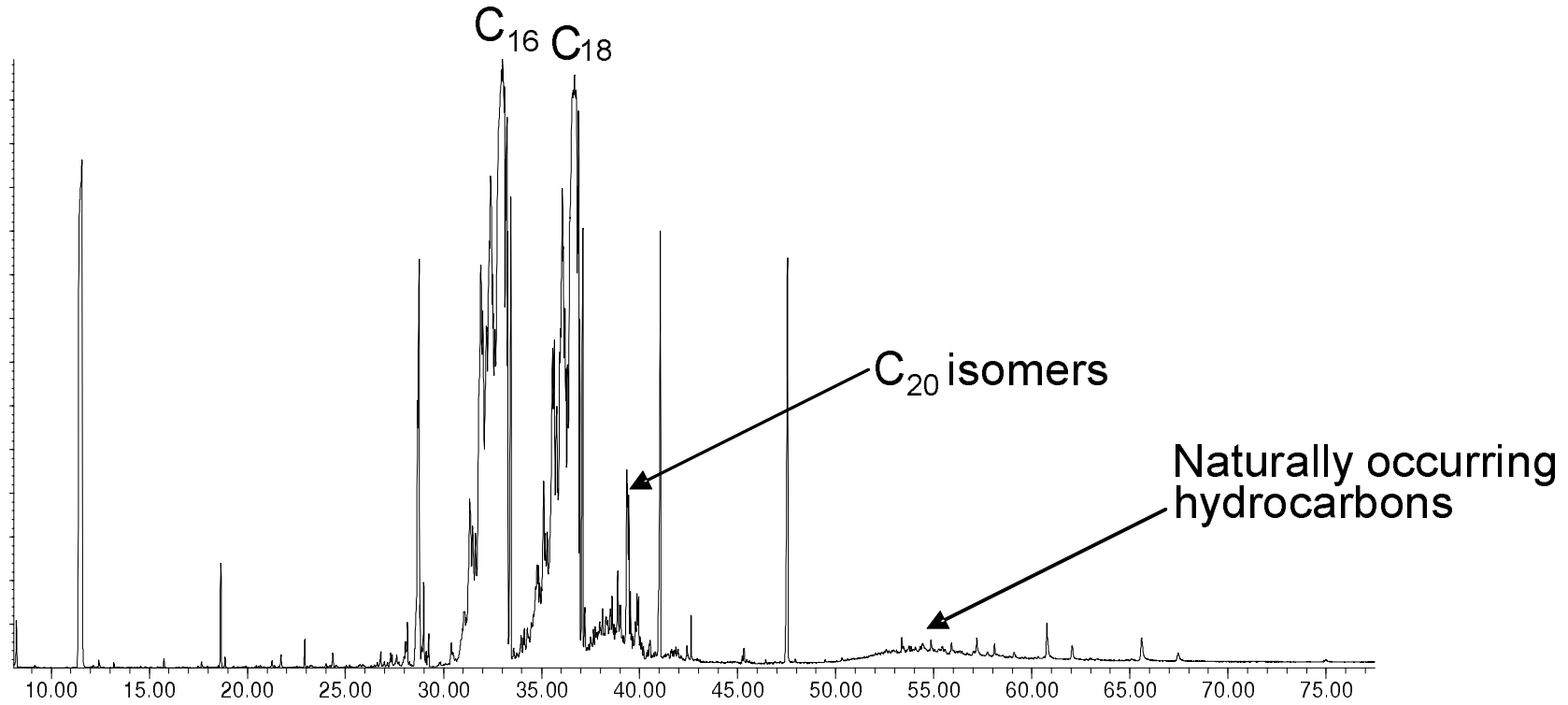

Figure 8-11. Representative gas chromatogram of typical sediment sample from this study showing evidence for C_{20} synthetic olefin isomers and naturally occurring hydrocarbons, both classes of which contribute to excess total petroleum hydrocarbons relative to synthetic based fluid concentrations. (Sample from near-field Station 5, Eugene Island 346).

There was a strong relationship between concentrations of SBF and TPH at each of the four continental shelf study sites (Table 8-6). Therefore, further statistical analysis was conducted on only the SBF concentrations. Concentrations of SBF were statistically analyzed using a linear model approach to determine if concentrations at the continental shelf study sites and continental slope study sites varied between the two cruises and/or among the three zones (near-field, mid-field, and far-field).

Table 8-6. Correlation between synthetic based fluid and total petroleum hydrocarbon concentrations at the continental shelf study sites.

Study Site	Spearman's ρ	Probability
Eugene Island 346	0.95	$p<0.0001$, Significant
Main Pass 288	0.71	$p<0.0001$, Significant
Main Pass 299	0.73	$p<0.0001$, Significant
South Timbalier 160	0.47	$p<0.0004$, Significant

The initial step in the analysis of variance of the continental shelf study sites was to test for interactions between cruises and zones, which was done using randomization methodology. Because the SBF concentrations varied over multiple orders of magnitude, the response variable for the analyses was the logarithmic transformation (base 10) of the SBF concentration.

The analysis of variance revealed significant interactions ($p<0.05$) for EI 346, MP 288, and ST 160. To examine these interactions in more detail, specific Bonferroni comparisons were made for each of the three study sites where a significant interaction was observed:

- Sampling Cruise 1, far-field vs. Sampling Cruise 2, far-field;
- Sampling Cruise 1, mid-field vs. Sampling Cruise 2, mid-field;
- Sampling Cruise 1, near-field vs. Sampling Cruise 2, near-field;
- Sampling Cruise 1, far-field vs. Sampling Cruise 1, mid-field;
- Sampling Cruise 1, far-field vs. Sampling Cruise 1, near-field;
- Sampling Cruise 1, mid-field vs. Sampling Cruise 1, near-field;
- Sampling Cruise 2, far-field vs. Sampling Cruise 2, mid-field;
- Sampling Cruise 2, far-field vs. Sampling Cruise 2, near-field; and
- Sampling Cruise 2, mid-field vs. Sampling Cruise 2, near-field.

The significant differences identified by the Bonferroni analysis are summarized and presented in Tables 8-7 and 8-8. These results indicated that SBM cuttings occur in very close proximity to the discharge point, i.e., mean SBF concentrations in the near-field were significantly greater than those in the far-field and/or mid-field. At ST 160, there was clear evidence of recovery in the near-field (Figure 8-6).

Table 8-7. Summary of the Bonferroni analyses to examine interactions between zones for each of the two Sampling Cruises. An arrow indicates that the Bonferroni comparison detected a significant difference between the mean concentrations of the two zones, and the direction of the arrow indicates the zone with the greater mean concentration. An "=" sign indicates that the Bonferroni comparison did not detect a statistically significant difference.

Eugene Island 346		
Sampling Cruise 1	Mid-field	Far-field
Near-field	=	←
Mid-field		←
Sampling Cruise 2	Mid-field	Far-field
Near-field	=	←
Mid-field		←
South Timbalier 160		
Sampling Cruise 1	Mid-field	Far-field
Near-field	←	←
Mid-field		←
Sampling Cruise 2	Mid-field	Far-field
Near-field	=	←
Mid-field		=
Main Pass 288		
Sampling Cruise 1	Mid-field	Far-field
Near-field	←	←
Mid-field		=
Sampling Cruise 2	Mid-field	Far-field
Near-field	=	←
Mid-field		←

Table 8-8. Summary of the Bonferroni analyses to examine interactions between the two Sampling Cruises for each of the zones. The "<" and ">" signs indicate that the Bonferroni comparison detected one Sampling Cruise mean was statistically greater than the other. An "=" sign indicates that the Bonferroni comparison did not detect a statistically significant difference.

Study Site	Near-field	Mid-field	Far-field
Eugene Island 346	SC1=SC2	SC1=SC2	SC1<SC2
South Timbalier 160	SC1>SC2	SC1<SC2	SC1<SC2
Main Pass 288	SC1>SC2	SC1=SC2	SC1=SC2

SC1 = Sampling Cruise 1.
SC2 = Sampling Cruise 2.

For the study site where interactions between cruises and zones were not detected, a two-way analysis of variance was conducted. A significant difference between the two cruises was detected at MP 299. The mean SBF concentration for the second cruise was lower than the mean concentration for the first cruise, a result that may indicate recovery at this site.

The analysis detected significant ($p<0.05$) differences among the zones at MP 299. To examine these differences, Bonferroni comparisons were made:

- far-field vs. mid-field;
- far-field vs. near-field; and
- mid-field vs. near-field.

The results of this analysis are presented in Table 8-9. These results also indicated that SBM cuttings settle in close proximity to the discharge point at this continental shelf site. Overall, the statistical results indicated that deposition of SBM discharges occurred in the near vicinity of the discharge location and that recovery occurred between the two Sampling Cruises.

Table 8-9. Significant differences identified by the Bonferroni analysis to examine differences between synthetic based mud concentrations at Main Pass 299.

Study Site	Significant Bonferroni Comparison
Main Pass 299	far-field < mid-field
	far-field < near-field

In addition to surface samples, sediment core samples were obtained at selected study sites. At each drillsite, a core was taken from a different location during Sampling Cruises 1 and 2. The concentration versus depth profiles for SBF measured in cores from EI 346, MP 299, MP 288, and ST 160 are shown in Figure 8-12. While direct comparisons among cores from different drillsites or between cores from the same drillsite taken on different cruises cannot be performed, a general depth pattern is shared among the cores. Not surprisingly, higher concentrations of SBF are noted at or near the surface, with lower concentrations measured with depth. This observation suggests that some SBF residues are being either buried or physically mixed with underlying subsurface sediment. The shapes and slopes of these SBF concentration profiles varied from drillsite to drillsite—probably a reflection of the dynamics of mixing of the cuttings with bottom sediments as the drill cuttings fall to the seabed floor.

8.3.3 Continental Slope Study Sites

Three of the four continental slope study sites, MC 496, EW 963, and GC 112, were drilled with an IO synthetic based drilling mud. It is notable that the general trends in spatial distribution of TPH and SBF were quite similar among these sites, even between Sampling Cruises 1 and 2 (Figures 8-8 through 8-10). With the exception of one sample (MF-4, Sampling Cruise 2, EW 963), the highest SBF and TPH concentrations at all three sites were found in the near-field. Concentrations of SBF in mid-field samples were detectable but generally lower than those in the near-field. At all three of these sites, when SBF residues were found, the corresponding TPH concentrations were higher. As noted above in Section 8.3.2, this observation was attributed to inherent compositional differences between the IO formulation used to drill the wells and the IO fluid used as an analytical instrument calibration standard, as well as

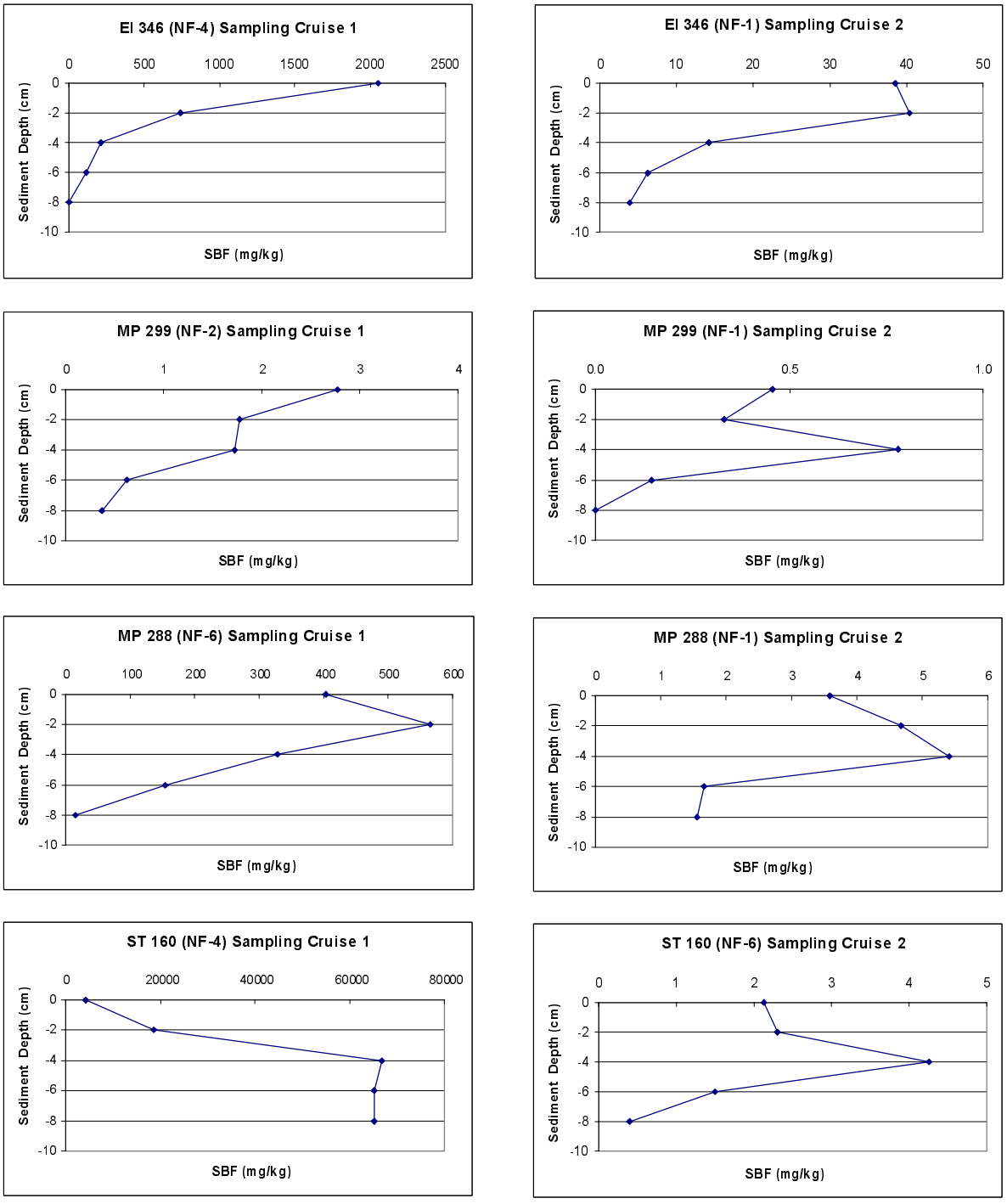

Figure 8-12. Synthetic based fluid (SBF) concentration profiles for cores from continental shelf study sites.

to the presence of naturally occurring hydrocarbons. The presence of C_{20} synthetic isomers in the field samples (unaccounted for by the analytical reference standard) plus any naturally occurring hydrocarbons outside of the SBF molecular weight range lead to a positive bias between the ratio of TPH and SBF measured in affected sediments. As with the continental shelf sediment samples, there was no chromatographic evidence for the presence of crude or refined petroleum that could have led to the somewhat greater relative TPH to SBF concentrations.

The TPH and SBF concentrations were found to decrease at each drillsite between Sampling Cruise 1 and Sampling Cruise 2 in a manner similar to that observed for the continental shelf study sites.

Viosca Knoll 783 was drilled with an ester SBF. During Sampling Cruises 1 and 2, the chemical signature for the ester SBF was found in several of the near-field and one of the mid-field stations at VK 783, but only at low level concentrations, literally near the background level of TPH. A number of hypotheses may explain this observation, including 1) the drill cuttings for this fluid did not migrate far enough from the discharge area to be found in the near- or mid-field stations sampled for this program, or 2) the cuttings fell to the seafloor in non-homogenous "clumps," and were not encountered during sampling, or 3) the fluid residues exhibited *in situ* degradation prior to sampling.

There was a strong relationship between concentrations of SBF and TPH at each of the four continental slope study sites (Table 8-10). Therefore, further statistical analysis was conducted on only the SBF concentrations. Concentrations of SBF were statistically analyzed using a linear model approach to determine if concentrations at the continental shelf study sites and continental slope study sites varied between the two cruises and/or among the three zones (near-field, mid-field, and far-field).

Table 8-10. Correlation between synthetic based fluid and total petroleum hydrocarbon concentrations at the continental slope study sites.

Study Site	Spearman's ρ	Probability
Viosca Knoll 783	0.63	$p<0.0001$, Significant
Ewing Bank 963	0.97	$p<0.0001$, Significant
Green Canyon 112	0.92	$p<0.0001$, Significant
Mississippi Canyon 496	0.86	$p<0.0001$, Significant

Statistical analysis of the logarithmic transformed SBF concentrations revealed significant interaction between cruises and zones at MC 496. Significant differences identified by the Bonferroni comparisons to examine this significant interaction were

- Sampling Cruise 1, far-field > Sampling Cruise 2, far-field;
- Sampling Cruise 1, far-field < Sampling Cruise 1, mid-field;
- Sampling Cruise 1, far-field < Sampling Cruise 1, near-field; and
- Sampling Cruise 2, far-field < Sampling Cruise 2, near-field.

These results indicated that the occurrence of SBM cuttings at this continental slope study site was restricted to close proximity to the discharge point.

If there was no interaction between cruises and zones at a site (EW 963, GC 112, and VK 783), a two-way analysis of variance was conducted. A significant difference between the two cruises was detected at EW 963. The mean SBF concentration at EW 963 for Sampling Cruise 2 was lower than the mean concentration for Sampling Cruise 1, a result that suggests recovery at this site.

The analysis detected significant ($p<0.05$) differences among the zones at EW 963, GC 112, and VK 783. To investigate the differences among the three zones, pairwise Bonferroni comparisons (near-field to mid-field, near-field to far-field, mid-field to far-field) were made. The results of the Bonferroni comparisons are presented in Table 8-11. These results also indicated that SBM cuttings settle in close proximity to the discharge point at these continental slope study sites.

Table 8-11. Significant differences identified by the Bonferroni analysis to examine differences in mean synthetic based fluid concentration between zones at Ewing Bank 963, Green Canyon 112, and Viosca Knoll 783. Data are from the two Sampling Cruises.

Study Site	Significant Bonferroni Comparison
Ewing Bank 963	far-field < mid-field
	far-field < near-field
Green Canyon 112	far-field < mid-field
	far-field < near-field
Viosca Knoll 783	far-field < near-field
	mid-field < near-field

Core samples from three continental slope study sites contained sufficient hydrocarbons to assess trends in SBF concentration with depth (Figure 8-13). These cores exhibited similar trends in decreasing SBF concentrations with depth, as was noted for the continental shelf cores. Again, the shape and slopes of these SBF concentration-depth profiles varied from drillsite to drillsite—probably a reflection of the dynamics of mixing of the cuttings with bottom sediments as the drill cuttings fall to the seabed floor.

8.4 CONCLUSIONS

Concentrations of TPH and SBF were measured in sediments from the vicinity of four continental shelf and four continental slope study sites in the Gulf of Mexico during two cruises (Sampling Cruise 1 and Sampling Cruise 2) separated in time by 1 year (May 2001 and May 2002). Surficial sediment samples (and a select few depth-discrete samples) were collected from six stations in the near-field (within 100 m), six stations in the mid-field (100 to 250 m), and six stations in the far-field (3,000 to 6,000 m) zones of the drillsites in order to determine the spatial distribution and behavior of SBM cuttings at these sites.

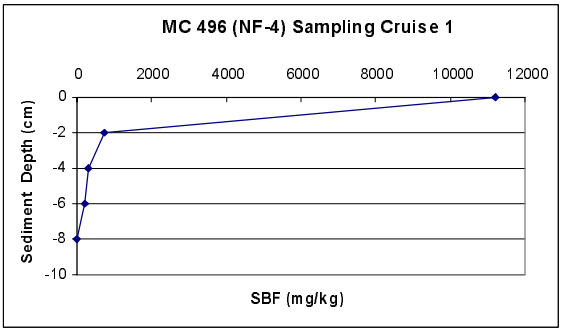

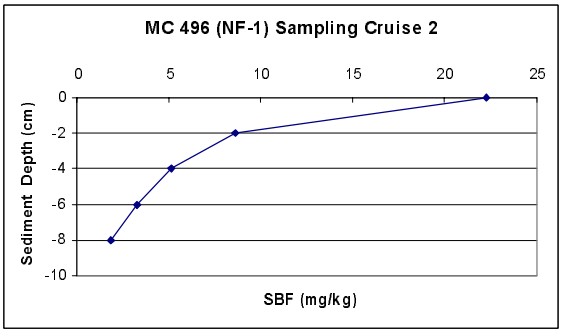

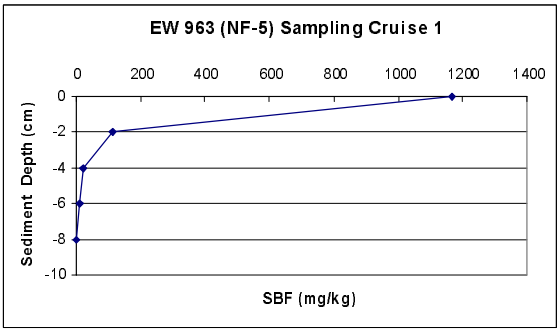

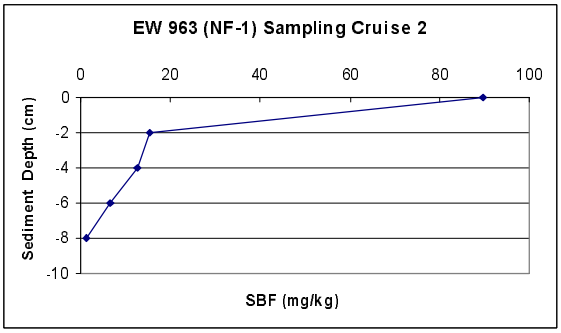

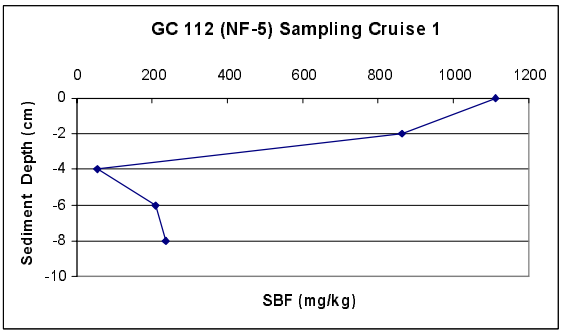

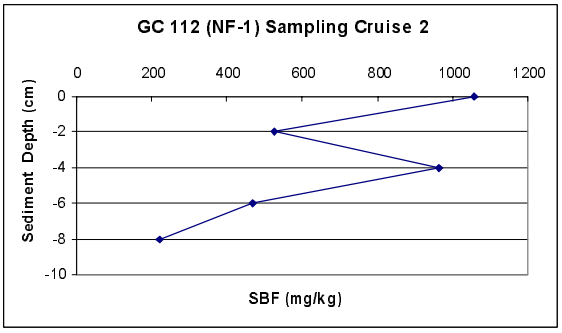

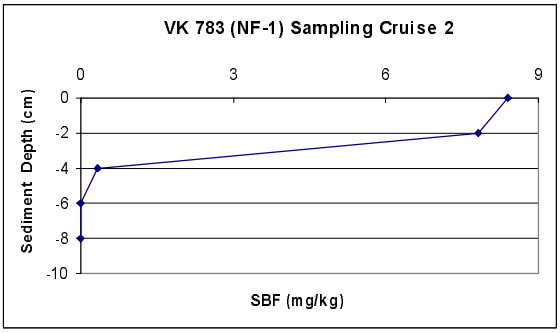

Figure 8-13. Synthetic based fluid (SBF) concentration profiles for cores from continental slope study sites.

There were striking similarities in the spatial distributions of SBF and TPH residues in sediments among the continental shelf and continental slope study sites found for both Sampling Cruises. As a general observation, SBF residues were found at the highest concentrations and greatest frequency in near-field sediment zones. Less frequent findings and lower concentrations of SBF were found in mid-field zone sediments. At study sites where substantial concentrations of SBF were observed in the near-field during Sampling Cruise 1, concentrations were up to an order of magnitude lower during Sampling Cruise 2. This strongly suggested ongoing recovery in the near-field sediments at these sites.

Only sporadic, low-level detections (<5 mg/kg) of SBF residues were found in the continental shelf or continental slope far-field surface sediment stations, demonstrating that the impressions of SBM cuttings are limited to sediments in close proximity to drillsites. This observation points to the utility of far-field stations as suitable reference stations for studies of the chemical and biological impacts of SBM cuttings to both shallow and deepwater benthic environments.

Chapter 9
METALS AND REDOX CHEMISTRY IN SEDIMENTS

John H. Trefry, Robert P. Trocine, Robert D. Rember, and Michelle L. McElvaine
Florida Institute of Technology

9.1 INTRODUCTION

The metals and redox program for sediments was designed to help identify spatial and temporal trends in 1) the presence of drilling discharges and 2) redox conditions in sediments at each site. Concentrations of indicator metals (Al, Ba, Fe, and Mn) and TOC were determined for surface sediments (0-2 cm) and for sediment cores from the primary sites during Sampling Cruise 1 (May 2001) and Sampling Cruise 2 (May 2002). In addition, concentrations of As, Cd, Cr, Cu, Hg, Ni, Pb, V, and Zn were determined for a subset of the surface and subsurface sediment samples from the Screening Cruise (July 2000). Vertical profiles for DO and Eh were determined for >90% of the stations during Sampling Cruises 1 and 2. Pore water was collected from six near-field and six far-field stations from Sampling Cruises 1 and 2, such that each of the six primary sites was sampled at one near-field and one far-field station during each of the two cruises.

The four indicator metals investigated throughout the study (Al, Ba, Fe, and Mn) provide insight to sediment composition, the presence of drilling discharges, and sediment redox conditions. Aluminum is a good indicator of the relative abundance of clay minerals and other aluminosilicates. Concentrations of Ba help identify the presence of drilling discharges because barite ($BaSO_4$) is a common component of drilling fluids. Elevated levels of Ba in sediments, in the absence of SBFs, help support the presence of WBMs. Concentrations of Fe generally correlate well with concentrations of Al and support identification of the terrigenous fraction of sediment. Manganese is a redox-sensitive metal that can be depleted in nearshore reducing sediment relative to Mississippi River suspended sediment and is greatly enriched in slowly accumulating and oxidizing slope sediment relative to river suspended sediment (Trefry and Presley, 1982). Concentrations of TOC vary with sediment accumulation rate and biological productivity in the overlying water column. The rate of accumulation of organic carbon helps control the redox state of the sediment.

Concentrations of DO in sediment and the overall Eh of the sediment column are primarily controlled by the input rate of organic matter as influenced by the following factors: 1) biological productivity in the surface water and benthic environment, 2) the rate at which terrestrial organic matter is added via rivers, and/or 3) introduction of organic matter from discharges of various municipal and industrial waste materials. Changes in redox environment at the sediment-water interface and in the upper layers of the sediment column can play a role in controlling the spatial distribution of benthic fauna. Hydrocarbons that can be metabolized by sediment bacteria are contained in SBFs. The presence of this additional source of sediment organic matter may alter the background redox environment.

In this chapter, the results for metals and TOC are presented first. This information helps to define the sediment composition at near-field (<100 m from drilling site) and mid-field (100 to 250 m from drilling site) locations relative to background sediments at far-field (3,000 to 6,000 m from drilling site) locations. Then, results for vertical profiles for DO and Eh in sediment cores (and pH in some cores) will be introduced along with limited data for sediment pore water. The collective data will be used to test for significant differences in sediment composition and properties 1) between sites containing SBF and background locations and 2) between Sampling

Cruises 1 and 2. The continental shelf sites (MP 299, MP 288, and EI 346) are discussed separately from sites on the continental slope (MC 496, EW 963, and GC 112) because of inherent, natural differences in sediment composition and redox conditions between the shelf and slope environments, as discussed later in this chapter.

9.2 METHODS

9.2.1 Sampling and Field Measurements

Sediments were collected from the Gulf of Mexico using a stainless steel box corer (50 cm x 50 cm x 50 cm) as described in Chapter 3. For metals, the surface 2 cm of sediment were removed using a Teflon® spatula and placed in a plastic vial. The vial was sealed with a layer of Parafilm® and stored frozen. At 12 stations during each cruise, the box core was carefully subsampled by pushing a Teflon® tube into the sediment. The sediment was extruded from the top, and 2-cm sections were sliced off, placed in plastic vials, and stored frozen.

One subsample from each box core was collected for probe measurements of DO and Eh. Values for pH were determined in selected cores on Sampling Cruise 1 as time permitted. Each core was immediately analyzed for oxygen using a 5-cm long microprobe (Microelectrodes, Inc. MI-730 O_2 probe, Figure 9-1) lowered from the top of the core. The probe was mounted on a microscope stage that was fixed vertically above the core. By lowering the microscope stage in millimeter increments, oxygen measurements were taken to the depth of oxygen depletion. Next, Eh and pH were measured through holes pre-drilled at 2-cm intervals in the wall of the core tube. The holes were covered with tape during sampling, and the tape was removed immediately before inserting a probe. The Eh was measured first (Orion Model 96-78-00 Platinum Redox Electrode, Figure 9-1), and pH and temperature measurements followed (Sentron Red Line pH probe).

All probes were calibrated prior to use for each core. The oxygen probe was calibrated using two beakers of water, one that was equilibrated with the atmosphere using an air stone and one that was deoxygenated by purging with nitrogen. The oxygen meter was adjusted to 20.9% while the probe was immersed in the first solution and was zeroed with the probe submerged in deoxygenated water. A one-point calibration with an Orion redox standard was performed for the Eh probe. The pH probe was calibrated with pH 7 and 10 buffers.

9.2.2 Pore Water Collection and Analysis

To obtain pore water, a 7-cm diameter subcore was transferred to a whole core squeezer similar to that described by Bender et al. (1987) for pore water extraction (Figure 9-1). By raising the lower piston to apply pressure to the core, 16 pore water samples were simultaneously collected from depths of 0 to 34 cm. Samples were collected directly into acid-washed glass syringes at 1-cm intervals in the uppermost 5 cm, 2-cm intervals from 5 to 13 cm, and 3-cm intervals below 13 cm. At the completion of pore water collection, samples were filtered through Type A/E glass fiber filters and divided for analysis. A 1-mL portion was diluted five-fold and analyzed for phosphate using the ascorbic acid method (Clesceri et al., 1989). A 0.5-mL portion was diluted four-fold and analyzed for ammonia using the oxidation method (Matsunaga and Nishimura, 1974). All colorimetric analyses performed aboard ship were carried out within 24 hours of sample collection using a Spectronic Instruments Spec 20 Genysis. The remainder of each pore water sample was divided into three portions (frozen, acidified, and unaltered) for further analysis at the Florida Institute of Technology (FIT).

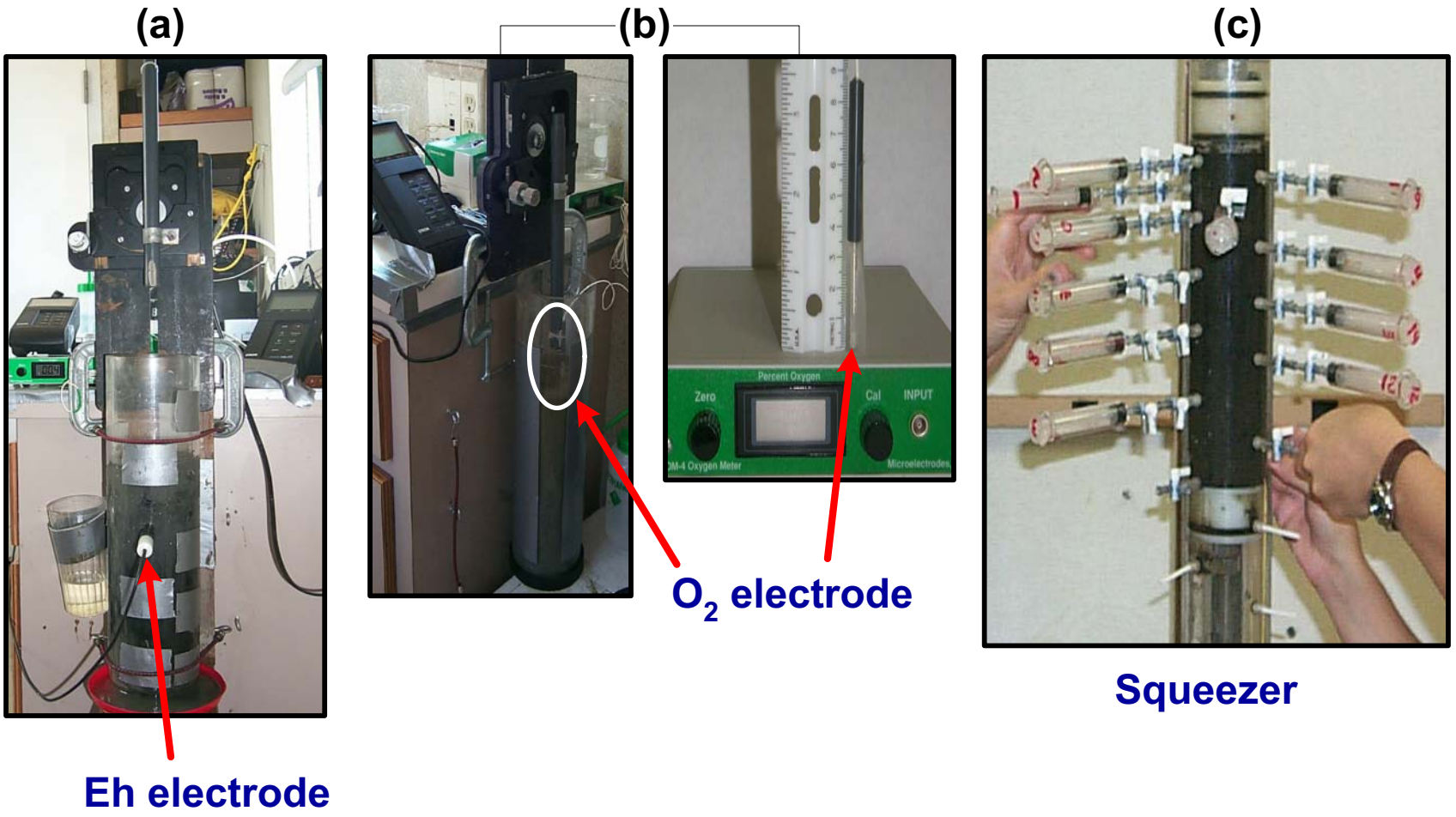

Figure 9-1. Photographs showing (a) Eh electrode inserted in sediment core, (b) oxygen probe inserted in top of sediment core and close-up of electrode and electronic control box, and (c) whole-core squeezer.

The frozen samples (≥3 mL) were thawed upon return from the field and used to determine concentrations of nitrate and sulfate using a Dionex DX-600 ion chromatograph. Before injection into the system, samples and standards were passed through Dionex OnGuard II® Ag cartridges to remove chloride. Standards were prepared from mixtures of standard seawater (from the International Association for the Physical Sciences of the Ocean [IAPSO]) and Dionex Five Anion Standard. The ion chromatograph was operated under the following conditions: 9-mM Na_2CO_3 eluent, 1.00-mL/minimum flow rate, Dionex IonPac® AS9-HC 4-mm column, 100-mA suppressor current, and 35°C oven temperature.

The acidified portion (1.5 to 2 mL) was prepared immediately upon collection by adding 20 µL of 6 N HCl. It was later analyzed for Fe and Mn by atomic absorption spectrometry (AAS) using a Perkin-Elmer Model 4000 instrument. To eliminate the effects of dissolved salts, samples were diluted by a factor of four before analysis. Standards and blanks were prepared in 1:4 seawater:DIW. The concentrations of Fe and Mn measured in the pore water represent the dissolved fraction and will be referred to as Fe^{2+} and Mn^{2+} concentrations.

The unaltered pore water sample was used for chlorinity and alkalinity analysis. Chlorinity was determined by Mohr titration whereby a 0.5-mL sample was added to 20 mL of DIW and titrated with ~0.04 N $AgNO_3$. Standard seawater (IAPSO) was titrated and used to standardize the analysis. Alkalinity was determined by titrating a 2-mL sample with 0.01 N HCl until the pH reached 4.00 or lower. The pH probe used to monitor the titration was first calibrated with pH 4 and 7 buffers. The volume of acid and final pH is used to calculate the alkalinity using an equation modified from Strickland and Parsons (1972).

9.2.3 Laboratory Analysis

9.2.3.1 Metals. After being transported to FIT, sediment samples were freeze-dried to a constant mass over 48 hours. For analysis of Al, Ba, Fe, and Mn, about 20 mg of sediment were digested in Teflon® beakers with $HClO_4$-HNO_3-HF and diluted to 20 mL (Trefry and Metz, 1984). For samples determined to have very high concentrations of Ba, based on residual white solid after digestion, a smaller mass of sample (≤10 mg of sediment) was digested and re-analyzed for Ba. The digested samples were analyzed for Al, Fe, and Mn by flame atomic absorption spectrometry (FAAS) using a Perkin-Elmer Model 4000 instrument. Concentrations of Ba were determined by inductively-coupled plasma-mass spectrometry (ICP-MS) using a Perkin-Elmer ELAN® 5000 instrument. A certified reference material (CRM), MESS-2, a marine sediment from the National Research Council (NRC) of Canada, also was digested and analyzed for Al, Fe, Mn, and Ba to check the accuracy of the method. Method detection limits (MDLs) and data quality information are listed in Appendix E.

For analysis of sediments collected during the Screening Cruise for As, Cd, Cr, Cu, Hg, Ni, Pb, V, and Zn, samples were initially brought to room temperature, then each wet sediment sample was homogenized in the original 75-mL plastic vial using a Teflon® mixing rod. Then, a portion (~2 g) of each sample was transferred into a pre-weighed plastic vial to determine water content. Once transferred, the wet sediment and the vial were reweighed. In addition, 2 to 4 g of sample were transferred into polypropylene-copolymer centrifuge tubes to determine the Hg content of the sediments. Samples to be used for determining water content were frozen, freeze-dried, and reweighed to obtain the water content. The dried sediment samples were again homogenized using a Teflon® mixing rod.

About 0.45 g of freeze-dried, homogenized sediment and CRM (MESS-2) were totally digested in Teflon® beakers using concentrated, high purity HF-HNO_3-$HClO_4$. Total digestion of the sediments is preferred as a starting point in environmental evaluations because then no doubt remains about the absolute amount of metal associated with a sample. In the digestion process, 1 mL of $HClO_4$, 1 mL of HNO_3, and 3 mL of HF were added to the sediment in the Teflon® beaker and heated at 50°C with a Teflon® watch cover in place until a moist paste formed. The mixture was heated for another 3 hours at 80°C with an additional 2 mL of HNO_3 and 3 mL of HF before bringing the sample to dryness. Finally, 1 mL of HNO_3 and about 30 mL of DIW were added to the sample and heated strongly to dissolve perchlorate salts and reduce the volume. The completely dissolved and clear samples were diluted to 20 mL with DIW. This technique is 100% efficient with no loss of the elements studied and has been used successfully in the laboratory at FIT for many years with a variety of sediment types.

Sediment samples to be analyzed for Hg were digested by heating 2 to 4 g of wet sediment in acid-washed, polypropylene-copolymer centrifuge tubes with 4 mL of HNO_3 and 2 mL of H_2SO_4. Sample tubes were heated for 1 hour in a 90°C water bath and allowed to cool. Each tube was centrifuged at 2,000 rpm, and the supernatant was decanted into a 25-mL graduated cylinder. The sediment pellet was rinsed twice with 5 mL of DIW, centrifuged, and decanted into the graduated cylinder before diluting to a final volume of 20 mL with DIW.

Sediment samples, CRMs, and procedural and reagent blanks were analyzed by FAAS, graphite furnace atomic absorption spectrometry (GFAAS with Zeeman or Continuum background correction), cold vapor atomic absorption spectrometry (CVAAS), or ICP-MS. Mercury concentrations were measured by CVAAS using a Laboratory Data Control Model 1235 Mercury Monitor. Concentrations of Cr, Cu, Ni, and Zn were determined by FAAS. Concentrations of As were determined by GFAAS using a Perkin-Elmer Model 5100 instrument. Concentrations of Cd and Pb were determined by ICP-MS. The corresponding MDLs are presented in Appendix E. All analytical techniques followed manufacturers' specifications and SOPs on file at FIT. These methods are closely akin to the USEPA methods described for FAAS, Series 7000 and GFAAS, Series 7470 CVAAS and Series 6010A ICP-MS as described in USEPA (1991).

Labware used in the digestion process was acid washed with hot, 8 N HNO_3 and rinsed three times with DIW. Two procedural blanks, two duplicate samples, and two CRMs were prepared with each set of 40 samples.

9.2.3.2 Total Organic Carbon. A 0.5- to 1-g portion of the freeze-dried sediment was placed in a 10-mL Pyrex® beaker and wetted with 10% H_3PO_4 to remove any inorganic carbon present. The sediment was dried at 60°C and reweighed to determine the increase in weight due to the formation of $CaHPO_4$ as a result of adding phosphoric acid. Then, approximately 200 to 400 mg of pre-treated sediment were weighed into ceramic boats and combusted at 900°C in a Shimadzu TOC-5050A carbon system with a SSM-5000A solid sampling module following the manufacturer's instructions. Total organic carbon content of the sediment samples was determined using a four-point calibration curve with pure sucrose as the standard and MESS-2 as the SRM. Total organic carbon concentrations were corrected to account for increases in sediment mass following addition of H_3PO_4. The calibration curve was checked every ten samples by analyzing pure sucrose.

9.2.3.3 Radionuclides. Sediment geochronology was determined using ^{137}Cs and excess ^{210}Pb following methods described by Kang et al. (2000). Vials containing about 10 g of freeze-dried

sediment were counted for 2 to 3 days until peak areas were sufficient to provide <10% counting error for total ^{210}Pb. The activities of ^{210}Pb, ^{214}Pb, ^{214}Bi, and ^{137}Cs were determined using a well-type, intrinsic germanium detector (WiGe, Princeton Gamma Tech). Detector efficiency was determined using the following: NBS 4350B, river sediment and NBS 4354, freshwater lake sediment from National Institute of Standards and Technology (NIST), and RGU-1 and RGTh-1 from the International Atomic Energy Agency. The specific activity (dpm/g) of each sediment sample was calculated from the detector efficiency, gamma intensity, geometry factor, and sample weight (Kang et al., 2000). All values were decay-corrected to the date of coring. Errors are shown on the basis of 1-sigma counting statistics.

9.2.4 Quality Control and Quality Assurance

9.2.4.1 Sample Tracking Procedure. All samples were collected, transported, and stored by personnel from FIT. Upon return to the laboratory, each sample was carefully inspected to ensure that it was intact and that the identification number was clearly readable. All sediment was kept frozen (-20°C) until processed for analysis.

9.2.4.2 Quality Control Measurements for Analysis. For this project, QC measures included balance calibration, instrument calibration (FAAS, GFAAS, CVAAS, ICP-MS, TOC analyzer, and *in-situ* instrument sensors), matrix spike analysis for each metal, duplicate sample analysis, analysis of CRMs and SRMs, procedural blank analysis, and standard checks. With each batch of up to 40 samples, two procedural blanks, two CRMs or SRMs, two duplicate samples, and two matrix-spiked samples were analyzed. Data quality objectives for these QC measurements are provided in Table 9-1.

Table 9-1. Data quality objectives and criteria.

Element or Sample Type	Minimum Frequency	Data Quality Objective/Acceptance Criteria
Initial Calibration	Prior to every batch of samples	Three- to five-point curve and a blank. Standard curve correlation coefficient r=0.999 for all analytes
Continuing Calibration	Must end every analytical sequence; for flame, repeat all standards every five samples; for graphite furnace and ICP-MS, recheck standard after every eight to ten samples	%RSD=15% for all analytes
Reference Materials	One per batch of 20 samples	Values must be within 20% of accepted values for >85% of the certified analytes and within 25% for mercury
Method Blank	One per batch of 20 samples	No more than 2 analytes to exceed five times the MDL unless analyte not detected in associated sample(s)
Matrix Spike and Spike Method Blank	One per batch of 20 samples	%RSD=80%-120%
Lab Duplicate	One per batch of 20 samples	%RSD=<25% for 65% analytes

ICP-MS = Inductively-coupled plasma-mass spectrometry.
MDL = Method detection limit.
RSD = Relative standard deviation.

9.2.4.3 Instrument Calibration. Electronic balances used for weighing samples and reagents were calibrated prior to each use with certified (NIST traceable) standard weights. All pipettes (electronic or manual) were calibrated prior to use. Each of the spectrometers used for metals analysis was initially standardized with a three- to five-point calibration. A linear correlation coefficient of $r \geq 0.999$ was required before experimental samples could be analyzed. Analysis of complete three- to five-point calibrations and/or single standard checks alternated every five to ten samples until all the analyses were complete. The relative standard deviation (RSD) between complete calibration and standard check was required to be <15%, or recalibration and reanalysis of the affected samples were performed.

9.2.4.4 Matrix Spike Analysis. Matrix spikes were prepared for a minimum of 5% of the total number of samples analyzed and included each metal to be determined. Results from matrix spike analysis using the method of standard additions provide information on the extent of any signal suppression or enhancement due to the sample matrix. If necessary (i.e., spike results outside 80% to 120% limit), spiking frequency was increased to 20% and a correction applied to the metal concentrations of the experimental samples.

9.2.4.5 Duplicate Sample Analysis. Duplicate samples from homogenized field samples (as distinct from field replicates) were prepared in the laboratory for a minimum of 5% of the total samples. These laboratory duplicates were included as part of each set of sample digestions and analyses and provide a measure of analytical precision.

9.2.4.6 Procedural Blank Analysis. Two procedural blanks were prepared with each set of 40 samples to monitor potential contamination resulting from laboratory reagents, glassware, and processing procedures. These blanks were processed using the same analytical scheme, reagents, and handling techniques as used for the experimental samples.

9.2.4.7 CRM and SRM Analysis. A common method used to evaluate the accuracy of environmental data is to analyze reference materials, samples for which consensus or "accepted" analyte concentrations exist. The following CRMs and SRMs were used: Marine Sediments, CRM MESS-2 (NRC), SRM Buffalo River Sediment 2704 (NIST), and SRM Trace Elements in Water 1643d (NIST). Metal concentrations obtained for the reference materials were required to be within 20% of accepted values for >85% of other certified analyses (Appendix E).

Data for quality assurance (QA)/QC measurements for each cruise are given with the complete data sets in Appendix E.

9.3 INDICATOR METALS AND TOTAL ORGANIC CARBON IN SURFACE SEDIMENTS

9.3.1 Shelf Sites MP 299, MP 288, and EI 346

Concentrations of indicator metals and TOC in sediments help identify the horizontal and vertical distribution of drilling discharges as well as provide a preliminary assessment of the redox state of the sediments. Means, standard deviations, maximums, and minimums for concentrations of Al, Ba, Fe, Mn, and TOC are summarized by site below in groups that include surface (0 to 2 cm) samples from near-field, mid-field, and far-field random stations. The complete data sets are presented in Appendix E. Comparisons for concentrations of Al, Fe, Mn, Ba, and TOC between cruise and zone will be discussed on a site-by-site basis for surface sediments. The shelf sites (MP 299, MP 288, and EI 346) are discussed separately in this chapter because of inherent, natural differences in sediment composition and redox conditions

between the continental shelf versus continental slope environments. Water depths for the three shelf sites are as follows: MP 299 at 60 m, MP 288 at 119 m, and EI 346 at 92 m.

At MP 299, mean concentrations of Al and Fe in surface sediments collected during Sampling Cruises 1 and 2 varied by <15% among near-field, mid-field, and far-field stations (Table 9-2). The mean Fe/Al ratio of 0.52 for sediments from MP 299 is close to a value of about 0.53 for suspended sediment (4.61% Fe/8.65% Al) from the Mississippi River (Trefry and Presley, 1982), even though the absolute values for Al and Fe at MP 299 were about 10% to 20% lower than in Mississippi River suspended sediment. This close comparison in the Fe/Al ratios is consistent with a terrigenous source of Al and Fe for these samples. Concentrations of Mn in surface sediments at MP 299 varied by as much as a factor of four (Table 9-2) and reflect differences in the degree of early chemical diagenesis of Mn from station to station at this site. Concentrations of Mn in suspended sediment from the Mississippi River are reported at ~1,300 ± 200 µg/g (Trefry and Presley, 1982); therefore, sediments from MP 299 contained about 15% to 75% less Mn than river particles. These lower values are consistent with a flux of Mn^{2+} from reducing sediments to the overlying water column (Trefry and Presley, 1982). This is a natural process and provides insight to the redox state of the sediments at each station. At MP 299, lower concentrations of Mn in the sediments from all stations show that the sediments were reducing. This information will be further considered in discussions regarding the redox state of the sediment.

Table 9-2. Means, standard deviations (SD), minimums (Min.), and maximums (Max.) for surface (0 to 2 cm) sediment from near-field (NF), mid-field (MF), and far-field (FF) random stations at Main Pass 299 (n=6 for all data points) for Sampling Cruises 1 and 2 (S1 and S2).

Main Pass 299	Al (%)	Al (%)	Ba (%)	Ba (%)	Fe (%)	Fe (%)	Mn (µg/g)	Mn (µg/g)	TOC (%)	TOC (%)
NF	S1	S2	S1	S2	S1	S2	S1	S2	S1	S2
Mean	7.13	7.61	0.464	0.276	3.38	3.75	451	673	1.28	1.15
SD	0.28	0.42	0.332	0.138	0.016	0.22	103	135	0.30	0.13
Min.	6.66	6.90	0.108	0.194	3.21	3.46	337	513	0.80	0.95
Max.	7.42	8.14	0.930	0.552	3.55	4.10	638	902	1.70	1.29
MF	S1	S2	S1	S2	S1	S2	S1	S2	S1	S2
Mean	7.24	7.74	0.303	0.237	3.53	3.79	663	740	1.28	1.26
SD	0.11	0.37	0.112	0.081	0.19	0.18	105	152	0.04	0.11
Min.	7.11	7.05	0.211	0.171	3.23	3.46	562	523	1.22	1.16
Max.	7.41	8.04	0.467	0.386	3.74	3.95	810	937	1.34	1.43
FF	S1	S2	S1	S2	S1	S2	S1	S2	S1	S2
Mean	7.15	7.84	0.130	0.101	3.41	3.86	1,120	763	1.23	1.24
SD	0.27	0.24	0.054	0.028	0.18	0.16	282	206	0.09	0.09
Min.	6.85	7.42	0.078	0.074	3.14	3.59	703	559	1.16	1.14
Max.	7.41	8.06	0.198	0.153	3.61	4.04	1,440	1,070	1.39	1.39

Mean concentrations of Ba in near-field stations at MP 299 were more than double values at far-field stations (Table 9-2 and Figure 9-2). Statistical testing for Ba followed the analysis of variance approach described in Chapter 8 where the initial step was to test for interactions between cruises and zones using randomization methodology (Table 9-3). The concentrations of Ba, but not Mn, were logarithmically transformed (base 10). As described in Chapter 8, Bonferroni comparisons were made for each study site where significant interactions were observed among zones. The results (Table 9-3) for MP 299 show that concentrations of Ba in near-field and mid-field sediments were significantly greater than in far-field sediments, yet Ba levels in near-field sediments were not significantly different from mid-field sediments (Table 9-3). Furthermore, Ba levels in sediments from all three zones at MP 299 were not significantly different between Sampling Cruise 1 and Sampling Cruise 2 (Table 9-3 and Figure 9-2). However, the loading of Ba, and therefore drilling discharges, at MP 299 was low. Concentrations of TOC, like Al and Fe, were quite uniform among zones and cruises, with <10% variations in mean values that averaged ~1.2% (Table 9-2 and Figure 9-2).

To help visualize the distribution of drilling discharges at each site, separate schematic diagrams for Ba are presented for 1) far-field and 2) near-field + mid-field sediments. In each diagram, data for Ba are plotted adjacent to the mark that identifies a far-field, mid-field, or near-field location from Sampling Cruise 1 or 2. An asterisk has been placed after the Ba concentration for each station where the levels of SBF are >0.01%. At MP 299, located near the Mississippi River delta, concentrations of Ba were <1% in sediment from all sites and only one station (NF-6, Sampling Cruise 1) had sediment with >0.01% SBF (and 0.8% Ba) (Figures 9-3 and 9-4). Although generally low, mean concentrations of Ba at mid-field and near-field stations were about double and triple background (far-field) levels, respectively. No distinct spatial trends were observed for concentrations of Ba in the near-field/mid-field zones (Figure 9-4).

At MP 288, mean concentrations of Al and Fe were 20% to 40% lower at far-field stations than at near-field and mid-field stations (Table 9-4). This difference is observed because sediments from Stations FF-1, FF-2, and FF-6 from Sampling Cruise 1 and FF-1, FF-2, and FF-3 from Sampling Cruise 2 for MP 288 contained >50% quartz sand that is naturally low in Al and Fe. This sandy texture was not found at any near-field, mid-field, or other far-field stations at MP 288. The presence of more sandy sediment at selected far-field stations is believed to be a remnant of an ancient river delta to the west of the site.

Despite lower levels of Al and Fe at some far-field stations, the Fe/Al ratio for the far-field sediments averaged 0.53, thereby identifying the Mississippi River as the dominant source of aluminosilicates at this site. Concentrations of Mn in surface sediments at MP 288 were variable (average CV = 50% based on means and standard deviations for three zones from two cruises, Table 9-4), as observed at MP 299. Thus, the same discussion regarding Mn diagenesis is applicable.

Mean concentrations of Ba in near-field stations at MP 288 were 4 to 20 times greater than at far-field stations (Table 9-4 and Figure 9-5). Statistical results (Table 9-3 and Figure 9-5) show that concentrations of Ba in near-field, mid-field, and far-field sediments were significantly different during Sampling Cruise 1, with Ba levels in near-field (2%) > mid-field (0.4%) > far-field (0.1%). During Sampling Cruise 2, Ba levels followed a hierarchy of mid-field (0.4%) ≈ near-field (0.3%) > far-field (0.1%). Concentrations of Ba in surface sediments at near-field stations from MP 288 were significantly lower during Sampling Cruise 2 than Sampling Cruise 1, with a five-fold decrease in mean concentrations of Ba in near-field sediments collected during Sampling Cruise 2 compared to Sampling Cruise 1 (Table 9-4).

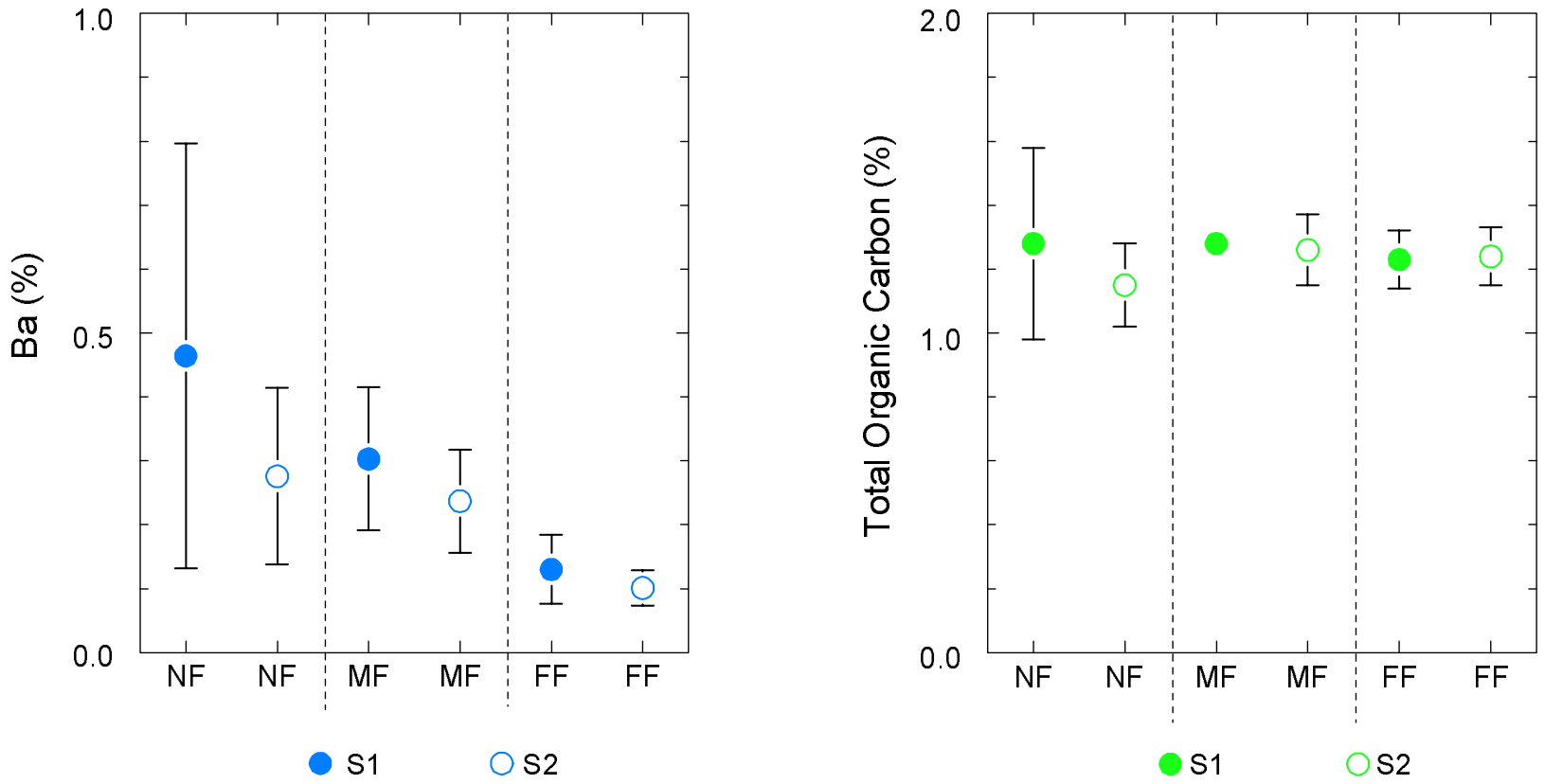

Figure 9-2. Means (circles) and standard deviations (solid lines) for concentrations of barium (Ba) and total organic carbon in surface sediments (0 to 2 cm) from random stations in near-field (NF), mid-field (MF), and far-field (FF) zones at Main Pass 299 for Sampling Cruises 1 and 2 (S1 and S2).

Table 9-3. Results of statistical comparisons for concentrations of barium (Ba as log_{10}) and manganese (Mn) among zones and cruises for sites on the continental shelf. Upper table for each element shows tests of significance by cruise and zone. Lower table for each element shows detailed comparisons by zone at each site (near-field = NF, mid-field = MF, and far-field = FF).

Study Site	Metal	Main Effect	Probability>F	Interpretation
Main Pass 299	Ba	Cruise	p>0.10	Not Significantly Different
		Zone	p<0.01	Significantly Different
Main Pass 288	Ba	Cruise	p<0.02	Significantly Different
		Zone	p<0.01	Significantly Different
Eugene Island 346	Ba	Cruise	p>0.06	Not Significantly Different
		Zone	p<0.01	Significantly Different

Study Site	Metal	Bonferroni Comparison	Probability>F	Interpretation
Main Pass 299	Ba	FF vs. MF	p<0.03	Significantly Different
		NF vs. FF	p<0.03	Significantly Different
		NF vs. MF	p>0.75	Not Significantly Different
Main Pass 288	Ba	FF vs. MF	p<0.03	Significantly Different
		NF vs. FF	p<0.03	Significantly Different
		NF vs. MF	p<0.03	Significantly Different
Eugene Island 346	Ba	FF vs. MF	p<0.03	Significantly Different
		NF vs. FF	p<0.03	Significantly Different
		NF vs. MF	p>0.15	Not Significantly Different

Study Site	Metal	Main Effect	Probability>F	Interpretation
Main Pass 299	Mn	Cruise	p>0.20	Not Significantly Different
		Zone	p<0.01	Significantly Different
Main Pass 288	Mn	Cruise	p>0.05	Not Significantly Different
		Zone	p>0.05	Not Significantly Different
Eugene Island 346	Mn	Cruise	p>0.08	Not Significantly Different
		Zone	p<0.01	Significantly Different

Study Site	Metal	Bonferroni Comparison	Probability>F	Interpretation
Main Pass 299	Mn	FF vs. MF	p<0.03	Significantly Different
		NF vs. FF	p<0.03	Significantly Different
		NF vs. MF	p>0.03	Significantly Different
Main Pass 288	Mn	FF vs. MF	p>0.05	Not Significantly Different
		NF vs. FF	p>0.05	Not Significantly Different
		FF vs. MF	p>0.05	Not Significantly Different
Eugene Island 346	Mn	FF vs. MF	p<0.03	Significantly Different
		NF vs. FF	p<0.03	Significantly Different
		NF vs. MF	p>0.75	Not Significantly Different

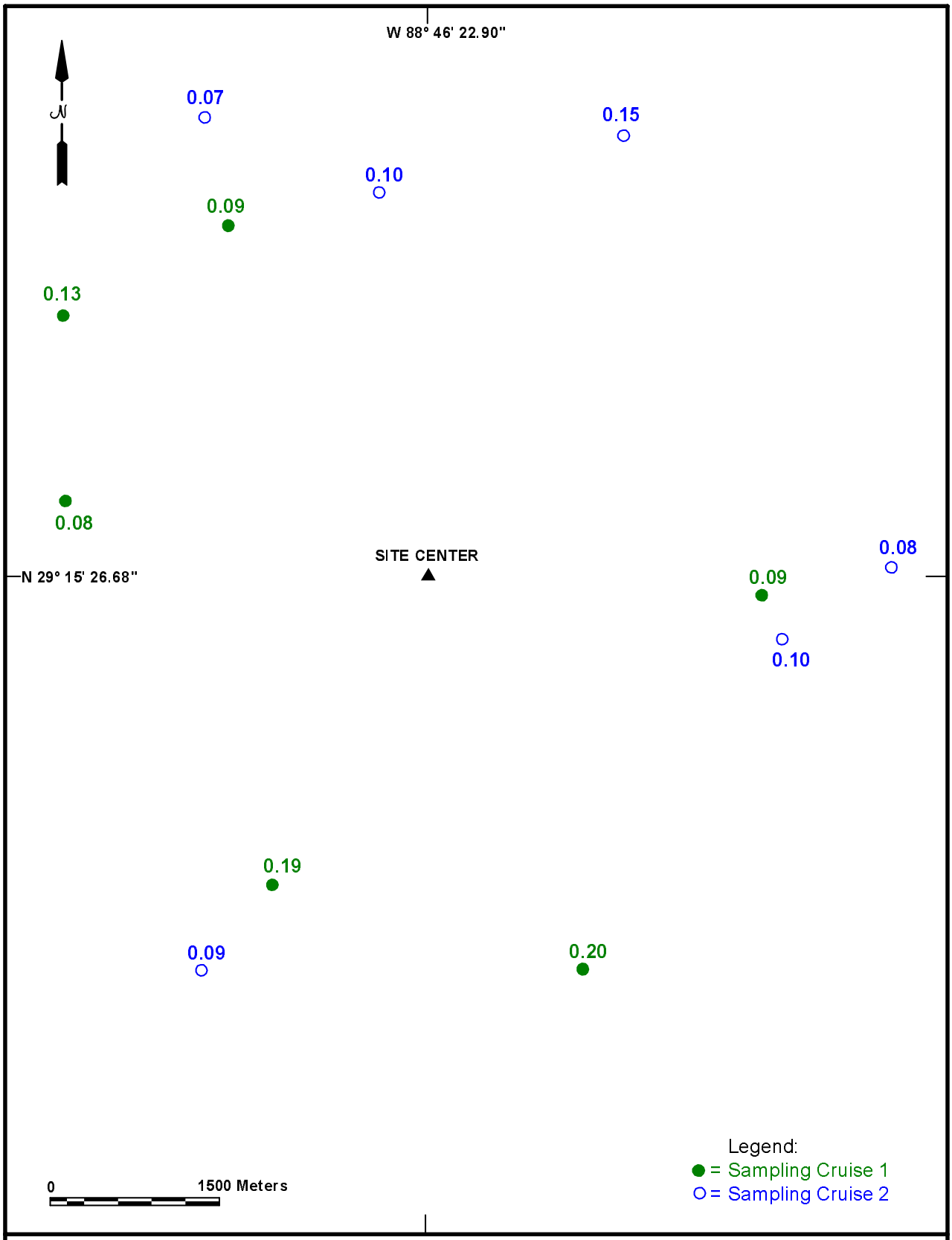

Figure 9-3. Concentrations of barium (Ba [%]) at far-field stations from Main Pass 299 for Sampling Cruises 1 and 2.

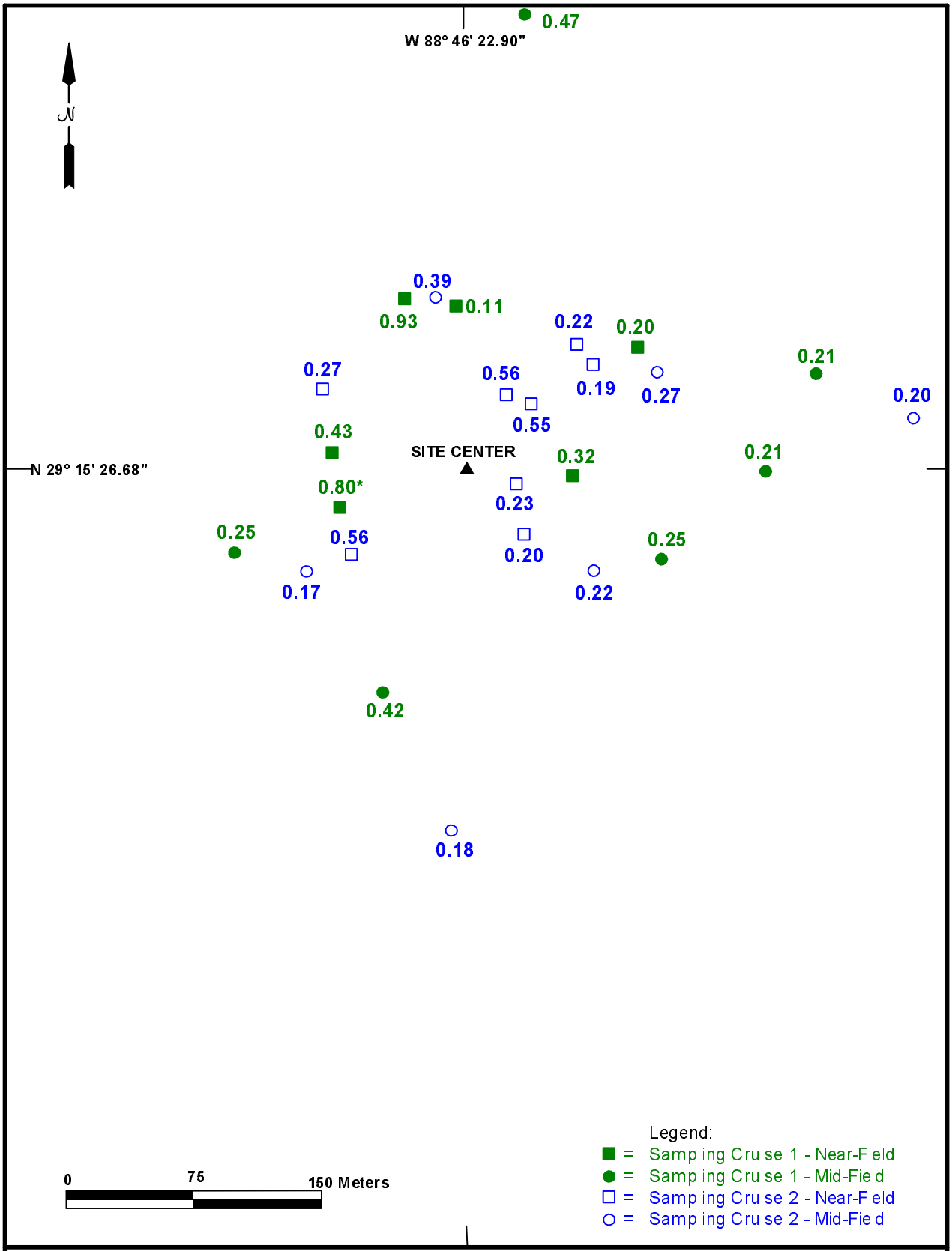

Figure 9-4. Concentrations of barium (Ba [%]) at near-field (including discretionary) and mid-field stations from Main Pass 299 for Sampling Cruises 1 and 2. Asterisks denote sediments with >0.01% synthetic based fluid.

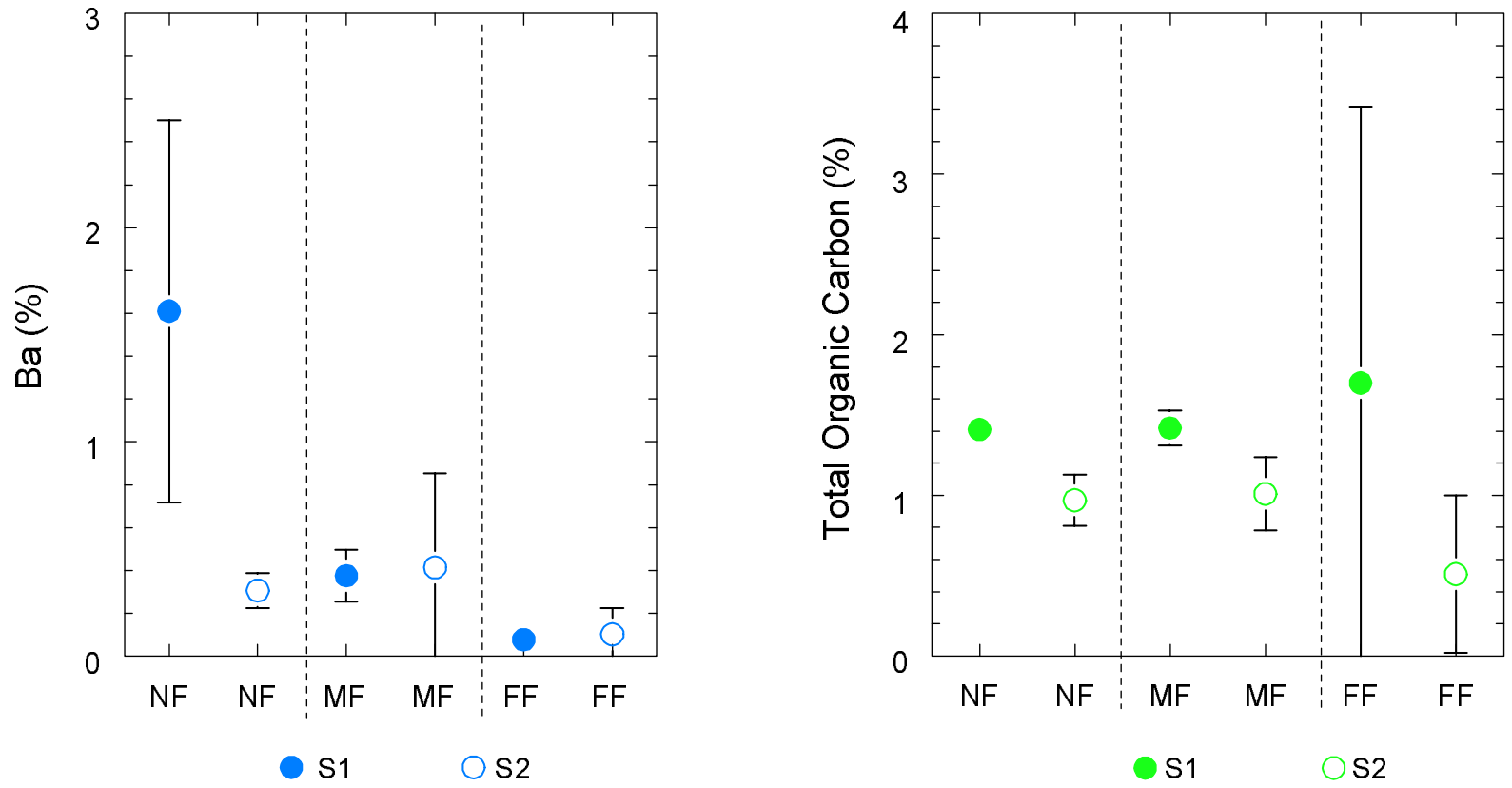

Figure 9-5. Means (circles) and standard deviations (solid lines) for concentrations of barium (Ba) and total organic carbon in surface sediments (0 to 2 cm) from random stations in near-field (NF), mid-field (MF), and far-field (FF) zones at Main Pass 288 for Sampling Cruises 1 and 2 (S1 and S2).

Table 9-4. Means, standard deviations (SD), minimums (Min.), and maximums (Max.) for surface (0 to 2 cm) sediment from near-field (NF), mid-field (MF), and far-field (FF) random stations at Main Pass 288 (n=6 for all data points) for Sampling Cruises 1 and 2 (S1 and S2).

Main Pass 288	Al (%)	Al (%)	Ba (%)	Ba (%)	Fe (%)	Fe (%)	Mn (µg/g)	Mn (µg/g)	TOC (%)	TOC (%)
NF	S1	S2	S1	S2	S1	S2	S1	S2	S1	S2
Mean	6.32	6.92	1.61	0.306	3.09	3.54	553	682	1.41	0.97
SD	0.41	0.25	0.892	0.081	0.24	0.10	162	240	0.10	0.16
Min.	5.84	6.61	0.598	0.203	2.68	3.41	438	413	1.29	1.17
Max.	7.03	7.30	2.73	0.427	3.35	3.69	873	945	1.56	0.75
MF	S1	S2	S1	S2	S1	S2	S1	S2	S1	S2
Mean	6.84	7.03	0.375	0.413	3.31	3.55	918	800	1.42	1.01
SD	0.48	0.21	0.121	0.441	0.13	0.16	329	304	0.11	0.23
Min.	6.10	6.74	0.204	0.175	3.10	3.35	591	449	1.28	0.73
Max.	7.57	7.26	0.562	1.31	3.45	3.78	1,520	1,170	1.54	1.30
FF	S1	S2	S1	S2	S1	S2	S1	S2	S1	S2
Mean	5.05	3.98	0.076	0.101	2.65	2.17	1,082	335	1.70	0.51
SD	3.17	3.43	0.029	0.123	1.25	1.53	924	243	1.72	0.49
Min.	1.19	0.94	0.035	0.011	1.09	0.71	237	167	0.35	0.08
Max.	7.98	8.25	0.107	0.334	3.78	4.10	2,720	803	5.05	1.24

Concentrations of Ba in surface sediments were <0.15% at all far-field stations from MP 288 during both cruises, except at FF-4 (0.33%) during Sampling Cruise 2 (Figure 9-6). Barium concentrations ≤0.05% were found in the sandy, far-field sediments to the west and northwest of the site (Figure 9-6). Surface sediments from four near-field stations and one mid-field station located north of the center of site MP 288 had Ba levels >1%, all from Sampling Cruise 1 (Figure 9-7). The three near-field stations from Sampling Cruise 1 with >1% Ba were the only surface samples collected during Sampling Cruise 1 or Sampling Cruise 2 from MP 288 with >0.01% SBF (Figure 9-7). The observed lower levels of Ba and SBF (Chapter 8) in near-field stations during Sampling Cruise 2 versus Sampling Cruise 1 are consistent with the data for TOC that show 30% lower concentrations of TOC during Sampling Cruise 2 relative to Sampling Cruise 1 (Table 9-4).

In contrast with MP 299 and MP 288, mean concentrations of Al and Fe at EI 346 were 30% to 40% lower at near-field stations relative to far-field stations (Table 9-5). This difference was observed because near-field sediment from EI 346 contained greater amounts of non-clay material than observed at the other two shelf sites. For example, at Station NF-4 (EI 346, Sampling Cruise 1), the sediment Ba concentration was 20.5% (or ~39% industrial barite based on an average Ba content of 53% for industrial barite [Trefry et al., 2003]). An Al concentration of 4.37% at Station NF-4 is consistent with a 42% dilution of ambient sediment (mean of 7.5% Al at far-field stations) with drilling material (in this case, predominantly barite). Overall, the mean levels of Al and Fe at near-field stations for EI 346 support the presence of 20% to 40% drilling discharges in the sediment.

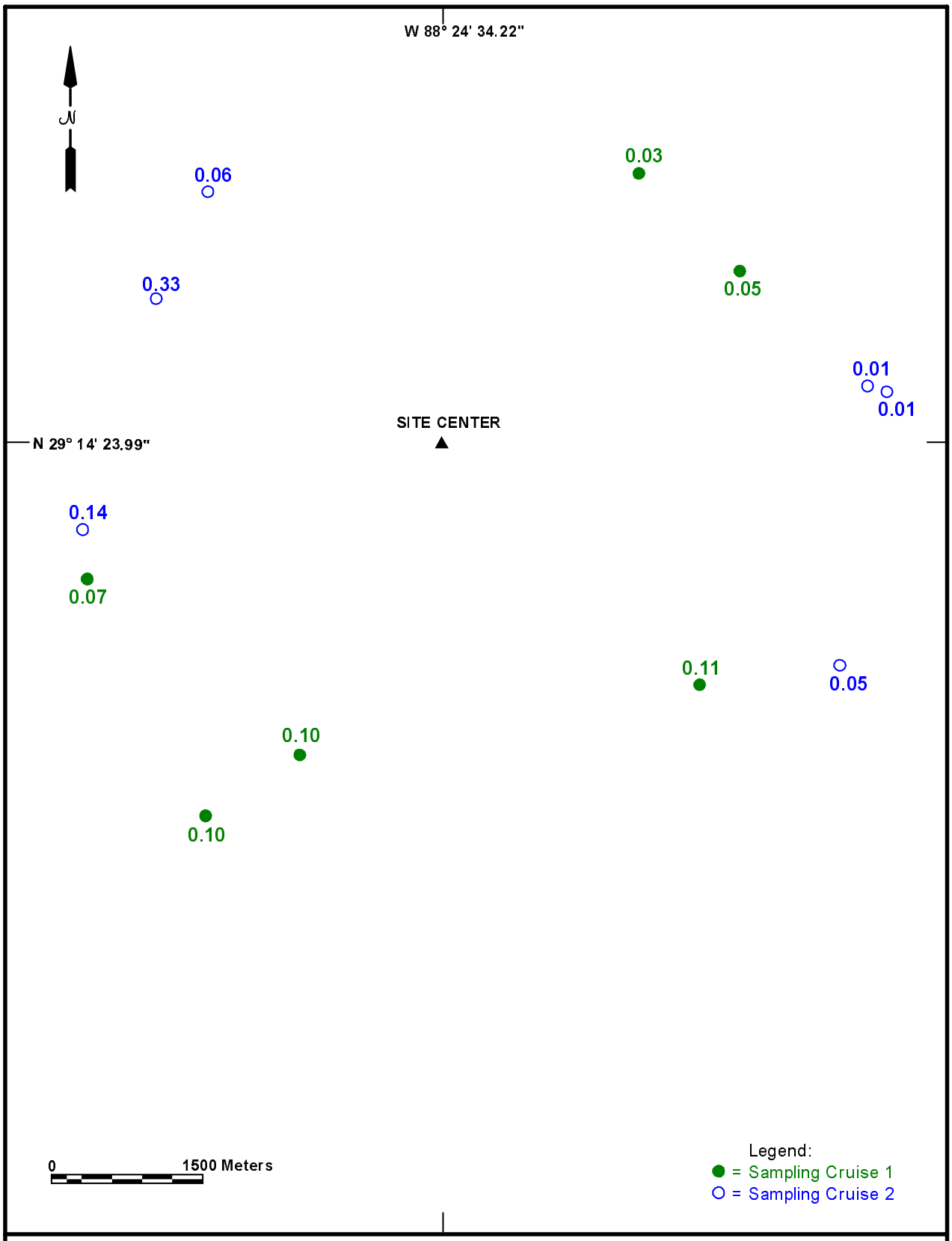

Figure 9-6. Concentrations of barium (Ba [%]) at far-field stations from Main Pass 288 for Sampling Cruises 1 and 2.

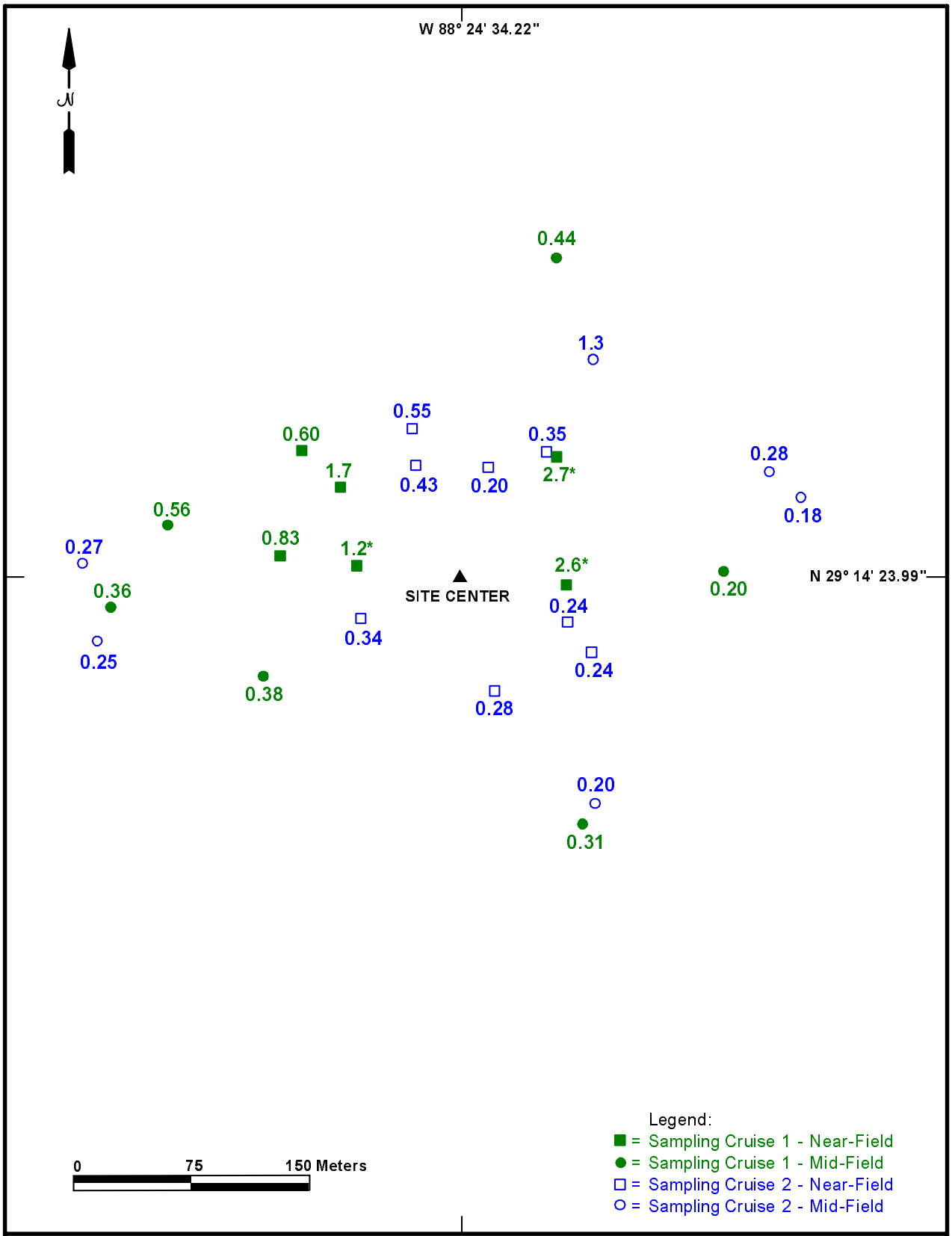

Figure 9-7. Concentrations of barium (Ba [%]) at near-field (including discretionary) and mid-field stations from Main Pass 288 for Sampling Cruises 1 and 2. Asterisks denote sediments with >0.01% synthetic based fluid.

Table 9-5. Means, standard deviations (SD), minimums (Min.), and maximums (Max.) for surface (0 to 2 cm) sediment from near-field (NF), mid-field (MF), and far-field (FF) random stations at Eugene Island 346 (n=6 for all data points) for Sampling Cruises 1 and 2 (S1 and S2).

Eugene Island 346	Al (%)	Al (%)	Ba (%)	Ba (%)	Fe (%)	Fe (%)	Mn (µg/g)	Mn (µg/g)	TOC (%)	TOC (%)
NF	S1	S2	S1	S2	S1	S2	S1	S2	S1	S2
Mean	4.98	4.67	6.51	15.2	2.18	2.37	409	275	2.84	1.55
SD	1.49	1.69	6.95	10.4	0.56	0.60	91	85	2.32	0.73
Min.	2.37	3.04	2.48	2.84	1.28	1.64	313	212	0.76	0.73
Max.	6.75	7.62	20.5	26.3	3.00	3.43	521	429	6.01	2.63
MF	S1	S2	S1	S2	S1	S2	S1	S2	S1	S2
Mean	5.37	6.15	3.64	6.07	2.38	2.82	391	374	1.69	1.05
SD	1.52	1.70	1.58	8.03	0.41	0.73	96	142	1.74	0.27
Min.	3.04	3.85	1.75	1.62	1.72	1.71	273	174	0.68	0.79
Max.	6.88	7.54	5.49	22.3	2.74	3.39	511	600	5.21	1.56
FF	S1	S2	S1	S2	S1	S2	S1	S2	S1	S2
Mean	7.50	7.68	0.146	0.168	3.33	3.54	1,130	1,180	0.91	0.86
SD	0.18	0.14	0.051	0.079	0.14	0.05	368	196	0.13	0.03
Min.	7.27	7.51	0.077	0.123	3.16	3.45	655	938	0.78	0.82
Max.	7.70	7.91	0.216	0.326	3.51	3.59	1,690	1,510	1.14	0.92

Concentrations of Mn in surface sediments at near-field and mid-field stations at EI 346 averaged about one-third of the mean values found in far-field sediments (Table 9-5). In addition, levels of TOC at the near-field and mid-field stations (mean of 1.8%) were double the mean value of ~0.9% in far-field sediments. Together, lower concentrations of Mn and higher levels of TOC in mid-field and near-field sediments at EI 346 support a more reducing environment in near-field and mid-field sediments relative to background (far-field) stations at EI 346, a point to be further discussed in the redox section of this chapter.

Mean concentrations of Ba in near-field stations at EI 346 were 45 to 90 times greater than at far-field stations for Sampling Cruises 1 and 2, respectively (Table 9-5 and Figure 9-8). No significant differences were observed for Ba levels as a function of cruise or between near-field and mid-field sediments (Table 9-3). Mean Ba values in surface sediments follow the same hierarchy of near-field (6.5% Ba) > mid-field (3.6% Ba) > far-field (0.15% Ba) during Sampling Cruise 1 and near-field (15% Ba) > mid-field (6.1% Ba) > far-field (0.17% Ba) during Sampling Cruise 2. Concentrations of Ba for near-field and mid-field sediments were significantly greater than in far-field sediments for both cruises (Tables 9-3 and 9-5). However, Ba levels at near-field, mid-field, and far-field stations were not significantly different between cruises (Table 9-3). Even though mean values of Ba at near-field and mid-field stations during Sampling Cruise 2 were ~2 times greater than during Sampling Cruise 1 (Table 9-5), the large standard deviations for Ba concentrations at near-field and mid-field stations for EI 346 during both cruises yield the result of no significant differences between cruises (Table 9-5 and Figure 9-8).

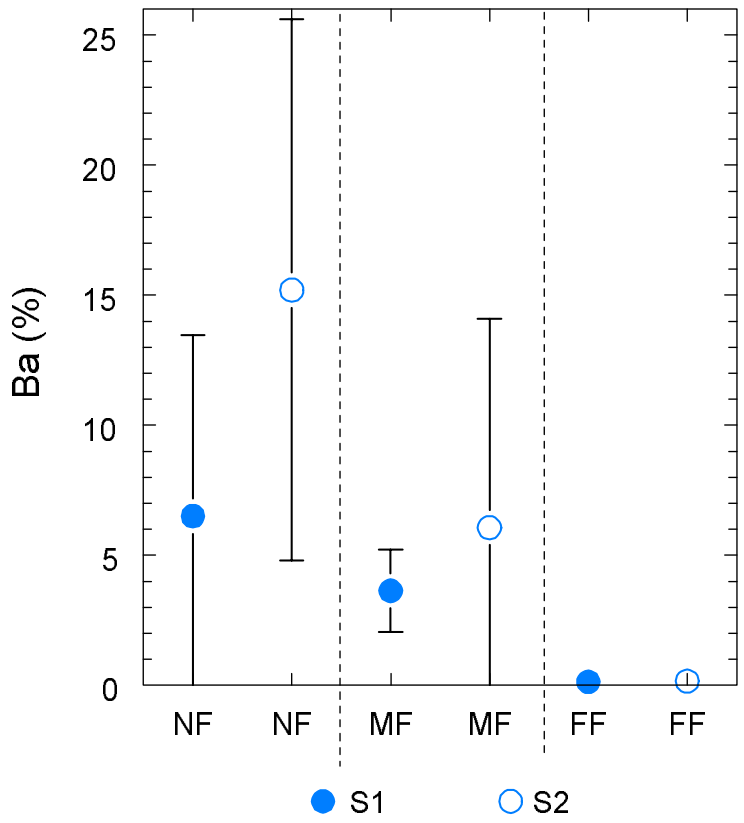

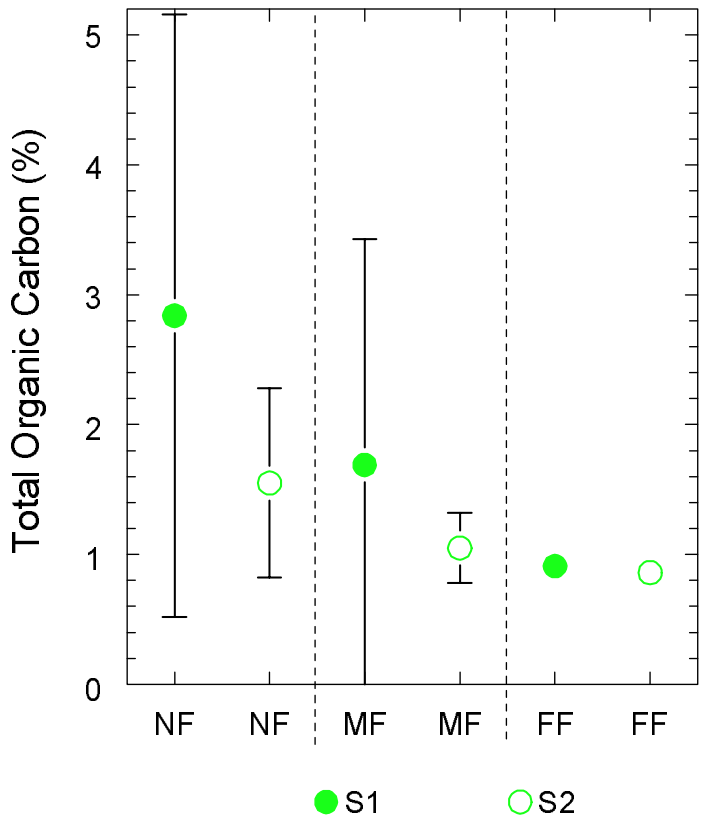

Figure 9-8. Means (circles) and standard deviations (solid lines) for concentrations of barium (Ba) and total organic carbon in surface sediments (0 to 2 cm) from random stations in near-field (NF), mid-field (MF), and far-field (FF) zones at Eugene Island 346 for Sampling Cruises 1 and 2 (S1 and S2).

Concentrations of Ba in surface sediments were ≤0.3% at far-field stations from EI 346 during Sampling Cruises 1 and 2 (Figure 9-9). In contrast, all surface sediments from near-field and mid-field stations at EI 346 from Sampling Cruises 1 and 2 contained >1% Ba (Figure 9-10). Eleven of the 26 near-field + mid-field samples from stations located mostly to the east of the site center contained >5% Ba (Figure 9-10). Concentrations of SBF in the sediment were >0.01% at 11 of the 26 near-field and mid-field stations (Figure 9-10). However, several sites with <3% Ba had >0.01% SBF, whereas other sites with >10% Ba had <0.01% SBF. Eight of the 11 sediments with >0.01% SBF were collected during Sampling Cruise 1, and the other three were collected during Sampling Cruise 2. The clear distinction between Ba-rich and (Ba + SBF)-rich drilling discharges is discussed in more detail after the overviews for each site are presented.

9.3.2 Slope Sites MC 496, EW 963, and GC 112

The continental slope sites (MC 496, EW 963, and GC 112) are discussed in this section. Water depths for the three slope sites are as follows: MC 496 at 556 m, EW 963 at 540 m, and GC 112 at 534 m. Background levels of Al (8.0%) and Fe (3.9%) in surficial sediment at far-field stations on the continental slope were ~20% greater than observed on the shelf (6.5% Al and 3.2% Fe) due to the increased presence of more fine-grained, Al- and Fe-rich clays. The distinction between shelf and slope was even greater for Mn, with average Mn concentrations of 6,700 µg/g in surface sediments at far-field stations for the three slope sites relative to Mn levels of ~900 µg/g in surface sediments at far-field stations for the three shelf sites. Concentrations of TOC averaged about 1.1% in far-field sediments from both the shelf and slope; however, the rate of deposition of TOC in shelf sediments is generally several times greater due to differences in sedimentation rates of ~0.5 cm/yr at shelf sites to ~0.2 cm/yr on the slope sites, as discussed below.

At MC 496, mean concentrations of Al and Fe were 10% to 20% lower at near-field stations relative to far-field stations in an indirect relationship with the fraction of drilling discharges (Table 9-6). Concentrations of Mn in surface sediments at MC 496 were variable (average CV = 65% based on means and standard deviations for three zones from two cruises) with Mn levels at the far-field stations being statistically equal to those at mid-field stations for both cruises and with the near-field stations only for Sampling Cruise 2 (Table 9-7).

Mean concentrations of Ba in near-field stations at MC 496 were ~30 and ~70 times greater than at far-field stations for Sampling Cruises 1 and 2, respectively (Table 9-6 and Figure 9-11). Concentrations of Ba were significantly greater at near-field and mid-field stations during Sampling Cruise 1 than during Sampling Cruise 2 (Table 9-7). Concentrations of Ba in surface sediments were ≤0.12% at far-field stations from MC 496 during Sampling Cruises 1 and 2 (Figure 9-12). All near-field surface sediments and 8 of 12 mid-field surface sediments contained >0.8% Ba (Figure 9-13). Barium concentrations were >5% at five near-field stations and one mid-field station, all located along a NW-SE line just east of the site center (Figure 9-13). Levels of SBF in the sediment were >0.01% at 14 of the 26 near-field and mid-field stations (Figure 9-13).

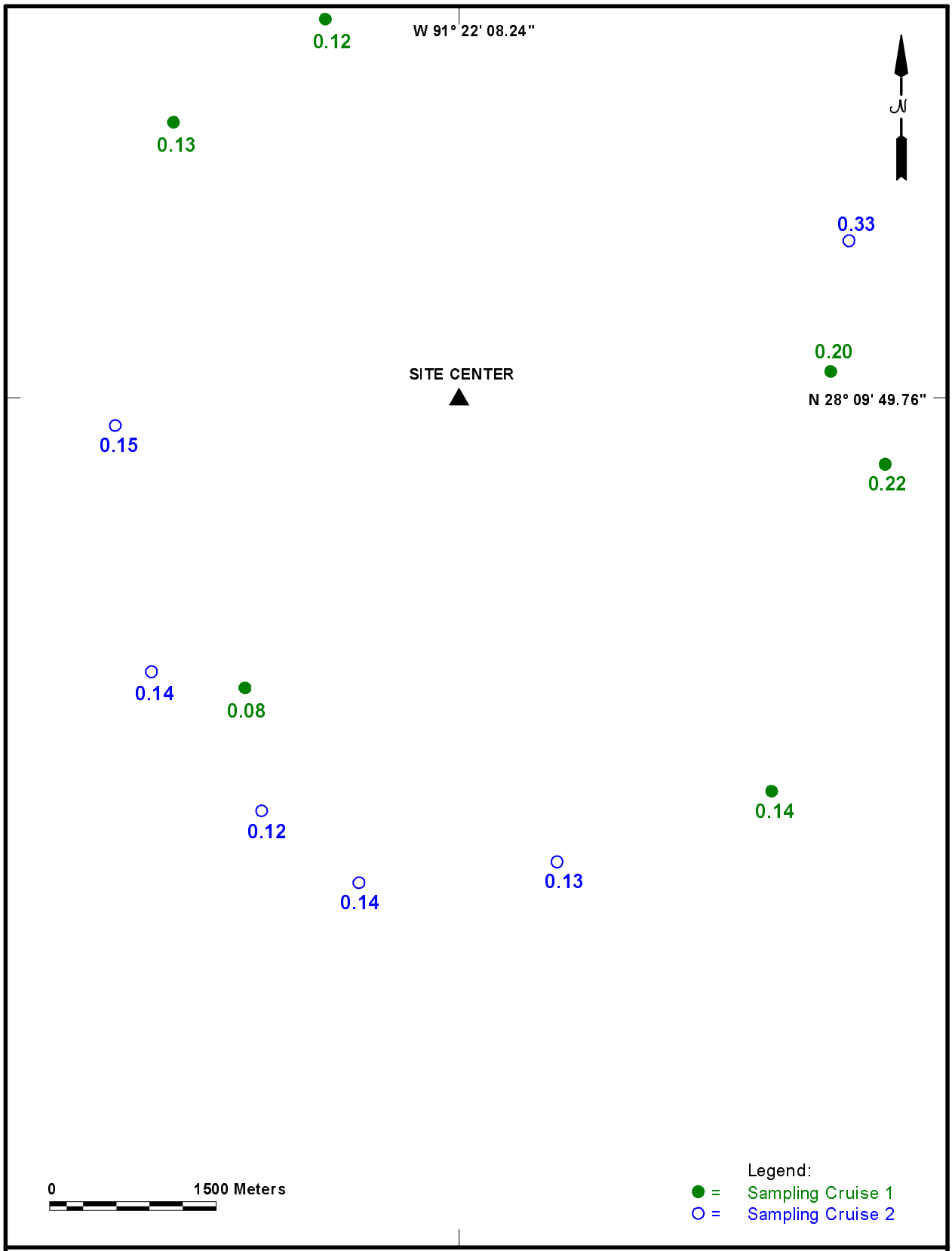

Figure 9-9. Concentrations of barium (Ba [%]) at far-field stations from Eugene Island 346 for Sampling Cruises 1 and 2.

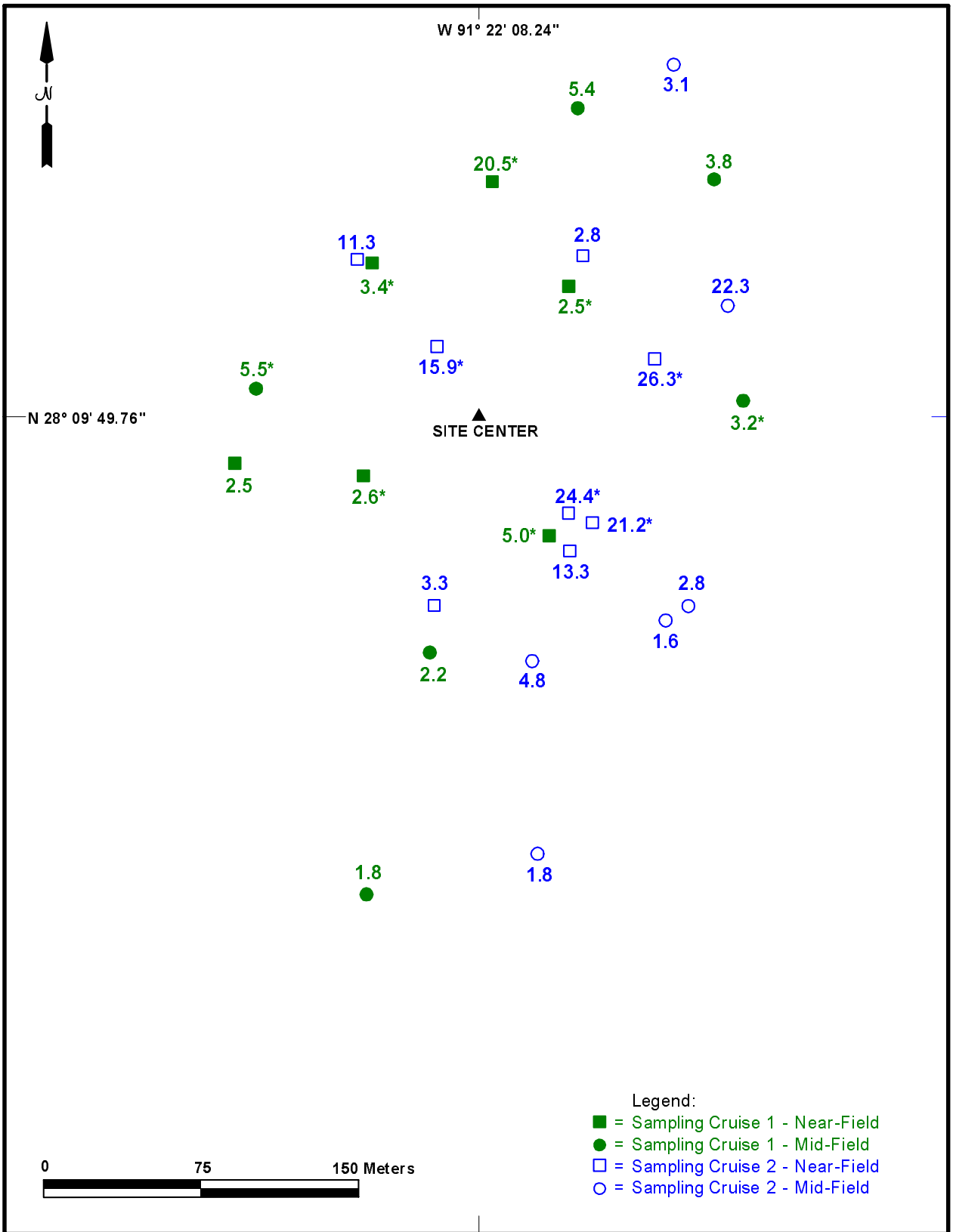

Figure 9-10. Concentrations of barium (Ba [%]) at near-field (including discretionary) and mid-field stations from Eugene Island 346 for Sampling Cruises 1 and 2. Asterisks denote sediments with >0.01% synthetic based fluid.

Table 9-6. Means, standard deviations (SD), minimums (Min.), and maximums (Max.) for surface (0 to 2 cm) sediment from near-field (NF), mid-field (MF), and far-field (FF) random stations at Mississippi Canyon 496 (n=6 for all data points) for Sampling Cruises 1 and 2 (S1 and S2).

Mississippi Canyon 496	Al (%)	Al (%)	Ba (%)	Ba (%)	Fe (%)	Fe (%)	Mn (µg/g)	Mn (µg/g)	TOC (%)	TOC (%)
NF	S1	S2	S1	S2	S1	S2	S1	S2	S1	S2
Mean	7.62	7.64	6.93	2.24	3.34	3.95	920	5,510	2.89	1.66
SD	1.44	0.26	6.27	1.66	0.61	0.22	575	3,400	2.58	0.57
Min.	5.22	7.16	1.71	0.885	2.31	3.55	472	1,100	0.85	1.08
Max.	8.78	7.88	17.4	5.17	3.86	4.13	2,050	9,470	7.36	2.71
MF	S1	S2	S1	S2	S1	S2	S1	S2	S1	S2
Mean	8.04	7.96	3.16	0.619	3.66	4.17	3,530	7,940	1.63	1.30
SD	0.36	0.15	2.67	0.542	0.19	0.14	3,800	2,730	0.37	0.20
Min.	7.42	7.79	0.956	0.211	3.32	3.95	398	3,080	1.19	0.95
Max.	8.29	8.20	7.85	1.56	3.83	4.35	8,670	11,300	2.22	1.54
FF	S1	S2	S1	S2	S1	S2	S1	S2	S1	S2
Mean	8.70	8.34	0.101	0.079	4.20	4.55	4,850	6,710	1.20	1.29
SD	0.19	0.25	0.020	0.027	0.16	0.13	3,620	3,420	0.12	0.13
Min.	8.38	8.03	0.069	0.049	4.02	4.41	558	2,920	1.01	1.06
Max.	8.89	8.66	0.125	0.112	4.45	4.77	9,450	12,200	1.39	1.42

At slope site EW 963, concentrations of Ba in surface sediments at near-field stations averaged 8.7% and 4.4% during Sampling Cruises 1 and 2, respectively (Table 9-8); however, this difference was not significant (Table 9-7) due to large standard deviations (Table 9-8 and Figure 9-14). Although mean Ba levels in surface sediment from mid-field stations were about 50% lower than at near-field stations, the differences were not significant (Table 9-7) due to large standard deviations in Ba concentrations (Table 9-8 and Figure 9-14). Barium levels in far-field sediments from EW 963 averaged 0.21% ± 0.09%, suggesting that background levels of Ba in surface samples at slope sites, such as EW 963, are higher than values of 0.06% to 0.10% in sediments from shelf sites. This difference in values for far-field sediments between the shelf and slope is due to natural diagenetic effects that sometimes yield Ba-rich layers in surficial sediments from the slope (e.g., Van Os et al., 1991) as well as proportionally greater deposition of biogenic barite in the more slowly accumulating sediments of the slope.

In contrast with shelf sediments, Mn levels in surface sediments from far-field stations at slope site EW 963 were very high due to diagenetic remobilization (Table 9-8) and were not significantly different from Mn levels at mid-field stations (Table 9-7). Surficial sediments from the upper slope in the Gulf of Mexico are enriched in Mn because reduction/dissolution of manganese oxides occur at depths of 5 to >10 cm in the sediment column, with subsequent diffusion of Mn^{2+} up toward the sediment-seawater interface where the Mn reoxidizes (Trefry and Presley, 1982). Because the sedimentation rate on the slope is slow, a sizeable Mn-rich layer of sediment can build up at the sediment-water interface where upwardly migrating Mn^{2+} precipitates. Average Mn levels at near-field stations were significantly lower than at mid-field and far-field stations (Table 9-7) because inputs of drilling discharges and lower levels of DO promote the dissolution of manganese oxides at the sediment water interface with diffusive loss

of Mn^{2+} to the overlying water column. The data also suggest that the redox environment at mid-field stations is more like that at far-field stations, even though significantly enhanced levels of Ba were found at mid-field versus far-field stations (Table 9-7).

Table 9-7. Results of statistical comparisons that test differences in concentrations of barium (Ba as $\log_{10}$) and manganese (Mn) among zones and cruises for study sites on the continental slope. Upper table for each element shows test of significance by cruise and zone. Lower table for each element shows detailed comparisons by zone at each site (near-field = NF, mid-field = MF, and far-field = FF).

Study Site	Metal	Main Effect	Probability>F	Interpretation
Mississippi Canyon 496	Ba	Cruise	p<0.10	Significantly Different
		Zone	p<0.01	Significantly Different
Ewing Bank 963	Ba	Cruise	p>0.21	Not Significantly Different
		Zone	p<0.01	Significantly Different
Green Canyon 112	Ba	Cruise	p>0.95	Not Significantly Different
		Zone	p<0.01	Significantly Different

Study Site	Metal	Bonferroni Comparison	Probability>F	Interpretation
Mississippi Canyon 496	Ba	FF vs. MF	p<0.03	Significantly Different
		NF vs. FF	p<0.03	Significantly Different
		NF vs. MF	p<0.03	Significantly Different
Ewing Bank 963	Ba	FF vs. MF	p<0.03	Significantly Different
		NF vs. FF	p<0.03	Significantly Different
		NF vs. MF	p>0.18	Not Significantly Different
Green Canyon 112	Ba	FF vs. MF	p<0.03	Significantly Different
		NF vs. FF	p<0.03	Significantly Different
		NF vs. MF	p<0.03	Significantly Different

Study Site	Metal	Main Effect	Probability>F	Interpretation
Mississippi Canyon 496	Mn	Cruise	p<0.01	Significantly Different
		Zone	p<0.04	Significantly Different
Ewing Bank 963	Mn	Cruise	p<0.01	Significantly Different
		Zone	p<0.01	Significantly Different
Green Canyon 112	Mn	Cruise	p>0.43	Not Significantly Different
		Zone	p<0.01	Significantly Different

Study Site	Metal	Bonferroni Comparison	Probability>F	Interpretation
Mississippi Canyon 496	Mn	FF vs. MF	p>0.95	Not Significantly Different
		NF vs. FF	p>0.09	Not Significantly Different
		NF vs. MF	p>0.51	Not Significantly Different
Ewing Bank 963	Mn	FF vs. MF	p>0.95	Not Significantly Different
		NF vs. FF	p<0.03	Significantly Different
		NF vs. MF	p>0.03	Significantly Different
Green Canyon 112	Mn	FF vs. MF	p<0.03	Significantly Different
		NF vs. FF	p<0.03	Significantly Different
		NF vs. MF	p<0.03	Significantly Different

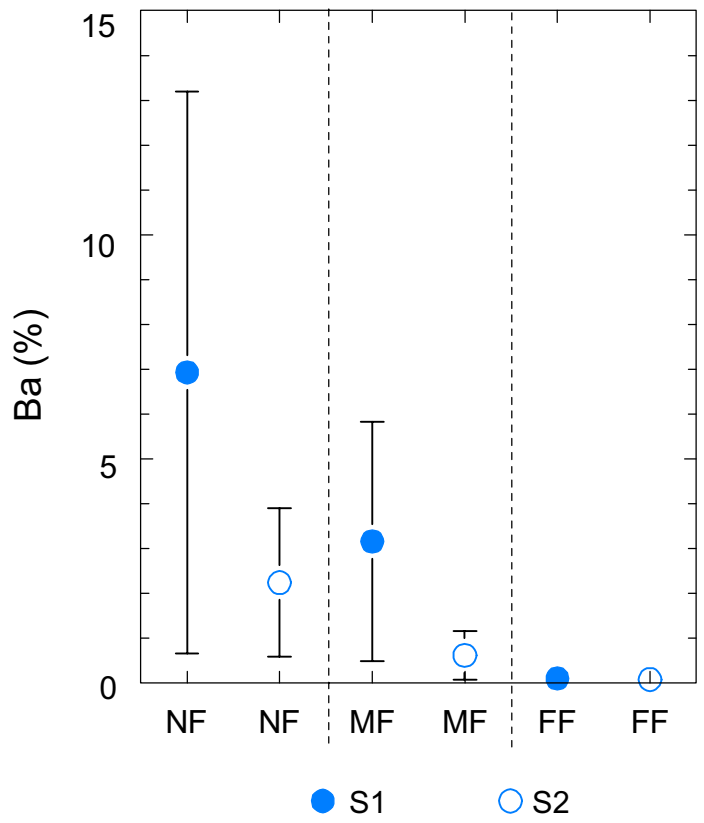

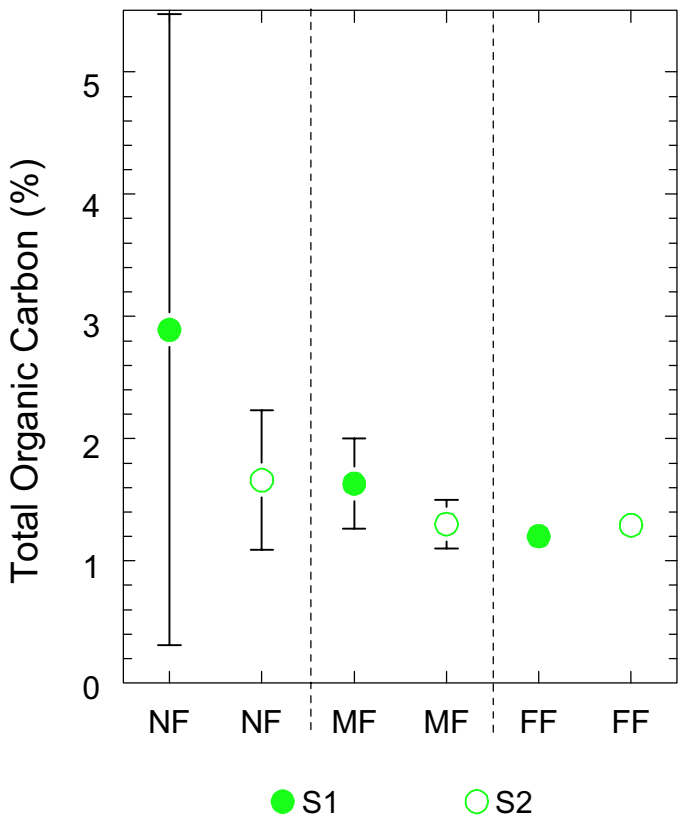

Figure 9-11. Means (circles) and standard deviations (solid lines) for concentrations of barium (Ba) and total organic carbon in surface sediments (0 to 2 cm) from random stations in near-field (NF), mid-field (MF), and far-field (FF) zones at Mississippi Canyon 496 for Sampling Cruises 1 and 2 (S1 and S2).

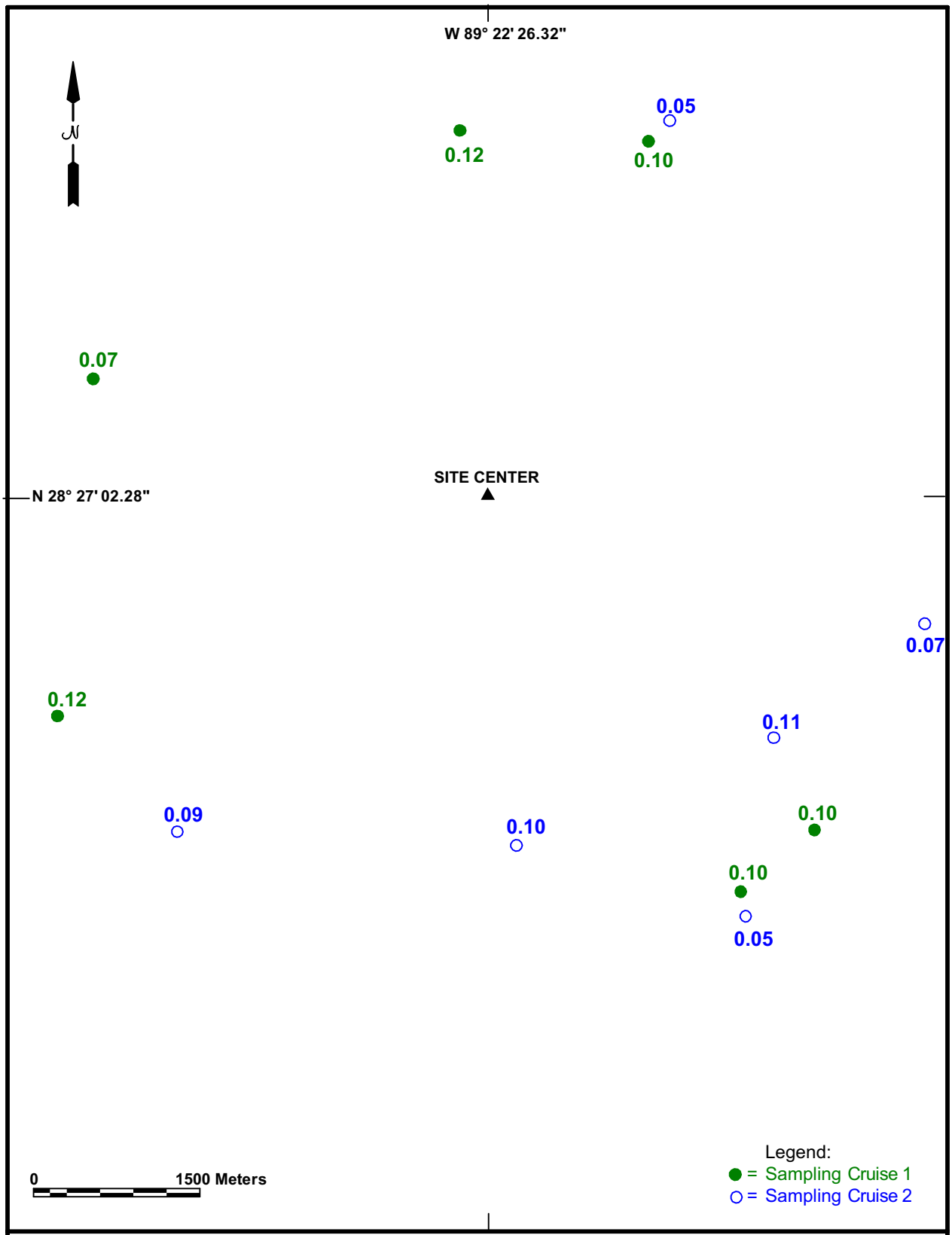

Figure 9-12. Concentrations of barium (Ba [%]) at far-field stations from Mississippi Canyon 496 for Sampling Cruises 1 and 2.

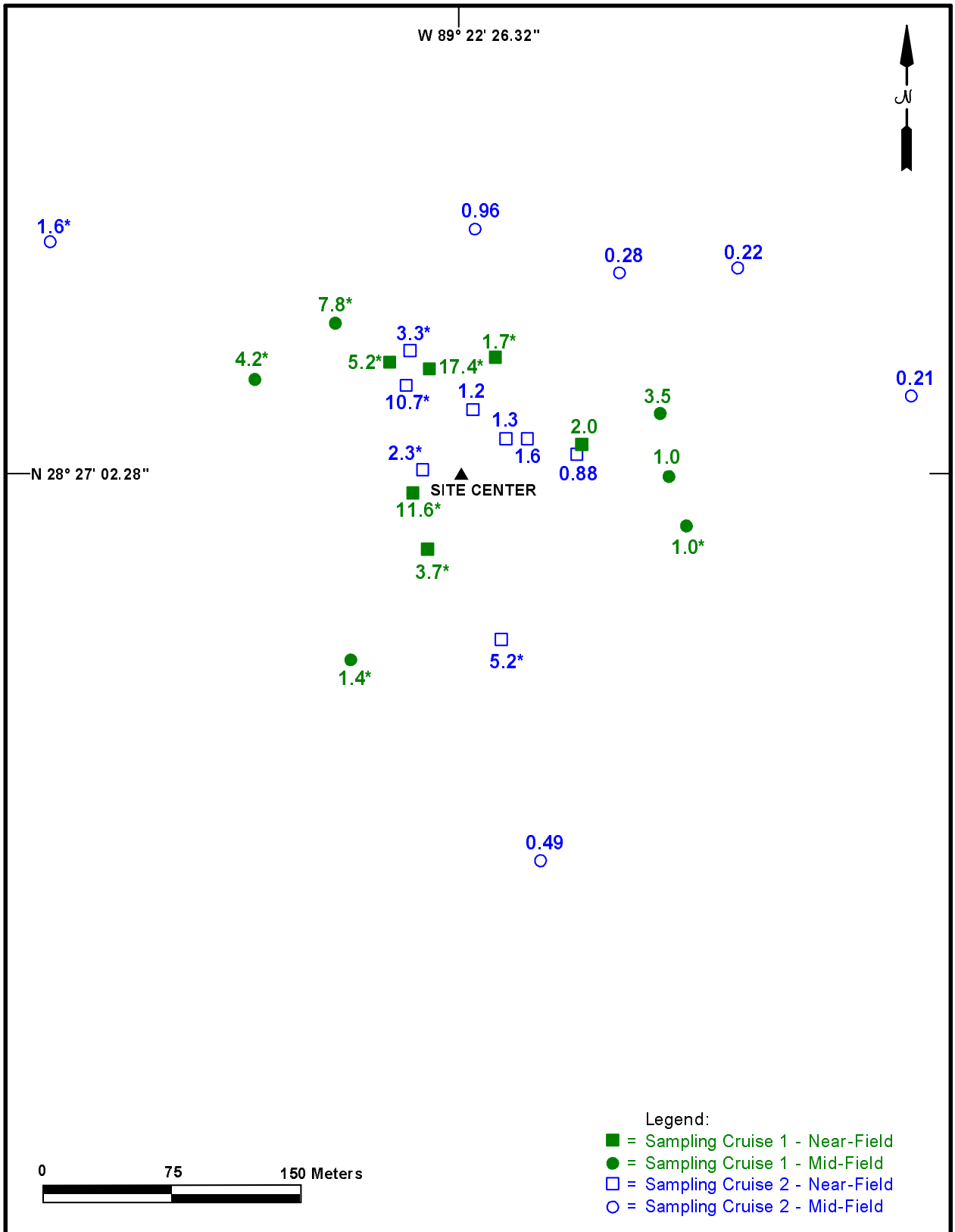

Figure 9-13. Concentrations of barium (Ba [%]) at near-field (including discretionary) and mid-field stations from Mississippi Canyon 496 for Sampling Cruises 1 and 2. Asterisks denote sediments with >0.01% synthetic based fluid.

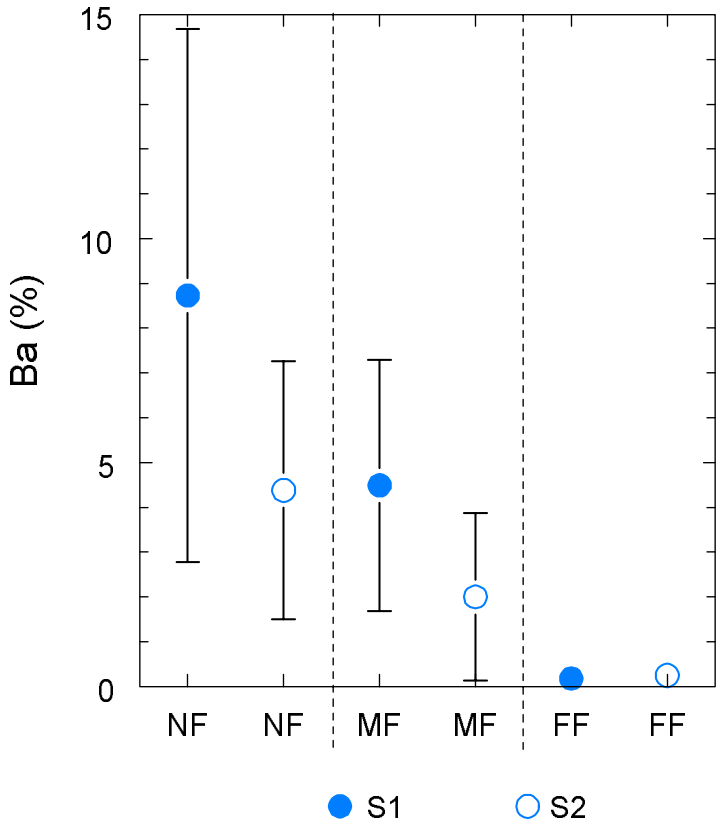

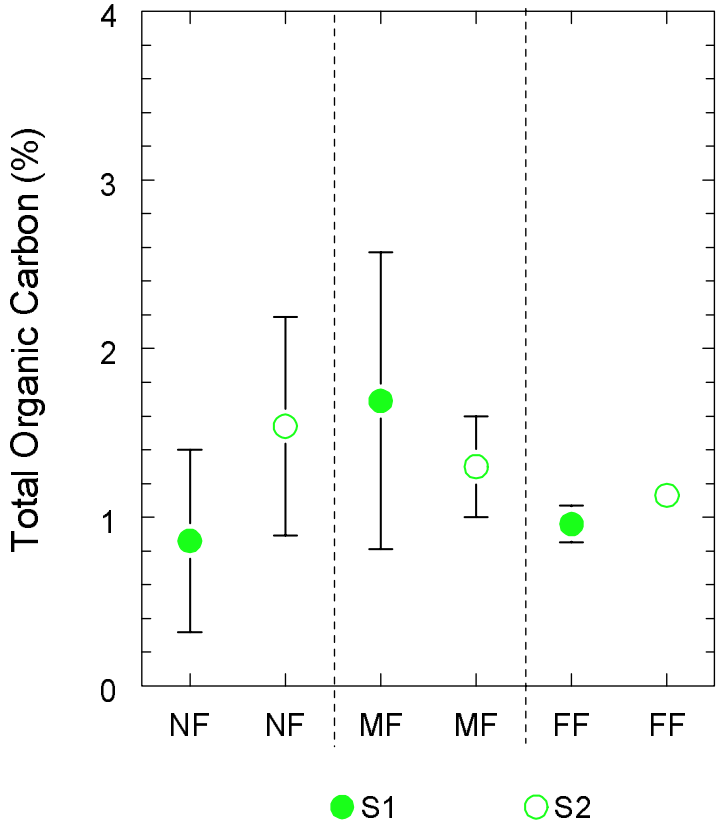

Figure 9-14. Means (circles) and standard deviations (solid lines) for concentrations of barium (Ba) and total organic carbon in surface sediments (0 to 2 cm) from random stations in near-field (NF), mid-field (MF), and far-field (FF) zones at Ewing Bank 963 for Sampling Cruises 1 and 2 (S1 and S2).

Table 9-8. Means, standard deviations (SD), minimums (Min.), and maximums (Max.) for surface (0 to 2 cm) sediment from near-field (NF), mid-field (MF), and far-field (FF) random stations at Ewing Bank 963 (n=6 for all data points) for Sampling Cruises 1 and 2 (S1 and S2).

Ewing Bank 963	Al (%)	Al (%)	Ba (%)	Ba (%)	Fe (%)	Fe (%)	Mn (µg/g)	Mn (µg/g)	TOC (%)	TOC (%)
NF	S1	S2	S1	S2	S1	S2	S1	S2	S1	S2
Mean	5.84	7.67	8.73	4.38	2.97	3.78	1,020	4,990	0.86	1.54
SD	2.26	0.67	5.95	2.88	1.11	0.29	554	4,080	0.54	0.65
Min.	2.88	6.70	0.483	0.407	1.77	3.50	311	2,050	0.38	1.15
Max.	8.95	8.59	16.2	8.79	4.33	4.30	1,770	12,700	1.87	2.80
MF	S1	S2	S1	S2	S1	S2	S1	S2	S1	S2
Mean	7.97	7.80	4.49	2.00	3.45	4.14	7,210	10,780	1.69	1.30
SD	1.57	0.21	2.80	1.87	0.38	0.61	4,590	4,490	0.88	0.30
Min.	6.74	7.52	0.984	0.450	3.03	3.83	2,430	3,560	0.82	1.06
Max.	11.0	8.14	8.13	5.15	4.03	5.39	12,800	15,600	3.13	1.89
FF	S1	S2	S1	S2	S1	S2	S1	S2	S1	S2
Mean	7.82	8.05	0.176	0.247	3.61	3.93	5,620	10,800	0.96	1.13
SD	0.35	0.17	0.066	0.114	0.20	0.05	3,230	3,930	0.11	0.06
Min.	7.29	7.81	0.074	0.177	3.28	3.87	1,880	6,080	0.85	1.03
Max.	8.31	8.23	0.279	0.464	3.81	4.00	10,500	16,400	1.16	1.20

Concentrations of Ba were <0.3 % at all far-field stations except FF-1 (Sampling Cruise 2), where the Ba content of the sediment was 0.46% (Figure 9-15). The relative importance of natural diagenetic causes versus drilling discharges for elevated Ba levels in far-field sediments is difficult to determine without more detailed study. Barium levels were >1% in surface sediments at 21 of 26 near-field and mid-field stations (Figure 9-16). Concentrations of Ba were >5% in surface sediments at seven near-field and four mid-field stations (Figure 9-16). Levels of SBF were >0.01% in surface sediments at 14 of the 26 near-field and mid-field stations (Figure 9-16). In the deeper water at EW 963, elevated concentrations of Ba and SBF at mid-field stations extended to greater distances from the site center than those observed at the shelf sites.

Barium concentrations in surface sediments at near-field stations from GC 112 averaged 12.1% for Sampling Cruise 1 and 11.8% for Sampling Cruise 2 (Table 9-9). Barium levels at near-field stations (overall mean = 12%) were significantly higher than at mid-field stations (overall mean = 4.6%) and far-field stations (overall mean = 0.45%) (Tables 9-7 and 9-9). In each case, no significant differences in Ba levels were observed within a given zone between cruises (Table 9-7 and Figure 9-17). Levels of Al and Fe were correspondingly 20% to 40% lower in the near-field sediments relative to far-field sediments (Table 9-9). Concentrations of Mn at near-field stations averaged about ten times lower than at far-field stations, whereas TOC levels at near-field stations were about double those at far-field stations (Table 9-9 and Figure 9-17), a trend observed at all three slope sites.

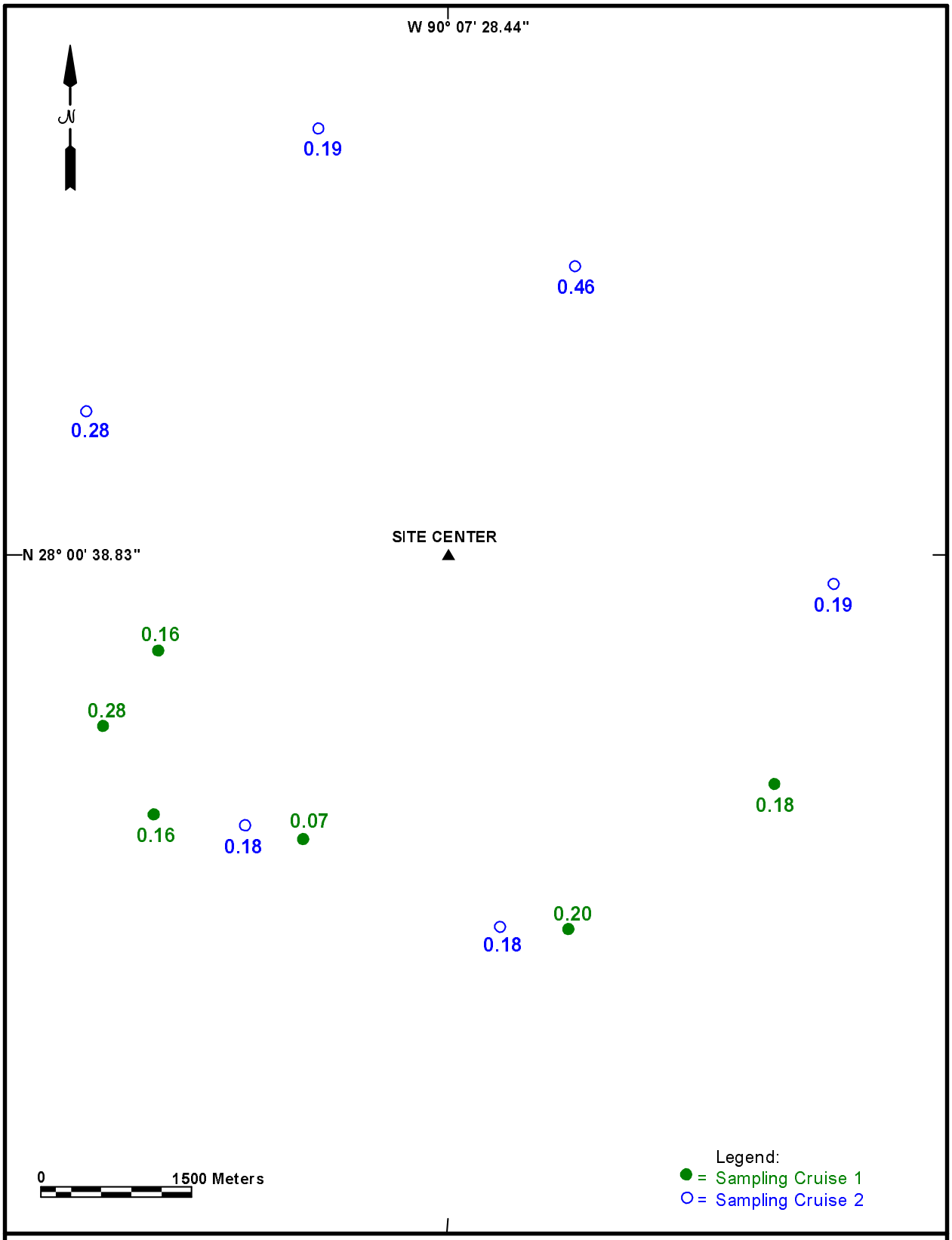

Figure 9-15. Concentrations of barium (Ba [%]) at far-field stations from Ewing Bank 963 for Sampling Cruises 1 and 2.

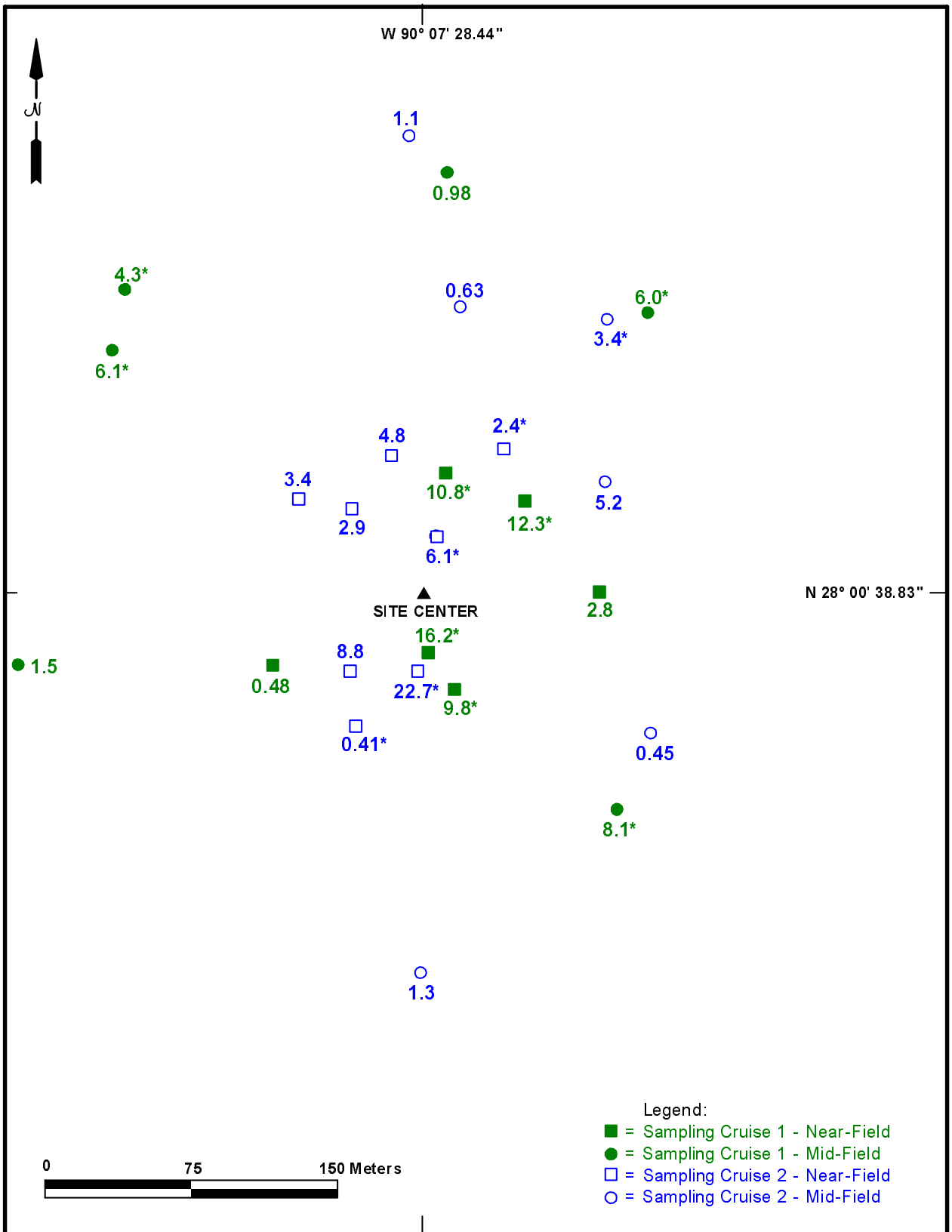

Figure 9-16. Concentrations of barium (Ba [%]) at near-field (including discretionary) and mid-field stations from Ewing Bank 963 for Sampling Cruises 1 and 2. Asterisks denote sediments with >0.01% synthetic based fluid.

Table 9-9. Means, standard deviations (SD), minimums (Min.), and maximums (Max.) for surface (0 to 2 cm) sediment from near-field (NF), mid-field (MF), and far-field (FF) random stations at Green Canyon 112 (n=6 for all data points) for Sampling Cruises 1 and 2 (S1 and S2).

Green Canyon 112	Al (%)	Al (%)	Ba (%)	Ba (%)	Fe (%)	Fe (%)	Mn (µg/g)	Mn (µg/g)	TOC (%)	TOC (%)
NF	S1	S2	S1	S2	S1	S2	S1	S2	S1	S2
Mean	4.99	6.36	12.1	11.8	2.39	3.10	661	662	1.55	1.92
SD	1.90	0.62	5.47	4.73	0.60	0.39	278	793	1.17	0.62
Min.	2.65	5.55	4.79	2.90	1.32	2.65	247	293	0.61	1.02
Max.	7.46	7.42	21.4	15.4	2.94	3.83	981	2,280	3.75	2.76
MF	S1	S2	S1	S2	S1	S2	S1	S2	S1	S2
Mean	7.24	7.04	2.82	6.40	3.11	3.44	2,890	3,400	1.37	1.62
SD	0.51	1.39	2.81	8.78	0.42	0.61	3,330	2,980	0.55	0.62
Min.	6.36	4.24	0.189	0.406	2.36	2.22	537	265	0.93	0.97
Max.	7.59	7.84	7.18	24.1	3.54	3.79	8,640	7,670	2.08	2.79
FF	S1	S2	S1	S2	S1	S2	S1	S2	S1	S2
Mean	7.58	7.76	0.612	0.288	3.58	3.68	5,790	6,590	1.06	0.89
SD	0.24	0.09	0.394	0.123	0.59	0.15	3,150	1,620	0.18	0.14
Min.	7.27	7.63	0.098	0.091	3.20	3.44	890	3,750	0.73	0.64
Max.	7.86	7.88	1.28	0.393	4.73	3.87	10,100	8,290	1.22	1.05

Overall, Ba levels in surface sediments for far-field stations at GC 112 were higher than at other sites, with five values >0.5%, four of which were at stations to the northeast (Figure 9-18). These five values may be related to dispersion of drilling discharges to greater distances at this deeper water site, or they may have been derived from five wells drilled in adjacent blocks GC 66, 67, and 69. All but two of the values for Ba at near-field and mid-field stations were >1% (Figure 9-19). Fifteen of the 26 Ba concentrations were >5%; however, only one of these values was found at a mid-field station. Levels of SBF were >0.01% at 18 stations, including six mid-field stations (Figure 9-19). Especially striking are results for NF-1 (Sampling Cruise 1) with 11% Ba and 0.004% SBF relative to Station NF-4 (Sampling Cruise 1) with 21.4% Ba and 6.3% SBF.

9.4 METALS AND TOTAL ORGANIC CARBON IN SEDIMENT CORES

Sediment cores provide a third dimension to the overall distribution patterns for drilling discharges and key parameters in sediments. At every site, a 3-cm diameter subcore was collected from the box core, extruded, and briefly examined to describe the different layers of sediment. The depth of penetration of the subcore was generally ~40 cm. The results of these observations are presented in Tables 9-10 and 9-11. These field data provide an additional resource to help explain observations from other aspects of the study. For example, sediment samples for toxicity testing and infaunal organisms were collected from the top 5 cm or more of the sediment column, whereas only the top 2 cm were investigated for chemical parameters in most instances. In some cases, the depth of sediment containing drilling discharges was limited to 1 or 2 cm, whereas in others it extended to depths >20 cm. The descriptive data also help with interpretation of the vertical profiles for concentrations of metals, SBF, oxygen, and redox in sediments as well as the SPI data.

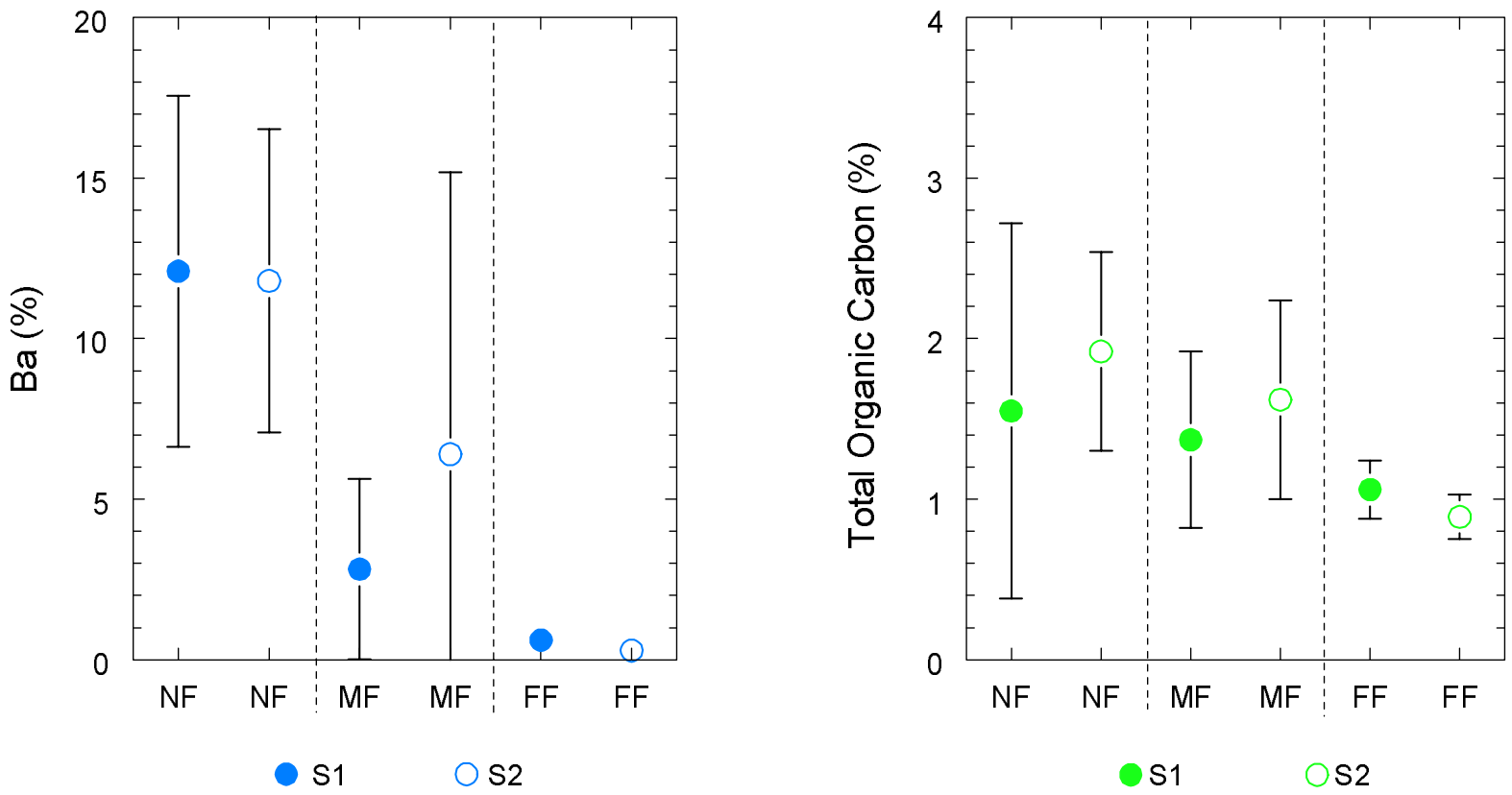

Figure 9-17. Means (circles) and standard deviations (solid lines) for concentrations of barium (Ba) and total organic carbon in surface sediments (0 to 2 cm) from random stations in near-field (NF), mid-field (MF), and far-field (FF) zones at Green Canyon 112 for Sampling Cruises 1 and 2 (S1 and S2).

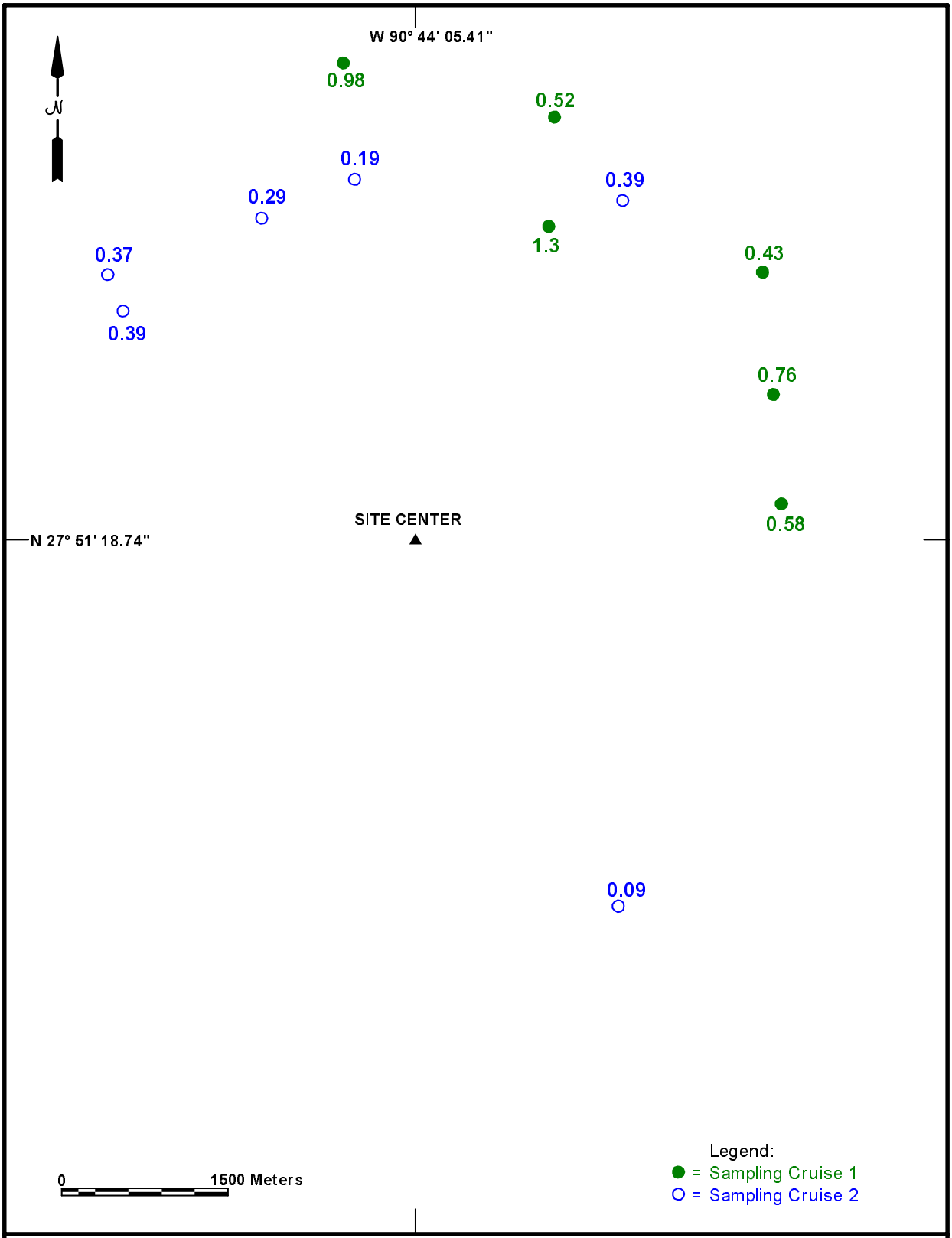

Figure 9-18. Concentrations of barium (Ba [%]) at far-field stations from Green Canyon 112 for Sampling Cruises 1 and 2.

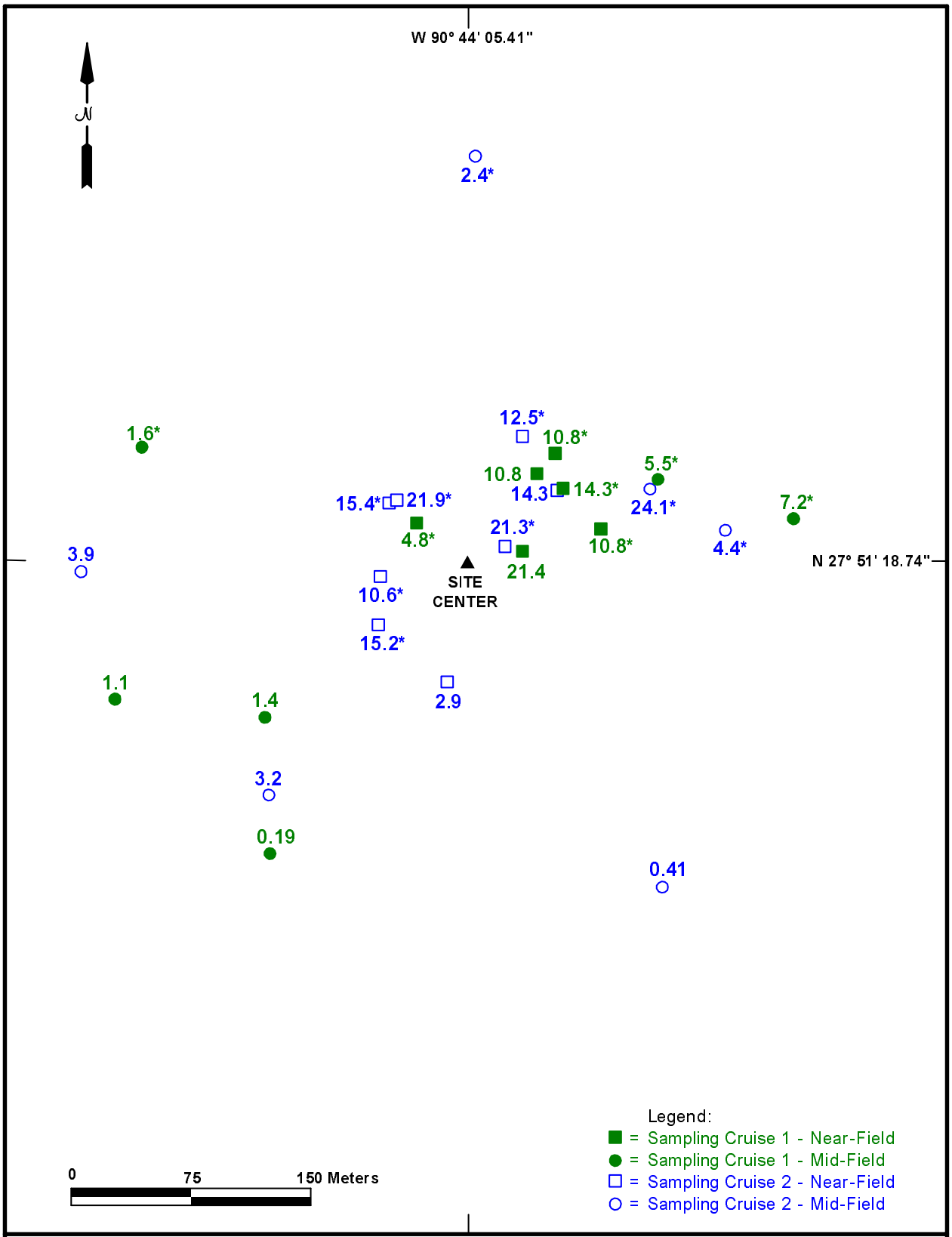

Figure 9-19. Concentrations of barium (Ba [%]) at near-field (including discretionary) and mid-field stations from Green Canyon 112 for Sampling Cruises 1 and 2. Asterisks denote sediments with >0.01% synthetic based fluid.

Table 9-10. Descriptions of sediment column for Sampling Cruise 1 (May 2001).

Site	Station	Thickness of Surface Oxic Layer (cm)	Black Layer (cm)	Other Layers (cm)	Depth at Start of Mississippi Delta Clay (cm)	Comments (* denotes table column to which comment applies)
Main Pass 299	NF-1	0	0-10	10-22*	22	Transition zone
	NF-2	<0.5	<0.5-11.5	11.5-19*	19	Transition zone
	NF-3	0	0-8	8-11*	11	Transition zone
	NF-4	<0.5	<0.5-6.5*	-	6.5	Minor black streaks
	NF-5	<0.5	<0.5-15	15-20*	20	Transition zone
	NF-6	0	0-15	-	15	
	MF-1	<0.5	–	-	<0.5	
	MF-2	<0.5	<0.5-14*	-	14	Some black mottled layers
	MF-3	<0.5	-	-	<0.5	
	MF-4	<0.2	<0.2-8	-	8	
	MF-5	<0.5	-	-	<0.5	
	MF-6	<0.5	<0.5-3	3-10*	10	Black streaks at 3-10 cm
	FF-1-6	<0.5	-	-	<0.5	
Main Pass 288	NF-1	<0.5	<0.5-18	-	18	
	NF-2	<0.2	<0.2-14	14-16*	16	Transition zone
	NF-3	3	3-5	-	8	
	NF-4	<0.2	<0.2-14	14-16*	16	Transition zone
	NF-5	<0.2	<0.2-6	6-18*	18	Transition zone
	NF-6	<0.5	<0.5-8.5	8.5-14*	14	Transition zone
	MF-1	1.0	1-12	1-5*	17	Olive black
	MF-2	0	-	-	0	
	MF-3	<0.5	<0.5-12*	-	12	Mottled
	MF-4	1	1-16*	-	16	Olive with some black
	MF-5	<0.5	<0.5-17	-	17	
	MF-6	<0.5	<0.5-15	-	15	
	FF-1	<0.5	-	-	-	Sandy
	FF-2	0	-	-	0	
	FF-3	<0.5	-	-	-	Sandy/gravelly
	FF-4	0	-	-	0	
	FF-5	0*	-	-	0	Top disturbed
	FF-6	0	-	-	-	Coarse, sandy with gray fine fraction
Eugene Island 346	NF-1*	0	0->30*	-	-	0-14 cm black, fine-grained, 14-30 cm coarse-grained, mostly black, 30 cm black-stained clay
	NF-2	<0.5	-	<0.5-8*	8	Black-stained, gray clay
	NF-4	3	3-13	-	13	
	NF-5	0	-	0-15*	15	0-8 cm black and coarse, 8-15 cm black and clayey

Table 9-10. (Continued).

Site	Station	Thickness of Surface Oxic Layer (cm)	Black Layer (cm)	Other Layers (cm)	Depth at Start of Mississippi Delta Clay (cm)	Comments (* denotes table column to which comment applies)
Eugene Island 346 (cont.)	NF-6	0	-	0-8*	8	0-5 cm black-stained clay, 5-8 cm minor black staining
	MF-1	0	0-19.5	-	19.5	
	MF-2	<0.2	<0.2-4	-	4	
	MF-3	0	-	0-9*	9	0-0.5 cm gray, 0.5-5 cm black, medium coarse, 5-9 cm black-stained clay
	MF-4	<0.2	-	-	>0.2	
	MF-5	<0.1	<0.1-2	2-10*	10	Transition zone
	MF-6	-	18.5	-	18.5	
	FF-1-6	<0.5	-	-	<0.5	
Mississippi Canyon 496	NF-1	<0.5	<0.5-5	-	5	
	NF-2	<0.5	<0.5-4*	-	4	Mottled, obvious black drilling mud in top 1-4 cm
	NF-3	<0.5	<0.5-4	-	4	
	NF-4	<0.5	<0.5-8	-	8	
	NF-5	<0.5	<0.5-8	-	8	
	NF-6	<0.5	<0.5-5.5*	-	<0.5	Distinct gray, minor black streaks
	MF-1	1	-	1-5*	5	Stiff, clumpy clay; no obvious black
	MF-2	<0.5	<0.5-3.5*	-	<0.5	Small, black streaks
	MF-3	<0.5	<0.5-5	-	5	
	MF-4	1	-	-	1*	Signs of drilling mud on corer, not sample
	MF-5	1	1-3*	-	3	Mottled
	MF-6	<0.5	<0.5-8	-	8	
	FF-1	<0.5	-	-	<0.5	
	FF-2	<0.5	-	-	<0.5	
	FF-3	<0.5	-	0.5-5*	5	Stiff, clumpy clay
	FF-4	<0.5	-	-	<0.5	
	FF-5	<0.5	-	-	<0.5	
	FF-6	<0.5	-	0.5-8*	<0.5	Stiff, clumpy clay
Ewing Bank 963	NF-1	<0.5	<0.5-2	2-25*	25	2-5 cm tan, 5.5-12 cm dark gray/black, 12-13 cm tan, 13-17 cm light gray, 17-25 cm deep brown w/black highlights
	NF-2	<0.5	<0.5-5	-	5	

Table 9-10. (Continued).

Site	Station	Thickness of Surface Oxic Layer (cm)	Black Layer (cm)	Other Layers (cm)	Depth at Start of Mississippi Delta Clay (cm)	Comments (* denotes table column to which comment applies)
Ewing Bank 963 (cont.)	NF-4	0	0-21*	-	21	0-8 cm black with obvious clumps, 8-15 cm dark black, 15-21 cm black/gray
	NF-5	<0.5	<0.5-6	6-8*	8	Brown
	NF-6	<0.5	<0.5-6	6-13*	13	6-9 cm black/tan, 9-13 cm dark brown (as in NF-1)
	MF-1	<0.5	<0.5-2	-	2	
	MF-2	<0.5	<0.5-5	5-6.5*	6.5	Transition zone
	MF-3	1	1-3*	-	3	Minor black streaks
	MF-4	<0.5	-	-	<0.5	
	MF-5	<0.5	<0.5-3	-	3	
	FF-1-6	0.5-1	-	-	1	
Green Canyon 112	NF-1	0	0-23	-	23	
	NF-2	<0.5	<0.5-13	-	13	
	NF-3	0	0-8	0-3*	11	Tan/light brown
	NF-4	0	-	0-23*	23	0-10 cm black, 10-20 cm tan, overall strong H_2S smell
	NF-5	0	0-10*	-	10	0-5 cm black, 5-10 cm black mud
	NF-6	0	7-13	0-7*	13	0-7 cm tan mud, 7-13 cm black mud
	MF-1	<0.5	<0.5-13	-	13	
	MF-2	<0.5	<0.5-7	-	7	
	MF-3	1	-	-	1	
	MF-4	7	-	-	7	
	MF-5	2	2-4	-	6	
	FF-1	5	-	-	5	
	FF-2	<0.5	-	<0.5-13*	13	Gray/brown
	FF-3	9	-	-	9	
	FF-4	1.5	-	1.5-2.5*	2.5	Gray/brown
	FF-5	6	-	-	6	
	FF-6	<0.2	-	<0.2-11*	11	0.2-4.5 cm dark brown, 4.5-11 cm light brown

Table 9-11. Descriptions of sediment column for Sampling Cruise 2 (May 2002).

Site	Station	Thickness of Surface Oxic Layer (cm)	Black Layer (cm)	Other Layers (cm)	Depth at Start of Mississippi Delta Clay (cm)	Comments (* denotes table column to which comment applies)
Main Pass 299	DISC-1	1	1-5*	-	5	Black patches
	DISC-2	1.5	1.5-10.5	-	10.5	
	NF-1	1	-	-	1.0	
	NF-2	1	-	1-4*	4	Brown clay w/ black streaks
	NF-3	5.0	-	5-11* 17-20*	5	Brown with black streaks
	NF-4-6	1	-	-	1	
	MF-1	0	-	-	0	
	MF-2	0.2	-	-	0.2	
	MF-3	0.1	-	-	0.1	
	MF-4	<0.1	-	-	<0.1	
	MF-5	0	-	-	0	
	MF-6	0	-	0-6*	6	Gray clay with black streaks
	FF-1	1	-	1-3*	3	Brown clay
	FF-2-3	0	-	-	0	
	FF-4	3	-	-	3	
	FF-5	<0.5	-	-	<0.5	
	FF-6	5	-	-	5	
Main Pass 288	DISC-1	<0.5	-	-	<0.5	
	DISC-2-1	0	-	-	0	Black patches
	DISC-2-2	3	-	3-10*	10	Gray clay with black patches
	NF-1	0	-	0-5*	5	Gray clay with black streaks
	NF-2	<0.5	-	<0.5-7*	7	Gritty; gray clay with black patches
	NF-3	0.1	-	-	0.1	
	NF-4	0	-	-	0	
	NF-5-6	<0.5	-	-	<0.5	
	MF-1	<0.5	<0.5-9	-	9	
	MF-2	0.5	-	-	0.5	
	MF-3	<0.5	-	-	<0.5	
	MF-4	<0.5	-	<0.5-10*	10	Black streaks
	MF-5	<0.5	5-7	<0.5-7*	7	Gray clay
	MF-6	<0.5	-		<0.5	
	FF-1	0	-	-	22	0-8 cm sandy, 8-22 cm silty clay
	FF-2	0	-	-	-	Sandy
	FF-3	<0.5	-	-	-	Olive gray, sandy
	FF-4-5	0			0	
	FF-6	<0.5			<0.5	

Table 9-11. (Continued).

Site	Station	Thickness of Surface Oxic Layer (cm)	Black Layer (cm)	Other Layers (cm)	Depth at Start of Mississippi Delta Clay (cm)	Comments (* denotes table column to which comment applies)
Eugene Island 346	DISC-1	0	0-14	-	14	
	DISC-2	0.5	<0.5-8.5	-	8.5	
	NF-1	0	1-14	0-1*	14	Gritty, gray/brown
	NF-2	<0.5	<0.5-8	-	8	
	NF-3	<0.5	<0.5-13	-	13	
	NF-5	0	0-8	-	8	
	MF-1	1	-	-	1	
	MF-2	0	-	0-2.5*	2.5	0-1.5 brown/gray layer, 1.5-2.5 gray/black layer
	MF-3	1	-	-	1	
	MF-4	0.2	0.2-17	-	17	
	MF-5	1	1-8	-	8	
	MF-6	0	-	0-4*	4	Gray/brown
	FF-1	1	-	-	1	
	FF-2	1	-	-	1	
	FF-3	0.5	-	-	0.5	
	FF-4	1	-	-	1	
	FF-5	2	-	-	2	
	FF-6	1.5	-	-	1.5	
Mississippi Canyon 496	DISC-1	0.5	-		0.5	
	DISC-2	<0.5	<0.5-3	-	3	
	NF-1	<0.5	-	-	<0.5	
	NF-2	1	-	-	1	
	NF-3	<0.5	<0.5-3	3-3.2*	3.2	Light brown
	NF-4	<0.5	1-6	<0.5-1*	6	Gray
	NF-5	1	-	-	1	
	NF-6	1	-	-	1	
	MF-1	1	-	-	1	
	MF-2-5	1	-	-	1	
	MF-6	1	2-8	1-2*	8	Gray
	FF-1	1	-	1-5*	5	Brown/gray clay
	FF-2	2.0	-	-	2	
	FF-3	1	-	-	1	
	FF-4	2	-	-	2	
	FF-5	<0.5	-	<0.5-6*	6	Clumpy, sticky, gray/olive clay
	FF-6	2	-	2-8*	8	Brown/gray clay
Ewing Bank 963	DISC-1	0	-	0-7*	7	Sticky, gray/olive clay
	DISC-2	0	0-13	-	13	Black streaks to 20 cm
	NF-1, 4	1	-	-	1	
	NF-2	1	-	1-10*	10	Gray w/ black/brown streaks

Table 9-11. (Continued).

Site	Station	Thickness of Surface Oxic Layer (cm)	Black Layer (cm)	Other Layers (cm)	Depth at Start of Mississippi Delta Clay (cm)	Comments (* denotes table column to which comment applies)
Ewing Bank 963 (cont.)	NF-5	0	-	0-8*	8	Gray with black patches
	NF-6	1	-	-	1	
	MF-1	1.5	-	-	1.5	
	MF-2	2.5	-	2.5-6*	6	Transition zone
	MF-3	1	-	1-4*	4	Brown/gray
	MF-4	<0.5	-	<0.5-6	6	Gray with black streaks
	MF-5	3	-	-	3	
	MF-6	1	-	-	1	
	FF-1	3	-	-	3	
	FF-2	1.5	-	-	1.5	
	FF-3	2	-	-	20	
	FF-4	4	-	-	4	
	FF-5	1.5	-	-	1.5	
	FF-6	2.	-	-	2	
Green Canyon 112	DISC-1	0	0-14	-	14	
	DISC-2	<1	<1-9	-	9	
	NF-1	1	1-8	-	8	
	NF-2	<1	-	<1-11*	11	Gritty, gray with black streaks
	NF-3	0.1	1-6, 10-14	<0.1-1* 6-10*	14	Gray
	NF-4	0.5	0.5-13	-	13	
	NF-5	0.2	1-6	0.2-1*	6	Gray
	NF-6	<0.5	<0.5-5, 10-13	5.0-10*	13	Gray
	MF-1	<0.5	-	<0.5-4*	4	Transition zone
	MF-2	<1	-	-	<1	
	MF-3	<0.5	-	-	<0.5	
	MF-4	<0.5	-	<0.5-6*	6	Gray, brown/black streaks
	MF-5	<0.2	<0.2-7	-	7	
	MF-6	<0.5	1.5-6	<0.5-1.5*	6	Gray/brown
	FF-1	2.5	-	-	2.5	
	FF-2	3.5	-	-	3.5	
	FF-3	2	-	2-14	14	Gritty; gray/brown
	FF-4	1.5	-	-	1.5	
	FF-5-6	3	-	-	3	

The depth of the oxic layer listed in Tables 9-10 and 9-11 was based on sediment color. The presence of a slight brownish color, rather than a gray or black color, was used as an indicator of oxic sediment. The depth of any black layer is listed because no such layers were observed in sediments from far-field stations. In most cases, such black layers were highly reducing. The black layer can be either drilling discharges or a combination of drilling discharges and reducing natural sediment bearing iron sulfides. Other layers and transitional depths also are described in Tables 9-10 and 9-11. For example, at MP 299, the sediment profile at Station NF-1 (Sampling Cruise 1, Table 9-10) was characterized by 10 cm of black material, followed by a mixture of black mud and Mississippi gray clay to a depth of 22 cm. Below a depth of 22 cm, the core contained typical Mississippi gray clay. Data for most far-field cores show the perceived depth of the oxic layer (based on color) with no additional comment, thereby implying that the core is predominantly Mississippi gray clay. In some cases (e.g., EW 963, Sampling Cruise 1, NF-1), the subcore contained a variety of distinct and different layers (Table 9-10).

In addition to the surface samples and 3-cm diameter subcores collected for core descriptions, 10-cm diameter Teflon® subcores were collected from the box core at 12 locations during Sampling Cruise 1 and 24 locations during Sampling Cruise 2. Each subcore was subdivided into five 2-cm sections. The sections were not always contiguous to ensure that sampling extended deep enough to collect what appeared to be background sediment. Five sections per core were analyzed for Al, Ba, TOC, SBF (as reported in Chapter 8), Fe, and Mn. The full data sets are given in Appendix E. Vertical profiles for 14 selected cores are given in Figures 9-20 to 9-33, and profiles for the remaining 22 cores are presented in Appendix E.

At far-field stations from MP 299, concentrations of Al, Ba, TOC, and Fe were uniform with depth, Mn levels were slightly elevated in the top-most layer, and no SBF was detected (Figure 9-20 and Appendix E). In sediment from Station NF-2 (Sampling Cruise 1), an 11.5-cm thick black layer with 0.3% Ba was observed, most likely containing drilling discharges (Table 9-10 and Appendix E). However, no SBF was detected in the core from Station NF-2 (Sampling Cruise 1, MP 299), even though Ba levels were about three times higher than expected background levels. At Station NF-1 (Sampling Cruise 2), no black layer, no elevated levels of Ba, and no SBF were found (Appendix E). During Sampling Cruise 2, cores collected from DISC–1 and DISC–2 contained 5 cm of black patches (Figure 9-21) and 10.5 cm of black mud, respectively, at the top of the core (Table 9-11). Consequently, concentrations of Ba in both discretionary cores (Sampling Cruise 2) were 0.6% to 0.8%, relative to background levels of ~0.1%, and levels of SBF were <0.01% but detectable (Figure 9-21 and Appendix E).

Far-field sediments from MP 288 also contained background levels of Ba with no detectable SBF and low levels of TOC (<1%), especially in the sandy layers (Tables 8-10 and 8-11, Figure 9-22, and Appendix E) previously described for this site. In the top 8 cm of sediment at Station NF-6 (Sampling Cruise 1, Table 9-10), the observed black layer contained elevated levels of Ba (1.2% to 3.5%), low levels of Mn (<500 µg/g), and minor amounts of SBF (~0.02% to 0.006%). A somewhat similar trend was observed for Station NF-1 (Sampling Cruise 2, Appendix E). At Station DISC-2 (Sampling Cruise 2), concentrations of Ba and SBF were slightly elevated above background levels (Figure 9-23), and no detectable change from natural conditions was found at Station DISC-1 (Sampling Cruise 2).

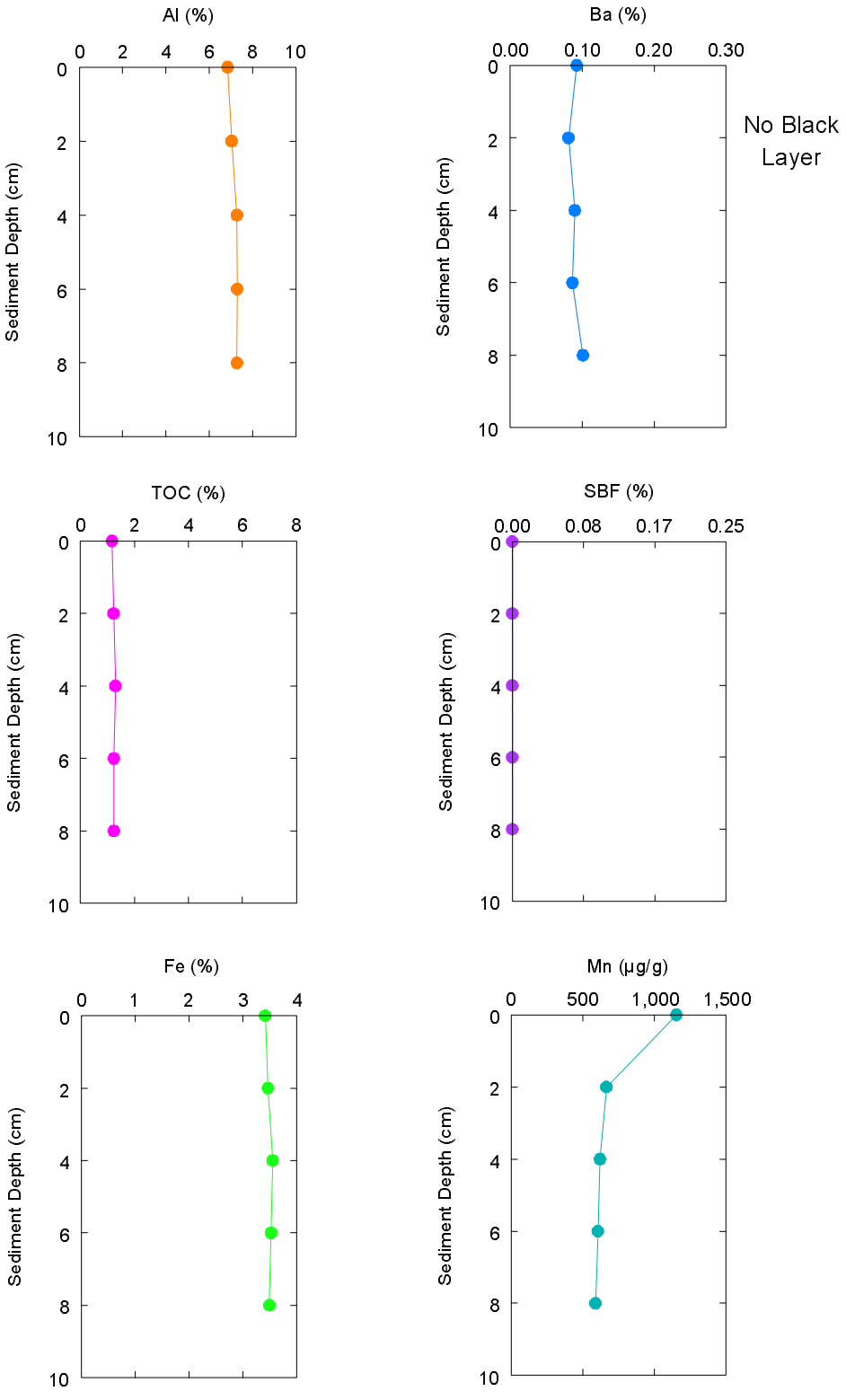

Figure 9-20. Vertical profiles for aluminum (Al), barium (Ba), total organic carbon (TOC), synthetic based fluid (SBF), iron (Fe), and manganese (Mn) in sediment from Main Pass 299, Station FF-2, Sampling Cruise 1.

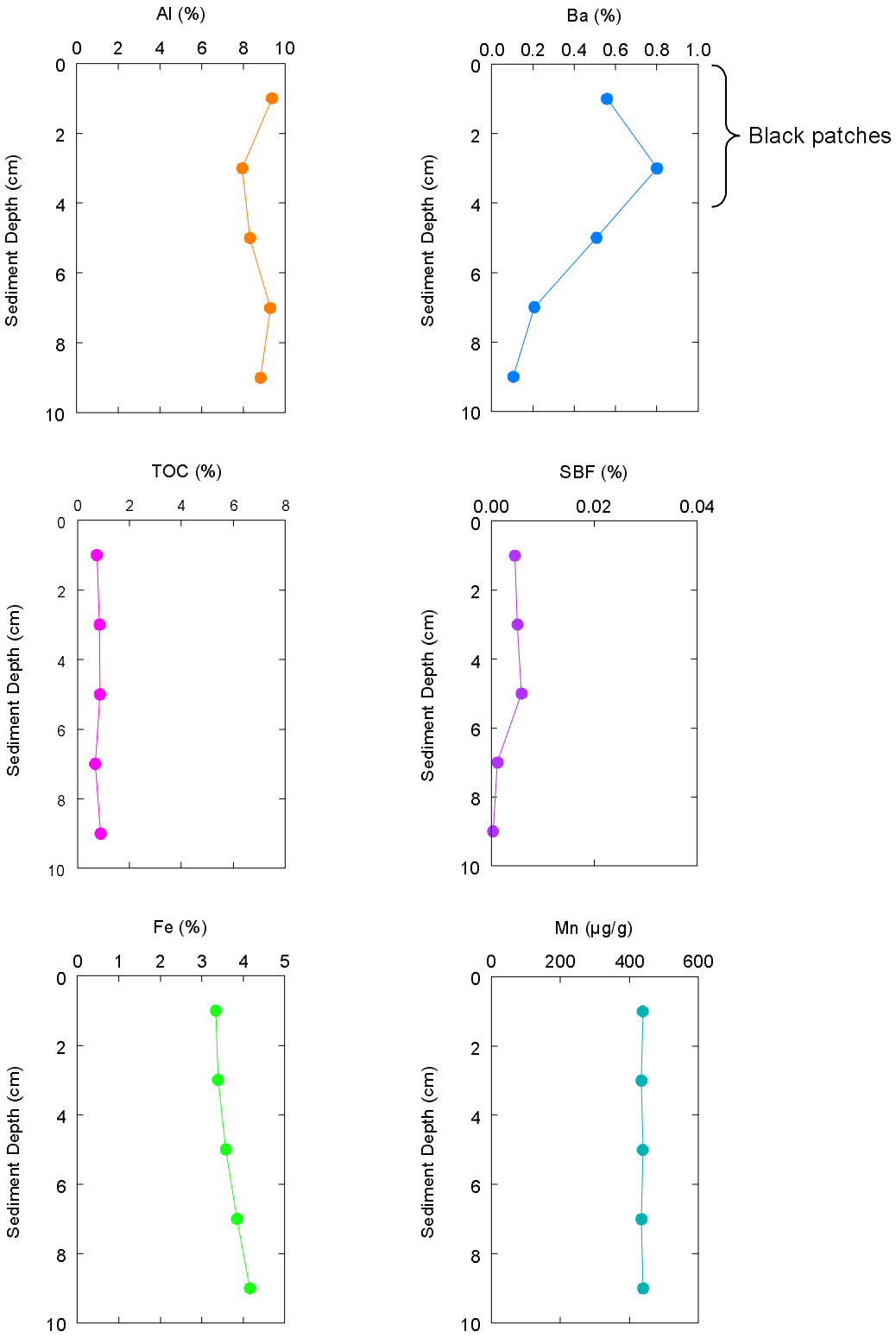

Figure 9-21. Vertical profiles for aluminum (Al), barium (Ba), total organic carbon (TOC), synthetic based fluid (SBF), iron (Fe), and manganese (Mn) in sediment from Main Pass 299, Station DISC-1, Sampling Cruise 2.

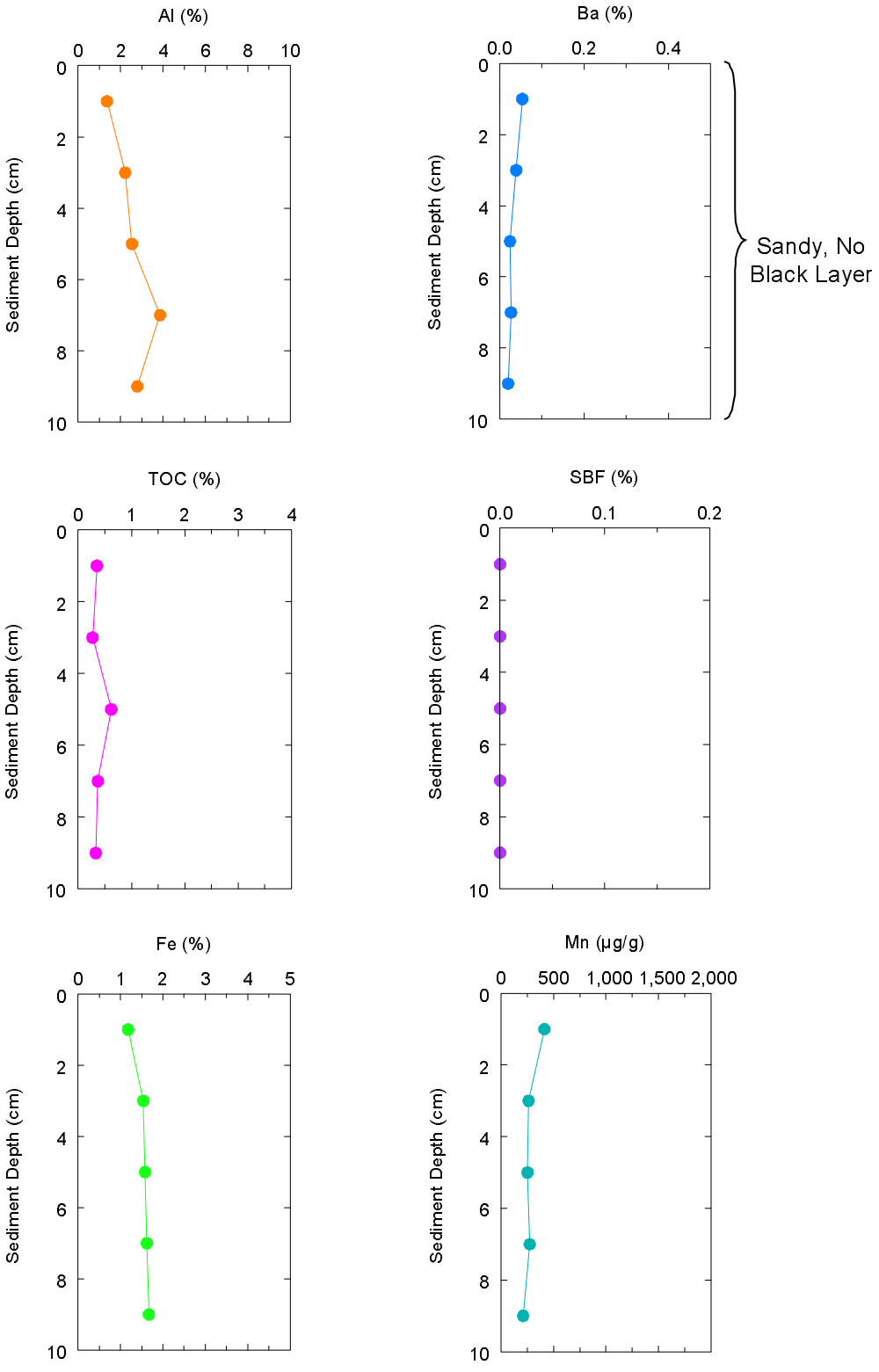

Figure 9-22. Vertical profiles for aluminum (Al), barium (Ba), total organic carbon (TOC), synthetic based fluid (SBF), iron (Fe), and manganese (Mn) in sediment from Main Pass 288, Station FF-3, Sampling Cruise 1.

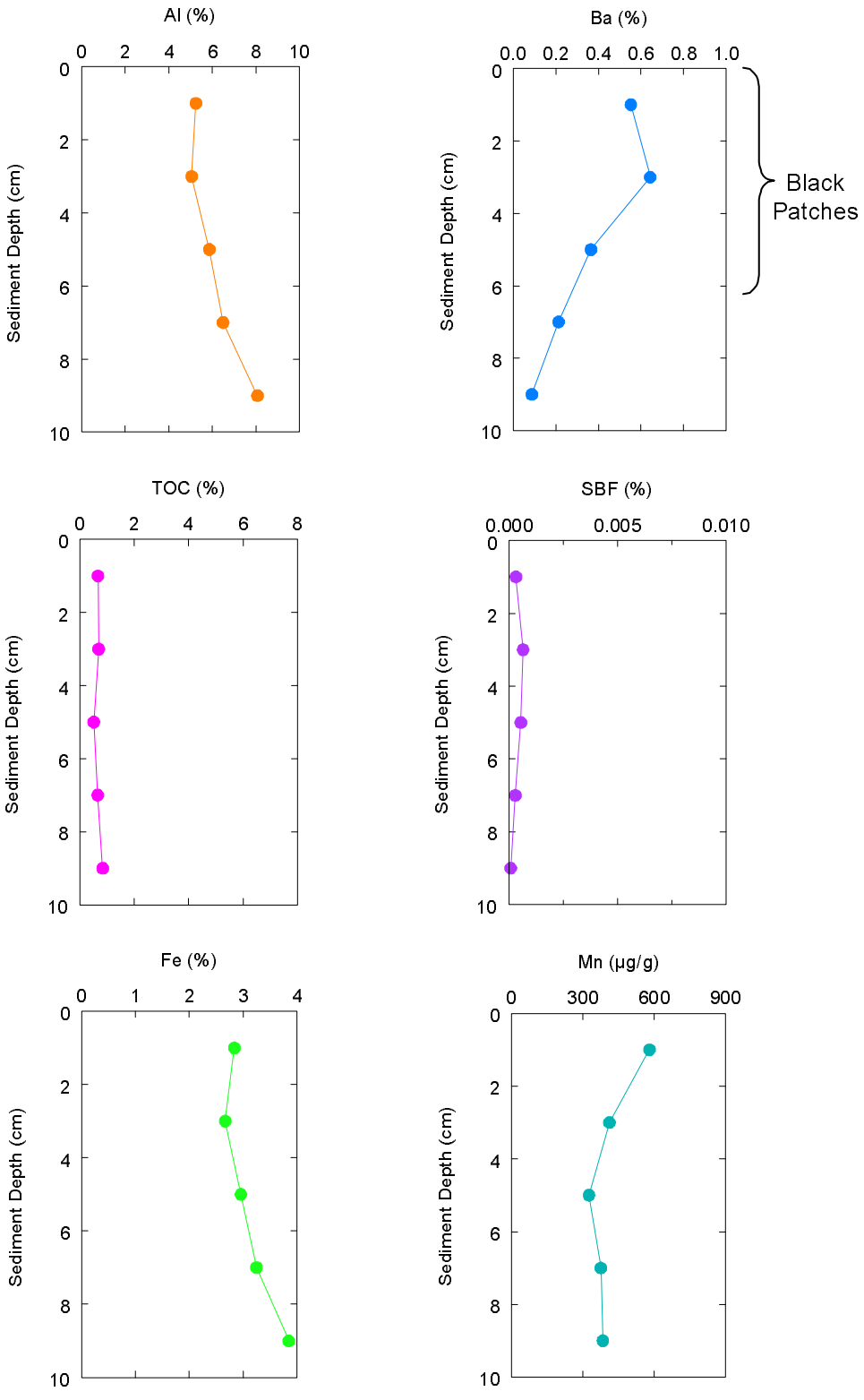

Figure 9-23. Vertical profiles for aluminum (Al), barium (Ba), total organic carbon (TOC), synthetic based fluid (SBF), iron (Fe), and manganese (Mn) in sediment from Main Pass 288, Station DISC-2, Sampling Cruise 2.

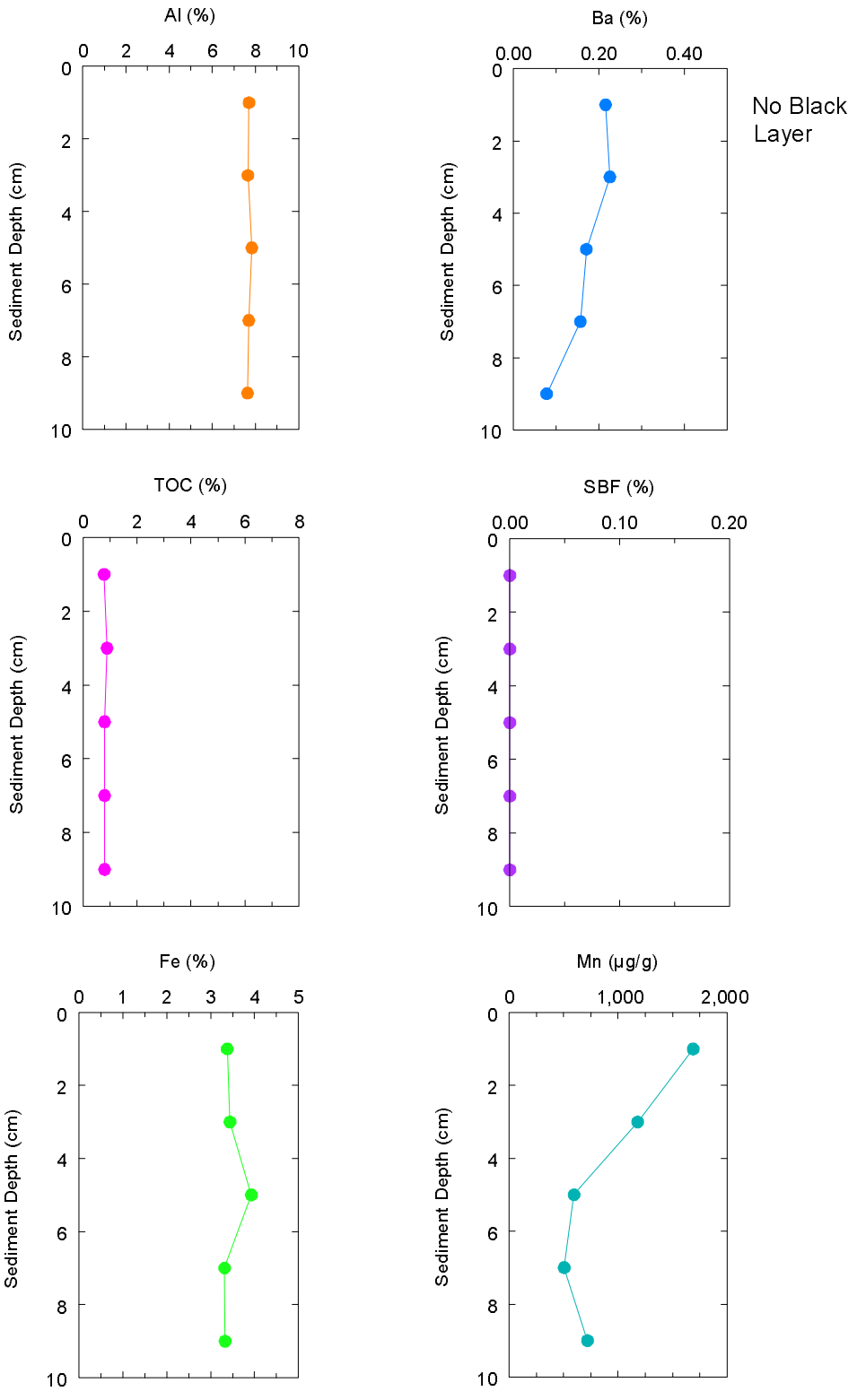

Figure 9-24. Vertical profiles for aluminum (Al), barium (Ba), total organic carbon (TOC), synthetic based fluid (SBF), iron (Fe), and manganese (Mn) in sediment from Eugene Island 346, Station FF-2, Sampling Cruise 1.

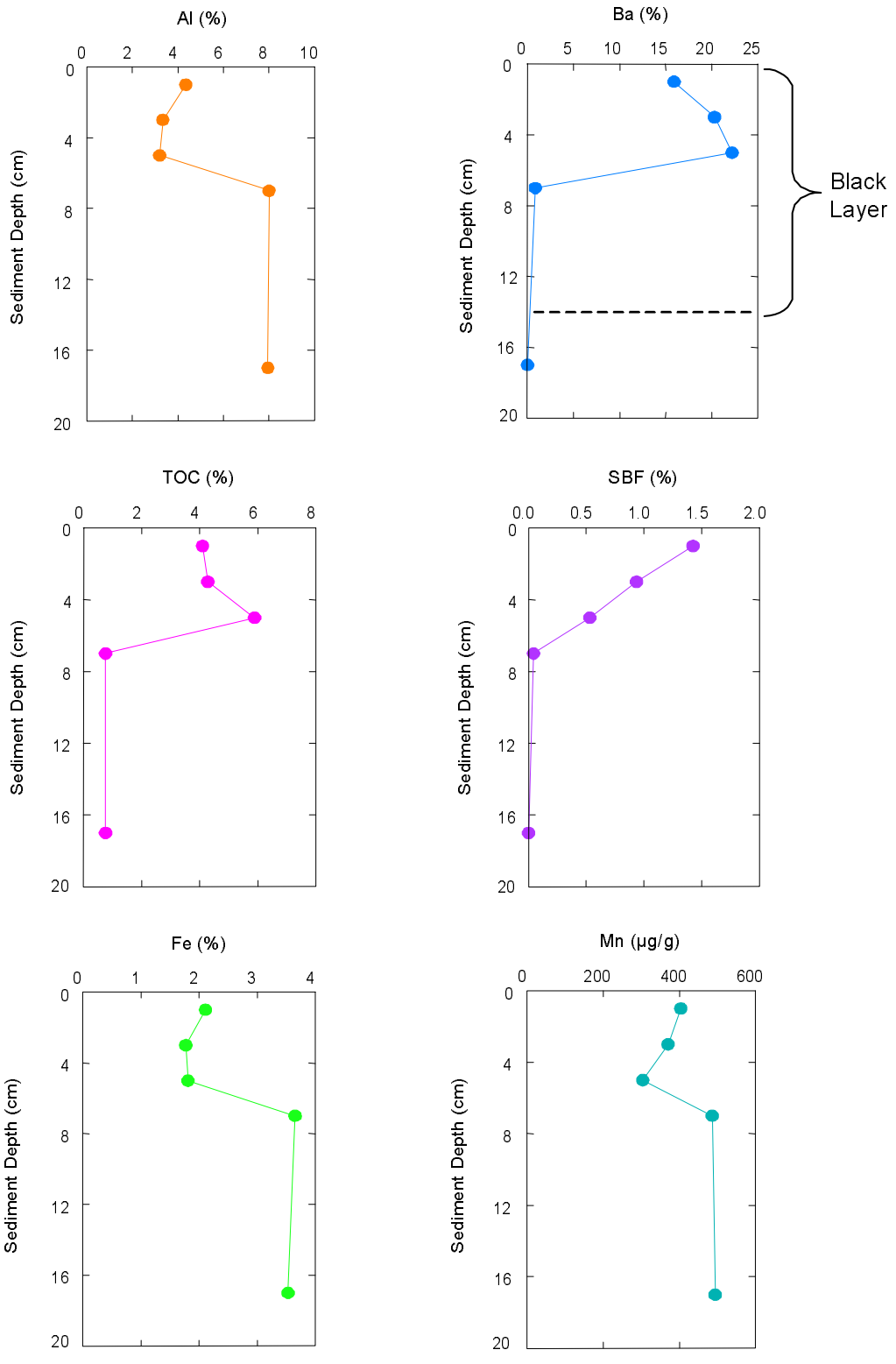

Figure 9-25. Vertical profiles for aluminum (Al), barium (Ba), total organic carbon (TOC), synthetic based fluid (SBF), iron (Fe), and manganese (Mn) in sediment from Eugene Island 346, Station DISC-1, Sampling Cruise 2.

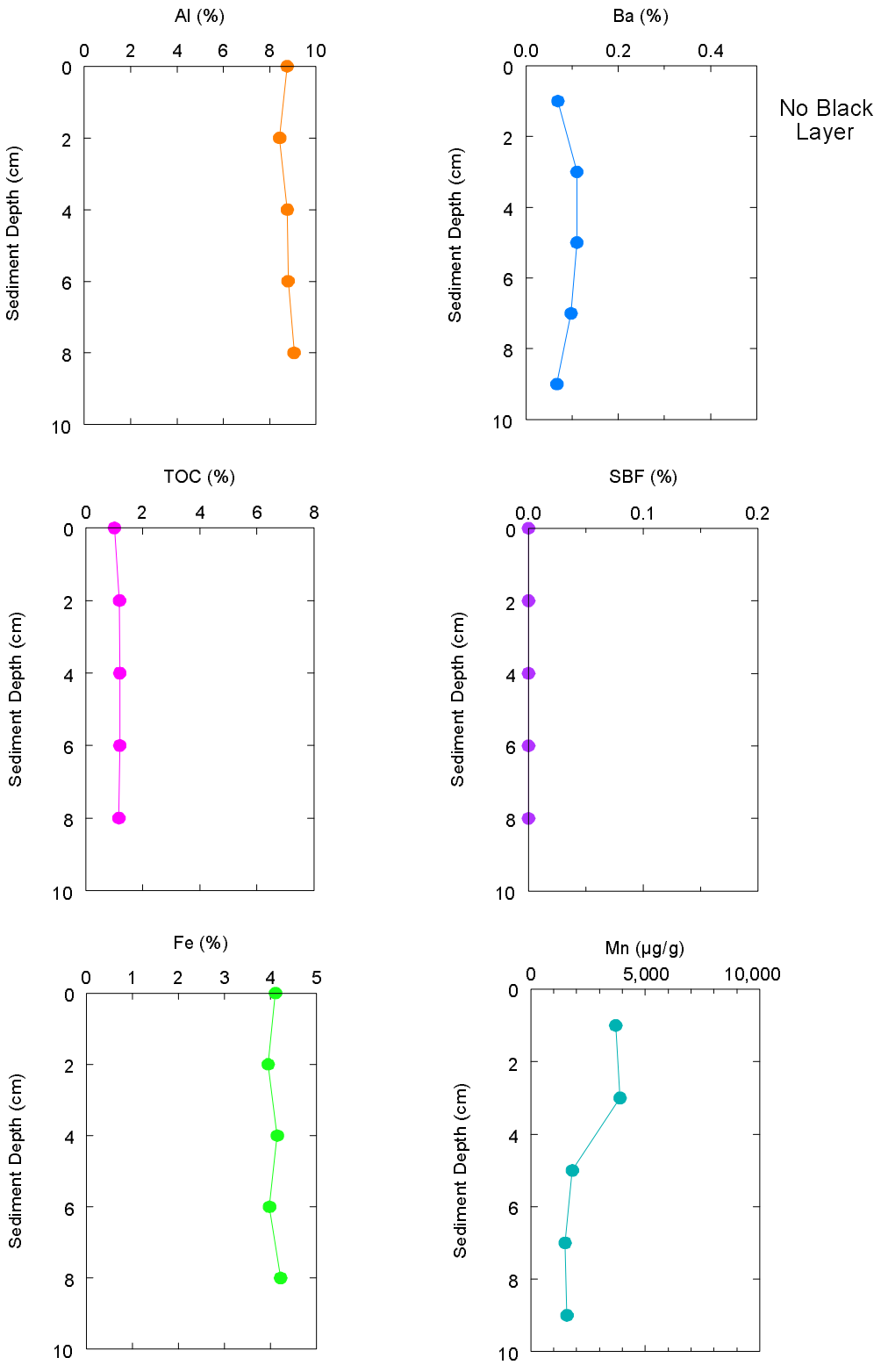

Figure 9-26. Vertical profiles for aluminum (Al), barium (Ba), total organic carbon (TOC), synthetic based fluid (SBF), iron (Fe), and manganese (Mn) in sediment from Mississippi Canyon 496, Station FF-5, Sampling Cruise 1.

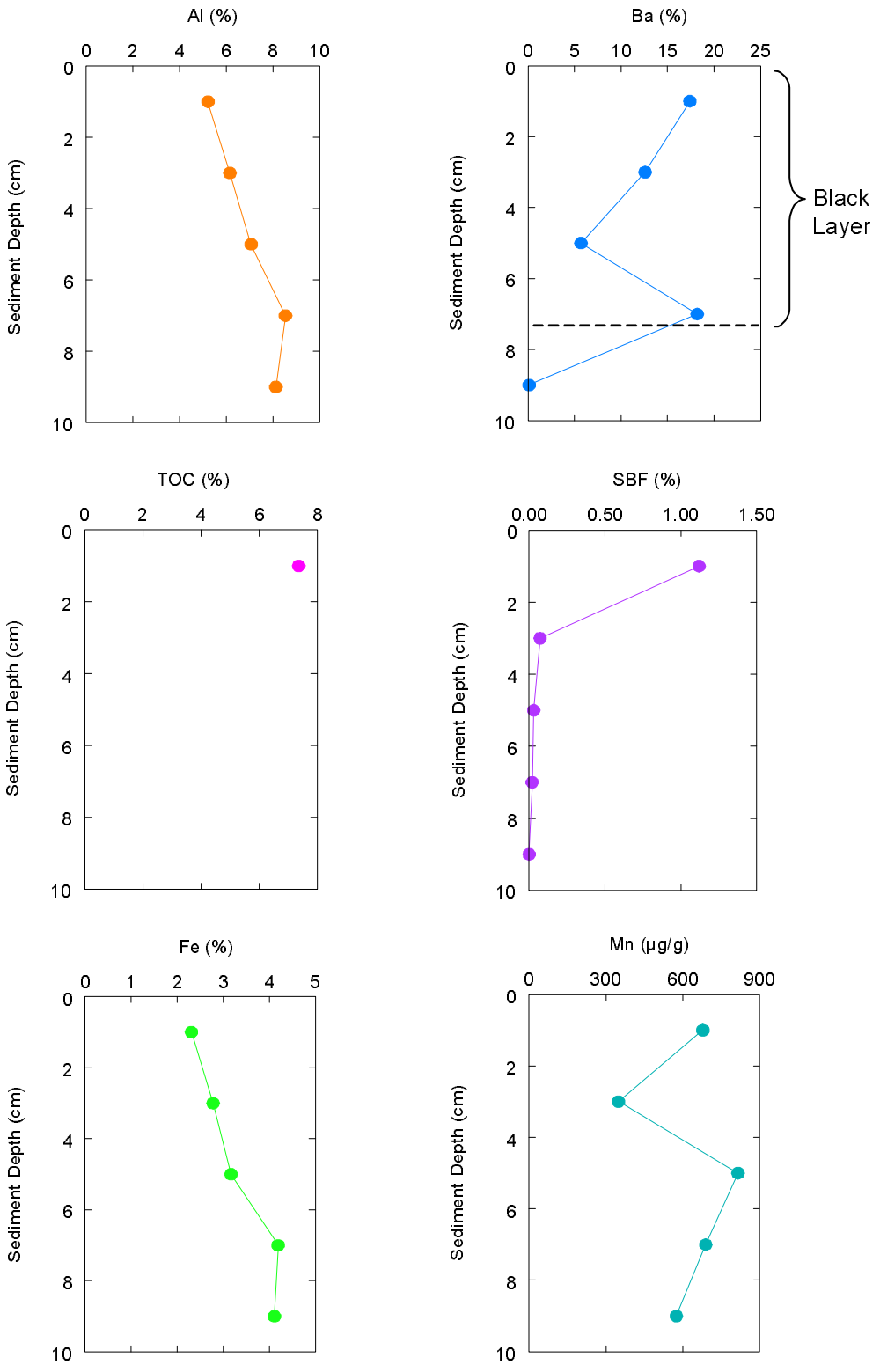

Figure 9-27. Vertical profiles for aluminum (Al), barium (Ba), total organic carbon (TOC), synthetic based fluid (SBF), iron (Fe), and manganese (Mn) in sediment from Mississippi Canyon 496, Station NF-4, Sampling Cruise 1.

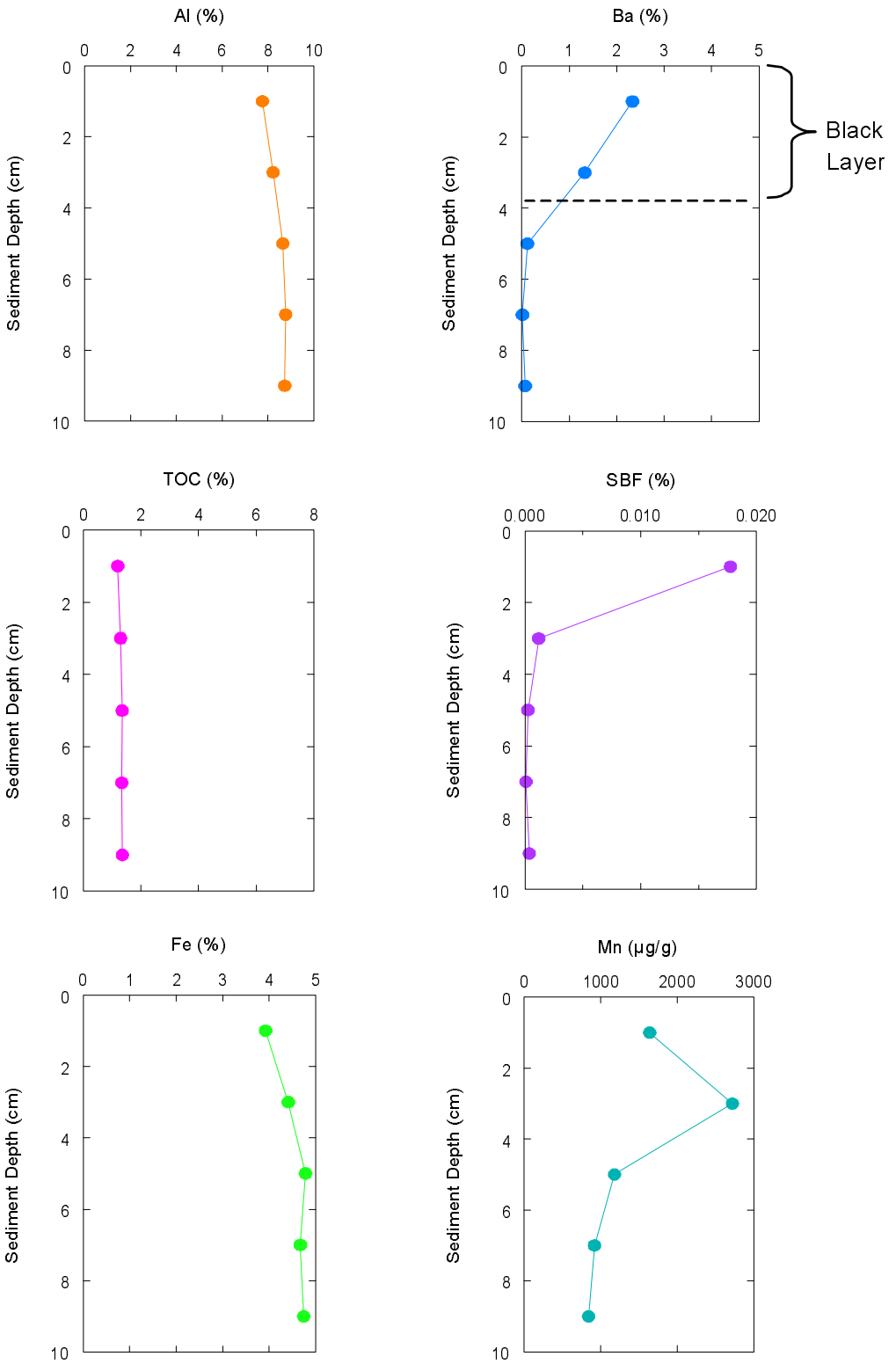

Figure 9-28. Vertical profiles for aluminum (Al), barium (Ba), total organic carbon (TOC), synthetic based fluid (SBF), iron (Fe), and manganese (Mn) in sediment from Mississippi Canyon 496, Station DISC-2, Sampling Cruise 2.

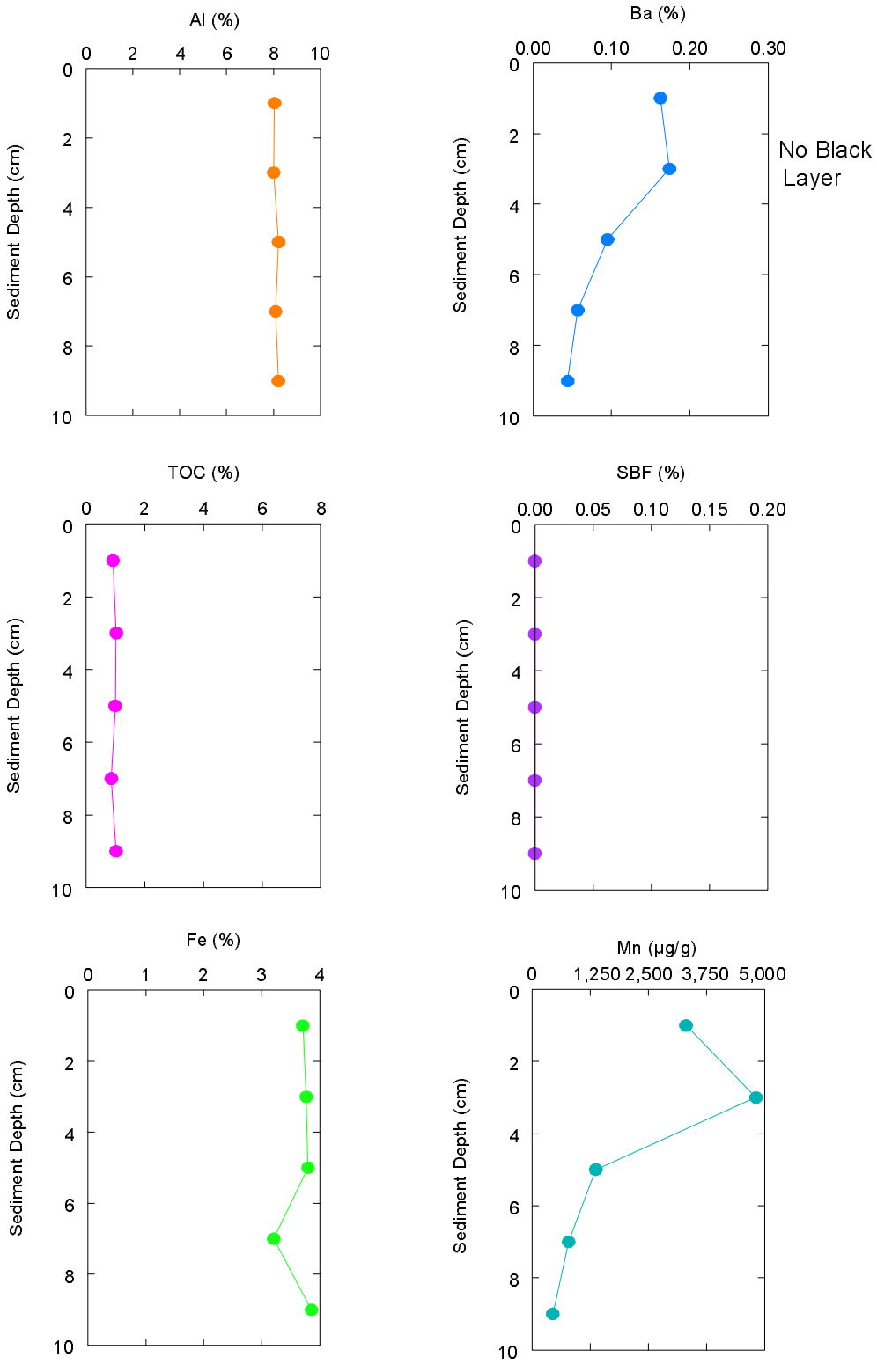

Figure 9-29. Vertical profiles for aluminum (Al), barium (Ba), total organic carbon (TOC), synthetic based fluid (SBF), iron (Fe), and manganese (Mn) in sediment from Ewing Bank 963, Station FF-5, Sampling Cruise 1.

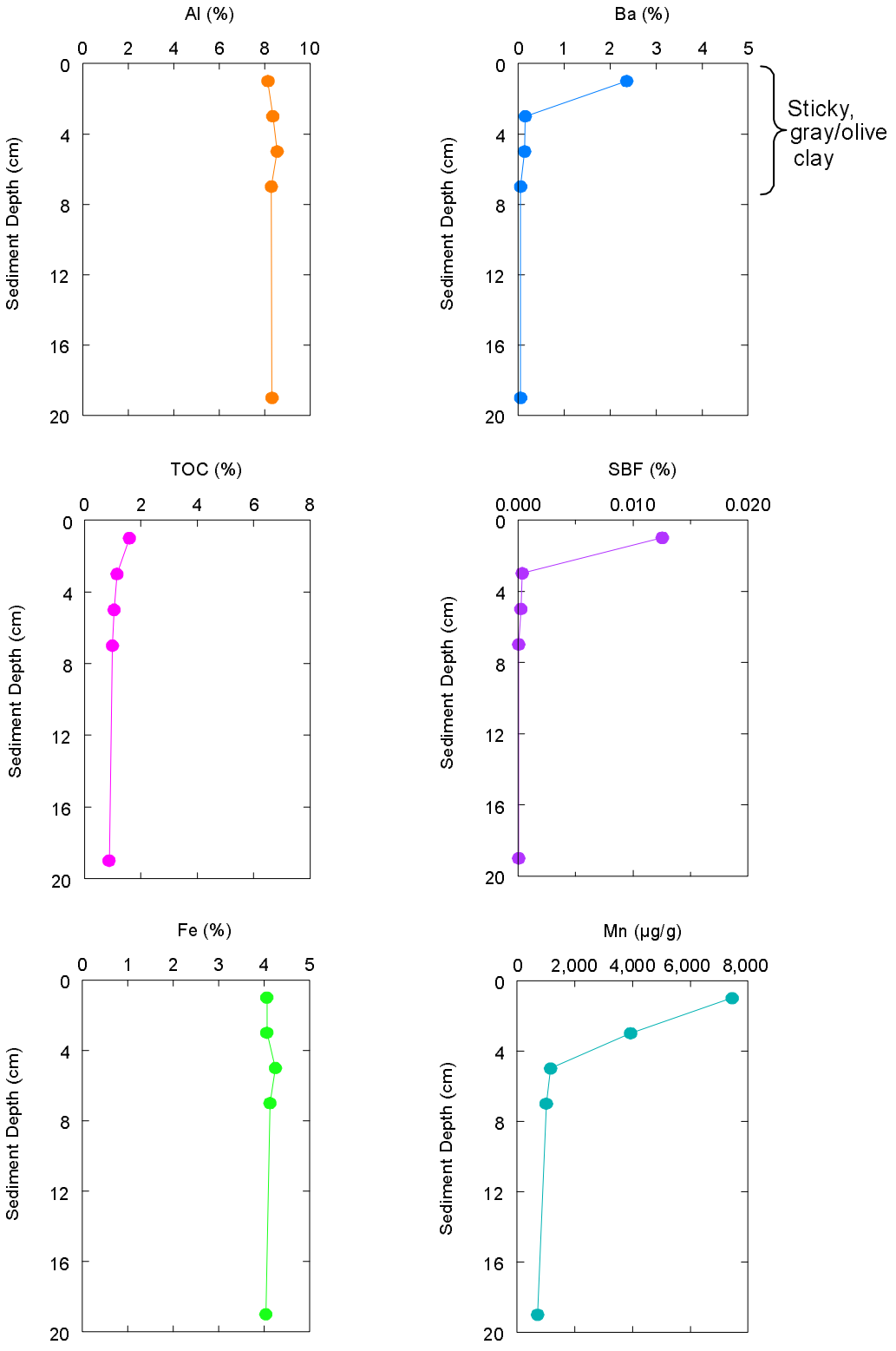

Figure 9-30. Vertical profiles for aluminum (Al), barium (Ba), total organic carbon (TOC), synthetic based fluid (SBF), iron (Fe), and manganese (Mn) in sediment from Ewing Bank 963, Station DISC-1, Sampling Cruise 2.

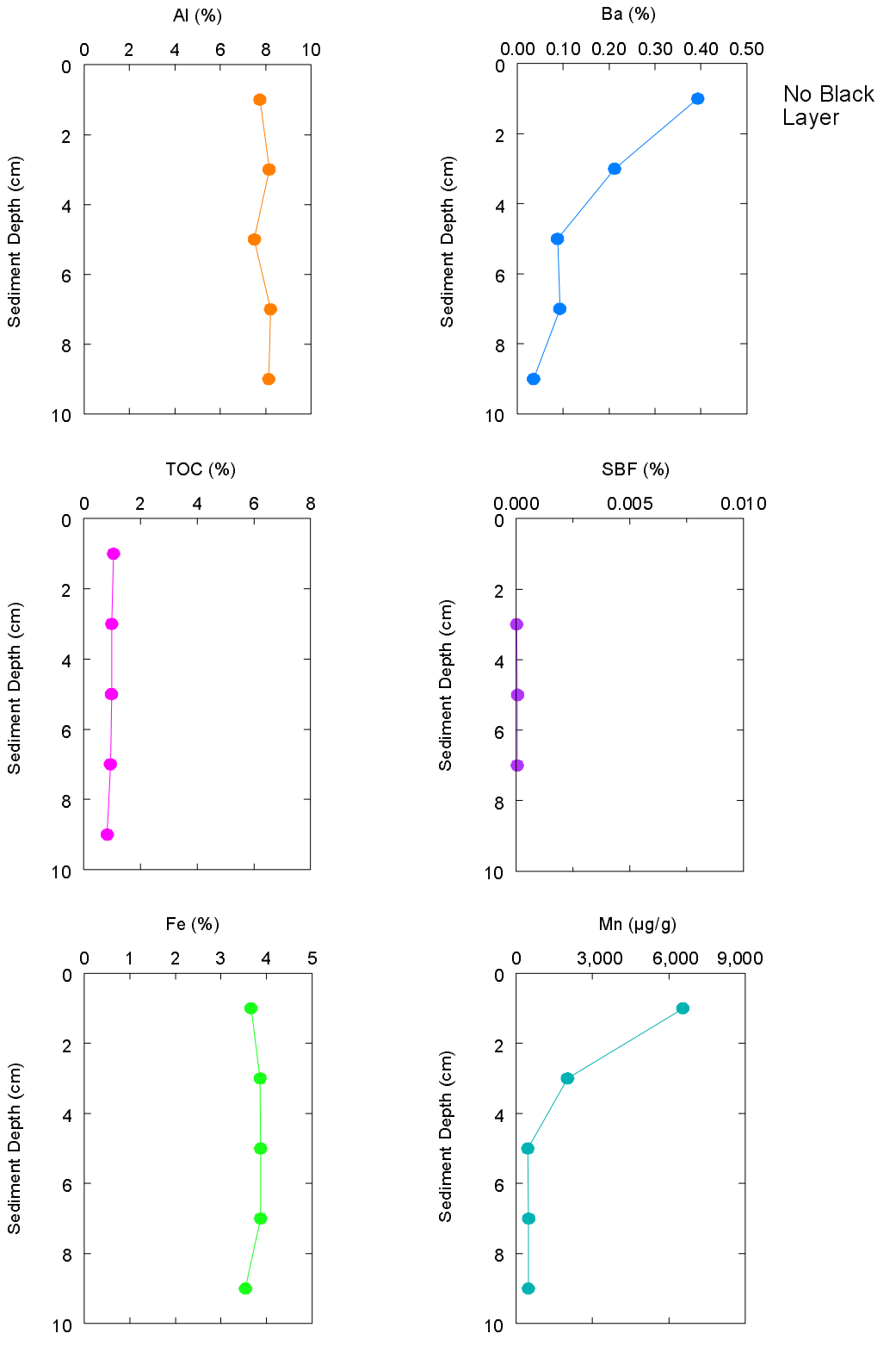

Figure 9-31. Vertical profiles for aluminum (Al), barium (Ba), total organic carbon (TOC), synthetic based fluid (SBF), iron (Fe), and manganese (Mn) in sediment from Green Canyon 112, Station FF-1, Sampling Cruise 2.

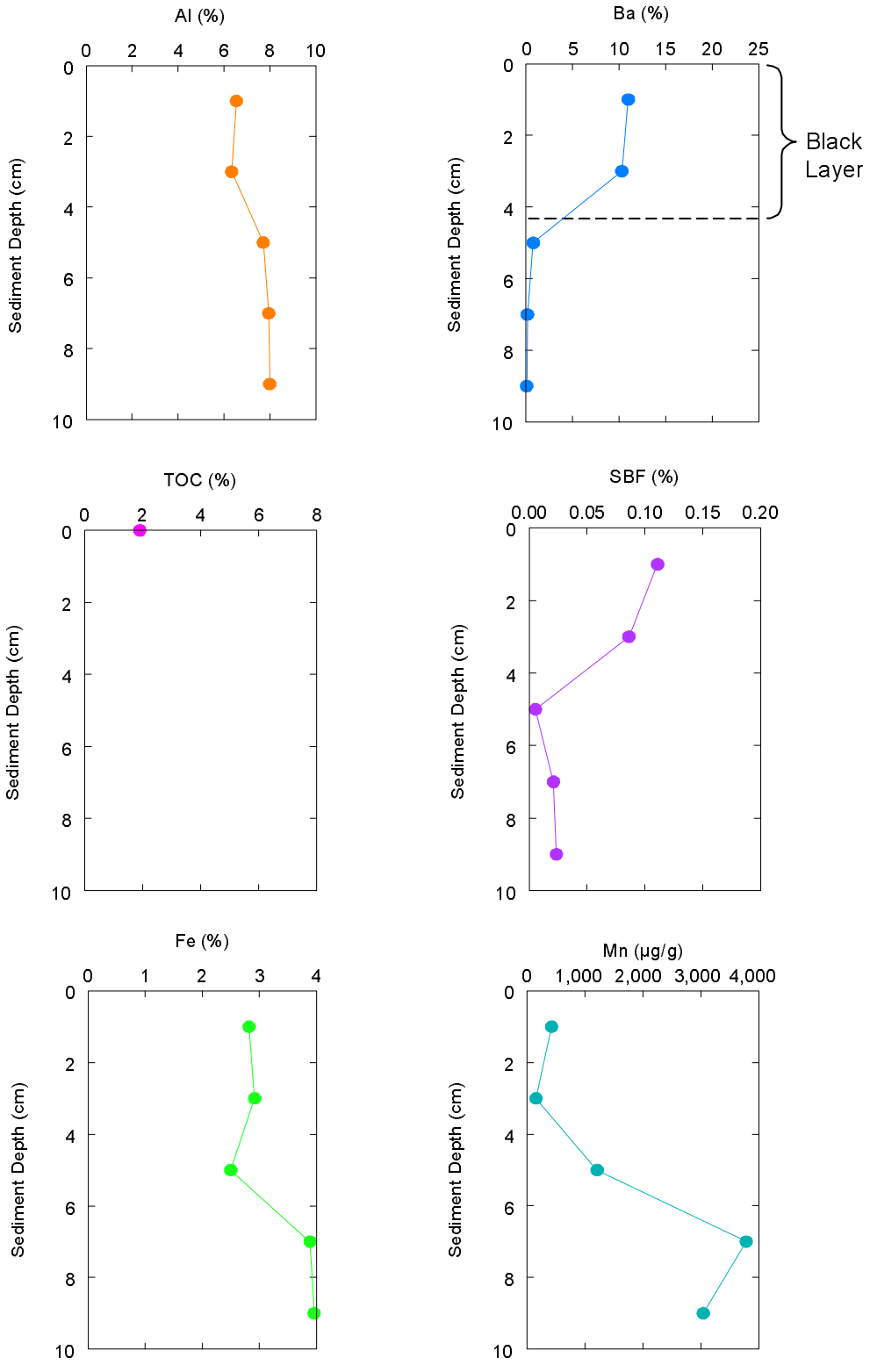

Figure 9-32. Vertical profiles for aluminum (Al), barium (Ba), total organic carbon (TOC), synthetic based fluid (SBF), iron (Fe), and manganese (Mn) in sediment from Green Canyon 112, Station NF-5, Sampling Cruise 1.

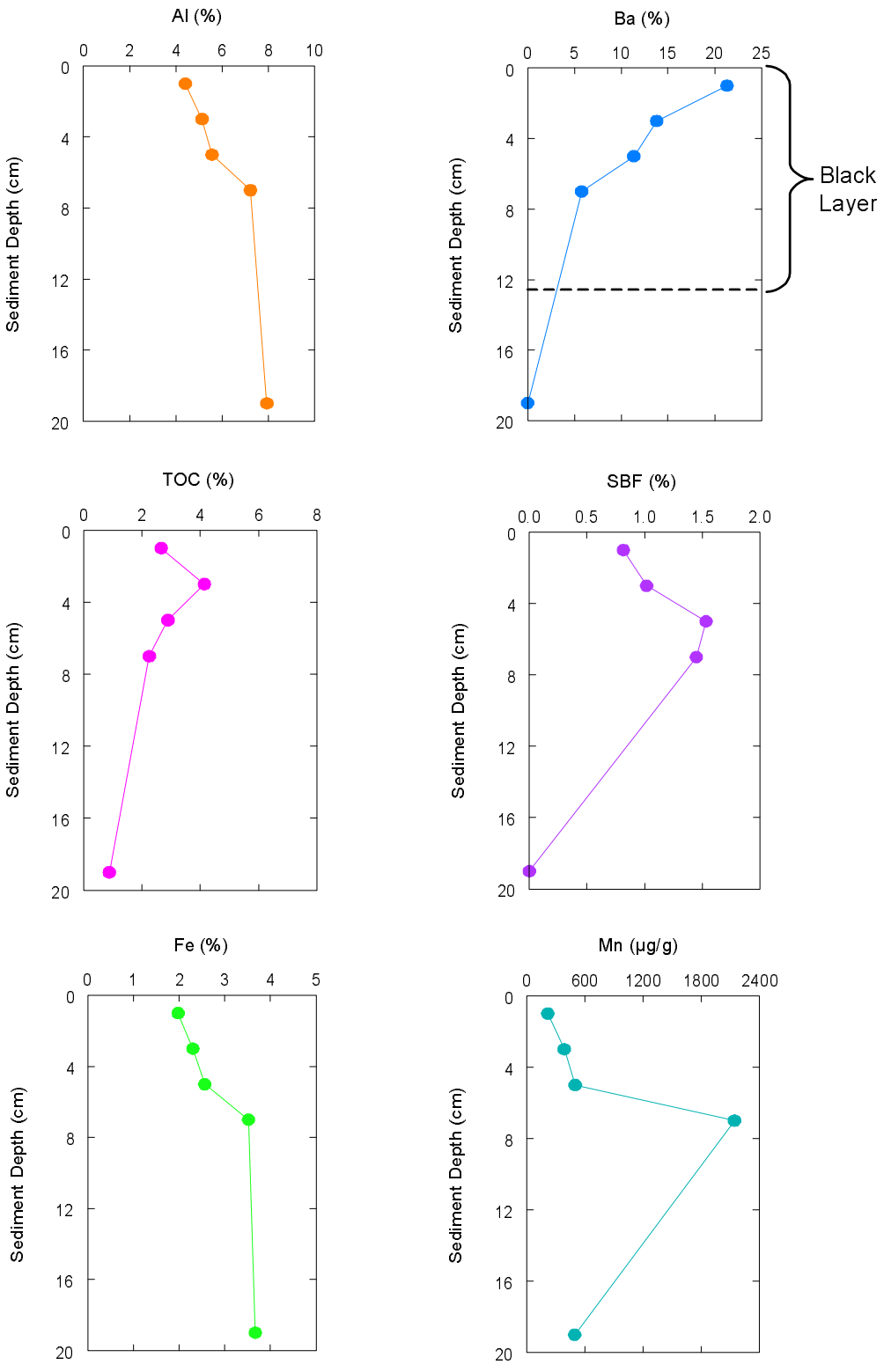

Figure 9-33. Vertical profiles for aluminum (Al), barium (Ba), total organic carbon (TOC), synthetic based fluid (SBF), iron (Fe), and manganese (Mn) in sediment from Green Canyon 112, Station DISC-1, Sampling Cruise 2.

At far-field stations from EI 346, concentrations of Al, Fe, and TOC were uniform with depth and no SBF was detected (Figure 9-24). Concentrations of Mn, and to a lesser degree Ba, were elevated in the upper layers of sediment (top 2 to 6 cm) (Figure 9-24 and Appendix E). These surface enrichments are due to remobilization of Mn^{2+} and Ba^{2+} in oxygen- and sulfate-depleted pore water at depths >8 to 10 cm in the core, and precipitation of the two metals as an oxide and sulfate phase, respectively, in the uppermost layers of the sediment column where sufficient oxygen and sulfate are present.

Barium concentrations were >10%, SBF levels were >0.5%, and TOC content was >4% in the top three layers (0 to 6 cm) at Station DISC-1 (Sampling Cruise 2) (Figure 9-25). Background conditions were observed at a sediment depth of 16 to 18 cm in the core from DISC-1 (Sampling Cruise 2) (Figure 9-25). In sediment from Station NF-4 (Sampling Cruise 1) at EI 346, a 13-cm thick layer of black mud was observed with 20.5% Ba and 0.2% SBF in the 0 to 2 cm section with decreasing concentrations with increasing depth. A similar trend, but with lower levels of Ba (<3%) and SBF (<0.01%), was observed at Station NF-1 (Sampling Cruise 2).

At MC 496 on the continental slope, the core from Station FF-5 represents the natural environment with uniform concentrations of Al, TOC, and Fe, and no SBF (Figure 9-26). Concentrations of Mn were ~4,000 µg/g in the top 4 cm, decreasing to 1,500 to 1,000 µg/g at depths of about 6 cm (Figure 9-26). Manganese levels as high as 12,000 µg/g were found in the top 2 cm of other cores from far-field stations at MC 496. As previously discussed, the vertical distribution of Mn is influenced by natural diagenetic processes. Concentrations of Mn are much greater in the top layers of sediment from the continental slope because of the thicker layer of oxic sediment that leads to oxidative precipitation of MnO_2. Surface enrichment of Ba concentrations was observed at Station FF-1 (Sampling Cruise 2, Appendix E) but not in sediment from Station FF-5 (Sampling Cruise 1, Figure 9-26).

At Station NF-4, MC 496, an 8-cm thick black layer was observed during Sampling Cruise 1. This layer contained concentrations of Ba at 17% and SBF at 1.1% in the top 2 cm (Figure 9-27). Concentrations of Al, Fe, and especially Mn were low in the layer containing Ba and SBF. Below 2 cm, concentrations of Ba and SBF decreased to ambient levels at 8 to 10 cm (Figure 9-27). Similar trends with lower amounts of Ba and SBF are observed for Stations DISC-2 (Sampling Cruise 2, Figure 9-28), NF-1 (Sampling Cruise 2), and DISC-1 (Sampling Cruise 2) at MC 496 (Appendix E).

Vertical distributions of Al, Fe, TOC, Ba, and Mn for far-field stations at EW 963 (Figure 9-29) were very similar to those described for MC 496, with elevated levels of Mn in the top 4 cm of the sediment column. Likewise, sediment layers of variable thicknesses that contained drilling discharges were found at near-field and discretionary stations for EW 963 (e.g., Figure 9-30). These layers contained 2% to >15% Ba and 0.01% to 0.12% SBF.

At GC 112, concentrations of Al, TOC, and Fe were relatively uniform in far-field cores and no SBF was detected (Figure 9-31). Samples at 0-2 cm and 2-4 cm had elevated levels of Ba that are most likely a natural phenomenon. Concentrations of Mn peaked at >6,000 µg/g in the top 2 cm (Figure 9-31). As shown on Figure 9-32, a black layer was observed in the top 5 cm of the core from Station NF-5 (Sampling Cruise 1). This 5-cm layer contained SBF >0.1%, >10% Ba, Mn levels <500 µg/g, and ~10% to 20% lower levels of Al and Fe. Thus, elevated levels of SBF and barite were observed to a depth of 5 cm. A similar trend was found for Station DISC-1 on Sampling Cruise 2, where even higher levels of Ba and SBF were observed (Figure 9-33). The depth of the black layer at Station DISC-1 (Sampling Cruise 2) was ~14 cm, with supporting

chemical data for the drilling discharges in the top 8 cm (Figure 9-33). The sample collected at 18 to 20 cm from this station was clearly background sediment (Figure 9-33).

Overall, black layers or patches of black were observed at 32 of 36 near-field stations during Sampling Cruise 1 and 32 of 48 near-field + discretionary stations during Sampling Cruise 2. At mid-field stations, 24 of 36 samples during Sampling Cruise 1 and 16 of 36 samples during Sampling Cruise 2 contained black layers. No black layers or patches of black were observed at any far-field stations. When observed, the black layers or layers with black patches were typically 2- to 15-cm thick with only one layer (at EI 346) thicker than 30 cm. Sediments from all of the black layers contained Ba at above background levels. Concentrations of SBF were >0.01% at ~ 60% of these near-field + mid-field stations during Sampling Cruise 1 and ~35% of the near-field (including discretionary) + mid-field stations during Sampling Cruise 2.

9.5 SEDIMENT RADIONUCLIDES

Vertical profiles for the activities of ^{137}Cs and excess ^{210}Pb in sediments were produced for the far-field stations from the following four sites that represent the complete range in water depths: MP 288 (water depth 119 m), VK 783 (water depth 338 m), MC 496 (water depth 556 m), and GC 112 (water depth 534 m). The radionuclide data for these stations provide information on sedimentation rates for the different environments. Such information can be used to help interpret vertical profiles for DO, redox, and other sediment and pore water parameters. A fifth profile was obtained for a discretionary station at GC 112 to investigate use of excess ^{210}Pb to differentiate background sediment from drilling discharges that may include cuttings.

The vertical profile for excess ^{210}Pb for Station FF-3 at MP 288 has a correlation coefficient of 0.99 and yields a sedimentation rate of 0.13 cm/yr. This ^{210}Pb-based sedimentation rate is in reasonably good agreement with a rate of 0.12 ± 0.03 cm/yr based on the ^{137}Cs data (6 ± 2 cm of sediment since 1950) (Figure 9-34). The sediment accumulation rate at this shallow water station is lower than rates of 0.3 to >0.5 cm/yr on the shelf near the Mississippi River delta (Nelsen et al., 1994). Main Pass 288 is marked by sandy layers to the east and may be an area of more active sediment movement and somewhat lower amounts of sediment deposition. In contrast, the sediment accumulation rate at VK 783 was 0.25 cm/yr (Figure 9-35). The VK 783 site is ~55 km farther from the mouth of the Mississippi River in deeper water. At deeper water sites MC 496 (Figure 9-36) and GC 112 (Figure 9-37), the sedimentation rates of ~0.2 cm/yr are remarkably similar to the value obtained for VK 783. These rather uniform rates are compatible with those obtained for sites at similar depths on the outer Mississippi delta (Nelsen and Trefry, 1986) and suggest that sediment deposition at these depths across this area are quite similar. As a further point of comparison, sedimentation rates for three sites at water depths of ~1,000 m (from an MMS study of SBF) were 0.05, 0.07, and 0.14 cm/yr.

One test of concept for differentiating background detrital sediment from drilling discharges and associated cuttings was carried out with data for a sediment core from Station DISC-1 at GC 112 collected during Sampling Cruise 2 (Figure 9-37). The results for the DISC-1 core from GC 112 showed levels of excess ^{210}Pb in the top 2 cm to be 1 dpm/g relative to 42 dpm/g in the 0-2 cm layer from Station FF-1 at GC 112 (Figure 9-37). Drilling fluids and associated cuttings are assumed to contain no excess ^{210}Pb because they contain materials that have not had a long exposure in recent seawater to scavenge excess ^{210}Pb and/or are older than the 100 to 120 year life-time of excess ^{210}Pb (half life = 22.3 yr). Based on the results from the FF-1 station, the top 2 cm of sediment from Station DISC-1 contained <5% background sediment ([1 dpm/g]/[42 dpm/g] x 100% = 2.4%). The sample from Station DISC-1 (0-2 cm)

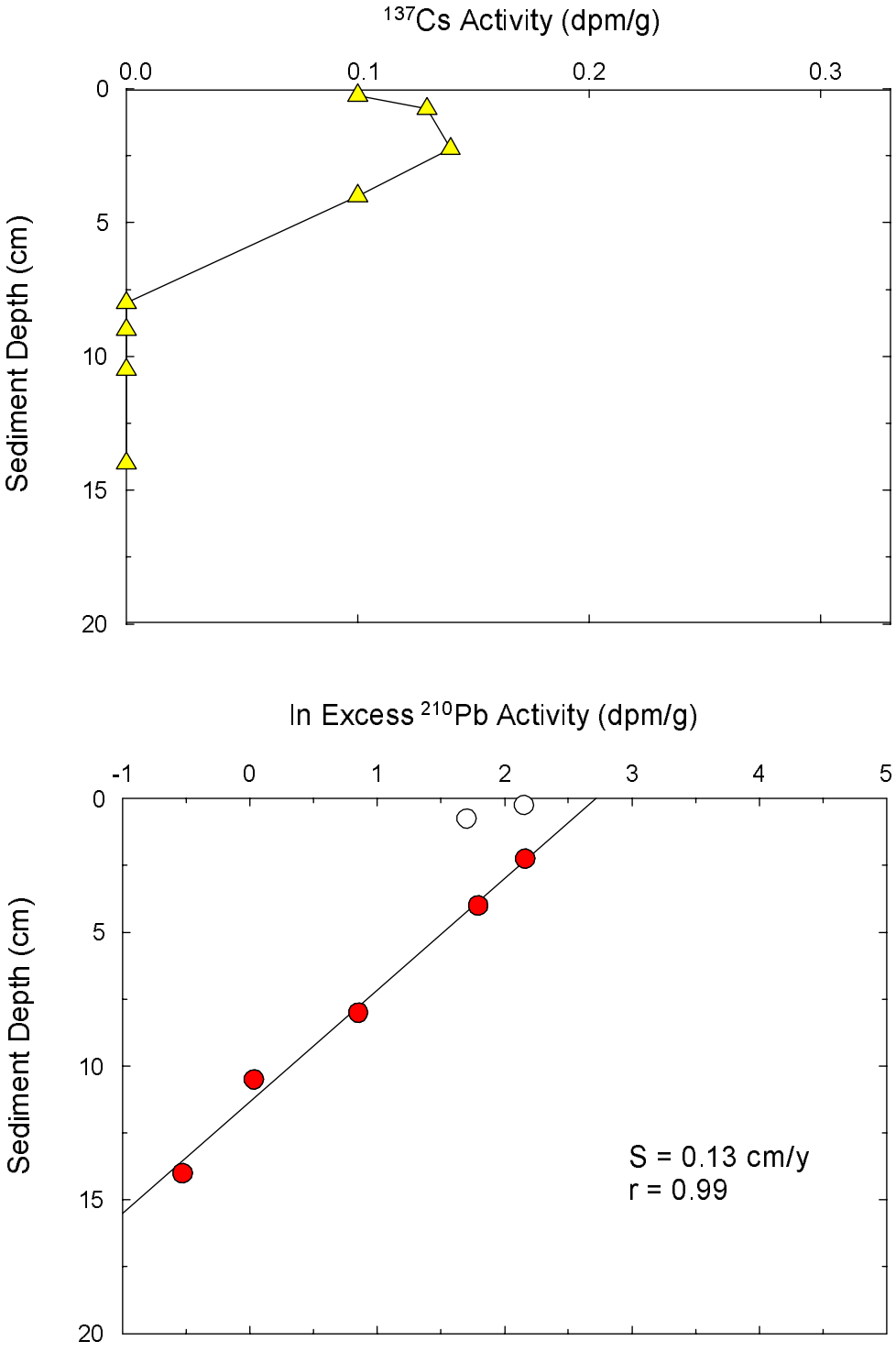

Figure 9-34. Vertical profiles for ^{137}Cs and excess ^{210}Pb in sediment core from Main Pass 288, Station FF-3 during the Screening Cruise. Sedimentation rate (S) and correlation coefficient for linear regression (r) for excess ^{210}Pb are shown on lower graph. The activities for excess ^{210}Pb represented by open circles appear to be part of a surface mixed layer and are not included in the linear regression.

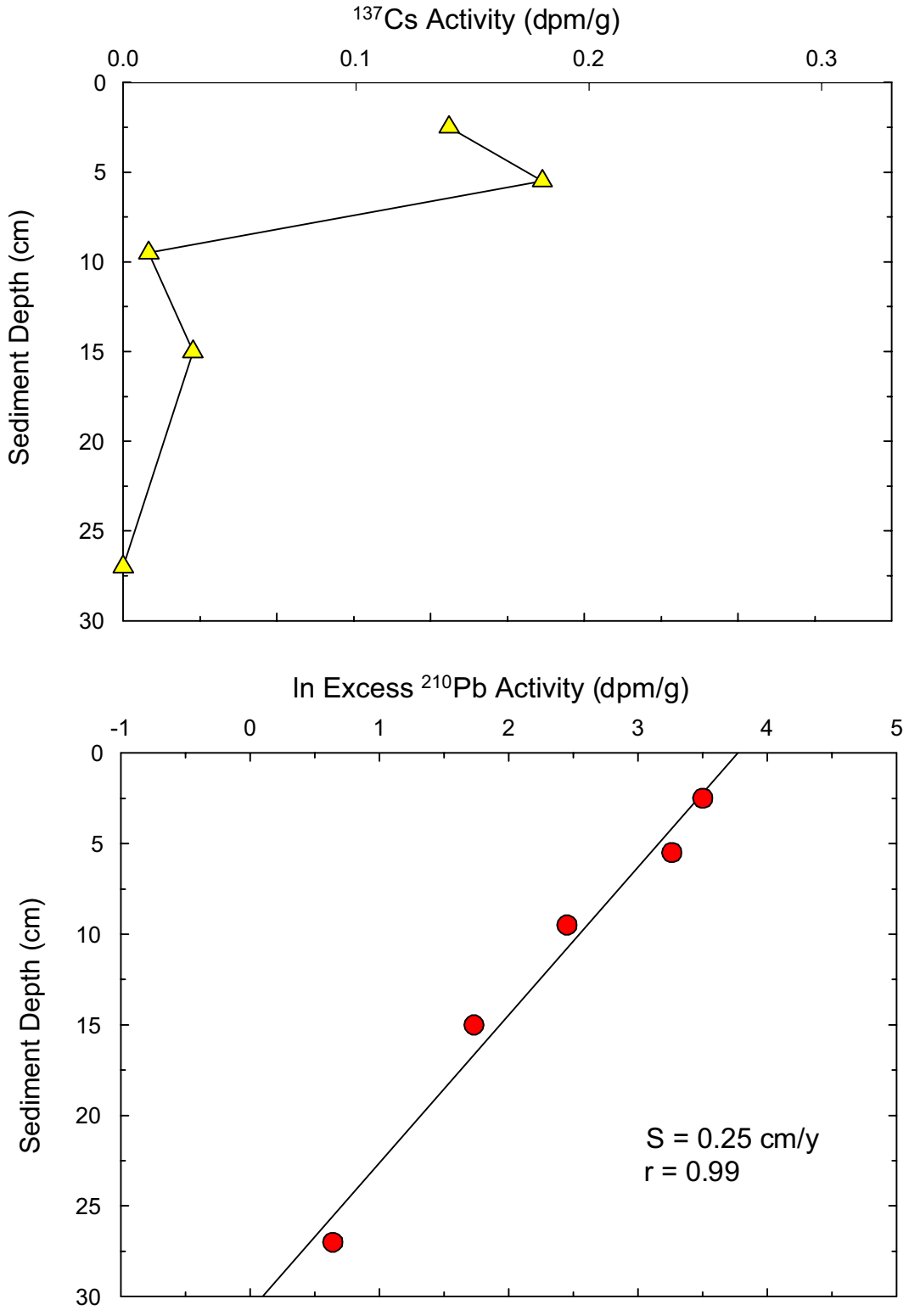

Figure 9-35. Vertical profiles for ^{137}Cs and excess ^{210}Pb in sediment core from Viosca Knoll 783, Station FF-5 during Sampling Cruise 1. Sedimentation rate (S) and correlation coefficient for linear regression (r) for excess ^{210}Pb are shown on lower graph.

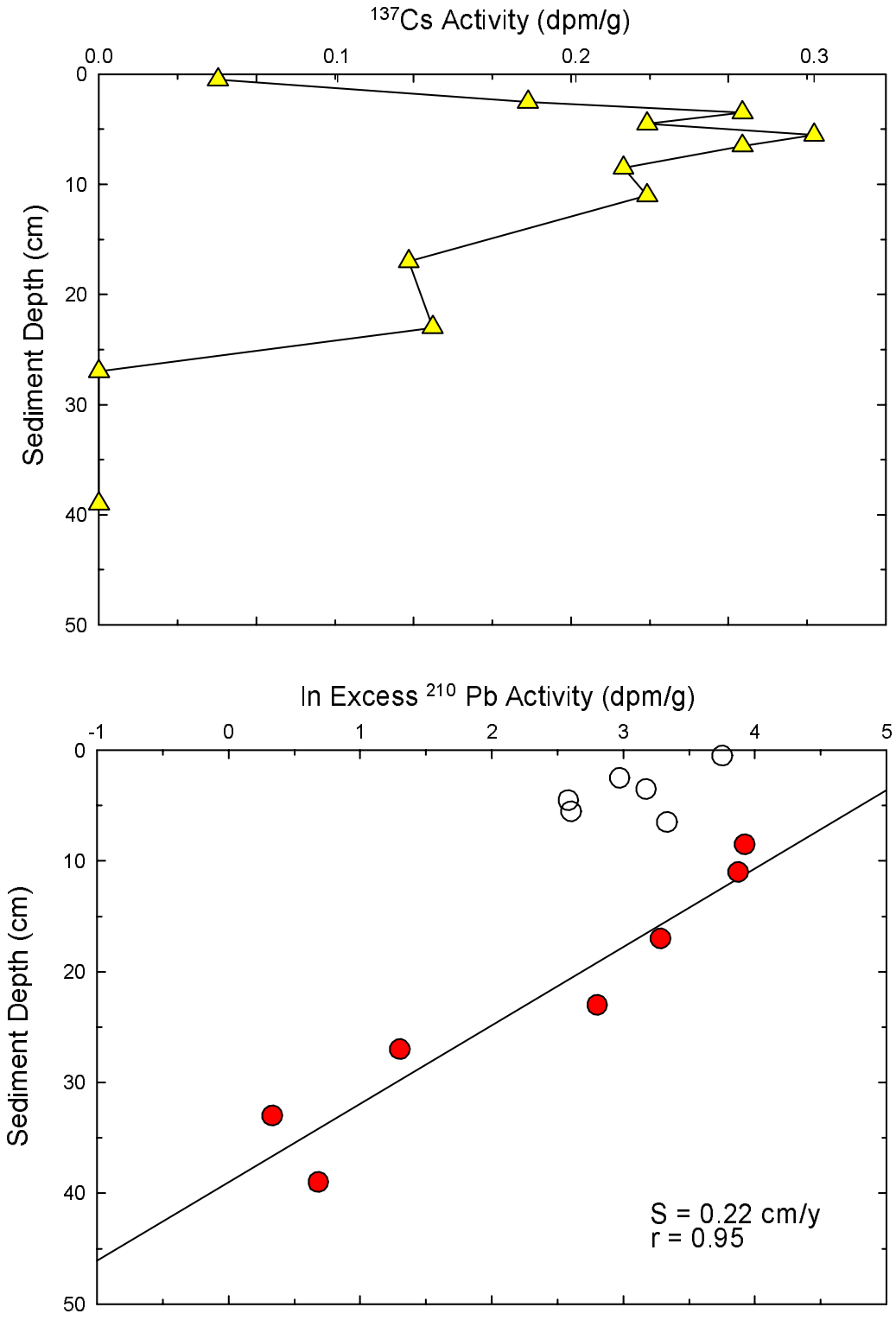

Figure 9-36. Vertical profiles for ^{137}Cs and excess ^{210}Pb in sediment core from Mississippi Canyon 496, Station FF-5 during Sampling Cruise 1. Sedimentation rate (S) and correlation coefficient for linear regression (r) for excess ^{210}Pb are shown on lower graph. The activities for excess ^{210}Pb represented by open circles appear to be part of a surface mixed layer and are not included in the linear regression.

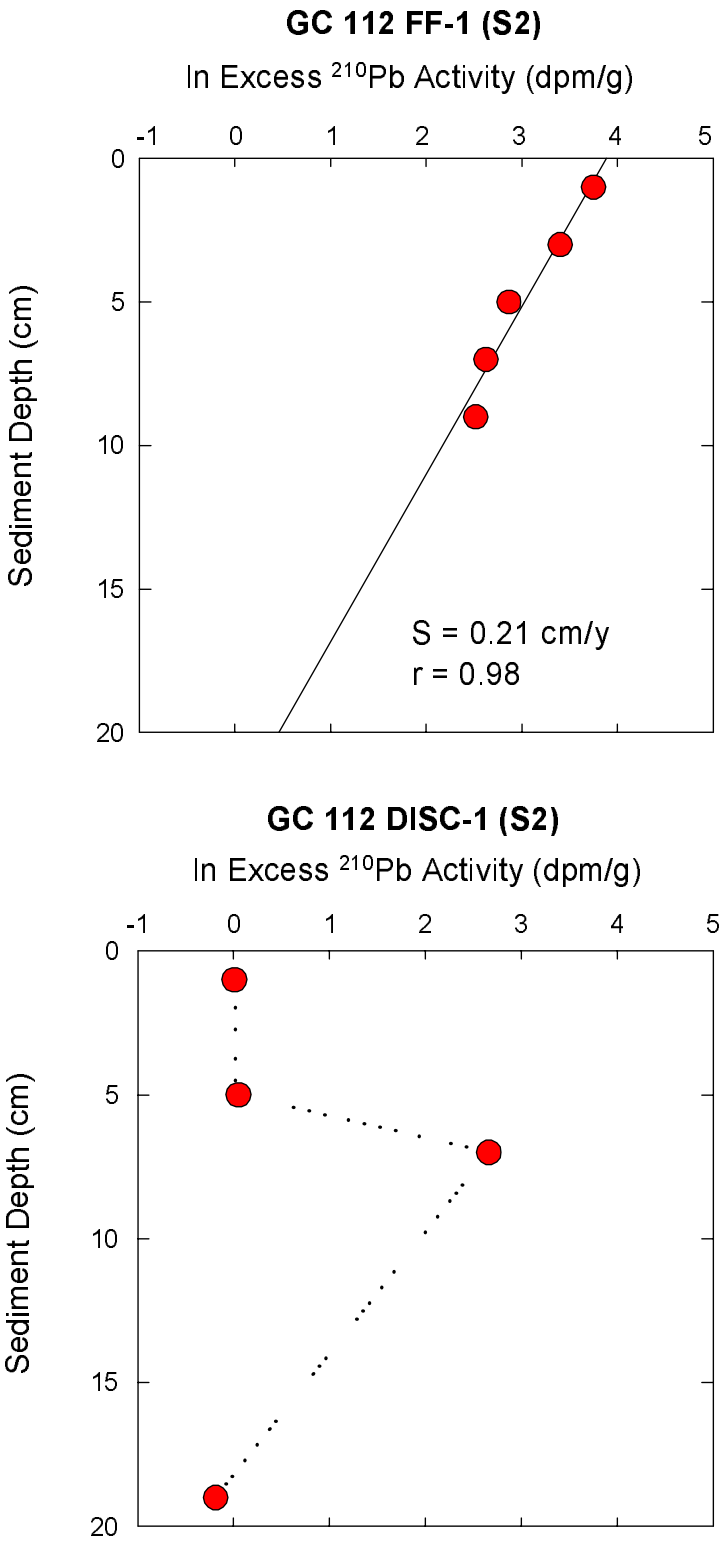

Figure 9-37. Vertical profiles for excess ^{210}Pb in sediment cores from Green Canyon 112 (GC 112), Stations FF-1 and DISC-1 during Sampling Cruise 2 (S2). Sedimentation rate (S) and correlation coefficient for linear regression (r) for excess ^{210}Pb are shown on upper graph.

contained 21.3% Ba (40% barite) and 4.4% Al (~50% clay for clay that contains about 8% Al). Thus, essentially all the Al in the sample is associated with drilling clays or discharged cuttings. The same scenario holds for the sample collected at 4-6 cm. However, at 6-8 cm, the activity of excess ^{210}Pb was 14.3 dpm/g and is similar to the value of 13.8 dpm/g at a depth of 6-8 cm at Station FF-1 (GC 112) (Figure 9-37). Concentrations of Al and Ba in the 6-8 cm layer were 7.2% and 5.8%, respectively. The data for excess ^{210}Pb suggest that a fraction of the aluminosilicate material was recently deposited (past 50 years) detrital material. The actual fraction of detrital sediment in the 6-8 cm layer depends on how this layer is identified relative to the far-field sediment. For example, if the detrital aluminosilicates in the 6-8 cm layer at Station DISC-1 have an excess ^{210}Pb activity of 42 dpm/g (as in the top 2 cm at Station FF-1), then the detrital component is 33% of the total sediment in that layer ([14 dpm/g]/[42 dpm/g] x 100%). This scenario implies that the drilling discharges have been deposited over the normal sediment from the area.

The sediment sample from 18-20 cm at Station DISC-1 from GC 112 had an excess ^{210}Pb activity of 0.8 dpm/g and background levels of Ba and Al. If 42 dpm/g is used as the initial activity of excess ^{210}Pb, then the sample at 18-20 cm is ~120 years old. Use of excess ^{210}Pb shows the absence or fraction of background detrital sediment in a layer that contains drilling discharges but cannot alone differentiate clays associated with drilling fluids from natural clays associated with drill cuttings.

9.6 INTERELEMENT RELATIONSHIPS IN SURFICIAL SEDIMENTS

The collective data set for Al, Ba, Fe, Mn, SBF, and TOC can be used to help discern broad trends in composition and categorize sediments with respect to differences in redox environment and the composition of drilling discharges. Concentrations of Ba in background sediments were generally ≤0.15% in shelf sediments and ≤0.3% to 0.4% in slope sediments, based on results for far-field samples in Figure 9-38a and data previously presented in Tables 9-2, 9-4, and 9-5. Pure barite contains Ba at levels of ~58.8%, and industrial barite typically contains 50% to 56% Ba. Thus, a marked shift in the Ba/Al relationship occurs as the fraction of barite in the sediments increases (Figure 9-38b). At Ba levels >5%, concentrations of Al (representing the clay fraction of sediment) decrease proportionally with the increase in Ba (Figure 9-38b). For example, a sample with ~26% Ba most likely contains about one-half barite. Consequently, samples with Ba levels at ~26% contain ~4% Al, or half the Al (clay) content of typical Gulf of Mexico sediment (Figure 9-38b). This information can be used to adjust calculations for natural loadings of metals in sediments and to help identify whether barite is a source of possible contaminants such as Hg (Trefry et al., 2003).

When Ba concentrations are plotted versus levels of SBF (Figure 9-39), the relative proportions of the two additives can be determined, and the presence of a WBM, relative to an SBM, can sometimes be identified. A wide range in proportions of Ba and SBF were observed in this study, showing the large diversity in proportions of the two drilling fluid additives. For example, sediment from Stations NF-1 and NF-5 from EI 346 contained >2% SBF and <5% Ba, whereas several samples from near-field stations at EI 346 contained >20% Ba and <0.3% SBF (Figure 9-39a). Yet, at Station NF-4 from GC 112, concentrations of both SBF and Ba were high (Figure 9-39a). These observations suggest that drilling discharges with low levels of SBF (in this case drilling discharges are identified from Ba data) and drilling residues with high SBF can be found within reasonably close proximity in the area of the same drillsite. This apparent diversity in the types and concentrations of drilling fluid additives in the surficial sediment may complicate the process of independently evaluating the impact of SBF in some cases.

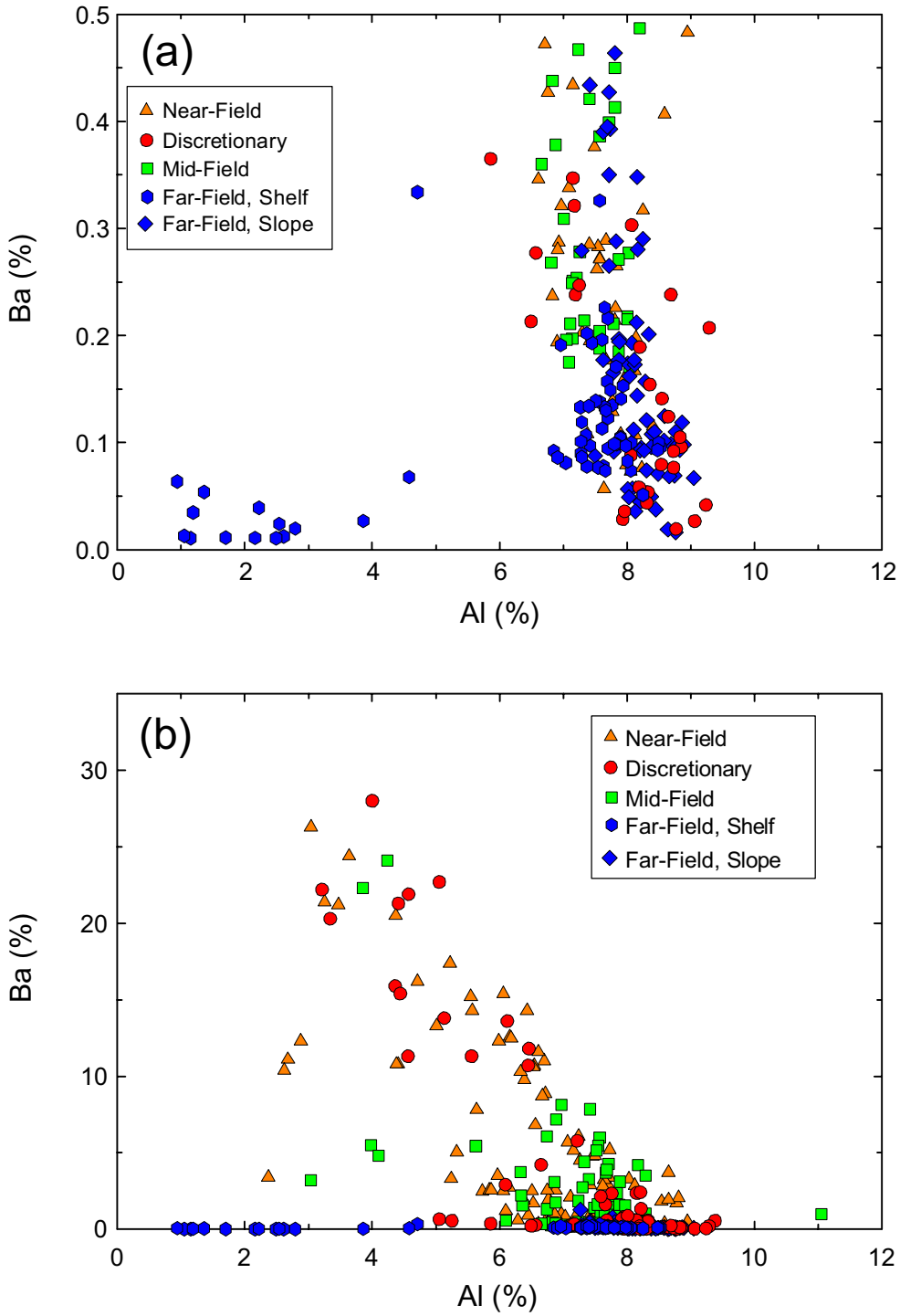

Figure 9-38. Concentrations of aluminum (Al) versus barium (Ba) in sediments from near-field, discretionary, mid-field, and far-field stations for (a) sediment with <0.5% Ba and (b) all sediments.

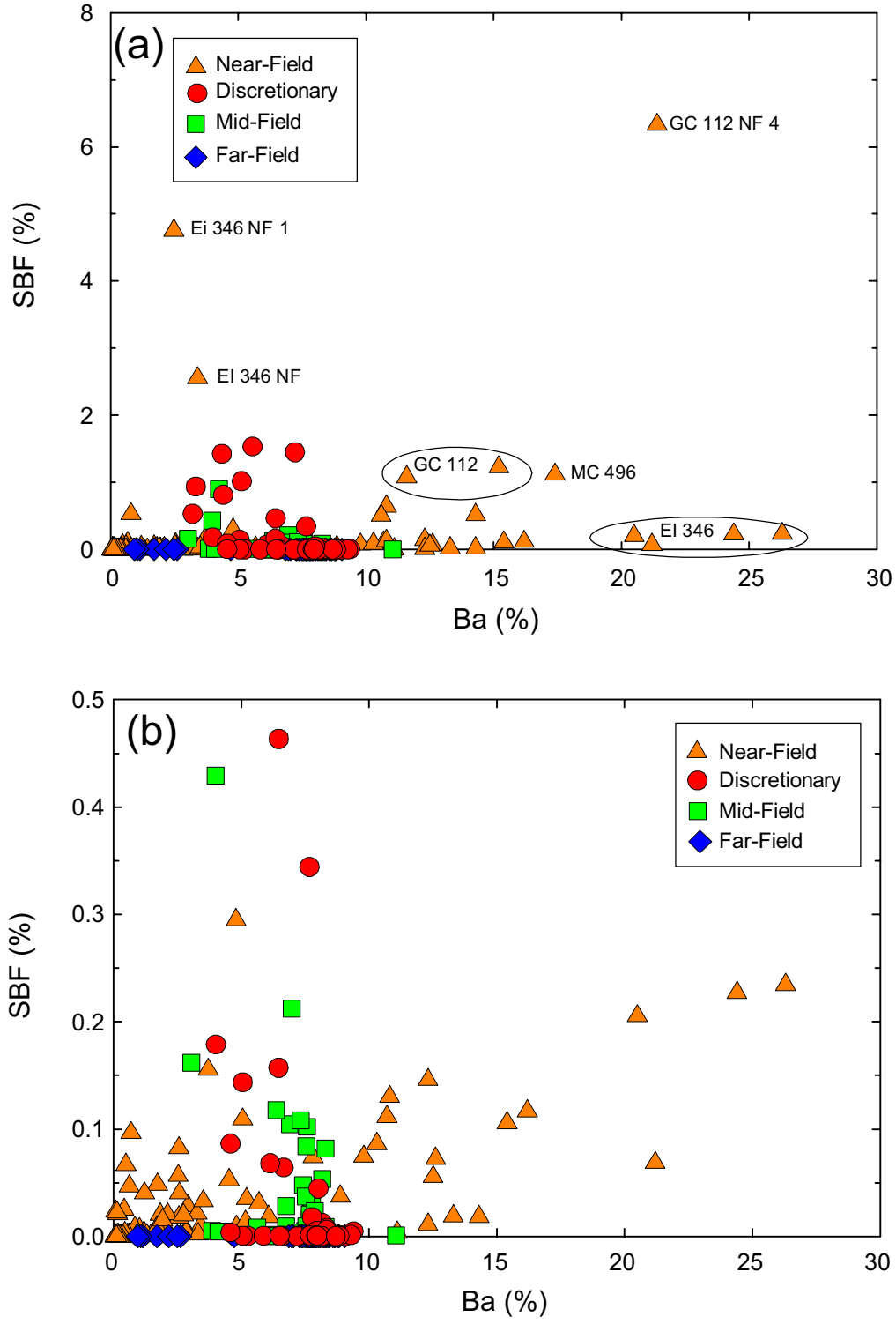

Figure 9-39. Concentrations of barium (Ba) versus synthetic based fluid (SBF) in sediments from near-field (NF), discretionary, mid-field, and far-field stations for (a) SBF at 7% full scale and (b) SBF at 1% full scale.

Concentrations of TOC in sediment ranged from <0.4% to 7.4% (Figure 9-40). In sediment from the far-field stations, concentrations of TOC tended to be higher in the more Al-rich, finer-grained sediment (Figure 9-40a). Much greater variation in the TOC/Al ratio was observed for the mid-field and near-field stations (Figure 9-40a). In some cases, higher TOC levels at near-field and mid-field stations were due to the presence of SBF, whereas at others it is possibly related to another source of organic matter. In most cases, SBF accounted for <15% of the TOC (Figure 9-40b). Two data points in Figure 9-40b plot above the 1:1 line, implying that the level of SBF is greater than that of TOC. This discrepancy is most likely related to the fact that the SBF and TOC sediments were taken from different subsamples of the box core and the distribution of black layers within a given box core from near-field stations was sometimes variable.

Concentrations of Mn in surficial sediment show the following two distinct trends:
1) concentrations in background (far-field) sediments from most slope sites are more than four times greater than at shelf sites (Tables 9-2, 9-4, 9-5, 9-6, 9-8, and 9-9) and 2) concentrations are significantly lower at near-field stations than at far-field stations (Tables 9-3 and 9-7, Figure 9-41). As previously described, surficial sediment from the upper slope in the Gulf of Mexico is enriched in Mn because reduction/dissolution of manganese oxides occurs at depths of 5 to >10 cm in the sediment column, with subsequent diffusion of Mn^{2+} up toward the sediment-seawater interface where the Mn reoxidizes (Trefry and Presley, 1982). At the continental slope stations, concentrations of Mn were ≥1% (10,000 µg/g) in some samples (Figure 9-41b).

Surficial sediment from the shelf stations was less enriched with Mn (Figure 9-41a) because new sediment is accumulating more rapidly, thereby lessening the depth and rate at which O_2 can diffuse down into the sediment and facilitate the oxidation of Mn. In some cases, upwardly migrating Mn^{2+} passes out into the bottom water. Thus, concentrations of Mn in the top 2 cm of the sediment column at the far-field sites on the shelf were typically 500 to 2,000 µg/g. With respect to the second point, concentrations of Mn were consistently lower at near-field stations because inputs of drilling discharges (with lower Mn/Al ratios) and lower levels of DO promote the dissolution of manganese oxides at the sediment water interface with diffusive loss of Mn^{2+} to the overlying water column. Concentrations of Mn in surficial sediments are a useful indicator of the redox environment with high Mn concentrations (>2,000 µg/g) typical for oxic, slowly accumulating sediments and low Mn concentrations (<1,000 µg/g) common where sediments are reducing.

9.7 DISTRIBUTIONS OF SELECTED TRACE METALS IN SEDIMENTS

Concentrations of nine trace metals (As, Cd, Cr, Cu, Hg, Ni, Pb, V, Zn) were determined in 42 surface sediments (0 to 2 cm) and 16 subsurface sediments (from eight cores) collected during the Screening Cruise (July 2000). The trace metal data complement results for Al, Ba, Fe, Mn, and TOC for the same samples. The data set is used here to evaluate possible sediment contamination from trace metals at the following drilling sites: MP 299, MP 288, MC 496, GC 112, GB 128, MC 28, VK 780, and VK 783. Only the first four sites listed above were incorporated into the final six primary sites for Sampling Cruises 1 and 2; however, the results for all eight sites are included in this metals discussion.

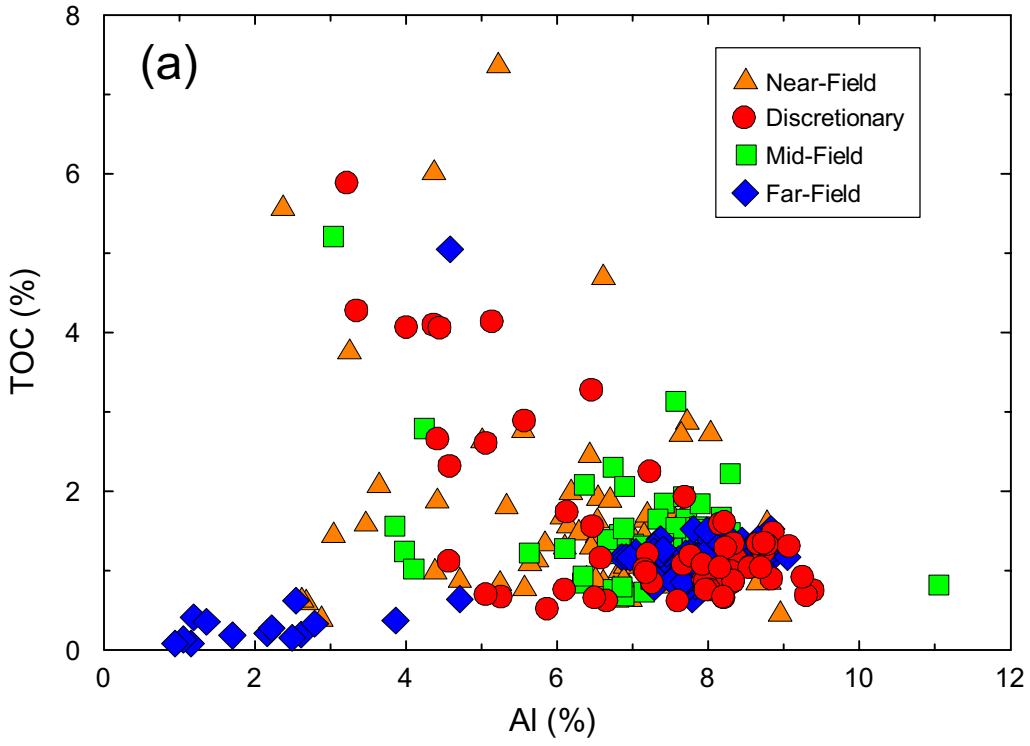

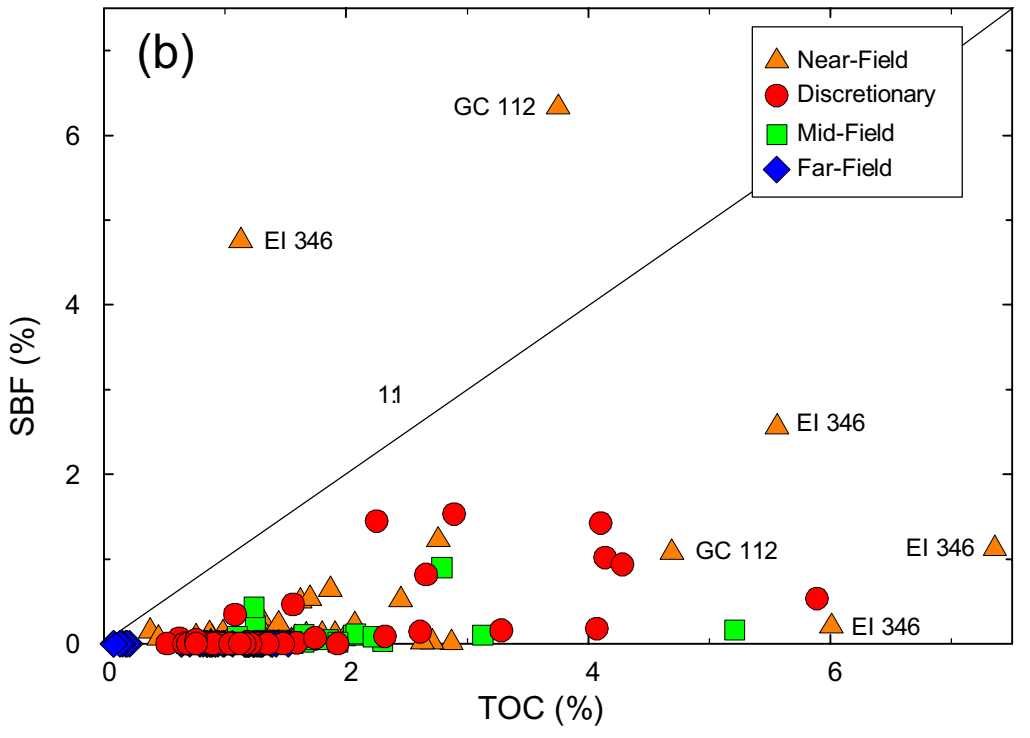

Figure 9-40. Concentrations of (a) aluminum (Al) versus total organic carbon (TOC) and (b) TOC versus synthetic based fluid (SBF) for near-field, discretionary, mid-field, and far-field stations.

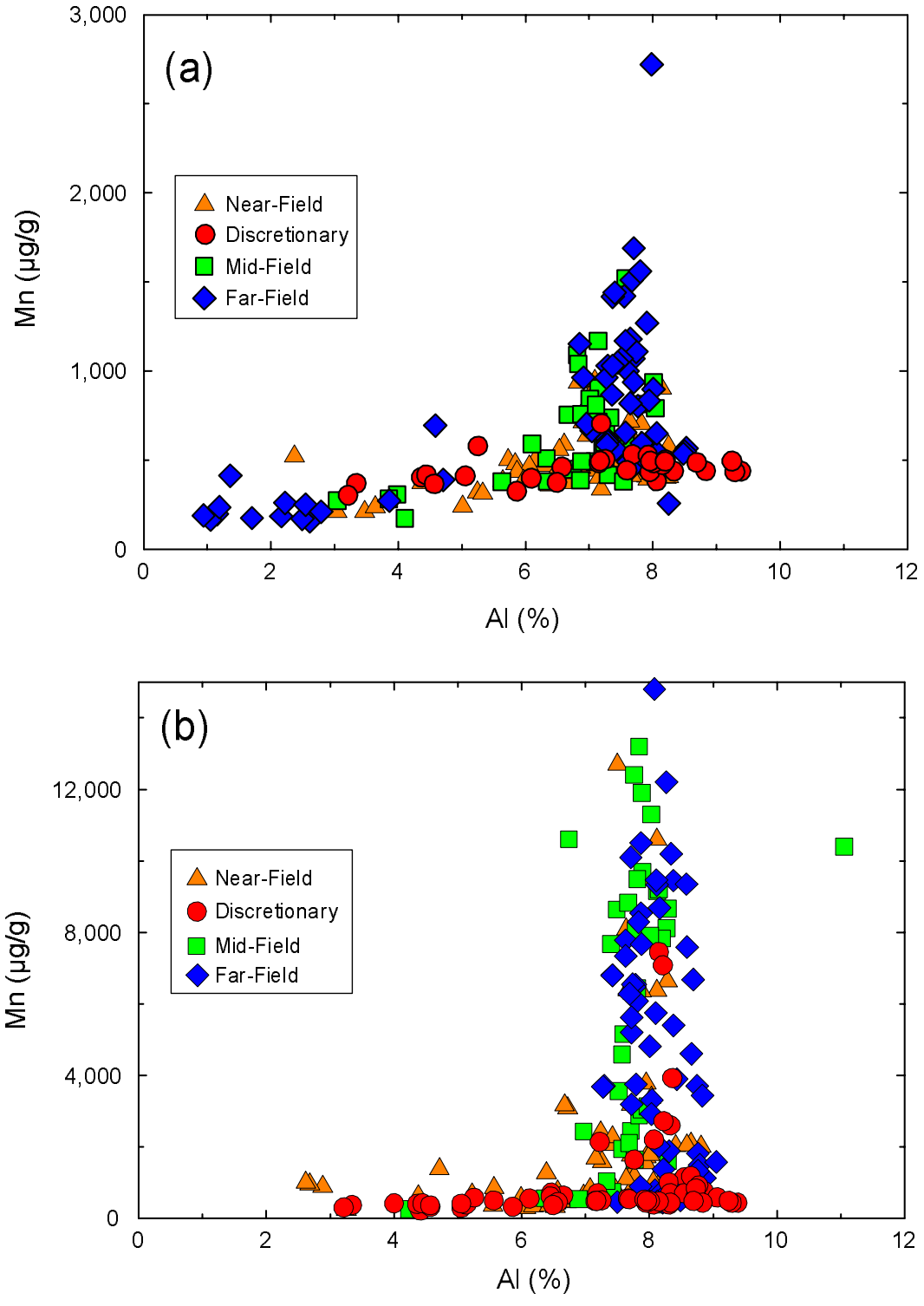

Figure 9-41. Concentrations of aluminum (Al) versus manganese (Mn) for near-field, discretionary, mid-field, and far-field stations at (a) all shelf sites and (b) all slope sites.

Concentrations of Fe in sediments from far-field stations follow a strong, positive linear trend versus Al (r = 0.97, Figure 9-42a). The slope of the linear regression line is 0.53, the same value as the Fe/Al ratio of Mississippi River suspended sediment, the dominant source material for the study area. Most other data points for near-field, mid-field, and discretionary stations plot close to the line established with the far-field samples. Lower concentrations of Fe (<2%) and Al (<4%) in some discretionary and near-field sediments result from mixing of Mississippi delta clay with material from drilling discharges, as enumerated below. Two points from discretionary stations appear to be enriched in Al relative to Fe, possibly the result of drilling mud and cuttings that contained more Al-rich clays (Figure 9-42a). One Fe-rich, far-field sample may be influenced by natural diagenetic processes that led to enhanced levels of Fe in surface layers.

Concentrations of trace metals in sediments generally correlate well with concentrations of Al and Fe because concentrations of most metals are very low in quartz sand or carbonate shell material and much higher in fine-grained aluminosilicates. Aluminum and Fe are rarely introduced by anthropogenic processes and are present at percent levels in most sediment relative to part per million (µg/g) levels for trace metals. Concentrations of Al and Fe often can be used to normalize concentrations of trace metals and thereby incorporate the metal-controlling variables of grain size, organic carbon content, and mineralogy. In the ideal case, under natural conditions, a good linear correlation is observed between concentrations of a trace metal and Al and/or Fe.

Concentrations of V in far-field samples correlated well with Al (r = 0.96, Figure 9-42b). The good linear fit for Al versus V is consistent with the mixing of relatively uniform composition, metal-rich aluminosilicate phases with smaller amounts of metal-poor sand and shell. Aluminum was chosen for normalization in this study because it is the major element least affected by chemical weathering and diagenesis and it works well for these sediments. None of the data points for samples from discretionary and near-field stations deviate greatly from the linear relationship developed for the far-field samples, and thus no V contamination is observed in sediments at any of the drilling sites. Plots of trace metal concentrations versus Fe or Al have been used in various forms for many years to identify sediment metal contamination (e.g., Trefry and Presley, 1976; Schropp et al., 1990).

No large deviations in the trend for Ni/Al ratio developed for far-field sediments was observed for any discretionary or near-field samples (Figure 9-43a). Four samples were enriched in Cr relative to the trend observed for the far-field samples (Figure 9-43b); however, no straightforward source for these enrichments has been identified. Because the data set for the far-field samples in this study is small (n = 8), prediction intervals were not added for some metals, such as Cr. However, large obvious positive deviations from the linear trend developed with the far-field samples are used to identify possible anthropogenic inputs of that metal, as enumerated in more detail below.

When concentrations of sediment Al (in %) were plotted versus Ba (in %) for the complete data set, an overall indirect trend was observed (Figure 9-44a). As the fraction of drilling discharges increases (as represented by Ba), the proportion of terrigenous clay (as represented by Al) decreases. Data for samples from far-field stations have low levels of Ba (<0.2%) relative to those where drilling discharges are present and thus plot along the baseline on Figure 9-44a.

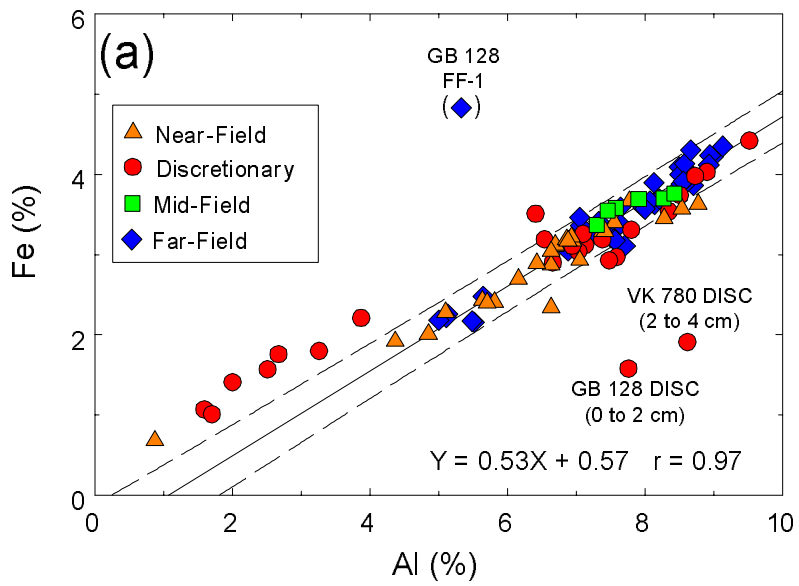

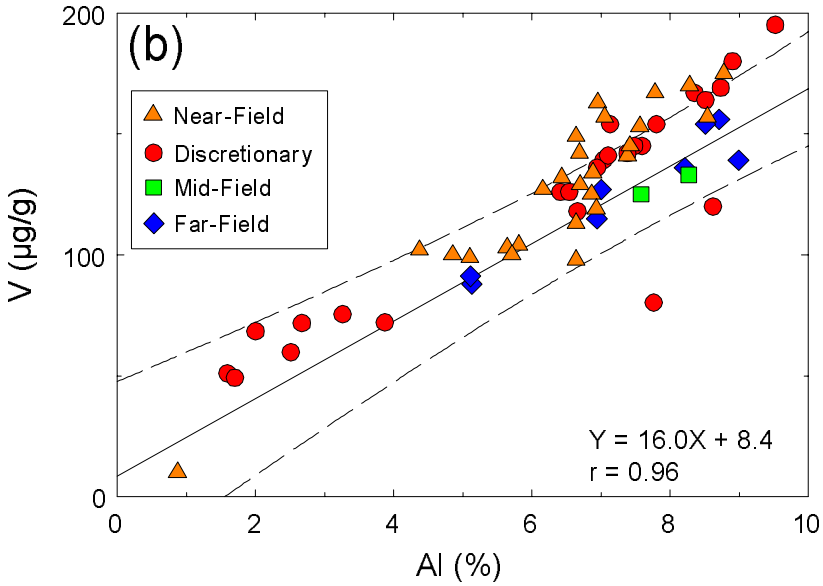

Figure 9-42. Concentrations of aluminum (Al) versus (a) iron (Fe) and (b) vanadium (V) for sediments collected during the Screening Cruise. Equations are from linear regression calculations using data for far-field stations, r is the correlation coefficient (point in parentheses not used in linear regression). Dashed lines above and below the solid regression lines show 95% prediction intervals.

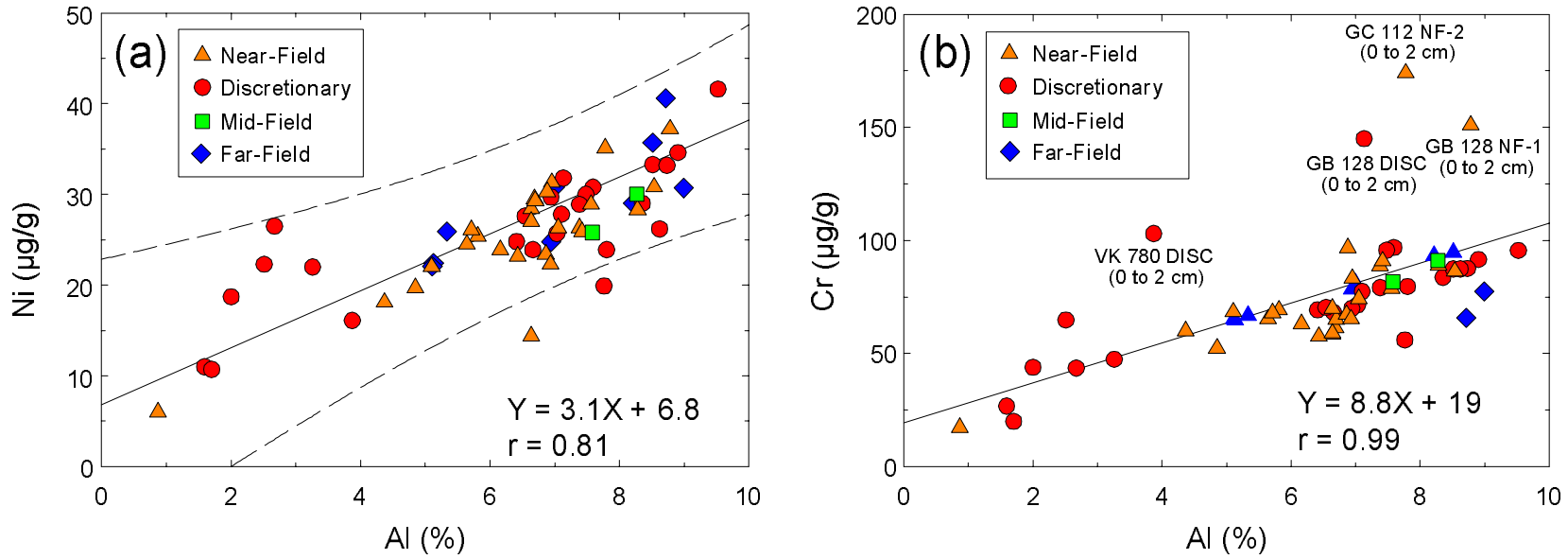

Figure 9-43. Concentrations of aluminum (Al) versus (a) nickel (Ni) and (b) chromium (Cr) for sediments collected during the Screening Cruise with labels for selected near-field (NF) and discretionary (DISC) stations. Equations and solid lines are from linear regression calculations for far-field samples, r is the correlation coefficient. Dashed lines above and below the solid regression line show 95% prediction interval.

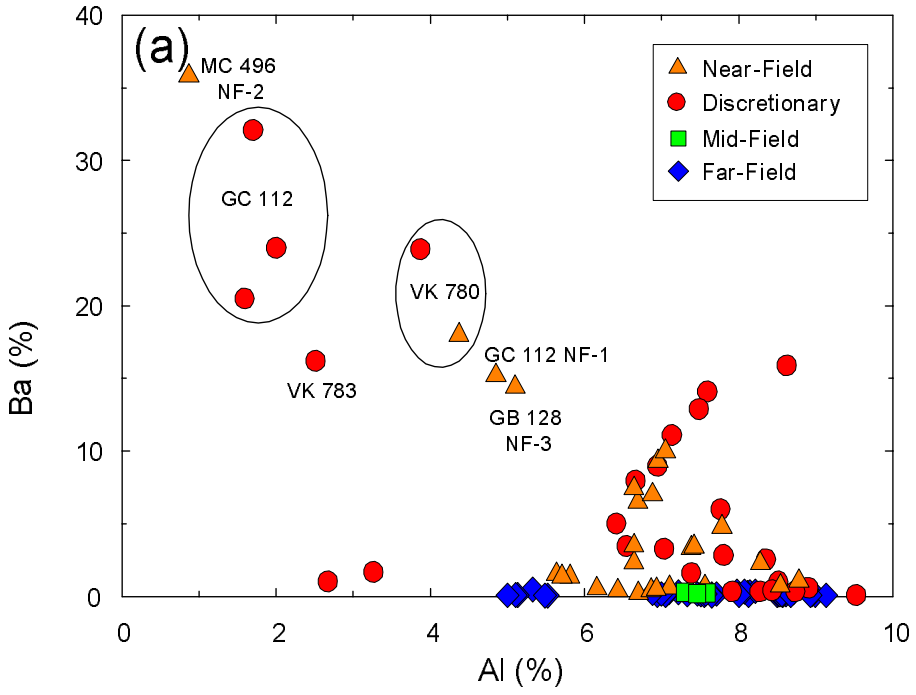

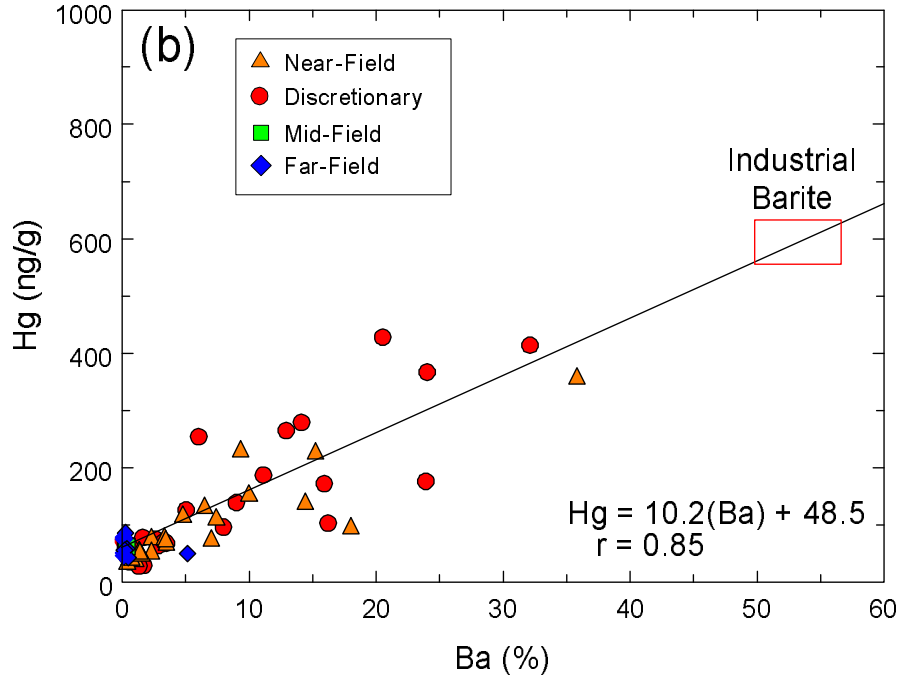

Figure 9-44. Concentrations of (a) aluminum (Al) versus barium (Ba) and (b) Ba versus mercury (Hg) for sediments collected during the Screening Cruise with labels for selected near-field (NF) and discretionary stations. Equation and solid line on (b) are from linear regression calculation for all samples, r is the correlation coefficient. Rectangle shows range of values for Ba in industrial barite for the extrapolated Hg levels defined by the line.

Considerable interest has been generated regarding concentrations of Hg in sediments adjacent to drilling sites because concentrations of total Hg near drilling sites are often two to ten times higher than in nearby background sediments (Neff, 2002b). This Hg is known to be a natural impurity in barite (Kramer et al., 1980; Trefry and Smith, 2003). As a separate but related part of this project, a detailed study of the distribution of total Hg and methylmercury in sediments from the same drilling sites was carried out and is reported elsewhere (Trefry et al., 2003). The previously unreported data for total Hg that accompanies the other trace metal results from the Screening Cruise are presented here (Figure 9-44b).

Concentrations of Hg increase directly with concentrations of Ba (Figure 9-44b). Correlations between concentrations of Ba and total Hg can be used to help confirm that excess total Hg in sediment is associated with barite. The correlation coefficient of 0.85 for Hg versus Ba in Figure 9-44b is good, considering that it is based on data from eight different drilling sites. Trefry et al. (2003) obtained values of $r>0.92$ for Ba versus Hg in sediments adjacent to drilling sites when sufficient data were available to create separate plots for each site. The strong correlation between concentrations of Ba and Hg can be used to estimate the Hg content of discharged barite, assuming that barite is the primary source of excess Hg in the sediment. The Ba versus Hg relationship can be used to calculate the concentration of total Hg in the barite used at a particular site. Barite has been specifically identified by x-ray diffraction in many near-field samples from the SBM study area (Chapter 7). If the regression line in Figure 9-44b is extrapolated to pure barite at 58.8% Ba, the concentration of total Hg is 648 ng/g (obtained by substituting 58.8% for Ba in the equation in Figure 9-44b). Typical “industrial barite” contains 85% to 95% barite (i.e., 50% to 56% Ba). Based on the range of Ba levels in industrial barite (50% to 56% Ba), the overall average for the total Hg content of barite used at all eight sites is 589 ng/g (from the average of 558 ng/g at 50% Ba and 620 ng/g at 56% Ba). These calculated values are in line with USEPA regulations that allow a maximum Hg level of 1,000 ng/g in barite (USEPA, 1993).

When concentrations of Hg are normalized to concentrations of Al, about 20 samples have Hg levels that are elevated above the trend observed in the Hg/Al ratio for far-field sediments (Figure 9-45a). Most of these sediments also contain elevated levels of Ba (Figure 9-44). As previously discussed, most of the excess Hg (that present above natural levels) seems to be associated with barite. Previous work, as summarized by Trefry and Smith (2003), shows that the barite-bound Hg has a very low degree of bioavailability.

Concentrations of Pb in sediments from this study ranged from 6 to 77 µg/g, with about 10 samples having Pb levels that are above the background trend for Pb/Al in far-field samples (Figure 9-45b). Concentrations of Cd and Zn vary by almost a factor of ten among samples (Figure 9-46). In each case, about 20 samples plot above the metal/Al trend by a factor of two or more.

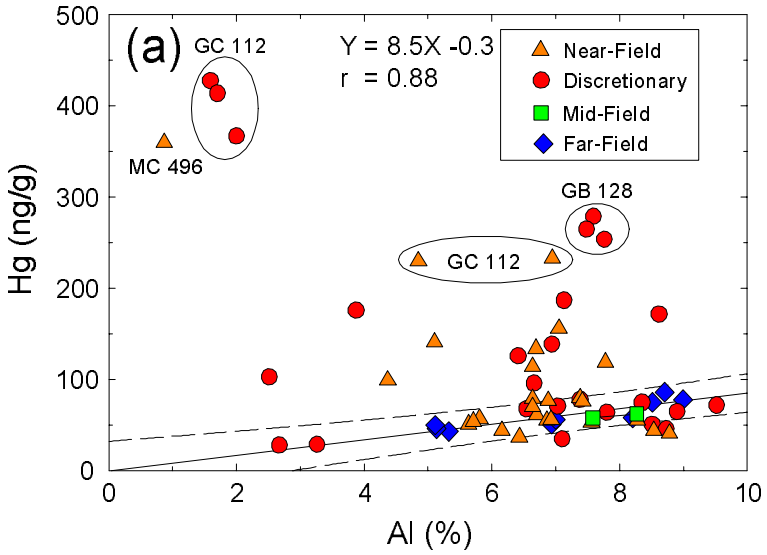

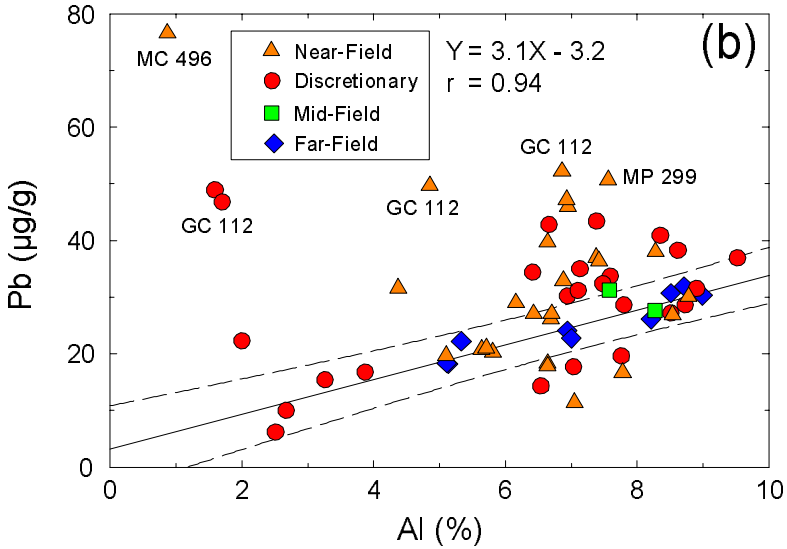

Figure 9-45. Concentrations of aluminum (Al) versus (a) mercury (Hg) and (b) lead (Pb) for sediments collected during the Screening Cruise. Equations are from linear regression calculations for far-field samples, r is the correlation coefficient. Dashed lines above and below the solid regression line show 95% prediction interval.

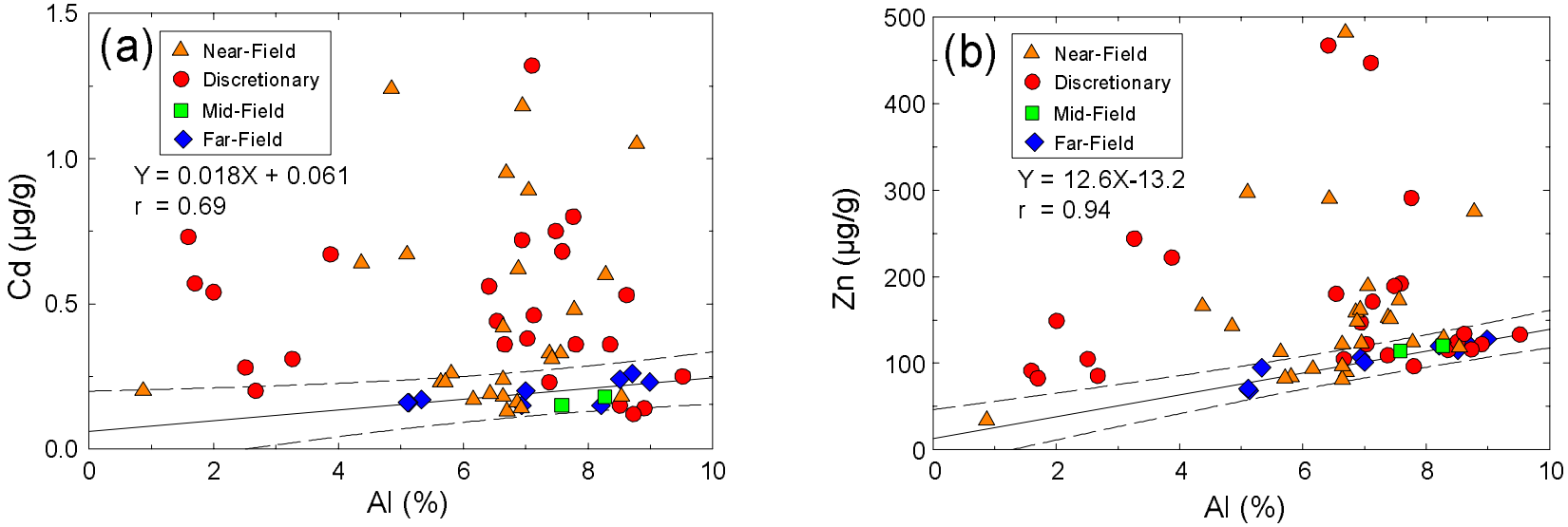

Figure 9-46. Concentrations of aluminum (Al) versus (a) cadmium (Cd) and (b) zinc (Zn) for sediments collected during the Screening Cruise. Equations are from linear regression calculations for far-field samples, r is the correlation coefficient. Dashed lines above and below the solid regression line show 95% prediction interval.

9.8 SEDIMENT OXYGEN LEVELS AND REDOX CONDITIONS

9.8.1 Probe Data for Sediment Oxygen, Eh, and pH

9.8.1.1 Shelf Sites MP 299, MP 288, EI 346, and ST 160. Vertical profiles for DO (O_2) and Eh were obtained using probes at far-field, mid-field, near-field, and discretionary stations during Sampling Cruises 1 and 2 for shelf sites MP 299, MP 288, and EI 346. In addition, probe data for sediments from shelf site ST 160 (water depth 37 m) were collected; however, only supporting data for TOC (Appendix E) and SBF (Chapter 8) were obtained. Measurement of pH was carried out at as many stations as time permitted. The complete data sets for oxygen, Eh, and pH are presented in tabular and graphical forms in Appendix E.

Values for Eh represent the sum of all oxidation/reduction reactions that are occurring in the sediment. An approximate Eh value can be given for the occurrence of various redox reactions (Figure 9-47). For example, the onset of bacterial reduction of nitrate (a replacement oxidizing agent for oxygen) to ammonia occurs at an Eh <200 mV. The onset of sulfate reduction to H_2S occurs as Eh values decrease below 0 to -100 mV (Figure 9-47).

At MP 299, concentrations of DO in the sediment ranged from ~150 µM (or 4.7 mg/L where 1 mg/L = 31.2 µM) in the bottom water collected in the box core (bottom water value is plotted at a depth of 0.0 cm on each graph) to <2 µM at varying depths in the cores (Figure 9-48). Concentrations of DO in the overlying water from the box core probably do not provide an exact measure of O_2 levels in near-bottom water; however, they provide a comparable and reasonable point of reference for each sediment core. Oxygen values for the overlying water are plotted at 0 cm on the pertinent graphs and tabulated at 0 cm in Appendix E. Dissolved oxygen levels in the overlying water, at 1 to 2 m above bottom, were typically in the range of 200 to 250 µM.

Concentrations of DO in sediment from the far-field stations at MP 299 were non-detectable (<2 µM) at variable depths of 0.5 to 2.2 cm. The depth in the sediment column where O_2 levels were not detectable decreased to 0.3 to 1.5 cm at mid-field stations and 0.1 to 0.5 cm at near-field stations (Table 9-12 and Figure 9-48). Main Pass 299 is located closer to the Mississippi River delta than any other site and is characterized by extensive offshore activity. The vertical profiles for oxygen showed little to no oxygen in most of the near-field stations, with only slightly greater amounts of O_2 at mid-field to far-field stations (Figure 9-48 and Table 9-12).

To help summarize and simplify the O_2 data for this report, the results for DO also are presented as the integrated (total) amount of oxygen (ΣO_2) in the sediment column (as nmoles/cm^2 over the length of the sediment column until levels of zero oxygen are reached). These oxygen inventories are presented as the average and standard deviation for near-field, mid-field, and far-field stations from each site for Sampling Cruises 1 and 2. At MP 299 during Sampling Cruise 1, the ΣO_2 in the sediments averaged 3 to 5 times more at mid-field and far-field stations than at near-field stations (Figure 9-49). However, the ΣO_2 in the sediment during Sampling Cruise 2 was not significantly different at near-field versus mid-field and far-field stations (Figure 9-49). The increase in ΣO_2 for near-field stations at MP 299 for Sampling Cruise 2 relative to Sampling Cruise 1 is supported by data for the depth to zero oxygen and the lower limit of Eh values at near-field stations (Table 9-12). The Eh at 10 cm ($Eh_{10\ cm}$) was <0 at all near-field stations except NF-4 for Sampling Cruise 1 (Table 9-12); however, the lowest $Eh_{10\ cm}$ for Sampling Cruise 2 was +60. The lowest Eh values in any core (-178 mV at 2 cm and -171 mV at 10 cm at Station NF-6, Sampling Cruise 1) were found where concentrations of SBF were 0.5%, relative to <0.05% at the other near-field, mid-field, and far-field stations. All values

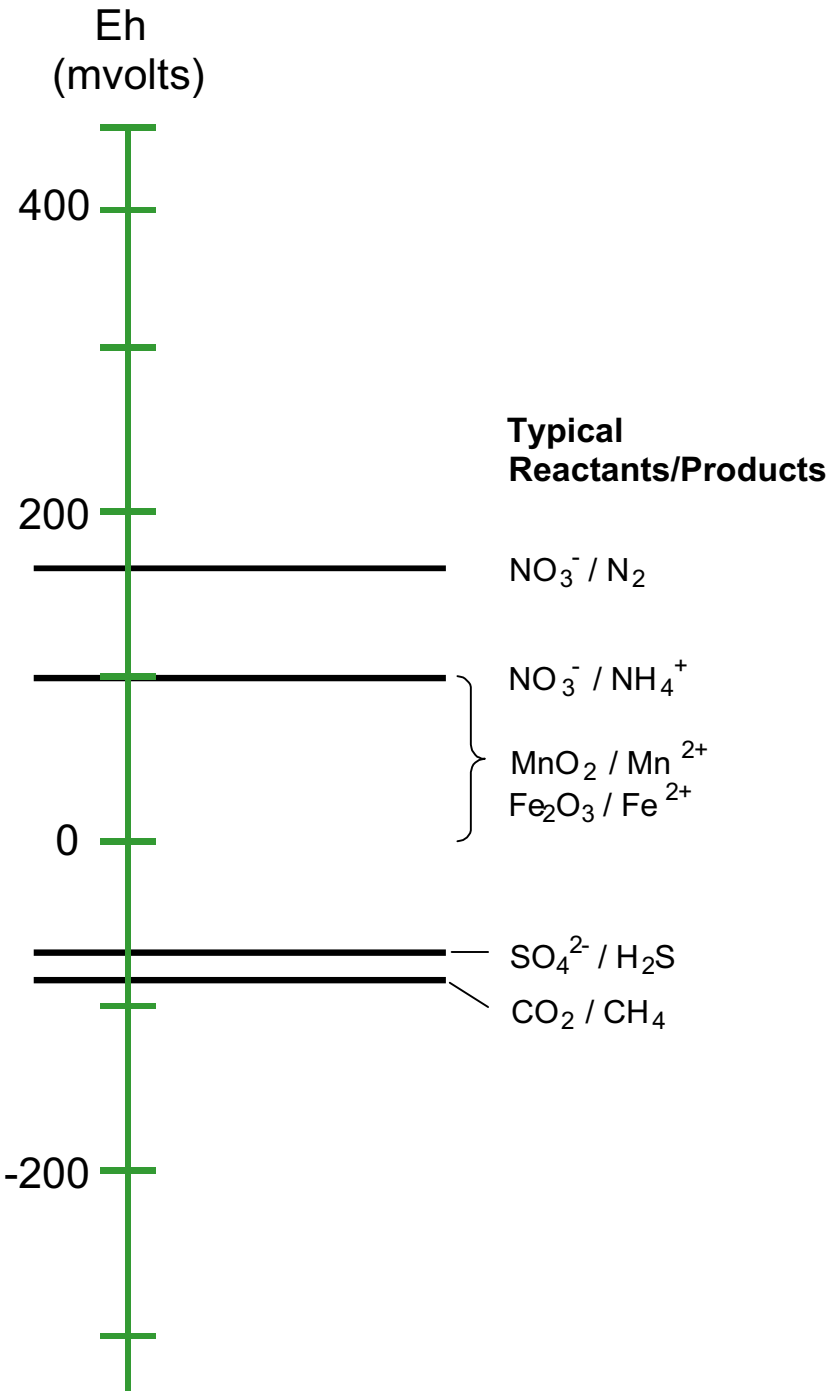

Figure 9-47. Approximate redox potential (Eh) values at which various redox reactions occur in water (From: Drever, 1997).

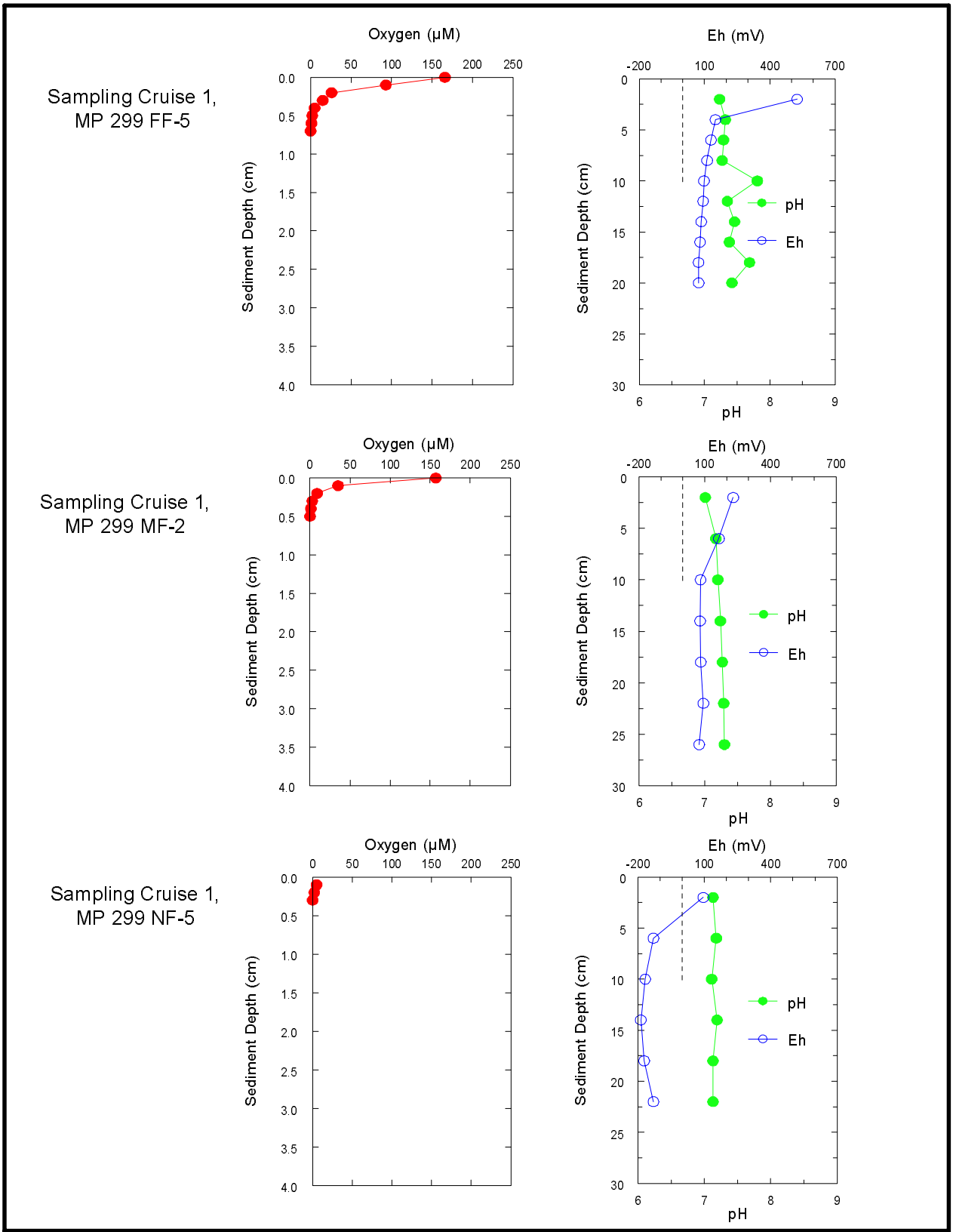

Figure 9-48. Vertical profiles for dissolved oxygen, pH, and redox potential (Eh) in sediments from representative near-field (NF), mid-field (MF), and far-field (FF) stations at Main Pass (MP) 299 for Sampling Cruise 1.

for $Eh_{10\ cm}$ at mid-field and far-field stations were >0 mV and averaged +84 ± 26 mV relative to -73 ± 110 mV at near-field stations. However, the distribution of the SBF alone cannot explain trends in oxygen inventories or Eh, as shown in more detail below. Overall at MP 299, average levels of ΣO_2 for Sampling Cruises 1 and 2 were not significantly different for mid-field versus far-field stations (Table 9-13). However, average values for ΣO_2 at near-field stations were significantly higher during Sampling Cruise 2 (Table 9-13).

Table 9-12. Summary data for dissolved oxygen, redox potential (Eh), and pH for sediment from shelf sites.

Site (Shallow Water)	Station	Zero O_2 depth (cm)	$Eh_{1\ cm}$ range (mV)		$Eh_{10\ cm}$ range (mV)		pH
Main Pass 299	NF (S1)	0.1-0.5	+537	-178	+94	-171	6.8-7.3
	(S2)	0.1-1.2	+519	+82	+136	+60	-
	MF (S1)	0.3-1.5	+405	+102	+108	+74	7.0-7.4
	(S2)	0.2-0.7	+450	+134	+167	+81	-
	FF (S1)	0.5-2.2	+513	+110	+119	+20	6.8-7.8
	(S2)	0.1-0.9	+541	+78	+120	+65	-
Main Pass 288	NF (S1)	0.2-0.8	+580	+134	+120	-81	7.1-7.7
	(S2)	0.1-0.9	+527	+161	+176	+76	-
	MF (S1)	0.5-2.3	+306	+90	+70	-50	7.3-8.0
	(S2)	0.1-1.6	+540	+91	+162	+7	-
	FF (S1)	0.7-1.9	+503	+226	+150	+71	7.2-7.7
	(S2)	0.1->3.1	+570	+42	+204	-91	-
Eugene Island 346	NF (S1)	0.0-0.6	+112	-215	-6	-272	7.3-8.2
	(S2)	0-0.8	+130	-174	+68	-183	-
	MF (S1)	0.1-1.5	+105	-164	+53	-164	-
	(S2)	0.2-1.1	+481	-123	+85	-154	-
	FF (S1)	1.7-5.3	+521	+470	+101	+54	-
	(S2)	0.3-2.9	+535	+103	+117	+55	-
South Timbalier 160	NF (S1)	0.0-0.4	+45	-181	-90	-183	-
	(S2)	0.1-0.5	+461	-159	+149	-190	-
	MF (S1)	0.4-2.2	+101	+71	-7	-	-
	(S2)	0.3-0.5	+461	+191	+143	+93	-
	FF (S1)	0.4	+290	-	+283	-	-
	(S2)	0.3	+457	+163	+128	+88	-

S1 = Sampling Cruise 1.
S2 = Sampling Cruise 2.

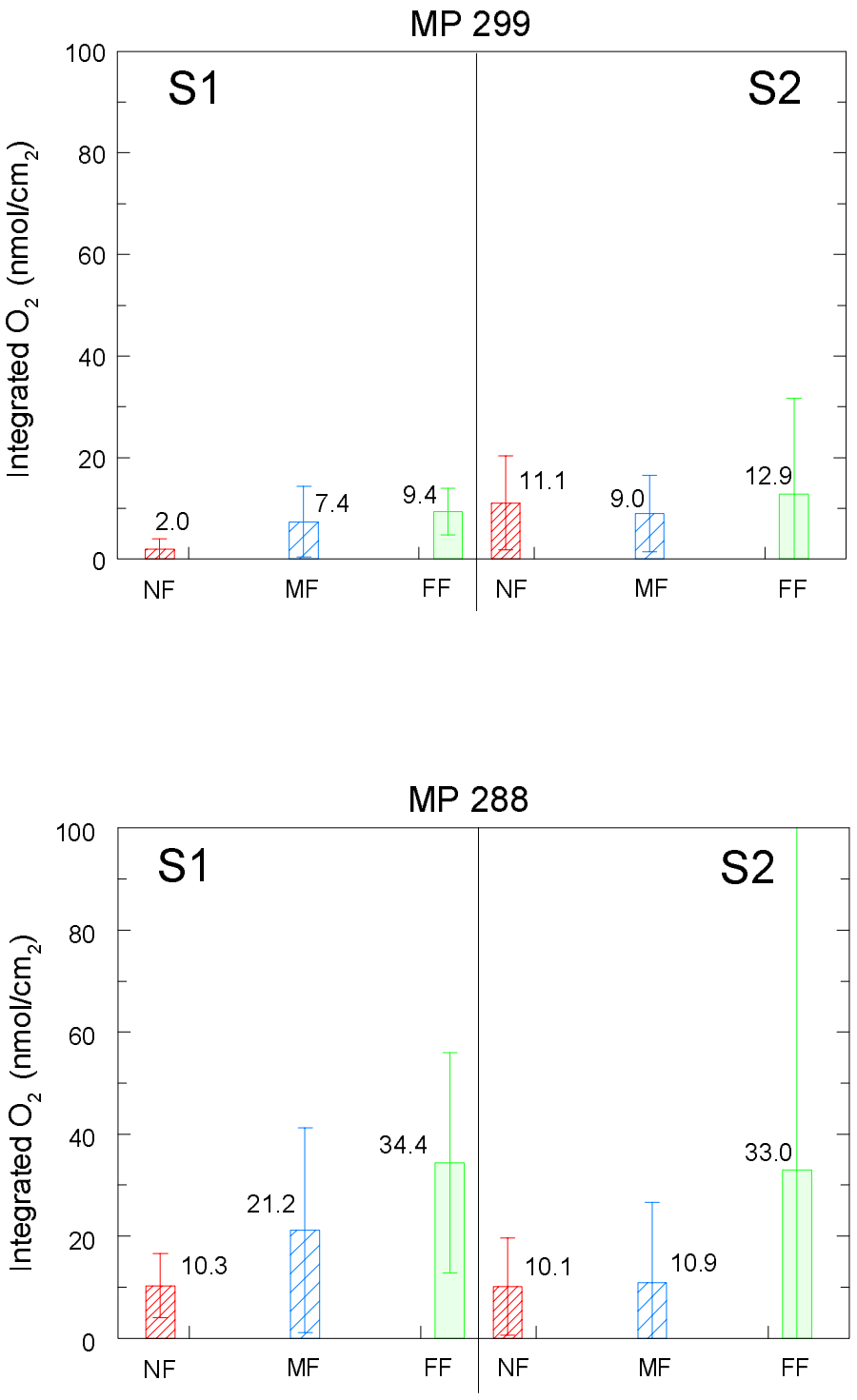

Figure 9-49. Integrated amounts of oxygen in sediment column for near-field (NF), mid-field (MF), and far-field (FF) stations at Main Pass (MP) 299 and MP 288 for Sampling Cruises 1 and 2 (S1 and S2). Bar and number show mean, and line shows standard deviation.

Table 9-13. Means and standard deviations for integrated amounts of dissolved oxygen in sediments from shelf sites during Sampling Cruises 1 and 2.

Site (Cruise)	Near-Field ($nmol/cm^2$)	Mid-Field ($nmol/cm^2$)	Far-Field ($nmol/cm^2$)
Main Pass 299 (Sampling Cruise 1)	2.0 ± 2.1	7.4 ± 7.0	9.4 ± 4.6
Main Pass 299 (Sampling Cruise 2)	11 ± 9	9.0 ± 7.5	13 ± 19
Main Pass 288 (Sampling Cruise 1)	10 ± 6	21 ± 20	34 ± 22
Main Pass 288 (Sampling Cruise 2)	10 ± 9.5	11 ± 16	33 ± 69
Eugene Island 346 (Sampling Cruise 1)	4.6 ± 3.6	10 ± 12	71 ± 45
Eugene Island 346 (Sampling Cruise 2)	4.0 ± 6.3	14 ± 17	50 ± 39

The ΣO_2 in the far-field sediments at MP 288 averaged 34 $nmole/cm^2$ during Sampling Cruise 1 and 33 $nmole/cm^2$ during Sampling Cruise 2, about 3 times greater than found in sediment from the far-field stations at MP 299 (Figure 9-49 and Table 9-13). This difference in oxygen inventory at the far-field stations may occur because MP 288 is farther away from the Mississippi delta in an area where sedimentation rates in these sandy sediments are slower than at MP 299. At MP 288, the oxygen profiles extend about 3 times deeper into the sediment at the far-field stations than at the mid-field and near-field stations (Figure 9-50 and Table 9-12). Values for Eh were similar in the top 2 cm at the near-field, mid-field, and far-field stations (Table 9-12). However, Eh values at 10 cm averaged about 100 mV less in the near-field sediment than in the far-field sediment (Table 9-12). Depletion of oxygen at shallower depths, along with the parallel decrease in Eh, leads to the lower O_2 inventory at the near-field stations. This distinction may be partly due to low levels of SBF in the near-field stations (~0.02% to 0.05%) relative to non-detectable levels of SBF at the far-field stations. Differences in ΣO_2 between Sampling Cruises 1 and 2 are not significant.

At EI 346, the depth of penetration of oxygen and the ΣO_2 at far-field stations were ~1.5 to 2 times higher than observed at MP 288 (Table 9-12, Figures 9-51 and 9-52), most likely a function of lower natural rates of deposition of sediment and organic matter at EI 346. Values for ΣO_2 in sediment at near-field and mid-field stations at EI 346 were significantly lower than at far-field stations (Figure 9-52, Table 9-13). This trend was observed during both Sampling Cruises 1 and 2.

The low levels of ΣO_2 in near-field sediments from EI 346 (Figure 9-52) were consistent with data for Eh that show most values are below -100 mV and therefore are anoxic and rich in H_2S. Concentrations of SBF were >0.01% (maximum 4.75%) in all near-field sediments from EI 346 during Sampling Cruise 1 and >0.01% (maximum 1.4%) during Sampling Cruise 2, relative to non-detectable levels of SBF at far-field stations.

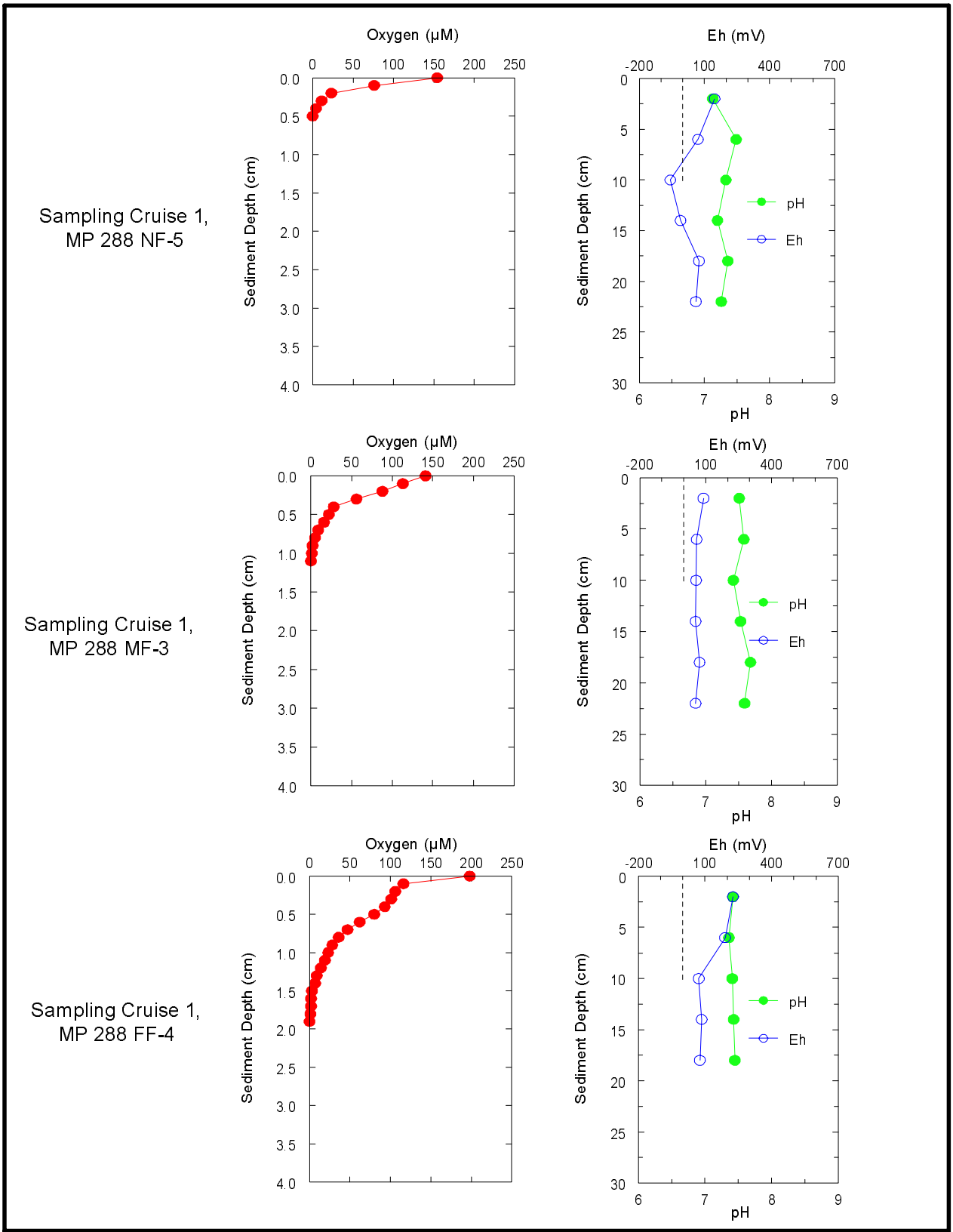

Figure 9-50. Vertical profiles for dissolved oxygen, pH, and redox potential (Eh) in sediments from representative near-field (NF), mid-field (MF), and far-field (FF) stations from Main Pass (MP) 288 for Sampling Cruise 1.

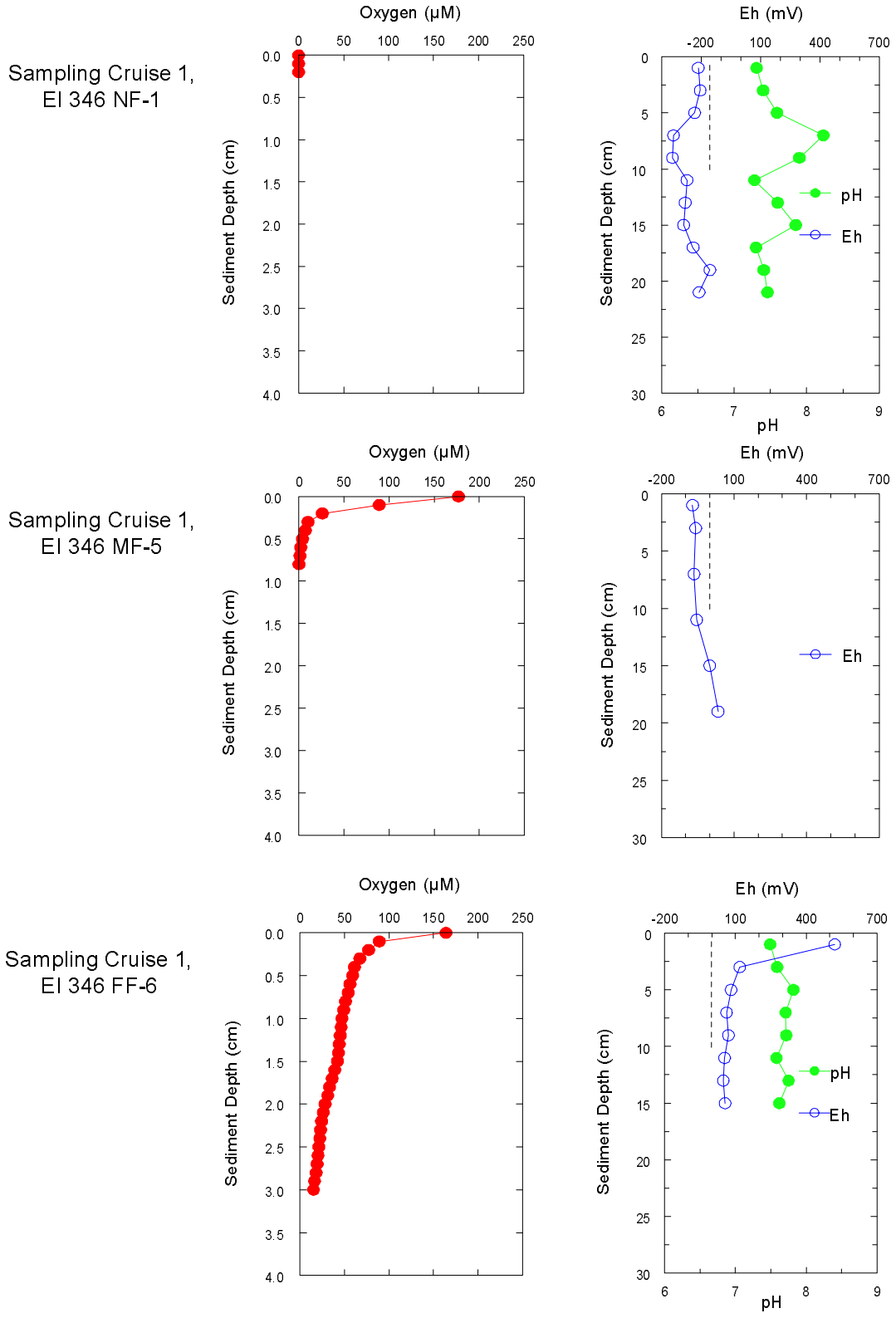

Figure 9-51. Vertical profiles for dissolved oxygen, pH, and redox potential (Eh) in sediments from representative near-field (NF), mid-field (MF), and far-field (FF) stations from Eugene Island (EI) 346 for Sampling Cruise 1.

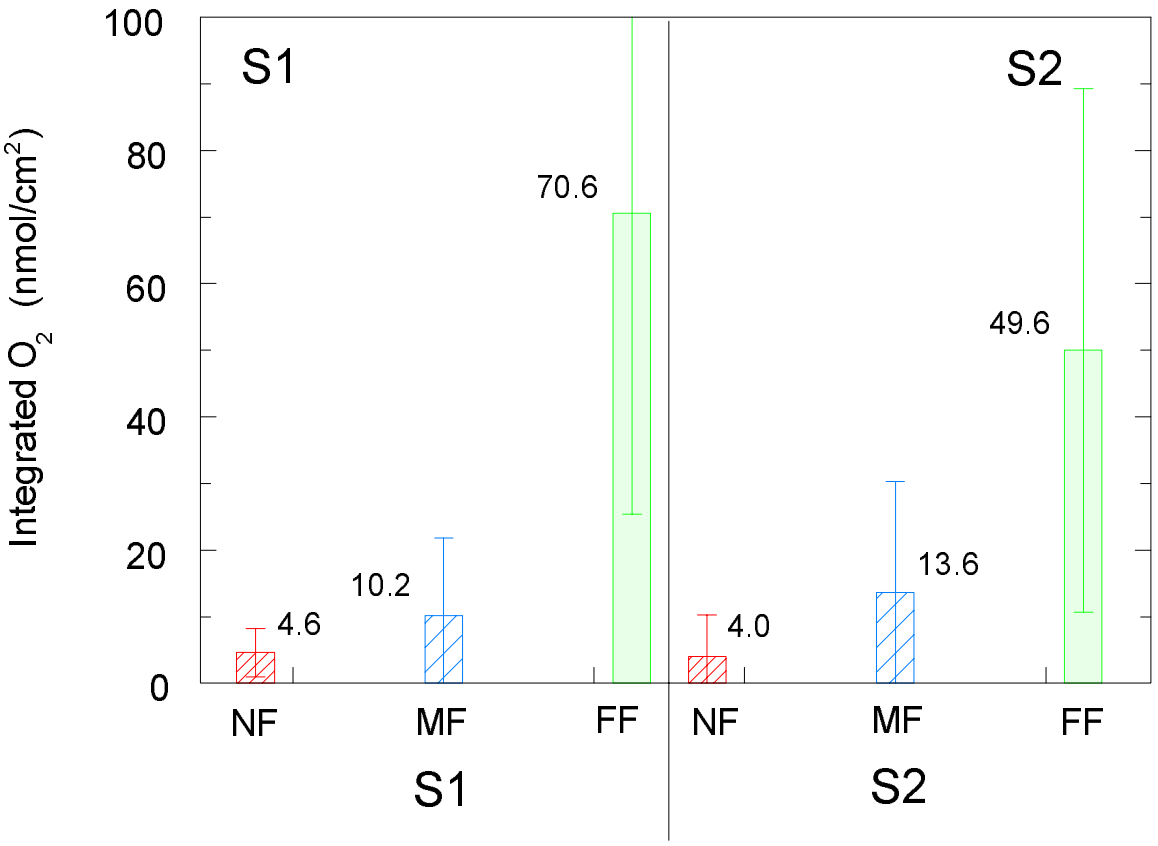

Figure 9-52. Integrated amounts of oxygen in sediment columns from near-field (NF), mid-field (MF), and far-field (FF) stations at Eugene Island (EI) 346 for Sampling Cruises 1 and 2 (S1 and S2). Bar and number show mean, and line shows standard deviation.

9.8.1.2 Slope Sites MC 496, EW 963, and GC 112 (Water Depths >500 m). At MC 496, the oxygen profiles (Figure 9-53) and oxygen inventories (Figure 9-54) are not significantly different among the near-field, mid-field, and far-field sites or between cruises. These similarities in levels of ΣO_2 occur despite sharp decreases in the concentrations of SBF from Sampling Cruise 1 to Sampling Cruise 2 at mid-field and near-field stations, as discussed in the next section of this chapter. Mississippi Canyon 496 is closer to the Mississippi River, and the inventory of O_2 in the far-field stations was about 25% to 40% lower than at other slope sites GC 112 and EW 963 (to be shown later in this chapter). Results for Eh and depth to zero oxygen also were similar at near-field, mid-field, and far-field stations at MC 496 (Table 9-14).

Table 9-14. Summary data for dissolved oxygen, redox potential (Eh) and pH for sediment from continental slope sites at near-field (NF), mid-field (MF), and far-field (FF) stations. Data for discretionary stations are included with NF stations.

Site (Deepwater)	Station	Zero O_2 depth (cm)	$Eh_{1\ cm}$ range (mV)		$Eh_{10\ cm}$ range (mV)		pH
Mississippi Canyon 496	NF (S1)	0.4-3.7	+490	+320	+177	+44	-
	(S2)	0.3-2.3	+546	+180	+130	+74	-
	MF (S1)	0.5-3.7	+485	+105	+66	+38	-
	(S2)	0.2-2.4	+564	+490	+123	+96	-
	FF (S1)	1.2-2.3	+223	+204	+90	+71	7.6-8.0
	(S2)	0.1-2.8	+541	+106	+423	+86	-
Green Canyon 112	NF (S1)	0.3-2.5	+350	-280	+76	-198	7.4-7.9
	(S2)	0.5-1.7	+516	-91	+162	-108	-
	MF (S1)	0.3-4.4	+501	+126	+425	+82	-
	(S2)	0.2-1.9	+521	+259	+272	+89	-
	FF (S1)	2.6-4.9	+498	+155	+294	+81	7.4-7.6
	(S2)	2.2-3.1	+542	+472	+333	+128	-
Ewing Bank 963	NF (S1)	0.2-3.6	+319	-144	+165	-157	7.6-8.3
	(S2)	0-1.8	+529	-137	+286	+74	-
	MF (S1)	0.6-3.7	+541	-63	+360	-69	-
	(S2)	1.9-2.4	+535	+282	+345	+108	-
	FF (S1)	2.8-3.6	+382	+240	+280	+114	7.4-7.8
	(S2)	2.1-3.3	+537	+339	+315	+103	-
Viosca Knoll 783	NF (S1)	1.9-2.5	+411	+131	+141	+82	7.3-7.6
	(S2)	0.2-1.7	+510	+151	+159	+107	-
	MF (S1)	1.3-2.4	+436	+130	+222	+87	7.1-8.1
	(S2)	1.8-2.5	+475	+242	+238	+79	-
	FF (S1)	0.4-2.2	+585	+250	+289	+111	7.1-7.9
	(S2)	1.1-2.3	+525	+171	+140	+101	-

S1 = Sampling Cruise 1.
S2 = Sampling Cruise 2.

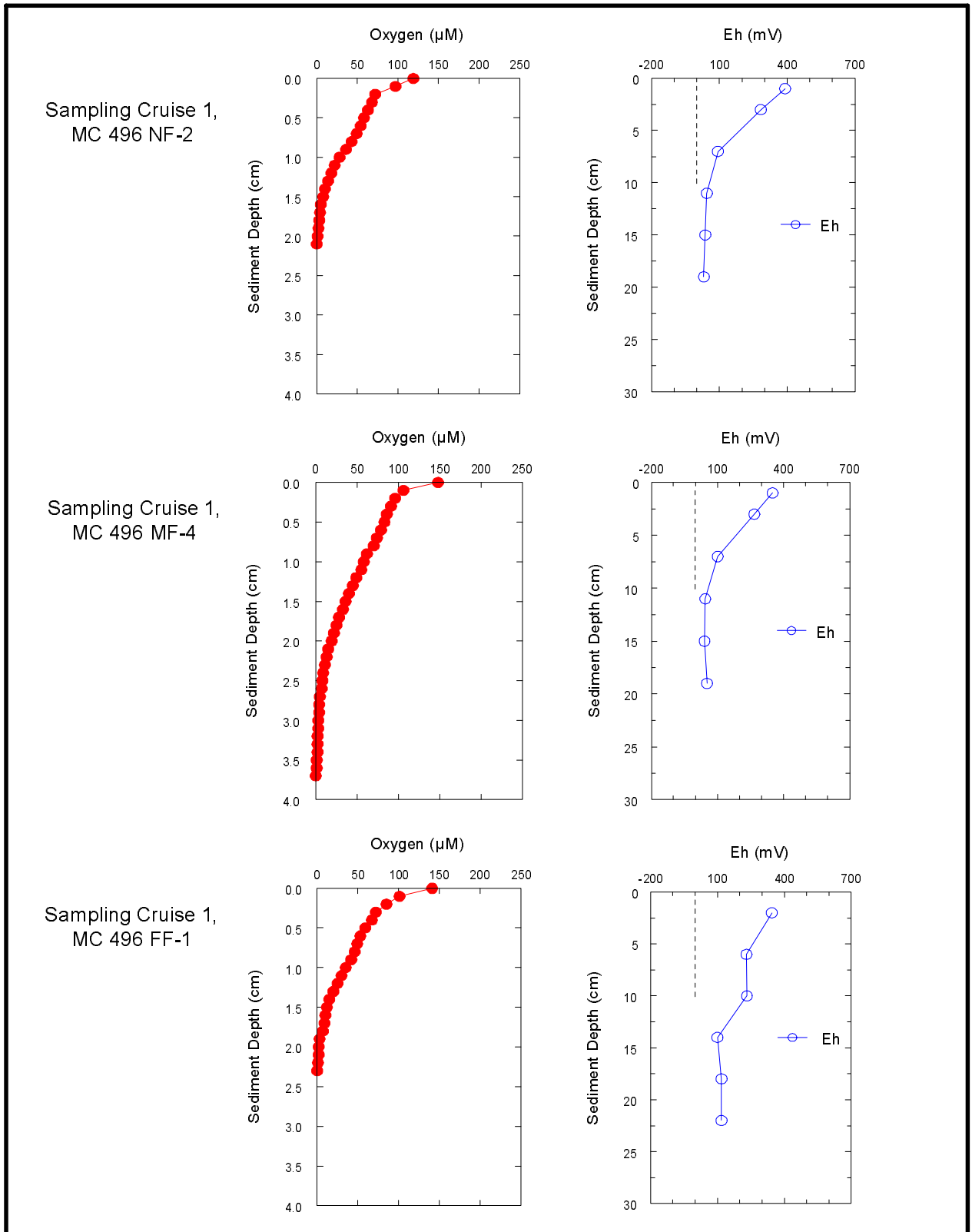

Figure 9-53. Vertical profiles for dissolved oxygen and redox potential (Eh) in sediment from representative near-field (NF), mid-field (MF), and far-field (FF) stations from Mississippi Canyon (MC) 496 for Sampling Cruise 1.

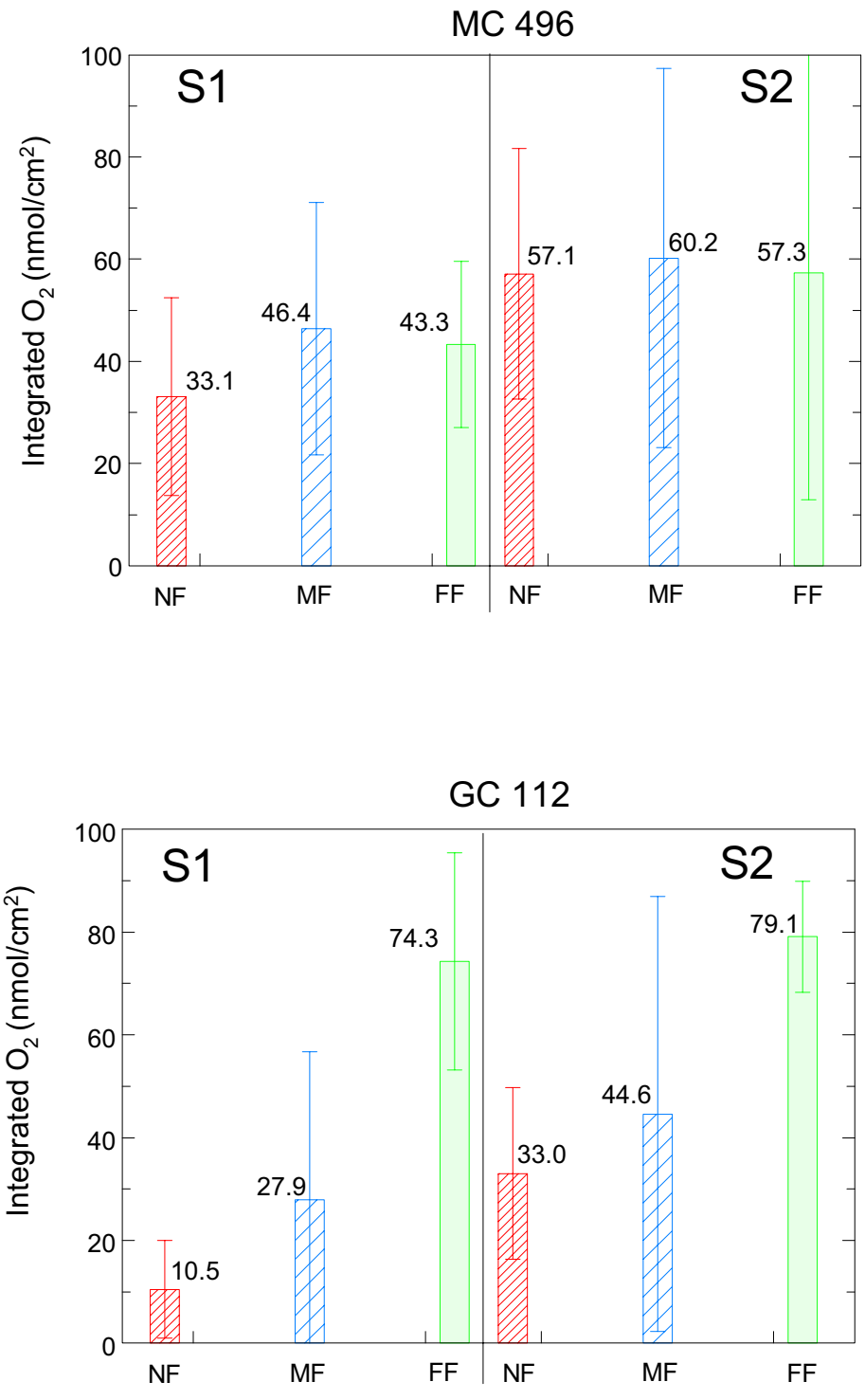

Figure 9-54. Integrated amounts of oxygen in sediment column at near-field (NF), mid-field (MF), and far-field (FF) stations at continental slope sites Mississippi Canyon (MC) 496 and Green Canyon (GC) 112 for Sampling Cruises 1 and 2 (S1 and S2). Bar and number show mean, and line shows standard deviation.

For sediment at GC 112, the far-field stations had an average ΣO_2 that was 2.7 and 1.8 times greater than at mid-field stations for Sampling Cruises 1 and 2, respectively (Figure 9-54). At near-field stations during Sampling Cruise 1, the ΣO_2 was 7 times lower than at far-field stations; however, the ΣO_2 during Sampling Cruise 2 was significantly greater (by a factor of 3) than during Sampling Cruise 1 (Figure 9-54 and Table 9-15).

Table 9-15. Means and standard deviations for integrated amounts of dissolved oxygen in sediments from continental slope sites during Sampling Cruises 1 and 2.

Site (Cruise)	Near-Field ($nmol/cm^2$)	Mid-Field ($nmol/cm^2$)	Far-Field ($nmol/cm^2$)
Mississippi Canyon 496 (Sampling Cruise 1)	33 ± 19	46 ± 25	43 ± 16
Mississippi Canyon 496 (Sampling Cruise 2)	57 ± 24	60 ± 37	57 ± 44
Green Canyon 112 (Sampling Cruise 1)	11 ± 9.5	28 ± 3	74 ± 21
Green Canyon 112 (Sampling Cruise 2)	33 ± 17	45 ± 42	79 ± 11
Ewing Bank 963 (Sampling Cruise 1)	13 ± 13	50 ± 31	87 ± 27
Ewing Bank 963 (Sampling Cruise 2)	39 ± 21	68 ± 12	88 ± 26

Values for Eh at GC 112 were consistent with the DO data (Figure 9-55). The Eh was <0 mV throughout the near-field core (shown in Figure 9-55), 100 to 300 mV in the representative mid-field core, and 400 mV to 100 mV over the top 10 cm in the representative far-field core. Production of H_2S is predicted in sediment from many near-field stations but not at the mid-field and far-field stations. Discussion of results for pore water will be provided in a later section of this chapter to help link the DO and Eh data to ongoing chemical reactions in the sediments.

Values for Eh at 1 cm are much more variable in the near-field stations than at mid-field and far-field stations from GC 112 partly because the near-field stations around the same site have considerable variability in the amount of SBF present and the thickness of black layers containing drilling discharges (Table 9-14). In some cases, the variability can be partly explained by concentrations of SBF. For example, at NF-4 (Sampling Cruise 1), levels of SBF were 6.3% and Eh was -280 mV in the top centimeter. The highest level of SBF at any other station at GC 112 was 0.3%, and all Eh values in the top centimeters of sediment at the other sites were >-50 mV. At a depth of 10 cm in the sediment column for GC 112, the lowest Eh values at the near-field stations were about 100 to 200 mV lower than the lowest values at the mid-field and far-field stations (Table 9-14). In the cores from GC 112, values for pH ranged from 7.4 to 7.9 (Table 9-14). The pH decreases as levels of CO_2 and H_2S increase. Typical pH levels in sediment range from about 7 to 8. Addition of drilling fluid can cause pH levels to increase above 8 or even 9.

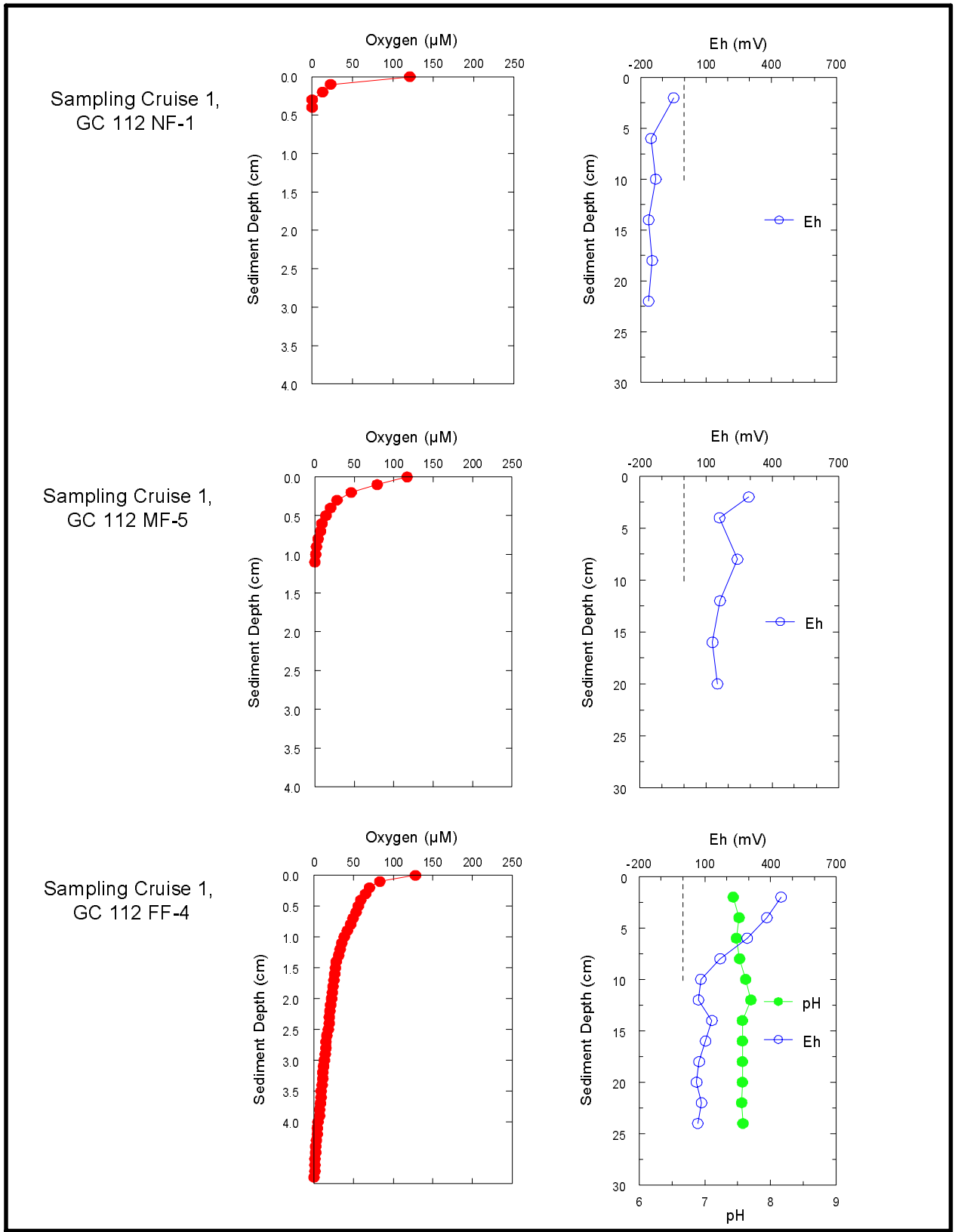

Figure 9-55. Vertical profiles for dissolved oxygen, pH, and redox potential (Eh) in sediments from representative near-field (NF), mid-field (MF), and far-field (FF) stations from Green Canyon (GC) 112 for Sampling Cruise 1.

Vertical profiles for dissolved O_2 at EW 963 (Figure 9-56) are similar to those observed at GC 112. Furthermore, oxygen inventories at far-field stations at EW 963 (Figure 9-57) also are within 10% to 20% of values for GC 112 (Table 9-15). Levels of ΣO_2 at far-field stations from EW 963 are 87 nmole/cm^2 for Sampling Cruise 1 and 88 nmole/cm^2 for Sampling Cruise 2 (Figure 9-57), about 75% and 30% higher, respectively, than levels at mid-field stations. The amounts of ΣO_2 at near-field stations from EW 963 are significantly lower than at mid-field and far-field stations. However, levels of SBF at near-field stations for EW 963 are all <0.2%, with the exception of 0.64% at NF-4 (Sampling Cruise 1).

Levels of ΣO_2 at near-field stations from slope sites GC 112 and EW 963 are significantly higher in Sampling Cruise 2 sediments than in Sampling Cruise 1 sediments. This trend is consistent with overall lower amounts of SBF in sediments collected during Sampling Cruise 2 (Chapter 8).

9.8.2 Factors Controlling Redox Conditions in Sediments.

One goal of the redox portion of this study is to determine the influence of SBF on the redox state of the sediment. As previously suggested, the rate of input of organic matter may be a primary controlling parameter. In the absence of detailed rate data, the relationships developed in this chapter are between the oxygen inventory (ΣO_2) of the sediment and concentrations of SBF and TOC. The oxygen inventory seems to be a useful parameter for comparing sites. Comparisons of oxygen inventory with concentrations of SBF and TOC are directly linked to biochemical oxygen demand in the sediment.

9.8.2.1 Shelf Sites MP 299, MP 288, and EI 346. The ΣO_2 ranged from ~0 to 120 nmole/cm^2 at far-field stations from the shelf sites, even though no SBF was detected at any of the far-field stations (Figure 9-58). Thus, the ΣO_2 varies greatly and independently of SBF at the background (far-field) stations on the shelf. Lower levels of ΣO_2 for far-field stations at MP 299 and MP 288 relative to EI 346 result from 25% and 40% higher levels of TOC at MP 288 and MP 299, respectively (Figure 9-59). At mid-field stations on the shelf, concentrations of ΣO_2 were <25 nmol/cm^2 at all stations except one from MP 288 that had a ΣO_2 of almost 50 nmol/cm^2 (Figure 9-58). Levels of SBF at mid-field stations were <0.05% at all stations except two at EI 346 (Figure 9-58). Once again, values for ΣO_2 varied independently of concentrations of SBF. At the near-field stations, levels of ΣO_2 were lower than at far-field stations, especially for EI 346 (Figure 9-58). However, concentrations of SBF were >0.05% at only 9 of 34 near-field stations, with 8 of those stations at EI 346 (Figure 9-58). Evidence of drilling discharges based on sediment Ba concentrations was found at all near-field stations on the shelf. Thus, the presence of SBF alone at the shallow-water shelf locations seems to be a less important variable in controlling redox state at shelf sites than the presence of non-SBF drilling discharges or other components with high oxygen demand. Concentrations of TOC (Figure 9-59) do not correlate with oxygen inventories, as most TOC levels at all stations were rather closely grouped at 1% to 2%. However, sediments containing SBF at levels >0.05% (Figure 9-58) to TOC >2% (Figure 9-59) most definitely have low levels of ΣO_2 (<10 nmol/cm^2, Figure 9-58). A near-field effect on the redox state of the sediment is observed, with the best explanation being the presence of 2- to 20-cm thick black layers that were rapidly deposited relative to ambient sediments and contain some drilling discharges.

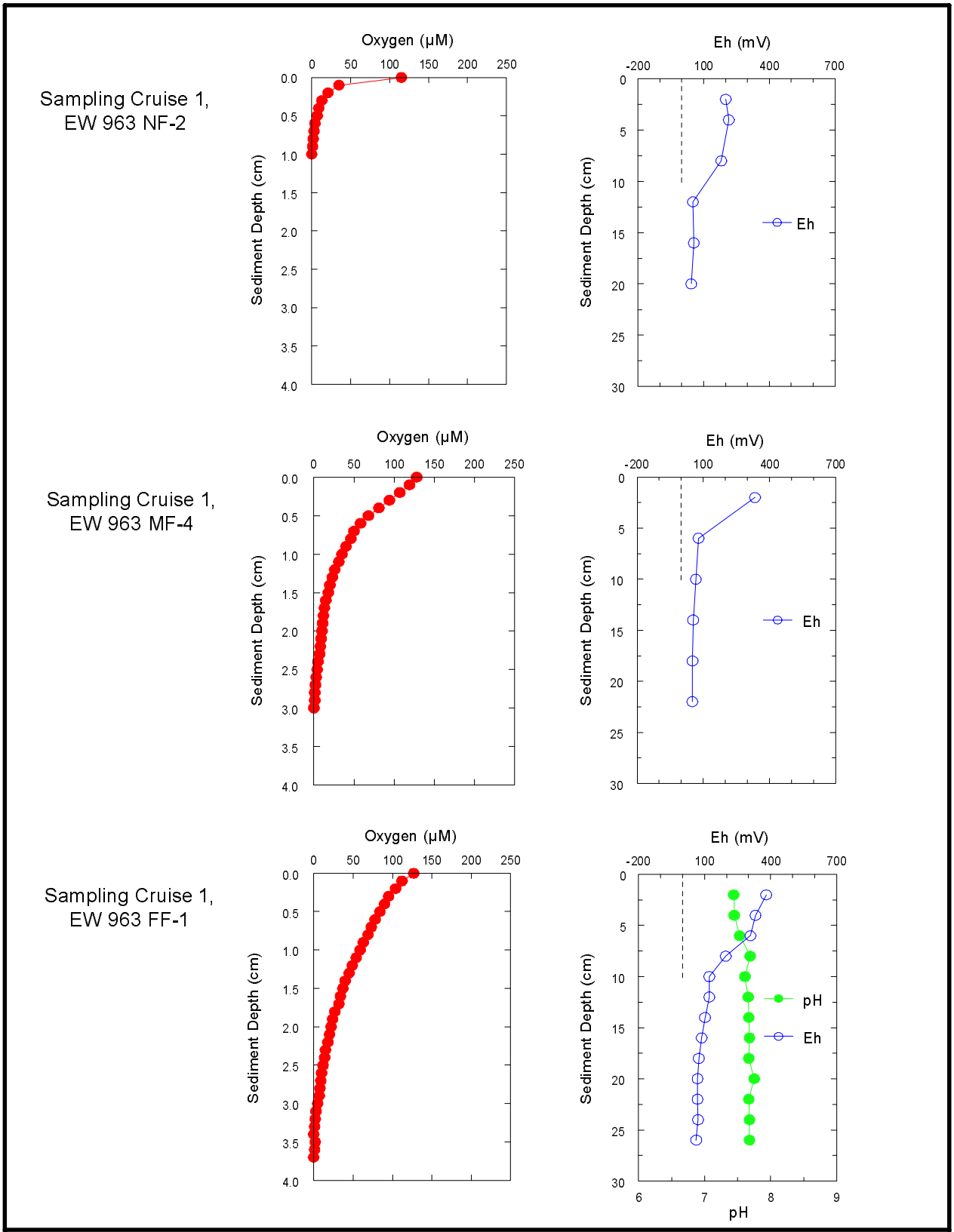

Figure 9-56. Vertical profiles for dissolved oxygen, pH, and redox potential (Eh) in sediments from representative near-field (NF), mid-field (MF), and far-field (FF) stations from Ewing Bank (EW) 963 for Sampling Cruise 1.

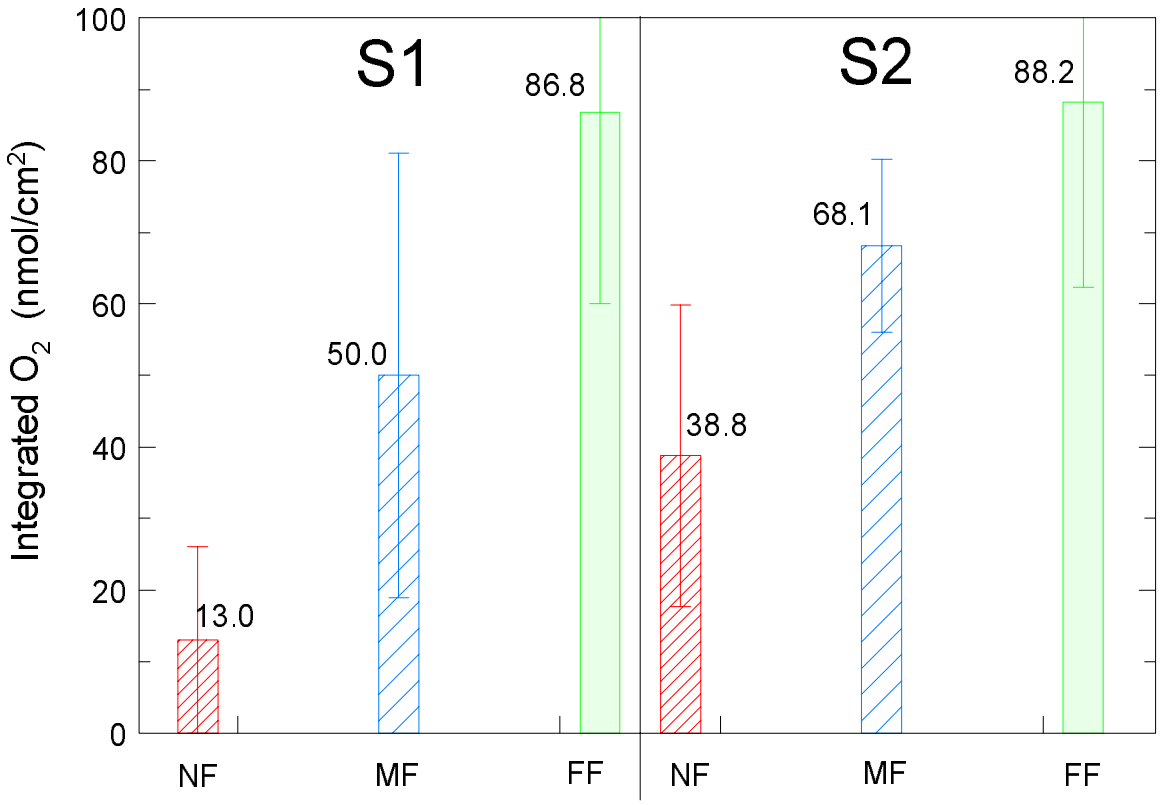

Figure 9-57. Integrated amounts of oxygen in sediment column at near-field (NF), mid-field (MF), and far-field (FF) stations at continental slope site Ewing Bank (EW) 963 for Sampling Cruises 1 and 2 (S1 and S2). Bar and number show mean, and line shows standard deviation.

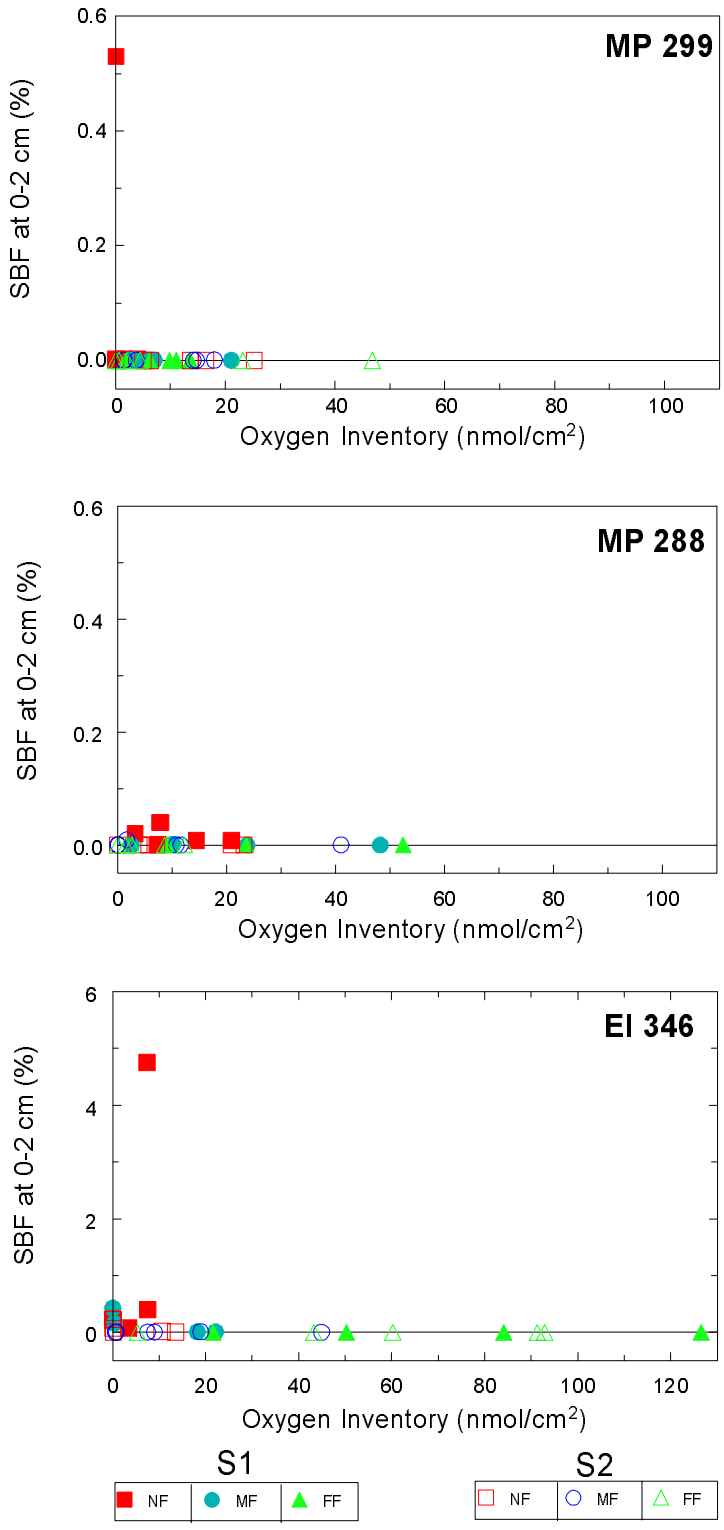

Figure 9-58. Oxygen inventories versus concentrations of synthetic based fluid (SBF) for near-field (NF), mid-field (MF), and far-field (FF) stations from continental shelf sites Main Pass (MP) 299, MP 288, and Eugene Island (EI) 346 for Sampling Cruises 1 and 2 (S1 and S2). Horizontal line at SBF = 0%.

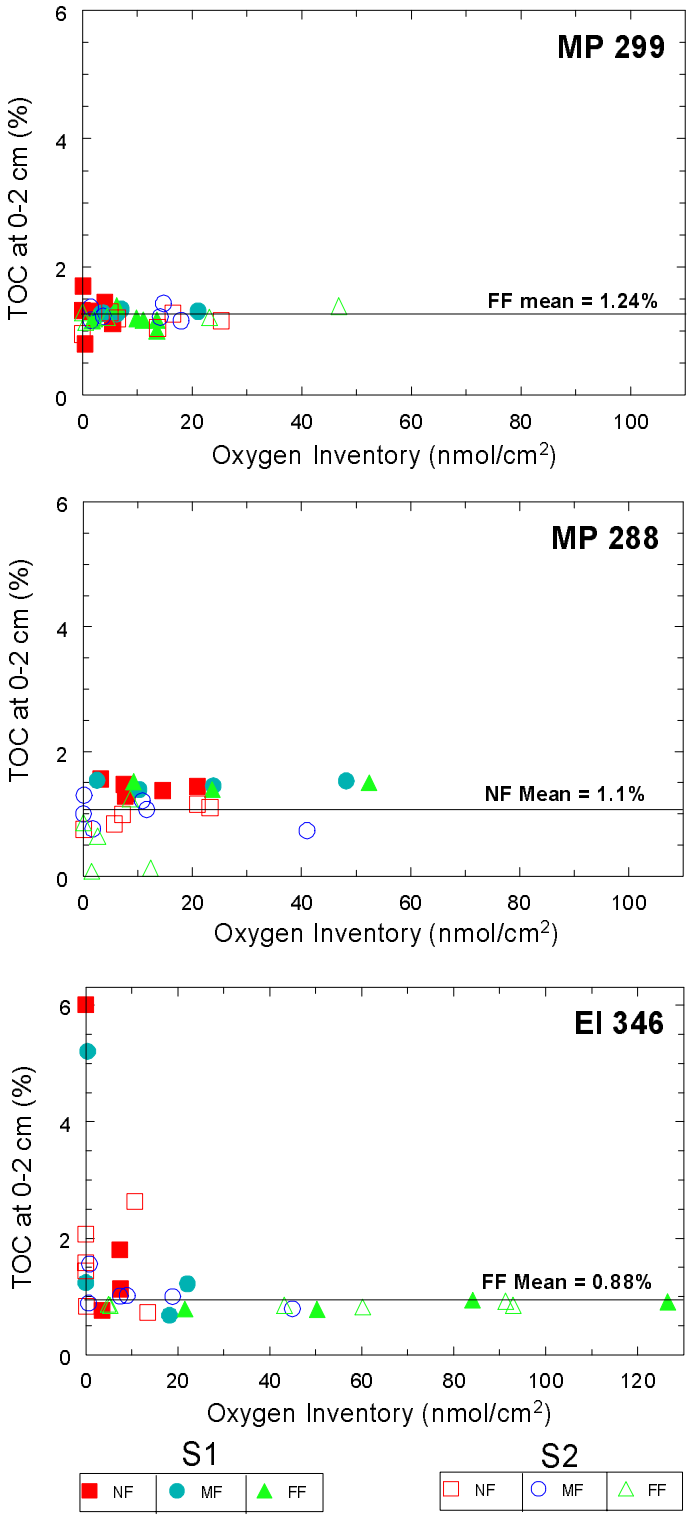

Figure 9-59. Oxygen inventories versus concentrations of total organic carbon (TOC) for near-field (NF), mid-field (MF), and far-field (FF) stations from continental shelf sites Main Pass (MP) 299, MP 288, and Eugene Island (EI) 346 for Sampling Cruises 1 and 2 (S1 and S2). Horizontal lines show mean levels of SBF for FF stations.

9.8.2.2 Slope Sites MC 496, EW 963, and GC 112. Values for ΣO_2 at far-field stations from the continental slope ranged from ~30 to 130 nmole/cm^2, even though no SBF was detected (Figure 9-60). Thus, once again, the ΣO_2 varies independently of SBF at background (far-field) stations. In the mid-field area, concentrations of SBF >0.05% were found at eight stations, and the oxygen inventory was <30 nmole/cm^2 at 10 stations (Figure 9-60). At the near-field stations, SBF was detected in all samples except one and was >0.05% in most of the samples. The ΣO_2 was <60 nmole/cm^2 at all near-field stations and <30 nmole/cm^2 at about two-thirds of the near-field stations (Figure 9-60). Although the oxygen inventory can vary widely in the absence of SBF, the presence of SBF does correspond with lower ΣO_2 values.

Comparisons of ΣO_2 with concentrations of TOC (Figure 9-61) show similar trends to that observed for SBF in that higher levels of TOC at some mid-field and near-field stations were consistent with low inventories of oxygen. Neither of the two variables introduced here explains all the low inventories of oxygen at mid-field and near-field stations. However, a near-site effect of lowering the redox state of the sediment is observed at most near-field and some mid-field stations.

9.8.3 Pore Water Composition

Pore water was collected at one far-field and one near-field station from each of the six sites on both cruises to complement the overall perspective on the redox state of the sediment. The pore water data will be used here to show how well the DO and Eh data predict the reactants and products of bacterial decomposition of organic matter in sediments. The pore water data, along with the oxygen and Eh data, also will be used to further identify changes in the redox state of the sediments in the presence of drilling discharges. The pore water data are tabulated in Appendix E, and vertical profiles for selected chemical species in several cores are presented below.

As background information, Table 9-16 shows some of the reactions that may occur as oxygen and subsequent oxidizing agents are used by bacteria to facilitate energy production from the oxidation of organic matter. As oxygen is depleted during oxidation of organic matter, nitrate and nitrite are produced (Eq. 1, Table 9-16). The shift from oxic decomposition of detrital organic matter by bacteria can occur abruptly at rather shallow depths in the sediment, as described in the previous sections of this chapter, to sub-oxic (nitrate reduction) decomposition (Eq. 2, Table 9-16). Upon depletion of oxygen and nitrate, other less efficient oxidizing agents, such as Mn and Fe oxides and sulfate, are used by resident bacteria (Eqs. 3 and 4, Table 9-16). Levels of Mn^{2+} and Fe^{2+} in pore water increase as metal oxides are chemically reduced.

Table 9-16. Selected reactions showing the decomposition of organic matter by various oxidizing agents (After: Froelich et al., 1979).

$(CH_2O)_{106}(NH_3)_{16}H_3PO_4 + 138\ O_2 = 106\ CO_2 + 16\ HNO_3 + H_3PO_4 + 122\ H_2O$	(Eq. 1)
$(CH_2O)_{106}(NH_3)_{16}H_3PO_4 + 94.4\ HNO_3 = 106\ CO_2 + 55.2\ N_2 + H_3PO_4 + 177.2\ H_2O$	(Eq. 2)
$(CH_2O)_{106}(NH_3)_{16}H_3PO_4 + 212\ MnO_2 + 424\ H^+ = 106\ CO_2 + 16\ NH_3 + H_3PO_4 + 212\ Mn^{2+} + 318\ H_2O$	(Eq. 3)
$(CH_2O)_{106}(NH_3)_{16}H_3PO_4 + 212\ Fe_2O_3$ (or 424 FeOOH) + 848 $H^+ = 106\ CO_2 + 16\ NH_3 + H_3PO_4 + 424\ Fe^{2+} + 530\ H_2O$ (or 742 H_2O)	(Eq. 4)
$(CH_2O)_{106}(NH_3)_{16}H_3PO_4 + 53\ SO_4^{2-} + 424\ H^+ = 106\ CO_2 + 16\ NH_3 + H_3PO_4 + 53\ S^{2-} + 318\ H_2O$	(Eq. 5)

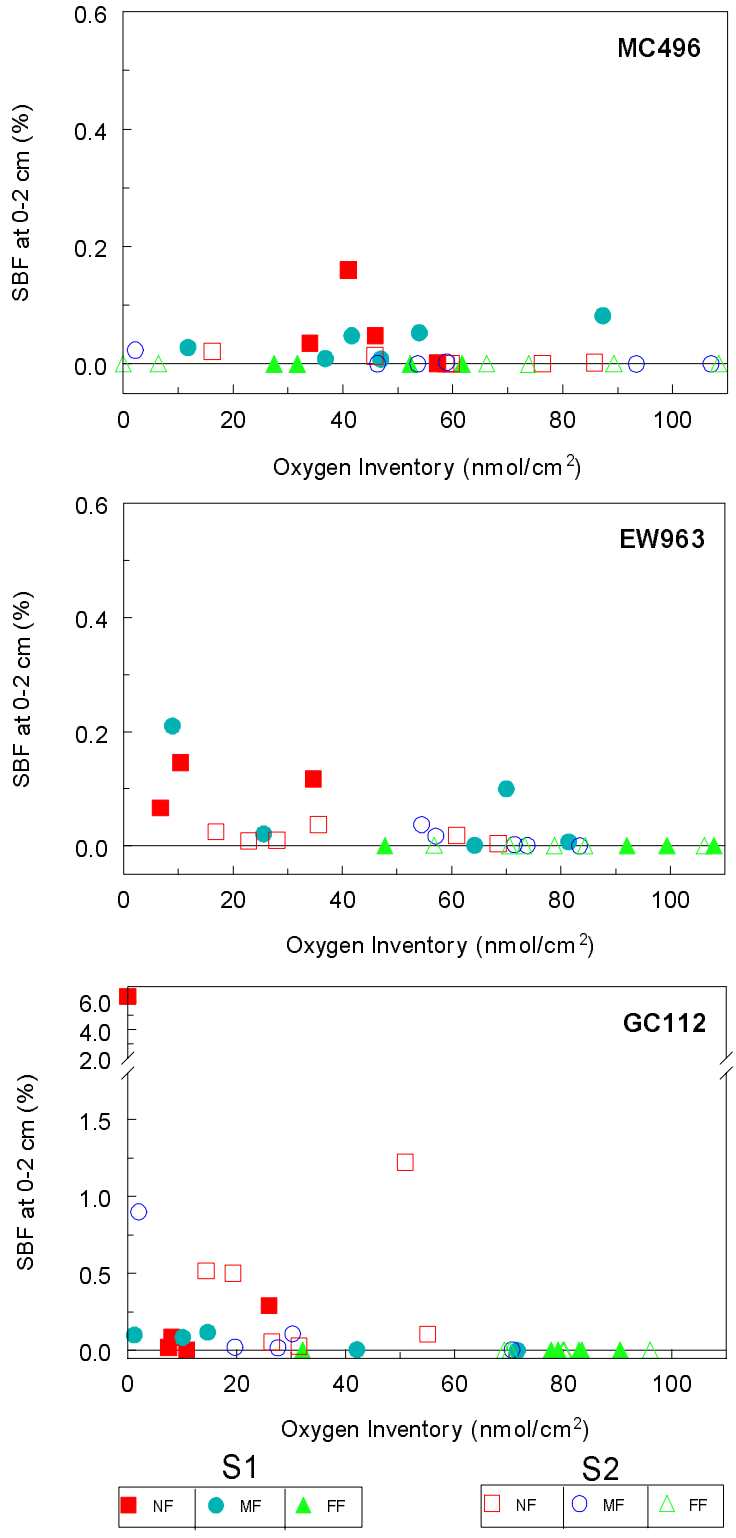

Figure 9-60. Oxygen inventories versus concentrations of synthetic based fluid (SBF) for near-field (NF), mid-field (MF), and far-field (FF) stations from continental slope sites Mississippi Canyon (MC) 496, Ewing Bank (EW) 963, and Green Canyon (GC) 112 for Sampling Cruises 1 and 2 (S1 and S2). Horizontal line at SBF = 0%.

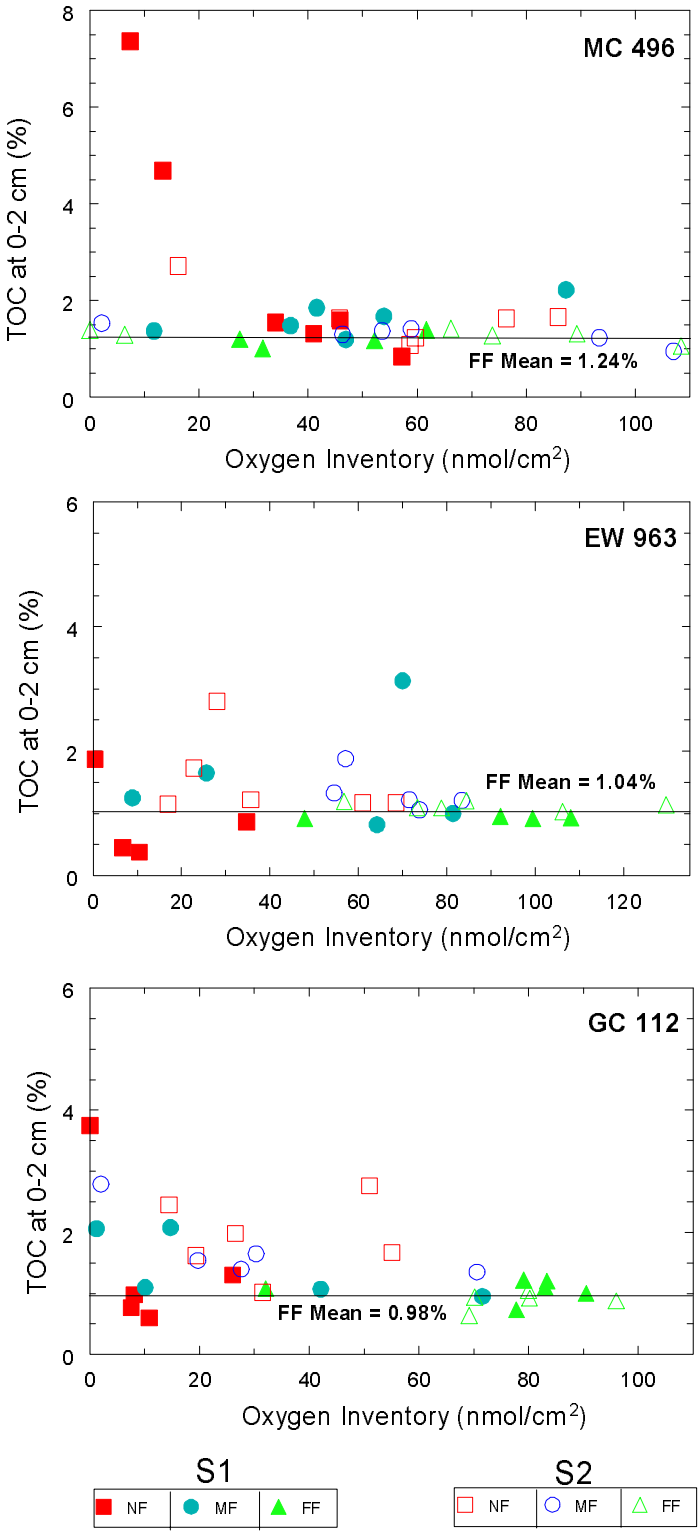

Figure 9-61. Oxygen inventories versus concentrations of total organic carbon (TOC) for near-field (NF), mid-field (MF), and far-field (FF) stations from continental slope sites Mississippi Canyon (MC) 496, Ewing Bank (EW) 963, and Green Canyon (GC) 112 for Sampling Cruises 1 and 2 (S1 and S2). Horizontal lines show mean levels of SBF for FF stations.

After sediment pore water becomes depleted of dissolved O_2, other oxidizing agents including dissolved NO_3^-, substrate-bound MnO_2 and Fe_2O_3, and dissolved sulfate are consumed (Eq. 4, Table 9-16). Throughout the process of organic matter decomposition, concentrations of various by-products (e.g., dissolved ammonia, H_2S, CO_2, and phosphate) increase (Eqs. 1-4, Table 9-16).

Detailed comparisons of pore water data for one far-field versus one near-field core from MP 299 (Sampling Cruise 1) on the continental shelf provide an example of how differences in concentrations of DO and Eh manifest in the chemical composition of the pore water (Figures 9-62 and 9-63). The ΣO_2 was 13.6 nmol/cm^2 in the far-field core versus 4.1 nmol/cm^2 in the near-field core, with depths of O_2 penetration to 2 cm and 0.1 cm, respectively, at far-field and near-field stations. The Eh was +100 mV in the far-field core versus -100 to -150 mV in the near-field core.

Sediment from Station NF-1 at MP 299 contained a black layer from 0 to 10 cm and black patches from 10 to 22 cm. The entire core from Station FF-3 at MP 299 and at sediment depths >22 cm at Station NF-1 consisted of Mississippi delta clay. Sediment composition for the FF-3 and NF-1 stations at MP 299 (Sampling Cruise 1) were as follows: Ba levels of 0.08 % Ba (far-field) versus 0.43% (near-field), concentrations of TOC at 1.2% (far-field) versus 1.4% (near-field), SBF levels of <0.000002% (far-field) and 0.003% (near-field), sediment Mn level of 960 µg/g (far-field) versus 400 µg/g (near-field), and Al and Fe levels that varied only slightly (<4% relative difference).

The Eh of +100 mV in the core from Station FF-3 at MP 299 is consistent with sub-oxic conditions with no detectable nitrate, no detectable sulfide (<2 µM), and reasonably high concentrations of dissolved Mn^{2+} and Fe^{2+} (Figure 9-62). Thus, the dominant reactions in the far-field core were those described for Eqs. 3 and 4 (Table 9-16 and Figure 9-47).

The Eh values of -100 to -150 mV in the core from Station NF-1 at MP 299 (Figure 9-63) are consistent with an anoxic environment wherein dissolved sulfide (H_2S) is produced according to Eq. 5 in Table 9-16 (Figure 9-63). Ten times greater concentrations of dissolved phosphate and two times greater levels of alkalinity in the top 10 cm of the core from the near-field versus the far-field stations at MP 299 are consistent with greater production of the decomposition products of early chemical diagenesis (Table 9-16) in the near-field sediments. Pore water salinities were similar at both sites (~36 g/kg).

The good relationship of the probe results for oxygen and Eh with the pore water data for MP 299 support direct interpretation of the probe results for other stations from MP 299 with the redox reactions described in Figure 9-7 and Table 9-16.

Another comparison of pore water results for far-field versus near-field sediments is described below for slope site EW 963 (Figures 9-64 and 9-65). In this example, the sediment core from Station NF-5 had an 8-cm thick black layer with 16.2% Ba and 0.117% SBF relative to 0.18% Ba and non-detectable levels of SBF in sediment from Station FF-1. Levels of TOC in the sediment were similar, with 0.95% in the far-field core and 0.87% in the near-field core. The ΣO_2 was 92 nmol/cm^2 in the far-field core versus 35 nmol/cm^2 in the near-field core, with depths of O_2 penetration to 3.3 cm and 2.6 cm, respectively, at far-field and near-field stations. The Eh decreased from +400 mV to +100 mV over 10 cm in the far-field core and from +300 mV to +100 mV over about 3 cm in the near-field core. Nitrate was measured in the top 2 cm in both the far-field and near-field cores, and no dissolved sulfide was detected (<2 µM) in either core (Figures 9-64 and 9-65). Vertical profiles for ammonia (Figures 9-64 and 9-65), phosphate, and sulfate were similar for both the far-field and near-field cores.

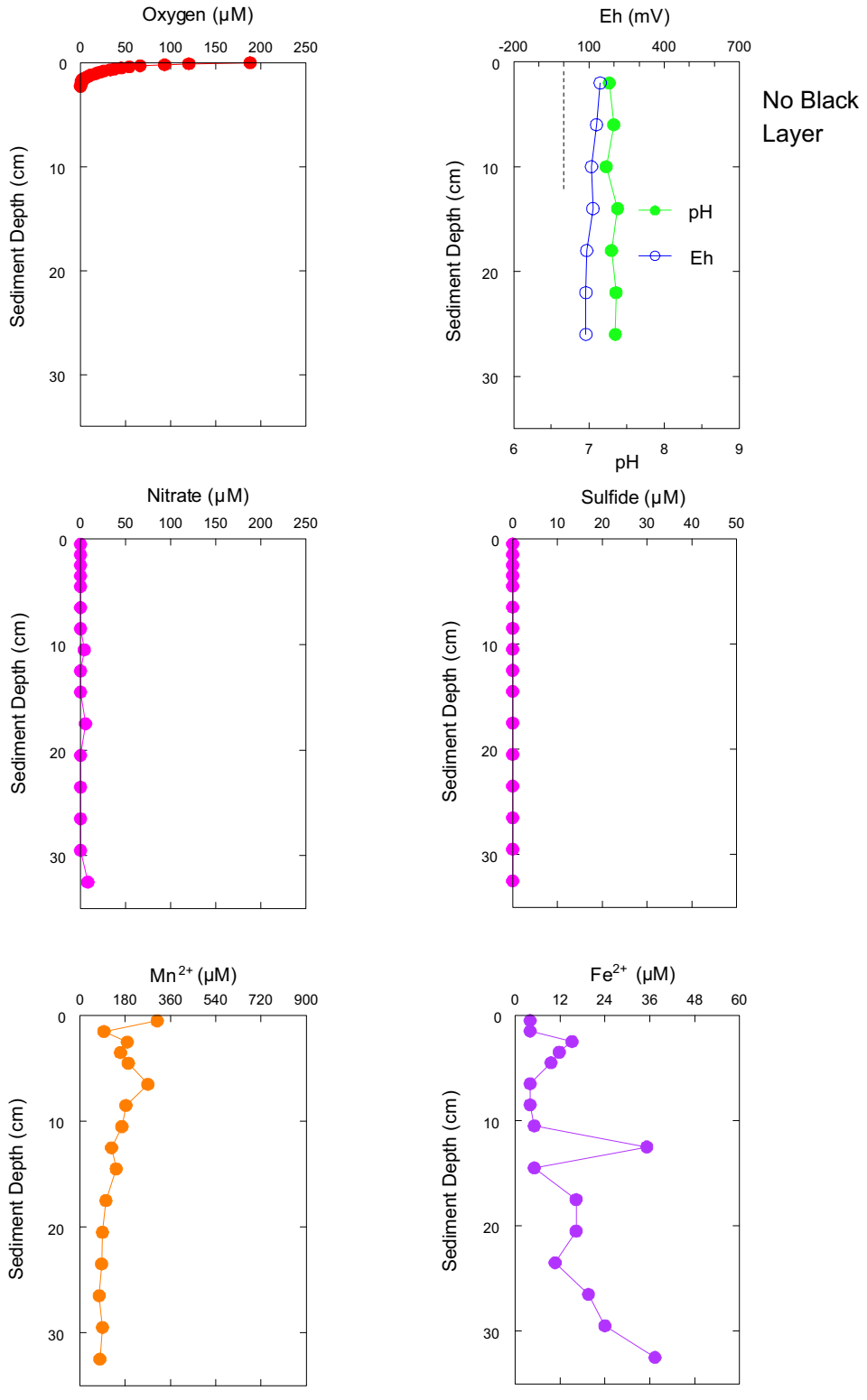

Figure 9-62. Vertical profiles for dissolved oxygen, redox potential (Eh), nitrate, sulfide, manganese (Mn^{2+}), and iron (Fe^{2+}) for pore water from Main Pass 299, Station FF-3 for Sampling Cruise 1.

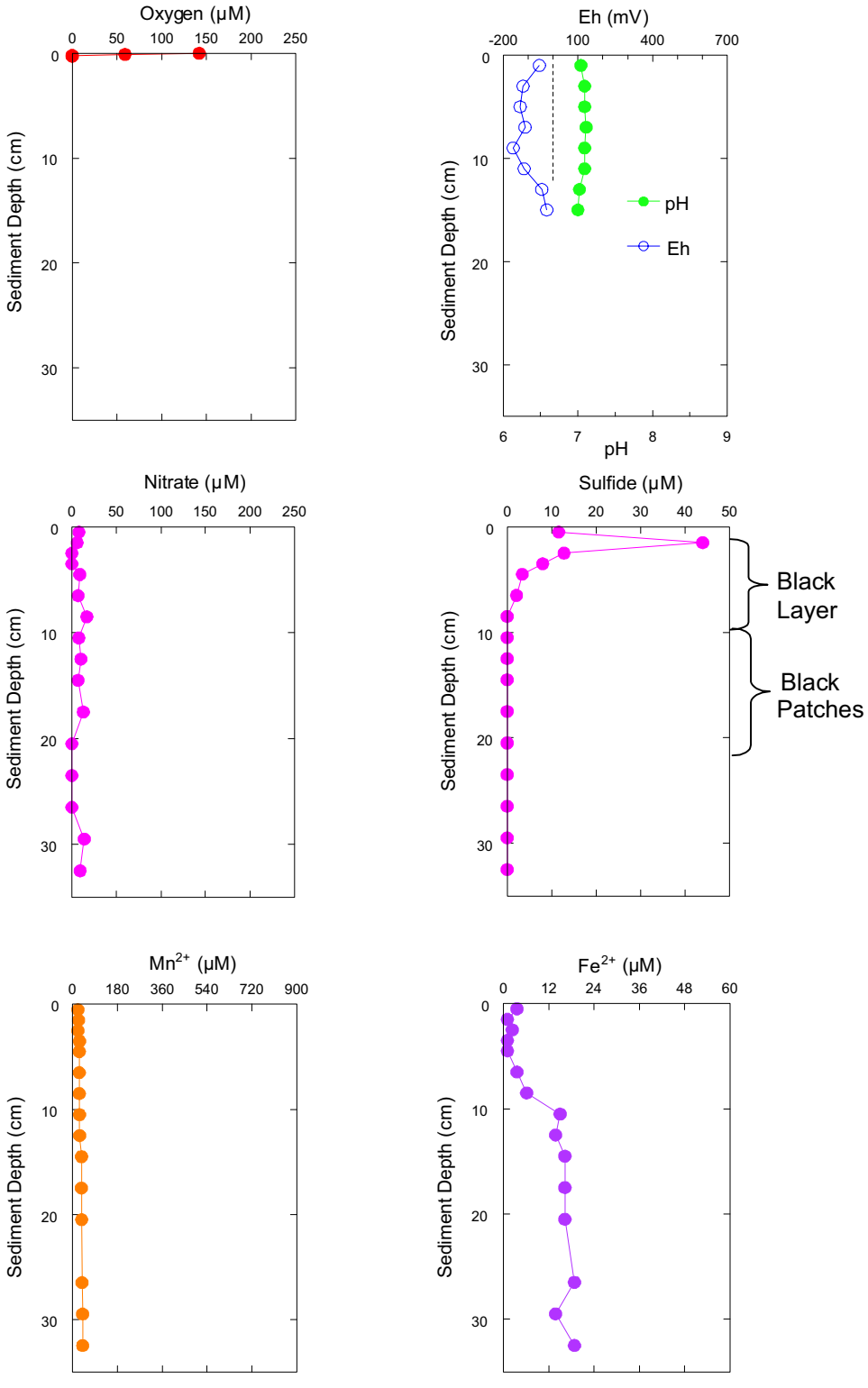

Figure 9-63. Vertical profiles for dissolved oxygen, redox potential (Eh), nitrate, sulfide, manganese (Mn^{2+}), and iron (Fe^{2+}) for pore water from Main Pass 299, Station NF-1 for Sampling Cruise 1.

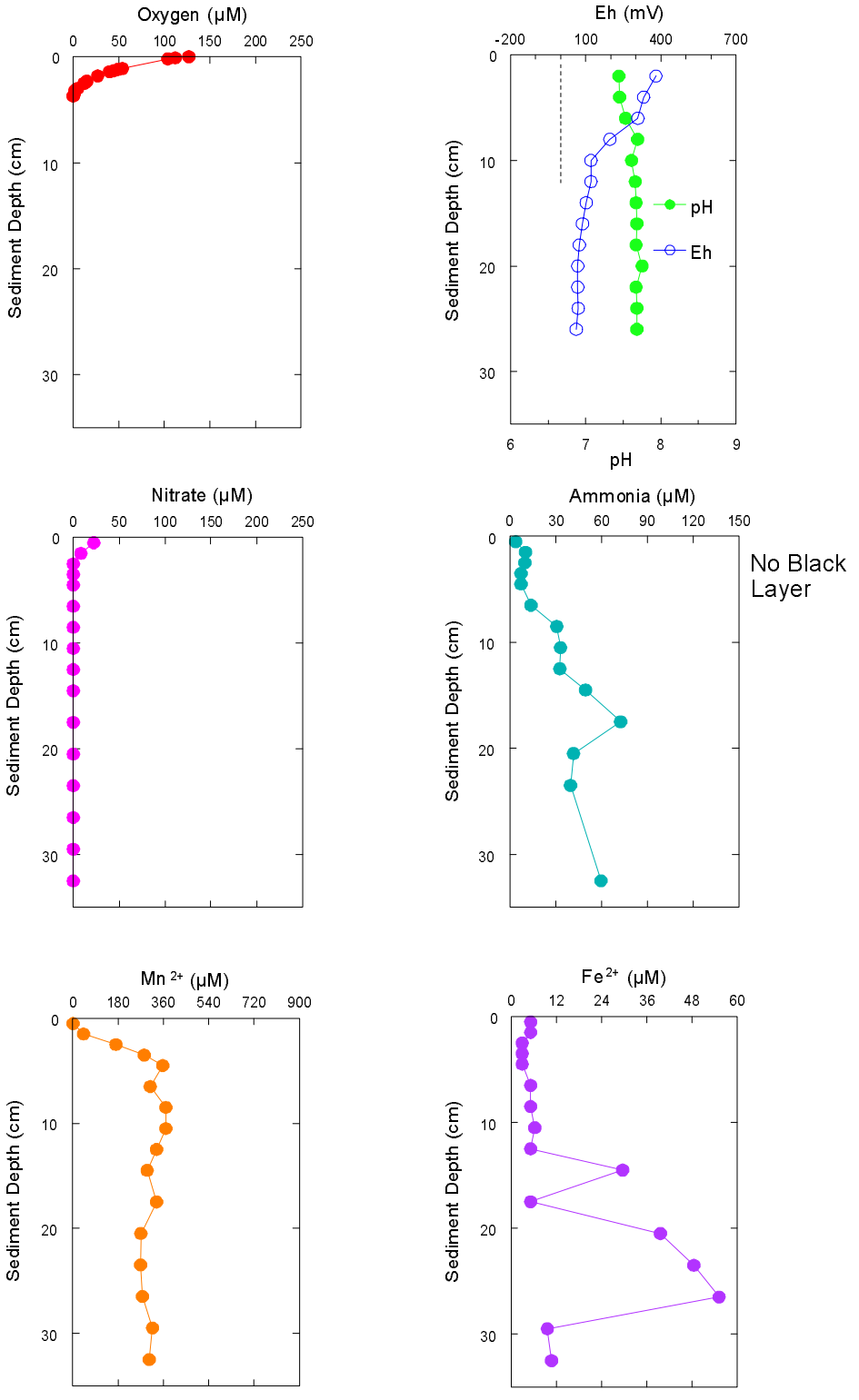

Figure 9-64. Vertical profiles for dissolved oxygen, redox potential (Eh), nitrate, ammonia, manganese (Mn^{2+}), and iron (Fe^{2+}) for pore water from Ewing Bank 963, Station FF-1 for Sampling Cruise 1.

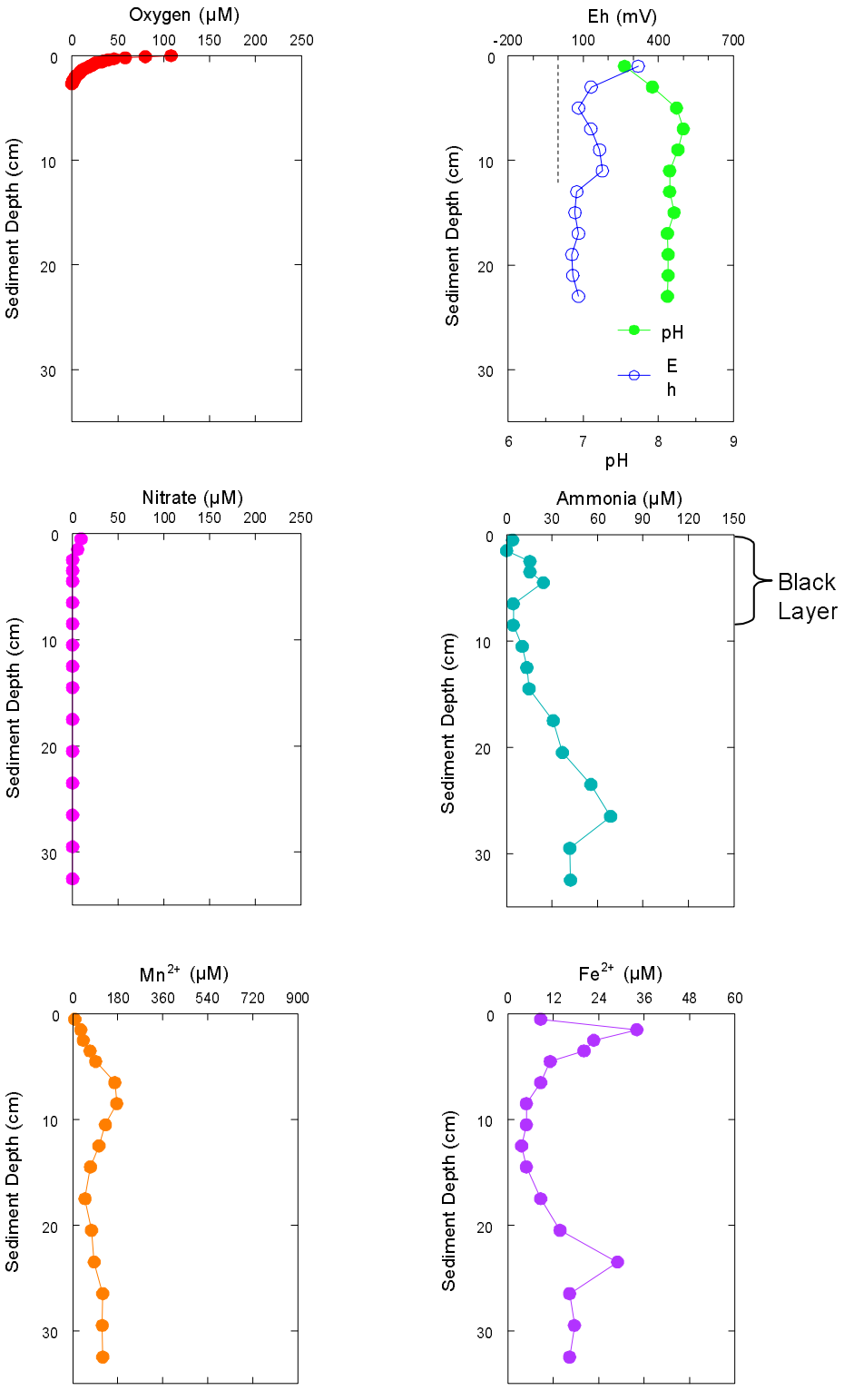

Figure 9-65. Vertical profiles for dissolved oxygen, redox potential (Eh), nitrate, ammonia, manganese (Mn^{2+}), and iron (Fe^{2+}) for pore water from Ewing Bank 963, Station NF-5 for Sampling Cruise 1.

Concentrations of dissolved Mn in the pore water were <10 µM in the top layer of both the far-field and near-field cores from EW 963 due to the presence of oxygen (Figures 9-64 and 9-65). With increasing depth in both cores, concentrations of Mn^{2+} in the pore water increased. However, the maximum level was about two times higher in the far-field core relative to the near-field core. Concentrations of sediment Mn were <2,000 µg/g in the top 8 cm of the near-field core and 10,600 µg/g at 8-10 cm. At Station FF-1, the sediment Mn content in the top 2 cm of the core was 7,800 µg/g and most likely increased with increasing depth. Thus, a far greater source of available Mn was present in the background sediment than in the layer of drilling discharges to support higher levels of Mn in the pore water at the far-field station. Once again, the DO and Eh data fit the trends observed for various constituents in the pore water. The presence of an 8-cm thick black layer had a discernible but minor impact on the overall redox state of the sediment, with the exception of Mn.

Pore water data from the other two slope sites (MC 496 and GC 112) show distributions remarkably similar to those found for EW 963. Nitrate is not present, except in the topmost layer from the far-field sites. Profiles for Eh, pH, alkalinity, and ammonia were similar at far-field and near-field stations, whereas concentrations of pore water Mn^{2+} are significantly higher in the far-field sediment that is richer in solid-phase Mn.

A further comparison of pore water composition between far-field and near-field stations is developed below using data from Sampling Cruise 2 for dissolved Mn^{2+} and dissolved ammonia (as NH_4^+). These two chemical species are common to the sub-oxic environments found at most of the sites studied. In each of the comparisons for dissolved Mn and ammonia (Figures 9-66 and 9-67), a black line was drawn on the profile for the discretionary station to show the presence of a black layer at all discretionary stations except at EW 963. No black layers were observed at the far-field stations.

At MP 299, the profiles for dissolved Mn are very similar for the far-field and discretionary stations (Figure 9-66), as are values for ΣO_2 (4 nmol/cm^2 for far-field and 3 nmol/cm^2 for discretionary), Eh (+100 mV for both), and total sediment Mn (552 µg/g for far-field and 532 µg/g for discretionary). However, concentrations of dissolved ammonia in the pore water from the discretionary stations were about double those at the far-field station (Figure 9-67). To support this increased ammonia, the sediment at the discretionary station contained 1.9% TOC relative to 1.2% at the far-field station. Furthermore, concentrations of dissolved Fe were 50 to 70 µM in the top few centimeters of the discretionary core relative to 1 to 5 µM in the far-field core. Thus, production of greater amounts of dissolved ammonia in the discretionary core can be explained by greater amounts of TOC and greater reduction of iron oxides (Eq. 4, Table 9-16). However, the greater TOC at the discretionary station is not due to SBF because levels of SBF are 0.001% at DISC-2 and <0.0001% at FF-1. The important point here is that the redox state of the sediment is delicately poised by a variety of chemical reactions and minor shifts are common. Furthermore, the DO and Eh data are consistent with the results for the pore water.

At MP 288, EI 346, MC 496, and GC 112, concentrations of dissolved Mn in the pore water are greater at the discretionary stations than at the far-field stations (Figure 9-66). The individual differences in the vertical profiles from site to site are somewhat different and reflect, for example, high oxygen levels in the top 3 cm of sediment at FF-3 (GC 112) and no oxygen in pore water from FF-5 at MC 496. As described above for MP 299, concentrations of dissolved ammonia are higher at the discretionary stations in all cases except MP 288. At MP 288, TOC levels were 1.2% at the far-field station relative to 0.7% at the discretionary station, and the production of dissolved Mn (Eq. 3, Table 9-16) was much greater in pore water from the far-field station with no significant production of dissolved Fe at either the discretionary or far-field station.

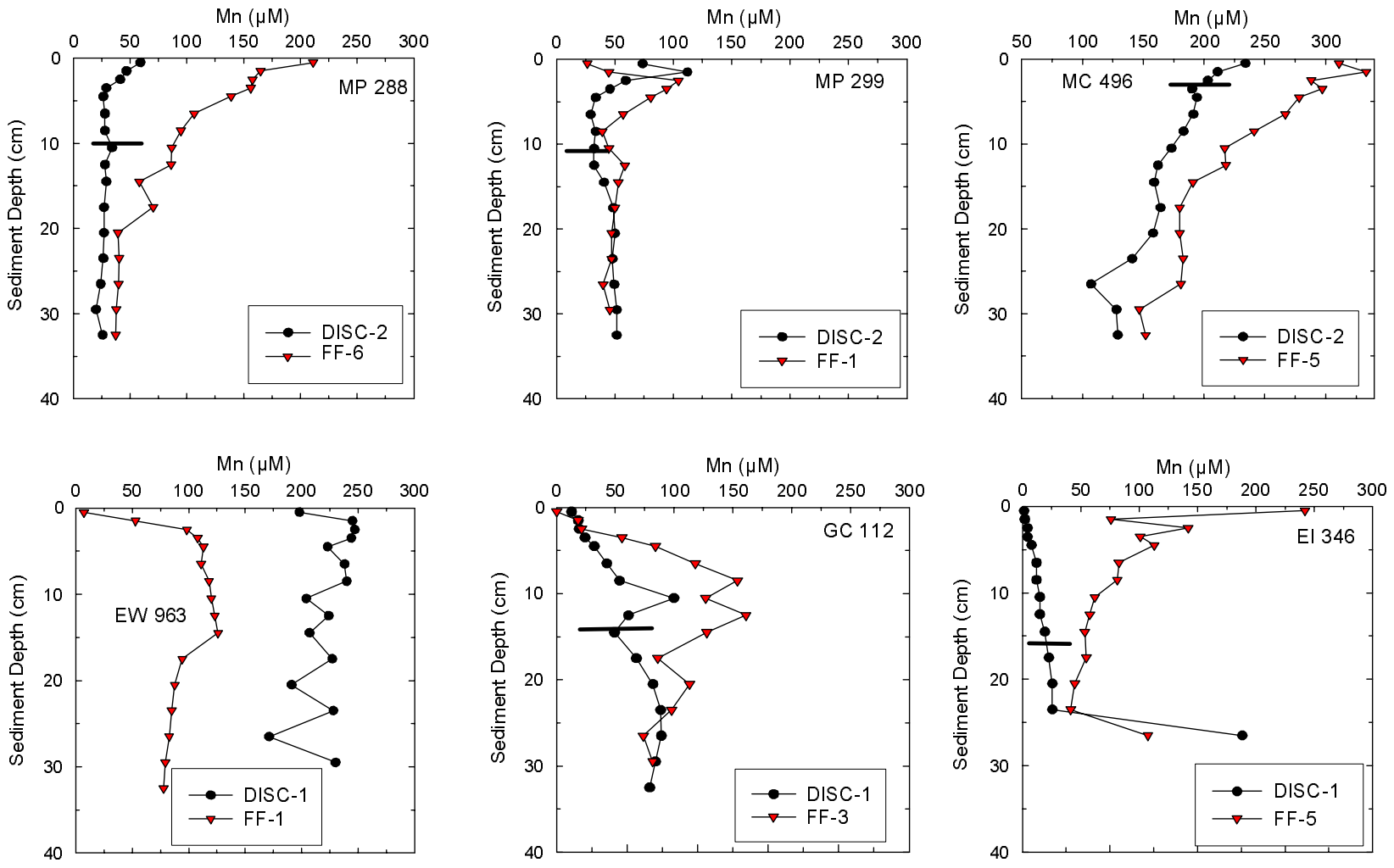

Figure 9-66. Vertical profiles for dissolved Mn^{2+} in pore water from discretionary (DISC) and far-field (FF) stations from Main Pass (MP) 288, MP 299, Mississippi Canyon (MC) 496, Ewing Bank (EW) 963, Green Canyon (GC) 112, and Eugene Island (EI) 346 from Sampling Cruise 2. Black line across profile for DISC stations (except EW 963) shows depth of black layer from the top of the core.

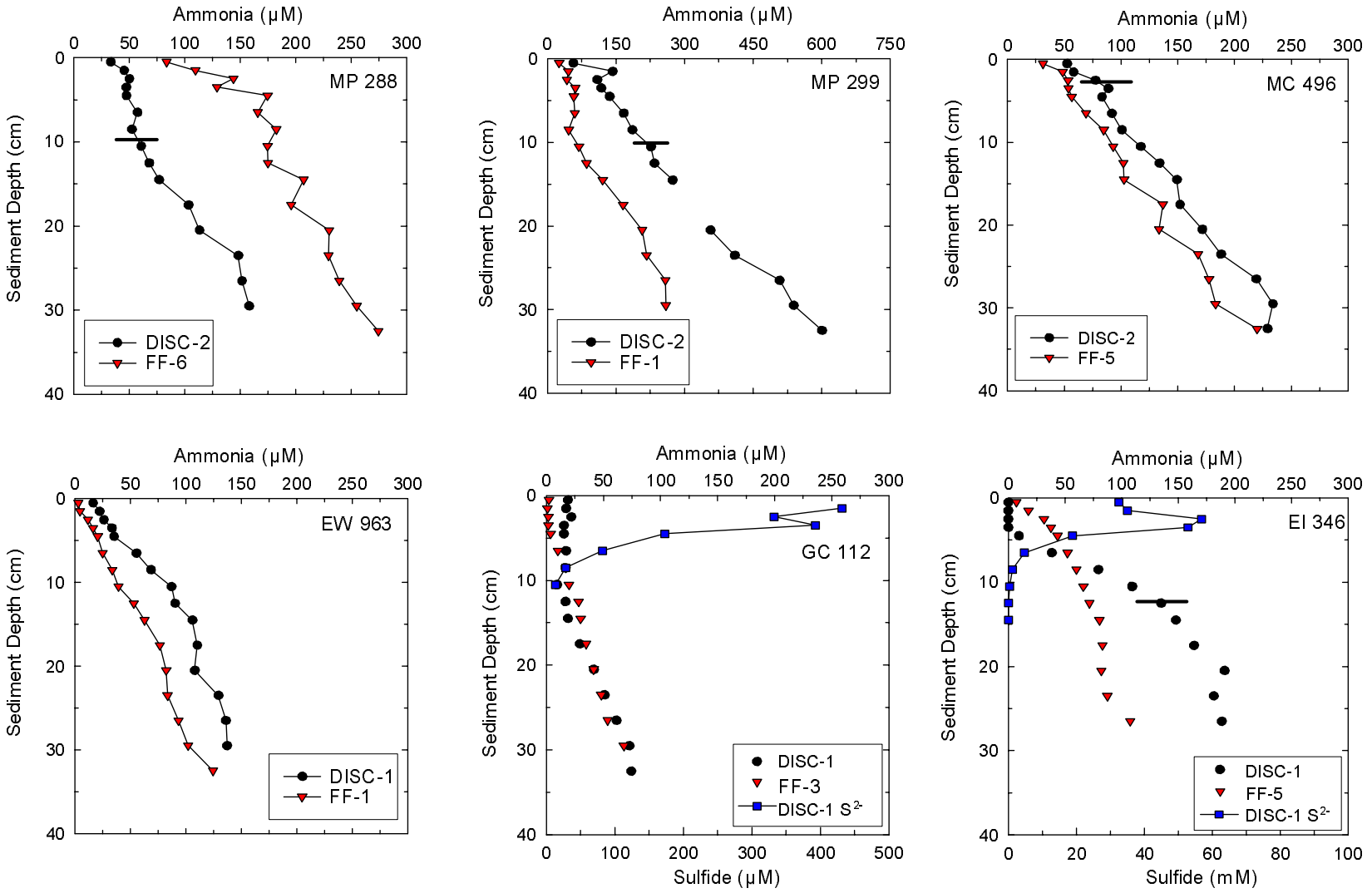

Figure 9-67. Vertical profiles for dissolved ammonia in pore water from discretionary (DISC) and far-field (FF) stations from Main Pass (MP) 288, MP 299, Mississippi Canyon (MC) 496, Ewing Bank (EW) 963, Green Canyon (GC) 112, and Eugene Island (EI) 346 from Sampling Cruise 2. Black line across profile for DISC stations (except EW 963) shows depth of black layer from the top of the core.

Sulfide was detected (>2 μM) in pore water at the following 4 of the 24 stations where pore water was collected: MP 299 (NF-1, Sampling Cruise 1), EI 346 (NF-1, Sampling Cruise 1 and DISC-1, Sampling Cruise 2), and GC 112 (DISC-1, Sampling Cruise 2). Only these 4 of the 24 stations with pore water data had Eh values <-100 mV. Thus, the Eh profiles can be used to predict the presence of sulfide in the pore water. The results described above for Station NF-1 from MP 299 (Sampling Cruise 1) provide an excellent example of the vertical distribution of sulfide relative to Eh (Figure 9-63). Sulfide profiles for GC 112 and EI 346 are shown in Figure 9-67. At EI 346, on both Sampling Cruises 1 and 2, concentrations of dissolved sulfide were extremely high (>20 mM or >20,000 μM) (Figure 9-67).

Overall, the pore water profiles for ammonia, nitrate, and iron from near-field and far-field samples do not vary greatly. Profiles for Mn^{2+} seem to show the greatest sensitivity to a changing redox environment. In the extreme cases of highly reducing sediment at near-field or discretionary stations, sulfide is present. One reason for the apparent overlaps in profiles for selected chemical species is that the effect of the black layers or the presence of SBF is limited to the top few centimeters of the sediment column, and the pore water profiles expand the picture to look over 30 cm.

9.9 CONCLUSIONS

Results from the metals and redox study for sediments have met the goals of identifying spatial and temporal trends in the presence of drilling discharges and in redox conditions for sediments collected around drilling sites. Concentrations of Ba were above background levels in >95% of the sediments collected from near-field stations (<100 m from site center), with levels as high as 35% Ba relative to background Ba concentrations of 0.1% to 0.3%. Elevated levels of Ba extended well into the mid-field zone (100 to 250 m from site center) at slope sites where horizontal dispersion was extended due to greater water depths (500 m versus about 100 m on the shelf).

Black layers were observed at 32 of 36 near-field stations during Sampling Cruise 1 and 32 of 48 near-field stations during Sampling Cruise 2. At mid-field stations, 24 of 36 samples during Sampling Cruise 1 and 16 of 36 samples collected during Sampling Cruise 2 contained black layers. These black layers were all characterized by elevated levels of Ba. Concentrations of SBF were >0.01% at 60% of the near-field and mid-field stations during Sampling Cruise 1 and ~35% of the near-field (including discretionary) + mid-field stations during Sampling Cruise 2. The black layers were typically 2- to 15-cm thick, with only one layer (at EI 346) thicker than 30 cm. Limited data for excess ^{210}Pb showed that a black layer from GC 112 with 40% barite and about 50% clay contained <5% detrital sediment. Thus, much of the material in the black layers is drilling fluid solids and cuttings. Unfortunately, the data for excess ^{210}Pb could not be used to distinguish clays in drilling fluids from clays in cuttings. However, the approach does seem to distinguish detrital sediment from drilling discharges.

Concentrations of Mn in sediments provided useful insight to redox conditions in the sediments. Levels of Mn in sediments were consistently lower at near-field stations than at far-field stations. This occurs because the more reducing environment in the near-field zone promotes dissolution of manganese oxides with subsequent loss of dissolved Mn^{2+} to the overlying water column, thereby depleting the sediments with solid-phase Mn.

Concentrations of Cd, Hg, Pb, and Zn were elevated by factors of 2 to ~5 above background levels (far-field) in sediments from >20 of the 58 samples of sediment analyzed for metals.

Based on sediment profiles for oxygen, the average ΣO_2 of oxygen in the sediment column at near-field stations was 2 to 7 times less than at far-field stations. The more reducing environment at near-field stations was coincident with the presence of black layers with elevated levels of Ba and in some cases TOC and SBF. These layers were definitely deposited quickly (several centimeters per year) relative to ambient sedimentation rates of about 0.2 cm/yr at several sites. This rapid influx of sediment and organic matter supports increase consumption of oxygen in the sediments. Data for pore water from 24 of the 156 stations sampled support predictions with respect to the presence of sulfide, Mn^{2+}, ammonia, and other products of early chemical diagenesis in sediments.

Chapter 10
SEDIMENT TOXICITY

Roy K. Kropp and Valerie I. Cullinan
Battelle Marine Sciences Laboratory

10.1 INTRODUCTION

Acute toxicity testing of Gulf of Mexico SBMs was performed in 2001 and 2002 following guidance provided in Methods for Assessing the Toxicity of Sediment-Associated Contaminants with Estuarine and Marine Amphipods, Test Method 100.4 (USEPA, 1994), the Standard Guide for Conducting 10-day Static Sediment Toxicity Tests with Marine and Estuarine Amphipods (ASTM, 1999), and Methods for Assessing the Chronic Toxicity of Marine and Estuarine Sediment-Associated Contaminants with the Amphipod *Leptocheirus plumulosus* – First Edition (USEPA, 2001b).

The primary objective of benthic toxicity testing is to determine the potential impact of whole sediment on benthic organisms at or near the site being evaluated. Ideally, that testing would involve the use of species found at the site. However, this is most frequently not practical because of difficulties associated with the collection of suitable numbers of individuals of a single, easily identifiable species to be used in testing. This is particularly true for deep water sites such as those evaluated during this program. Therefore, easily cultured or collected species typically are used as surrogates for those resident at or near study sites. The species selected for testing should be representative of appropriately sensitive infaunal species inhabiting the site. Amphipods are often selected for toxicity testing because it is well-known that they are sensitive to many contaminants, including petroleum hydrocarbons. *L. plumulosus*, the species used in this program, has recently been advocated as a suitable species for toxicity testing because it is intimately associated with sediments due to its burrowing lifestyle and because it ingests sediment (USEPA, 2001b). It is the organism required in the NPDES general permit. Extending the results of the laboratory toxicity testing to field populations is tempered by the observation that what is true for one species (i.e., the surrogate) is not necessarily true for another (i.e., the resident species).

The following sections briefly describe the bioassay test procedures and present the analyses of the test results from the 3 years of the study. The toxicity data not only provide an estimate of the relative toxicity of the samples collected during the program but also can be used in conjunction with sediment chemistry and infaunal data to provide an overall characterization of sediment quality in the areas included in the study.

10.2 LABORATORY AND STATISTICAL METHODS

10.2.1 Test Organism Sources

The marine amphipod *Leptocheirus plumulosus* was used to evaluate the toxicity of the test sediments. *L. plumulosus* used for the toxicity tests were obtained from in-house cultures at the Battelle Marine Sciences Laboratory (MSL) or from Chesapeake Cultures (CC), Hayes, Virginia. Organisms exhibiting abnormal behavior or appearance were not used in toxicity tests.

10.2.2 Sediment Sample Preparation

In each year of testing, shipments of sediments were received from CSA. In 2000, sediment temperatures, as measured upon receipt at MSL, ranged from 13.6ºC to 19.5ºC. The jars containing two of the samples designated for testing (API SCR GB128NF-3ST and API SCR MP288 NF3-ST) were broken during transit. Some sediment was recovered from each of these jars but not enough to test the required five replicates. In 2001 and 2002, sediment temperatures ranged from 0.6ºC to 7.8ºC and from 3.7ºC to 6.7ºC, respectively. All containers were in good condition.

10.2.3 *Leptocheirus plumulosus* Solid-Phase (Benthic) Acute Toxicity Test Conditions

Benthic acute toxicity testing was performed using subadult *L. plumulosus* in a 10-day static exposure (i.e., no water renewals) with mortality as the endpoint. *L. plumulosus* was exposed to 30, 54, and 108 discrete samples of Gulf of Mexico test sediments in 2000, 2001, and 2002, respectively (Battelle, 2000, 2001, 2002). Because of the numbers of sediments to be tested, the 2001 and 2002 toxicity tests were conducted in three and six batches of 18 samples, respectively. Each batch included a laboratory control sample and a concurrent reference toxicant test, with cadmium chloride as the toxicant. The sediments assigned to each test batch, the amphipod source, and the dates of the testing are listed in Table 10-1.

Table 10-1. Batch assignments, amphipod source, and testing dates for the synthetic based mud *Leptocheirus plumulosus* testing program.

Batch	Site	Amphipod Source[1]	Test Initiation Date	Test Termination Date
1	Main Pass 288, Main Pass 299, Garden Banks 128, Viosca Knoll 780, Viosca Knoll 783	MSL	22 August 2000	1 September 2000
1	Main Pass 299	CC	21 May 2001	31 May 2001
2	Main Pass 288	CC	5 June 2001	15 June 2001
3	Eugene Island 346	MSL	12 June 2001	22 June 2001
1	Main Pass 288	CC	24 May 2002	3 June 2002
2	Main Pass 299	CC	28 May 2002	7 June 2002
3	Mississippi Canyon 496	CC	4 June 2002	14 June 2002
4	Eugene Island 346	CC	11 June 2002	21 June 2002
5	Green Canyon 112	CC	18 June 2002	28 June 2002
6	Ewing Bank 963	CC	25 June 2002	5 July 2002

[1]MSL = Battelle Marine Sciences Laboratory; CC = Chesapeake Cultures.

After preliminary water quality monitoring measurements of the conditions (temperature, pH, DO, and salinity) in each container were made, the test was initiated by introducing 20 organisms into each test chamber. During the test these parameters were monitored in one replicate on Days 2, 5, and 7 but were measured in all replicates at test termination. Organisms were randomly allocated to treatments, and treatment replicates were randomly positioned on water tables. The discrete random number generator in Microsoft® Excel spreadsheet software

was used to assign random positions on the water tables for test chambers (Figure 10-1). Amphipods were not fed during the test. In addition to the test sediments, each batch of the bioassay included a concurrent, 96-h, water-only, reference toxicant (cadmium chloride at seven concentrations) test to assess the sensitivity of each test population. Specific test conditions for the benthic toxicity test are provided in Table 10-2.

Table 10-2. *Leptocheirus plumulosus* solid-phase acute toxicity test conditions.

Parameter	*Leptocheirus plumulosus*
Treatments	30 Gulf of Mexico sediments (1 batch of 30) during the Screening Cruise 54 Gulf of Mexico sediments (3 batches of 18) in 2001 108 Gulf of Mexico sediments (6 batches of 18) in 2002 1 native control (Sequim Bay) sediment with each batch
Test Runs	10
Replicates	5
Test Population	20 individuals per replicate; total per treatment, n = 100
Temperature	25°C ± 2°C
Sediment Volume	175 mL per container
Water Volume	950 mL per container
Dissolved Oxygen	>50% saturation (>3.6 mg/mL at 25°C, 20‰)
pH	7.0–9.0
Salinity	20‰ ± 2‰
Feeding	None
Reference Toxicant (1 concurrent with each batch)	Cadmium chloride at 0, 0.16, 0.31, 0.63, 1.25, 2.5, 5.0, and 7.0 mg/L 20 individuals per replicate

At test termination, final water quality measurements were made, and the amphipods remaining in each container were carefully removed by rinsing the sediment over a 0.5-mm mesh sieve. The numbers of living, dead, and missing amphipods were recorded on data sheets. The proportion of amphipods surviving in each test container and the mean and standard deviation of the proportion surviving were calculated for each test sediment. The mean proportion surviving for each sediment was used in the statistical analyses.

10.2.4 Ammonia and Sulfide Measurements

The possible influence of sediment pore water ammonia and/or sulfide concentrations on the test results was evaluated in 2002. To permit measurement of the initial (Day 0) and final (Day 10) pore water ammonia concentrations, two surrogate containers for each test sediment were placed on the water tables along with the remaining test containers. The Day 0 surrogate containers were removed just prior to test initiation. The Day 10 surrogate containers each received an aliquot of 20 animals during initiation of the 10-day test. Day 10 surrogate containers were removed from the water table just prior to test termination. Pore waters were collected by pouring off the overlying water and centrifuging the sediment sample at 2,500 rpm for 30 minutes. Pore water aliquots were placed in separate containers for ammonia or sulfide analyses. Pore waters were shipped to Columbia Analytical Services, Inc. (CAS), Kelso, Washington for analyses. At CAS, pore water ammonia and sulfide concentrations were determined by following Methods EPA 350.3 and EPA 376.2, respectively. Pore water ammonia and sulfide concentrations are listed in Appendix F.

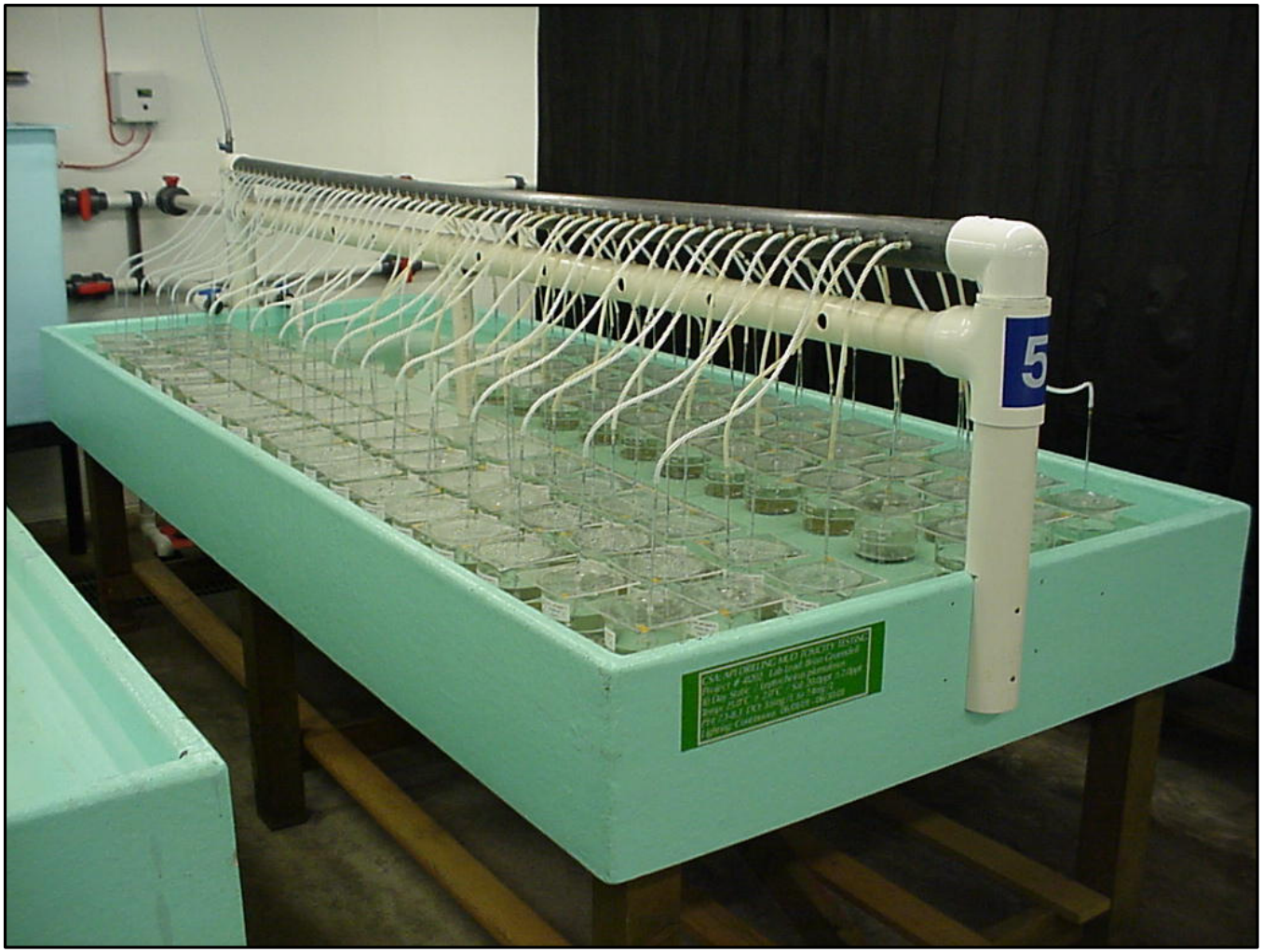

Figure 10-1. *Leptocheirus plumulosus* toxicity test set-up, 2001.

10.2.5 Statistical Methods for Sediment Toxicity Analysis

The statistical analysis focused on the levels and spatial patterns of sediment toxicity associated with sediment TPH concentrations (Chapter 8) around six selected sites sampled during the Screening Cruise (August 2000), Sampling Cruise 1 (May 2001), and Sampling Cruise 2 (May 2002). Sites that were sampled and evaluated for sediment toxicity during the Screening Cruise were not used in the statistical analysis but were used in the spatial analyses. Sediments from each sampling effort were collected from randomly selected stations positioned within three zones (near-field, mid-field, and far-field). This design is appropriate for producing unbiased estimates of each zone's population parameters, assuming homogeneity of response within zones. Additionally, this design allows comparisons between zones within a sampling period and comparisons between sampling periods within zones (i.e., temporal differences within a site area).

Descriptive statistics including the mean, standard deviation, CV, median, and the first and third quartiles (Q1 and Q3, respectively) of the toxicity data were used to characterize zones. One-way analysis of variance (ANOVA) on the arcsine square-root transformed proportion survival was used to compare the mean toxicity between zones within a sampling period and between sampling periods within zones. If the transformation was unsuccessful at reducing the heterogeneity of the within-class variances, the Kruskal-Wallis test and Tukey's Honest Significant Difference (HSD) based on rank transformed survival were used to make comparisons.

Based on the original intent to evaluate spatial patterns of sediment toxicity, an alternative analysis ignoring zones also was conducted. Tukey's HSD on the transformed proportion survival was used to determine the significant differences between mean survival for each sampling site within a site and year regardless of zones. Four toxicity classes (T-class) based on proportion survival also were developed to highlight proportional survival less than 0.25, between 0.25 and 0.5, between 0.5 and 0.75, and greater than 0.75. The general relationships between the T-class groups were determined by using a pair-wise comparison (Tukey's HSD). The resulting statistical groupings were then combined with the toxicity classes to produce plots of relative toxicity for each site.

Relative toxicity areal plots were made by using scatter plots of the box core locations classified by the combined statistical and toxicity classes as defined in Table 10-3. Classes and symbols used for each class are consistent for each site. Larger, bold symbols indicated locations with greater sediment toxicity, and smaller symbols indicated locations with little or no sediment toxicity.

Table 10-3. Definition of relative toxicity groups. Note that groups with the same pair-wise comparison letter are not significantly different.

T-class	Range of Proportion Survival	Pair-Wise Comparison Based on Tukey's HSD (α = 0.05)
1	s < 0.25	A
2	0.25 < s < 0.50	AB
3	0.50 < s < 0.75	BC
4	s > 0.75	C

All statistical analyses were conducted using Minitab (Minitab Statistical Software, Release 13.3, Minitab, Inc.).

10.3 TOXICITY TEST RESULTS

Test endpoint data for individual replicates were previously presented in the reports submitted at the completion of each year of testing. A summary of any water quality deviations, reference toxicant test results, and pore water ammonia and sulfide concentrations from the 2002 testing is provided in Appendix F.

10.3.1 General Results

Samples from three sites (MP 299, MP 288, and EI 346) were evaluated for sediment toxicity using data from Sampling Cruise 1 and Sampling Cruise 2 (Table 10-4; Appendix F, Table F-9). Samples from sites MC 496, GC 112, and EW 963 were evaluated only for Sampling Cruise 2 because they were added to the study in 2002 to provide broader coverage. Zones sampled during the Screening Cruise had three observations each for the near-field and far-field zones. No observations were made in the mid-field zones on sediment toxicity during the Screening Cruise. All other sampling periods contained six observations of toxicity per zone.

Table 10-4. Descriptive statistics of proportion survival for each cruise, site, and zone.

Cruise	Site	Zone	N	Mean	Standard Deviation
Screening Cruise	MP 299	Near-Field	3	0.25	0.38
Screening Cruise	MP 299	Far-Field	3	0.96	0.01
Sampling Cruise 1	MP 299	Near-Field	6	0.74	0.37
Sampling Cruise 1	MP 299	Mid-Field	6	0.98	0.02
Sampling Cruise 1	MP 299	Far-Field	6	0.97	0.03
Sampling Cruise 2	MP 299	Near-Field	6	0.92	0.04
Sampling Cruise 2	MP 299	Mid-Field	6	0.91	0.06
Sampling Cruise 2	MP 299	Far-Field	6	0.93	0.02
Screening Cruise	MP 288	Near-Field	3	0.80	0.17
Screening Cruise	MP 288	Far-Field	3	0.94	0.04
Sampling Cruise 1	MP 288	Near-Field	6	0.79	0.22
Sampling Cruise 1	MP 288	Mid-Field	6	0.94	0.03
Sampling Cruise 1	MP 288	Far-Field	6	0.96	0.03
Sampling Cruise 2	MP 288	Near-Field	6	0.97	0.02
Sampling Cruise 2	MP 288	Mid-Field	6	0.97	0.01
Sampling Cruise 2	MP 288	Far-Field	6	0.96	0.02
Sampling Cruise 1	EI 346	Near-Field	6	0.58	0.46
Sampling Cruise 1	EI 346	Mid-Field	6	0.77	0.30
Sampling Cruise 1	EI 346	Far-Field	6	0.97	0.02
Sampling Cruise 2	EI 346	Near-Field	6	0.31	0.28
Sampling Cruise 2	EI 346	Mid-Field	6	0.56	0.20
Sampling Cruise 2	EI 346	Far-Field	6	0.87	0.07
Sampling Cruise 2	MC 496	Near-Field	6	0.85	0.10
Sampling Cruise 2	MC 496	Mid-Field	6	0.84	0.12
Sampling Cruise 2	MC 496	Far-Field	6	0.89	0.07
Sampling Cruise 2	GC 112	Near-Field	6	0.27	0.30
Sampling Cruise 2	GC 112	Mid-Field	6	0.56	0.35
Sampling Cruise 2	GC 112	Far-Field	6	0.93	0.02
Sampling Cruise 2	EW 963	Near-Field	6	0.65	0.21
Sampling Cruise 2	EW 963	Mid-Field	6	0.75	0.23
Sampling Cruise 2	EW 963	Far-Field	6	0.89	0.05

EI = Eugene Island.
EW = Ewing Bank.
GC = Green Canyon.
MC = Mississippi Canyon.
MP = Main Pass.

The mean proportion survival for samples from each zone and sampling period (Figure 10-2) tended to be greatest in the far-field (ranging from 0.87 to 0.97) and least in the near-field (ranging from 0.25 to 0.97). The near-field results also were the most variable, with CVs in survival between stations within a zone ranging from 2% to 153%. In contrast, the far-field CVs in survival ranged from 1% to 8%. Further, the far-field proportion survival for all replicates and sites ranged from 0.75 to 1.0 and may represent a single statistical population. Three observations with a proportional survival less than 0.84 may be outliers or just the extreme values of the population response (Figure 10-3).

Significant differences between the near-field and far-field zones were detected among samples from three sites (GC 112, EW 963, and EI 346; Table 10-5). A significant difference between the near-field and far-field samples was detected for both Sampling Cruises at EI 346. Differences between these two zones at MP 299 were not detected because of the high variability in survival in samples from the near-field zone.

Table 10-5. Statistical comparison of the mean proportion survival between zones for a given site and sampling period.

Cruise	Site	Near-Field Compared to Mid-Field		Significance (α = 0.05)	Near-Field Compared to Far-Field		Significance (α = 0.05)	Mid-Field Compared to Far-Field		Significance (α = 0.05)
Sampling Cruise 1	MP 299	0.74	0.98	NS	0.74	0.97	NS	0.98	0.97	NS
	MP 288	0.79	0.94	NS	0.79	0.96	NS	0.94	0.96	NS
	EI 346	0.58	0.77	NS	0.58	0.97	S	0.77	0.97	S
Sampling Cruise 2	MP 299	0.92	0.91	NS	0.92	0.93	NS	0.91	0.93	NS
	MP 288	0.97	0.97	NS	0.97	0.96	NS	0.97	0.96	NS
	EI 346	0.31	0.56	NS	0.31	0.87	S	0.56	0.87	S
	MC 496	0.85	0.84	NS	0.85	0.89	NS	0.84	0.89	NS
	GC 112	0.27	0.56	NS	0.27	0.93	S	0.56	0.93	S
	EW 963	0.65	0.75	NS	0.65	0.89	S	0.75	0.89	NS

NS = Not significant. EI = Eugene Island. GC = Green Canyon. MP = Main Pass.
S = Significant. EW = Ewing Bank. MC = Mississippi Canyon.

None of the drilling sites or sampling periods showed a significant difference in the mean proportion survival between samples from the near-field and mid-field zones even though the proportion survival in the mid-field was almost double that of the near-field at two of the sites (GC 112 and EI 346; Table 10-5). Again, a lack of significance is a function of the within-stratum variability and the small sample size.

Only one site showed a significant difference (α = 0.05) in the mean proportion survival between sampling periods for a given zone and site (Table 10-6). The observed mean proportion survival for near-field samples at MP 288 was 0.79 for Sampling Cruise 1 and 0.97 for Sampling Cruise 2. The locations sampled during Sampling Cruise 1 were not resampled during Sampling Cruise 2. The spatial distribution of sediment toxicity was not homogeneous in the near-field at this site.

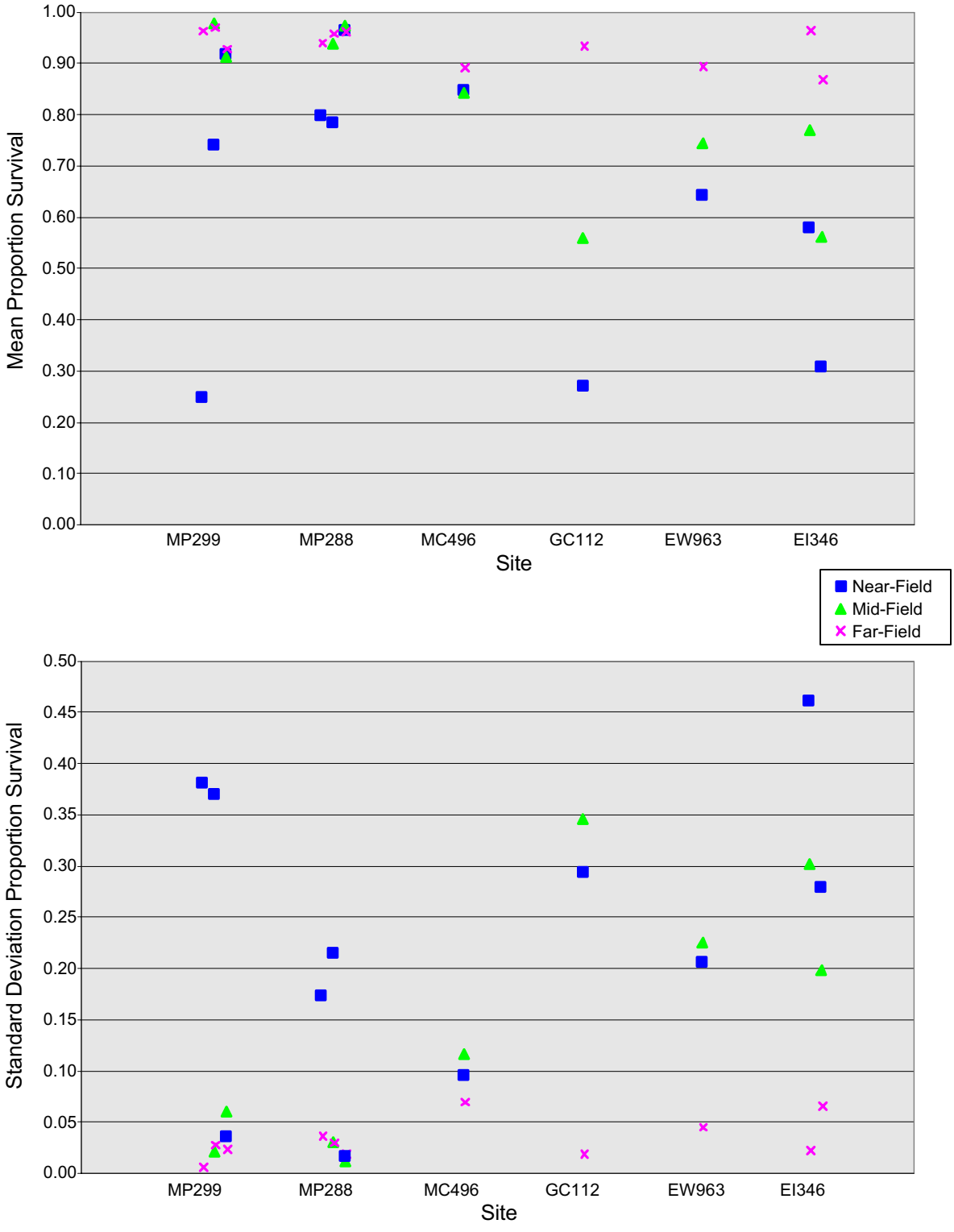

Figure 10-2. Mean and standard deviation of the proportion survival for each site and zone.

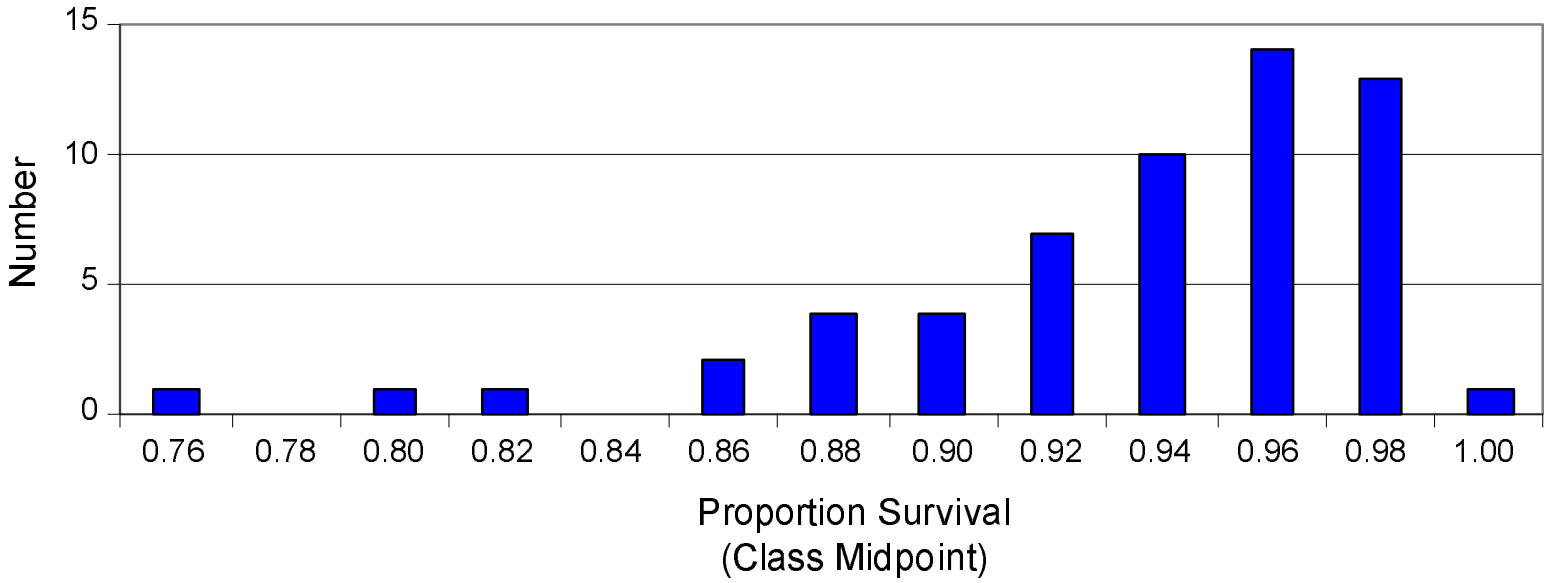

Figure 10-3. Histogram of the proportion survival for all sampling periods and site replicates of the far-field stations.

Table 10-6. Statistical significance (α = 0.05) of comparisons of the mean proportion survival between sampling periods for a given zone and site.

Site	Sampling Cruise 1 Compared to Sampling Cruise 2		
	Near-Field	Mid-Field	Far-Field
Main Pass 299	NS	NS	NS
Main Pass 288	S*	NS	NS
Eugene Island 346	NS	NS	NS

NS = Not significant.
S = Significant.
* Mean survival during Sampling Cruise 2 was significantly greater than during Sampling Cruise 1.

An alternative analysis, ignoring zones, was conducted to determine if patterns of sediment toxicity were detectable in the data for near- and mid-field samples. All far-field sample data had proportional survival greater than or equal to 0.75 and were not used in this analysis. To compile as much spatial information as possible, survival data for samples from all sampling periods for a given site were combined. This may confound patterns that may be related to changes in site operation or other unknown factors, and the variability associated with the toxicity testing in the laboratory. However, laboratory control data suggested very little variability between batch analyses, indicating that the test procedures and test animal responses were consistent among all 3 years. All control replicates had a proportional survival greater than or equal to 0.90 (10 batches spanning 2000 to 2002 with five replicates for each batch; Appendix F, Figure F-1). In fact, 78% of the replicates had 100% survival. Thus, the major component of variation in proportional survival for test sediments across the sampling periods is not likely to be from laboratory variation.

10.3.2 Site Results

10.3.2.1 Main Pass 299. A plot of the relative toxicity as defined by T-class (Table 10-3) about site MP 299 suggested that there was variability across sampling periods potentially associated with site operation or environmental changes (Figure 10-4). The two low survival data points north of the site center were for samples collected during the Screening Cruise. All remaining points within the same area that showed relatively low toxicity were from samples obtained during Sampling Cruises 1 and 2. Concentrations of TPH were higher in sediments associated with higher toxicity (Figure 10-5), with a significant response probably occurring at just less than 1,000 mg/kg TPH.

10.3.2.2 Main Pass 288. Sediments from MP 288 had relatively little toxicity (Appendix F, Figure F-2). All sediments that showed slightly elevated toxicity were collected during the Screening Cruise and Sampling Cruise 1. Note that these same locations are associated with the higher TPH concentrations at the site (Appendix F, Figure F-3).

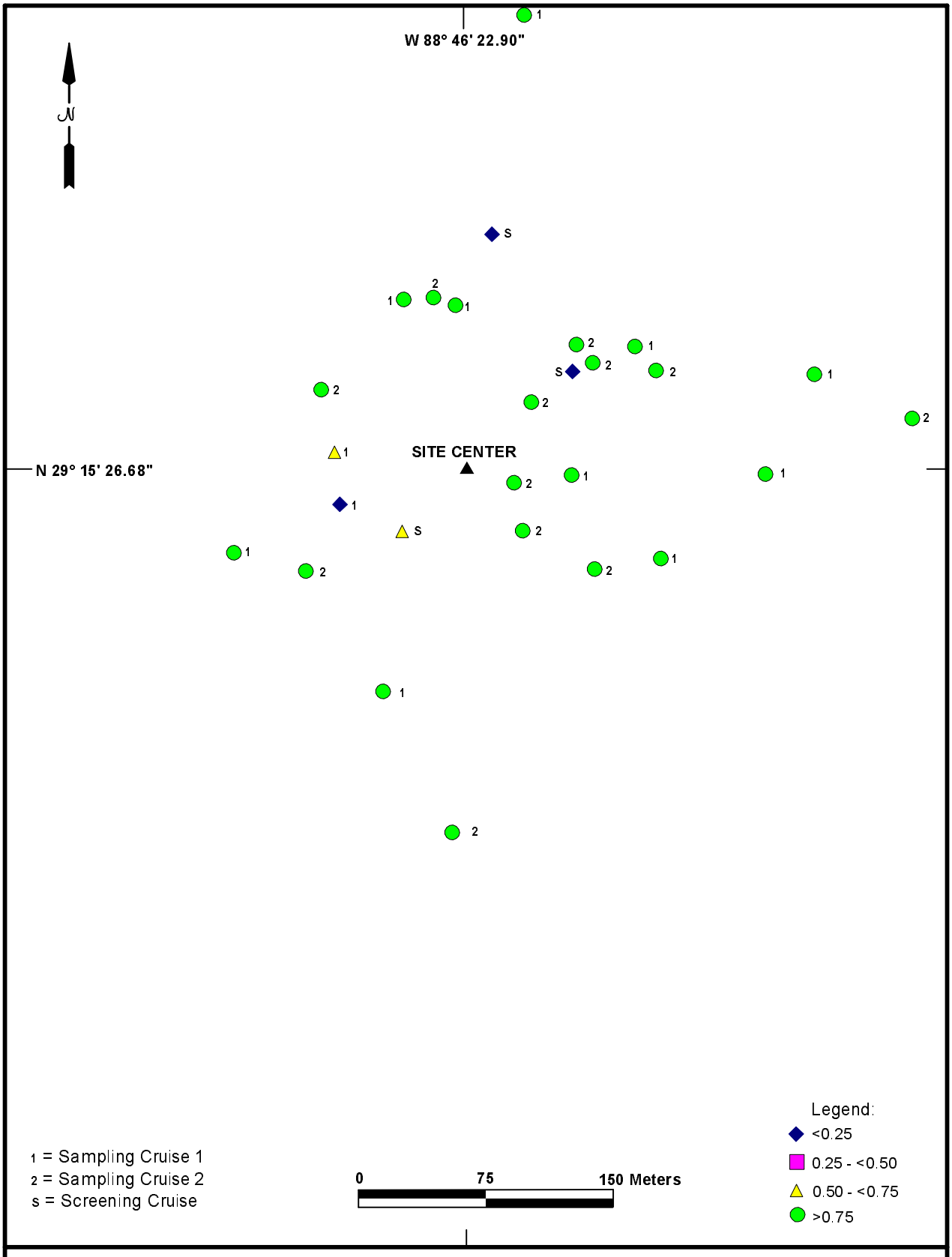

Figure 10-4. Plot of the sediment toxicity around Main Pass 299 site. Legend defines survival levels.

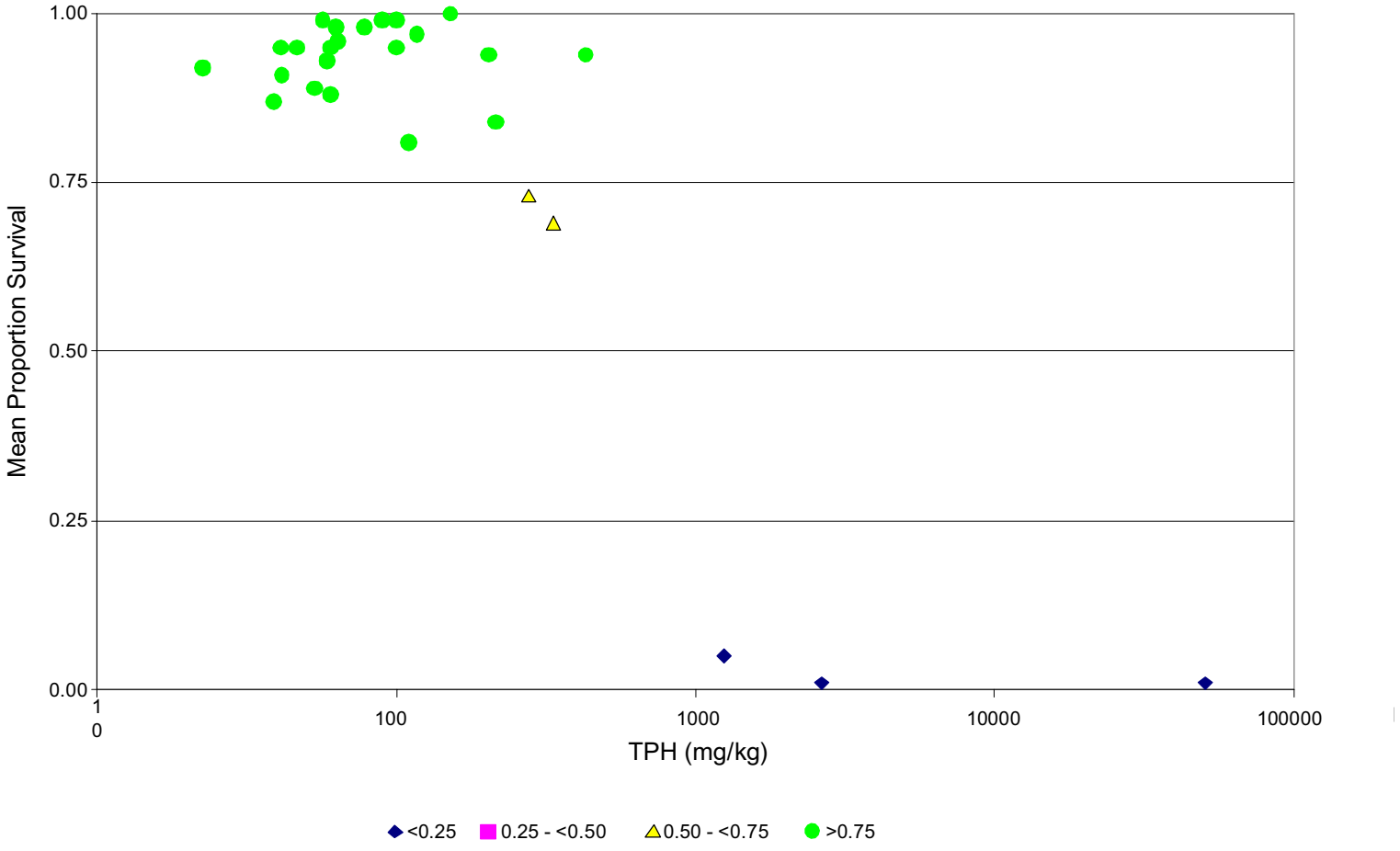

Figure 10-5. Scatter plot of the mean proportion survival against the total petroleum hydrocarbons (TPH) associated with sediments collected from the near- and mid-field strata of Main Pass 299 during the Screening Cruise and Sampling Cruises 1 and 2. Total petroleum hydrocarbon data are from Chapter 8.

10.3.2.3 Eugene Island 346. Eugene Island 346 had the greatest level of sediment toxicity relative to all other sites (Figure 10-6). The highest levels of toxicity were distributed south of the site. All of the T-class 4 relative toxicity observations (survival >0.75) were from sediments collected during Sampling Cruise 1. Interestingly, sediments from this site had lower survival that did not appear to be related to TPH (Figure 10-7). One observation with 0% survival and nearly 5,000 mg/kg TPH also had high levels of pore water sulfides (124 mg/L). However, none of the other observations of high toxicity had elevated total ammonia levels or detectable sulfides. Therefore, it is not likely that either was a factor in the relatively anomalous toxicity results for sediments from this site. Sediment toxicity apparently was related to some unmeasured factor.

10.3.2.4 Mississippi Canyon 496. Mississippi Canyon 496 had the lowest level of sediment toxicity relative to all other sites (Appendix F, Figure F-4). There were only two observations with survival less than 75% (0.67 and 0.68). Sediments from this site also had the lowest levels of TPH (Appendix F, Figure F-5).

10.3.2.5 Green Canyon 112. Green Canyon 112 had relatively high levels of sediment toxicity (Appendix F, Figure F-6). Survival was highly correlated with TPH ($r = -0.76$), with the highest responses at a TPH concentration of about 1,000 mg/kg or greater (Appendix F, Figure F-7). Three of the four samples classified in T-class 1 (survival <0.25) had high initial (Test Day 0) pore water sulfide concentrations, ranging from 4.5 to 52 mg/L (Appendix F), in addition to high TPH concentrations (>1,000 mg/kg).

10.3.2.6 Ewing Bank 963. Ewing Bank 963 had a moderate level of sediment toxicity relative to all other sites (Appendix F, Figure F-8). Most of the toxicity was observed in sediments running in a band from the northeast to southwest through the center of the site. TPH concentrations also were moderate relative to the other sites (Appendix F, Figure F-9). However, a distinct toxicity response with TPH concentration was evident, with the greatest response at about 1,000 mg/kg.

10.4 CONCLUSIONS

The mean proportion survival for each zone and sampling period tended to be greatest in the far-field (ranging from 0.87 to 0.97) and least in the near-field (ranging from 0.25 to 0.97). The near-field results also were the most variable, with CVs in survival between stations within a zone ranging from 2% to 153%.

Significant differences in survival between samples from the near-field and far-field zones were detected at three sites (GC 112, EW 963, and EI 346). No significant differences in survival between near-field and far-field zones were detected for the remaining sites (MC 496, MP 288, and MP 299) because of generally low toxicity in all zones and the presence of a single sample with low survival in near-field samples. A significant difference between the near-field and far-field samples was detected for samples collected during Sampling Cruises 1 and 2 at EI 346.

None of the drilling sites or sampling periods showed a significant difference in the mean proportion survival between samples from the near-field and mid-field zones.

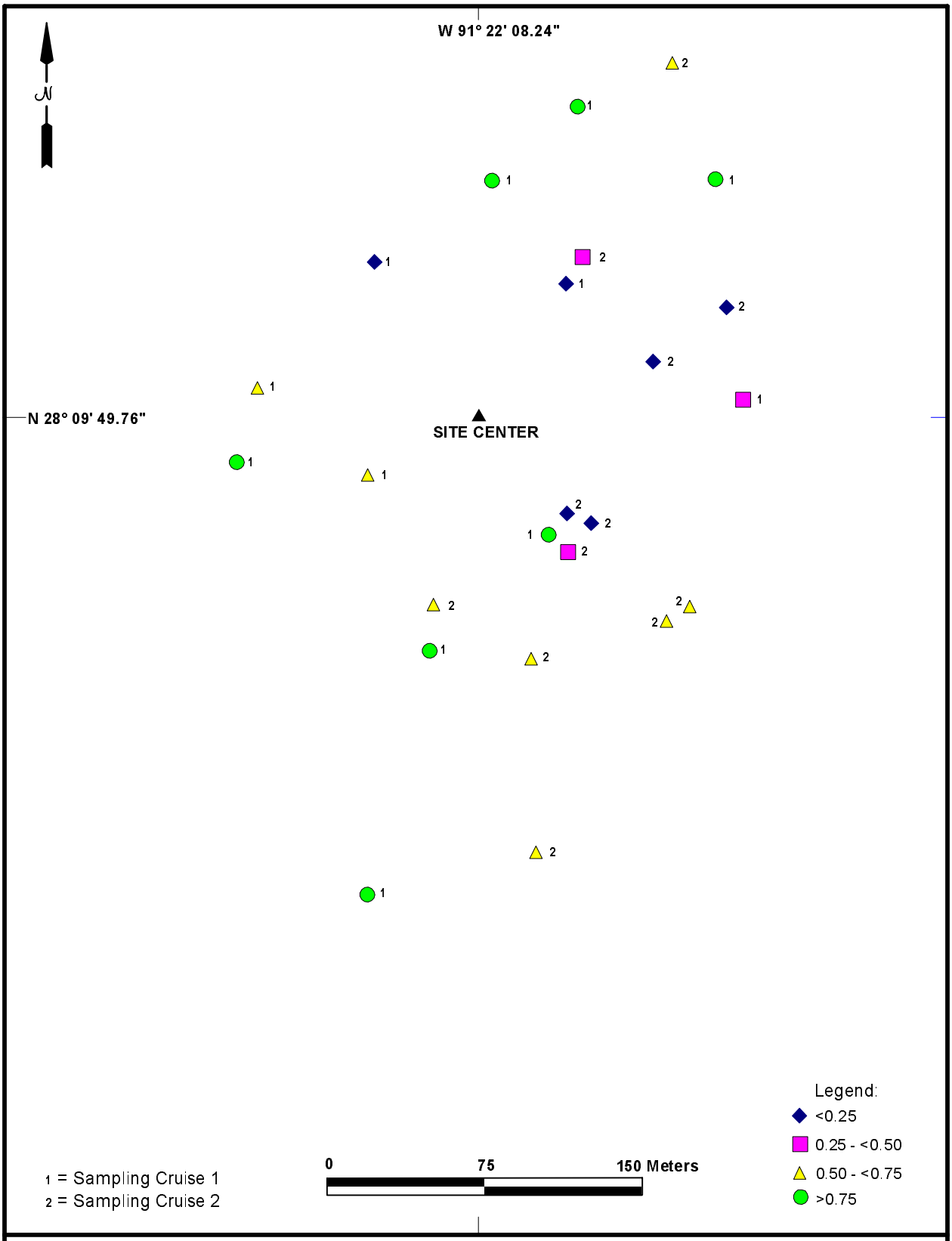

Figure 10-6. Plot of the sediment toxicity around Eugene Island 346 site. Legend defines survival levels.

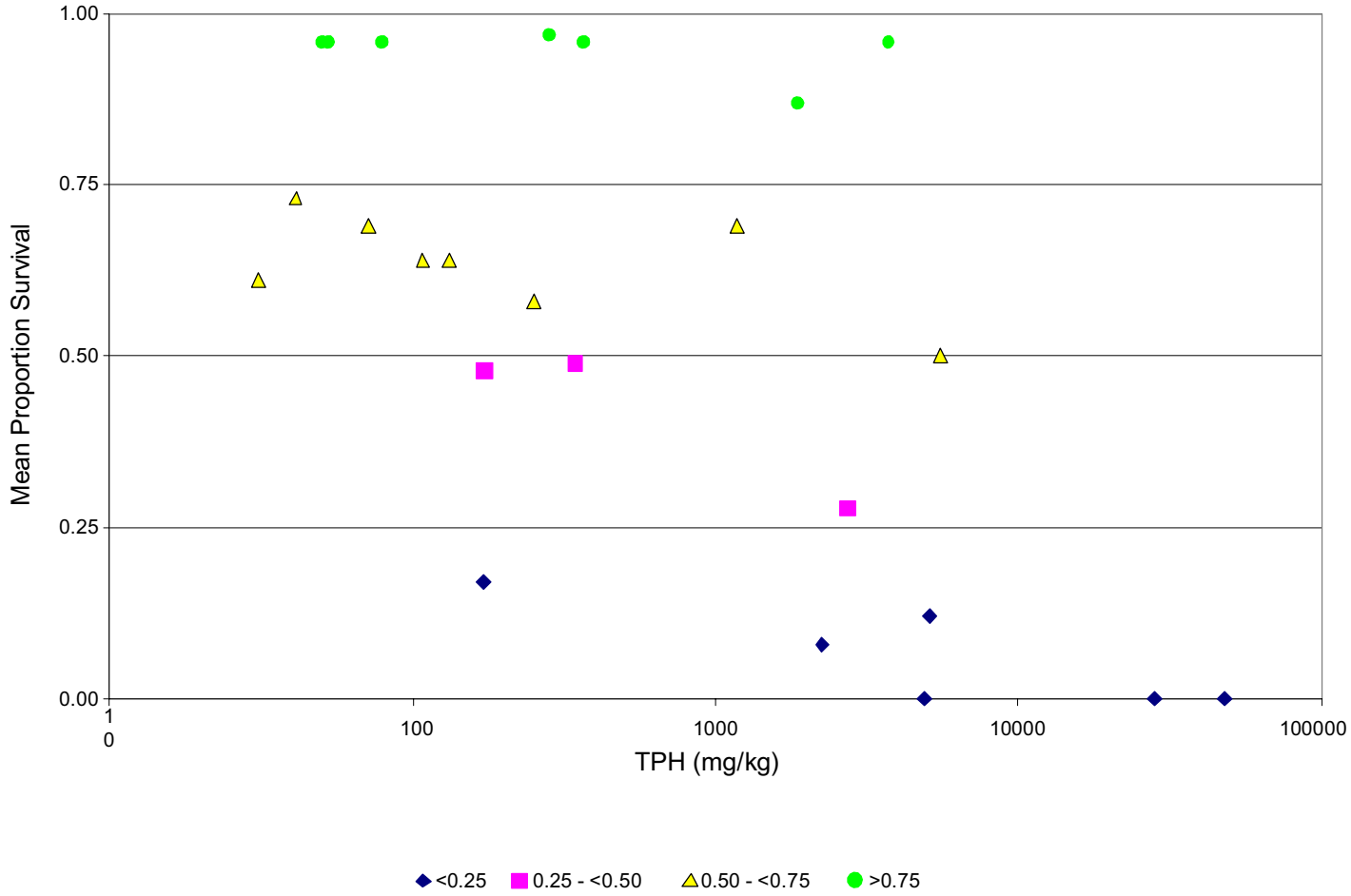

Figure 10-7. Scatter plot of the mean proportion survival against the total petroleum hydrocarbons (TPH) associated with sediments collected from the near- and mid-field zones of Eugene Island 346 during Sampling Cruises 1 and 2. Total petroleum hydrocarbon data are from Chapter 8.

Only one site showed a significant difference ($\alpha = 0.05$) in the mean proportion survival between sampling periods for a given zone and site. The mean survival for samples from the near-field zone at MP 288 was significantly greater for Sampling Cruise 2 (0.97) than it was for Sampling Cruise 1 (0.79).

An alternative analysis, ignoring zones, was conducted to determine if patterns of sediment toxicity were detectable in the near- and mid-field data. All far-field data had proportional survival greater than or equal to 0.75 and were not used in this analysis.

Based on the existing spatial coverage, samples from EI 346 had the greatest level and samples from MC 496 had the lowest level of sediment toxicity relative to samples from all other sites. Sediments from all sites had unique patterns of sediment toxicity generally associated with concentrations of TPH. Higher mortality levels were usually associated with TPH concentrations greater than 1,000 mg/kg.

Samples collected from EI 346 showed wide variability. There were samples with high survival at moderate TPH levels (e.g., 96% and 87% survival at 3,700 and 1,900 mg/kg TPH, respectively), as well as low survivals at low TPH levels (e.g., 17% survival at 170 mg/kg TPH). None of these samples had high pore water ammonia or sulfide concentrations. Therefore, toxicity could have been related to some factor that was not measured.

Chapter 11
SEDIMENT PROFILE IMAGING

Robert J. Diaz
Virginia Institute of Marine Science

11.1 INTRODUCTION

In order to help characterize the benthic habitats at selected oil and gas development sites in the Gulf of Mexico, sediment profile imaging (SPI) surveys were conducted in 2000, 2001, and 2002. However, SPI was not the central measurement method for this project; its use was limited to a few photographs at a site during individual cruises and thus only provides a general impression of benthic habitats. Rhoads and Cande (1971) developed sediment profiling as a means of obtaining *in situ* data to investigate processes structuring the sediment-water interface. The technology of remote ecological monitoring of the seafloor (REMOTS – Rhoads and Germano, 1982) or SPI has allowed for the development of a better understanding of the complexity of sediment dynamics, from both biological and physical points of view (for examples see Rhoads and Germano, 1986; Diaz and Schaffner, 1988; Valente et al., 1992; Diaz et al., 1994; Bonsdorff et al., 1996; Nilsson and Rosenberg, 2000; and Rosenberg et al., 2001). This approach to evaluating the environment and potential impacts can be easily combined with classical approaches to habitat and impact assessment, providing scientists and managers with a more holistic ecosystem view. In addition, SPI serves to provide ground-truth data for acoustic methods such as side-scan and multibeam sonar.

11.2 MATERIALS AND METHODS

11.2.1 Field Methods

An SPI survey was conducted during the Screening Cruise and two Sampling Cruises of the Gulf of Mexico Comprehensive Synthetic Based Muds Monitoring Program. At each station, a sediment profile camera was deployed three to five times.

On the Screening Cruise, sediment profile images were collected at 28 stations from nine different sites. On Sampling Cruise 1, images were obtained at 20 stations from MP 288 and MP 299. No images were collected at the other six sites due to a failure of the camera system that was not detected during the cruise (Table 11-1). On Sampling Cruise 2, images were obtained at 82 stations at eight different sites. A summary of stations with SPI data is contained in Table 11-1.

11.2.2 Sediment Profile Camera Details

A modified Benthos Model 3731 sediment profile camera was used to collect images (Figure 11-1). The profile camera works like an inverted periscope with a deep-sea 35-mm camera mechanism mounted horizontally inside a water-tight housing on top of a wedge-shaped prism. A Plexiglas® faceplate is at the front of the prism, and a mirror placed at a 45° angle is at the back of the prism. The camera lens looks down at the mirror, and the image is reflected from the faceplate. An internal strobe is mounted inside the prism at the back of the wedge to provide illumination for the image, and the chamber within the prism is filled with distilled water, so the camera always has an optically clear path through which to shoot. A moveable carriage within a stainless steel frame houses the wedge assembly.

Table 11-1. Summary of sediment profile camera stations sampled during the Screening Cruise, Sampling Cruise 1, and Sampling Cruise 2. Blanks indicate the zone was not sampled. A zero indicates the zone was sampled, but no analyzable images were collected.

Site	Zone	Screening Cruise	Sampling Cruise 1	Sampling Cruise 2
Eugene Island 346	FF		0	2
	MF		0	4
	NF		0	5
Eugene Island 963	FF			0
	MF			1
	NF			0
Ewing Bank 305	FF	1		
	NF	1		
Ewing Bank 963	FF		0	3
	MF		0	3
	NF		0	3
Garden Banks 128	FF	1		
	NF	2		
Green Canyon 112	FF	1	0	3
	MF		0	2
	NF	2	0	3
Mississippi Canyon 28	FF	1		
	NF	2		
Mississippi Canyon 496	FF	1	0	2
	MF		0	3
	NF	2	0	0
Main Pass 288	FF	1	0	0
	MF		4	4
	NF	2	4	4
Main Pass 299	FF	1	3	2
	MF		5	4
	NF	2	4	4
South Timbalier 160	FF		0	6
	MF		0	6
	NF		0	6
Viosca Knoll 780	FF	1		
	NF	2		
Viosca Knoll 783	FF	1	0	4
	MF		0	5
	NF	4	0	0
Total		28	20	82

FF = Far-field.
MF = Mid-field.
NF = Near-field.

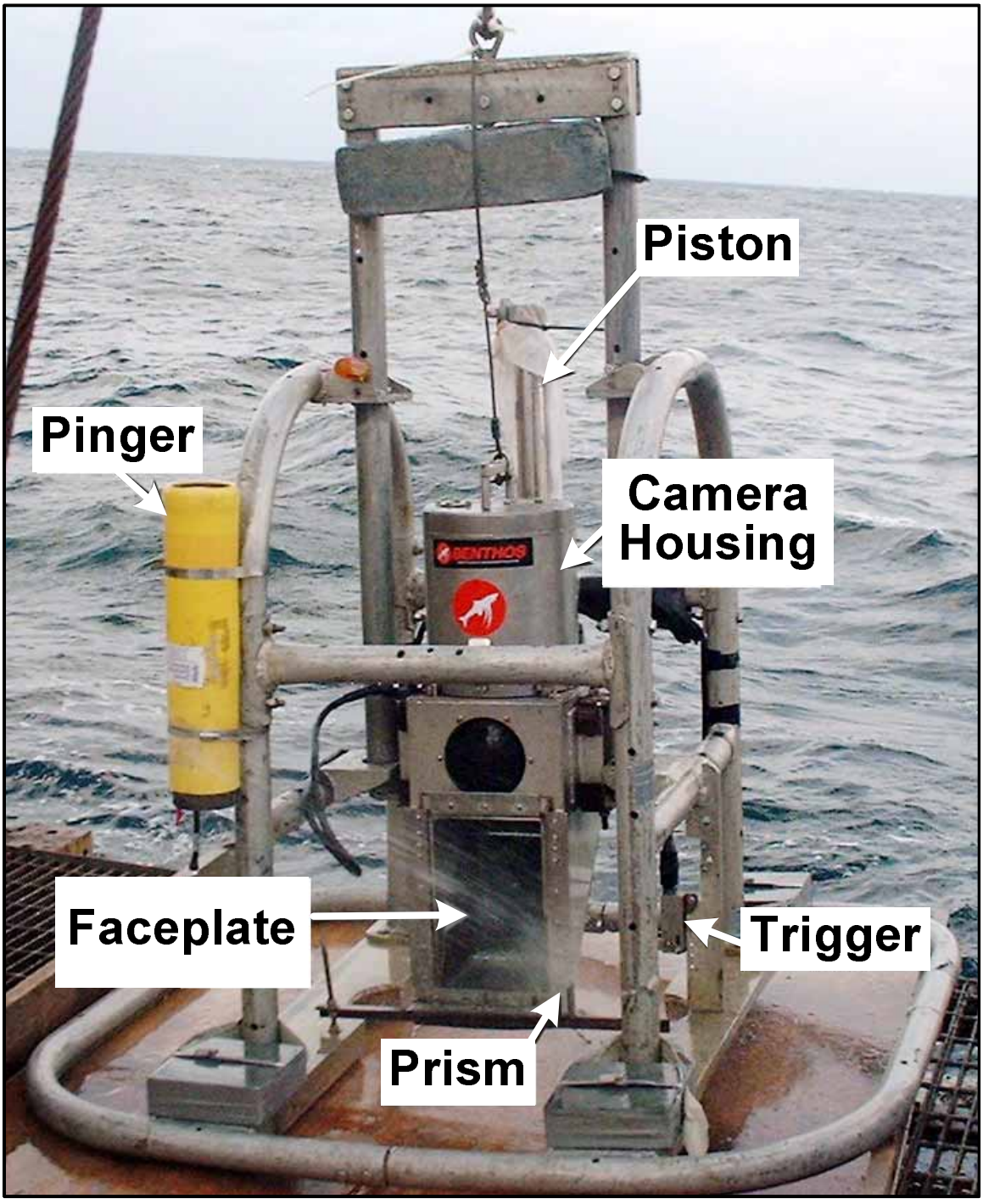

Figure 11-1. Sediment profile camera and frame. Faceplate is about 15 cm wide.

The frame is lowered to the seafloor on a winch wire, and the prism is held in its "up" position by the tension on the wire (Figure 11-2). When the frame comes to rest on the seafloor, the winch wire goes slack and the camera prism descends into the sediment at a slow rate that is controlled by the dampening action of a hydraulic piston so that the sediment-water interface is not disturbed. On the way down, the prism trips a trigger that activates a time-delay circuit to allow the camera to penetrate the seafloor before any image is taken. The knife-sharp edge of the prism transects the sediment, and the bottom then is penetrated by the prism. The strobe is discharged twice with each lowering to obtain two cross-sectional images of the upper 20 cm of the sediment column at 2 and 15 seconds after triggering. Stitching the two images together allows imaging of the sediment column to a greater depth than the prism window because of increased penetration in the 15-second image. In soft sediments, the two time-delayed images can be combined to increase the effective penetration of the prism to as much as 30 to 35 cm. After the two time-delayed images are obtained, the camera is then raised up about 2 to 3 m off the bottom to allow the strobe to recharge. The strobe recharges within 5 seconds, after which the camera is ready to be lowered again for another two images. The images that result give the viewer the same perspective as looking through the side of an aquarium half-filled with sediment.

Kodak Ektachrome® color slide film (ISO 100) was used throughout the study. At the beginning of each survey day, the time on the camera's internal data logger was synchronized with the internal clock on the computerized navigation system being used to conduct the survey. A Benthos Model 2216 Deep Sea pinger was attached to the camera frame and wired to the camera housing; when the strobe discharged, the ping rate doubled for 10 seconds. By monitoring the pinger signals through the use of a hydrophone on the research vessel, the scientist operating the camera was able to verify that a picture had been taken at each station.

Each SPI replicate is identified by the time recorded on the film and on disk along with vessel position. Even though multiple images were taken at each location, each image was assigned a unique frame number by the data logger and cross-checked with the time stamp in the navigational system's computer data file. Redundant sample logs were kept by the field crew.

Test exposures of the Jobo Color Checker® were fired on deck at the beginning and end of each roll of film to verify that all internal electronic systems were working to design specifications and to provide a color standard against which final film emulsion could be checked for proper color balance. Charged spare batteries were carried in the field at all times to ensure uninterrupted sample acquisition.

11.2.3 Image Analysis

Both the 1- and 15-second images were analyzed visually by projecting them and recording all features seen into a preformatted standardized spreadsheet file. The images then were digitized using a Nikon® LS-2000 scanner and analyzed using the Adobe PhotoShop®, Image Pro®, and NTIS Image® programs. Data from each image were sequentially saved to a spreadsheet file for later analysis. Details of how these data were obtained can be found in Rhoads and Germano (1986) and Diaz and Schaffner (1988). The following sections present a summary of major parameters measured.

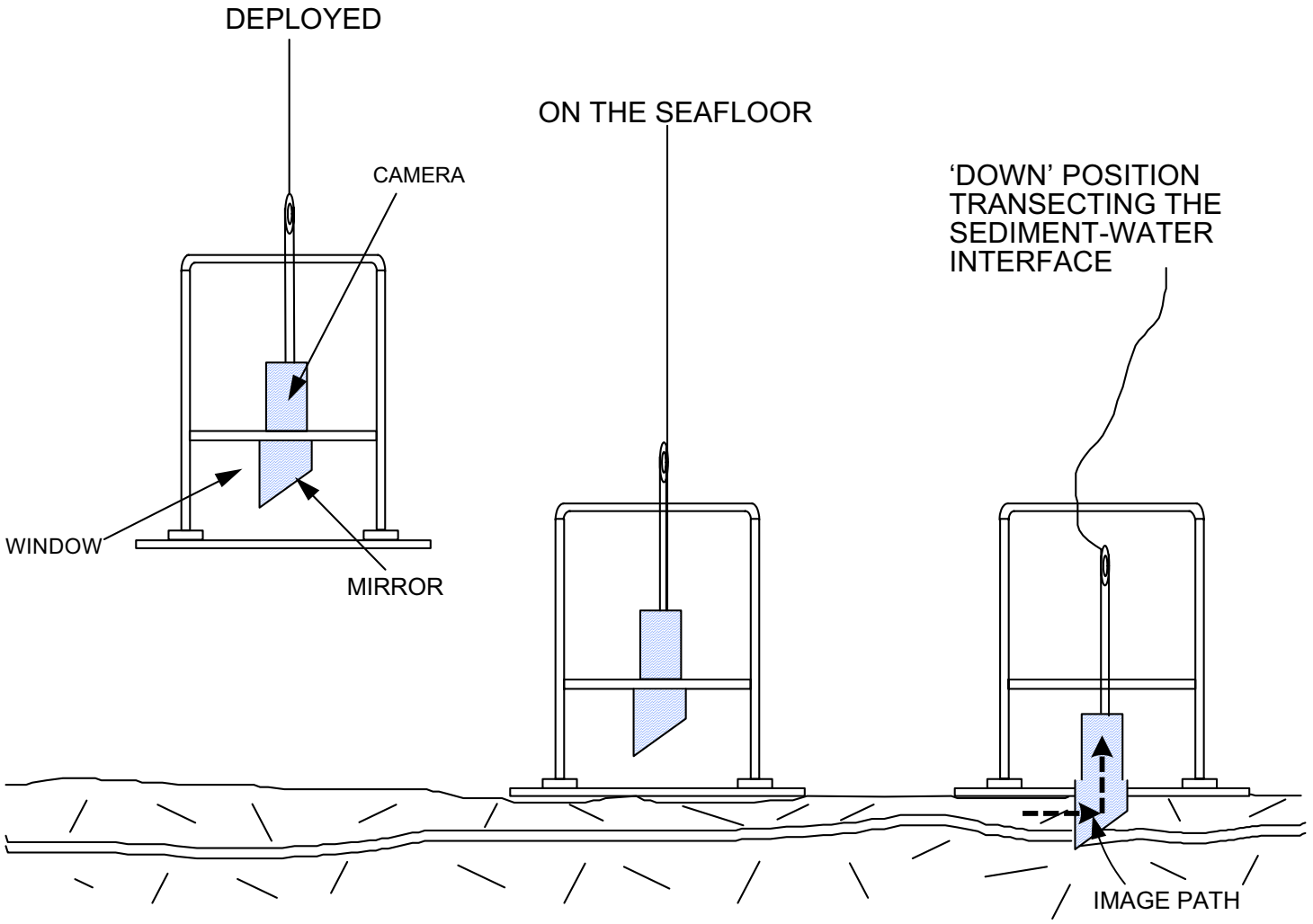

Figure 11-2. Sediment profile imaging photograph collection process (Modified from: Germano and Read, 2002).

11.2.3.1 Prism Penetration. This parameter provided a geotechnical estimate of sediment compaction with the profile camera prism acting as a dead weight penetrometer. The farther the prism entered into the sediment, the softer the sediments and more likely the higher the water content. Penetration was measured as the distance the sediment moved up the 23-cm length of the faceplate. The weight on the camera frame was kept at 200 lbs (weight in air), so prism penetration provided a means for assessing the relative compaction between stations.

11.2.3.2 Surface Relief. Surface relief or small-scale bed roughness, on the order of the prism faceplate width (15.2 cm), was the difference between maximum and minimum prism penetration. The origin of bed roughness can be determined from visual analysis of the images. In physically dominated habitats, features such as bedforms and sediment granularity cause bed roughness. In biologically dominated habitats, bed roughness is a result of biogenic activity such as tube structures, feeding mounds, feeding pits, or epifaunal organisms such as echinoderms or coelenterates.

11.2.3.3 Apparent Color Redox Potential Discontinuity Layer. This parameter is important in estimating benthic habitat quality (Rhoads and Germano, 1986; Diaz and Schaffner, 1988; Nilsson and Rosenberg, 2000) by providing an estimate of the depth to which sediments appear to be oxidized. The term apparent is used in describing this parameter because no actual measurement was made of the redox potential. It is assumed that given the complexities of iron and sulfate reduction-oxidation chemistry, the reddish-brown sediment color tones (Diaz and Schaffner, 1988; Rosenberg et al., 2001) indicate sediments are in an oxidative geochemical state or at least are not intensely reducing. This is in accordance with the classical concept of RPD layer depth, which associates redox potential with sediment color (Fenchel, 1969; Vismann, 1991). The apparent color RPD has been very useful in assessing the quality of a habitat for epifauna and infauna from both physical and biological points of view. Rhoads and Germano (1986), Diaz and Schaffner (1988), Valente et al. (1992), Bonsdorff et al. (1996), Nilsson and Rosenberg (2000), and Rosenberg et al. (2001) all found the depth of the RPD layer from sediment profile images to be directly correlated to the quality of the benthic habitat. These authors all found that deeper RPD layers were always associated with higher benthic habitat quality.

11.2.3.4 Sediment Grain Size. Grain size is an important parameter for determining the nature of the physical forces acting on a habitat and is a major factor in determining benthic community structure (Rhoads, 1974). The sediment type descriptors used for image analysis follow the Wentworth classification as described in Folk (1974) and represent the major modal class for each image. Grain size was determined by comparison of collected images with a set of standard images for which mean grain size had been determined in the laboratory. Table 11-2 is provided as a means of comparing phi scale sizes corresponding to sediment descriptors used in the current analysis.

Table 11-2. Phi scale and sediment descriptors used in sediment profile imaging (SPI) analysis.

Phi Scale	Upper Limit Size (mm)	Grains per cm of Image	SPI Descriptor	Sediment Size Class
8 to 6	<0.0039	>320	SICL	Silty-clay
>8	<0.0005	>2,560	CL	Clay

11.2.3.5 Surface Features. These parameters included a wide variety of features (bedforms, biogenic mounds, shells, amphipod tubes, worm tubes, bacterial mats). Each contributes information on the type of habitat and its quality for supporting benthic species. The presence of certain surface features is indicative of the overall nature of a habitat. For example, bedforms are always associated with physically dominated habitats, whereas the presence of worm tubes or feeding pits would be indicative of a more biologically accommodated habitat (Rhoads and Germano, 1986; Diaz and Schaffner, 1988). The presence of bacterial mats also is indicative of a low DO environment because mats form only over a narrow range of DO, typically from 0.2 to 0.5 mg/L (Rosenberg and Diaz, 1993). While no measurements of DO were made within the benthic boundary layer, other studies have shown that when bacterial mats are present in SPI images, bottom DO was low (Rosenberg and Diaz, 1993; Rosenberg et al., 2001). Surface features were visually evaluated from each image and compiled by type and frequency of occurrence.

11.2.3.6 Subsurface Features. Like surface features, these parameters included a wide variety of features and revealed a great deal about physical and biological processes influencing the bottom (e.g., infauna, burrows, water filled voids, gas voids, sediment layering). For example, habitats with grain size layers or homogeneous color layers are generally dominated by physical processes, while habitats with burrows, infaunal feeding voids, and/or visible infauna are generally dominated by biological processes (Rhoads and Germano, 1986; Diaz and Schaffner, 1988; Valente et al., 1992; Nilsson and Rosenberg, 2000). Subsurface features were visually evaluated from each image and compiled by type and frequency of occurrence.

11.2.4 Statistics

Analysis of variance was used to test for differences between and within sites and zones. Normality was checked with the Shapiro-Wilk test and homogeneity of variance with Bartlett's test (Zar, 1999). Data were square-root or log (x + 1) transformed when necessary. Tukey's HSD test was used to determine which groups in the analysis of variance were different (Zar, 1999). For statistical analysis, only RPD layers that were directly measured were included. Estimates of RPD layers from images that were over-penetrated, indicated by >0.1 in Appendix G, were excluded from all statistical comparisons. Also, for statistical comparisons that involved prism penetration, images that were over-penetrated were assigned a value of 23.0 cm. This approach provided a conservative estimate of differences in prism penetration between stations.

11.3 RESULTS AND DISCUSSION

Sediment profile imaging data are contained in Appendix G. All images have been processed to highlight the apparent color RPD layer and other sedimentary features. Individual stations in the text are identified as site-zone-station-replicate. For example, VK780FF3-1 is replicate one at far-field (FF) zone station 3 in site Viosca Knoll (VK) 780. Locations of sites, zones, and stations are provided in Chapter 3. The number of images analyzed from each site-zone is summarized in Table 11-1. The only site-zones that were sampled on all three cruises were MP288-NF, MP299-FF, and MP299-NF. The mid-field zone was sampled only on Sampling Cruises 1 and 2. A summary of SPI data is provided in Tables 11-3 and 11-4.

Table 11-3. Summary of sediment profile imaging parameters by site and zone. All numbers are means for a zone. Standard deviations are presented in Table 11-4.

Cruise	Site	Zone	N	Penetration (cm)	Surface Relief (cm)	RPD (cm)	Layers (image)	Layer 1 Thickness (cm)	Layer 2 Thickness (cm)	Layer 3 Thickness (cm)	Layer 4 Thickness (cm)	Tubes (image)	Infauna (image)	Burrows (image)	Oxic Voids (cm)	Oxic Voids Depth (cm)	Anaerobic Voids (image)	Anaerobic Voids Depth (cm)	Modal Grain Size	Sediment Color	Low DO**	Bacterial Mat
Screening	EW 305	FF	3	17.0	0.6	1.9	1.7	4.0	9.7	--	--	0.0	0.0	0.0	4.0	8.8	0.0	0.0	SICL	Light/Dark Gray	NO	NO
Screening	EW 305	NF	3	20.0	0.5	0.0	4.0	4.5	4.1	3.5	4.5	0.0	0.0	0.0	0.0	--	2.3	2.3	SICL	Dark Gray with White Spots	YES	YES
Screening	GB 128	FF	3	16.9	1.1	2.5	0.0	--	--	--	--	1.3	0.3	5.3	6.0	14.3	0.0	0.0	SICL	Light Gray	NO	NO
Screening	GB 128	NF	6	19.3	2.0	0.1	2.2	4.7	6.6	--	--	1.0	0.2	0.0	0.0	--	7.7	7.7	SICL	Dark/Light Gray	YES	YES
Screening	GC 112	FF	3	23.2	3.0	4.0	1.0	4.1	--	--	--	0.3	0.0	4.7	5.3	13.6	0.0	0.0	CL	Light Gray	NO	NO
Screening	GC 112	NF	6	20.9	2.3	0.5	1.8	7.2	5.2	--	--	42.8	2.2	0.2	0.3	15.6	4.7	4.7	SICL	Light/Dark Gray with White	YES	NO
Screening	MC 28	FF	3	23.1	2.1	7.8	0.7	5.5	--	--	--	3.0	0.3	2.7	5.3	16.1	0.0	0.0	SICL	Light Gray	NO	NO
Screening	MC 28	NF	6	22.1	1.3	2.1	2.3	3.3	9.9	--	--	1.8	0.0	1.5	4.5	15.4	0.5	0.5	SICL	Light/Dark Gray	NO	NO
Screening	MC 496	FF	3	25.3	--	6.1	0.0	--	--	--	--	--	0.0	5.0	2.3	11.2	0.7	0.7	CL	Light Gray	NO	NO
Screening	MC 496	NF	6	21.6	1.1	2.4	1.5	3.6	3.1	2.9	3.8	0.4	0.3	4.0	5.5	19.2	0.8	0.8	CL	Light/Dark Gray	NO	NO
Screening	MP 288	FF	3	23.7	2.1	4.8	0.0	--	--	--	--	1.0	0.3	1.0	3.3	14.7	0.0	0.0	SICL	Light Gray	NO	NO
Screening	MP 288	NF	6	20.1	1.8	1.1	1.8	4.6	9.4	--	--	0.3	0.7	0.5	0.0	--	1.3	1.3	SICL	Light/Dark Gray	YES?	NO
Screening	MP 299	FF	3	21.9	1.6	3.8	0.3	6.8	--	--	--	1.3	0.0	1.7	4.0	8.5	0.0	0.0	CL	Light Gray	NO	NO
Screening	MP 299	NF	6	20.4	1.1	0.4	2.0	4.1	8.8	--	--	4.0	0.5	0.0	0.0	--	0.5	0.5	SICL	Light/Dark Gray with White	YES	NO
Screening	VK 780	FF	3	22.4	2.5	2.5	0.0	--	--	--	--	0.0	0.0	3.0	5.0	18.5	0.0	0.0	CL	Light Gray	NO	NO
Screening	VK 780	NF	6	21.0	2.0	1.5	1.2	6.7	9.3	--	--	1.2	0.3	0.7	2.3	14.9	4.0	4.0	SICL	Light/Dark Gray with White	NO	NO
Screening	VK 783	FF	3	23.0	1.4	3.0	1.0	15.2	--	--	--	0.3	0.0	1.0	5.7	20.4	0.0	0.0	SICL	Light/Dark Gray	NO	NO
Screening	VK 783	NF	12	23.8	1.6	2.0	1.0	10.8	10.4	--	--	0.6	0.0	1.5	2.2	17.2	0.0	0.0	SICL	Light/Dark Gray	NO	NO
Sampling 1	MP 288	MF	4	18.2	1.4	2.5	0.5	4.9	--	--	--	1.3	0.3	2.3	3.5	12.0	0.0	0.0	SICL	Light/Dark Gray	NO	NO
Sampling 1	MP 288	NF	4	16.5	1.8	1.4	1.0	5.5	11.5	--	--	1.5	0.0	1.8	0.8	2.3	1.0	1.0	SICL	Greenish Gray to Light/Dark	NO	NO
Sampling 1	MP 299	FF	3	20.5	1.2	1.7	0.0	--	--	--	--	2.0	0.7	3.3	4.3	6.5	0.0	0.0	CL	Light Gray	NO	NO
Sampling 1	MP 299	MF	5	21.9	1.7	2.2	0.0	--	--	--	--	1.0	0.0	2.7	0.2	3.4	0.0	0.0	SICL	Light Gray	NO	NO
Sampling 1	MP 299	NF	4	18.0	1.2	0.5	0.0	--	--	--	--	1.0	0.3	0.3	0.0	--	0.0	0.0	SICL	Light Gray to Dark Gray with	YES	NO
Sampling 2	EI 346	FF	2	15.3	1.2	0.7	0.0	--	--	--	--	0.5	0.0	0.0	1.0	4.1	0.0	0.0	CL	Light Gray	NO	NO
Sampling 2	EI 346	MF	4	19.2	2.0	1.1	0.3	4.6	--	--	--	0.5	0.3	0.0	0.3	6.0	0.3	0.3	CL	Light Gray	NO	NO
Sampling 2	EI 346	NF	5	19.4	1.2	0.1	1.2	10.0	4.8	4.3	5.6	0.3	0.0	0.0	0.0	--	0.2	0.2	SICL	Dark/Medium Gray	YES	YES?
Sampling 2	EW 963	MF	1	16.3	0.8	0.6	2.0	1.5	5.3	--	--	2.0	1.0	1.0	0.0	--	0.0	0.0	SICL	Light/Dark/Medium Gray	NO	NO
Sampling 2	EW 963	FF	3	22.6	0.8	0.7	0.0	--	--	--	--	0.0	0.0	0.0	0.0	--	4.7	4.7	CL	Light Gray	NO	NO
Sampling 2	EW 963	MF	3	19.8	0.9	0.8	0.7	3.4	--	--	--	1.0	0.7	1.0	0.7	9.8	5.0	5.0	CL	Dark/Light Gray	YES?	NO
Sampling 2	EW 963	NF	3	21.9	2.3	1.2	1.3	5.3	16.0	--	--	1.0	0.0	0.7	1.7	14.3	1.3	1.3	SICL	Light/Dark Gray	NO	NO
Sampling 2	GC 112	FF	3	22.8	1.3	1.7	0.0	--	--	--	--	0.0	0.0	0.0	0.0	--	2.7	2.7	CL	Light Gray	NO	NO
Sampling 2	GC 112	MF	2	23.0	--	--	2.0	6.9	5.4	--	--	--	1.0	0.0	0.0	--	0.0	0.0	SICL	Dark/Light/Medium Gray	NO	NO
Sampling 2	GC 112	NF	3	22.3	0.4	1.4	1.7	6.2	15.9	--	--	1.5	0.3	0.0	0.3	14.2	0.0	0.0	SICL	Light/Dark/Medium Gray	NO	NO
Sampling 2	MC 496	FF	2	21.6	1.9	1.3	0.0	--	--	--	--	1.5	0.0	1.0	1.5	10.1	3.5	3.5	CL	Light Gray	NO	NO
Sampling 2	MC 496	MF	3	21.1	1.2	0.7	0.3	8.1	--	--	--	5.7	0.7	1.7	4.0	8.6	3.3	3.3	CL	Light Gray	NO	NO
Sampling 2	MP 288	MF	4	23.0	--	--	0.5	18.3	--	--	--	--	0.8	0.5	2.3	15.7	1.0	1.0	CL to SICL	Light to Dark/Medium Gray	NO	NO
Sampling 2	MP 288	NF	4	20.0	1.6	0.9	1.3	7.1	14.2	--	--	2.5	1.3	0.3	0.5	12.1	0.3	0.3	SICL	Dark/Medium Gray	NO	NO
Sampling 2	MP 299	FF	2	22.7	2.0	0.7	0.0	--	--	--	--	0.5	0.0	0.0	0.0	--	1.5	1.5	CL	Light Gray	NO	NO
Sampling 2	MP 299	MF	4	22.8	0.6	0.8	1.0	3.2	12.6	--	--	1.5	0.0	0.3	0.3	16.7	0.0	0.0	SICL	Light Gray	NO	NO
Sampling 2	MP 299	NF	4	21.1	1.5	0.8	0.5	8.6	--	--	--	1.5	1.3	0.5	1.8	12.5	0.5	0.5	CL to SICL	Light/Dark Gray with White	NO	NO
Sampling 2	ST 160	FF	6	11.9	1.8	1.7	0.2	8.7	--	--	--	6.7	0.0	0.2	0.2	6.3	0.3	0.3	CL	Light Gray	NO	NO
Sampling 2	ST 160	MF	6	11.1	1.0	0.8	0.3	11.9	--	--	--	0.0	0.2	0.0	0.2	5.3	1.7	1.7	CL	Light/Medium Gray	YES	YES?
Sampling 2	ST 160	NF	6	11.9	1.5	0.9	0.5	8.3	--	--	--	0.0	0.0	0.0	0.0	--	0.0	0.0	SICL	Dark Gray with White Spots	YES	YES?
Sampling 2	VK 783	NF	5	23.0	--	--	0.4	5.4	12.1	--	--	--	0.0	0.2	1.6	16.7	0.6	0.6	CL	Light Gray	NO	NO
Sampling 2	VK 783	FF	3	23.0	--	--	0.0	--	--	--	--	--	0.0	0.0	0.7	13.7	1.3	1.3	CL	Light Gray	NO	NO
Sampling 2	VK 783	MF	4	23.0	--	--	0.5	6.0	12.2	--	--	--	0.0	0.0	0.8	14.0	0.5	0.5	CL	Light Gray	NO	NO

CL= Clay.
DO = Dissolved oxygen.
RPD = Redox potential discontinuity.
SICL = Silty-clay.

** Visual interpretation from image if DO appeared to be low.
? = Questionable.
FF = Far-field; MF = Mid-field; NF = Near-field.

Table 11-4. Standard deviations for quantitative sediment profile imaging parameters listed in Table 11-3.

Cruise	Site	Zone	N	Penetration (cm)	Surface Relief (cm)	RPD (cm)	Layers (image)	Layer 1 Thickness (cm)	Layer 2 Thickness (cm)	Tubes (image)	Infauna (image)	Burrows (image)	Oxic Voids (image)	Oxic Voids Depth (cm)	Anaerobic Voids (image)	Anaerobic Voids Depth (cm)
Screening	Ewing Bank 305	FF	3	1.6	0.3	0.4	0.6	0.2	0.4	0.0	0.0	0.0	2.6	2.7	0.0	0.0
Screening	Ewing Bank 305	NF	3	1.4	0.2	0.0	0.0	1.5	0.5	0.0	0.0	0.0	0.0	--	1.2	1.2
Screening	Garden Banks 128	FF	3	1.3	0.7	1.0	0.0	--	--	2.3	0.6	4.9	1.0	2.6	0.0	0.0
Screening	Garden Banks 128	NF	6	5.1	1.4	0.2	0.4	1.4	2.6	1.7	0.4	0.0	0.0	--	4.4	4.4
Screening	Green Canyon 112	FF	3	3.3	1.4	0.1	0.0	0.2	--	0.6	0.0	0.6	3.1	4.6	0.0	0.0
Screening	Green Canyon 112	NF	6	4.1	2.1	0.9	0.8	7.2	0.8	88.0	2.6	0.4	0.5	0.4	4.5	4.5
Screening	Mississippi Canyon 28	FF	3	3.9	0.7	4.0	0.6	5.1	--	1.0	0.6	2.5	5.1	7.4	0.0	0.0
Screening	Mississippi Canyon 28	NF	6	2.7	0.7	0.8	0.5	0.9	2.5	2.1	0.0	0.8	2.6	7.5	1.2	1.2
Screening	Mississippi Canyon 496	FF	3	2.4	--	--	0.0	--	--	--	0.0	1.0	1.5	3.3	1.2	1.2
Screening	Mississippi Canyon 496	NF	6	8.7	0.5	0.7	2.0	0.8	0.5	0.9	0.5	2.6	4.3	6.7	1.3	1.3
Screening	Main Pass 288	FF	3	3.0	0.6	1.1	0.0	--	--	1.7	0.6	1.0	0.6	2.3	0.0	0.0
Screening	Main Pass	NF	6	3.7	1.2	0.6	0.4	1.2	3.4	0.8	0.5	0.5	0.0	--	2.8	2.8
Screening	Main Pass	FF	3	4.7	1.0	2.8	0.6	--	--	2.3	0.0	1.5	6.1	0.4	0.0	0.0
Screening	Main Pass	NF	6	0.9	0.8	0.3	0.0	0.5	3.8	5.2	0.8	0.0	0.0	--	0.5	0.5
Screening	Viosca Knoll 780	FF	3	2.3	0.2	1.3	0.0	--	--	0.0	0.0	1.0	3.6	4.9	0.0	0.0
Screening	Viosca Knoll 780	NF	6	1.9	1.2	0.8	0.4	3.0	--	1.6	0.5	0.8	3.1	7.1	4.9	4.9
Screening	Viosca Knoll 783	FF	3	1.6	0.7	0.6	0.0	1.5	--	0.6	0.0	0.0	1.5	2.8	0.0	0.0
Screening	Viosca Knoll 783	NF	12	2.5	1.3	0.9	0.7	5.8	2.3	1.2	0.0	1.5	1.7	6.1	0.0	0.0
Sampling 1	Main Pass 288	MF	4	4.6	0.3	0.5	0.6	1.0	--	2.5	0.5	1.7	3.5	5.4	0.0	0.0
Sampling 1	Main Pass 288	NF	4	3.8	0.4	0.7	0.8	2.7	--	3.0	0.0	1.7	1.0	0.2	2.0	2.0
Sampling 1	Main Pass 299	FF	3	0.9	0.2	0.7	0.0	--	--	1.0	1.2	1.5	2.5	2.9	0.0	0.0
Sampling 1	Main Pass 299	MF	5	2.1	0.8	0.9	0.0	--	--	1.7	0.0	1.5	0.4	--	0.0	0.0
Sampling 1	Main Pass 299	NF	4	5.3	0.9	0.6	0.0	--	--	1.0	0.5	0.6	0.0	--	0.0	0.0
Sampling 2	Eugene Island 346	FF	2	4.9	0.8	--	0.0	--	--	0.7	0.0	0.0	1.4	--	0.0	0.0
Sampling 2	Eugene Island 346	MF	4	1.7	1.0	0.6	0.5	--	--	1.0	0.5	0.0	0.5	--	0.5	0.5
Sampling 2	Eugene Island 346	NF	5	2.5	0.5	0.1	1.6	4.7	--	0.5	0.0	0.0	0.0	--	0.4	0.4
Sampling 2	Ewing Bank 963	MF	1	--	--	--	--	--	--	--	--	--	--	--	--	--
Sampling 2	Ewing Bank 963	FF	3	0.5	0.5	0.4	0.0	--	--	0.0	0.0	0.0	0.0	--	0.6	0.6
Sampling 2	Ewing Bank 963	MF	3	4.5	0.4	0.6	0.6	1.5	--	1.7	1.2	1.0	0.6	2.7	5.0	5.0
Sampling 2	Ewing Bank 963	NF	3	1.0	0.7	0.6	0.6	3.4	--	1.4	0.0	1.2	1.5	0.9	2.3	2.3
Sampling 2	Green Canyon 112	FF	3	0.2	0.0	0.6	0.0	--	--	0.0	0.0	0.0	0.0	--	2.5	2.5
Sampling 2	Green Canyon 112	MF	2	0.0	--	--	0.0	0.6	1.7	--	1.4	0.0	0.0	--	0.0	0.0
Sampling 2	Green Canyon 112	NF	3	1.0	0.1	0.5	0.6	6.1	0.3	0.7	0.6	0.0	0.6	--	0.0	0.0
Sampling 2	Mississippi Canyon 496	FF	2	0.7	0.7	--	0.0	--	--	2.1	0.0	1.4	2.1	--	0.7	0.7
Sampling 2	Mississippi Canyon 496	MF	3	1.1	0.5	0.1	0.6	--	--	3.5	1.2	2.1	4.0	3.5	3.5	3.5
Sampling 2	Main Pass 288	MF	4	0.0	--	--	0.6	2.4	--	--	0.5	1.0	1.9	6.3	2.0	2.0
Sampling 2	Main Pass 288	NF	4	2.1	0.8	0.3	0.5	6.6	--	3.8	1.9	0.5	0.6	2.6	0.5	0.5
Sampling 2	Main Pass 299	FF	2	0.4	--	--	0.0	--	--	0.7	0.0	0.0	0.0	--	2.1	2.1
Sampling 2	Main Pass 299	MF	4	0.4	--	--	1.2	0.7	4.5	3.0	0.0	0.5	0.5	--	0.0	0.0
Sampling 2	Main Pass 299	NF	4	1.3	0.6	0.3	0.6	2.4	--	1.9	1.3	1.0	1.5	6.8	1.0	1.0
Sampling 2	South Timbalier 160	FF	6	2.0	1.3	0.6	0.4	--	--	16.3	0.0	0.4	0.4	--	0.5	0.5
Sampling 2	South Timbalier 160	MF	6	2.2	0.7	0.9	0.5	0.2	--	0.0	0.4	0.0	0.4	--	2.6	2.6
Sampling 2	South Timbalier 160	NF	6	3.9	0.6	1.0	0.5	3.8	--	0.0	0.0	0.0	0.0	--	0.0	0.0
Sampling 2	Viosca Knoll 783	NF	5	0.0	--	--	0.9	--	--	--	0.0	0.4	1.8	3.2	0.9	0.9
Sampling 2	Viosca Knoll 783	FF	3	0.0	--	--	0.0	--	--	--	0.0	0.0	0.6	8.0	0.6	0.6
Sampling 2	Viosca Knoll 783	MF	4	0.0	--	--	1.0	--	--	--	0.0	0.0	1.5	--	1.0	1.0

FF = Far-field. MF = Mid-field. NF = Near-field. RPD = Redox potential discontinuity.

11.3.1 Sediments

Physical processes appeared to dominate the sediment surface at all but 1 of the 28 stations from the Screening Cruise and all stations from Sampling Cruises 1 and 2. Biological processes dominated surface sediments at Station GC112-NF1. Biogenic structures constructed by benthic organisms were abundant in surface sediments of this station, with an average of 42.8 tubes/image and a maximum of about 200 tubes/image. Apart from this station, there were few biogenic structures observed in images from any cruise. The maximum number of tubes for any single image was 40 at Station ST160-FF5. All these tubes were small (<1 mm in diameter) and short (<4 mm long).

The dominance of physical processes was most apparent in the uniform grain size and color layering of sediments (Table 11-3). Sediment grain size estimated from the sediment profile images was very uniform over the study sites and were within a narrow range of Folk textural classes (Folk, 1974) of silty-clay to clay (Table 11-3). Grain size analysis of the top 0 to 2 cm layer of sediment confirmed the uniformly fine texture of the sediments, with most stations being silty-clay or clay. A few stations had a significant sand component, such as MP288-NF2, which was 23% sand during Sampling Cruise 1 and 13% sand during Sampling Cruise 2 (see Chapter 7). Sandy layers, however, were not observed in any of the sediment profile images.

When all sites were combined by cruise, sediment grain size at far-field stations was evenly divided between silty-clay and clay for the Screening Cruise. For Sampling Cruises 1 and 2, all the far-field stations were clay. Sediments at mid-field stations for Sampling Cruise 1 were all silty-clay. For Sampling Cruise 2, there were more clay stations than silty-clay. Overall, far-field stations tended to be clay, while mid-field and near-field stations were silty-clay (Table 11-5).

Table 11-5. Summary of sediment types from sediment profile imaging analysis.

	Sediment Class		Ratio of SICL to CL
	SICL	CL	
Screening Cruise			
Far-field	14	13	1.1
Near-field	48	9	5.3
Sampling Cruise 1			
Far-field	0	3	
Mid-field	9	0	
Near-field	8	0	
Sampling Cruise 2			
Far-field	0	21	
Mid-field	12	19	0.6
Near-field	23	7	3.3

CL = Clay
SICL = Silty clay.

Average prism penetration, a proxy for sediment compaction, for a zone ranged from 11.1 cm (2.2 cm standard deviation [SD]) at mid-field stations in ST 160 for Sampling Cruise 2, to 25.3 cm (2.4 cm SD) at far-field stations in MC 496 for the Screening Cruise. The overall average for all cruises was 20.2 cm (4.4 cm SD). Variation in compaction likely reflected variation in the concentration of pore water, since sediment type was so similar over the study zone and there was no significant difference in penetration related to sediment type (Figure 11-3A). Average prism penetration at near-field, mid-field, and far-field zones was the same, 20.5 cm (0.63 cm standard error [SE]), 19.6 cm (0.72 cm SE), and 20.4 cm (0.45 cm SE), respectively (Figure 11-3B). Bed roughness or surface relief also was the same between zones, 1.6 cm (0.15 cm SE), 1.3 cm (0.19 cm SE), and 1.5 cm (0.11 cm SE), respectively. Bed roughness was formed primarily by sediment clasts, e.g., VK783-FF2 on the Screening Cruise.

Many of the stations had sediments that appeared to be layered. At all but one station, the layering was due to color change in the sediment and not grain size. These color layers varied from dark gray (MP288-NF Sampling Cruise 2) to light gray (MP299-MF Sampling Cruise 2), with a few greenish-gray layers (MP288-NF Sampling Cruise 1, Table 11-2). At Station GB128-NF1 from the Screening Cruise, sediment layers were dark and light gray with both silty-clay and clay present. Statistically, the number of color sediment layers was significantly greater in the near-field zone compared to mid-field and far-field zones (Kruskal-Wallis test, Chi-square = 47.1, $p = <0.0001$, Figure 11-4). On average, near-field stations had 1.4 layers/image (0.09 layers/image SE), while mid-field and far-field stations had 0.6 layers/image (0.14 layers/image SE) and 0.3 layers/image (0.28 layers/image SE), respectively (Figure 11-4).

Discharged cuttings drilled with SBF may have formed sediment layering at some near-field stations sampled during the Screening Cruise. As many as four layers were observed at EW305-NF and MC496-NF from the Screening Cruise and at EI346-NF from Sampling Cruise 2 (Table 11-2). The colors of these layers ranged from light gray to dark gray, with the gray being a darker shade compared to far-field stations (Figure 11-5). It is possible that at many near-field stations the prism did not penetrate below SBF deposits, but the analysis of sediment cores did not support the fact that surface sediments were composed entirely of SBF (see Chapter 8, Table 8-3). The surface sediment layers seen in the sediment profile images likely represent a mixture of SBF and natural sediments. A comparison of SBF data with the presence of layers in the sediment profile images from the Screening Cruise indicated that most of the color sediment layering observed was related to drilling activities. Synthetic based fluid was positively correlated with the presence of color layers, but barite presence, both from analysis and visual inspection of the sediment cores (see Chapter 9, Section 9.4), appeared to be negatively correlated with color layers (Table 11-6).

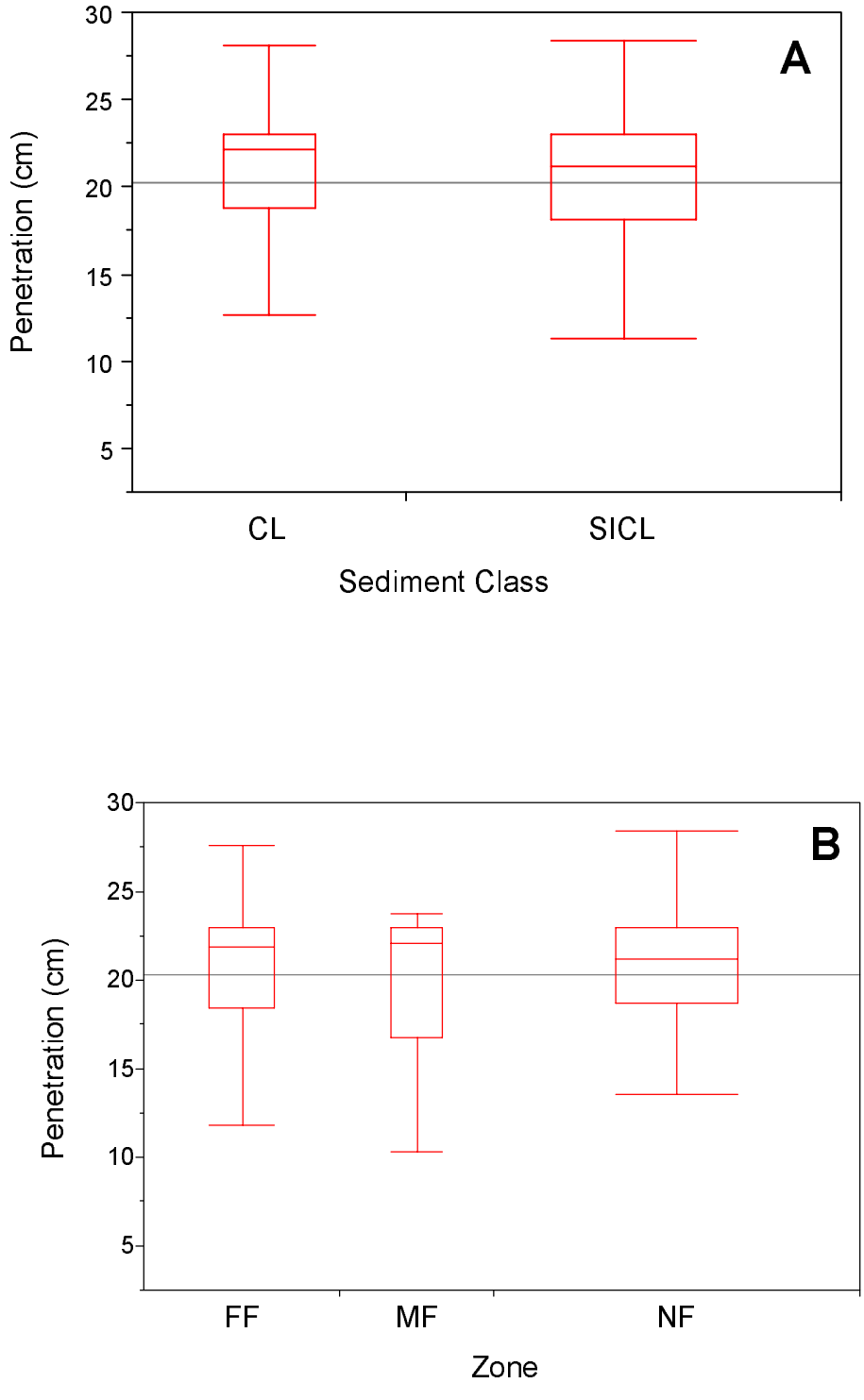

Figure 11-3. Box plots of prism penetration (cm) for all sediment profile images by sediment type (A) and zone (B). Box is interquartile range (IR), whiskers are 1.5IR, and bar in box is the median. The horizontal line is the grand mean. Width of the box is proportional to sample size.

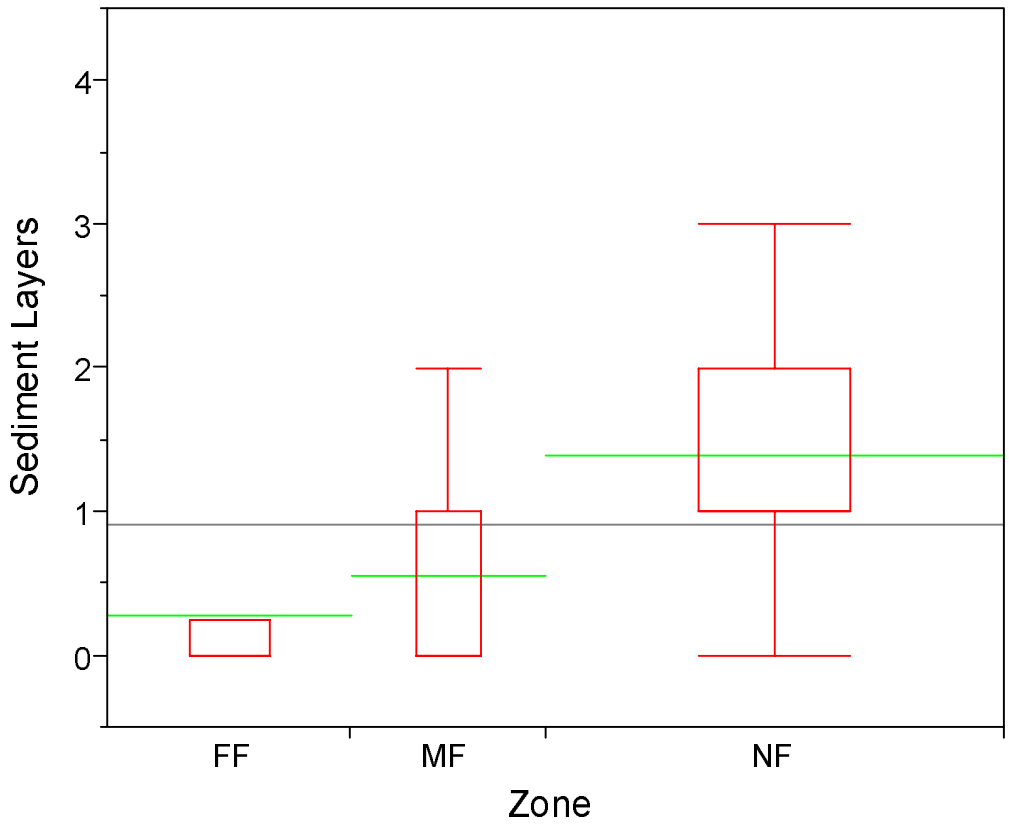

Figure 11-4. Box plots of the number of sediment layers for all sediment profile images by zone. Box is interquartile range (IR), whiskers are 1.5IR, and line extending from box is mean. The horizontal line is the overall mean. Width of the box is proportional to sample size.

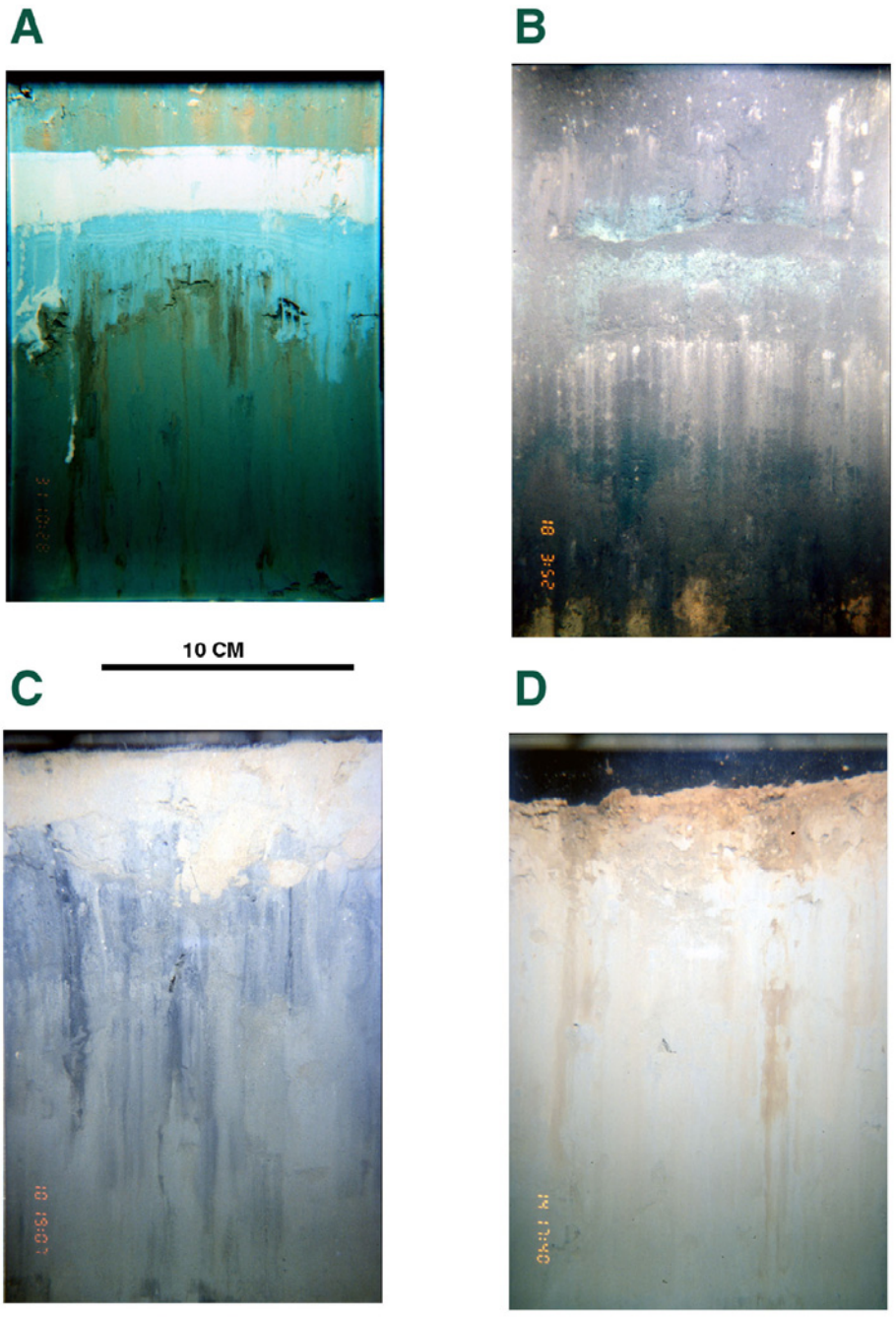

Figure 11-5. Sediment profile images from (A) MC 496-NF2 on Screening Cruise, (B) EI 346-NF2 on Sampling Cruise 2, (C) MP 299-MF3 on Sampling Cruise 2, and (D) MC 496-FF3 on Sampling Cruise 2. A and B show multiple layered sediments from the near-field zone. C and D are typical images from mid-field and far-field zones. Data for images are contained in Appendix G.

Table 11-6. Comparison of sediment layering in sediment profile imaging (SPI) with core analysis for synthetic based fluids (SBFs) (Chapter 8, Sections 8.3.2 and 8.3.3) and barite (Chapter 9, Section 9.4). Numbers are total stations within each category.

SPI Layers	Presence of SBF		
	No	Yes	Trace
No	5	0	1
Yes	5	13	0
SPI Layers	Presence of Barite (Analyzed)		
	No	Yes	Trace
No	4	1	1
Yes	15	2	1
SPI Layers	Presence of Barite (Visual)		
	No	Yes	
No	6	0	
Yes	17	1	

The thickness of the first color sediment layers ranged from 1.5 cm (mid-field) to 20.0 cm (mid-field); however, there were no statistically significant differences between near-field, mid-field, and far-field zones in the thickness of this layer (Table 11-7).

Table 11-7. Thickness of sediment layers from sediment profile imaging.

Zone	Thickness of First Sediment Layer (cm)				
	N	Minimum	Maximum	Mean	SE
Far-field	12	1.9	16.6	7.7	1.45
Mid-field	16	1.5	20.0	7.3	1.31
Near-field	72	1.9	18.9	6.3	0.50

N = Number of images.
SE = Standard error.

11.3.2 Apparent Color RPD Layer Depth and Low DO

Average RPD layer depths ranged from 0.0 cm at Station EW305-NF to 7.8 cm at Station MC28-FF, both on the Screening Cruise (Table 11-3), with the deeper measured RPD layers in sediments with higher levels of subsurface biogenic activity. Burrows convoluted the plane of the RPD layer and projected oxidized sediments >24 cm below the sediment-water-interface at two stations (MC496-NF1 and GC112-FF1 on the Screening Cruise). Shallowest RPD layer depths were associated with near-field stations, which included EW305-NF, GB128-NF, GC112-NF, MP288-NF, and MP299-NF from the Screening Cruise; MP299-NF from Sampling Cruise 1; and EI346-NF and ST160-NF from Sampling Cruise 2 (Table 11-5).

RPD layer depths were not related to sediment type, with the mean of clay stations being 1.9 cm (0.24 cm SE) and 1.5 cm (0.17 cm SE) for silt-clay sediments. However, zone averaged RPD layer depths were deeper at far-field relative to mid-field and near-field zones (ANOVA, degrees of freedom = 2, F = 7.5, p = 0.002, Figure 11-6, Table 11-8).

Table 11-8. Summary of redox potential discontinuity (RPD) layer depth from sediment profile images.

Zone	RPD Layer Depth (cm)				
	N	Min.	Max.	Mean	SE
Far-field	16	0.7	7.8	2.8	0.35
Mid-field	8	0.6	2.5	1.2	0.50
Near-field	17	0.0	2.4	1.0	0.34

N = Number of images.
SE = Standard error.

Most of the shallower RPD layer depths on all three cruises in the near-field zone were likely related to low levels of biogenic activity (Appendix G). The only mid-field zone stations with shallow RPD layers were in ST 160 and EW 963 on Sampling Cruise 2 (Table 11-2). In muddy sediments, those with a significant silt and clay component, physical diffusion limits oxygen penetration to <1 cm (Jørgensen and Revsbech, 1985). When the RPD layers in fine sediments are >1 cm, bioturbation by infauna (Rhoads, 1974) or major resuspension/deposition events (Don Rhoads, personal communication) are responsible for oxygenating sediments. The penetration of oxygen into the sediments (see Chapter 9) was less at Screening Cruise stations that appeared to have limited biogenic activity in the SPI images (Table 11-9).

Table 11-9. Summary of oxygen penetration depth into sediments (data from Chapter 9) based on level of biogenic activity in sediment profile images.

Biogenic Activity	Depth (mm) of Oxygen Penetration into Sediments				
	N	Min.	Max.	Mean	SE
NO	20	0.0	2.5	0.8	0.2
YES	7	0.0	0.4	0.1	0.1

N = Number of images.
SE = Standard error.

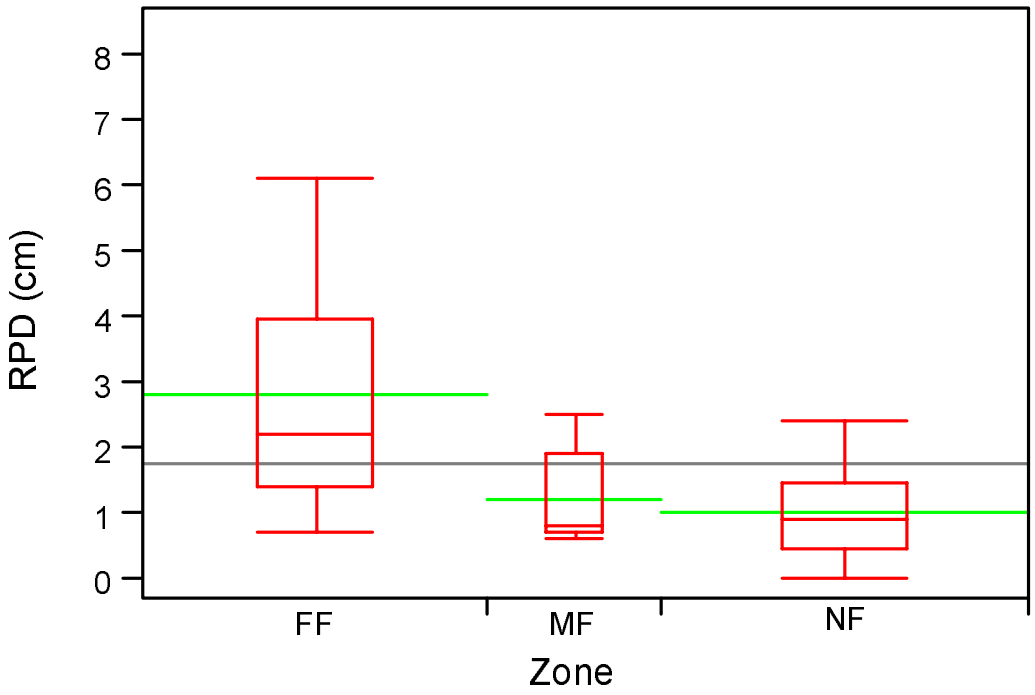

Figure 11-6. Box plots of apparent color redox potential discontinuity (RPD) layer depth for all sediment profile images by zone. Box is interquartile range (IR), whiskers are 1.5IR, line in box is the median, and line extending from box is the mean. The horizontal line is the overall mean. Width of the box is proportional to sample size.

The SPI data indicated that low DO may have been a factor regulating benthic communities at near-field zones, particularly those at EI 346, EW 305, GB 128, and ST 160 where there appeared to be bacterial mats on the sediment surface at the time of sampling. The presence of bacterial mats and macroinfauna at these near-field stations indicated that DO concentrations at the time of sampling were within the narrow range of 0.2 to 0.5 mg/L over which most bacterial mats form (Rosenberg and Diaz, 1993). Bacterial mats often are associated with naturally occurring deepwater oxygen minimum zones (OMZs) and anthropogenic coastal hypoxic zones (Diaz and Rosenberg, 1995).

Bacterial mats and other indicators of poor macrobenthic habitat, such as shallow RPDs, appeared to be temporally variable. At MP288-NF, two of six stations appeared to be stressed during the Screening Cruise, but all stations during Sampling Cruise 1 (four stations) and Sampling Cruise 2 (four stations) appeared normoxic. At MP 299, all six images from the Screening Cruise and two of four images from Sampling Cruise 1 appeared to indicate stress. During Sampling Cruise 2, none of the four near-field stations at MP 299 appeared to be stressed (Appendix G). For MP299-NF, there did appear to be a trend for increased benthic habitat quality from 2000 to 2002 (Table 11-10).

Table 11-10. Summary of redox potential discontinuity (RPD) layer depth from sediment profile imaging by year.

Site, Zone	RPD Layer Depth (cm)				
	Year	Min.	Max.	Mean	SE
Main Pass 288, Near-field	2000	0.4	1.8	1.0	0.24
	2001	0.9	2.4	1.4	0.34
	2002	0.7	1.2	0.9	0.14
Main Pass 299, Near-field	2000	0.1	0.9	0.4	0.13
	2001	0.0	1.2	0.5	0.35
	2002	0.5	1.1	0.8	0.14

SE = Standard error.

11.3.3 Biogenic Activity

The dominance of physical processes at all but one station (GC112-NF1 on the Screening Cruise) led to unstable surface sediments that prevented the development of a more advanced biogenic forming surface fauna. The most abundant biogenic surface feature was small worm tubes that occurred at 82% of the site-zones sampled. These small tubes likely belonged to pioneering successional Stage I species such as the spionid *Paraprionospio pinnata* or capitellid polychaetes, which were numerical dominants at the stations (see Chapter 12). Subsurface biogenic structures associated with infaunal organisms, mostly larger bodied polychaetes (see MP288-NF2 from the Screening Cruise or GC112-MF4 on Sampling Cruise 2), included active burrows at 65% (30 of 46) of the site-zones (see VK780-FF3 on the Screening Cruise), water filled oxic voids at 74% (34 of 46) that were zones of active feeding by head-down deposit feeders such as maldanid polychaetes (see MC28-FF1 on the Screening Cruise), water filled anaerobic voids that likely were abandoned feeding zones at 59% (27 of 46) (see EW963-MF1 on Sampling Cruise 2), and infaunal organisms at 48% (22 of 46) (see GC112-NF1 on Screening Cruise).

Subsurface biogenic activity was the most important factor in deepening the RPD layer with oxic feeding voids and burrows, the principal structures deepening the RPD layer (Table 11-2). Statistically, there were significantly more oxic voids at far-field zone stations than mid-field and near-field zones (ANOVA, F = 4.5, p = 0.017, Figure 11-7), which was an indication that benthic communities were more successionally advanced in the far-field relative to mid-field and near-field (Table 11-11).

Table 11-11. Summary of oxic voids from sediment profile imaging.

Zone	Average Number of Oxic Voids				
	N	Min.	Max.	Mean	SE
Far-field	17	0.0	6.0	2.9	0.54
Mid-field	11	0.0	4.0	1.1	0.44
Near-field	18	0.0	5.5	1.2	0.38

N = Number of images.
SE = Standard error.

The number of anaerobic voids was the same for all zones. Macroinfaunal samples also indicated that communities were not well developed in the near-field and mid-field zones.

11.4 SUMMARY

The distribution of sediment types within the study zone appeared to be dominated by physical processes with sediment instability and sediment layering controlling sediment surfaces. Biogenic activity of epifauna and infauna was not a predominant factor in structuring surface sediment at 185 of the 186 stations sampled. The only station where there was significant biological control over surface sediments was GC112-NF1 on the Screening Cruise. Zone averaged RPD layer depths were significantly deeper at far-field zones relative to mid-field and near-field zones, and the number of oxic voids (an indicator of subsurface biological activity) also was greater in the far-field zones relative to the mid- and near-field zones.

On average, stations within the near-field zones had lower benthic habitat quality than mid-field and far-field stations, as assessed by depth of the apparent color RPD layer (lower in the near-field zone and higher in mid-field and far-field zones) and amount of biogenic activity (less in the near-field zone and more in mid-field and far-field zones). Bacterial mats were associated primarily with the near-field zones (4 of 18 with bacterial mats). One mid-field zone appeared to have bacterial mats (Table 11-2). There were indications of improved habitat conditions from 2000 to 2002 at the near-field zones in MP 299. Unfortunately, equipment malfunctions precluded collecting enough data at the other sites to make general conclusions about the temporal trends in benthic habitat quality.

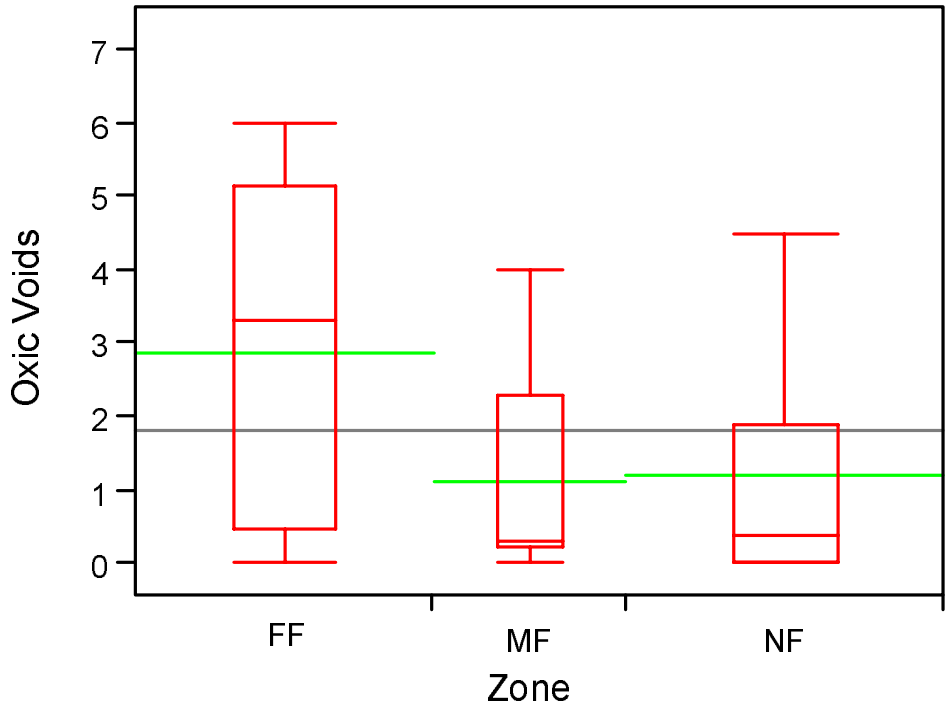

Figure 11-7. Box plots of the number of oxic voids per image by zone. Box is interquartile range (IR), whiskers are 1.5IR, line in box is the median, and line extending from box is the mean. The horizontal line is the overall mean. Width of the box is proportional to sample size.

Chapter 12
MACROINFAUNA

Nancy J. Maciolek and James A. Blake
ENSR Marine and Coastal Center

12.1 INTRODUCTION

The animals that live in the sediments of the seafloor, collectively known as the benthos, are considered to be indicative of ambient environmental conditions because they are relatively immobile and must be able to tolerate local conditions. Undisturbed habitats will support a variety of invertebrate populations reflective of parameters such as sediment grain size and temperature. Disturbed habitats may have increased levels of organic carbon or other changes in sediment parameters that affect the ability of the indigenous populations to maintain themselves; conversely, some changes may favor opportunistic species that will then become established to such a degree that they prohibit additional species from settling and surviving in the same area. The objective of this work element was to investigate the benthos at several sites where SBMs have been used in order to evaluate whether a zone of biological effect has developed related to the discharge of SBM cuttings.

Benthic infaunal samples were collected in August 2000 during the Screening Cruise at six study sites in two zones, a near-field zone (within 100 m of the platform or drillsite) and a far-field zone (3,000 to 6,000 m from the platform or drillsite). In addition to MP 288, MP 299, and EI 346, which were later selected for further study, GB 128 (near-field), VK 780 (near-field and far-field), and VK 783 (near-field and far-field) were sampled. For the Sampling Cruises, three zones were established within each site: the near-field zone was within 100 m of the drillsite, the mid-field zone was between 100 and 250 m from the drillsite, and the far-field zone was 3,000 to 6,000 m from the drillsite. At each of the three final study sites, 18 samples—six nonreplicated cores from each of the three zones—were collected on Sampling Cruise 1 in May 2001. Fifty-four samples—three replicates at each of six stations in each zone—were collected in May 2002 on Sampling Cruise 2. Stations were randomly selected on each cruise and were not resampled.

Samples were sieved through a 0.5-mm-mesh sieve, and each organism was recorded at the lowest practical identification level (LPIL). Identifications and compilation of the basic data were done by Barry A. Vittor & Associates, Inc. (BVA) of Mobile, Alabama. A list of all taxa identified from the samples taken during this study is presented in Appendix H.

The evaluation of the macroinfaunal data was performed by ENSR Marine & Coastal Center, Woods Hole, Massachusetts. Additionally, data on the grain size composition (Appendix C) and TOC content of the sediments (Appendix E) were provided to ENSR in order to facilitate evaluation of the infaunal data. This chapter presents the results of that analysis.

12.2 METHODS FOR DATA ANALYSIS

Each study site was considered separately. Initial inspection of the benthic data included production of summaries of species densities by sample, tables of species dominance, and lists of numbers of species and numbers of individuals per sample. The entire data set as produced by BVA was used for calculation of density and numerically dominant species, and a partially edited database was used for the calculation of diversity indices. Typically, only those organisms identified to the species level, whether named or not, would be used for the diversity

analyses. However, in the current data set, only approximately 60% to 80% of the organisms were identified to species level (MP 288: 59.3%, MP 299: 65.8%, EI 346: 78.6%). If all of the higher-level taxa were excluded, it would not have been possible to prepare community analyses because there would have been so few organisms remaining. Therefore, after judicious review of the data, many higher-level taxa were retained, in particular if there were fewer than two valid lower-level designations for that group. Retention of higher-level taxa has the undesired effect of introducing a bias toward higher diversity and higher similarity among samples than actually exists. The only way to avoid this problem is to increase the level of taxonomic discrimination as the organisms are identified.

A series of community parameters was calculated, along with multivariate statistics, to assess community patterns and structure. With MATLAB as an operating platform, programs written by Dr. Eugene Gallagher, University of Massachusetts, Boston, were used to calculate diversity values for single samples and rarefaction values for single and pooled replicates. Diversity indices incorporate two components of the sampled community: the number of species and the equitability (or evenness) with which individuals are distributed among the species. The Shannon-Wiener (or Shannon's) index H' (base 2), which has its basis in information theory, and its associated evenness value, J', was the primary index used to evaluate diversity. Fisher's logarithmic series model of the distribution of individuals among a number of species is summarized by the index *alpha* (Fisher et al., 1943; May, 1975) and is another measure of diversity. These indices are described and evaluated by Pielou (1975), Magurran (1988), and Hubbell (2001).

Another technique, rarefaction, is useful in comparing samples of different sizes. The rarefaction (ESN) method as modified by Hurlbert (1971) is more sensitive to rare species than is the Shannon-Wiener index. It produces estimates of the number of species that will be found if *n* number of individuals were pulled at random from the sample. Rarefaction curves were generated for each sample, with the number of estimation points set at 25, from 1 to the maximal number of specimens in the sample.

Some multivariate programs are included in COMPAH96, originally written by Dr. Donald Boesch and now available from Dr. Eugene Gallagher (http://www.es.umb.edu/edgwebp.htm). Patterns in benthic communities were analyzed by cluster analysis using CNESS (chord-normalized expected species shared) (Trueblood et al., 1994), which is related to Grassle and Smith's NESS (normalized expected species shared) (Grassle and Smith, 1976). CNESS includes several indices that can be made more or less sensitive to rare species in the community and as such is more versatile than another popular algorithm, Bray-Curtis similarity, which is influenced by dominant species. The rarefaction index and CNESS are both based on the sample-by-species matrix of hypergeometric probabilities, where hypergeometric probability (H) is the probability of sampling species *k* in sample *i* with a random draw of *m* individuals. For the CNESS analyses, the optimal sampling value of *m* was set at 10; at this sampling level, both numerically dominant and rare species influence the resulting clusters. Results of these analyses were inspected for patterns among the different times and sites sampled.

Nonmetric multidimensional scaling (MDS) was conducted using PRIMER (Plymouth Routines in Multivariate Ecological Research) (Clarke and Warwick, 2001). This analysis begins with a similarity or a dissimilarity matrix. For the analyses of the macroinfaunal data for this study, the Bray-Curtis dissimilarity was computed with logarithmic transformed abundances [log(x+1)]. The same data set used in the cluster analysis was used in the MDS analysis. The MDS constructs a "map" or configuration of the samples in a specified number of dimensions (two dimensions for these analyses). The constraint on the "map" (configuration of the samples) is

that all conditions imposed by the rank of dissimilarities in the dissimilarity matrix are satisfied. Because it is not generally possible to configure a realistic number of samples into a space with reduced dimensions in a manner such that the distances in the space and the ranks of the dissimilarities from the underlying dissimilarity matrix agree exactly, there is some distortion or stress between the distances and the corresponding dissimilarities. The objective of the MDS algorithm is to find a configuration of points that minimizes the degree of stress, which is essentially a measure of goodness-of-fit.

Two sediment parameters, mean phi and percent TOC, were plotted and inspected to determine whether differences in community structure could be explained by differences in sediment characteristics.

12.3 MAIN PASS 288

Main Pass 288 is located in 119 m water depth. During the Screening Cruise, three samples were taken in the near-field zone and three in the far-field zone. During Sampling Cruise 1, six benthic samples were taken in each of the three zones. During Sampling Cruise 2, three zones were again randomly sampled. Six stations were sampled in each of the three zones, but this time three replicates were taken at each of the stations. Therefore, six samples were collected at MP 288 during the Screening Cruise, 18 were collected during Sampling Cruise 1, and 54 were collected during Sampling Cruise 2. A total of 340 taxa was reported for the MP 288 samples. Of these, 41 were deleted for diversity calculations. Raw data for these samples are presented in Appendix H.

12.3.1 Dominant Infaunal Species

In the present context, dominant species are those represented by the greatest number of individuals in each sample (numerical dominance). Results from the two Sampling Cruises are tabulated separately below.

12.3.1.1 Screening Cruise. Table 12-1 shows the benthic species that were dominant in the samples in the near-field and far-field zones during the Screening Cruise. The near-field samples were dominated by the opheliid polychaete *Armandia maculata* (23.8%), and the spionid polychaete *Paraprionospio pinnata* was the second-ranked dominant in both the near- and far-field samples.

Table 12-1. Numerically dominant taxa at Main Pass 288 during the Screening Cruise.

Near-field			Far-field		
Rank	Taxon	% Contribution	Rank	Taxon	% Contribution
1	*Armandia maculata*	23.8	1	*Cirrophorus lyra*	18.3
2	*Paraprionospio pinnata*	18.0	2	*Paraprionospio pinnata*	11.7
3	*Scoletoma verrilli*	7.8	3	*Notomastus latericeus*	6.7
4	Aclididae Genus C	7.4	4	Spionidae (LPIL)	5.0
5	*Prionospio* (LPIL)	5.7	5	Bivalvia (LPIL)	4.2
6	*Cirrophorus lyra*	3.3	5	Capitellidae (LPIL)	4.2
6	Rhynchocoela (LPIL)	3.3	5	Maldanidae (LPIL)	4.2
7	*Mediomastus* (LPIL)	2.5	6	Cirratulidae (LPIL)	3.3
7	Semelidae (LPIL)	2.5	6	*Paramphinome* sp. B	3.3
8	*Ninoe* sp. B	2.0	6	Rhynchocoela (LPIL)	3.3
Cumulative Total		76.2	Cumulative Total		64.2
Total Density for 3 Samples		244	Total Density for 3 Samples		120

LPIL= Lowest practical identification level.

12.3.1.2 Sampling Cruise 1. Table 12-2 shows the benthic species that were dominant in the samples in each of the three sampling zones during Sampling Cruise 1. Although the samples are not replicates but are single samples taken at separate stations, each set was summarized for an evaluation of dominant species in each of the three zones.

12.3.1.2.1 Near-field. The spionid polychaete *Paraprionospio pinnata* dominated the six samples taken in the near-field zone. Overall, this species accounted for 16.9% of the fauna in that zone but ranged as high as 25.3% in the samples taken closest to the drillsite. The bivalve *Anodontia alba* and another polychaete, *Paramphinome* sp. B, also were numerous at the near-field stations.

12.3.1.2.2 Mid-field. The numerically dominant taxon in the mid-field samples was an unidentified bivalve that accounted for 13.5% of the organisms collected. It is not clear whether this taxon represents one or many species; this problem is the same for all taxa with designations above the species level. If the taxonomic level of discrimination is very low, as in this case where the record is at the class level, the uncertainty as to whether true dominants (and subsequently true species diversity) are being determined is very high. The mid-field samples shared six dominant taxa with the near-field samples, although the level of dominance as determined by the percent contribution to the community differed between species and zones.

12.3.1.2.3 Far-field. As in the mid-field, the numerically dominant taxon in the far-field samples was recorded as an unidentified bivalve. In this case, this taxon accounted for 7.3% of the organisms collected, but again it is not clear if this is the same organism that occurred in the mid-field samples or whether it represents more than one species. The only species shared as a dominant among the far-field, mid-field, and near-field zones is the polychaete *P. pinnata*. In contrast to the near-field samples, where *P. pinnata* accounted for 16.9% of the collections, this species accounted for only 4.9% in the far-field.

12.3.1.3 Sampling Cruise 2. Table 12-3 shows the benthic species that were dominant in the samples in each of the three sampling zones during Sampling Cruise 2. In this case, three replicates were taken at each station. Replicate counts at each station were summed for this presentation. As for Sampling Cruise 1, the stations in each zone were considered together to determine the dominant taxa. Dominants for each of the six stations within each zone can be found in Appendix H.

12.3.1.3.1 Near-field. When the 18 samples collected in the near-field zone are considered together, only about half of the taxa that were dominant during Sampling Cruise 1 were again dominant during Sampling Cruise 2. The polychaetes *P. pinnata*, *Sigambra tentaculata,* and *Ninoe* sp. B were again among the top numerically dominant species, but the bivalve *A. alba* and the polychaete *Paramphinome* sp. B, mentioned previously, dropped out.

12.3.1.3.2 Mid-field. The top four or five numerically dominant taxa in the mid-field zone were consistent between Sampling Cruise 1 and Sampling Cruise 2 (but note that two or three of these taxa are not species but higher level taxa). Also, the same top five taxa were dominant in both the mid-field and near-field zones.

Table 12-2. Numerically dominant taxa at Main Pass 288 during Sampling Cruise 1.

Near-field			Mid-field			Far-field		
Rank	Taxon	% Contribution	Rank	Taxon	% Contribution	Rank	Taxon	% Contribution
1	*Paraprionospio pinnata*	16.9	1	Bivalvia (LPIL)	13.5	1	Bivalvia (LPIL)	7.3
2	*Anodontia alba*	6.7	2	*Paraprionospio pinnata*	9.6	2	*Phascolion strombi*	6.8
3	*Paramphinome* sp. B	5.0	3	Cirratulidae (LPIL)	7.5	3	*Lucinoma filosum*	6.6
4	*Sigambra tentaculata*	4.8	4	Lineidae (LPIL)	4.0	4	*Paraprionospio pinnata*	4.9
5	*Spiophanes wigleyi*	4.2	5	*Sigambra tentaculata*	3.1	5	*Antalis ceratum*	4.6
6	Lineidae (LPIL)	3.5	6	*Nephtys incisa*	2.9	6	*Nucula proxima*	4.0
7	Rhynchocoela (LPIL)	3.4	7	*Scoletoma verrilli*	2.5	7	Onuphidae (LPIL)	2.3
8	Cirratulidae (LPIL)	3.2	7	Rhynchocoela (LPIL)	2.5	8	Capitellidae (LPIL)	2.2
9	*Cirrophorus lyra*	2.9	8	*Ninoe* sp. B	2.3	9	*Eusarsiella radiicosta*	1.9
10	*Ninoe* sp. B	2.7	8	Goneplacidae (LPIL)	2.3	10	Ophiuroidea (LPIL)	1.8
10	*Mediomastus* (LPIL)	2.7	9	Dentaliidae (LPIL)	2.1	10	*Nuculana acuta*	1.8
Cumulative Total		56.0	Cumulative Total		52.3	Cumulative Total		44.2
Total Density for 6 Samples		623	Total Density for 6 Samples		519	Total Density for 6 Samples		988

LPIL = Lowest practical identification level.

Table 12-3. Numerically dominant taxa at Main Pass 288 during Sampling Cruise 2.

Near-field			Mid-field			Far-field		
Rank	Taxon	% Contribution	Rank	Taxon	% Contribution	Rank	Taxon	% Contribution
1	Cirratulidae (LPIL)	9.6	1	Cirratulidae (LPIL)	9.2	1	Sipuncula (LPIL)	9.6
2	*Paraprionospio pinnata*	9.4	2	*Paraprionospio pinnata*	6.3	2	*Nucula proxima*	9.1
3	Lineidae (LPIL)	4.9	3	Lineidae (LPIL)	5.1	3	*Thyasira trisinuata*	5.3
4	*Sigambra tentaculata*	4.4	4	*Sigambra tentaculata*	5.0	4	*Notomastus daueri*	4.6
5	*Notomastus tenuis*	4.3	5	*Notomastus tenuis*	4.8	5	*Antalis ceratum*	4.5
6	Aclididae (LPIL)	3.5	6	Aclididae Genus C	3.6	6	*Poromya granulata*	3.6
7	Rhynchocoela (LPIL)	3.0	7	*Tubulanus* (LPIL)	2.6	7	*Nuculana acuta*	2.9
7	*Tubulanus* (LPIL)	3.0	8	*Notomastus latericeus*	2.5	7	Ophiuroidea (LPIL)	2.9
8	*Ninoe* sp. B	2.4	9	*Ninoe* sp. B	2.4	8	Cirratulidae (LPIL)	2.2
9	*Levinsenia reducta*	2.2	10	Maldanidae (LPIL)	2.3	9	*Tellina* (LPIL)	2.0
Cumulative Total		46.5	Cumulative Total		45.8	Cumulative Total		46.8
Total Density for 18 Samples		983	Total Density for 18 Samples		883	Total Density for 18 Samples		2,324

LPIL = Lowest practical identification level.

12.3.1.3.3 Far-field. Dominant taxa in the far-field zone differed considerably among the Screening Cruise and two Sampling Cruises. The common polychaete *P. pinnata* was dominant in both the Screening Cruise and Sampling Cruise 1 samples but was not among the dominants in Sampling Cruise 2 samples. When all samples collected in the far-field are considered together, only *Nucula proxima* and *Antalis ceratum* were among the numerical dominants in both Sampling Cruise 1 and Sampling Cruise 2 samples.

12.3.2 Infaunal Density

Density results presented here are based on the entire database submitted by BVA. Other parameters, including all of the diversity measures, are based on an edited database from which some higher-level taxa have been deleted.

12.3.2.1 Sampling Cruise 1. Table 12-4 presents the benthic community parameters for all samples taken at MP 288 during Sampling Cruise 1. The density of individuals per 0.1-m^2 ranged from 70 to 196 in the near-field, 44 to 133 in the mid-field, and 40 to 361 in the far-field. Two of the far-field stations (FF-1 and FF-3) had the highest densities, with 287 and 361 individuals per 0.1-m^2 sample, respectively.

Table 12-4. Benthic community parameters for Main Pass 288 during Sampling Cruise 1. Number of individuals is from the entire database; other parameters are based on the edited database.

Station	No. Indiv.	No. Taxa	H' Base 2	J'	LSA	ESN 2	ESN 8	ESN 50	ESN 100
Near-field									
NF-1	93	30	4.51	0.92	16.87	1.96	8.36	23.42	-
NF-2	112	28	4.25	0.88	11.98	1.94	7.80	20.32	26.96
NF-3	75	31	4.59	0.93	20.65	1.96	8.46	25.92	-
NF-4	77	28	4.36	0.91	16.62	1.95	8.16	22.91	-
NF-5	196	39	3.90	0.74	14.95	1.87	6.63	18.57	27.85
NF-6	70	30	4.46	0.91	20.87	1.95	8.25	25.41	-
Mid-field									
MF-1	101	25	3.85	0.83	11.74	1.90	7.01	19.21	-
MF-2	73	27	4.40	0.92	18.89	1.96	8.32	24.65	-
MF-3	133	39	4.50	0.85	20.35	1.93	7.79	24.64	36.06
MF-4	44	17	3.65	0.89	11.81	1.92	7.33	-	-
MF-5	100	38	4.84	0.92	22.78	1.96	8.60	27.27	-
MF-6	68	33	4.72	0.94	27.38	1.97	8.73	28.38	-
Far-field									
FF-1	287	50	4.67	0.83	18.75	1.94	7.88	23.37	33.58
FF-2	61	27	4.21	0.89	20.98	1.93	7.86	25.50	-
FF-3	361	70	5.23	0.85	26.95	1.96	8.45	27.72	41.31
FF-4	51	20	3.64	0.84	13.47	1.88	7.00	-	-
FF-5	40	13	3.17	0.86	7.13	1.87	6.42	-	-
FF-6	187	49	5.03	0.90	22.78	1.96	8.59	27.12	38.64

No. Indiv. = Number of individuals in three replicates.
No. Taxa = Number of taxa used for diversity analyses.
H' = Shannon diversity index, base 2.
J' = Evenness associated with H'.
LSA = log-series *alpha.*
ESN2-100 = estimated number of species if 2 to 100 individuals are drawn from the sample.

12.3.2.2 Sampling Cruise 2. Tables 12-5 and 12-6 present the benthic community parameters for all samples taken at MP 288 during Sampling Cruise 2, both averaged and for individual replicates. Figure 12-1 compares the mean densities of all samples within a zone for Sampling Cruises 1 and 2 and demonstrates the generally lower densities in the near-field and mid-field during Sampling Cruise 2 compared with Sampling Cruise 1. Densities in the far-field zone were extremely variable on both Sampling Cruises and are not statistically different between sampling times. During Sampling Cruise 2, the mean density of individuals per 0.1-m^2 ranged from 28 to 86 in the near-field, 34 to 61 in the mid-field, and 2 to 312 in the far-field (Figure 12-2). On both Sampling Cruises, far-field samples exhibited high variability among stations, with three stations on each Sampling Cruise having (mean) abundances of fewer than 100 individuals per sample and three stations having (mean) abundances of 150 to 361 individuals per sample. Within-station variability, measured only on Sampling Cruise 2, also was high at the far-field stations, indicating a heterogeneous environment. Within- and among-station variability was not as great at the near- or mid-field stations.

12.3.3 Species Diversity and Evenness

12.3.3.1 Sampling Cruise 1. Inspection of the diversity results (Table 12-4) suggests a very even distribution of species in the samples, with many samples having J' values greater than 0.9 (a value of 1 would represent perfect evenness, with all species having an equal number of individuals). It is not clear whether this high evenness is real or an artifact of the somewhat high proportion of individuals identified only to higher-than-species-level taxa. The lowest evenness value (0.74) was recorded at NF-5, where one species, *Prionospio pinnata*, accounted for 29% of the fauna.

Species richness (absolute number of taxa) was similar in both the near-field and mid-field zones, ranging from 28 to 39 in the near-field and 17 to 39 in the mid-field. Results from the far-field stations were highly variable, with 13 taxa recorded from FF-5 and 70 taxa recorded from FF-3.

H' (base 2) diversities were high in all three sampling zones, ranging from 3.90 to 4.59 in the near-field, 3.65 to 4.84 in the mid-field, and 3.17 to 5.23 in the far-field. As evidenced by the results for the far-field zone, within-zone variability was greater than among-zone variability. Diversity as measured by *alpha* showed similar patterns in terms of whether stations within and among zones were higher or lower in diversity than other stations. By both measures, the lowest diversity was seen at FF-5; however, the highest diversity as measured by H' was FF-3, whereas the highest *alpha* was seen at MF-6.

12.3.3.2 Sampling Cruise 2. Diversity and evenness values for MP 288 samples collected during Sampling Cruise 2 were generally similar to those values from the same zone taken 1 year earlier (Table 12-5; Figure 12-3, A-C). Because additional replicates were collected in each zone on Sampling Cruise 2, species richness (absolute number of taxa) appeared slightly higher in all three zones when samples from each station were pooled. Near-field stations ranged from 32 to 58 taxa, mid-field stations from 36 to 53, and far-field stations, again the most variable, had from 2 to 93 taxa. Mean H' (base 2) diversities ranged from 3.53 to 4.29 in the near-field, 3.79 to 4.45 in the mid-field, and 4.12 to 4.81 in the far-field (there are no results for FF-5 because of the low number of individuals recorded in those samples).

Table 12-5. Benthic community parameters for Main Pass 288 sampled on Sampling Cruise 2. Number of individuals is the average of three replicates (entire database); other parameters are based on replicates either pooled (No. Taxa, ESN) or averaged (No. Individuals, H', J', LSA) at each station (edited database).

Station	Mean No. Indiv.	SD	No. Taxa	Mean H' Base 2	Mean J'	Mean LSA	ESN 2	ESN 8	ESN 50	ESN 100
Near-field										
NF-1	27.7	18.4	32	3.53	0.96	15.18	1.96	8.45	25.63	-
NF-2	50.0	20.1	48	4.18	0.92	20.59	1.97	8.69	28.48	41.12
NF-3	48.7	13.6	44	4.15	0.93	19.20	1.95	8.20	25.92	38.02
NF-4	86.3	24.5	58	4.29	0.88	17.57	1.96	8.59	27.26	39.26
NF-5	55.3	29.9	52	4.23	0.92	20.64	1.96	8.49	27.70	41.77
NF-6	59.7	14.6	49	4.06	0.88	18.13	1.93	7.85	25.50	38.30
Mid-field										
MF-1	58.3	3.2	49	4.18	0.91	18.88	1.95	8.33	26.28	39.13
MF-2	35.7	4.2	39	4.12	0.94	23.19	1.96	8.60	27.04	38.81
MF-3	34.3	2.1	36	4.13	0.96	28.03	1.97	8.83	27.88	-
MF-4	58.0	15.6	53	4.45	0.93	24.89	1.96	8.63	29.35	43.48
MF-5	47.3	28.0	36	3.79	0.90	14.51	1.94	7.96	22.37	31.51
MF-6	60.7	8.1	50	4.34	0.93	18.87	1.97	8.75	28.72	40.95
Far-field										
FF-1	156.3	75.2	77	4.81	0.89	21.99	1.96	8.47	27.18	40.45
FF-2	311.5	212.8	88	4.78	0.85	22.41	1.95	8.10	25.15	37.87
FF-3	278.0	239.5	93	4.35	0.80	17.83	1.93	7.79	22.99	33.52
FF-4	63.7	21.7	59	4.46	0.92	26.23	1.96	8.54	29.84	45.66
FF-5	2.3	1.2	2	-	-	-	-	-	-	-
FF-6	66.7	24.5	50	4.12	0.90	18.54	1.94	8.12	26.78	39.48

Mean No. Indiv. = Mean number of individuals in three replicates.
SD = Standard deviation.
No. Taxa = Number of taxa used for diversity analyses.
H' = Shannon diversity index, base 2.
J' = Evenness associated with H'.
LSA = Log-series *alpha.*
ESN2-100 = estimated number of species if 2 to 100 individuals are drawn from the sample.

Table 12-6. Benthic community parameters for individual samples taken at Main Pass 288 on Sampling Cruise 2. See legend on Table 12-5 for explanation of column headings.

Station-Replicate	No. Indiv.	No. Taxa	H'	J'	LSA	ESN 2	ESN 8	ESN 50	ESN 100
NF1-1	42	23	4.31	0.95	24.67	1.97	8.66	-	-
NF1-2	34	19	4.03	0.95	20.87	1.96	8.39	-	-
NF1-3	6	5	2.25	0.97	-	-	-	-	-
NF2-1	69	30	4.46	0.91	22.01	1.95	8.27	26.01	-
NF2-2	29	16	3.81	0.95	16.51	1.95	8.18	-	-
NF2-3	52	27	4.27	0.90	23.26	1.94	8.04	26.67	-
NF3-1	58	29	4.38	0.90	24.83	1.95	8.17	27.24	-
NF3-2	55	23	4.13	0.91	16.50	1.94	7.98	23.00	-
NF3-3	33	17	3.95	0.97	16.26	1.96	8.38	-	-
NF4-1	62	22	3.56	0.80	12.92	1.85	6.63	20.03	-
NF4-2	86	28	4.30	0.89	15.48	1.94	7.98	22.27	-
NF4-3	111	41	5.01	0.94	24.31	1.97	8.81	28.69	39.97
NF5-1	89	36	4.65	0.90	25.55	1.95	8.33	27.15	-
NF5-2	45	23	4.27	0.94	20.11	1.96	8.45	-	-
NF5-3	32	17	3.79	0.93	16.26	1.94	7.89	-	-
NF6-1	76	32	4.15	0.83	21.42	1.91	7.35	24.66	-
NF6-2	55	21	3.82	0.87	12.85	1.92	7.32	20.31	-
NF6-3	48	23	4.22	0.93	20.11	1.96	8.31	-	-
MF1-1	56	25	4.24	0.91	19.90	1.95	8.12	25.00	-
MF1-2	62	29	4.49	0.92	24.83	1.96	8.48	27.26	-
MF1-3	57	20	3.82	0.88	11.90	1.92	7.39	19.65	-
MF2-1	39	21	4.11	0.94	20.14	1.96	8.29	-	-
MF2-2	37	23	4.26	0.94	29.18	1.96	8.59	-	-
MF2-3	31	18	3.98	0.95	20.26	1.96	8.41	-	-
MF3-1	36	20	4.16	0.96	22.82	1.97	8.65	-	-
MF3-2	35	22	4.35	0.98	41.57	1.98	9.15	-	-
MF3-3	32	17	3.88	0.95	19.69	1.96	8.31	-	-
MF4-1	76	30	4.46	0.91	20.20	1.95	8.22	25.33	-
MF4-2	48	27	4.46	0.94	29.72	1.96	8.63	-	-
MF4-3	50	26	4.42	0.94	24.76	1.96	8.58	-	-
MF5-1	23	15	3.71	0.95	18.71	1.95	8.18	-	-
MF5-2	41	18	3.86	0.93	13.38	1.94	7.82	-	-
MF5-3	78	23	3.79	0.84	11.44	1.90	7.06	18.74	-
MF6-1	56	24	4.20	0.92	16.91	1.95	8.07	23.36	-
MF6-2	70	28	4.44	0.92	18.66	1.96	8.34	24.61	-
MF6-3	56	25	4.36	0.94	21.04	1.96	8.45	-	-
FF1-1	118	39	4.94	0.93	22.47	1.97	8.73	28.07	38.32
FF1-2	243	49	4.62	0.82	19.26	1.94	7.89	22.53	32.86
FF1-3	108	40	4.88	0.92	24.24	1.96	8.61	27.57	39.63
FF2-1	146	49	5.05	0.90	27.13	1.96	8.62	28.23	41.77
FF2-2	218	50	4.66	0.83	21.01	1.94	7.86	23.64	35.15
FF2-3	259	50	4.64	0.82	19.09	1.94	7.86	22.84	33.38
FF3-1	166	43	4.43	0.82	19.62	1.93	7.64	21.97	33.14
FF3-2	553	66	4.43	0.73	19.94	1.90	7.20	21.11	30.83
FF3-3	115	30	4.18	0.85	13.94	1.92	7.55	20.95	29.20
FF4-1	80	36	4.83	0.93	29.76	1.97	8.72	29.98	-
FF4-2	39	23	4.38	0.97	29.18	1.97	8.92	-	-
FF4-3	72	29	4.16	0.86	19.75	1.91	7.58	24.51	-
FF5-1	3	2	-	-	-	-	-	-	-
FF5-2	3	3	-	-	-	-	-	-	-
FF5-3	1	1	-	-	-	-	-	-	-
FF6-1	91	26	4.17	0.89	13.80	1.93	7.76	21.41	-
FF6-2	67	22	3.91	0.88	13.84	1.92	7.47	21.16	-
FF6-3	42	24	4.27	0.93	27.97	1.96	8.45	-	-

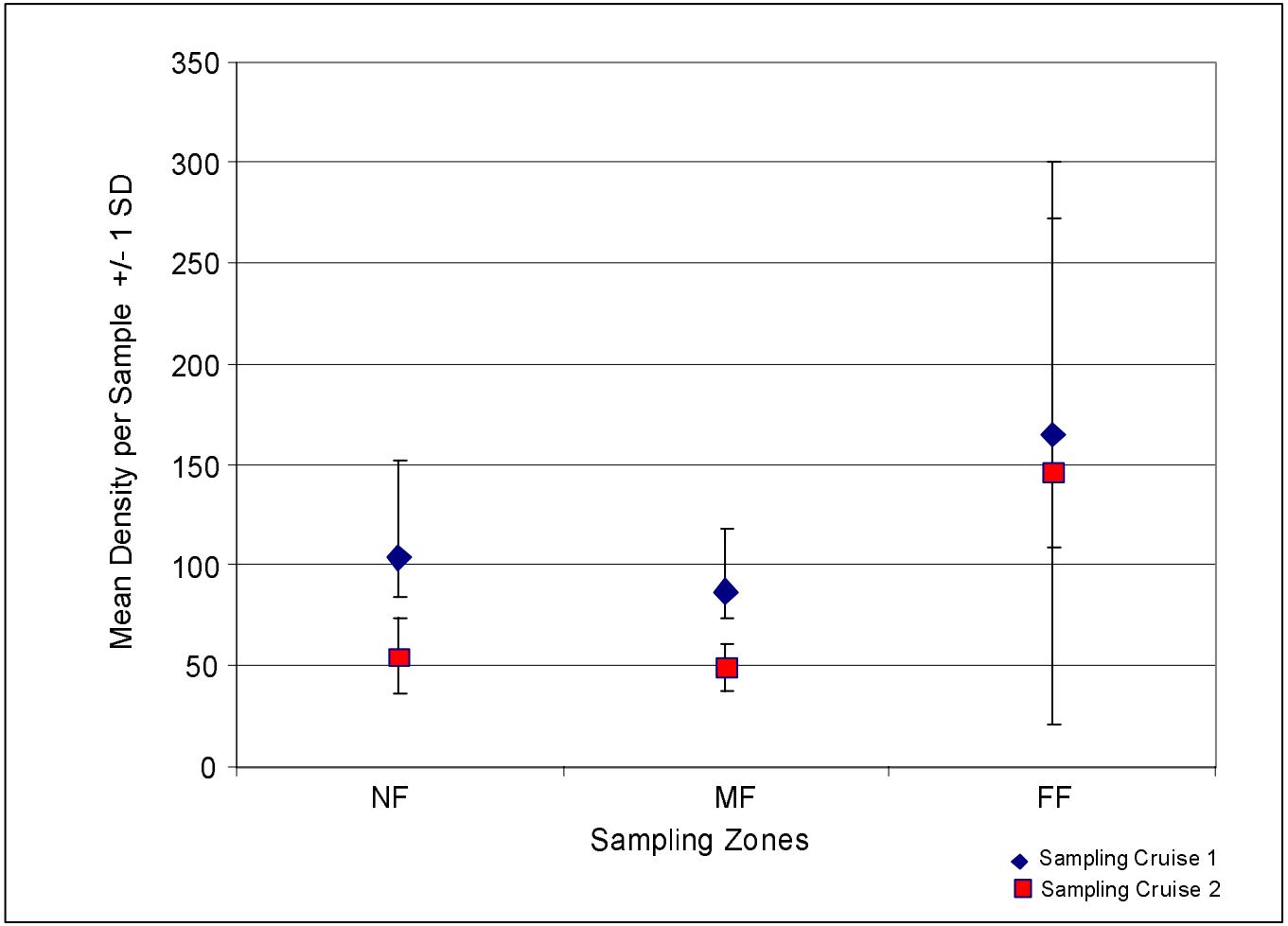

Figure 12-1. Comparison of mean infaunal densities in each of the three sampling zones (near-field [NF], mid-field [MF], and far-field [FF]) at Main Pass 288 during Sampling Cruises 1 and 2. Densities for Sampling Cruise 1 (6 samples) were based on single samples at each station; densities for Sampling Cruise 2 (18 samples) were the mean of three replicates at each station. Database was used without deletions.

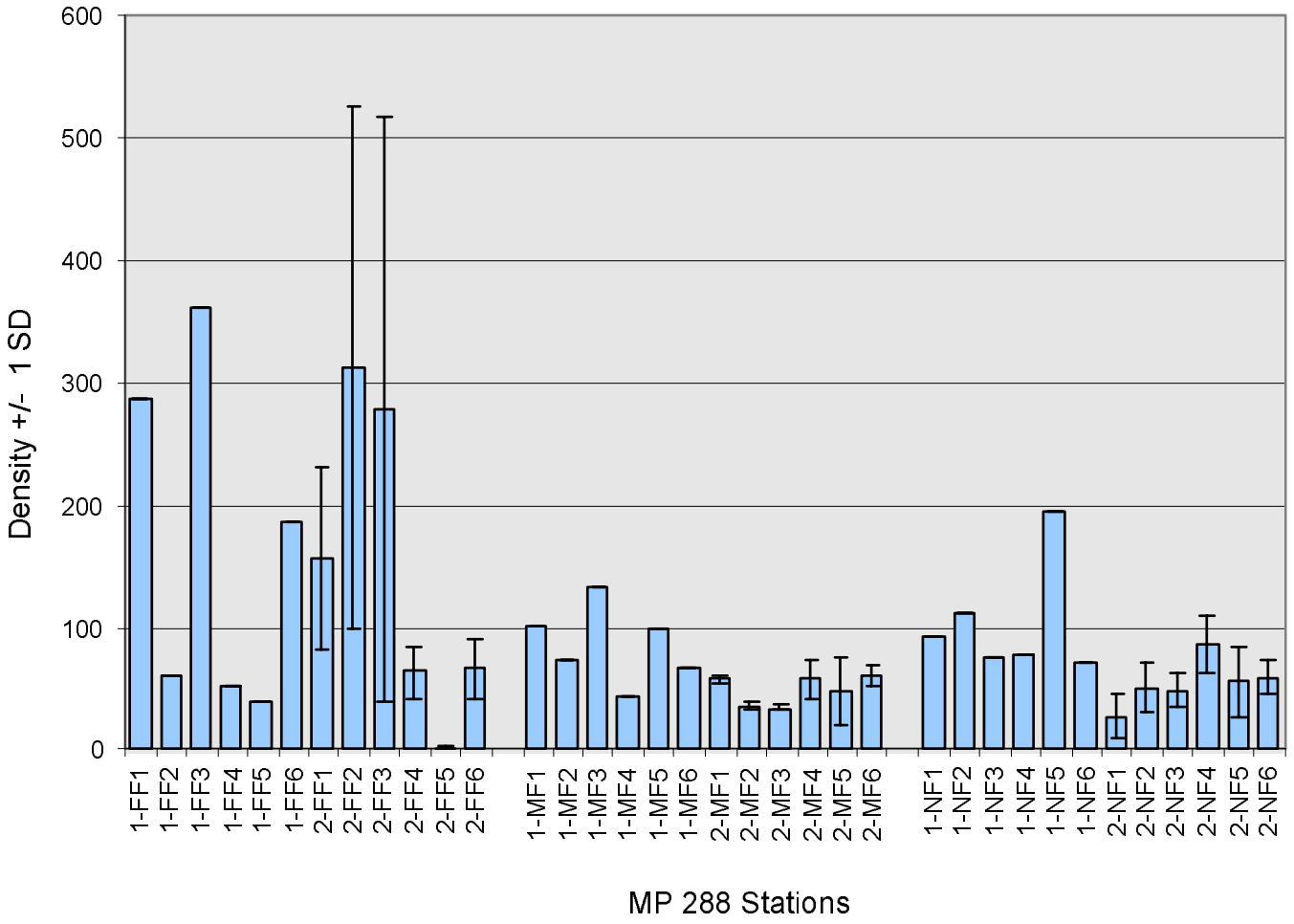

Figure 12-2. Infaunal densities at Main Pass 288 stations. Densities for Sampling Cruise 1 (stations labeled 1-) were based on single samples at each station; densities for Sampling Cruise 2 (labeled 2-) were the mean of three replicates at each station. Database was used without deletions.

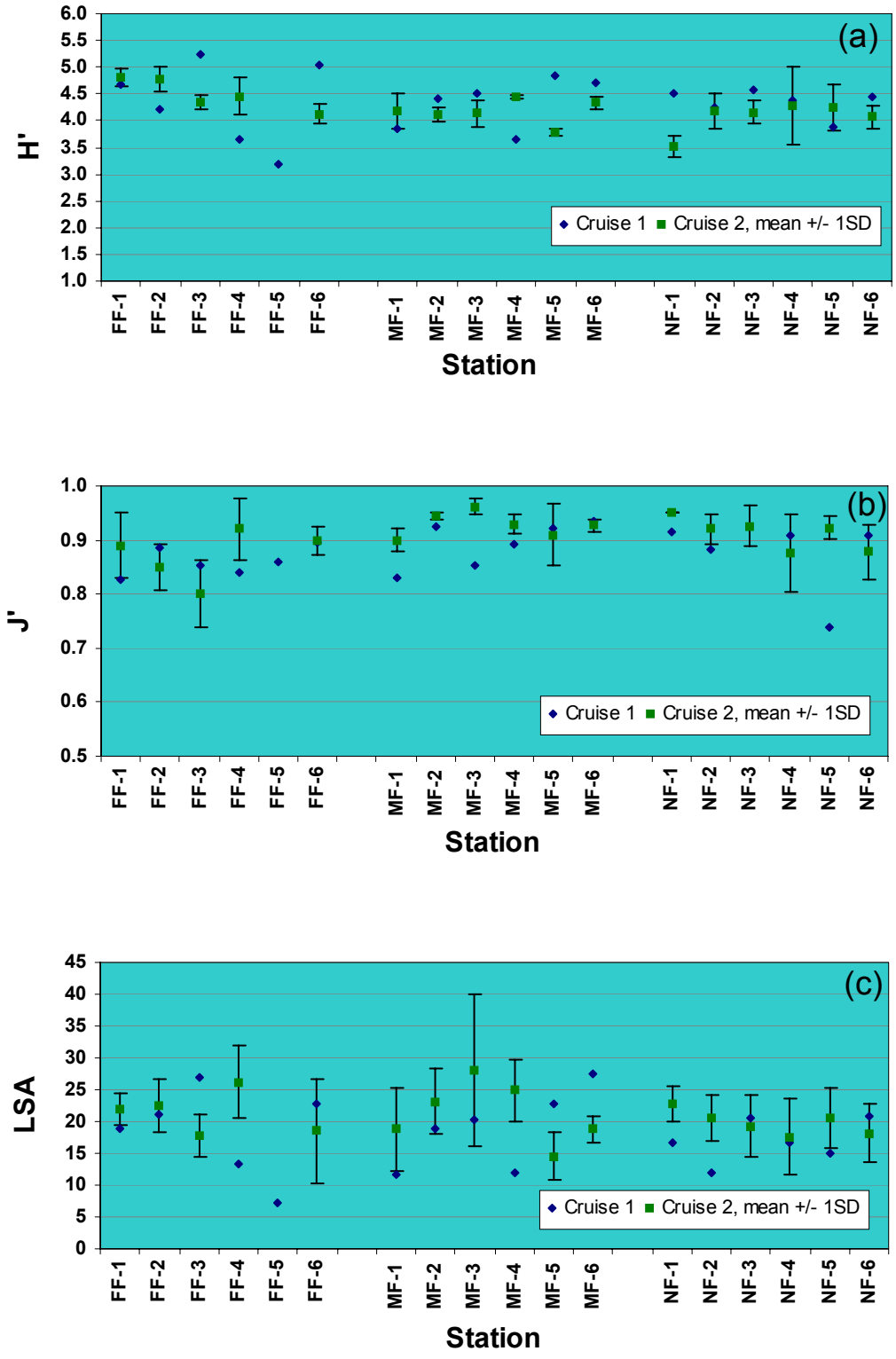

Figure 12-3. Benthic community diversity parameters at Main Pass (MP) 288. a: Shannon diversity; b: Evenness; c: Log-series *alpha* (LSA). Values for Sampling Cruise 1 were for single samples; values for Sampling Cruise 2 were mean of three replicates +/- one standard deviation (SD).

When individual samples are considered (Table 12-6), species richness ranged from 5 to 41 for samples taken in the near-field and 15 to 30 for mid-field samples. Results from the far-field stations were again highly variable, ranging from 1 to 3 taxa in the replicates from FF-5 to 66 taxa in a sample from FF-3. The far-field zone also had both the highest and lowest values recorded in terms of number of individuals in replicate samples, with a range from 1 individual (FF-5, replicate 3) to 553 individuals (FF-3, replicate 2). Species diversity (H') of individual samples ranged from 2.25 to 5.01 in the near-field, from 3.71 to 4.49 in the mid-field, and from 0 to 5.05 in the far-field. With the exception of the samples with the lowest diversities (NF-1, replicate 3 and all three replicates from FF-5), the results for individual replicates are equivalent to those obtained for samples from Sampling Cruise 1 (see Figure 12-3). As seen in results for Sampling Cruise 1, the highest diversity as measured by H' was in the far-field (FF-3), whereas the highest *alpha* was seen at MF-3 (replicate 2).

12.3.4 Rarefaction

The rarefaction technique produces curves that illustrate the diversity of each sample by estimating the number of species that would be found if *n* number of individuals were pulled at random from the sample. The curves produced for both the Sampling Cruise 1 and Sampling Cruise 2 samples are shown in Figures 12-4 through 12-6. Curves labeled 1 to 6 correspond to Stations 1 to 6 sampled during Sampling Cruise 1, and curves labeled 7 to 12 correspond to pooled replicates from Stations 1 to 6 taken during Sampling Cruise 2. Diversities for three pooled samples will appear higher compared with values obtained for single samples, which represent only one-third the sampling area. Values for the estimated number of species at four points (if the number of individuals in the sample allows calculation) are presented in Tables 12-4 through 12-6.

For both Sampling Cruises, the within-zone variability was as great or greater than the among-zone variability, with the result that samples from all three zones are mixed in relative position to each other and exhibit no clear trend of higher or lower diversity. In general, the curves for Sampling Cruise 2 samples indicate a higher diversity than those for Sampling Cruise 1 samples, but this is due to a larger area being sampled by three replicates compared with one replicate. The curves that do not reach an asymptote but continue to climb steeply indicate that the station has not been adequately sampled, and additional species would be added if additional individuals were collected. This circumstance is especially noticeable for the far-field samples, where 6 of the 12 curves are very steep.

12.3.5 Community Assemblage Patterns

Figure 12-7 shows the patterns resulting from multivariate cluster analysis of individual samples using the CNESS dissimilarity analysis. The lower the level at which two samples join, the more similar those two samples are to each other.

Far-field stations, whether sampled during Sampling Cruise 1 or Sampling Cruise 2, tended to differ from the near-field and mid-field stations. The two samples from FF-1 and FF-3 collected during Sampling Cruise 1 plus nine samples from Stations FF-1, FF-2, and FF-3 collected during Sampling Cruise 2 all form a discrete grouping or cluster, with some dissimilarity between the two Sampling Cruises. These samples are all from an area north of the site center, where sediments were much coarser than other sampling stations (see below). The very high level (1.33) at which this group of far-field samples joins the larger cluster of remaining samples suggests that the far-field and near-/mid-field are very different in terms of benthic community structure.

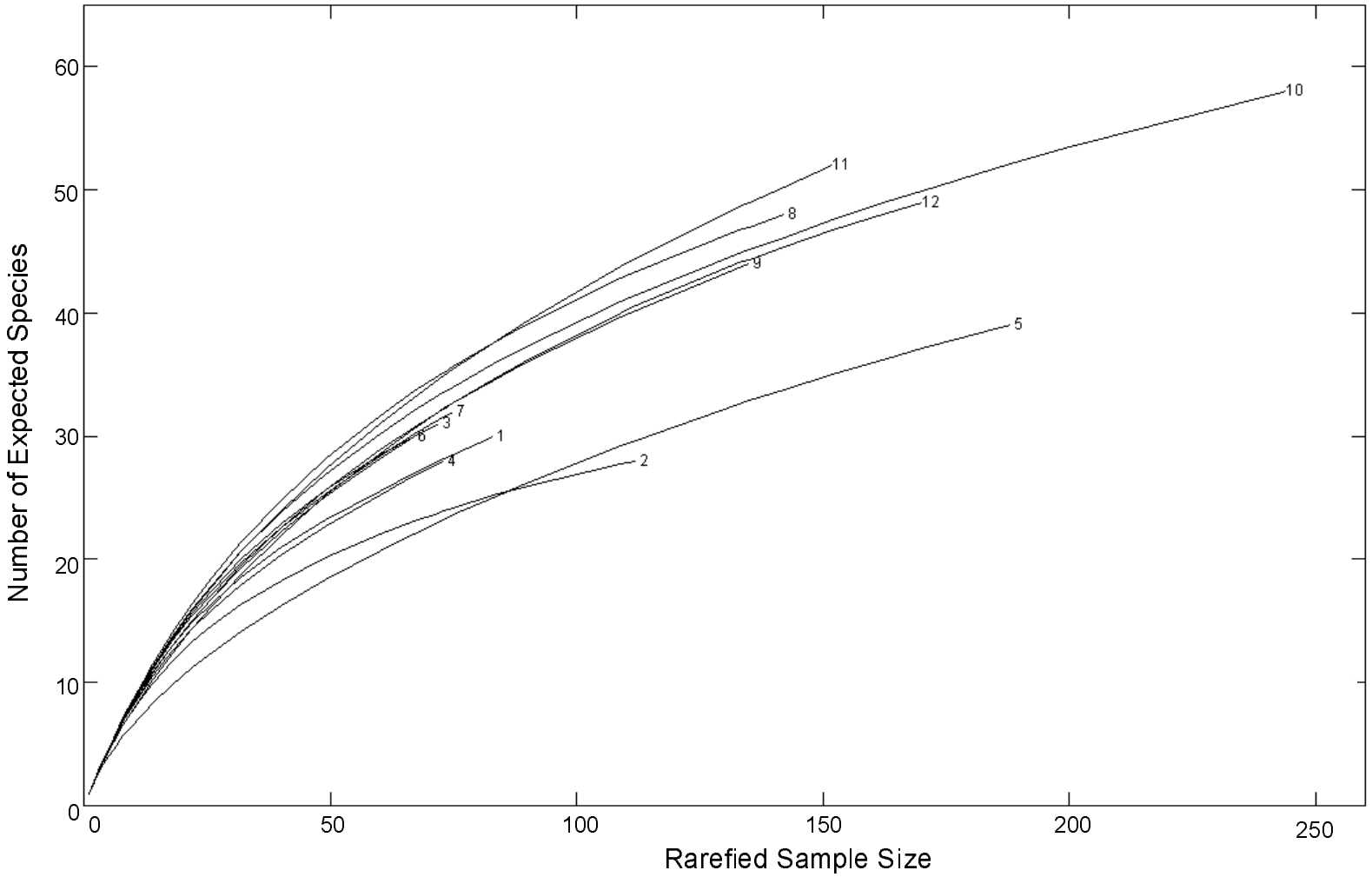

Figure 12-4. Rarefaction curves for Main Pass 288 near-field stations. In each area, curves labeled 1 to 6 correspond to Stations 1 to 6 sampled during Sampling Cruise 1, and curves labeled 7 to 12 correspond to pooled replicates from Stations 1 to 6 sampled during Sampling Cruise 2.

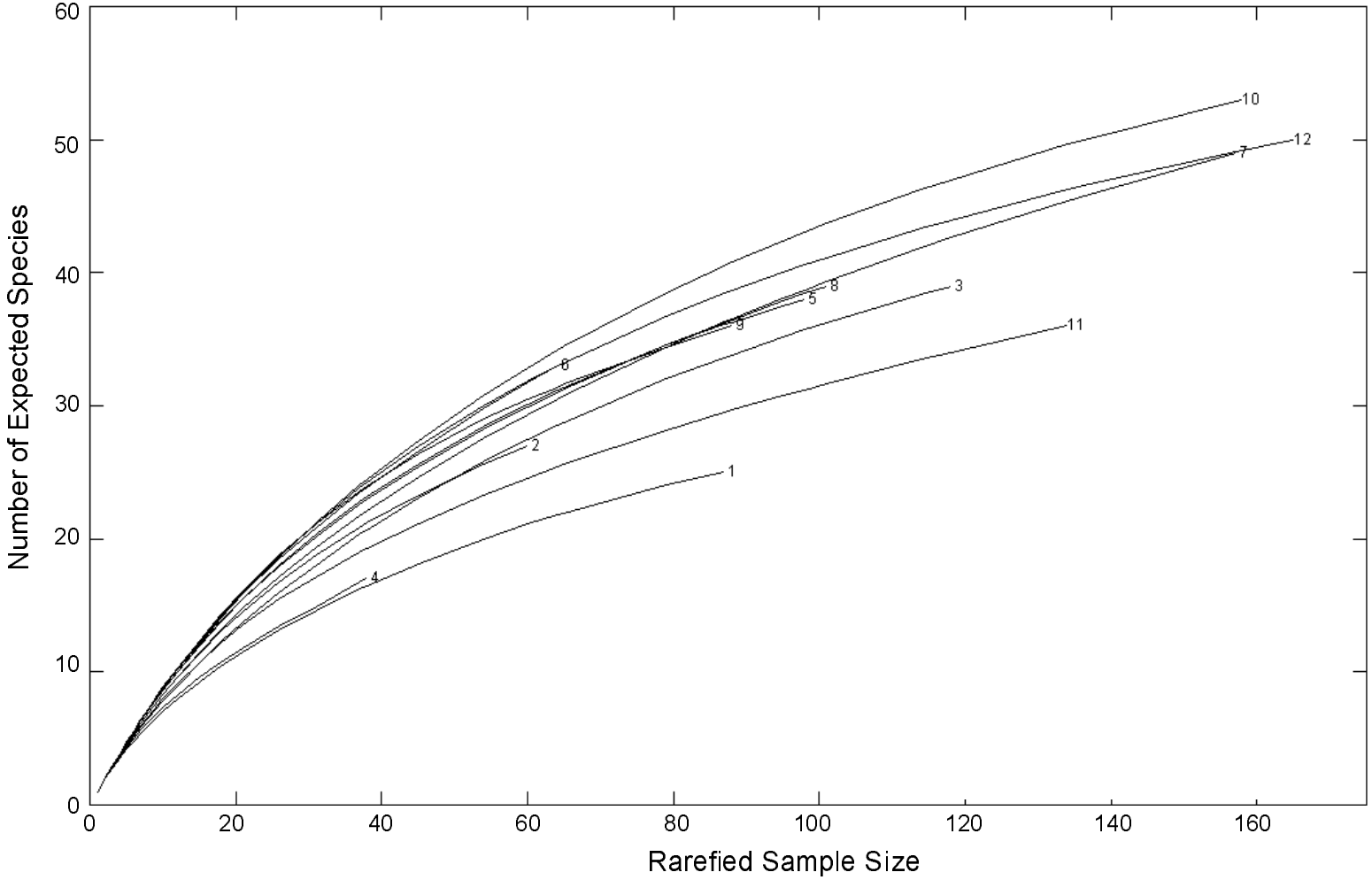

Figure 12-5. Rarefaction curves for Main Pass 288 mid-field stations. In each area, curves labeled 1 to 6 correspond to Stations 1 to 6 sampled during Sampling Cruise 1, and curves labeled 7 to 12 correspond to pooled replicates from Stations 1 to 6 sampled during Sampling Cruise 2.

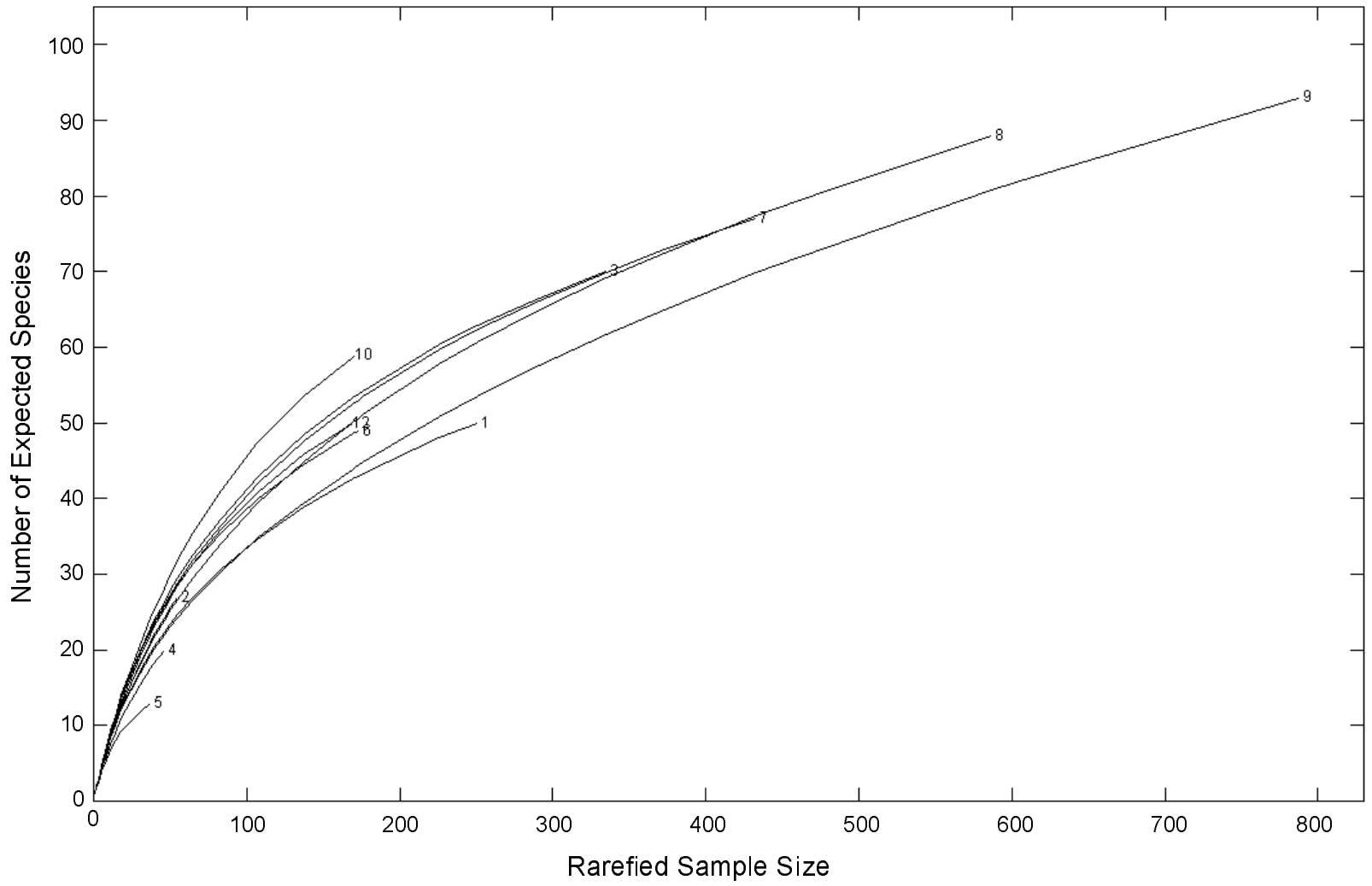

Figure 12-6. Rarefaction curves for Main Pass 288 far-field stations. In each area, curves labeled 1 to 6 correspond to Stations 1 to 6 sampled during Sampling Cruise 1, and curves labeled 7 to 12 correspond to pooled replicates from Stations 1 to 6 sampled during Sampling Cruise 2.

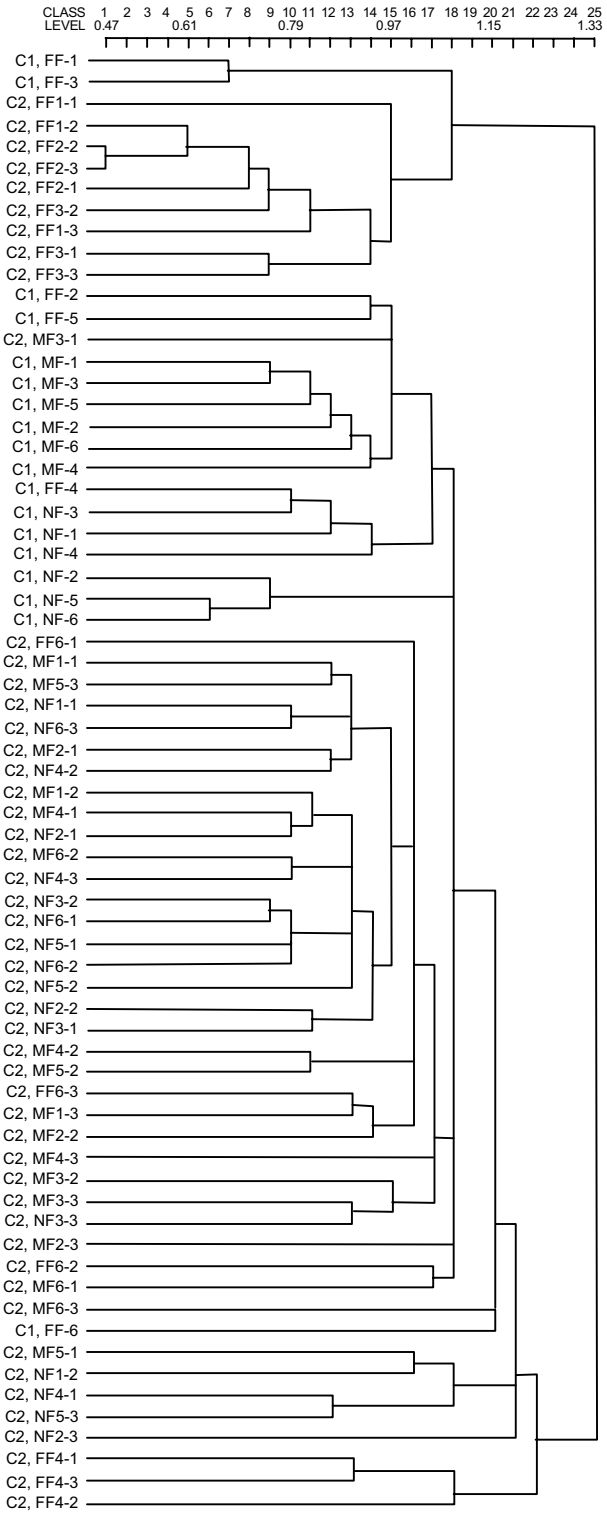

Figure 12-7. Cluster dendrogram for Main Pass 288 samples. Sample label C1 indicates Sampling Cruise 1 and C2 indicates Sampling Cruise 2.

All three Sampling Cruise 2 replicates from FF-4 form a small cluster that is highly dissimilar to any other station. Although this station also is to the north of the site center and closer to FF-3 (Sampling Cruise 2) than to any other station, these two stations were highly dissimilar in terms of sediment and species composition. The remaining far-field samples show some similarities to mid-field and/or near-field samples: FF-2 and FF-5 (Sampling Cruise 1) form a unit of two samples that cluster with mid-field Sampling Cruise 1 samples; similarly, the FF-4 (Sampling Cruise 1) sample joins a cluster of near-field Sampling Cruise 1 samples. Samples collected on Sampling Cruise 2 at FF-5 had too few animals (3, 3, and 1, in replicates 1, 2, and 3, respectively) to be included in this analysis and are not represented in Figure 12-7.

There also were some differences, although less pronounced, between samples from the near-field and mid-field zones. The dichotomy between near-field and mid-field samples was more pronounced during Sampling Cruise 1 than during Sampling Cruise 2, when some of the near-field replicates showed a high similarity to replicates from mid-field stations.

Figure 12-7 also indicates that Sampling Cruise 1 samples from all zones tended to differ from those collected on Sampling Cruise 2. With only a few exceptions, the near-field and mid-field samples tended to be more similar to samples collected on the same Sampling Cruise within the same zone than to samples collected on the alternate Sampling Cruise. The temporal clusters reflect the differences in faunal density between the two Sampling Cruises, as well as the differences in the species composition.

Results of the MDS analysis of the MP 288 samples agreed with those from the cluster analysis. The stress value for this MDS was 0.17, which corresponds to a useful 2-dimensional representation of the relationships among the samples. The samples collected during Sampling Cruise 1 were different from those collected during Sampling Cruise 2 (Figure 12-8). In addition, the near-field and mid-field samples were similar within each cruise but were different between the two cruises. Many of the far-field samples were different from the near-field and mid-field samples collected during the corresponding cruise.

12.3.6 Sediment Characteristics at Main Pass 288

Sediment grain size and TOC data (Appendices C and E, respectively) were plotted in order to examine whether differences in these parameters might explain why the far-field samples differed so much from the near-field and mid-field samples (Figure 12-9). Inspection of the plot of mean phi shows that the samples that clustered separately—FF-1 and FF-3 sampled during Sampling Cruise 1 and FF-1, FF-2, and FF-3 sampled during Sampling Cruise 2—all had much coarser sediments (lower mean phi value) and lower TOC than the remaining stations.

12.3.7 Main Pass 288 Summary

1. On both Sampling Cruises, infaunal abundance was highly variable among far-field stations, which exhibited both the highest and lowest abundances recorded at this site. Within-station variability, measured on Sampling Cruise 2, also was high at the far-field stations, indicating a heterogeneous environment. Within- and among-station variability was not as great at the near- or mid-field stations.

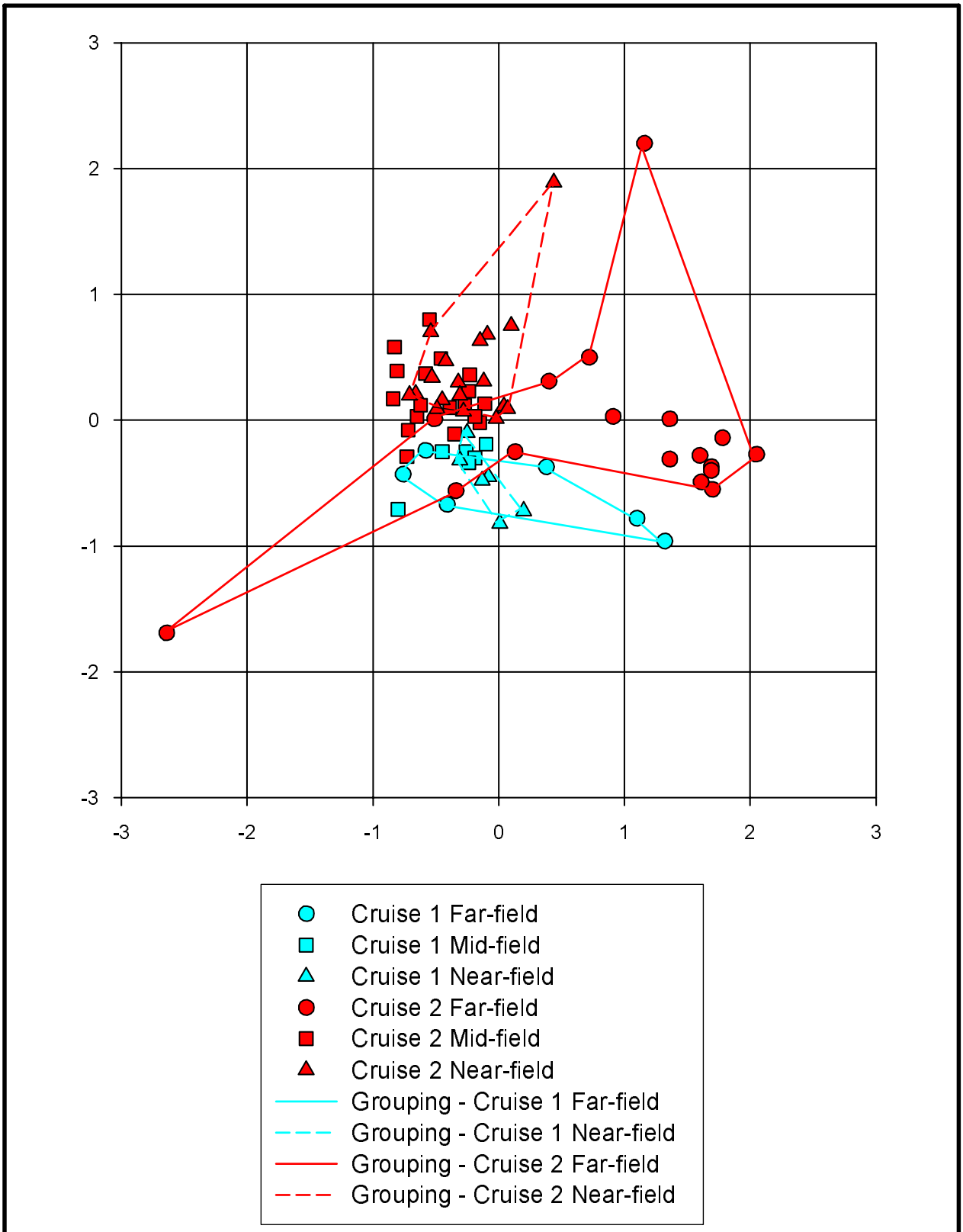

Figure 12-8. Results of nonmetric multidimensional scaling analysis for Main Pass 288.

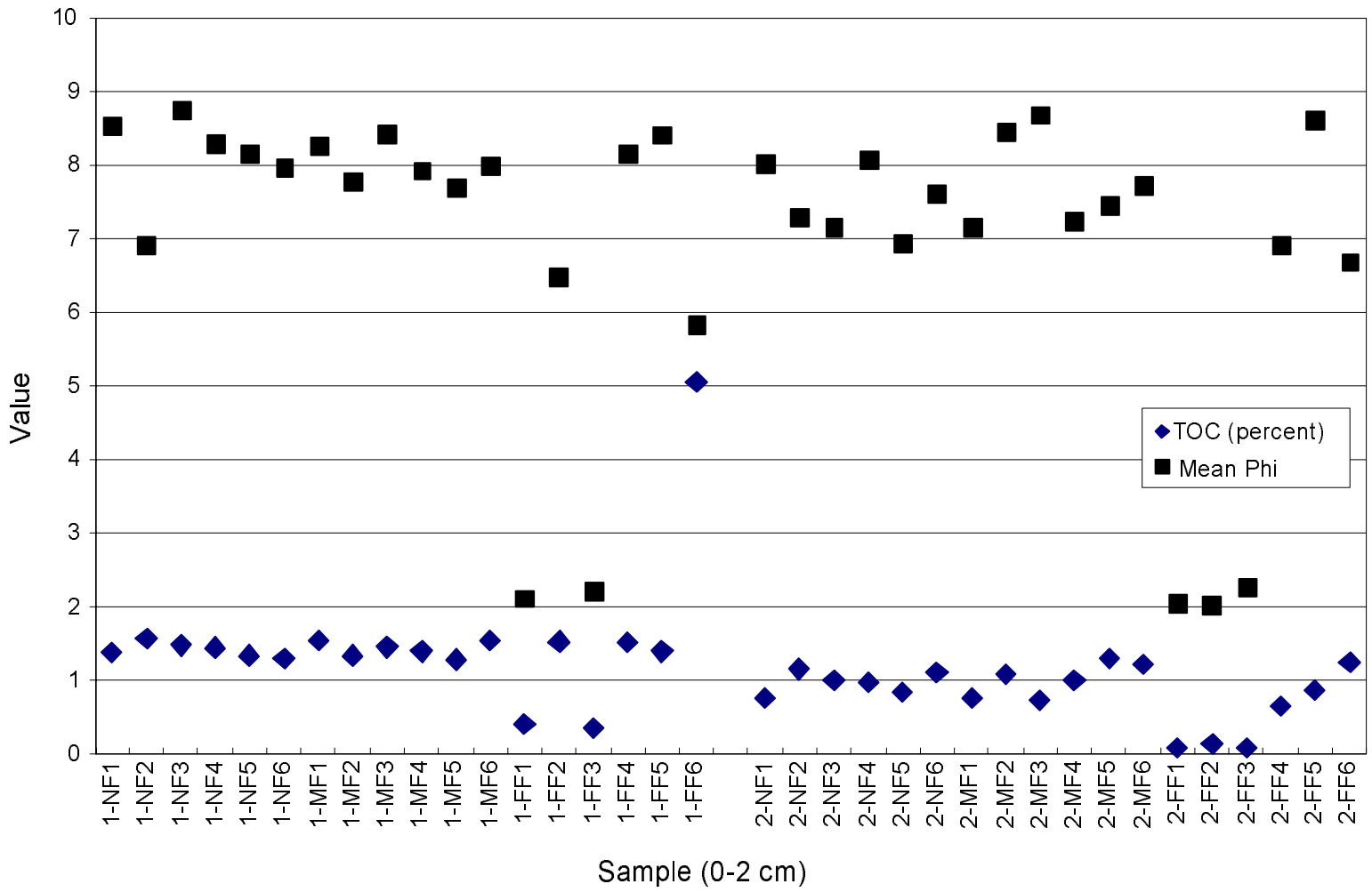

Figure 12-9. Percent total organic carbon (TOC) and mean phi of sediments at Main Pass 288. Values represent the top 2 cm of sediment taken from single samples. Sampling Cruise 1 stations are labeled 1- and Sampling Cruise 2 stations are labeled 2-.

2. Mean densities in the near-field and mid-field zones were significantly lower during Sampling Cruise 2 compared with Sampling Cruise 1.

3. The dominant organism at the near-field stations changed between the time of the Screening Cruise and the time of Sampling Cruise 1. During the Screening Cruise, the opheliid polychaete *Armandia maculata* accounted for nearly 24% of the infauna, whereas in later collections the spionid *Paraprionospio pinnata* generally dominated both the near-field and mid-field communities. Opheliid polychaetes are burrowing, deposit-feeding worms that are common in near-coastal marine habitats. Field studies of the recruitment and population ecology of opheliids are few (Blake, 2000), although Hermans (1978) suggested that *Armandia brevis* could produce as many as six generations during a single reproductive season, and Tamaki (1985) found that populations of other polychaetes tended to inhibit the settlement of *Armandia* sp. on a Japanese tidal flat. *Prionospio pinnata* is a common and widespread species in many Gulf of Mexico habitats. Neither *Armandia* nor *Paraprionospio* are considered to be indicative of disturbed or organically enriched environments.

4. The difference in species composition among the far-field stations is probably related to differences in sediment grain size composition. Several of the far-field stations had extremely coarse sediments, whereas the remaining stations had fine sediments with a high percentage of silt-plus-clay. Far-field stations with fine-grained sediments were more similar to near- and mid-field stations. The low level of taxonomic discrimination in the dataset (60% to 78% of organisms identified to species level) has assuredly resulted in higher levels of similarity among stations than would be the case if a higher percentage of organisms had been identified to species level.

5. Diversity and evenness values for MP 288 samples collected during Sampling Cruise 2 were generally similar to those values from the same sampling zone taken 1 year earlier.

6. Rarefaction diversity indicated that some stations remain undersampled, that is, additional species would be found if additional samples are taken.

7. Multivariate cluster analysis of individual samples indicated that some near-field replicates showed a high similarity to replicates from some of the mid-field stations. Also, with only a few exceptions, the near-field and mid-field samples tended to be more similar to samples collected on the same Sampling Cruise than to samples collected on the alternate Sampling Cruise. The majority of far-field stations, whether sampled during Sampling Cruise 1 or Sampling Cruise 2, differed considerably from the near-field and mid-field stations. The results of the MDS analysis generally agreed with those from the cluster analysis.

Conclusion: Infaunal community structure appears to be related primarily to grain size composition of sediments.

12.4 MAIN PASS 299

Main Pass 299 is located in 60 m water depth. During the Screening Cruise in August 2000, three samples were taken in the near-field zone and three in the far-field zone. During Sampling Cruise 1 in May 2001, six benthic samples were taken in each of the three sampling zones. During Sampling Cruise 2 in May 2002, three zones were again sampled randomly. Six stations were sampled in each of the three zones, but this time three replicates were taken at each of the stations. Therefore, six samples were collected at MP 299 during the Screening Cruise, 18 were collected during Sampling Cruise 1, and 54 were collected during Sampling

Cruise 2. A total of 281 taxa was reported for the MP 299 samples. Of these, 53 were deleted for diversity calculations. Raw data for these samples are presented in Appendix H.

12.4.1 Dominant Infaunal Species

In the present context, dominant species are those represented by the greatest number of individuals in each sample (numerical dominance). The results from the Sampling Cruises are tabulated separately below.

12.4.1.1 Screening Cruise. Table 12-7 shows the benthic species that were dominant in the samples in the near-field and mid-field during the Screening Cruise. The near-field samples were dominated by the polychaete *Capitella capitata*, which represented over half of the organisms (54.6%). Especially when dominating the benthic community to such an extent, this opportunistic species is considered to be indicative of environments stressed by either organic input or physical disturbances (e.g., Eagle and Rees, 1973). The opheliid polychaete *Armandia maculata*, which also was numerous at MP 288 near-field during the Screening Cruise, also was important at both near-field and far-field stations at MP 299, as was the common spionid *Paraprionospio pinnata*.

Table 12-7. Dominant taxa at Main Pass 299 during the Screening Cruise.

Near-field			Far-field		
Rank	Taxon	% Contribution	Rank	Taxon	% Contribution
1	*Capitella capitata*	54.6	1	*Paraprionospio pinnata*	10.3
2	*Armandia maculata*	17.2	2	*Armandia maculata*	9.3
3	Capitellidae (LPIL)	9.8	3	*Levinsenia gracilis*	7.3
4	*Capitella jonesi*	4.0	4	*Scoletoma verrilli*	7.0
4	*Nassarius vibex*	4.0	5	*Prionospio* (LPIL)	5.6
5	*Paraprionospio pinnata*	1.7	6	*Aricidea taylori*	5.3
6	Cirratulidae (LPIL)	1.1	6	*Cirrophorus* (LPIL)	5.3
7	*Apoprionospio dayi*	0.6	7	Cirratulidae (LPIL)	5.0
7	Bivalvia (LPIL)	0.6	8	Ampharetidae (LPIL)	3.6
7	*Cirrophorus* (LPIL)	0.6	9	*Amphicteis* (LPIL)	2.6
Cumulative Total		94.3	Cumulative Total		61.3
Total Density for 3 Samples		174	Total Density for 3 Samples		302

LPIL = Lowest practical identification level.

12.4.1.2 Sampling Cruise 1. Table 12-8 shows the benthic species that were dominant in the samples in each of the three zones during Sampling Cruise 1. Although the samples are not replicates but are single samples taken at each station, each set was summarized for an evaluation of dominant species in the three sampling zones. Inspection of the data shows that several species were dominant in all three sampling zones, implying a wide distribution of the fauna at this site.

Table 12-8. Numerically dominant species in Main Pass 299 sampling zones during Sampling Cruise 1.

Near-field			Mid-field			Far-field		
Rank	Taxon	% Contribution	Rank	Taxon	% Contribution	Rank	Taxon	% Contribution
1	Nuculanidae (LPIL)	10.6	1	*Antalis ceratum*	10.2	1	*Nephtys incisa*	13.5
2	*Capitella capitata*	9.6	2	*Diopatra cuprea*	8.4	2	Bivalvia (LPIL)	6.1
3	Bivalvia (LPIL)	6.7	3	*Nuculana acuta*	8.2	3	*Ampelisca* (LPIL)	5.5
4	*Paraprionospio pinnata*	6.0	4	*Nephtys incisa*	6.3	4	*Paraprionospio pinnata*	4.9
5	*Ampelisca* (LPIL)	3.9	5	Bivalvia (LPIL)	5.1	5	*Diopatra cuprea*	4.6
6	Lineidae (LPIL)	3.4	6	*Scoletoma verrilli*	4.9	6	*Volvulella texasiana*	4.6
7	*Nassarius* (LPIL)	2.6	7	*Paraprionospio pinnata*	4.7	7	*Armandia maculata*	4.0
7	*Scoletoma verrilli*	2.6	8	*Mediomastus* (LPIL)	2.5	8	Lineidae (LPIL)	3.5
7	*Nuculana acuta*	2.6	9	*Lumbrineris latreilli*	2.2	9	*Eudorella monodon*	3.2
8	*Diopatra cuprea*	2.3	10	*Pyrunculus caelatus*	2.2	10	*Apseudes* sp. A	2.9
8	*Armandia maculata*	2.3	10	*Volvulella texasiana*	2.2	10	*Paramphinome* sp. B	2.9
						10	Siphonodentaliidae (LPIL)	2.9
Cumulative Total		52.6	Cumulative Total		56.9	Cumulative Total		58.5
Total Density for 6 Samples		386	Total Density for 6 Samples		510	Total Density for 6 Samples		347

LPIL = Lowest practical identification level.

12.4.1.2.1 Near-field. The numerically dominant species at the near-field stations was a bivalve identified only at the family level (Nuculanidae). Another dominant in the MP 299 near-field zone was identified as *Nuculana acuta*, which belongs to the same family. Similarly, another dominant was identified at the class level (Bivalvia). It is not clear whether the family level or class level taxa represent one or many species, or whether the organisms identified as Bivalvia from the MP 299 samples are the same as those given the same designation in samples from the MP 288 stations. Dominants identified to the species level include the spionid polychaete *Paraprionospio pinnata* and the onuphid polychaete *Diopatra cuprea*, both of which also were dominant at the mid-field and far-field stations. The opportunistic species *Capitella capitata*, which accounted for more than half the individuals during the Screening Cruise, now ranked second with a much lower 9.6% contribution to the community, suggesting a possible improvement in benthic conditions. Similarly, *Armandia maculata* fell from comprising 17.2% to 2.3% of the fauna, and from second to eighth place in the numerical dominants.

12.4.1.2.2 Mid-field. The dominant species at the mid-field stations during Sampling Cruise 1 was a scaphopod mollusk, *Antalis ceratum*, which accounted for 10.2% of the infauna. Three taxa, *D. cuprea*, *P. pinnata*, and Bivalvia, were dominant in both the near-field and far-field samples.

12.4.1.2.3 Far-field. The numerical dominant at the far-field stations was the polychaete *Nephtys incisa*, which accounted for 13.5% of the recorded fauna. Several of the other dominants also were common at the near-field and mid-field stations.

12.4.1.3 Sampling Cruise 2. Table 12-9 shows the benthic species that were dominant in the samples in each of the three sampling zones during Sampling Cruise 2. In this case, three replicates were taken at each station.

12.4.1.3.1 Near-field. The dominant species in the near-field were very different from those that were recorded during Sampling Cruise 1. Several species, including *Capitella capitata*, *Paraprionospio pinnata*, *Diopatra cuprea*, and *Armandia maculata*, which were dominant during Sampling Cruise 1, did not appear among the top ten numerical dominants during Sampling Cruise 2. The near-field samples were dominated by a scaphopod, *Cadulus arctus*, which also was dominant at the mid-field and near-field stations. The third most common species was the polychaete *Nephtys incisa*, which had been important in the far-field during the previous Sampling Cruise.

12.4.1.3.2 Mid-field. The scaphopod that dominated the near-field samples also was dominant in the mid-field. This species, *C. arctus*, apparently replaced the scaphopod species *Antalis ceratum* that had been dominant during Sampling Cruise 1. As in the near-field, the other mid-field dominants were very different compared with Sampling Cruise 1, with an alpheid shrimp ranking first and the previously common polychaete and bivalve species (i.e., *P. pinnata*, *D. cuprea*, *Nephtys incisa*, *Scoletoma verrilli*, and *Nuculana acuta*) being replaced by turrid gastropods (*Compsodrilla eucosmia*) and other polychaetes (e.g., *Ampharete parvidentata*, *Owenia fusiformis*).

Table 12-9. Numerically dominant species in Main Pass 299 sampling zones during Sampling Cruise 2.

Near-field			Mid-field			Far-field		
Rank	Taxon	% Contribution	Rank	Taxon	% Contribution	Rank	Taxon	% Contribution
1	*Cadulus arctus*	8.4	1	*Alpheus* (LPIL)	12.1	1	*Cadulus arctus*	16.6
2	*Nuculana acuta*	5.6	2	*Cadulus arctus*	7.6	2	*Nephtys incisa*	6.1
3	*Nephtys incisa*	4.0	3	*Compsodrillia eucosmia*	5.6	3	*Paramphinome* sp. B	4.2
4	*Notomastus daueri*	3.7	4	Maldanidae (LPIL)	5.0	4	Lineidae (LPIL)	3.9
5	Lineidae (LPIL)	3.6	5	*Ampharete parvidentata*	4.4	5	*Nuculana acuta*	3.6
6	*Cirrophorus* (LPIL)	3.5	6	Cirratulidae (LPIL)	3.1	6	*Volvulella texasiana*	2.5
7	*Scoletoma verrilli*	3.3	6	*Owenia fusiformis*	3.1	7	*Scoletoma verrilli*	2.3
8	*Ampelisca agassizi*	3.1	7	*Magelona* sp. L	3.0	8	Aclididae Genus C	2.2
8	*Ninoe* sp. B	3.1	8	*Cosmioconcha calliglypta*	2.4	9	*Macoma pulleyi*	2.2
8	*Semele* (LPIL)	3.1	9	Turridae (LPIL)	2.3	9	*Cosmioconcha calliglypta*	2.1
8	*Cosmioconcha calliglypta*	3.1	10	*Ampelisca* (LPIL)	2.2			
			10	Vitrinellidae (LPIL)	2.2			
Cumulative Total		44.5	Cumulative Total		53.2	Cumulative Total		45.9
Total Density for 18 Samples		5,191	Total Density for 18 Samples		1,277	Total Density for 18 Samples		937

LPIL = Lowest practical identification level.

12.4.1.3.3 Far-field. The scaphopod *Cadulus arctus* dominated the far-field stations as well as the near- and mid-field stations, although in the far-field it accounted for an even greater percentage of the fauna. *Nephtys incisa* continued to be important at far-field stations, as did *Paramphinome* sp. B, Lineidae, and *Volvulella texasiana*. The remaining dominants differed from those recorded during Sampling Cruise 1.

12.4.2 Infaunal Density

Density results presented here are based on the entire database of 281 taxa as submitted by BVA. Other parameters, including all of the diversity measures, are based on an edited database from which 53 higher-level taxa were deleted.

12.4.2.1 Sampling Cruise 1. Table 12-10 presents the benthic community parameters for all samples taken at MP 299 during Sampling Cruise 1. Overall, densities were low at all MP 299 stations, especially in the far-field. Variability among stations was high in all three zones (Figures 12-10 and 12-11), with the greatest extreme seen in the mid-field between MF-4 and MF-5. The density of individuals per 0.1-m^2 sample ranged from 34 to 126 in the near-field, 17 to 172 in the mid-field, and 23 to 77 in the far-field.

12.4.2.2 Sampling Cruise 2. Tables 12-11 and 12-12 present the benthic community parameters for all samples taken at MP 299 during Sampling Cruise 2. Figure 12-10 compares the mean densities of all samples within a zone for both Sampling Cruises and demonstrates that, compared with Sampling Cruise 1, Sampling Cruise 2 mean densities were higher in the near-field zone but lower in both the mid-field and far-field zones. However, the standard deviation around the mean is so large that there is no significant difference between densities recorded in the three sampling zones, nor are the densities during Sampling Cruise 2 different from those recorded during Sampling Cruise 1. During Sampling Cruise 2, the mean density of individuals per 0.1-m^2 ranged from 49 to 107 in the near-field, 57 to 92 in the mid-field, and 18 to 119 in the far-field (Figure 12-11). Within-station variability, measured only on Sampling Cruise 2, was high at the majority of the stations in all three sampling zones, although some of the stations (FF-2, MF-1) had low variability as measured by the standard deviation around the mean.

12.4.3 Species Diversity and Evenness

12.4.3.1 Sampling Cruise 1. Inspection of the diversity results (Table 12-10, Figure 12-12) suggests that, with only one or two exceptions, there was a very even distribution of species in the samples. Many samples had J' values greater than 0.9 (a value of 1 would represent perfect evenness, with each individual representing a different species). The lowest value, 0.59, was found at NF-6, which also had the lowest diversity of all stations (see below). Species richness (absolute number of taxa) was highly variable in all three sampling zones, ranging from 10 to 40 in the near-field zone, 8 to 37 in the mid-field zone, and 11 to 31 in the far-field zone (Figure 12-12, A-C).

Each of the three zones had one station with low abundance and low diversity. NF-6 had a significantly lower H' (1.95) compared with other stations in that zone and with MP 299 as a whole. This station, with only 53 individuals distributed among 10 taxa, also had the lowest evenness (0.59) and the lowest *alpha* (3.72). Mid-field station MF-5 and far-field station FF-4 also had significantly lower H’ diversity values compared to other stations sampled either on Sampling Cruise 1 or Sampling Cruise 2. However, evenness and log-series alpha did not follow the same pattern, with values for those parameters at MF-5 and FF-4 falling within the range seen at other stations.

Table 12-10. Benthic community parameters for Main Pass 299 sampled on Sampling Cruise 1. Number of individuals was from the entire database; other parameters were calculated based on the edited database.

Station	No. Indiv.	No. Taxa	H' Base 2	J'	LSA	ESN 2	ESN 8	ESN 50	ESN 100
Near-field									
NF-1	39	14	3.57	0.94	9.18	1.93	7.47	-	-
NF-2	74	25	4.31	0.93	16.37	1.95	8.23	23.22	-
NF-3	60	14	3.59	0.94	11.71	1.94	7.69	-	-
NF-4	126	40	4.91	0.92	26.32	1.97	8.67	28.54	-
NF-5	34	14	3.58	0.94	14.06	1.94	7.83	-	-
NF-6	53	10	1.95	0.59	3.72	1.57	3.97	9.90	-
Mid-field									
MF-1	89	25	4.28	0.92	12.25	1.95	8.07	20.97	-
MF-2	56	17	3.82	0.93	9.07	1.94	7.64	17.00	-
MF-3	80	23	4.01	0.89	12.08	1.94	7.62	19.51	-
MF-4	172	37	4.22	0.81	15.51	1.92	7.35	20.66	29.98
MF-5	17	8	2.91	0.97	13.19	1.95	7.55	-	-
MF-6	96	34	4.58	0.90	19.69	1.95	8.26	24.87	-
Far-field									
FF-1	77	22	3.78	0.85	11.56	1.90	7.09	19.13	-
FF-2	56	20	3.91	0.91	13.16	1.93	7.68	-	-
FF-3	49	26	4.57	0.97	32.20	1.98	9.06	-	-
FF-4	23	11	3.18	0.92	10.90	1.91	7.17	-	-
FF-5	70	31	4.65	0.94	29.39	1.97	8.73	29.23	-
FF-6	72	23	3.90	0.86	12.70	1.92	7.35	19.70	-

No. Indiv. = Number of individuals in three replicates.
No. Taxa = Number of taxa used for diversity analyses.
H' = Shannon diversity index, base 2.
J' = Evenness associated with H'.
LSA = log-series *alpha.*
ESN2-100 = estimated number of species if 2 to 100 individuals are drawn from the sample.

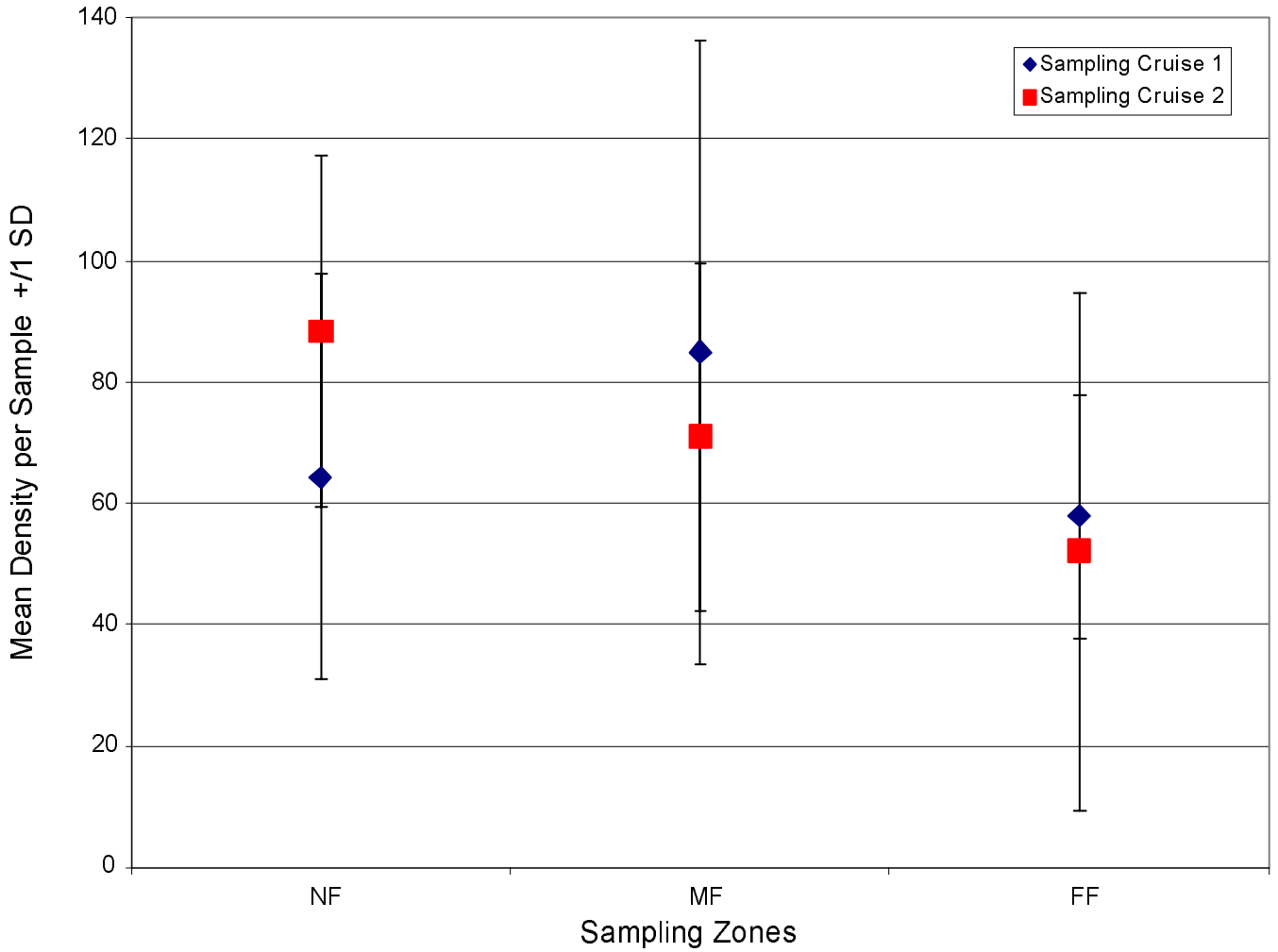

Figure 12-10. Comparison of mean infaunal densities in each of the three sampling zones (near-field [NF], mid-field [MF], and far-field [FF]) at Main Pass 299 during Sampling Cruises 1 and 2. Densities for Sampling Cruise 1 (6 samples) were based on single samples at each station; densities for Sampling Cruise 2 (18 samples) were the mean of three replicates at each station. Database was used without deletions.

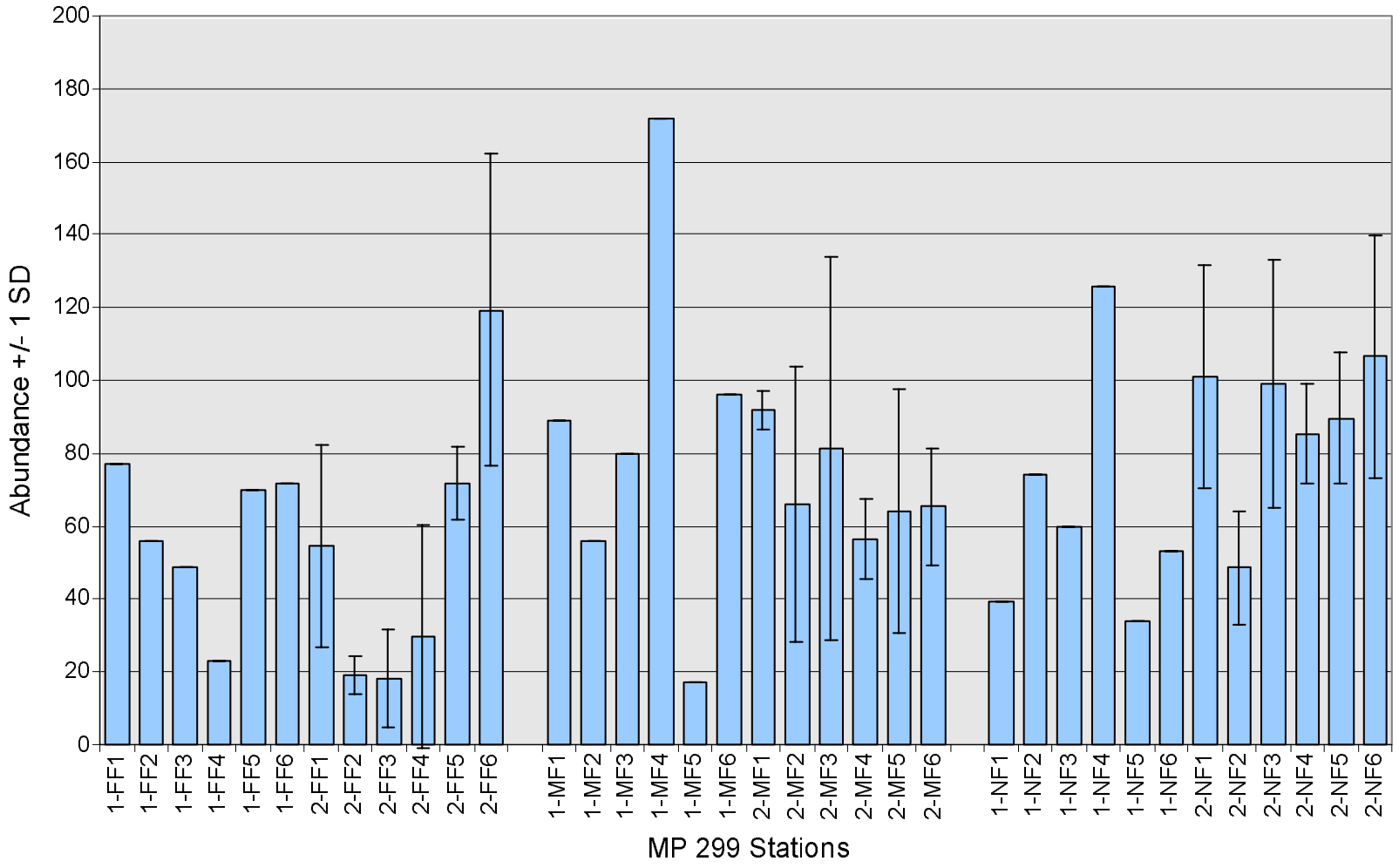

Figure 12-11. Infaunal densities at Main Pass (MP) 299 stations. Densities for Sampling Cruise 1(stations labeled 1-) were based on single samples at each station; densities for Sampling Cruise 2 (labeled 2-) were the mean of three replicates at each station. Database was used without deletions.

Table 12-11. Benthic community parameters for Main Pass 299 sampled on Sampling Cruise 2. Number of individuals is the mean and standard deviation (SD) of three replicates (entire database); other parameters were calculated based on replicates either pooled (No. Taxa, ESN) or averaged (No. Individuals, H', J', LSA) at each station (edited database).

Station	Mean No. Indiv.	SD	No. Taxa	Mean H' base 2	Mean J'	Mean LSA	ESN 2	ESN 8	ESN 50	ESN 100
Near-field										
NF-1	101.0	30.8	63	4.74	0.93	24.45	1.97	8.84	29.35	42.49
NF-2	48.7	15.6	46	4.15	0.93	19.31	1.97	8.72	28.36	40.52
NF-3	99.0	33.9	47	3.90	0.84	11.92	1.93	7.80	23.09	32.30
NF-4	85.3	13.8	53	4.59	0.93	21.12	1.96	8.55	26.46	37.64
NF-5	89.7	17.8	58	4.29	0.87	19.34	1.94	7.95	25.33	37.70
NF-6	106.7	33.3	59	4.23	0.86	17.21	1.94	8.03	25.27	37.40
Mid-field										
MF-1	92.0	5.2	54	4.56	0.90	20.53	1.95	8.31	26.14	37.85
MF-2	66.0	38.0	45	3.86	0.89	14.45	1.94	8.04	24.17	34.69
MF-3	81.3	52.8	55	3.83	0.87	13.03	1.93	7.92	24.90	36.56
MF-4	56.7	11.0	42	4.21	0.92	17.32	1.95	8.28	25.10	35.27
MF-5	64.3	33.5	46	4.17	0.91	18.40	1.95	8.26	25.38	36.27
MF-6	65.3	15.9	44	4.25	0.91	22.07	1.95	8.16	25.28	36.67
Far-field										
FF-1	54.7	27.7	54	4.05	0.91	22.09	1.96	8.51	28.99	44.29
FF-2	19.0	5.2	26	3.38	0.96	17.29	1.95	8.19	24.61	-
FF-3	18.0	13.4	23	2.29	0.64	12.43	1.96	8.43	-	-
FF-4	29.7	30.8	34	3.31	0.95	17.46	1.95	8.28	25.19	-
FF-5	71.7	10.1	48	4.01	0.85	16.77	1.93	7.88	25.25	36.79
FF-6	119.3	42.7	57	3.94	0.80	14.98	1.89	7.16	22.78	34.03

No. Indiv. = Number of individuals in three replicates.
No. Taxa = Number of taxa used for diversity analyses.
H': = Shannon diversity index, base 2.
J' = Evenness associated with H'.
LSA = log-series *alpha.*
ESN2-100 = estimated number of species if 2 to 100 individuals are drawn from the sample.

Table 12-12. Benthic community parameters for individual samples taken at Main Pass 299 on Sampling Cruise 2. See legend on Table 12-10 for explanation of column headings.

Station-Replicate	No. Indiv.	No. Taxa	H'	J'	LSA	ESN 2	ESN 8	ESN 50	ESN 100
NF1-1	109	36	4.85	0.94	20.73	1.97	8.72	26.91	-
NF1-2	127	42	4.83	0.90	25.47	1.96	8.43	27.09	40.58
NF1-3	67	28	4.53	0.94	27.15	1.97	8.67	-	-
NF2-1	63	28	4.50	0.94	22.83	1.96	8.54	26.52	-
NF2-2	32	14	3.55	0.93	11.14	1.93	7.55	-	-
NF2-3	51	27	4.41	0.93	23.95	1.96	8.45	27.00	-
NF3-1	77	25	3.91	0.84	13.43	1.90	7.22	20.36	-
NF3-2	138	33	4.09	0.81	14.33	1.89	7.13	21.27	29.74
NF3-3	82	19	3.69	0.87	8.00	1.91	7.06	15.89	-
NF4-1	80	26	4.38	0.93	14.43	1.96	8.27	22.60	-
NF4-2	101	35	4.74	0.92	21.74	1.96	8.56	26.48	-
NF4-3	75	32	4.65	0.93	27.20	1.96	8.62	28.35	-
NF5-1	77	27	4.33	0.91	16.80	1.95	8.15	23.17	-
NF5-2	82	32	4.21	0.84	24.02	1.91	7.52	26.03	-
NF5-3	110	34	4.34	0.85	17.20	1.93	7.66	23.14	32.99
NF6-1	69	24	4.10	0.89	15.91	1.93	7.80	22.57	-
NF6-2	119	34	4.43	0.87	17.20	1.94	7.97	22.61	32.81
NF6-3	132	35	4.15	0.81	18.53	1.89	7.18	23.10	34.34
MF1-1	89	34	4.65	0.91	21.00	1.96	8.42	25.87	-
MF1-2	89	32	4.50	0.90	20.27	1.95	8.19	25.16	-
MF1-3	98	34	4.54	0.89	20.31	1.95	8.18	24.88	-
MF2-1	104	33	4.32	0.86	16.80	1.93	7.71	22.68	32.56
MF2-2	66	27	4.25	0.89	20.98	1.94	7.97	25.50	-
MF2-3	28	10	3.02	0.91	5.56	1.89	6.34	-	-
MF3-1	119	33	4.35	0.86	15.98	1.93	7.79	22.10	31.43
MF3-2	21	10	3.04	0.92	7.96	1.90	6.73	-	-
MF3-3	104	31	4.11	0.83	15.16	1.90	7.30	21.62	30.72
MF4-1	56	25	4.27	0.92	19.39	1.95	8.22	24.71	-
MF4-2	46	20	4.10	0.95	14.96	1.96	8.26	-	-
MF4-3	68	27	4.27	0.90	17.60	1.95	8.01	23.51	-
MF5-1	45	22	4.19	0.94	22.84	1.96	8.42	-	-
MF5-2	103	31	4.23	0.85	16.14	1.93	7.60	22.11	-
MF5-3	45	21	4.09	0.93	16.21	1.95	8.13	-	-
MF6-1	74	25	4.20	0.90	15.82	1.94	7.95	22.65	-
MF6-2	75	29	4.23	0.87	21.22	1.93	7.78	25.11	-
MF6-3	47	23	4.32	0.95	29.18	1.97	8.75	-	-
FF1-1	84	32	4.43	0.89	21.42	1.94	8.03	25.44	-
FF1-2	29	18	3.93	0.94	32.72	1.96	8.54	-	-
FF1-3	51	19	3.79	0.89	12.12	1.93	7.45	-	-
FF2-1	25	13	3.43	0.93	10.92	1.93	7.39	-	-
FF2-2	16	10	3.19	0.96	13.11	1.94	7.69	-	-
FF2-3	16	12	3.51	0.98	27.85	1.97	8.71	-	-
FF3-1	3	2	0	-	-	-	-	-	-
FF3-2	22	13	3.58	0.97	16.10	1.96	8.21	-	-
FF3-3	29	11	3.28	0.95	8.75	1.93	7.25	-	-
FF4-1	65	26	4.41	0.94	16.31	1.96	8.37	23.64	-
FF4-2	9	5	2.20	0.95	-	-	-	-	-
FF4-3	15	11	3.32	0.96	18.60	1.95	8.12	-	-
FF5-1	81	33	4.64	0.92	22.85	1.96	8.47	26.83	-
FF5-2	73	22	3.16	0.71	11.56	1.76	5.76	18.69	-
FF5-3	61	24	4.23	0.92	15.91	1.95	8.11	22.85	-
FF6-1	157	38	4.06	0.77	17.68	1.87	6.90	21.59	32.58
FF6-2	128	28	3.93	0.82	11.37	1.89	6.98	19.43	26.21
FF6-3	73	27	3.82	0.80	15.89	1.87	6.91	21.51	-

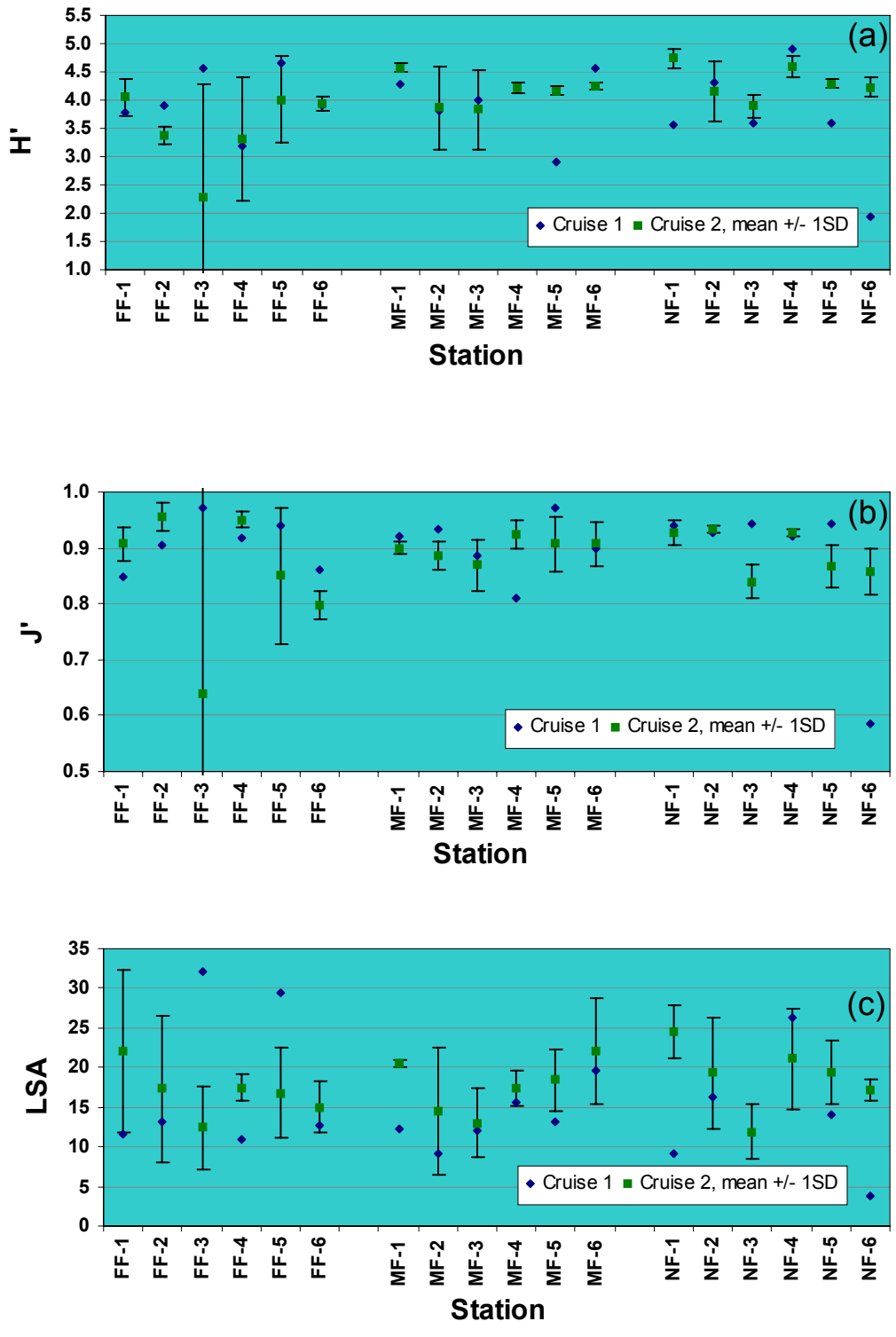

Figure 12-12. Benthic community diversity parameters at Main Pass (MP) 299. a: Shannon diversity H'; b: Evenness J'; c: Log-series *alpha* (LSA). Values for Sampling Cruise 1 were for single samples; values for Sampling Cruise 2 were mean of three replicates +/- one standard deviation (SD).

The highest H' diversity, 4.91, was recorded at NF-4; log-series alpha also was high at this station but was lower than alpha values recorded at FF-3 and FF-5 (Table 12-10).

12.4.3.2 Sampling Cruise 2. Because additional replicates were collected in each sampling zone on Sampling Cruise 2, species richness (absolute number of taxa) appeared slightly higher in all three zones when samples from each station were pooled. Near-field stations ranged from 46 to 63 taxa, mid-field stations from 42 to 54, and far-field stations had from 23 to 57 taxa. Shannon diversity values for MP 299 samples collected during Sampling Cruise 2 also were not as variable within each zone as they were during Sampling Cruise 1 (Tables 12-10 and 12-11, Figure 12-12A). The extreme low values seen, for example, at NF-6 during Sampling Cruise 1 were not recorded at any station sampled during Sampling Cruise 2. Mean H' (base 2) diversities ranged from 3.90 to 4.74 in the near-field, 3.83 to 4.56 in the mid-field, and 3.31 to 4.05 in the far-field. Evenness remained high at stations in all three zones; within-station variability of this parameter was high only at FF-3 and FF-5 (Figure 12-12B).

Results for individual samples are presented in Table 12-11. The far-field zone had both the highest and lowest values recorded for number of individuals in a sample, with a range from 3 individuals (FF-3, replicate 1) to 157 individuals (FF-6, replicate 1). Number of taxa in individual samples also was lowest in the far-field (two and five taxa at FF-3, replicate 1 and FF-4, replicate 2, respectively), and therefore the lowest diversities also were seen at these stations. The near-field zone had the highest number of taxa in a sample (42 at NF-1, replicate 2), and the highest Shannon diversities also were seen in near-field samples. With only a few exceptions in the far-field and near-field, log-series *alpha* diversity values for Sampling Cruise 2 samples were similar to those seen for Sampling Cruise 1 samples.

12.4.4 Rarefaction

The rarefaction technique produces curves that illustrate the diversity of each sample by estimating the number of species that would be found if *n* number of individuals were pulled at random from the sample. The curves produced for both the Sampling Cruise 1 and Sampling Cruise 2 samples are shown in Figures 12-13 through 12-15. Curves labeled 1 to 6 correspond to Stations 1 to 6 sampled during Sampling Cruise 2, and curves labeled 7 to 12 correspond to pooled replicates from the same stations (i.e., Stations 1 to 6) taken during Sampling Cruise 2. Values for the estimated number of species at four points (if the number of individuals in the sample allows calculation) are presented in Tables 12-10 through 12-12.

In the set of curves for the near-field samples, it can be seen, for instance, that NF-4 is more diverse than NF-6; in the mid-field stations, the diversities are all similar; and for the far-field stations, FF-3 and FF-5 have higher diversities than the other stations. However, all of the samples had a low number of individuals, and just the beginning portion of the curves where they are still climbing steeply and have not leveled off into the asymptote that denotes the station has been fully sampled is seen. The curves labeled 7 to 12 in each set are longer because they represent three pooled replicates. Many of these curves indicate a diversity similar to that seen in the Sampling Cruise 1 samples: e.g., far-field curves 3, 5, and 7 have identical slopes, even though the first two are shorter.

12.4.5 Community Assemblage Patterns

Cluster analyses of only the Sampling Cruise 1 data suggested that there was very low similarity among the 18 MP 299 samples, but there was an indication of a trend for samples in the different sampling zones to group with other samples from the same zone. However, when data

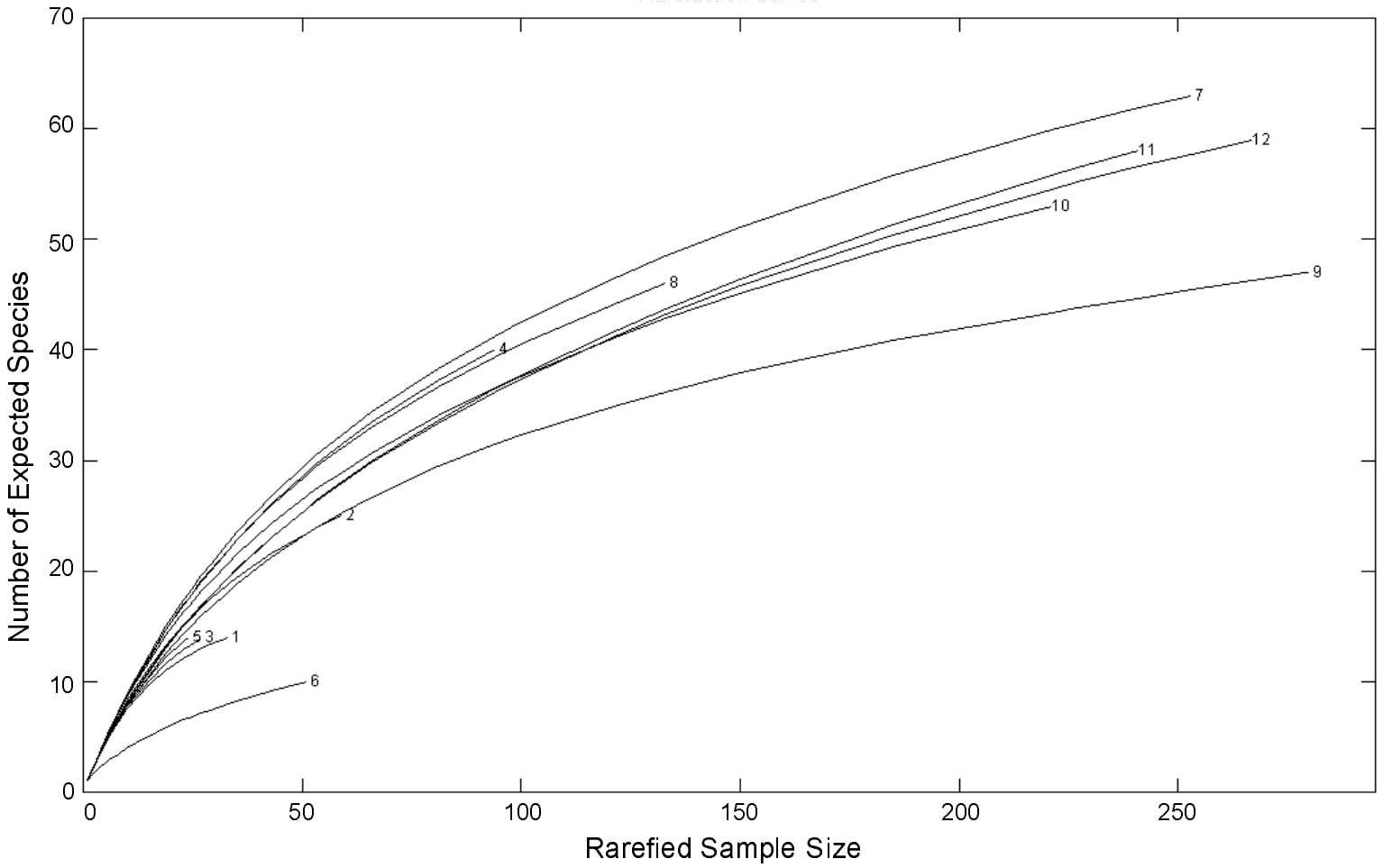

Figure 12-13. Rarefaction curves for Main Pass 299 near-field stations. In each area, curves labeled 1 to 6 correspond to Stations 1 to 6 sampled during Sampling Cruise 1, and curves labeled 7 to 12 correspond to pooled replicates from the same stations (i.e., Stations 1 to 6) taken during Sampling Cruise 2.

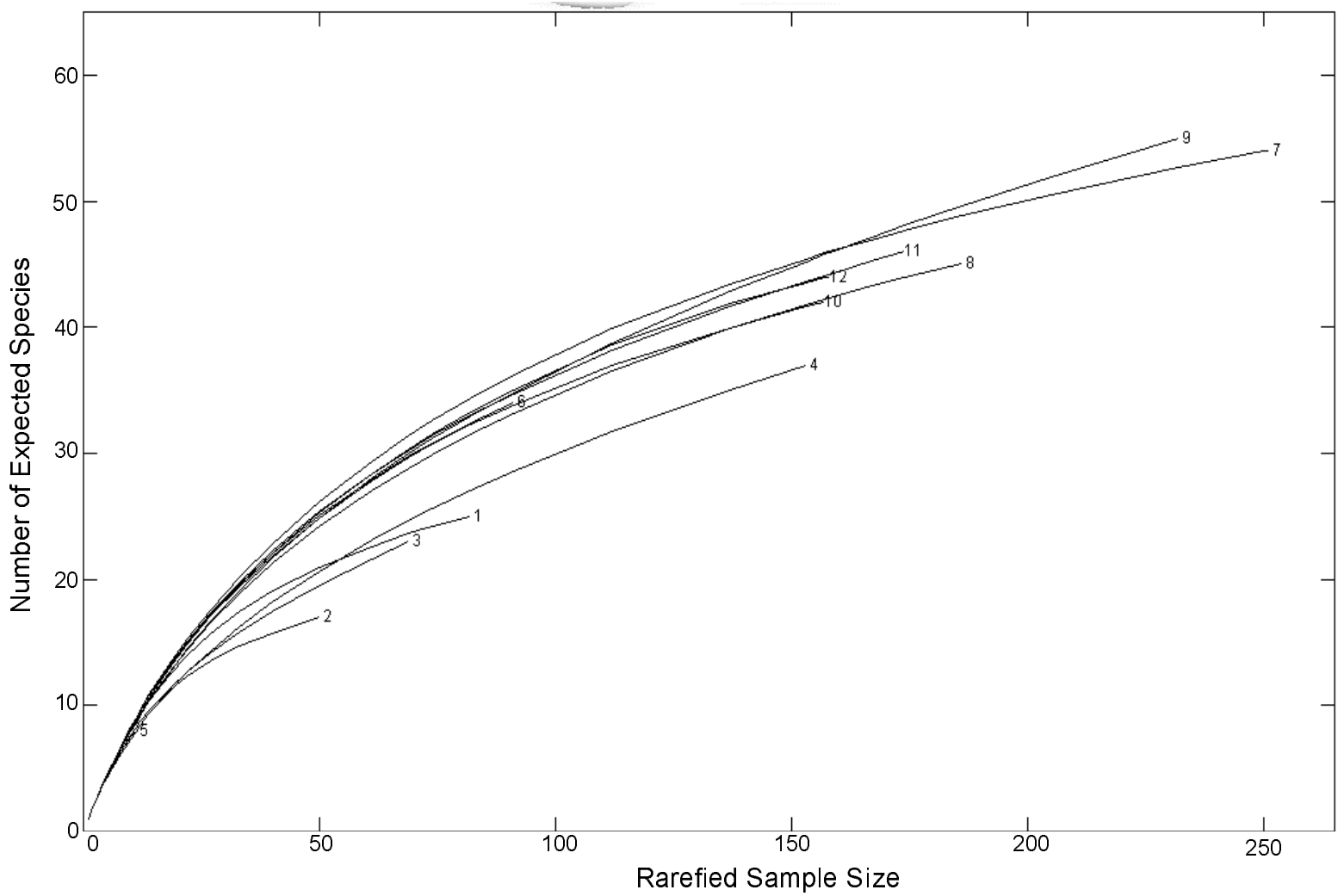

Figure 12-14. Rarefaction curves for Main Pass 299 mid-field stations. In each area, curves labeled 1 to 6 correspond to Stations 1 to 6 sampled during Sampling Cruise 1, and curves labeled 7 to 12 correspond to pooled replicates from the same stations (i.e., Stations 1 to 6) taken during Sampling Cruise 2.

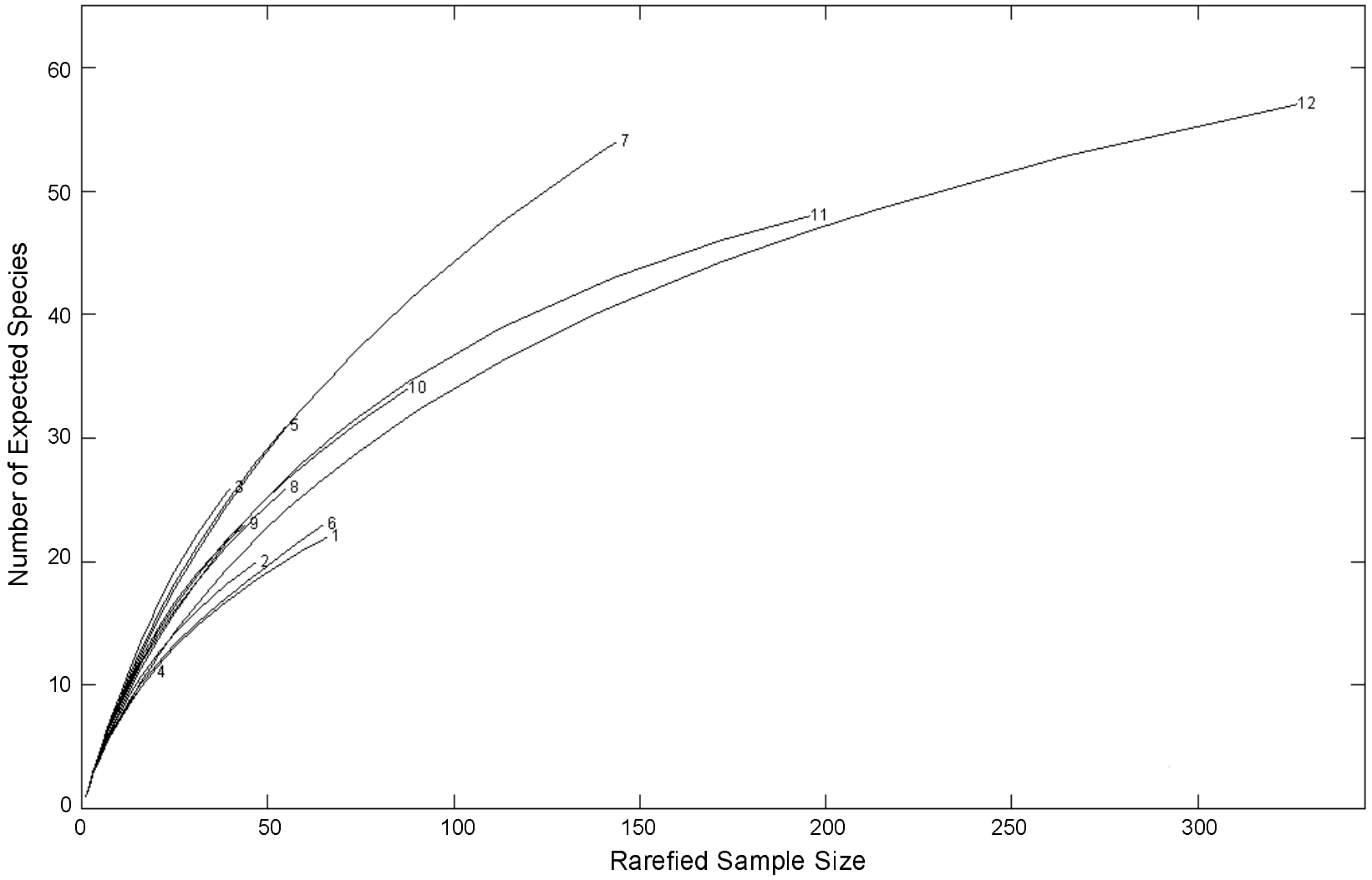

Figure 12-15. Rarefaction curves for Main Pass 299 far-field stations. In each area, curves labeled 1 to 6 correspond to Stations 1 to 6 sampled during Sampling Cruise 1, and curves labeled 7 to 12 correspond to pooled replicates from the same stations (i.e., Stations 1 to 6) taken during Sampling Cruise 2.

from both Sampling Cruises 1 and 2 were analyzed together, it was apparent that there was a clearer difference between the two Sampling Cruises than between the sampling zones (Figure 12-16). Within the Sampling Cruise 2 data, there are some cluster groups composed of samples from each of the sampling zones; in particular, mid-field samples tended to cluster together and secondarily joined with samples from the near-field stations. Far-field Stations 1 and 2, and Stations 3, 4, and 5 tended to form small groups that then showed affinities with the mid- and near-field groups. There were several outliers from both Sampling Cruises; these appear as samples with very low similarity to the major cluster composed of samples from both Sampling Cruises.

Results of the MDS analysis of the MP 299 samples agreed with those from the cluster analysis. The stress value for this MDS was 0.23, which indicates a useful 2-dimensional representation of the relationships among the samples. There was a clear temporal segregation of samples between the two Sampling Cruises. This difference was greater than differences among the three zones for the individual cruises (Figure 12-17). For Sampling Cruise 1, there appears to be a distinction between the near-field and far-field stations, and the mid-field stations were more similar to the near-field stations than to the far-field stations. For Sampling Cruise 2, there was more overlap among the near-field, mid-field, and far-field stations. This result suggested some level of recovery of the near-field and mid-field stations may have occurred during the time between the two Sampling Cruises.

12.4.6 Sediment Characteristics at Main Pass 299

Sediment grain size and TOC data were plotted in order to examine whether differences in these characteristics might explain why the Sampling Cruise 1 samples differed from the Sampling Cruise 2 samples. Figure 12-18 suggested that the sediments at the majority of stations sampled during Sampling Cruise 2 were slightly coarser (i.e., had a lower mean phi value) than sediments sampled the previous year. Two samples showed the reverse of this trend: MF-6 from Sampling Cruise 1 had a mean phi value that was more similar to those recorded during Sampling Cruise 2; however, this sample grouped solidly with other Sampling Cruise 1 mid-field samples (Figure 12-16), suggesting that the difference in sediment texture was not a major influence on the fauna at that station. Similarly, the sediment at FF- 2 during Sampling Cruise 2 was finer than at the other stations sampled during that cruise. The three FF-2 replicates clustered together in a small group, along with a Sampling Cruise 2 replicate from the mid-field (Figure 12-16). Total organic carbon values (percentages) were similar during both Sampling Cruises and do not appear to be influencing benthic community structure.

The sample that had the lowest Shannon H' diversity was NF-6 sampled on Sampling Cruise 1 in May 2001. Values for mean phi and percent TOC for this station were well within the range of values for all other samples collected on Sampling Cruise 1 and therefore do not account for the low diversity at this station.

12.4.7 Main Pass 299 Summary

1. During Sampling Cruise 1, densities were low at all MP 299 stations, especially in the far-field, and variability among stations was high in all three sampling zones. During Sampling Cruise 2, mean densities were higher in the near-field but lower in both the mid-field and far-field. However, within-station variability was very high, and there was no significant difference between densities recorded in the three sampling zones, nor were the densities during Sampling Cruise 2 different from those recorded from Sampling Cruise 1.

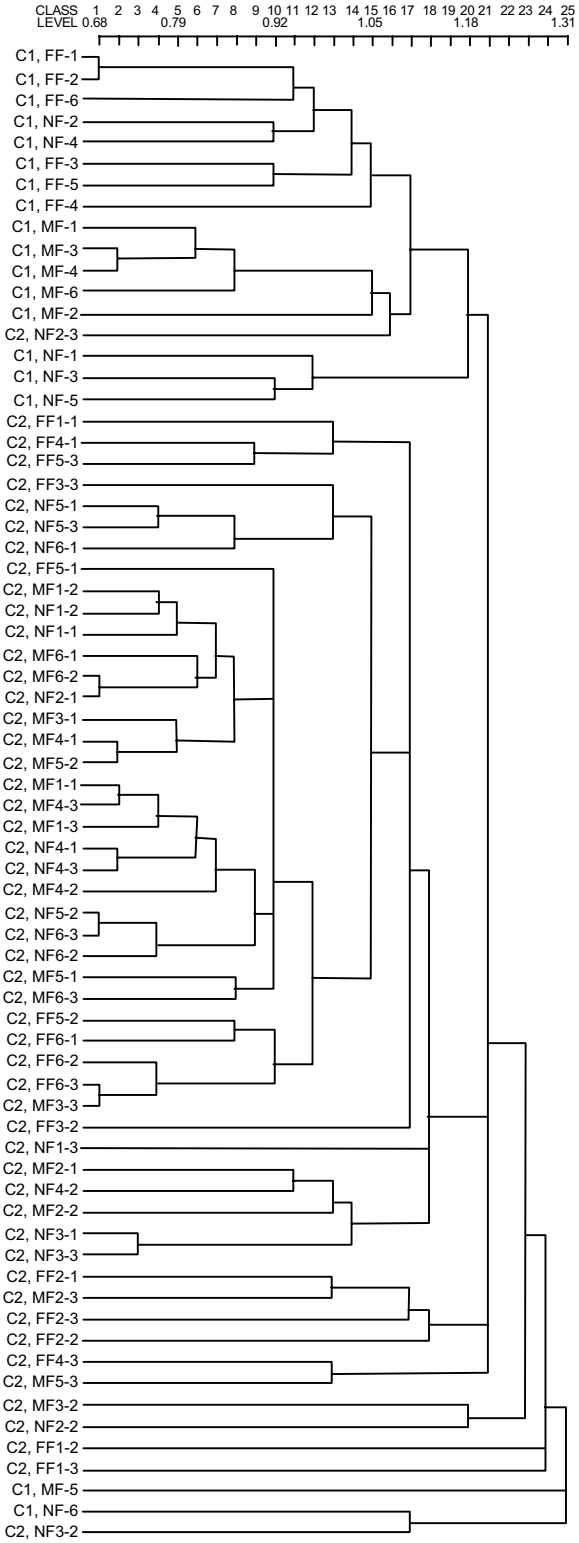

Figure 12-16. Cluster dendrogram for Main Pass 299. Sample label C1 indicates Sampling Cruise 1 and C2 indicates Sampling Cruise 2.

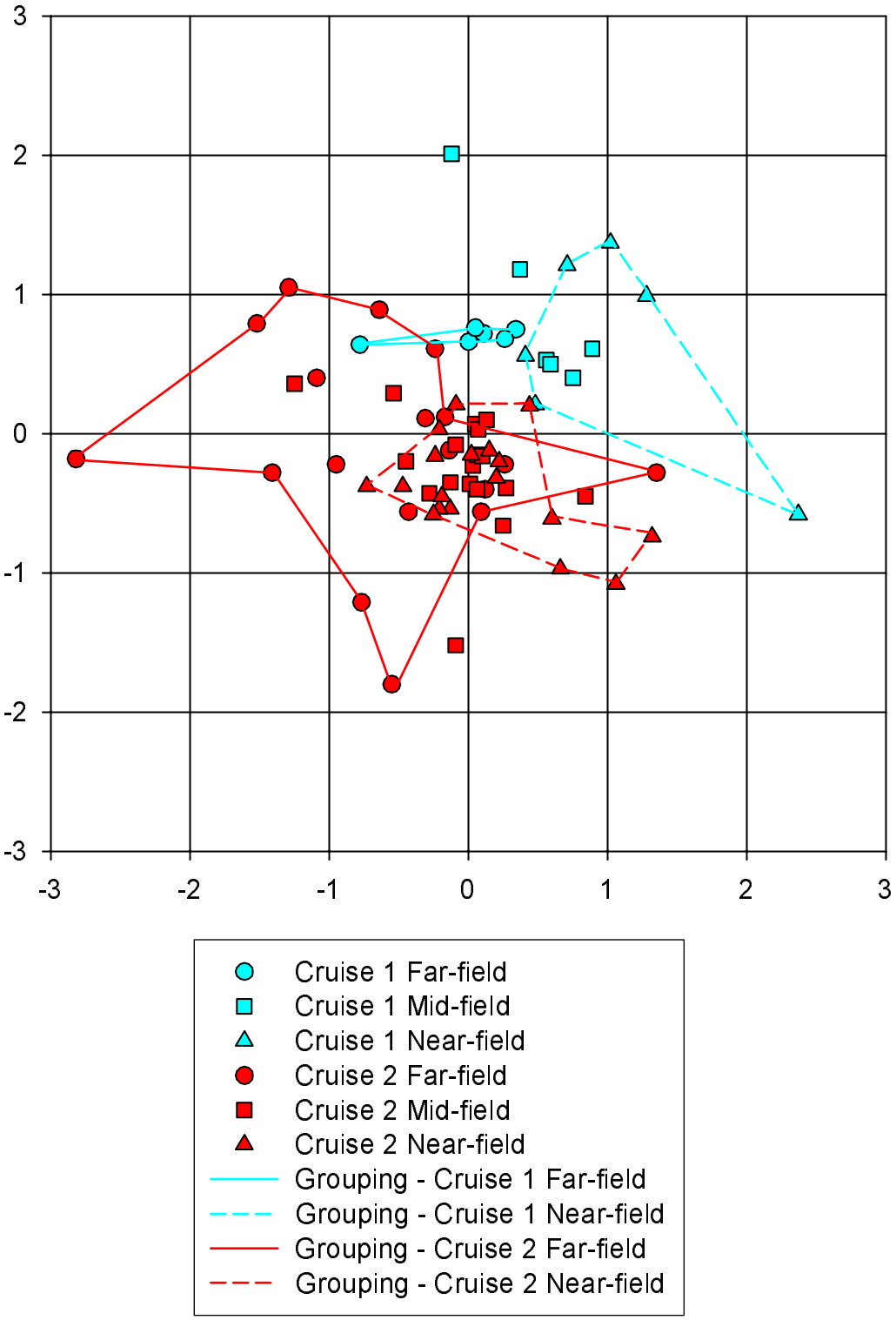

Figure 12-17. Results of nonmetric multidimensional scaling analysis for Main Pass 299.

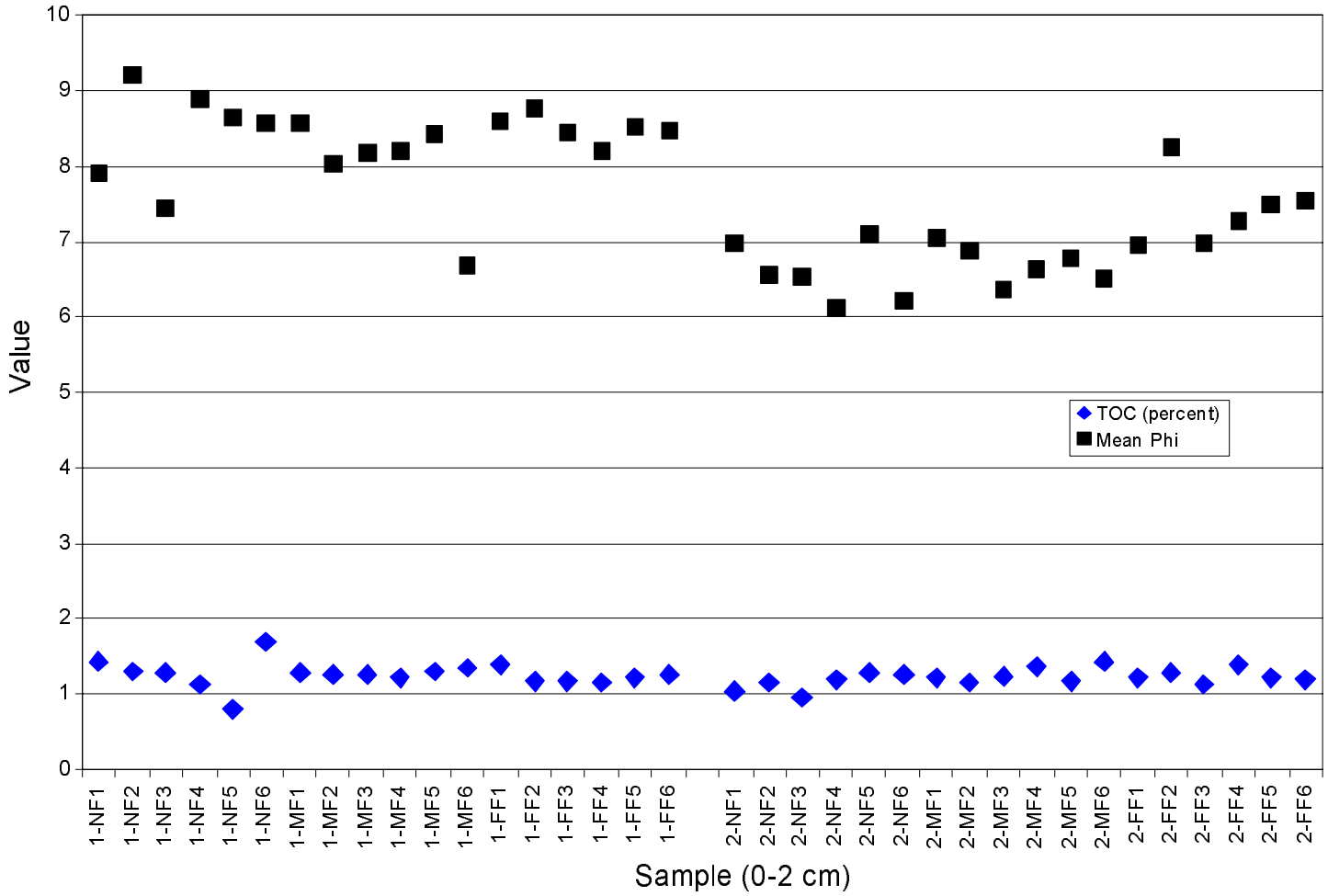

Figure 12-18. Percent total organic carbon (TOC) and mean phi of sediments at Main Pass 299. Values represent the top 2 cm of sediment taken from single samples. Sampling Cruise 1 stations are labeled 1- and Sampling Cruise 2 stations are labeled 2-.

2. The dominant organisms in all three sampling zones changed considerably between the Screening Cruise and Sampling Cruise 1 and between Sampling Cruise 1 and Sampling Cruise 2. An opportunistic species, *Capitella capitata*, accounted for over half the individuals collected on the Screening Cruise but for only 9.7% during Sampling Cruise 1, and it was not a numerical dominant during Sampling Cruise 2. None of the numerically dominant species from Sampling Cruise 2 are considered opportunistic, suggesting an improvement in bottom conditions.

3. Each of the three sampling zones had one station with low abundance and low diversity during Sampling Cruise 1: NF-6, MF-5, and FF-4 had significantly lower diversity values compared to other stations sampled either on Sampling Cruise 1 or Sampling Cruise 2. During Sampling Cruise 2, community parameters were less variable compared with Sampling Cruise 1 in all three zones. The extreme low values seen during Sampling Cruise 1 were recorded only at two far-field stations sampled during Sampling Cruise 2 (FF-3, replicate 1 and FF-4, replicate 2). Evenness was high at stations in all three zones; within-station variability of this parameter was high only at FF-5.

4. Rarefaction diversity indicated patterns similar to those seen with the Shannon diversity measurements.

5. Multivariate cluster analysis of individual samples indicates a clear difference between Sampling Cruises 1 and 2, reflecting the differences in species composition noted above. Samples from each zone were similar to samples from other zones, but some mixing of samples from different zones did occur. The temporal difference appears to be greater than the spatial difference. The results of the MDS analysis supported a similar interpretation.

6. Sediments were slightly coarser during Sampling Cruise 2, which may have influenced the differences in species composition, but TOC levels were the same during both Sampling Cruises.

Conclusion: The composition of the benthic communities at MP 299 appears very different from Sampling Cruises 1 and 2, reflected in the temporal separation of these sampling dates in multivariate community analysis. However, community parameters such as infaunal densities and species diversity at the near-field stations were similar between the two Sampling Cruises. Differences in mean phi and percent TOC of the sediments do not appear to account for the differences in species composition.

12.5 EUGENE ISLAND 346

EI 346 is located in 92 m water depth. This site was not sampled on the Screening Cruise in August 2000. During Sampling Cruise 1 (May 2001), six benthic samples were taken in each of three sampling zones, with the drillsite at the center. During Sampling Cruise 2 (May 2002), six stations were again occupied in each of the three sampling zones, but this time, three replicates were taken at each of the stations. Therefore, 18 samples were collected at EI 346 during Sampling Cruise 1, and 54 were collected during Sampling Cruise 2. A total of 345 taxa was reported for the EI 346 samples. Of these, 74 were deleted for diversity calculations. Raw data for these samples are presented in Appendix H.

12.5.1 Dominant Infaunal Species

In the present context, dominant species are those represented by the greatest number of individuals in each sample (numerical dominance). The results from the Sampling Cruises are tabulated separately below.

12.5.1.1 Sampling Cruise 1. Table 12-13 shows the benthic species that were dominant in the samples in each of the three sampling zones. Although the samples are not replicates, but are single samples taken at each station, each set was summarized for an evaluation of dominant species. Inspection of the data shows that different species were dominant in each of the three zones, implying a patchy distribution of the fauna and a low degree of similarity among the three zones (see results of Cluster Analysis, below).

12.5.1.1.1 Near-field. The numerically dominant species at the near-field stations was a bivalve, *Codakia costata*, which occurred in large numbers in four of the six near-field samples. Another lucinid bivalve, *Anodontia alba*, also was dominant in this zone.

12.5.1.1.2 Mid-field. The mid-field stations were dominated by another lucinid bivalve, *Lucina multilineata*, which accounted for 36.4% of the specimens collected in that zone. This species also was patchily distributed, with three samples having all but 3 of the 179 specimens collected. The polychaete *Capitella capitata* was the only species recorded in common between the mid-field and near-field zones, and the isopod *Gnathia* sp. was the only dominant shared with the far-field.

12.5.1.1.3 Far-field. The far-field zone was dominated primarily by the ostracod *Skogsbergia lerneri*, the gastropods *Philine sagra* and *Rissoina cancellata*, and the isopod *Gnathia*. None of these species accounted for more than 5.3% of the fauna, indicating a highly even community. The only shared dominant between the far-field and mid-field zones was the isopod *Gnathia*, and the only dominant common to all three zones was Lucinidae, a family-level category that represents bivalves that could not be identified to genus or species.

12.5.1.2 Sampling Cruise 2. Table 12-14 shows the benthic species that were dominant in each of the three sampling zones during Sampling Cruise 2. In this case, three replicates were taken at each station. Counts in the replicates at each station were summed for this presentation.

12.5.1.2.1 Near-field. A bivalve, *Lucina radians*, dominated the samples taken in the near-field zone, accounting for over 70% of the fauna.

12.5.1.2.2 Mid-field. The same bivalve that dominated the near-field also was the numerical dominant in the mid-field samples: *Lucina radians* accounted for slightly more than 50% of the fauna. This was a different species of *Lucina* than the one that dominated the same zone a year earlier. Several other mid-field dominants were shared with the near-field, notably Aclididae Genus C, *Paramphinome* sp. B, and *Macoma pulleyi*.

12.5.1.2.3 Far-field. The fauna in the far-field zone was very different during Sampling Cruise 2 compared with Sampling Cruise 1, with only one species, the polychaete *Paralacydonia paradoxa*, dominant during both Sampling Cruises. During Sampling Cruise 2, the bivalve *Thyasira trisinuata* accounted for nearly 12% of the far-field fauna, compared with the ostracod, isopod, and gastropods that were dominant during Sampling Cruise 1.

Table 12-13. Numerically dominant taxa at Eugene Island 346 during Sampling Cruise 1.

Near-field			Mid-field			Far-field		
Rank	Taxon	% Contribution	Rank	Taxon	% Contribution	Rank	Taxon	% Contribution
1	*Codakia costata*	75.45	1	*Lucina multilineata*	36.51	1	*Skogsbergia lerneri*	5.31
2	Lucinidae (LPIL)	5.20	2	*Capitella capitata*	8.09	2	*Gnathia* (LPIL)	4.11
2	*Anodontia alba*	5.04	3	Lucinidae (LPIL)	7.05	2	*Philine sagra*	4.11
2	*Capitella capitata*	1.79	4	Sipuncula (LPIL)	2.70	2	*Rissoina cancellata*	4.11
3	*Spiophanes wigleyi*	1.46	5	Ophiuroidea (LPIL)	2.28	3	Bivalvia (LPIL)	3.86
4	Genus C Aclididae	1.14	6	*Philine sagra*	2.28	4	*Paralacydonia paradoxa*	3.62
5	Bivalvia (LPIL)	0.73	7	*Spiophanes wigleyi*	2.28	5	Dentaliidae (LPIL)	3.14
6	*Nassarius albus*	0.73	7	*Gnathia* (LPIL)	2.07	6	*Eusarsiella radiicosta*	2.90
6	Tellinidae (LPIL)	0.65	8	*Nuculana* (LPIL)	2.07	6	*Harbansus paucichelatus*	2.90
6	*Sigambra tentaculata*	0.49	8	Bivalvia (LPIL)	1.87	6	Lucinidae (LPIL)	2.90
Cumulative Total		92.68	Cumulative Total		67.22	Cumulative Total		36.96
Total Density for 6 Samples		1,230	Total Density for 6 Samples		482	Total Density for 6 Samples		414

LPIL = Lowest practical identification level.

Table 12-14. Numerically dominant taxa at Eugene Island 346 during Sampling Cruise 2.

Near-field			Mid-field			Far-field		
Rank	Taxon	% Contribution	Rank	Taxon	% Contribution	Rank	Taxon	% Contribution
1	*Lucina radians*	71.35	1	*Lucina radians*	50.29	1	*Thyasira trisinuata*	11.99
2	Genus C Aclididae	4.12	2	Genus C Aclididae	10.20	2	Sipuncula (LPIL)	4.50
2	*Nassarius* sp. F	4.12	3	*Nuculana acuta*	3.42	3	*Paralacydonia paradoxa*	4.40
3	*Paramphinome* sp. B	2.31	4	*Semele* (LPIL)	2.64	4	*Antalis* (LPIL)	4.20
4	*Macoma* (LPIL)	1.44	5	*Phascolion strombi*	2.22	5	*Semele* (LPIL)	3.80
5	*Semele* (LPIL)	1.24	6	*Paramphinome* sp. B	2.02	6	*Alternochelata sikorai*	3.30
6	*Capitella capitata*	1.09	7	Sipuncula (LPIL)	1.37	7	Cirratulidae (LPIL)	3.20
7	*Spiophanes wigleyi*	1.07	8	Lineidae (LPIL)	1.21	8	*Levinsenia gracilis*	2.60
8	*Macoma pulleyi*	0.74	9	*Macoma pulleyi*	1.04	8	*Sternaspis scutata*	2.60
9	*Pagurus* (LPIL)	0.69	10	*Corbula* (LPIL)	1.01	9	*Nephtys incisa*	2.40
						10	*Sarsonuphis hartmanae*	1.90
Cumulative Total		88.17	Cumulative Total		75.42	Cumulative Total		44.86
Total Density for 18 Samples		4,320	Total Density for 18 Samples		3,068	Total Density for 18 Samples		1,001

LPIL = Lowest practical identification level.

12.5.2 Infaunal Density

Density results presented here are based on the entire database of 345 taxa as submitted by BVA. Other parameters, including all of the diversity measures, are based on an edited database from which 74 higher-level taxa were deleted.

12.5.2.1 Sampling Cruise 1. Table 12-15 presents the benthic community parameters for all samples taken at EI 346 during Sampling Cruise 1. Densities were highly variable, especially in the near-field, where they ranged from a low of 9 to 10 individuals per 0.1-m^2 sample at NF-5 and NF-1, respectively, to a high of 631 at NF-4, a station dominated by large numbers of the bivalve *Codakia costata*. Densities ranged from 40 to 157 individuals at the mid-field stations and from 36 to 103 individuals at the far-field stations.

Table 12-15. Benthic community parameters for Eugene Island 346 sampled during Sampling Cruise 1. Number of individuals is from the entire database; other parameters are calculated based on the edited database.

Station	No. Indiv.	No. Taxa	H' Base 2	J'	LSA	ESN 2	ESN 8	ESN 50	ESN 100
Near-field									
NF-1	10	2	0	-	-	-	-	-	-
NF-2	313	22	1.74	0.39	5.41	1.47	3.26	7.83	11.74
NF-3	94	11	1.56	0.45	3.27	1.44	3.22	8.10	-
NF-4	631	20	1.06	0.25	3.95	1.28	2.33	5.33	7.60
NF-5	9	3	0.99	-	-	-	-	-	-
NF-6	173	20	2.14	0.49	5.96	1.55	3.91	10.82	15.78
Mid-field									
MF-1	103	4	1.19	0.60	0.84	1.44	2.66	3.92	-
MF-2	75	25	4.31	0.93	21.04	1.96	8.35	-	-
MF-3	40	17	3.95	0.97	12.59	1.96	8.22	-	-
MF-4	44	17	3.60	0.88	11.81	1.91	7.16	-	-
MF-5	157	28	2.77	0.58	10.61	1.66	4.80	14.87	23.03
MF-6	63	13	2.54	0.69	5.01	1.76	4.68	11.54	-
Far-field									
FF-1	90	22	3.46	0.78	9.78	1.87	6.26	16.71	-
FF-2	50	22	4.12	0.92	18.66	1.95	8.13	-	-
FF-3	90	34	4.78	0.94	26.06	1.97	8.77	28.28	-
FF-4	103	39	4.86	0.92	32.15	1.96	8.67	29.65	-
FF-5	45	21	4.07	0.93	22.17	1.95	8.22	-	-
FF-6	36	17	3.75	0.92	18.34	1.94	7.87	-	-

No. Indiv. = Number of individuals in three replicates.
No. Taxa = Number of taxa used for diversity analyses.
H' = Shannon diversity index, base 2.
J' = Evenness associated with H'.
LSA = log-series *alpha.*
ESN2-100 = estimated number of species if 2 to 100 individuals are drawn from the sample.

12.5.2.2 Sampling Cruise 2. Tables 12-16 and 12-17 present the benthic community parameters for all samples taken at EI 346 during Sampling Cruise 2, both averaged and for individual replicates. Figure 12-19 compares the mean densities of all samples within a sampling zone for Sampling Cruise 1 and Sampling Cruise 2. Mean densities were slightly higher in the near-field, notably higher in the mid-field, and slightly lower in the far-field during Sampling Cruise 2 compared with Sampling Cruise 1. However, the standard deviations around the mean are very large, and the mean densities are not statistically different between zones or cruises.

Table 12-16. Benthic community parameters for Eugene Island 346 on Sampling Cruise 2. Number of individuals is the average of three replicates (entire database); other parameters are based on replicates either pooled (No. Taxa, ESN) or averaged (No. Individuals, H', J', LSA) at each station (edited database).

Station	Mean No. Indiv.	SD	No. Taxa	Mean H' base 2	Mean J'	Mean LSA	ESN 2	ESN 8	ESN 50	ESN 100
Near-field										
NF-1	242.7	15.9	50	2.19	0.47	7.40	1.56	4.03	11.88	18.53
NF-2	107.3	17.2	52	3.59	0.77	11.15	1.89	6.97	19.95	29.84
NF-3	428.3	71.7	41	1.60	0.35	4.94	1.43	3.15	8.21	12.32
NF-4	362.0	241.1	26	0.88	0.29	2.51	1.20	2.00	5.07	7.76
NF-5	186.3	243.4	13	0.87	0.30	1.69	1.15	1.74	3.90	5.56
NF-6	17.3	9.6	3	1.16	0.90	0.78	1.66	2.93	3.00	0.00
Mid-field										
MF-1	87.3	45.5	52	4.02	0.85	20.63	1.91	7.40	23.15	34.95
MF-2	68.7	3.1	64	4.44	0.89	29.26	1.95	8.23	28.32	45.50
MF-3	70.7	26.6	56	4.56	0.95	24.20	1.97	8.87	29.82	43.36
MF-4	532.3	133.5	27	0.45	0.12	2.41	1.11	1.55	3.45	5.39
MF-5	121.3	17.0	49	3.81	0.80	12.22	1.90	7.17	20.76	29.74
MF-6	142.3	69.6	68	3.78	0.75	17.99	1.82	6.45	21.88	34.45
Far-field										
FF-1	62.0	14.9	63	4.43	0.92	29.22	1.97	8.76	29.96	48.00
FF-2	56.7	17.0	54	4.48	0.95	33.08	1.97	8.97	31.71	47.59
FF-3	52.0	14.7	49	4.24	0.93	24.23	1.97	8.68	28.82	43.32
FF-4	76.7	14.3	54	3.72	0.78	19.83	1.84	6.66	22.49	35.40
FF-5	43.0	15.7	47	3.96	0.90	24.14	1.95	8.36	28.67	43.89
FF-6	43.3	7.2	46	4.23	0.96	88.92	1.97	8.95	32.22	0.00

Mean No. Indiv. = Mean number of individuals in three replicates.
SD = Standard deviation.
No. Taxa = Number of taxa used for diversity analyses.
H' = Shannon diversity index, base 2.
J' = Evenness associated with H'.
LSA = Log-series *alpha*.
ESN2-100 = estimated number of species if 2 to 100 individuals are drawn from the sample.

Table 12-17. Benthic community parameters for individual samples taken at Eugene Island 346 on Sampling Cruise 2. See legend on Table 12-16 for explanation of column headings.

Station-Replicate	No. Indiv.	No. Taxa	H'	J'	LSA	ESN 2	ESN 8	ESN 50	ESN 100
NF1-1	261	32	2.83	0.57	10.36	1.66	4.81	14.56	21.92
NF1-2	234	14	0.95	0.25	3.29	1.23	2.17	5.87	9.02
NF1-3	233	28	2.80	0.58	8.54	1.71	4.74	13.21	19.87
NF2-1	110	31	4.34	0.88	15.27	1.94	7.88	21.98	30.86
NF2-2	89	19	3.03	0.71	7.60	1.80	5.52	14.00	-
NF2-3	123	26	3.41	0.73	10.58	1.86	6.01	15.58	24.11
NF3-1	477	18	1.32	0.32	3.71	1.34	2.70	6.61	9.32
NF3-2	462	12	0.40	0.11	2.26	1.09	1.43	3.01	4.73
NF3-3	346	32	3.09	0.62	8.86	1.79	5.20	13.25	18.90
NF4-1	462	22	1.08	0.24	4.82	1.27	2.30	5.60	8.68
NF4-2	537	9	0.38	0.12	1.54	1.08	1.43	2.94	4.45
NF4-3	87	5	1.19	0.51	1.17	1.43	2.65	4.20	-
NF5-1	91	7	1.41	0.50	1.78	1.45	3.06	5.67	-
NF5-2	463	9	0.32	0.10	1.59	1.07	1.35	2.61	3.91
NF5-3	5	3	1.52	0.96	-	-	-	-	-
NF6-1	19	3	1.38	0.87	1.06	1.62	2.85	-	-
NF6-2	26	2	0.93	0.93	0.50	1.47	2.00	-	-
NF6-3	7	3	1.38	0.87	-	-	-	-	-
MF1-1	70	23	4.04	0.89	16.50	1.93	7.76	23.00	-
MF1-2	53	27	4.40	0.92	31.10	1.96	8.50	-	-
MF1-3	139	32	3.63	0.73	14.28	1.82	6.25	19.26	28.88
MF2-1	72	33	4.58	0.91	36.04	1.95	8.42	31.06	-
MF2-2	68	33	4.54	0.90	30.10	1.95	8.28	29.03	-
MF2-3	66	29	4.21	0.87	21.65	1.92	7.71	25.54	-
MF3-1	86	35	4.76	0.93	25.96	1.97	8.64	28.05	-
MF3-2	86	34	4.81	0.95	24.36	1.97	8.80	28.05	-
MF3-3	40	19	4.11	0.97	22.27	1.97	8.66	-	-
MF4-1	380	9	0.39	0.12	1.65	1.09	1.46	2.93	4.30
MF4-2	588	13	0.32	0.09	2.36	1.06	1.32	2.55	3.95
MF4-3	629	17	0.65	0.16	3.22	1.16	1.76	3.85	5.65
MF5-1	139	28	4.25	0.88	11.66	1.94	7.80	20.29	26.48
MF5-2	120	29	3.73	0.77	13.43	1.86	6.60	19.03	28.53
MF5-3	105	26	3.46	0.74	11.56	1.81	6.12	18.27	-
MF6-1	62	22	4.09	0.92	13.59	1.94	7.93	20.99	-
MF6-2	181	39	3.00	0.57	16.76	1.65	4.91	17.23	28.80
MF6-3	184	46	4.26	0.77	23.62	1.87	7.04	23.90	37.31
FF1-1	79	34	4.76	0.93	32.52	1.97	8.79	29.94	-
FF1-2	56	26	4.30	0.92	34.09	1.95	8.37	-	-
FF1-3	51	25	4.23	0.91	21.04	1.95	8.14	-	-
FF2-1	58	31	4.61	0.93	36.25	1.97	8.70	-	-
FF2-2	39	21	4.25	0.97	38.17	1.98	9.00	-	-
FF2-3	73	29	4.57	0.94	24.83	1.97	8.65	27.50	-
FF3-1	61	24	4.20	0.92	18.60	1.95	8.13	-	-
FF3-2	60	28	4.53	0.94	28.11	1.97	8.69	-	-
FF3-3	35	19	3.99	0.94	25.99	1.96	8.40	-	-
FF4-1	89	25	3.14	0.68	12.86	1.73	5.57	19.23	-
FF4-2	80	27	3.53	0.74	16.33	1.81	6.28	21.44	-
FF4-3	61	31	4.50	0.91	30.29	1.95	8.35	29.28	-
FF5-1	32	19	4.06	0.96	28.53	1.97	8.65	-	-
FF5-2	61	29	3.99	0.82	23.63	1.87	7.21	26.45	-
FF5-3	36	18	3.84	0.92	20.26	1.94	8.00	-	-
FF6-1	47	23	4.14	0.92	25.96	1.94	8.20	-	-
FF6-2	35	20	4.30	0.99	206.61	2.00	9.79	-	-
FF6-3	48	21	4.25	0.97	34.19	1.98	8.96	-	-

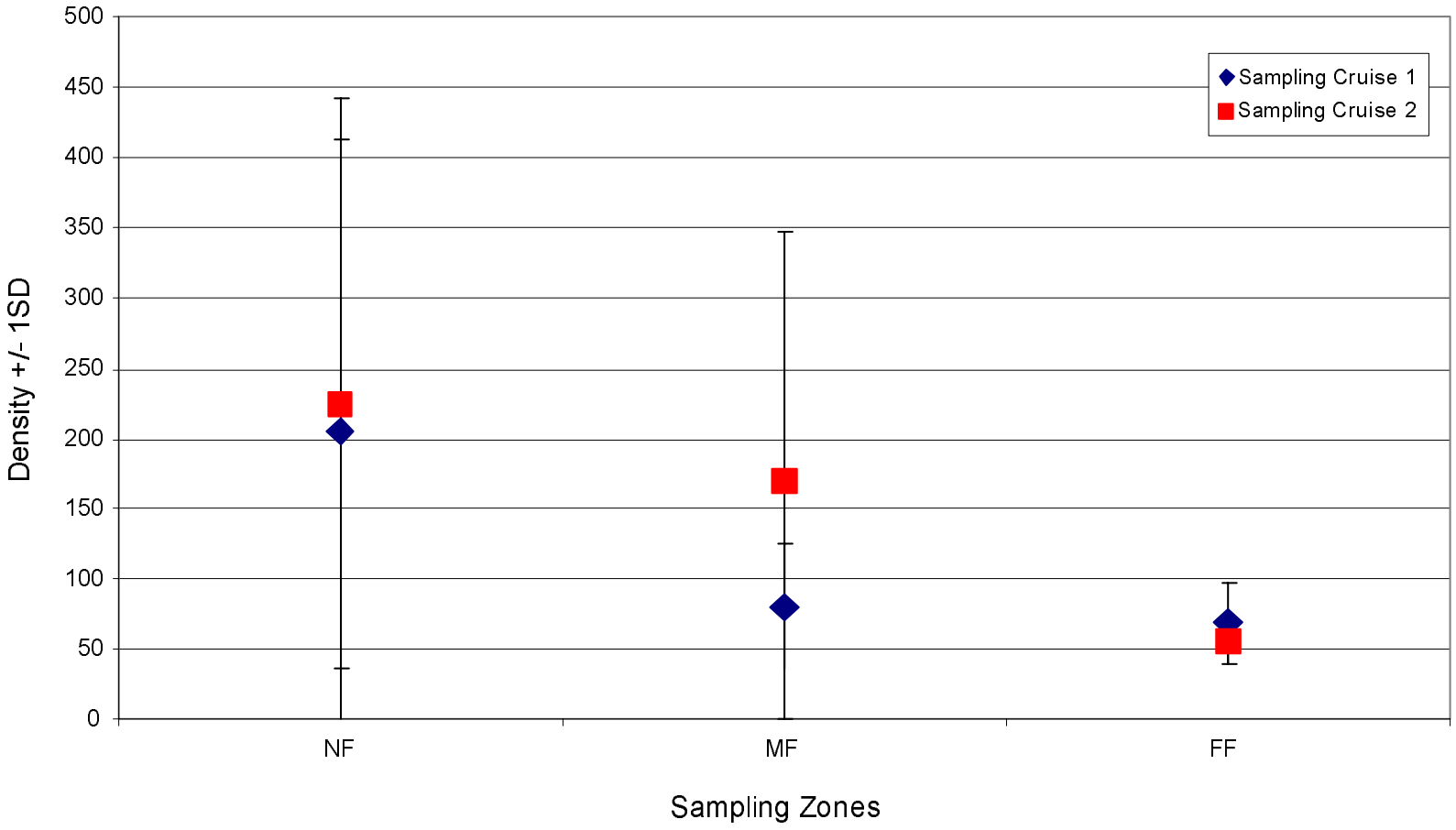

Figure 12-19. Comparison of mean infaunal densities in each of the three sampling zones (near-field [NF], mid-field [MF], and far-field [FF]) at Eugene Island 346 during Sampling Cruises 1 and 2. Densities for Sampling Cruise 1 (6 samples) were based on single samples at each station; densities for Sampling Cruise 2 (18 samples) were the mean of three replicates at each station. Database was used without deletion.

Figure 12-20 compares the density (Sampling Cruise 1) or mean density (Sampling Cruise 2) at each station in each of the three zones. During Sampling Cruise 2, the mean density of individuals per 0.1-m^2 was again highly variable in the near-field and mid-field, ranging from 17 to 428 in the near-field and from 68 to 532 in the mid-field, and less variable in the far-field, with a range from 43 to 77. Within-station variability was measured only on Sampling Cruise 2. Near-field stations NF-4 and NF-5, and to a lesser extent NF-3, showed high variability, whereas the samples from NF-1, NF-2, and NF-6 did not. Near-field stations NF-1 and NF-5 sampled on Sampling Cruise 1 and NF-6 sampled on Sampling Cruise 2 had significantly lower densities compared with other near-field stations, with the exception of NF-5 (Sampling Cruise 2), which had a range of 5 to 463 individuals in the three samples collected there. In the mid-field, MF-4 had significantly higher densities compared with other mid-field stations sampled on either Sampling Cruise 1 or Sampling Cruise 2.

12.5.3 Species Diversity and Evenness

12.5.3.1 Sampling Cruise 1. Species diversity, as measured by H' (base 2), was very low at the EI 346 near-field stations during Sampling Cruise 1. Stations NF-1 and NF-5, which had only two and three taxa, respectively, had H' values of less than 1.0. The remaining near-field stations had H' values ranging from 1.06 to 2.14, all of which can be considered to be very low. Diversity at the mid-field stations was intermediate between that found in the near-field and that found in the far-field; mid-field stations had H' values ranging between 1.19 and 4.31. Far-field stations exhibited the highest diversities, with H' values ranging from 3.46 to 4.86. Patterns in log-series *alpha* values were similar to those seen with H', with similar within- and among-zone variability.

The pattern of evenness (J') was similar to that for diversity, with the lowest values seen at the near-field stations, especially those dominated by *C. costata*, and the highest values seen at the far-field stations.

12.5.3.2 Sampling Cruise 2. Diversity and evenness values for EI 346 samples collected during Sampling Cruise 2 were generally similar to those values from the same sampling zone taken 1 year earlier (Table 12-16; Figure 12-21, A-C), with some near-field stations having the lowest diversities but considerable within-station variability. Because additional replicates were collected in each zone on Sampling Cruise 2, species richness (absolute number of taxa) was higher in all three zones. In the near-field, although one station again had only 3 taxa, the other stations had from 13 to 52 taxa, or twice as many as the maximum of 22 recorded in Sampling Cruise 1 samples. Mid-field samples ranged from 27 to 68 taxa and far-field samples from 46 to 63 taxa, representing a two- to three-fold increase in numbers of species recorded.

Shannon diversity values for EI 346 samples collected during Sampling Cruise 2 were as variable within each sampling zone as they had been during the previous Sampling Cruise (Tables 12-16 and 12-17; Figure 12-21A). Within-station variability also was very high, especially at near-field stations but also at a minimum of one station in each of the other zones (e.g., MF-6 and FF-4). Mean H' (base 2) diversities ranged from 0.87 to 3.59 in the near-field, 0.45 to 4.56 in the mid-field, and 3.72 to 4.48 in the far-field. Evenness was high at the far-field stations, and similarly high at five of the mid-field stations. All three samples from MF-4, however, had significantly lower values of evenness; this station also had the lowest diversity of any EI 346 station sampled on Sampling Cruise 2. Within-station variability of evenness was particularly high in the near-field but also was high at one or two stations in each of the other sampling zones (e.g., MF-6, FF-4).

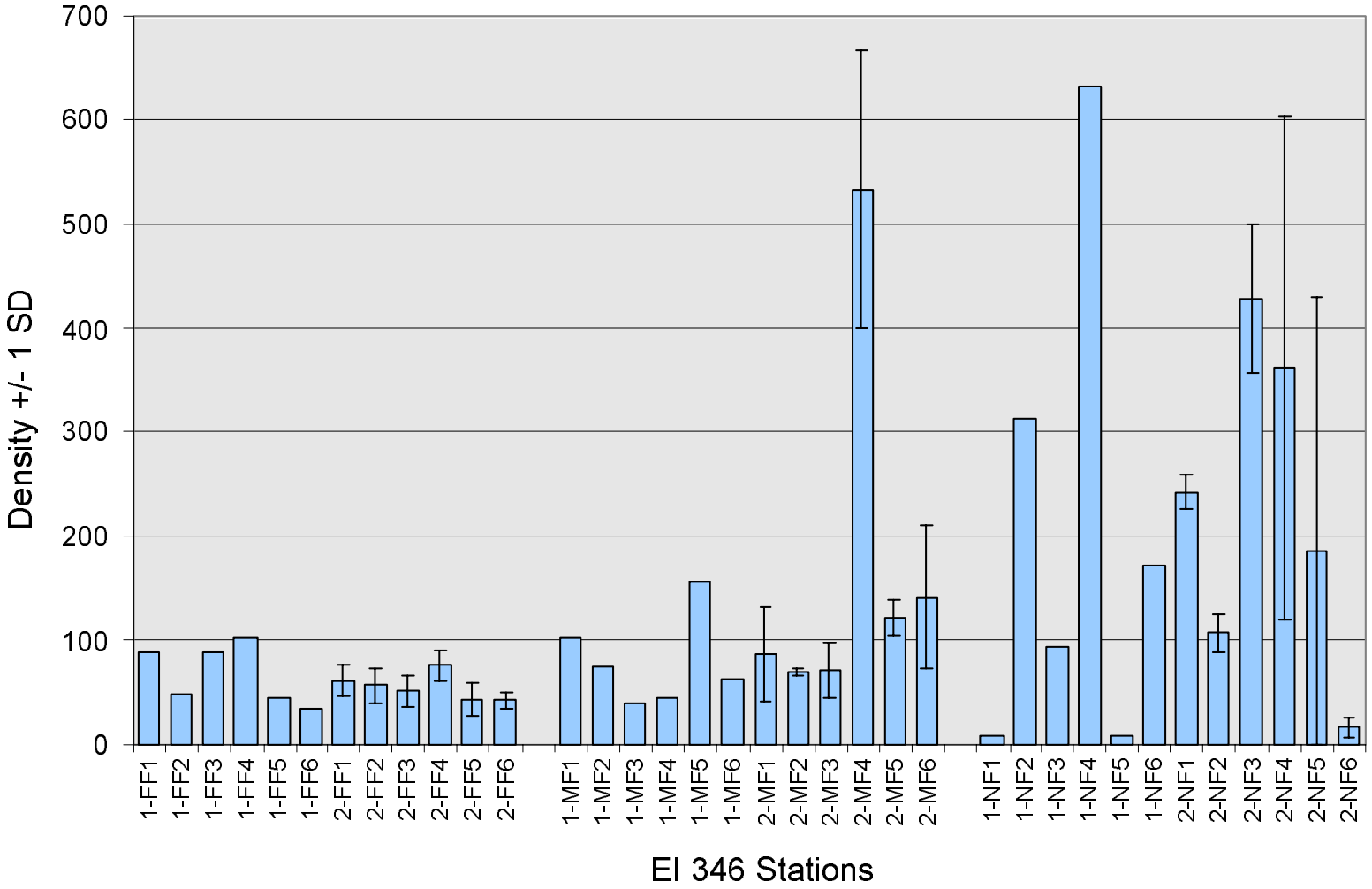

Figure 12-20. Infaunal densities at Eugene Island (EI) 346 stations. Densities for Sampling Cruise 1 (stations labeled 1-) were based on single samples at each station; densities for Sampling Cruise 2 (labeled 2-) were the mean of three replicates at each station. Database was used without deletions.

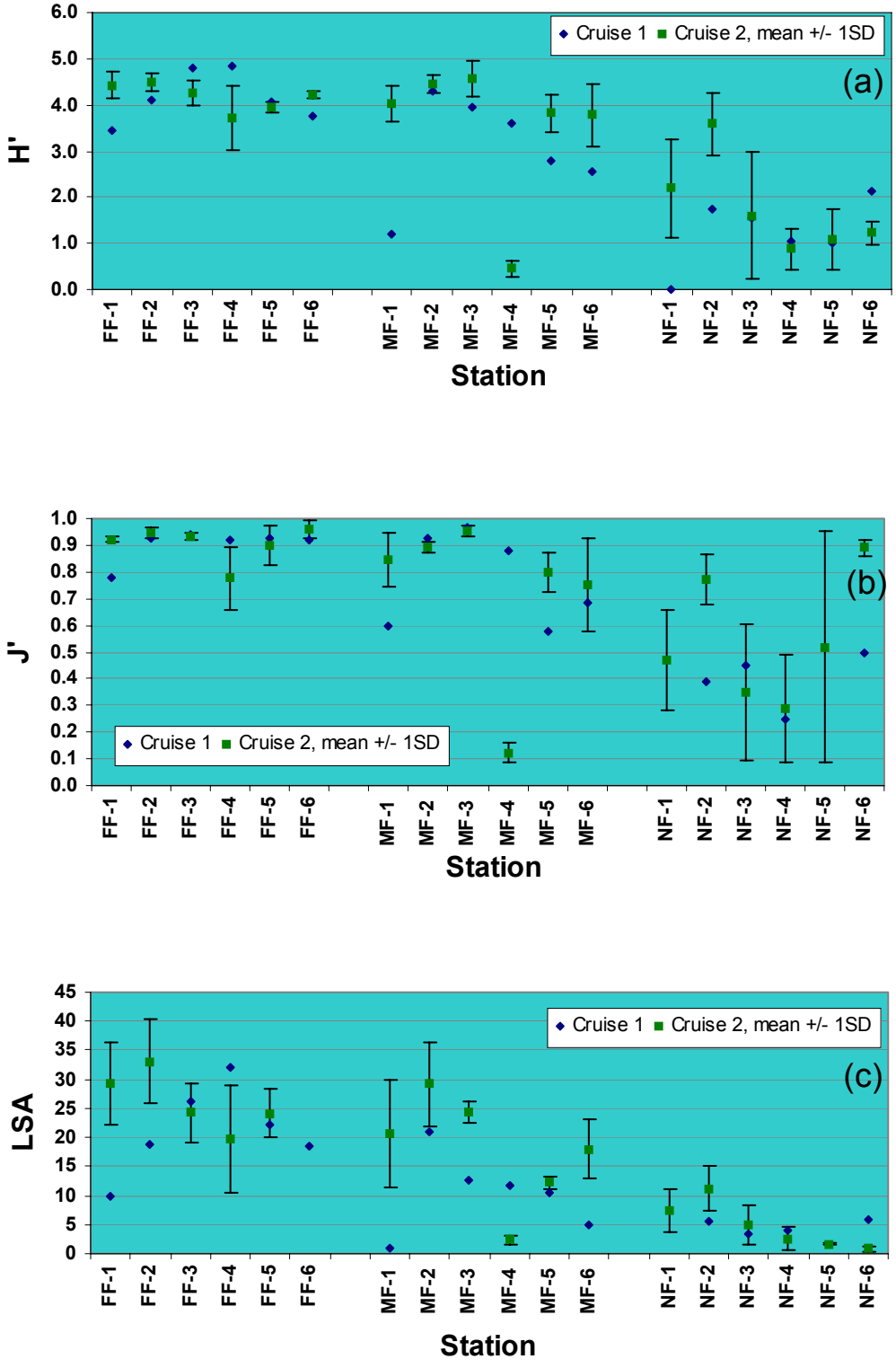

Figure 12-21. Benthic community diversity parameters at Eugene Island 346. a: Shannon diversity H'; b: Evenness J'; c: Log-series *alpha*. Values for Sampling Cruise 1 are for single samples; values for Sampling Cruise 2 are mean of three replicates +/- one standard deviation (SD). Log-series alpha value for FF-6, Sampling Cruise 2, is not plotted (see text).

Results for individual samples are presented in Table 12-17. The near-field zone had the lowest values recorded in terms of number of individuals and taxa in individual samples, with five individuals (NF-5, replicate 3) and two taxa (NF-6, replicate 2). The mid-field had the highest values in each category, with 629 individuals in MF-4, replicate 3, and 39 taxa in MF-6, replicate 2. Species diversity (H') of individual samples ranged from 0.32 to 4.34 in the near-field, from 0.32 to 4.81 in the mid-field, and from 3.14 to 4.76 in the far-field. Log-series alpha values generally tracked the trends seen with the H' values, with the highest diversities in the far-field and lower, wide-ranging values in the near- and mid-field. An extreme value of 206.61 was recorded for FF-6, replicate 2; this value appears inexplicably high and has not been plotted in Figure 12-21C.

12.5.4 Rarefaction

The rarefaction technique produces curves that illustrate the diversity of each sample by estimating the number of species that would be found if *n* number of individuals were pulled at random from the sample. The curves produced for both the Sampling Cruise 1 and Sampling Cruise 2 samples are shown in Figures 12-22 through 12-24. Curves labeled 1 to 6 correspond to Stations 1 to 6 sampled during Sampling Cruise 1, and curves labeled 7 to 12 correspond to pooled replicates from the same stations (i.e., Stations 1 to 6) taken during Sampling Cruise 2. Values for the estimated number of species at four points (if the number of individuals in the sample allows calculation) are presented in Tables 12-15 through 12-17.

The near-field samples were variable in the shape and slope of the rarefaction curves. Some samples had such a small number of individuals that the lines are essentially non-existent, (NF-1, Sampling Cruise 1) or flat (NF-6, Sampling Cruise 2). In the mid-field, the Sampling Cruise 1 sample from MF-1 has an extremely low diversity, but the shape of the curve implies that no additional species will be collected through additional sampling. With the exception of MF-4, Sampling Cruise 2 (labeled 10), the other mid-field stations appear to be undersampled, even with three replicates. The curves for the far-field samples show that the majority of stations had similar diversities, in contrast to the more variable near-field and mid-field.

12.5.5 Community Assemblage Patterns

Figure 12-25 shows the patterns resulting from cluster analysis of the EI 346 samples using the CNESS clustering algorithms. The lower the level at which two samples join, the more similar those two samples are to each other. Samples with fewer than ten individuals were dropped. All of the samples taken during Sampling Cruise 1 cluster separately from the samples taken during Sampling Cruise 2. The stations tended to cluster into three groups, according to the distance from the drillsite. The six far-field stations group together, although at very low levels of similarity, with two mid-field samples joining the group. The remaining four mid-field samples cluster together, with samples MF-1 and MF-6 showing a high level of similarity. The four near-field samples form a third unique group. Samples NF-2 and NF-4, which had large numbers of the dominant bivalve *Codakia costata*, form a highly similar sample pair.

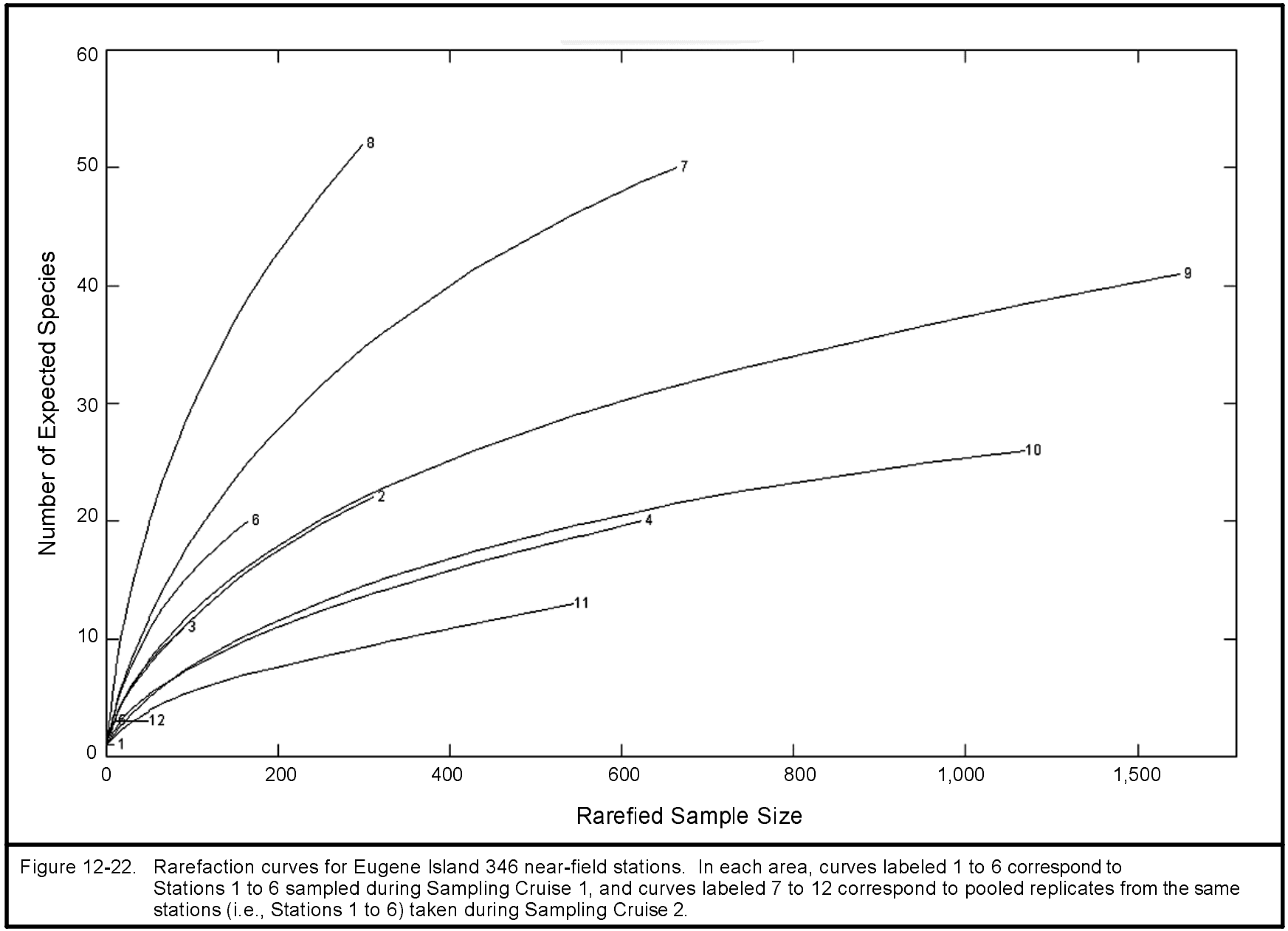

Figure 12-22. Rarefaction curves for Eugene Island 346 near-field stations. In each area, curves labeled 1 to 6 correspond to Stations 1 to 6 sampled during Sampling Cruise 1, and curves labeled 7 to 12 correspond to pooled replicates from the same stations (i.e., Stations 1 to 6) taken during Sampling Cruise 2.

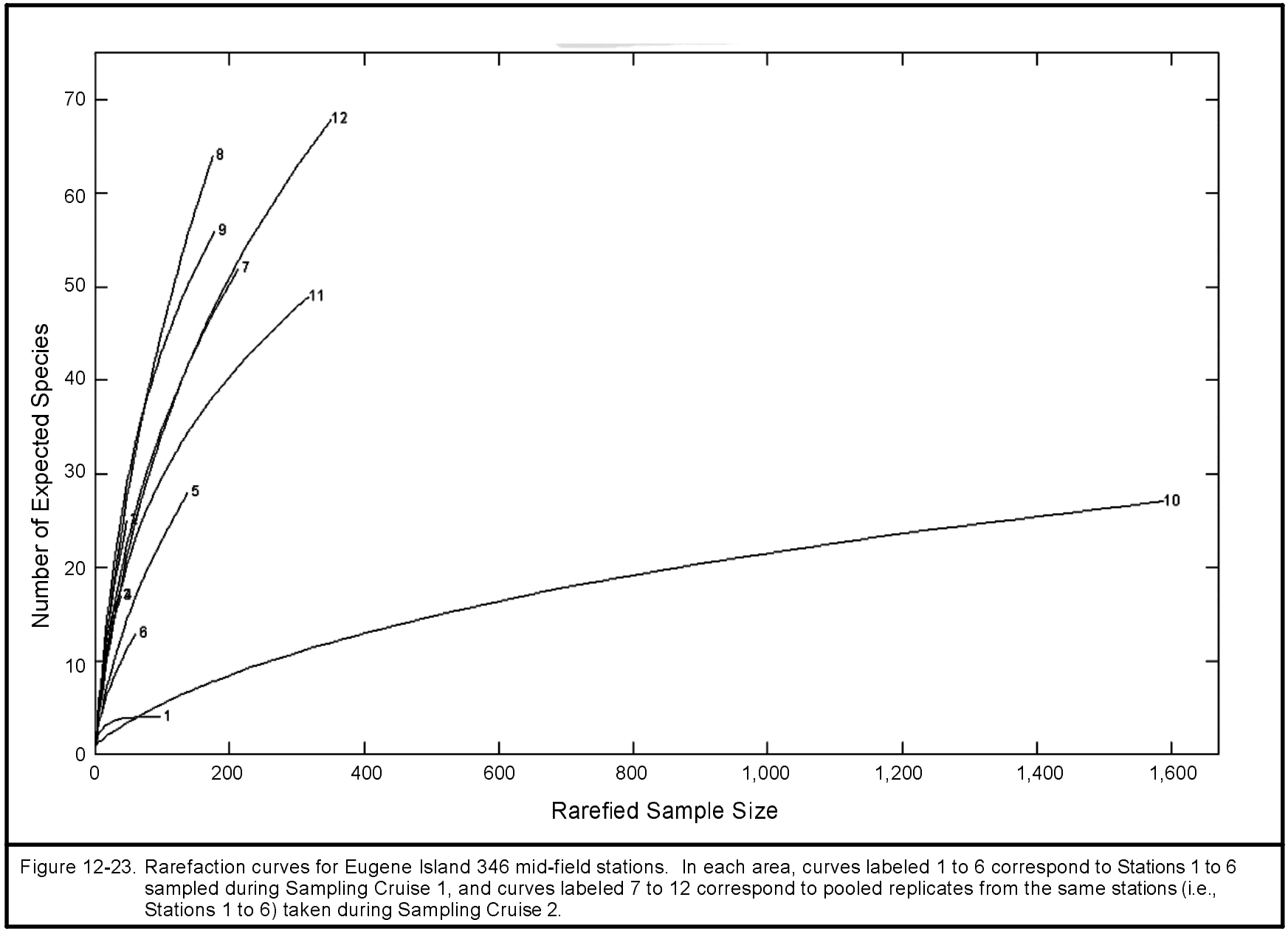

Figure 12-23. Rarefaction curves for Eugene Island 346 mid-field stations. In each area, curves labeled 1 to 6 correspond to Stations 1 to 6 sampled during Sampling Cruise 1, and curves labeled 7 to 12 correspond to pooled replicates from the same stations (i.e., Stations 1 to 6) taken during Sampling Cruise 2.

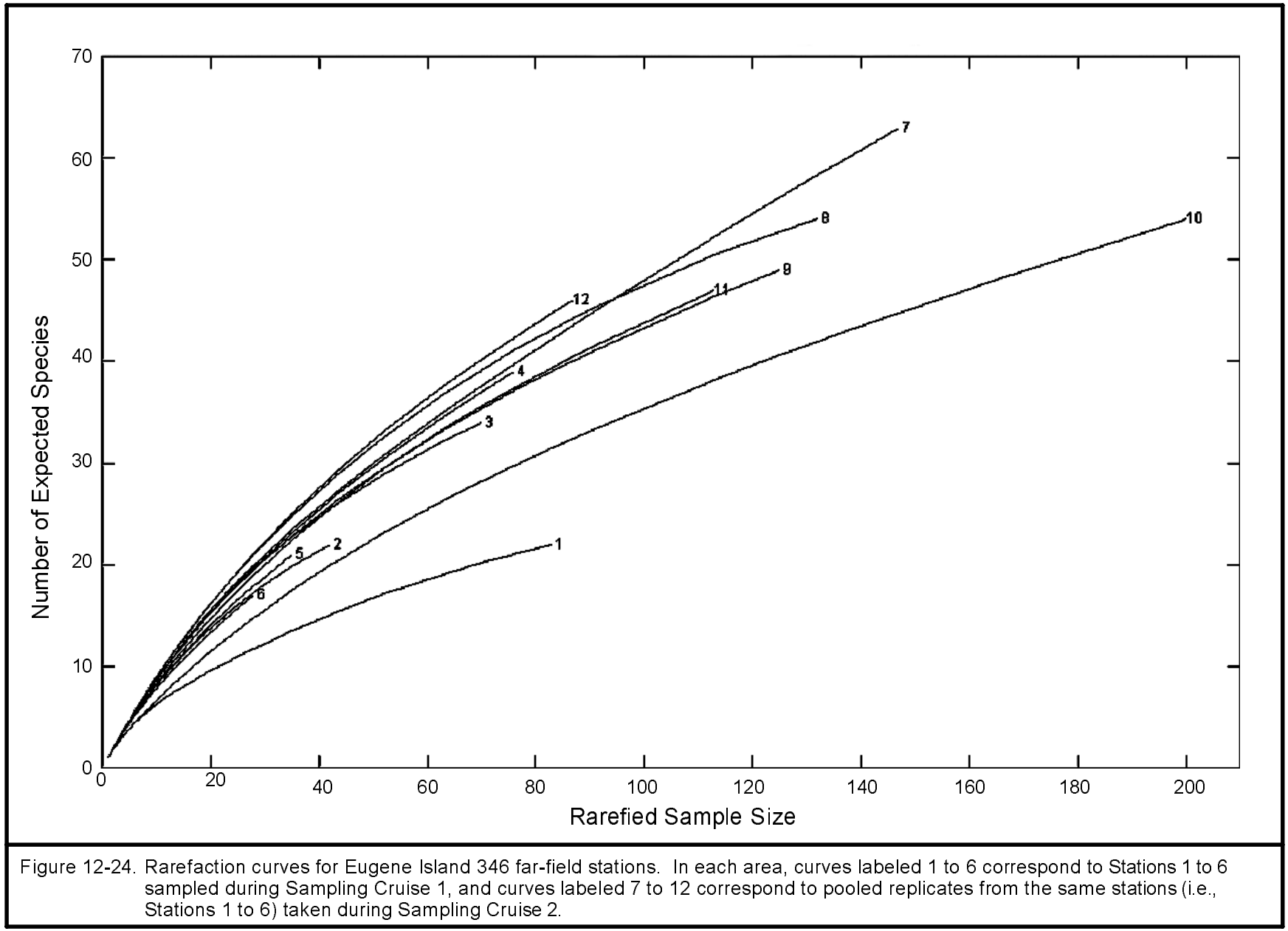

Figure 12-24. Rarefaction curves for Eugene Island 346 far-field stations. In each area, curves labeled 1 to 6 correspond to Stations 1 to 6 sampled during Sampling Cruise 1, and curves labeled 7 to 12 correspond to pooled replicates from the same stations (i.e., Stations 1 to 6) taken during Sampling Cruise 2.

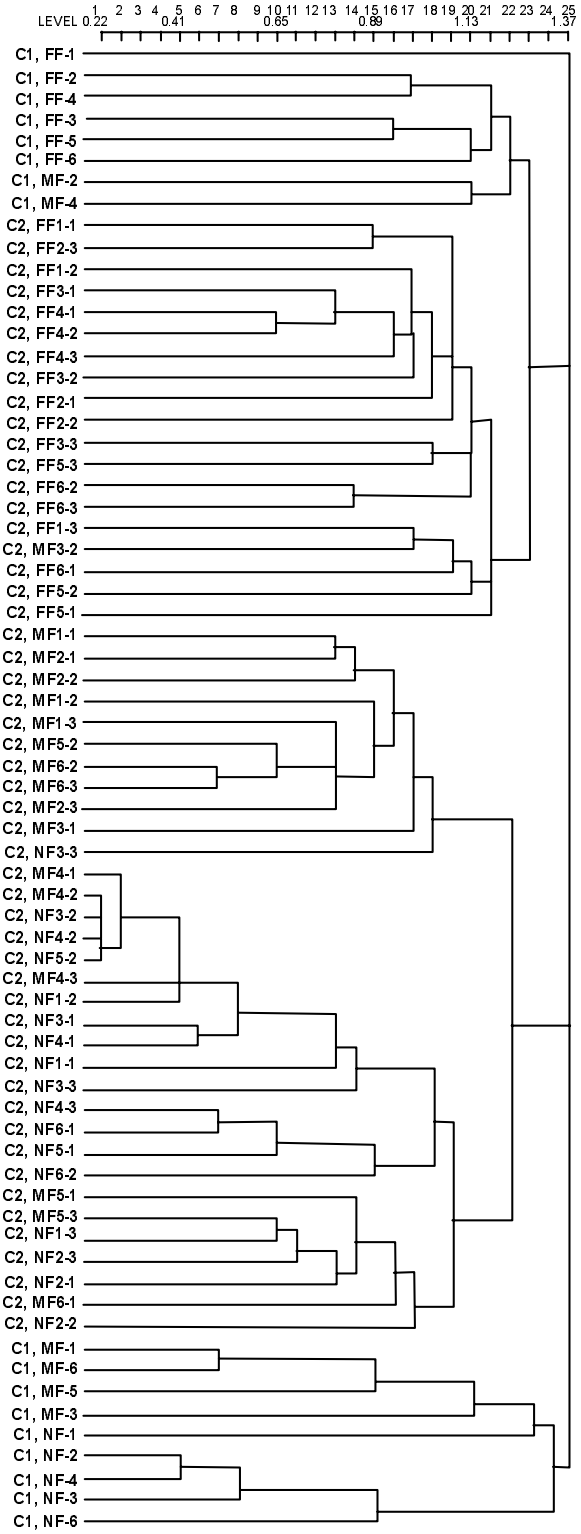

Figure 12-25. Cluster dendrogram for Eugene Island 346. Sample label C1 indicates Sampling Cruise 1 and C2 indicates Sampling Cruise 2.

All of the far-field samples form a major group within the cluster diagram. These samples are not very similar to each other, but along with two mid-field samples taken during Sampling Cruise 1, they do form a cohesive unit that differs from samples taken in the other sampling zones. The mid-field and near-field samples taken during Sampling Cruise 2 form a major group with two subgroups, each comprising a mix of samples from each zone. Samples MF4-1, MF4-2, NF3-2, and NF4-2 are very similar; these samples were characterized by large numbers of the bivalve *Lucina radians*.

This analysis suggests that the far-field fauna differs markedly from that found in the near-field and mid-field zones, and secondly, that the samples taken during Sampling Cruise 1 differ from those taken a year later during Sampling Cruise 2.

Results of the MDS analysis of the EI 346 samples agreed with those from the cluster analysis. The stress value for this MDS was 0.15, which indicates a useful 2-dimensional representation of the relationships among the samples. In addition to the distinction between the two cruises, which indicated temporal differences, there was a clear relationship among the three zones (Figure 12-26). For the individual cruises, the near-field samples were distinctly different from the far-field samples. Mid-field samples tended to be intermediate between the near-field and far-field samples. These results indicated that recovery of the near-field and mid-field had not progressed as far as was observed at the other two study sites.

12.5.6 Sediment Characteristics

Sediment grain size and TOC data were plotted in order to examine whether differences in these characteristics might explain some of the differences seen in the benthic infaunal communities. Figure 12-27 shows the highly variable sediment grain size composition and TOC content of the sediments at EI 346. The highest TOC recorded in this program, slightly more than 6%, was recorded at NF-4 during Sampling Cruise 1. Values of TOC during Sampling Cruise 1 at NF-5 and MF-6 also were high, 5.61% and 5.21%, respectively. A year later, during Sampling Cruise 2, mean TOC values at all stations were 3%. Sediment grain size composition within each zone was even more variable than TOC content. Sediment types ranged from clay (mean phi around 8 or 9) to sandy mud (mean phi around 5).

12.5.7 Eugene Island 346 Summary

1. Infaunal densities were highly variable at EI 346 stations, especially in the near-field. Compared with Sampling Cruise 1, mean densities during Sampling Cruise 2 were similar in the near-field and far-field zones but were significantly higher in the mid-field.

2. The near-field and mid-field stations were highly dominated during both Sampling Cruises by bivalves. In the near-field, *Codakia costata* and *Lucina radians* accounted for over 70% of the near-field fauna during Sampling Cruise 1 and Sampling Cruise 2, respectively. In the mid-field, *L. multilineata* and *L. radians* accounted for 37% and 50% of the fauna during Sampling Cruise 1 and Sampling Cruise 2, respectively. Dominant species at the far-field stations differed from those in the other zones and were more evenly distributed.

3. Species diversity was very low at the near-field stations during both Sampling Cruises; these stations often had only two or three taxa present in the samples. Diversity was highest in the far-field and was generally similar during Sampling Cruise 2 compared with Sampling Cruise 1.

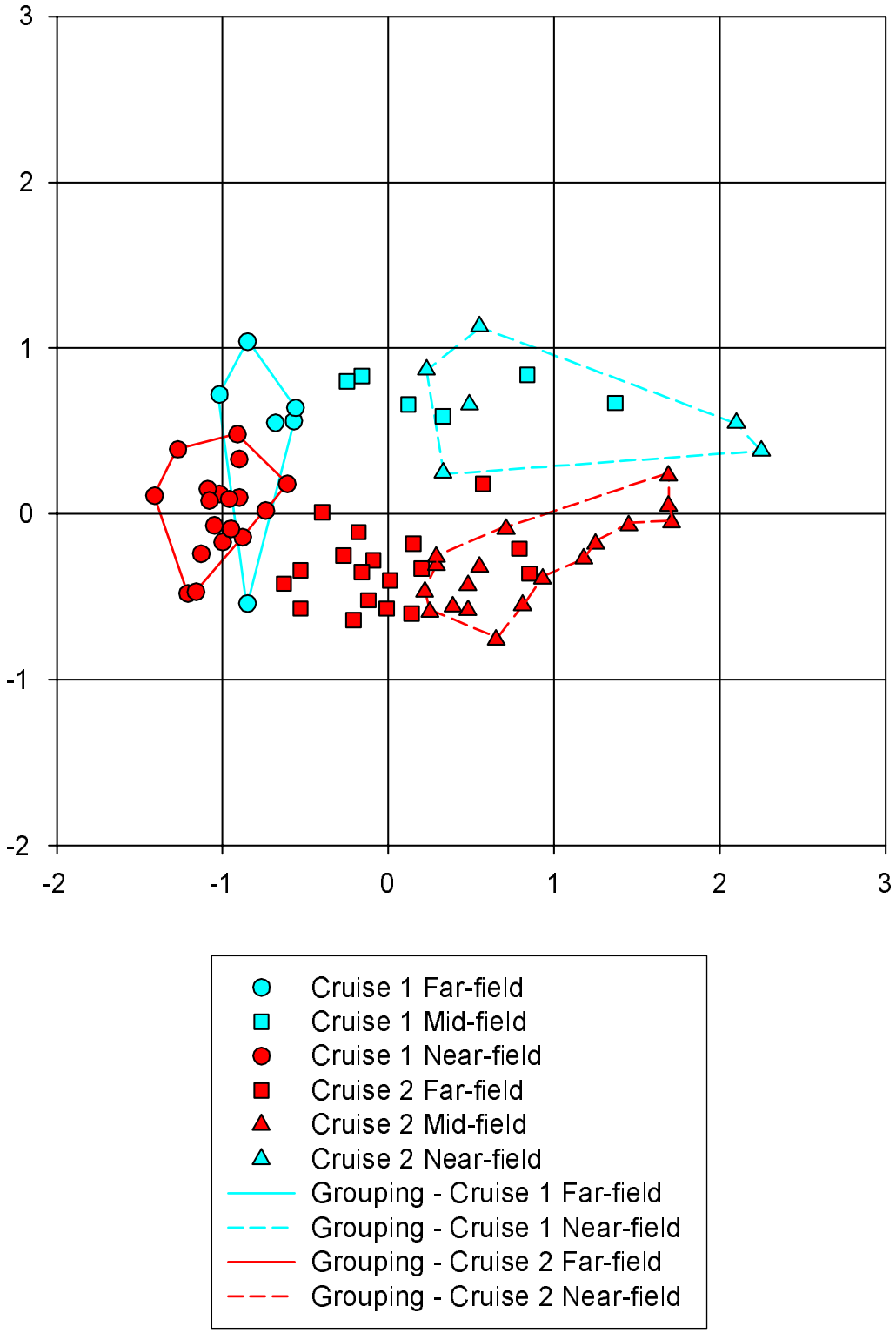

Figure 12-26. Results of nonmetric multidimensional scaling analysis for Eugene Island 346.

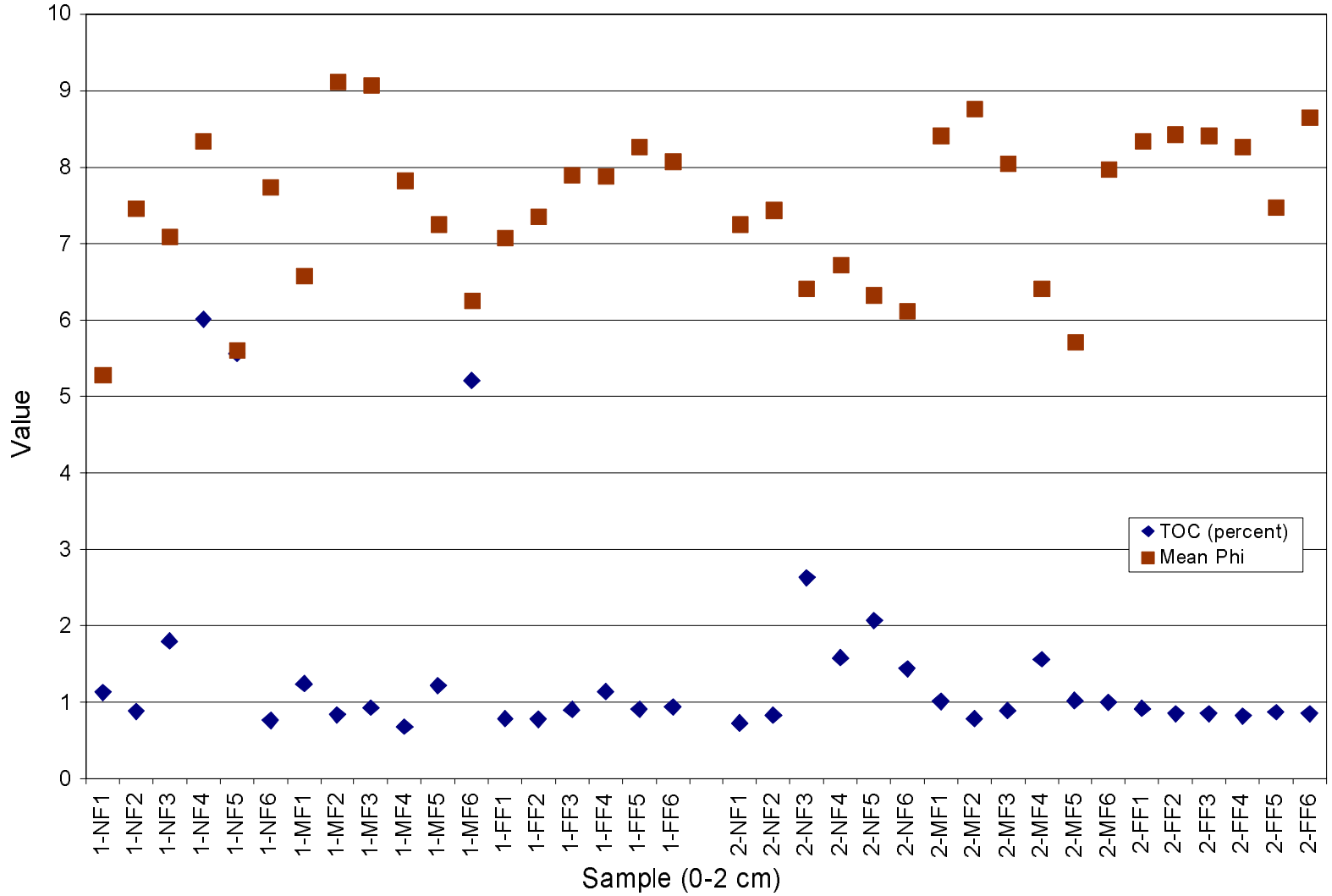

Figure 12-27. Total organic carbon (TOC) and mean phi of sediments at Eugene Island 346. Values represent the top 2 cm of sediment taken from single samples.

4. Rarefaction diversity curves reflect the variability found in the infaunal communities, with many mid-field and near-field samples having steeply sloping curves that indicate the fauna is undersampled, while others had very short but flat curves, indicating a low diversity and low expected species richness.

5. Multivariate cluster analysis of individual samples indicated both temporal and spatial differences, with the far-field samples in particular forming a distinct group. MDS analysis indicated that there were temporal and spatial differences. The intermediate position of the mid-field samples between the far-field samples and the near-field samples was evident at this site.

6. Sediment texture was highly variable at all stations, ranging from clay to sandy mud. Total organic carbon content was high at some near-field stations during Sampling Cruise 1 but was low at all stations during Sampling Cruise 2.

7. Concentrations of contaminants associated with drilling muds (Ba, TPH, and SBFs) were higher at EI 346 than at the two Main Pass sites. It is possible that drilling activities associated with alteration of the sediment (drilling muds, anchors, cables) account for reduced species diversity and faunal variability in the near-field and mid-field locations.

Conclusion: *The EI 346 area is characterized by high variability in all parameters examined, on both spatial and temporal scales. The extreme variability in sediment texture probably accounts for the differences in species composition between the far-field zone and the stations closer to the drilling site. It is possible that activities associated with drilling, including location of anchors, movement of cables, and deposition of drilling muds, can account for some of the faunal variability in the near-field and mid-field zones.*

12.6 SUMMARY

Benthic communities were studied at three locations in the Gulf of Mexico with the objective of determining whether SBMs have any effect on the infaunal communities. Two of the three sites were sampled on a Screening Cruise and then twice again, a year apart, during Sampling Cruise 1 (May 2001) and Sampling Cruise 2 (2002) to document the species composition and abundance of the infauna. The third site was sampled only during the Sampling Cruises. At each site, samples were collected in designated near-field, mid-field, and far-field zones, each being farther from the central drilling site where SBMs were discharged.

For all three study sites, meeting the study objective was hampered by the difficulty in identification of some organisms found in the samples. Only approximately 60% to 80% of the organisms were identified to species (MP 288: 59.3%, MP 299: 65.8%, EI 346: 78.6%); this is well below the expected 90% to 95% necessary for definitive evaluation of the composition of such communities. The low level of taxonomic discrimination assuredly resulted in higher levels of similarity among stations than would be the case if a higher percentage of organisms had been identified to species level. Even with these limitations, certain patterns were evident in the data from each of the study sites.

At MP 288, the majority of far-field stations, whether sampled in May 2001 or May 2002, differed considerably from the near-field and mid-field stations, which in several instances exhibited high similarity between areas. Also, with only a few exceptions, the near-field and mid-field samples

tended to be more similar to samples collected on the same Sampling Cruise than to samples collected on the alternate Sampling Cruise. Further differentiating the far-field from the other zones, infaunal abundance was highly variable among far-field stations, which exhibited both the highest and lowest abundances recorded at this site. The difference in species composition among the far-field stations is probably related to differences in sediment grain size composition. Several of the far-field stations had extremely coarse sediments, whereas the remaining stations had fine sediments with a high percentage of silt-plus-clay. The benthic community composition of those far-field stations that did have fine-grained sediments was similar to that of the near- and mid-field stations. Diversity and evenness values for samples collected on Sampling Cruise 2 were generally similar to those values from the same zone taken 1 year earlier. Rarefaction analysis indicated that for both cruises, there was no clear trend in diversity because the within-zone variability of diversity was as great or greater than the among-zone variability. The dominant organism at the near-field stations changed between the time of the Screening Cruise and the time of Sampling Cruise 1. In August 2000, the opheliid polychaete *Armandia maculata* accounted for nearly 24% of the infauna, whereas in later collections the spionid *Paraprionospio pinnata* generally dominated both the near-field and mid-field communities. *Paraprionospio pinnata* is a common and widespread species in many Gulf of Mexico habitats. Neither *Armandia* nor *Paraprionospio* are considered to be indicative of disturbed or organically enriched environments.

At MP 299, within-station variability was very high in all three sampling zones in terms of the number of organisms found in the sediments, and there was no significant difference in densities among the sampling zones. Similarly, densities from Sampling Cruise 2 were not statistically different from those recorded from Sampling Cruise 1, and calculated community parameters such as species diversity at the near-field stations also were similar between Sampling Cruises 1 and 2. However, the species composition of the benthic communities changed considerably between the Screening Cruise and Sampling Cruise 1 and also between the two Sampling Cruises. This change was reflected in the separation of the Sampling Cruises in multivariate community analysis. An opportunistic species, *Capitella capitata*, accounted for over half the individuals collected on the Screening Cruise but only for 9.7% during Sampling Cruise 1 and was not a numerical dominant during Sampling Cruise 2, suggesting an improvement in benthic conditions. None of the numerically dominant species during Sampling Cruise 2 are considered opportunistic. The scaphopod mollusk *Cadulus arctus* dominated samples in all three zones. Differences in mean phi and percent TOC of the sediments do not appear to account for the differences in species composition as they did at MP 288.

Eugene Island 346 was characterized by high variability in all parameters examined, on both spatial and temporal scales. Far-field samples in particular differed from the near-field and mid-field samples, both in terms of species composition and calculated parameters. Sediment texture was extremely variable at all stations, ranging from clay to sandy mud, and this variability probably accounted for the differences among target areas. Species richness and diversity were very low at the near-field stations during both Sampling Cruises; these stations often had only two or three taxa present in the samples. Diversity was highest in the far-field and was generally similar on Sampling Cruise 2 compared with Sampling Cruise 1. The near-field and mid-field stations were highly dominated during both Sampling Cruises by bivalves, including *Codakia costata* and species of *Lucina*. Dominant species at the far-field stations differed from those in the other areas and were more evenly distributed in the samples. Concentrations of contaminants associated with drilling muds (Ba, TPH, and SBF) were higher at EI 346 than at the two Main Pass sites, and it is possible that drilling activities associated with alteration of the sediment (deposition of drilling muds, location of anchors, movement of cables)

can account for reduced species diversity and faunal variability in the near-field and mid-field locations at the Eugene Island study site.

All three study sites showed spatial differences among zones, with the near-field and mid-field stations often similar to each other but the far-field stations usually having a different sediment type and therefore different species composition. Temporal differences were also observed at all three sites, with the species composition often changing between Sampling Cruises but the calculated diversity values remaining similar. Species composition of benthic communities is known to be related to sediment grain size composition, and many of the differences in the communities studied in this project can be related to variability in sediment parameters at the study sites.

Chapter 13
REFERENCES

American Petroleum Institute (API). 1989. *Fate and Effects of Drilling Fluid and Cuttings Discharges in Shallow, Nearshore Waters*. API Publication 4480. Report prepared by Continental Shelf Associates, Inc., Jupiter, FL, Geochemical and Environmental Research Group, College Station, TX, and Barry A. Vittor & Associates, Inc., Mobile, AL.

American Society for Testing and Materials (ASTM). 1992. *Standard Guide for Conducting 10-Day Static Sediment Toxicity Tests with Marine and Estuarine Amphipods.* ASTM E1367-92. American Society for Testing and Materials, Philadelphia, PA.

American Society for Testing and Materials (ASTM). 1999. *Method E 1367-99, Standard Guide for Conducting 10-day Static Sediment Toxicity Tests with Marine and Estuarine Amphipods*. ASTM West Conshohocken, PA.

Annis, M.R. 1997. *Retention of Synthetic-Based Drilling Material on Cuttings Discharged to the Gulf of Mexico*. Report for the American Petroleum Institute (API) *ad hoc* Retention on Cuttings Work Group under the API Production Effluent Guidelines Task Force. American Petroleum Institute, Washington, D.C. Various pages.

Battelle. 2000. *Acute Toxicity Testing of the Gulf of Mexico Synthetic-Based Drilling Muds, 2000 Screening Study*. Draft Report submitted to Continental Shelf Associates, Inc.

Battelle. 2001. *Acute Toxicity Testing of the Gulf of Mexico Synthetic-Based Drilling Muds, 2001 Cruise I*. Draft Report submitted to Continental Shelf Associates, Inc.

Battelle. 2002. *Acute Toxicity Testing of the Gulf of Mexico Synthetic-Based Drilling Muds, 2002 Cruise II*. Draft Report submitted to Continental Shelf Associates, Inc.

Bender, M.L., W. Martin, J. Hess, F. Sayles, L. Ball, and C. Lambert. 1987. A Whole-Core Squeezer for Interfacial Pore Water Sampling. *Limnology and Oceanography*. 32:1,214-1,225.

Blake, J.A. 2000. Family Opheliidae Malmgren, 1867. In J.A. Blake, B. Hilbig, and P.V. Scott, eds. *Volume 7. The Annelida Part 4 — Polychaeta: Flabelligeridae to Sternaspidae. Taxonomic Atlas of the Benthic Fauna of the Santa Maria Basin and Western Santa Barbara Channel*. Santa Barbara Museum of Natural History. pp. 145-168.

Bloys, B., N. Davis, B. Smolen, L. Bailey, O. Houwen, P. Reid, J. Sherwood, L. Fraser, and M. Hodder. 1994. Designing and Managing Drilling Fluid. *Oilfield Review.* April 1994:33-43.

Bonsdorff, E., R.J. Diaz, R. Rosenberg, A. Norkko, and G.R. Cutter. 1996. Characterization of Soft-Bottom Benthic Habitats of the Åland Islands, Northern Baltic Sea. *Marine Ecology Progress Series*. 142:235-245.

Boothe, P.N. and B.J. Presley. 1985. *Distribution and Behavior of Drilling Fluids and Cuttings Around Gulf of Mexico Drilling Sites*. American Petroleum Institute, Washington, D.C.

Boothe, P.N. and B.J. Presley. 1989. Trends in Sediment Trace Element Concentrations Around Six Petroleum Drilling Platforms in the Northwestern Gulf of Mexico. In F.R. Engelhardt, J.P. Ray, and A.H. Gilliam, eds. *Drilling Wastes*. Elsevier Applied Science, London. pp. 3-22.

Borja, A., J. Franco, and V. Pérez. 2000. A Marine Biotic Index to Establish the Ecological Quality of Soft-Bottom Benthos within European Estuarine and Coastal Environments. *Marine Pollution Bulletin.* 40:1,100-1,114.

Borja, A., I. Mixika, and J. Franco. 2003. The Application of a Marine Biotic Index to Different Impact Sources Affecting Soft-Bottom Benthic Communities Along European Coasts. *Marine Pollution Bulletin.* 46:835-845.

Brandsma, M.G. 1996. Computer Simulations of Oil-Based Mud Cuttings Discharges in the North Sea. In *The Physical and Biological Effects of Processed Oily Drill Cuttings (Summary Report).* E&P Forum, London. pp. 25-40.

Brannon, J.M., D. Gunnison, R.M. Smart, and R.L. Chen. 1984. Effects of Added Organic Matter on Iron and Manganese Redox Systems in Sediment. *Geomicrobiology Journal.* 3:319-341.

Breuer, E., J.A. Howe, G.B. Shimmield, D. Cummings, and J. Carroll. 1999. *Contaminant Leaching from Drill Cuttings Piles of the Northern and Central North Sea: A Review*. Report to NERC and UKOOA from the Scottish Association for Marine Science, Dunstaffnage Marine Laboratory, Oban, Scotland. 49 pp.

Brownlow, A.H. 1979. *Geochemistry*. Prentice Hall, Edgewood Cliff, NJ.

Burke, C.J. and J.A. Veil. 1995. Synthetic-Based Drilling Fluids Have Many Environmental Pluses. *Oil & Gas Journal*. 93:59-64.

Candler, J.E., J.H. Rushing, and A.J. Leuterman. 1993. *Synthetic-Based Mud Systems Offer Environmental Benefits Over Traditional Mud Systems*. SPE 259993. SPE/EPA Exploration and Production Environmental Conference, San Antonio, TX. Society of Petroleum Engineers, Inc., Richardson, TX.

Candler, J.E., S. Hoskin, M. Churan, C.W. Lai, and M. Freeman. 1995. Seafloor Monitoring for Synthetic-Based Mud Discharged in the Western Gulf of Mexico. In *SPE/EPA Exploration & Production Environment Conference*. Houston, TX, 27-29 March 1995. SPE 29694. Society of Petroleum Engineers, Inc., Richardson, TX. pp. 51-69.

Candler, J., R. Hebert, and A.J.J. Leuterman. 1997. Effectiveness of a 10-day ASTM Amphipod Sediment Test to Screen Drilling Mud Base Fluids for Benthic Toxicity. In *1997 SPE/EPA Exploration and Production Environmental Conference*. Dallas, TX, 3-5 March 1997. SPE 37890. Society of Petroleum Engineers, Inc., Richardson, TX. 19 pp.

Chapman, P.M. and E.R. Long. 1983. The Use of Bioassays as Part of a Comprehensive Approach to Marine Pollution Assessment. *Marine Pollution Bulletin.* 14:81-84.

Chapman, P.M., E.A. Power, R.N. Dexter, and H.B. Anderson. 1991. Evaluation of Effects Associated with an Oil Platform, Using the Sediment Quality Triad. *Environmental Toxicology and Chemistry.* 10:407-424.

Chapman, P.M., B. Anderson, S. Carr, V. Engle, R. Green, J. Hameedi, M. Harmon, P. Haverland, J. Hyland, C. Ingersoll, E. Long, J. Rodgers, Jr., M. Salazar, P.K. Sibley, P.J. Smith, R.C. Swartz, B. Thompson, and H. Windom. 1997. General Guidelines for Using the Sediment Quality Triad. *Marine Pollution Bulletin*. 34:368-372.

Churan, M., J.E. Candler, and M. Freeman. 1997. *Onsite and Offsite Monitoring of Synthetic-Based Drilling Fluids for Oil Contamination.* In Proceedings of the 1997 SPE/EPA Exploration and Production Environmental Conference. Society of Petroleum Engineers, Inc., Richardson, TX. pp. 179-192.

Clarke, K.R. and R.M. Warwick. 2001. *Change in Marine Communities: An Approach to Statistical Analysis and Interpretation.* 2nd Edition. PRIMER-E Ltd, Plymouth, United Kingdom.

Clesceri, P.R., A.E. Greenberg, and R.R. Trussel. 1989. *Standard Methods for the Examination of Water and Wastewater*. American Public Health Association.

Cogen, W.M. 1940. Heavy Mineral Zones of Louisiana and Texas Gulf Coast Sediments. *Bulletin of the American Association of Petroleum Geologists.* 24:2,069-2,101.

Cohen, J. 1977. *Statistical Power Analysis for the Behavioral Sciences.* Revised Edition. Academic Press, NY. 474 pp.

Constable, M., M. Charlton, F. Jensen, K. McDonald, G. Craig, and K.W. Taylor. 2003. An Ecological Risk Assessment of Ammonia in the Aquatic Environment. *Human and Ecological Risk Assessment*. 9:527-548.

Continental Shelf Associates, Inc. 1983. *Environmental Monitoring Program for Exploratory Well No. 3, Lease OCS-G 3316, Block A-384, High Island Area, South Extension Near the West Flower Garden Bank*. Final Report to Union Oil Co. 2 Volumes.

Continental Shelf Associates, Inc. 2000. *Post-Screening Cruise Data Report for the Gulf of Mexico Comprehensive Synthetic Based Muds Monitoring Program.* Prepared for the SBM Research Group. 80 pp.

Continental Shelf Associates, Inc. 2002. *Sampling Cruise 1 Data Report, Gulf of Mexico Comprehensive Synthetic Based Muds Monitoring Program*. Prepared for the SBM Research Group. 95 pp. + apps.

Cordah. 1998. *Review of Drill Cuttings Piles in the North Sea*. Report for the Offshore Decommissioning Communications Project. Cordah Environmental Consultants, Aberdeen Scotland. 90 pp.

Cornwell, J.C. and J.W. Morse. 1987. The Characterization of Iron Sulfide Minerals in Anoxic Marine Sediments. *Marine Chemistry.* 22:193-206.

Cranfield, D.E. 1989. Reactive Iron in Marine Sediments. *Geochimica et Cosmochimica Acta.* 53:619-632.

Daan, R., K. Booij, M. Mulder, and E.M. van Weerlee. 1996. Environmental Effects of a Discharge of Drill Cuttings Contaminated with Ester-Based Drilling Muds in the North Sea. *Environmental Toxicology and Chemistry*. 15:1,709-1,722.

Dando, P.R. and A.J. Southward. 1986. Chemoautotrophy in Bivalve Molluscs of the Genus *Thyasira*. *Journal of the Marine Biological Association of the United Kingdom.* 66:915-929.

Delvigne, G.A.L. 1996. Laboratory Investigations on the Fate and Physicochemical Properties of Drill Cuttings After Discharge into the Sea. In *The Physical and Biological Effects of Processed Oily Drill Cuttings (Summary Report).* E&P Forum, London. pp. 16-24.

Diaz, R.J. and R. Rosenberg. 1995. Marine Benthic Hypoxia: A Review of Its Ecological Effects and the Behavioural Responses of Benthic Macrofauna. *Oceanography and Marine Biology Annual Review*. 33:245-303.

Diaz, R.J. and L.C. Schaffner. 1988. Comparison of Sediment Landscapes in the Chesapeake Bay as Seen by Surface and Profile Imaging. In M.P. Lynch and E.C. Krome, eds. *Understanding the Estuary; Advances in Chesapeake Bay Research*. Chesapeake Res. Consort. Pub. 129, CBP/TRS 24/88. pp. 222-240.

Diaz, R.J., G.R. Cutter, and D.C. Rhoads. 1994. The Importance of Bioturbation to Continental Slope Sediment Structure and Benthic Processes off Cape Hatteras, North Carolina. *Deep-Sea Research II*. 41:719-734.

Drever, J.I. 1997. *The Geochemistry of Natural Waters*. Prentice Hall, Upper Saddle River, NJ.

Eagle, R.A. and E.I.S. Rees. 1973. Indicator Species – A Case for Caution. *Marine Pollution Bulletin.* 4(2):25.

Environmental & Resource Technology Ltd. (ERT Ltd.). 1994. *Bioconcentration Assessment Report. Assessment of the Bioconcentration Factor (BCF) of ISO-TEQ Base Fluid in the Blue Mussel* Mitilus edulis. ERT 94/061. Report to Baker Hughes INTEQ, Houston, TX.

Fechhelm, R.G., B.J. Gallaway, and J.M. Farmer. 1999. Deepwater Sampling at a Synthetic Drilling Mud Discharge Site on the Outer Continental Shelf, Northern Gulf of Mexico. In *1999 SPE/EPA Exploration and Production Environmental Conference*. Austin, TX, 28 February-3 March 1999. SPE 52744. Society of Petroleum Engineers, Inc., Richardson, TX. pp. 509-513.

Fenchel, T. 1969. The Ecology of Marine Microbenthos. IV. Structure and Function of the Benthic Ecosystem, Its Chemical and Physical Factors and Microfauna Communities with Special Reference to the Ciliated Protozoa. *Ophelia*. 6:1-182.

Fillio, J.P., T.A. Hamacker, S.M. Koraido, R.G. Stefanacci, J.T. Tallon, and D. Wesolowski. 1987. *Production Waters Associated with the Production, Processing, Transmission, and Storage of Natural Gas: A Literature Study.* Technical Report GRI-87/0126 to the Gas Research Institute, Chicago, IL.

Fisher, R.A., A.G. Corbett, and C.B. Williams. 1943. The Relation Between Number of Species and the Number of Individuals in a Random Sample of an Animal Population. *Journal of Animal Ecology.* 12:42-58.

Folk, R.L. 1974. *Petrology of Sedimentary Rocks*. Hemphill's, Austin, TX. 170 pp.

Folk, R.L. and W.C. Ward. 1957. Brazos River Bar, A Study in the Significance of Grain-size Parameters. *Journal of Sedimentary Petrology*. 27:3-27.

Förstner, U. and G.T.W. Wittmann. 1981. *Metal Pollution in the Aquatic Environment*. 2nd Revised Edition. Springer Verlag, Berlin.

Friedheim, J.E. 1994. *Drilling with Synthetic Fluids in the North Sea - An Overview*. Presented at the IBC Conference on Drilling Technology. Aberdeen, November 1994. 13 pp. + figures.

Friedheim, J.E. and H.L. Conn. 1996. *Second Generation Synthetic Fluids in the North Sea: Are They Better?* In IADC/SPE Drilling Conference. New Orleans, 12-15 March 1996. IADC/SPE 35061. Society of Petroleum Engineers, Inc., Richardson, TX. pp. 215-228.

Friedheim, J.E. and R.M. Pantermuehl. 1993. Superior Performance with Minimal Environmental Impact: A Novel Nonaqueous Drilling Fluid. In *1993 SPE/IADC Drilling Conference.* Amsterdam, 23-25 February 1993. SPE/IADC 25753. Society of Petroleum Engineers, Inc., Richardson, TX. pp. 713-726.

Friedheim, J.E. and A. Patel. 1999. Technical Solutions for Environmental Problems: Novel Drilling Formulations to Minimize Environmental Impact. In *1999 SPE/EPA Exploration and Production Environmental Conference*. Austin, TX, 28 February-3 March 1999. SPE 52741. Society of Petroleum Engineers, Inc., Richardson, TX.

Froelich, P.N., G.P. Klinkhammer, M.L. Bender, N.A. Luedtke, G.R. Heath, D. Cullen, P. Dauphi, D. Hammond, B. Hartman, and V. Maynard. 1979. Early Oxidation of Organic Matter in Pelagic Sediments of the Eastern Equatorial Atlantic: Suboxic Diagenesis. *Geochimica et Cosmochimica Acta*. 43:1,075-1,090.

Gallaway, B.J., R.G. Fechhelm, G.F. Hubbard, and S.A. MacLean. 1998. *Opportunistic Sampling at a Synthetic Drilling Fluid Discharge Site on the Continental Slope of the Northern Gulf of Mexico: The Pompano Development, 13-14 March 1998.* Report to BP Exploration, Inc., Houston, TX. LGL Ecological Research Associates, Inc., Bryan, TX. Various pages.

Germano, J.D. and L.B. Read. 2002. *Natural Recovery at a Submarine Wood Waste Site.* In R.E. Hinchee, A. Porta, and M. Pellei, eds. Remediation and Beneficial Reuse of Contaminated Sediments. Proceedings of the First International Conference on Remediation of Contaminated Sediments, Venice, Italy, 10-12 October 2001. Battelle Memorial Institute Press, Columbus, OH. pp. 395-402.

Getliff, J., A. Roach, J. Toyo, and J. Carpenter. 1997. *An Overview of the Environmental Benefits of LAO Based Drilling Fluids for Offshore Drilling*. Report from Schlumberger Dowell. 10 pp.

Goldstein, A. 1942. Sedimentary Petrologic Provinces of the Northern Gulf of Mexico. *Journal of Sedimentary Petrology.* 12:77-84.

Grassle, J.F. and W. Smith. 1976. A Similarity Measure Sensitive to the Contribution of Rare Species and Its Use in Investigation of Variation in Marine Benthic Communities. *Oecologia*. 25:13-22.

Growcock, F.B., S.L. Andrews, and T.P. Frederick. 1994. Physicochemical Properties of Synthetic Drilling Fluids. In *1994 IADC/SPE Drilling Conference.* Dallas, TX, 15-18 February 1994. IADC/SPE 27450. International Association of Drilling Contractors/Society of Petroleum Engineers, Inc. (IADC/SPE), Richardson, TX. pp. 181-190.

Gundersen, J.K., B.B. Jørgensen, E. Larsen, and H.W. Jannasch. 1992. Mats of Giant Sulfur Bacteria on Deep-Sea Sediments Due to Fluctuating Hydrothermal Flow. *Nature London.* 360:454-455.

Harland, W.B., R.L. Armstrong, A.V. Cox, L.E. Craig, A.G. Smith, and D.G. Smith. 1990. *A Geologic Time Scale,* 1989 edition. Cambridge University Press, Cambridge. 263 pp.

Hartley, J.P. 1996. Environmental Monitoring of Offshore Oil and Gas Drilling Discharges – A Caution on the Use of Barium as a Tracer. *Marine Pollution Bulletin.* 32:727-733.

Hartley, J., R. Trueman, S. Anderson, J. Neff, K. Fucik, and P. Dando. 2003. *Drill Cuttings Initiative: Food Chain Effects Literature Review*. United Kingdom Offshore Operators Association, Aberdeen, Scotland.

Hawker, D.W. and D.W. Connell. 1985. Relationships Between Partition Coefficient, Uptake Rate Constant, Clearance Rate Constant, and Time to Equilibrium for Bioaccumulation. *Chemosphere.* 14:1,205-1,219.

Hawker, D.W. and D.W. Connell. 1986. Bioconcentration of Lipophilic Compounds by Some Aquatic Organisms. *Ecotoxicology and Environmental Safety.* 11:184-197.

Hermans, C.O. 1978. Metamorphosis in the Opheliid Polychaete *Armandia brevis*. In F. Chia and M.E. Rice, eds. *Settlement and Metamorphosis of Marine Invertebrate Larvae*. Elsevier, NY. pp. 113-126.

Hubbell, S.P. 2001. *The Unified Neutral Theory of Biodiversity and Biogeography*. Princeton University Press, Princeton & Oxford. 375 pp.

Hudgins, C.M. 1991. *Chemical Usage in North Sea Oil and Gas Production and Exploration Operations.* Report prepared for Oljeindustriens Landsforening (OLF). The Norwegian Oil Industry Association, Environment Committee, Stavanger, Norway.

Hurlbert, S.H. 1971. The Non-Concept of Species Diversity: A Critique and Alternative Parameters. *Ecology.* 52:577-586.

Inman, D.L. 1952. Measures for Describing the Size Distribution of Sediments. *Journal of Sedimentary Petrology.* 22(3):125-245.

Isphording, W.C. 1983. Interpretive Mineralogy: Examples from Miocene Coastal Plain Formations. *Transactions of the Gulf Coast Association of Geological Societies.* 33:295-305.

Jenkins, K.D., S. Howe, B.M. Sanders, and C. Norwood. 1989. Sediment Deposition, Biological Accumulation and Subcellular Distribution of Barium Following Drilling of an Exploratory Well. In F.R. Engelhardt, J.P. Ray, and A.H. Gillam, eds. *Drilling Wastes.* Elsevier Applied Sciences, London. pp. 587-608.

Jones, F.V., C. Hood, and G. Moiseychenko. 1996. International Methods of Evaluating the Discharge of Drilling Fluids in Marine Environments. In *1998 SPE International Conference on Health, Safety and Environment in Oil and Gas Exploration and Production.* Caracas, Venezuela, 7-10 June 1998. SPE 46825. Society of Petroleum Engineers, Inc., Richardson, TX. 18 pp.

Jørgensen, N. and N.P. Revsbech. 1985. Diffusive Boundary Layers and the Oxygen Uptake of Sediments and Detritus. *Limnology and Oceanography*. 30:111-122.

Kang, W.J., J.H. Trefry, T.A. Nelsen, and H.R. Wanless. 2000. Direct atmospheric inputs versus runoff fluxes of mercury to the lower Everglades and Florida Bay. *Environmental Science and Technology*. 34:4,058-4,063.

Kennicutt, M.C., II, P.N. Boothe, T.L. Wade, S.T. Sweet, R. Rezak, F.J. Kelly, J.M. Brooks, B.J. Presley, and D.A. Wiesenburg. 1996. Geochemical Patterns in Sediments Near Offshore Production Platforms. *Canadian Journal of Fisheries and Aquatic Sciences*. 53:2,554-2,566.

Kenny, P. 1993. Ester-Based Muds Show Promise for Replacing Some Oil-Based Muds. *Oil and Gas Journal.* 91:88-91.

Kingston, P.F. 1992. Impact of Offshore Oil Production Installations on the Benthos of the North Sea. *ICES Journal of Marine Science.* 49:45-53.

Kjeilen, G., S.J. Cripps, and T.G. Jacobsen. 2001. *Survey of Information on Cuttings Piles in the Norwegian Sector*. RF Report 773/654853 to the Norwegian Oil Industry Association (OLF).

Kramer, J.R., H.D. Grundy, and L.G. Hammer. 1980. Occurrence and Solubility of Trace Metals in Barite for Ocean Drilling Operations. In *Research on Environmental Fate and Effects of Drilling Fluids and Cuttings, Vol. II*. Courtesy Associates, Washington, D.C. pp. 789-798.

Krumbein, W.C. and F.J. Pettijohn. 1938. *Manual of Sedimentary Petrology.* Appleton, Century, and Crofts, Inc., NY. 549 pp.

Lee, B. 1998. The Use of Synthetics in Well Drilling Fluids for the Offshore Oil Field. American Chemical Society, Division of Fuel Chemistry. *Preprints of Symposia.* 43(2):233-237.

Lenihan, H.S., C.H. Peterson, S.L. Kim, K.E. Conlan, R. Fairey, C. McDonald, J.H. Grabowski, and J.S. Oliver. 2003. Variation in Marine Benthic Community Composition Allows Discrimination of Multiple Stressors. *Marine Ecology Progress Series*. 261:63-73.

Leuterman, A., I. Still, I. Johnson, J. Christie, and N. Butcher. 1997. *A Study of Trace Metals from Barites: Their Concentration, Bioavailability, and Potential for Bioaccumulation.* Proceedings of the Offshore Mediterranean Conference and Exhibition, Ravenna, Italy. OMC97.

LGL Ecological Research Associates, Inc. 1997. *Opportunistic Sampling at a Synthetic Drilling Fluid Discharge Site on the Continental Slope of the Northern Gulf of Mexico: The Pompano Development*. Report dated November 1997.

Limia, J.M. 1996. *Seabed Surveys: The Best Means to Assess the Environmental Impact of Drilling Fluid Discharges?* SPE 36048. Society of Petroleum Engineers, Inc., Richardson, TX. pp. 803-813.

Long, E.R. and P.M. Chapman. 1985. A Sediment Quality Triad: Measures of Sediment Contamination, Toxicity and Infaunal Community Composition in Puget Sound. *Marine Pollution Bulletin.* 16:405-415.

Luther, G.W., III, J.E. Kostka, T.M. Church, B. Sulzberger, and W. Stumm. 1992. Seasonal Iron Cycling in the Salt-Marsh Sedimentary Environment: The Importance of Ligand Complexes with Fe(II) and Fe(III) in the Dissolution of Fe(III) Minerals and Pyrite, Respectively. *Marine Chemistry.* 40:81-103.

Magurran, A.E. 1988. *Ecological Diversity and Its Measurement*. Princeton University Press, Princeton, NJ. 179 pp.

Matsunaga, K. and M. Nishimura. 1974. A Rapid and Sensitive Method for Determination of Submicrogram Amounts of Ammonia in Fresh and Sea Waters. *Analytica Chimica Acta*. 73:204-208.

Maurer, D., R.T. Keck, J.C. Tinsman, W.A. Leathem, C. Wethe, C. Lord, and T.M. Church. 1986. Vertical Migration and Mortality of Marine Benthos in Dredged Material: A Synthesis. *Internationale Revue der Gesamten Hydrobiologie.* 71:49-63.

May, R.M. 1975. Patterns of Species Abundance and Diversity. In M.L. Cody and J.M. Diamond, eds. *Ecology and Evolution of Communities.* Belknap Press, Cambridge. pp. 81-120.

McKee, J.D.A., K. Dowrick, and S.J. Astleford. 1995. A New Development Towards Improved Synthetic Based Mud Performance. In *1995 SPE/IADC Drilling Conference. Amsterdam, 28 February-2 March 1995.* SPE/IADC Drilling Conference. SPE/IADC 29405. Society of Petroleum Engineers, Inc., Richardson, TX. pp. 613-621.

Meinhold, A.F. 1999. Framework for a Comparative Environmental Assessment of Drilling Fluids Used Offshore. In *1999 SPE/EPA Exploration and Production Environmental Conference.* SPE 52746. Society of Petroleum Engineers, Inc., Richardson, TX. pp. 515-524.

Mirza, F.B. and J.S. Gray. 1981. The Fauna of Benthic Sediments from the Organically Enriched Oslofjord, Norway. *Journal of Experimental Marine Biology and Ecology*. 54:181-207.

Monnin, C., C.G. Dupre, H. Elderfield, and M.M. Mottl. 2001. Barium Geochemistry in Sediment Pore Waters and Formation Waters of the Oceanic Crust on the Eastern Flank of Juan de Fuca Ridge (ODP Leg 168). *Geochemistry, Geophysics, and Geosystems 2*. 15 pp.

National Oceanic and Atmospheric Administration (NOAA). 1998. Trace Organic Analytical Procedures. In *Sampling and Analytical Methods of the National Status and Trends Program Mussel Watch Project: 1993-1996 Update*. NOAA Technical Memorandum NOS/ORCA/CMBAD 130. National Oceanic and Atmospheric Administration, Silver Spring, MD.

National Research Council. 1983. *Drilling Discharges in the Marine Environment.* National Academy Press, Washington, D.C. 180 pp.

Neff, J.M. 1987. Biological Effects of Drilling Fluids, Drill Cuttings, and Produced Waters. In D.F. Boesch and N.N. Rabalais, eds. *Long-Term Environmental Effects of Offshore Oil and Gas Development*. Elsevier Applied Science Publishers, London. pp. 469-538.

Neff, J.M. 2002a. *Bioaccumulation in Marine Organisms. Effects of Contaminants from Oil Well Produced Water*. Elsevier Science Publishers, Amsterdam. 452 pp.

Neff, J.M. 2002b. *Fates and Effects of Mercury from Oil and Gas Exploration and Production Operations in the Marine Environment.* Report to the American Petroleum Institute, Washington, D.C. 164 pp.

Neff, J.M. and T.C. Sauer, Jr. 1995. *Barium in Produced Water: Fate and Effects in the Marine Environment.* API Publication 4633. American Petroleum Institute, Washington, D.C.

Neff, J.M., N.N. Rabalais, and D.F. Boesch. 1987. Offshore Oil and Gas Development Activities Potentially Causing Long-Term Environmental Effects. In D.F. Boesch and N.N. Rabalais, eds. *Long-Term Effects of Offshore Oil and Gas Development*. Elsevier Applied Science Publishers, London. pp. 149-174.

Neff, J.M., M.H. Bothner, N.J. Maciolek, and J.F. Grassle. 1989. Impacts of Exploratory Drilling for Oil and Gas on the Benthic Environment of Georges Bank. *Marine Environmental Research.* 27:77-114.

Neff, J.M., S. McKelvie, and R.C. Ayers, Jr. 2000. *Environmental Impacts of Synthetic Based Drilling Fluids.* OSC Study MMS 2000-064. U.S. Department of the Interior, Minerals Management Service, Gulf of Mexico OCS Region, New Orleans, LA. 121 pp.

Nelsen, T.A. and J.H. Trefry. 1986. Pollutant-Particle Relationships in the Marine Environment: A Study of Particulates and Their Fate in a Major River-Delta-Shelf System. *Rapports et Proces-verbaus des Réunions. Conseil International pour l'Exploration de la Mer.* 186:115-127.

Nelsen, T.A., P. Blackwelder, T. Hood, B. McKee, N. Romer, C. Alvarez-Zarikian, and S. Metz. 1994. Time-Based Correlation of Biogenic, Lithogenic and Authigenic Sediment Components with Anthropogenic Inputs in the Gulf of Mexico. *Estuaries.* 17:873-885.

Nilsson, H.C. and R. Rosenberg. 2000. Succession in Marine Benthic Habitats and Fauna in Response to Oxygen Deficiency: Analyzed by Sediment Profile Imaging and by Grab Samples. *Marine Ecology Progress Series*. 197:139-194.

Norman, M. 1997. Esters - *The Only Synthetic Option for the Next Millennium?* Presented at the 5th International [IBC] Conference of Minimizing the Environmental Effects of Drilling Operations. Aberdeen, Scotland. 13 pp.

Norwegian Oil Industry Association Working Group. 1996. Criteria for Selection and Approval of Drilling Fluids: With Respect to Effects on Human Workers and Marine Ecological Systems. Norwegian Oil Industry Association, Stavanger, Norway. 70 pp.

Olsgard, F. and J.S. Gray. 1995. A Comprehensive Analysis of the Effects of Offshore Oil and Gas Exploration and Production on the Benthic Communities of the Norwegian Continental Shelf. *Marine Ecology Progress Series.* 122:277-306.

Park, S., D. Cullum, and A.D. McLean. 1993. *The Success of Synthetic-Based Drilling Fluids Offshore Gulf Of Mexico: A Field Comparison to Conventional Systems.* SPE 26345. 68th Annual Technical Conference and Exhibition of the Society of Petroleum Engineers, Houston, TX. Society of Petroleum Engineers, Inc., Richardson, TX.

Payne, J.F., J. Kiceniuk, A. Rahimtula, U. Williams, L. Fancey, W. Melvin, and R.A. Addison. 1989. Bioaccumulation of Polycyclic Aromatic Hydrocarbons in Flounder (*Pseudopleuronectes americanus*) Exposed to Oil-Based Drill Cuttings. In F.R. Engelhardt, J.P. Ray, and A.H. Gillam, eds. *Drilling Wastes.* Elsevier Applied Science Publishers, London. pp. 427-438.

Paytan, A., S. Mearon, K. Cobb, and M. Kastner. 2002. Origin of Marine Barite Deposits: Sr and S Isotope Characterization. *Geology*. 30:747-750.

Pearson, T.H. and R. Rosenberg. 1978. Macrobenthic Succession in Relation to Organic Enrichment and Pollution of the Marine Environment. *Oceanography and Marine Biology Annual Review*. 16:229-311.

Phillips, E.J.P., E.R. Landa, T. Kraemer, and R. Zielinski. 2001. Sulfate-Reducing Bacteria Release Barium and Radium from Naturally Occurring Radioactive Material in Oil-Field Barite. *Geomicrobiology Journal.* 18:167-182.

Pielou, E.C. 1975. *Ecological Diversity.* John Wiley & Sons, New York, NY. 165 pp.

Rabke, S.P., J. Candler, and C. Trial. 1998. *Development of Acute Benthic Toxicity Testing for Monitoring Synthetic-Based Muds Discharged Offshore*. Presented at the IBC Conference on Monitoring the Environmental Effects of Offshore Drilling, Houston, TX. 26 pp.

Rabke, S.P., K. Satterlee, C. Johnston, L. Henry, S. Wilson, T. Sharpe, and J. Ray. 2003. *Achieving Regulatory Compliance with Synthetic-Based Drilling Fluids*. SPE 80588. Paper presented at the SPE/EPA/DOE Exploration and Production Environmental Conference, San Antonio, TX. Society of Petroleum Engineers, Inc., Richardson, TX. 10 pp.

Randall, D.J. and T.K.N. Tsui. 2002. Ammonia Toxicity in Fish. *Marine Pollution Bulletin.* 45:17-23.

Rhoads, D.C. 1974. Organism Sediment Relations on the Muddy Sea Floor. *Oceanography and Marine Biology Annual Review*. 12:263-300.

Rhoads, D.C. and S. Cande. 1971. Sediment Profile Camera for In Situ Study of Organism-Sediment Relations. *Limnology and Oceanography*. 16:110-114.

Rhoads, D.C. and J.D. Germano. 1982. Characterization of Organism-Sediment Relations Using Sediment Profile Imaging: An Efficient Method to Remote Ecological Monitoring on the Seafloor (REMOTS System). *Marine Ecology Progress Series*. 8:115-128.

Rhoads, D.C. and J.D. Germano. 1986. Interpreting Long-Term Changes in Benthic Community Structure: a New Protocol. *Hydrobiologia*. 142:291-308.

Robin, E., C. Barouille, G. Martinez, I. Lefevre, J.L. Reyss, P. van Beek, and C. Jeandel. 2003. Direct Barite Determination Using SEM/EDS-ACC System: Implication for Constraining Barium Carriers and Barite Preservation in Marine Sediments. *Marine Chemistry.* 82:289-306.

Rosen, N.C. 1969. Heavy Minerals and Size Analysis of the Citronelle Formation of the Gulf Coastal Plain. *Journal of Sedimentary Petrology.* 39:1,552-1,565.

Rosenberg, R. and R.J. Diaz. 1993. Sulphur Bacteria (*Beggiatoa* spp.) Mats Indicate Hypoxic Conditions in the Inner Stockholm Archipelago. *Ambio*. 22:32-36.

Rosenberg, R., H.C. Nilsson, and R.J. Diaz. 2001. Response of Benthic Fauna and Changing Sediment Redox Profiles over a Hypoxic Gradient. *Estuarine, Coastal and Shelf Science*. 53:343-350.

Rushing, J.H., M.A. Churan, and F.V. Jones. 1991. Bioaccumulation from Mineral Oil-Wet and Synthetic Liquid-Wet Cuttings in an Estuarine Fish, *Fundulus grandis*. In The First International Conference on Health, Safety and Environment. The Hague, The Netherlands, 10-14 November 1991. SPE 23350. Society of Petroleum Engineers, Inc., Richardson, TX. pp. 311-320.

Russell, R.D. 1937. Mineral Composition of Mississippi River Sands. *Geological Society of America Bulletin*. 48:1,307-1,348.

Santschi, P., P. Höhener, G. Benoit, and M. Buchholtz-ten-Brink. 1990. Chemical Processes at the Sediment-Water Interface. *Marine Chemistry.* 30:269-315.

Sayle, S., M. Seymour, and E. Hickey. 2002. *Assessment of Environmental Impacts from Drilling Muds and Cuttings Disposal Offshore Brunei*. SPE 73930. In SPE International Conference on Health, Safety and Environment in Oil and Gas Exploration and Production, Kuala Lumpur, Malaysia. Society of Petroleum Engineers, Inc., Richardson, TX. 12 pp.

Schaanning, M., K. Hylland, R. Lichtenthaler, and B. Rygg. 1996. *Biodegradation of Anco Green and Novaplus Drilling Muds on Cuttings Deposited in Benthic Chambers.* Report SNO 3475-96. Norwegian Institute for Water Research, Oslo, Norway. 77 pp. + app.

Schropp, S.J., F.G. Lewis, and H.L. Windom. 1990. Interpretation of Metal Concentrations in Estuarine Sediments of Florida Using Aluminum as a Reference Element. *Estuaries.* 13(3):227-235.

Shepard, F.P. 1954. Nomenclature Based on Sand-Silt-Clay Ratios. *Journal of Sedimentary Petrology.* 24:151-158.

Shimmield, G. and E. Breuer. 2000. *A Geochemical & Radiochemical Appraisal of Offshore Drill Cuttings as a Means of Predicting Possible Environmental Impact After Site Abandonment.* Report to NERC and UKOOA from the Scottish Association for Marine Science, Dunstaffnage Marine Laboratory, Oban, Scotland. 22 pp.

Shimmield, G.B. and T.F. Pedersen. 1990. The Geochemistry of Reductive Trace Metals and Halogens in Hemipelagic Continental Margin Sediments. *Aquatic Sciences.* 3:255-279.

Shimmield, G.B., E. Breuer, D.G. Cummings, O. Peppe, and T. Shimmield. 2000. *Contaminant Leaching from Drill Cuttings Piles of the Northern and Central North Sea: Field Results from Beryl "A" Cuttings Pile*. Report UKOOA from the Scottish Association for Marine Science, Dunstaffnage Marine Laboratory, Oban, Scotland. 28 pp.

Slomp, C.P., J.F.P. Malschaert, L. Lohse, and W. van Raaphorst. 1997. Iron and Manganese Cycling in Different Sedimentary Environments on the North Sea Continental Margin. *Continental Shelf Research.* 17:1,083-1,117.

Stagg, R.M. and A. McIntosh. 1996. The Effects of Drill Cuttings on the Dab (*Limanda limanda*). In *The Physical and Biological Effects of Processed Oily Drill Cuttings*. E&P Forum Report No. 2.61/202. E&P Forum, London. April 1996. pp. 79-103.

Strickland, J.D.H. and T.R. Parsons. 1972. *A Practical Handbook of Seawater Analysis*. Fisheries Research Board of Canada.

Tamaki, A. 1985. Inhibition of Larval Recruitment of *Armandia* sp. (Polychaeta: Opheliidae) by Established Adults of *Psuedopolydora paucibranchiata* (Okuda) (Polychaeta: Spionidae) on an Intertidal Sand Flat. *Journal of Experimental Marine Biology and Ecology*. 87:167-182.

Tankére, S.P.C., P.J. Statham, and N.B. Price. 2000. Biogeochemical Cycling of Mn and Fe in an Area Affected by Eutrophication: The Adriatic Sea. *Estuarine, Coastal and Shelf Science.* 51:491-506.

Thamdrup, B., R.N. Glud, and J.W. Hansen. 1994. Manganese Oxidation and In Situ Manganese Fluxes from a Coastal Sediment. *Geochimica et Cosmochimica Acta.* 58:2,563-2,570.

Thode-Andersen, S. and B.B. Jørgensen. 1989. Sulfate Reduction and the Formation of ^{35}S-labeled FeS, FeS_2, and S^o in Coastal Marine Sediments. *Limnology and Oceanography.* 34:793-806.

Trefry, J.H. and S. Metz. 1984. Selective Leaching of Trace Metals from Sediments as a Function of pH. *Analytical Chemistry*. 56(4):745-749.

Trefry, J.H. and B.J. Presley. 1976. Heavy Metals in Sediment from San Antonio Bay and the Northwest Gulf of Mexico. *Environmental Geology*. 1:283-294.

Trefry, J.H. and B.J. Presley. 1982. Manganese Fluxes from Mississippi Delta Sediments. *Geochimica et Cosmochimica Acta*. 46:1,715-1,726.

Trefry, J.H. and J.P. Smith. 2003. *Forms of Mercury in Drilling Fluid Barite and Their Fate in the Marine Environment: A Review and Synthesis*. SPE Paper 80571 presented at the 2003 SPE/DOE/EPA Exploration and Production Environmental Conference, San Antonio, TX, March 10-12, 2003.

Trefry, J.H., R.P. Trocine, M. McElvaine, R. Rember, and L. Hawkins. 2003. *Concentrations of Total and Methylmercury in Sediment Adjacent to Oil Platforms in the Gulf of Mexico*. SPE Paper 80569 presented at the SPE/DOE/EPA Exploration and Production Environmental Conference, San Antonio, TX, March 10-12, 2003.

Trueblood, D.D., E.D. Gallagher, and D.M. Gould. 1994. The Three Stages of Seasonal Succession on the Savin Hill Cove Mudflat, Boston Harbor. *Limnology and Oceanography.* 39:1,440-1,454.

Uhler, A.D. and J.M. Neff. 1998. *Survey of Monitoring Approaches for the Detection of Oil Contamination in Synthetic-based Drilling Muds (SBMs).* Final Report submitted to American Petroleum Institute.

Ulrich, G.A., G.N. Breit, I.M. Cozzarelli, and J.M. Suflita. 2003. Sources of Sulfate Supporting Anaerobic Metabolism in a Contaminated Aquifer. *Environmental Science and Technology.* 37:1,093-1,099.

U.S. Department of the Interior, Minerals Management Service (USDOI, MMS). 2000. *Gulf of Mexico Deepwater Operations and Activities: Environmental Assessment*. Gulf of Mexico OCS Region. MMS OCS/EIS-EA 2000-001. Available on the Internet at http://www/gomr.mms.gov/homepg/watsnew/techann/Deepwater.pdf

U.S. Environmental Protection Agency (USEPA). 1991. *Methods for the Determination of Metals in Environmental Samples*. EPA/600/4-91/010. U.S. Environmental Protection Agency, Office of Research & Development, Cincinnati, OH.

U.S. Environmental Protection Agency (USEPA). 1993. Oil and Gas Extraction Point Source Category, Offshore Subcategory; Effluent Limitations Guidelines and New Source Performance Standards. *Federal Register*. 58(41):12,454-12,512.

U.S. Environmental Protection Agency (USEPA). 1994. *Methods for Assessing the Toxicity of Sediment-Associated Contaminants with Estuarine and Marine Amphipods*. EPA 600/R-94/025. June 1994. U.S. Environmental Protection Agency Office of Research and Development, Washington, D.C.

U.S. Environmental Protection Agency (USEPA). 1996. 40 CFR Part 435 [FRL-5648-4] RIN 2040-AB72 Final Effluent Limitations Guidelines and Standards for the Coastal Subcategory of the Oil and Gas Extraction Point Source Category. December 16, 1996. *Federal Register.* 61(242):66,086-66,130.

U.S. Environmental Protection Agency (USEPA). 1999. 40 CFR Part 435 [FRL-6215-1] RIN 2040-AD14 Effluent Limitations Guidelines and New Source Performance Standards for Synthetic-Based and Other Non-Aqueous Drilling Fluids in the Oil and Gas Extraction Point Source Category, Proposed Rule. February 3, 1999. *Federal Register.* 64(22):5,487-5,554.

U.S. Environmental Protection Agency (USEPA). 2001a. 40 CFR Parts 9 and 435 [FRL-6929-8] RIN 2040-AD14 Effluent Limitations Guidelines and New Source Performance Standards for the Oil and Gas Extraction Point Source Category; OMB Approval Under the Paperwork Reduction Act: Technical Amendment; Final Rule. January 22, 2001. *Federal Register.* 66(14):6,850-6,919.

U.S. Environmental Protection Agency (USEPA). 2001b. *Methods for Assessing the Chronic Toxicity of Marine and Estuarine Sediment-associated Contaminants with Amphipod Leptocheirus plumulosus* - First Edition. March 2001. EPA/600/R-01/020.

U.S. Environmental Protection Agency (USEPA). 2001c. [FRL-7119-5] Notice of Final NPDES General Permit; Final NPDES General Permit for New and Existing Sources and New Dischargers in the Offshore Subcategory of the Oil and Gas Extraction Category for the Western Portion of the Outer Continental Shelf of the Gulf of Mexico (GMG290000). December 18, 2001. *Federal Register.* 66(243):65,209-65,210.

Valente, R.M., D.C. Rhoads, J.D. Germano, and V.J. Cabelli. 1992. Mapping of Benthic Enrichment Patterns in Narragansett Bay, Rhode Island. *Estuaries*. 15:1-17.

Van Cappellen, P. and Y. Wang. 1995. Metal Cycling in Surface Sediments: Modeling the Interplay of Transport and Reaction. In H.E. Allen, ed. *Metal Contaminated Aquatic Sediments*. Ann Arbor Press, Inc., Chelsea, MI. pp. 21-64.

van der Zee, C., W. van Raaphorst, W. Helder, and H. de Heij. 2003. Manganese Diagenesis in Temporal and Permanent Depositional Areas of the North Sea. *Continental Shelf Research.* 23:625-646.

Van Os, B.J.H., J.J. Middelburg, and G.J. de Lange. 1991. Possible diagenetic mobilization of barium in sapropelic sediment from the eastern Mediterranean. *Marine Geology.* 100:125-136.

Veil, J.A. and J.M. Daly. 1999. Innovative regulatory approach for synthetic-based drilling fluids. In *1999 SPE/EPA Exploration and Production Environmental Conference. Austin, TX, 28 February-3 March 1999.* SPE 52737. Society of Petroleum Engineers, Inc., Richardson, TX. 5 pp.

Veil, J.A., C.J. Burke, and D.O. Moses. 1996. Synthetic-Based Muds Can Improve Drilling Efficiency Without Polluting. *Oil & Gas Journal*. 94(10)49-54.

Vik, E.A., S. Dempsey, and B.S. Nesgard. 1996a. *Evaluation of Available Test Results from Environmental Studies of Synthetic Based Drilling Muds*. Version 4. OLF Project. Acceptance Criteria for Drilling Fluids. Aquateam Report Number: 96-010. Aquateam-Norwegian Water Technology Centre A/S, Oslo, Norway. 127 pp.

Vik, E.A., B.S. Nesgard, J.D. Berg, S.M. Dempsey, D.R. Johnson, L. Gawel, and E. Dalland. 1996b. Factors Affecting Methods for Biodegradation Testing of Drilling Fluids for Marine Discharge. In *International Conference on Health, Safety & Environment, New Orleans, Louisiana, 9-12 June 1996.* SPE 35981. Society of Petroleum Engineers, Inc., Richardson, TX. pp. 697-711.

Vismann, B. 1991. Sulfide Tolerance: Physiological Mechanisms and Ecological Implications. *Ophelia*. 34:1-27.

Wang, F. and P.M. Chapman. 1999. Biological Implications of Sulfide in Sediment – A Review Focusing on Sediment Toxicity. *Environmental Toxicology and Chemistry.* 18:2,526-2,532.

Weisbart, S.B., H.T. Wilson, D.G. Heimbuch, H.L. Windom, and J.K. Summers. 2000. Comparison of Sediment Metal: Aluminum Relationships Between the Eastern and Gulf Coasts of the United States. *Environmental Monitoring and Assessment.* 61:373-385.

Wilhelm, S.M. 2001. *Mercury in Petroleum and Natural Gas: Estimation of Emissions from Production, Processing, and Combustion*. EPA-600/R-01-066. U.S. Environmental Protection Agency, Office of Research and Development, Washington, D.C. 70 pp.

Windom, H.L., S.J. Schropp, F.D. Calder, J.D. Ryan, R.G. Smith, L.C. Burney, F.G. Lewis, and C.H. Rawlinson. 1989. Natural Trace Metal Concentrations in Estuarine and Coastal Marine Sediments of the Southeastern United States. *Environmental Science and Technology.* 23:314-320.

Wu, R.S.S. 2002. Hypoxia: From Molecular Responses to Ecosystem Responses. *Marine Pollution Bulletin.* 45:35-45.

Zar, J.H. 1999. *Biostatistical Analysis.* 4th ed., Prentice Hall, Upper Saddle River, NJ.